ADRIADAPT D.3.3.1

Detailed quantification of climate change signal in the region of interest with special emphasis on severe impacting events

Authors: CMCC, ARPAE, DHMZ

contact person: enrico.scoccimarro@cmcc.it

TABLE OF CONTENTS

1 ABBREVIATIONS 9

2 INTRODUCTION 10

3 DESCRIPTION OF MODELS AND PARAMETERS 11

3.1 Regional Climate Models 11

3.2 Statistical Downscaling schemes (SDs) 15

4 DESCRIPTION OF THE WHOLE DATA SET AVAILABLE (DYNAMICAL AND STATISTICAL DOWNSCALED DATA) AVAILABLE 20

5 FUTURE PROJECTIONS AS RESULTING FROM DYNAMICAL DOWNSCALING OVER THE WHOLE ADRIADAPT DOMAIN 22

5.1 Temperature related indices projections 22

5.1.1 Averaged temperature 22

5.1.2 Extreme temperature 27

5.1.3 Heat wave duration 32

5.1.4 Tropical nights 37

5.1.5 Frost days 40

5.2 Precipitation related indices projections 43

5.2.1 Averaged precipitation 43

5.2.2 Intense precipitation 48

5.2.3 Extreme precipitation 53

5.2.4 Consecutive dry days 58

6 FUTURE PROJECTIONS OVER THE CASE STUDIES 64

6.1 Case study 1: Knin 64
6.1.1 Dynamically downscaled results 64
6.1.1.1 Temperature related indices projections 64
6.1.1.1.1 Averaged 2 meter air temperature 64
6.1.1.1.2 Extreme high temperature... 67
6.1.1.1.3 Extreme high maximum temperature 69
6.1.1.1.4 Extreme rare high temperature 71
6.1.1.1.5 Extreme rare high maximum temperature...................................... 73
6.1.1.2 Precipitation related indices projections 75
6.1.1.2.1 Averaged precipitation 75
6.1.1.2.2 Intense precipitation 77
6.1.1.2.3 Extreme precipitation 79
6.1.1.3 Surface relative humidity projections.. 81
6.1.1.4 Extra rare humidex projections... 83
6.1.2 Statistically downscaled results 85
6.1.2.1 Temperature related indices projections 85
6.1.2.1.1 Minimum and maximum air temperature.. 85
6.1.2.1.2 Extreme temperature 90
6.1.2.1.3 Heat wave duration 94
6.1.2.1.4 Tropical nights... 96
6.1.2.1.5 Frost days 97
6.1.2.2 Precipitation related indices projections 100
6.1.2.2.1 Amount of precipitation 100
6.1.2.2.2 Intense precipitation 102
6.1.2.2.3 Consecutive dry days.. 103

6.2 Case study 2: Šibenik 106
6.2.1 Dynamically downscaled results 106
6.2.1.1 Temperature related indices projections 106

6.2.1.1.1 Averaged 2 meter air temperature 106
6.2.1.1.2 Extreme high temperature... 109
6.2.1.1.3 Extreme high maximum temperature 111
6.2.1.1.4 Extreme rare high temperature 113
6.2.1.1.5 Extreme rare high maximum temperature.................................... 115
6.2.1.2 Precipitation related indices projections 117
6.2.1.2.1 Averaged precipitation 117
6.2.1.2.2 Intense precipitation 119
6.2.1.2.3 Extreme precipitation 121
6.2.1.3 Surface relative humidity projections... 123
6.2.1.4 Extra rare humidex projections... 125
6.2.2 Statistically downscaled results 127
6.2.2.1 Temperature related indices projections 127
6.2.2.1.1 Seasonal minimum and maximum temperature........................... 127
6.2.2.1.2 Extreme temperature 132
6.2.2.1.3 Heat wave duration 136
6.2.2.1.4 Tropical nights.. 138
6.2.2.1.1 Frost days 140
6.2.2.2 Precipitation related indices projection... 143
6.2.2.2.1 Amount of precipitation 143
6.2.2.2.2 Intense precipitation 146
6.2.2.2.3 Consecutive dry days.. 148
6.3 Case study 3: Vodice 151
6.3.1 Dynamically downscaled results 151
6.3.1.1 Temperature related indices projections 151
6.3.1.1.1 Averaged 2 meter air temperature 151
6.3.1.1.2 Extreme high temperature... 154
6.3.1.1.3 Extreme high maximum temperature 156
6.3.1.1.4 Extreme rare high temperature 158

6.3.1.1.5 Extreme rare high maximum temperature.................................... 160
6.3.1.2 Precipitation related indices projections... 162
6.3.1.2.1 Averaged precipitation 162
6.3.1.2.2 Intense precipitation.. 164
6.3.1.2.3 Extreme precipitation 166
6.3.1.2.4 Heavy precipitation index... 168
6.3.1.2.5 Maximum number of consecutive dry days.................................. 170
6.3.1.3 Extra rare humidex projections.. 172

6.4 Case study 4: Cervia 174
6.4.1 Dynamically downscaled results... 174
6.4.1.1 Temperature related indices projections 174
6.4.1.1.1 Averaged 2 meter air temperature 174
6.4.1.1.2 High temperature 177
6.4.1.1.3 High maximum temperature... 179
6.4.1.1.4 Extreme high temperature.. 181
6.4.1.1.5 Extreme high maximum temperature... 183
6.4.1.1.6 Extreme rare high temperature 185
6.4.1.1.7 Extreme rare high maximum temperature.................................... 187
6.4.1.1.8 Warm spell days index 189
6.4.1.1.9 Heat wave duration index... 191
6.4.1.2 Precipitation related indices projections... 193
6.4.1.2.1 Averaged precipitation 193
6.4.1.2.2 Intense precipitation.. 195
6.4.1.2.3 Extreme precipitation 197
6.4.1.2.4 Heavy precipitation index... 199
6.4.1.2.5 Maximum number of consecutive dry days.................................. 201
6.4.1.3 Extra rare humidex projections.. 203
6.4.1.4 Wind projections... 205
6.4.1.4.1 Averaged wind module.. 205

6.4.1.4.2 Maximum wind module 207
6.4.2 Statistically downscaled results 209
6.4.2.1 Temperature related indices projections 209
6.4.2.1.1 Seasonal and annual minimum and maximum temperature........ 209
6.4.2.1.2 Extreme temperature 214
6.4.2.1.3 Heat wave duration 219
6.4.2.1.4 Tropical nights........ 221
6.4.2.1.5 Frost days 222
6.4.2.2 Precipitation related indices projection........ 225
6.4.2.2.1 Amount of precipitation 225
6.4.2.2.2 Intense precipitation........ 227
6.4.2.2.3 Consecutive dry days........ 229
6.5 Case study 5: Cesena 231
6.5.1 Dynamically downscaled results 231
6.5.1.1 Temperature related indices projections 231
6.5.1.1.1 Averaged 2 meter air temperature 231
6.5.1.1.2 High temperature 234
6.5.1.1.3 High maximum temperature........ 236
6.5.1.1.4 Extreme high temperature........ 238
6.5.1.1.5 Extreme high maximum temperature........ 240
6.5.1.1.6 Extreme rare high temperature 242
6.5.1.1.7 Extreme rare high maximum temperature........ 244
6.5.1.1.8 Warm spell days index 246
6.5.1.1.9 Heat wave duration index........ 248
6.5.1.2 Precipitation related indices projections 250
6.5.1.2.1 Averaged precipitation 250
6.5.1.2.2 Intense precipitation........ 252
6.5.1.2.3 Extreme precipitation 254
6.5.1.2.4 Heavy precipitation index........ 256

6.5.1.2.5 Maximum number of consecutive dry days 258
6.5.1.3 Extra rare humidex projections 260
6.5.1.4 Wind projections 262
6.5.1.4.1 Averaged wind module 262
6.5.1.4.2 Maximum wind module 264
6.5.2 Statistically downscaled results 266
6.5.2.1 Temperature related indices projections 266
6.5.2.1.1 Seasonal minimum and maximum temperature 266
6.5.2.1.2 Extreme temperature 271
6.5.2.1.3 Heat wave duration 276
6.5.2.1.4 Tropical nights 278
6.5.2.1.5 Frost days 279
6.5.2.2 Precipitation related indices projection 282
6.5.2.2.1 Amount of precipitation 282
6.5.2.2.2 Intense precipitation 284
6.5.2.2.3 Consecutive dry days 286
6.6 Case study 6: Verghereto 288
6.6.1 Dynamically downscaled results 288
6.6.1.1 Temperature related indices projections 288
6.6.1.1.1 Averaged 2 meter air temperature 288
6.6.1.1.2 High temperature 291
6.6.1.1.3 High maximum temperature 293
6.6.1.1.4 Extreme high temperature 295
6.6.1.1.5 Extreme high maximum temperature 297
6.6.1.1.6 Extreme rare high temperature 299
6.6.1.1.7 Extreme rare high maximum temperature 301
6.6.1.1.8 Warm spell days index 303
6.6.1.1.9 Heat wave duration index 305
6.6.1.2 Precipitation related indices projections 307

6.6.1.2.1 Averaged precipitation 307
6.6.1.2.2 Intense precipitation 309
6.6.1.2.3 Extreme precipitation 311
6.6.1.2.4 Heavy precipitation index 313
6.6.1.2.5 Maximum number of consecutive dry days 315
6.6.1.3 Extra rare humidex projections 317
6.6.1.4 Wind projections 319
6.6.1.4.1 Averaged wind module 319
6.6.1.4.2 Maximum wind module 321
6.6.2 Statistically downscaled results 323
6.6.2.1 Temperature related indices projections 323
6.6.2.1.1 Seasonal minimum and maximum temperature 323
6.6.2.1.2 Extreme temperature 328
6.6.2.1.3 Heat wave duration 332
6.6.2.1.4 Tropical nights 334
6.6.2.1.5 Frost days 335
6.6.2.2 Precipitation related indices projection 338
6.6.2.2.1 Amount of precipitation 338
6.6.2.2.2 Intense precipitation 340
6.6.2.2.3 Consecutive dry days 342

7 CONCLUSIONS 344

8 ACKNOWLEDGEMENTS 345

9 REFERENCES 346

10 ANNEXES 348

Document History

Name (Institution)	Date	Version
CMCC (Enrico Scoccimarro Andrea Borrelli, Giovanni Zizzi, Silvio Gualdi)	01/07/2020	V0
DHMZ (Lidija Cvitan, Ivan Guettler, Leonardo Patalen, Lidija Srnec)	11/12/2020	V2
ARPAE: Rodica Tomozeiu, Roberta Monti, Fabrizio Nerozzi	11/12/2020	V3
DHMZ (Lidija Cvitan, Ivan Guettler, Leonardo Patalen, Lidija Srnec)	13/12/2020	V4
CMCC (Enrico Scoccimarro Andrea Borrelli, Giovanni Zizzi, Silvio Gualdi)	16/12/2020	V5
CMCC (Enrico Scoccimarro Andrea Borrelli, Giovanni Zizzi, Silvio Gualdi)	17/12/2020	V6
DHMZ (Lidija Cvitan, Ivan Guettler, Leonardo Patalen, Lidija Srnec)	18/12/2020	V6
ARPAE: Rodica Tomozeiu, Roberta Monti, Fabrizio Nerozzi	21/12/2020	V7
CMCC, ARPAE,DHMZ	23/12/2020	V8
Name of reviewer	**Date**	
DOOR Dunja Mazzocco Dvar	18/01/2021	V9

Declaration of originality:
This deliverable contains original unpublished work, except where it is clearly indicated otherwise. Acknowledgement of previously published material and of the intellectual property of other(s) has been stated through citation, quotation or both.

1 Abbreviations

AR5:	5th Assessment Report of the Intergovernmental Panel on Climate Change
CCA:	Canonical Correlation Analysis
CGCMs:	Fully coupled General Circulation Models
CMIP5:	5th phase of the Coupled Model Intercomparison Project
CMCC:	Fondazione Centro euro-Mediterraneo sui Cambiamenti Climatici
CORR:	Correlation Coefficient
DJF:	December-January February
ENS:	Ensemble Average
GCMs:	General Circulation Models
IPCC:	Intergovernmental Panel on Climate Change
JJA:	June-July-August
MAM:	March-April-May
MSLP:	Mean Sea Level Pressure
NetCDF:	Network Common Data Form
RCMs:	Regional Climate Models
RCP4.5:	Representative Concentration Pathway to a radiative forcing of 4.5 W/m2 at the end of 2100 wrt preindustrial values
RCP8.5:	Representative Concentration Pathway to a radiative forcing of 8.5 W/m2 at the end of 2100 wrt preindustrial values
RMSE:	Root Mean Square Error
SON:	September-October-November
SD:	Statistical Downscaling
Z500:	Geopotential at 500hPa

2 Introduction

This document (D3.3.1) provides a description of the projections of climate indicators over different periods and radiative scenarios based on data delivered by CMCC, Arpae and DHMZ to the ADRIADAPT project users, both in terms of dynamical (see deliverables D3.2.1), and statistical (see deliverable D3.2.2) downscaling outputs. Within the ADRIADAPT project, the simulated data cover the period 1961 to 2100, following historical forcing up to 2005 and two different possible radiative emission scenarios to the end of the century: a business as usual (RCP8.5) and a more moderate one (RCP4.5). Result for future periods will be mainly presented as deviation from the base line historical period (1986-2005, named P0) over different time slices: 2021:2040, 2041:2060, 2061:2080, 2081:2100 named respectively P1, P2, P3, P4.
The used tools are shortly presented in Section 2, the climatic variables delivered within the project are presented in Section 3, as recap of D3.2.1 and D3.2.2.
Section 4 focuses on the projections resulting from the dynamical downscaling over the whole domain and section 5 focuses on projections over the case study cities, as resulting from both dynamical and statistical downscaling approach. Projections for the main parameters required by stakeholders and project users, case study by case study, have been considered.

3 Description of Models and parameters

3.1 Regional Climate Models

One of the ways to investigate the climate system and its variability is through climate models. Considering the global scale, a climate model can be an atmosphere (or ocean)-only general circulation model (GCM) or a fully coupled general circulation model (CGCM). To improve the ability of a climate model in representing small-scale features, instead of a general circulation model, regional climate model (RCM) and statistical downscaling technique (SD) can be used: this approach makes it possible to increase the spatial resolution, reducing the extension of the domain considered. In fact, the performance and the spatial resolution of GCMs have continuously improved in the recent years, but the typical state of the art spatial scale is still too coarse to realistically reproduce present climate and eventually project climate change signals on local scales, especially in the presence of complex orography (Rummukainen, 2010; IPCC, 2001) such as over the European domain.

The EURO-CORDEX (COordinated Regional climate Downscaling EXperiment) (Nikulin et al., 2012) on the 12.5 km EUR-11 spatial domain is one source of data foreseen within ADRIADAPT and in the next chapters we will evaluate model ability in representing the climate over the ADRIADAPT domain (Figure 2-1), not only in terms of averages but also extremes, comparing them with observational data-sets.

EURO-CORDEX is the European branch of the international CORDEX (COordinated Regional climate Downscaling EXperiment) initiative, which is sponsored by the World Climate Research Program (WRCP) to organize an internationally coordinated framework to produce improved regional climate change projections, through regional climate models, for all land regions world-wide (http://www.euro-cordex.net/). The CORDEX-results serve as input for climate change impact and adaptation studies within the timeline of the Fifth Assessment Report (AR5) of the Intergovernmental Panel on Climate Change (IPCC) and beyond. The experiments used to provide the RCM dataset described in this report are based on the standard setup of the model for the CORDEX ensemble simulations (Nikulin et al., 2012, Vautard et al. 2013) over the EUR-11 domain thus over the European domain with a horizontal resolution of 12.5 km. This means that the RCMs compute the “climate equations” over each grid cell (one cell represent an area of 12.5km x 12.5km), based on previous values (the model time step is of the order for few minutes) and adjacent cell values. The model is able to evolve in time, with the only constrain of radiative forcing (atmospheric concentration of greenhouse gasses, ozone and aerosols) and boundary conditions: ocean conditions are expected at the lower boundary of the RCM (such as sea surface temperature, current velocities, etc.) and atmospheric conditions (temperature, wind, water fluxes, etc.) of the surrounding area are expected at

the border of the cube on which the model is planned to simulate. As already stated in this way the model is able to evolve in time, providing also long term time series of climate data, based on different potential assumptions in terms of radiative forcing.
Four RCMs are considered in this contest (Scoccimarro et al. 2017). Table 1 lists the considered RCMs. In Table 1 the list of the driving GCMs, furnishing boundary conditions to the relative RCM is also provided. Model biases typically depend on the region analyzed and are partly related to parametric uncertainty and choices in model configuration and can be affected by internal variability as well as by uncertainties of the observational reference data themselves (Kotlarski et al. 2014).

Table 2 lists the raw and derived fields that we already compared to observations in D3.2.1. This is a subsample of the Table 2 and Table 3 parameters defined in D3.1.1.
Anyway, at this stage, all of the raw data required for the computation of derived indices are available on the CMCC ftp server (see below for ftp credentials).

Model name	**Driving GCM**	**Institute**
MPI-CCLM4	MPI-ESM-LR	Max Plank Institute fur Meteorology
KNMI-RACMO22E	ICHEC-EC-EARTH	Royal Netherlands Meteorological Institute
INERIS-WRF331F	IPSL-CM5A-MR	IPSL (Institut Pierre Simon Laplace) and INERIS (Institut National de l Environnement industriel et des RISques)
CNRM-CCLM4	CNRM-CM5-LR	Centre National de Recherches Meteorologiques

Table 1: Regional Climate Models involved in ADRIADAPT data collection.

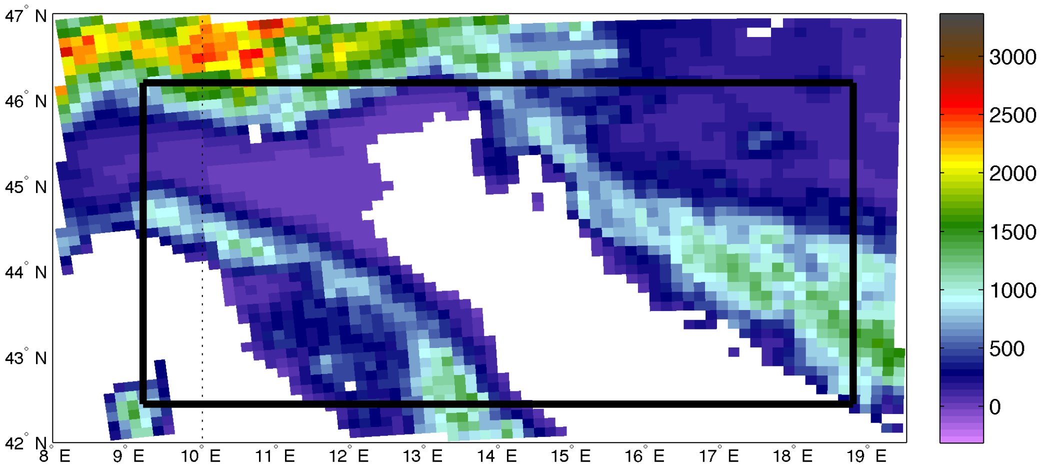

Figure 2-1: Domain selected (black contour) for the provision of climate (table 2) and extreme (table 4) parameters within ADRIADAPT. Colours represent the local orography. Units are [m].

The data format used is NetCDF (http://www.unidata.ucar.edu/software/netcdf/). NetCDF is an abstraction that supports a view of data as a collection of self-describing, portable objects that can be accessed through a simple interface. Array values may be accessed directly, without knowing details of how the data are stored. Auxiliary information about the data, such as what units are used, is stored with the data. Generic utilities and application programs can access NetCDF datasets and transform, combine, analyse, or display specified fields of the data.

Data are now available through the CMCC ftp server (download.cmcc.bo.it – user and password sent privately to the ADRIADAPT partner reference person).

Field Description (the corresponding code in D3.1.1, table 4, is also indicated)	**Field Acronym**	**Vertical level**	**Field Unit**	**Relative validation figures**
2 meter Air Temperature	tas	2 meter	[°C]	2,3,4
99 percentile of temperature: rare events of high temperature (7)	tas_99 (about 100 events in 30y)	2 meter	[°C]	5
99.9 percentile of temperature: extremely rare events of high temperature (7bis)	tas_99.9(about 10 events in 30y)	2 meter	[°C]	6
99 percentile of max daily temperature: rare events of high temperature (8)	tasmax_99 (about 100 events in 30y)	2 meter	[°C]	7
99.9 percentile of max daily temperature: extremely rare events of high temperature (8bis)	tasmax_99.9 (about 10 events in 30y)	2 meter	[°C]	8
99.9 percentile of Perceived Temperature: extremely rare events (20bis)	Humidex_99.9(about 10 events in 30y)	2 meter	[]	9
Precipitation	pr	Surface	[mm/d]	10,11,12
Extreme precipitation (1)	pr_99	Surface	[mm/d]	13
Intense Precipitation (2)	pr_95	Surface	[mm/d]	14

Table 2: List of meteorological fields investigated in D3.2.1 (in brackets the relative parameter number consistent with table 2 of D3.1.1) for model evaluation.

The indices presented in Table 2 were selected within the list defined in D3.1.1 to describe the frequency and the intensity of some extreme events and used to evaluate model performances in D3.2.1. The extreme events are here defined based on threshold percentile (STARDEX (http://www.cru.uea.ac.uk/stardex).

In order to give an idea on the percentile approach, considering daily data, over the whole year, the 99 percentile of a 30-year time series of temperature data, corresponds to the temperature value reached in about 100 days only: about 4 days in a year. For the identification of even more rare and potentially impacting events, also the 99.9 percentile

is taken into account for some of the investigated parameters, representing events happening 10 times only in a 30y time series of daily values: one event every three years. In other words, the 95th/99th/and 99.9th percentiles are used to represent moderately rare / rare / extremely rare events in the right tail of the event distribution.
For the performance evaluation of dynamical models, in terms of their ability to represent extreme events the reader is referred to ADRIADAPT deliverable 3.2.1.

3.2 Statistical Downscaling schemes (SDs)

The statistical downscaling (SD) is a tool used to perform simulations at local scale, stations or grid points. There are different statistical downscaling tools applied in the climatology, ranging from Perfect-Prog (PP) approaches to Model Output Statistics (MOS). Perfect Prog is based on the assumption that the local climate is correlated with the state of the large-scale fields and the local features such as topography or land-sea distribution (Von Storch 1995,Wilks 2006). Taking into account these assumptions, the local climate information is derived from the construction of a statistical relationship that links *observed* large –scale atmospheric fields (*predictors*) with *observed* local fields (*predictands*). As regards the Model Output Statistics technique (MOS) this is based on a statistical scheme that is calibrated using *simulated* predictors and *observed* predictands.
In the present project the Perfect Prog approaches is used by Arpae to simulate seasonal future climate changes over the case studies. The link between local climate and large scale is detected through the canonical correlation analysis –CCA-(Von Storch 1995). The most important patterns provided by the CCA are used in a multivariate regression SD schemes -CCAReg (Tomozeiu et al., 2007; 2014).
The main advantages of SD are that they are computationally inexpensive and allow the direct downscaling of indices related to extreme weather events, even up to local scale (station or grid point). The SD disadvantages refer to the fact that they need long and homogeneous observational time series for calibration and validation of the statistical relationship.
In the present work, the SD is implemented at *seasonal time scale* for the following domain:
- Cervia (Figure 2-2, "**C**"-yellow area) and Savio Valley Municipalities Union (Figure 2-2, "**SVMU"**-green area), both of them belong to Emilia-Romagna region and are referred in the report as Italy case studies (Figure 2-2). The ***SVMU*** area includes: Cesena, Mercato Saraceno, Sarsina, Bagno di Romagna and Verghereto municipalities. The grid points that belong to ***C*** and ***SVMU*** are presented in ANNEXES in Table A, information

extracted from Eraclito climatic data set available at https://arpaeprv.datamb.it/dataset/erg5-eraclito.

- Sibenik (***S***) and Knin (***K***) meteorological stations - referred in the report as Croatia case studies.

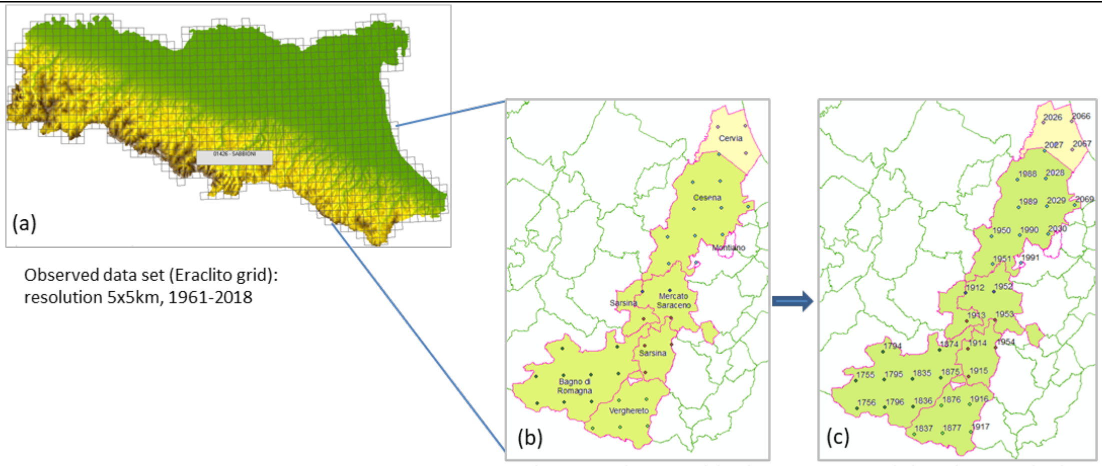

Observed data set (Eraclito grid): resolution 5x5km, 1961-2018

Italian case studies: Cervia (**C**) and municipaties that belong to of Savio Union (**SVMU**)

Map with the grid points and code extacted from Eraclito data set that belong to **C** and **SVMU**

Figure 2-2: (a) Resolution of observed data set of temperature and precipitation –Eraclito data set; Italian case studies: Cervia-C- (yellow) and the Savio Valley Union Municipalities- SVMU (green); (b) Eraclito grid points and associated codes (c)

A description of SD implemented in ADRIADAPT project is summarised in two steps:

- ***Step1: calibration and validation of SD (CCAReg scheme)***

In this step of SD implementation, the model/scheme is calibrated and validated using *observed* data, namely: large-scale *predictors* from ECMWF-ERA40 + ERA-interim *re-analysis* (https://www.ecmwf.int/en/forecasts/datasets/archive-datasetsand local *observational predictands* from Italy and Croatia. The calibration (construction) of SD is done over the period 1961-1985 and 2006-2010 while the **validation** is done over 1986-2005. Before the calibration, firstly the local and large scale fields are filtered through empirical orthogonal functions (EOFs) then is performed the CCA analysis. A subset of CCA pairs is then used in the multivariate linear statistical model (CCAReg) to estimate the *seasonal predictands* (Tomozeiu et al.,2007, 2014).

The **predictands** are represented by the **seasonal mean and extreme indices of temperature and precipitation** over the Italian and Croatian case studies. The seasonal climate indices are described in Table 3, and are computed from daily observed minimum, maximum temperature and precipitation.

As regards Cervia and Savio Valley Municipalities predictands, these are computed using daily data of temperature and precipitation from Eraclito climatic data set, available online at https://arpaeprv.datamb.it/dataset/erg5-eraclito. This data set has a spatial resolution of 5kmx5km, cover the period 1961-2015 (Figure 2a), data deeply described by Antolini et al (2015). The observed Croatia predictands, seasonal climate indices (Table 3), are derived from daily temperature and precipitation from Sibenik and Knin stations over 1961-2010 period, data provided by the Croatian project partner. The indices presented in Table 3 are selected within the list defined in D3.1.1 and describe the frequency and the intensity of extreme events. Some indices are based on threshold percentile (STARDEX, https://crudata.uea.ac.uk/projects/stardex/), and represent part of indices simulated also by dynamical downscaling.

As regards **predictors**, these are the large scale fields: namely geopotential at 500hPa (Z500), mean sea level pressure (MSLP), temperature at 850hPa derived from ERA40 and ERA interim ECMWF archives (https://www.ecmwf.int/en/forecasts/datasets/archive-datasetscover the window 90°W-90°E and 0°-90°N and the period 1961-2013 period.

Taking into account the different periods available for predictands and predictors, we choose a common period of analysis, namely 1961-2010.

Field	**Field Acronym**	**Field Description**	**Unit**
Precipitation	pr	Amount of seasonal precipitation	[mm]
Maximum temperature	tasmax	Seasonal average of maximum temperature	[C]
Minimum temperature	tasmin	Seasonal average of minimum temperature	[C]
Intense Precipitation	pr_90p	Seasonal 90th percentile of daily precipitation	[mm]
Consecutive dry days	cdd	Seasonal maximum number of consecutive days with precipitation lower than 1 mm	[d]
High maximum temperature	tasmax_95p	Seasonal 95th percentile of daily maximum temperature	[C]
Low minimum temperature	tasmin_5p	Seasonal 5th percentile of daily minimum temperature	[C]
Frost days	fd	Seasonal number of days with minimum temperature below 0°C	[days]
Tropical night index	tr	Seasonal number of days with minimum temperature greater than 20°C	[days]

Heat Wave Duration index	hwd	Seasonal maximum number of consecutive days with maximum temperature greater than 90th percentile	[days]

Table 3: List of local fields (climate indices) used in statistical downscaling (SD) over ADRIADAPT case studies

An important step in SD is the validation process. The SD models are built for each season and index, choosing each time a different subset of predictors, fields extracted from the ECMWF re-analysis. Finally, only the optimum SD scheme for each field and each season is retained and used then for future projections.

The validation of SDs over 1986-2005 period helps to select the best SD model. The performance (skill) of the downscaling model is quantified at grid point/station for each index/season in terms of: BIAS, correlation coefficient (CORR), root-mean square-error (RMSE). Tomozeiu et al (2007) underlined that the skill of the downscaling models is dependent on: predictands, predictors (large-scale field, single or combined), domain (area) of predictors, and filtered data process. The sensitivity of SDs to these factors is also tested in this work.

Another important aspect in SD is to test how work the SDs when is feed with predictors from GCMs (Table 4) simulated during control run/historical period. In this case, the results depend by the performance of GCMs to reproduce the predictors. This analysis is also done in the report.

- ***Step2: simulations of future changes of local climate (grid points/stations spatial resolution)***

In the second step, ones the schemes built and selected the best ones for each season and index, these SDs are then applied to the future anomalies of predictors simulated by GCM from CMIP5 experiments (https://pcmdi.llnl.gov/mips/cmip5/terms-of-use.html) in the framework of RCP4.5 and RCP8.5, in order to obtain seasonal future changes of local indices over ADRIADAPT case studies.

The ***future*** periods are: 2021-2040, 2041-2060, 2061-2080, 2081-2100 while the historical period is 1986-2005 period. The list of GCM CMIP5 experiments used to feed the SDs scheme for the ADRIADAPT case studies is presented in Table 4.

Global Climate Model (GCMs name)	**Modelling Centre**
CMCC-CM	Centro Euro-Mediterraneo per i Cambiamenti Climatici

MPI ESM-MR	Max Planck Institute for Meteorology
CNRM -CM5	Centre National de Recherches Meteorologiques
Can-ESM2	Canadian Centre for Climate Modelling and Analysis

Table 4: List of GCMs from CMIP5 experiment that feed the statistical downscaling scheme (CCAReg scheme) in ADRIADAPT project

For the performance evaluation of statistical downscaling, in terms of ability to represent extreme events the reader is referred to ADRIADAPT deliverable 3.2.2.

4 Description of the whole data set available (dynamical and statistical downscaled data) available

The aim of this section is to list the full dataset obtained following the two downscaling approaches. Table 5 shows the data availability for historical and future scenarios as from dynamical downscaling (results from the four models listed in table 1 are available for all of the mentioned parameters).

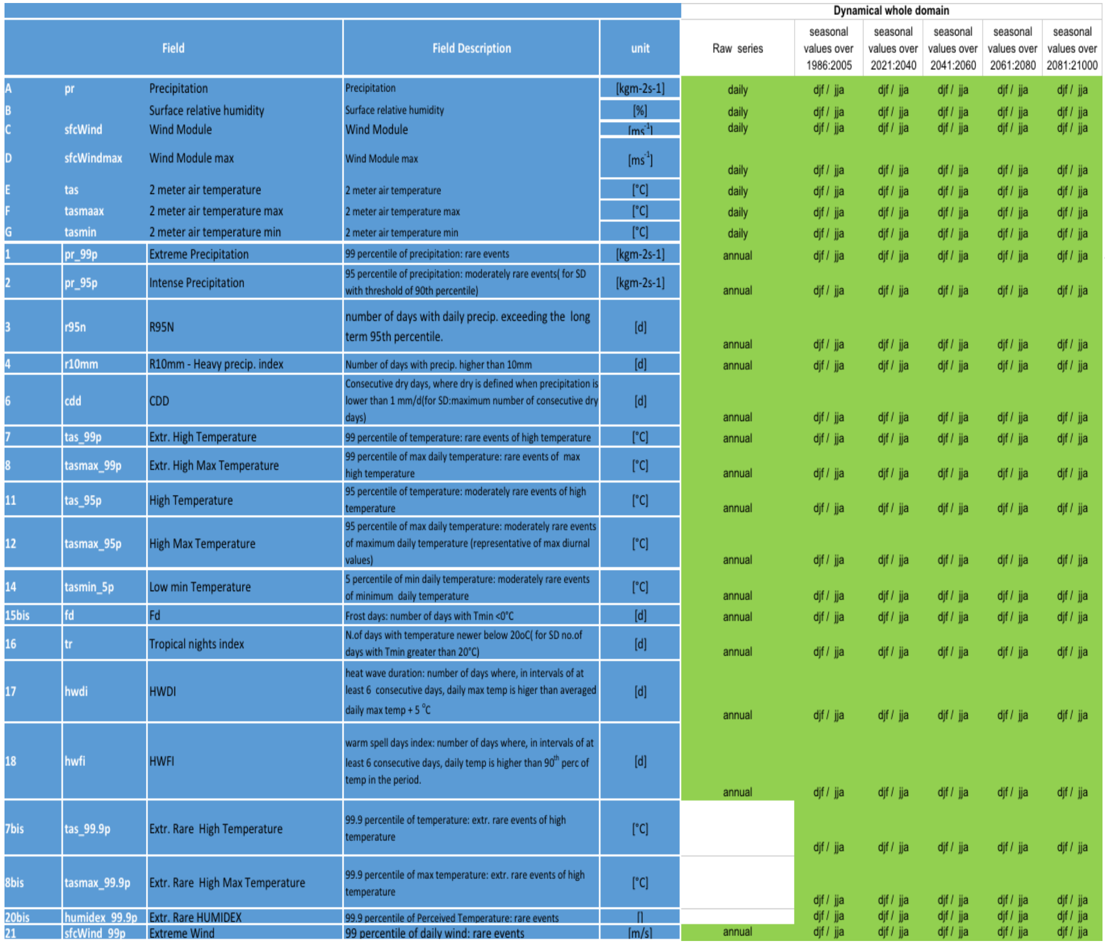

Field			Field Description	unit	Dynamical whole domain					
					Raw series	seasonal values over 1986:2005	seasonal values over 2021:2040	seasonal values over 2041:2060	seasonal values over 2061:2080	seasonal values over 2081:21000
A	pr	Precipitation	Precipitation	[kgm-2s-1]	daily	djf / jja	djf / jja	djf / jja	djf / jja	djf / jja
B		Surface relative humidity	Surface relative humidity	[%]	daily	djf / jja	djf / jja	djf / jja	djf / jja	djf / jja
C	sfcWind	Wind Module	Wind Module	[ms^{-1}]	daily	djf / jja	djf / jja	djf / jja	djf / jja	djf / jja
D	sfcWindmax	Wind Module max	Wind Module max	[ms^{-1}]	daily	djf / jja	djf / jja	djf / jja	djf / jja	djf / jja
E	tas	2 meter air temperature	2 meter air temperature	[°C]	daily	djf / jja	djf / jja	djf / jja	djf / jja	djf / jja
F	tasmaax	2 meter air temperature max	2 meter air temperature max	[°C]	daily	djf / jja	djf / jja	djf / jja	djf / jja	djf / jja
G	tasmin	2 meter air temperature min	2 meter air temperature min	[°C]	daily	djf / jja	djf / jja	djf / jja	djf / jja	djf / jja
1	pr_99p	Extreme Precipitation	99 percentile of precipitation: rare events	[kgm-2s-1]	annual	djf / jja	djf / jja	djf / jja	djf / jja	djf / jja
2	pr_95p	Intense Precipitation	95 percentile of precipitation: moderately rare events(for SD with threshold of 90th percentile)	[kgm-2s-1]	annual	djf / jja	djf / jja	djf / jja	djf / jja	djf / jja
3	r95n	R95N	number of days with daily precip. exceeding the long term 95th percentile.	[d]	annual	djf / jja	djf / jja	djf / jja	djf / jja	djf / jja
4	r10mm	R10mm - Heavy precip. index	Number of days with precip. higher than 10mm	[d]	annual	djf / jja	djf / jja	djf / jja	djf / jja	djf / jja
6	cdd	CDD	Consecutive dry days, where dry is defined when precipitation is lower than 1 mm/d(for SD:maximum number of consecutive dry days)	[d]	annual	djf / jja	djf / jja	djf / jja	djf / jja	djf / jja
7	tas_99p	Extr. High Temperature	99 percentile of temperature: rare events of high temperature	[°C]	annual	djf / jja	djf / jja	djf / jja	djf / jja	djf / jja
8	tasmax_99p	Extr. High Max Temperature	99 percentile of max daily temperature: rare events of max high temperature	[°C]	annual	djf / jja	djf / jja	djf / jja	djf / jja	djf / jja
11	tas_95p	High Temperature	95 percentile of temperature: moderately rare events of high temperature	[°C]	annual	djf / jja	djf / jja	djf / jja	djf / jja	djf / jja
12	tasmax_95p	High Max Temperature	95 percentile of max daily temperature: moderately rare events of maximum daily temperature (representative of max diurnal values)	[°C]	annual	djf / jja	djf / jja	djf / jja	djf / jja	djf / jja
14	tasmin_5p	Low min Temperature	5 percentile of min daily temperature: moderately rare events of minimum daily temperature	[°C]	annual	djf / jja	djf / jja	djf / jja	djf / jja	djf / jja
15bis	fd	Fd	Frost days: number of days with Tmin <0°C	[d]	annual	djf / jja	djf / jja	djf / jja	djf / jja	djf / jja
16	tr	Tropical nights index	N.of days with temperature newer below 20oC(for SD no.of days with Tmin greater than 20°C)	[d]	annual	djf / jja	djf / jja	djf / jja	djf / jja	djf / jja
17	hwdi	HWDI	heat wave duration: number of days where, in intervals of at least 6 consecutive days, daily max temp is higer than averaged daily max temp + 5 °C	[d]	annual	djf / jja	djf / jja	djf / jja	djf / jja	djf / jja
18	hwfi	HWFI	warm spell days index: number of days where, in intervals of at least 6 consecutive days, daily temp is higher than 90th perc of temp in the period.	[d]	annual	djf / jja	djf / jja	djf / jja	djf / jja	djf / jja
7bis	tas_99.9p	Extr. Rare High Temperature	99.9 percentile of temperature: extr. rare events of high temperature	[°C]		djf / jja	djf / jja	djf / jja	djf / jja	djf / jja
8bis	tasmax_99.9p	Extr. Rare High Max Temperature	99.9 percentile of max temperature: extr. rare events of high temperature	[°C]		djf / jja	djf / jja	djf / jja	djf / jja	djf / jja
20bis	humidex_99.9p	Extr. Rare HUMIDEX	99.9 percentile of Perceived Temperature: rare events	[]		djf / jja	djf / jja	djf / jja	djf / jja	djf / jja
21	sfcWind_99p	Extreme Wind	99 percentile of daily wind: rare events	[m/s]	annual	djf / jja	djf / jja	djf / jja	djf / jja	djf / jja

Table 5: List of fields (climate indices), descriptions and periods of availability, delivered by dynamical downscaling for the whole ADRIADAPT domain. "DJF" indicates December to February period. "JJA" indicates June to August period.

Table 6 shows the data availability within the project, derived from statistical downscaling techniques (SD) over the grid points that belong to Cervia (***C***), Union Valley Municipalities (***SVMU***) (Table A from ANNEXES of deliverable 3.2.2) and for Sibenik (***S***), Knin (***K***) stations. As could be noted, the outputs are seasonal. The seasons are defined standard, namely: winter includes December, January and February (djf); spring includes March, April, May (mam); summer includes June, July, August (jja) and autumn includes September, October and November (son).

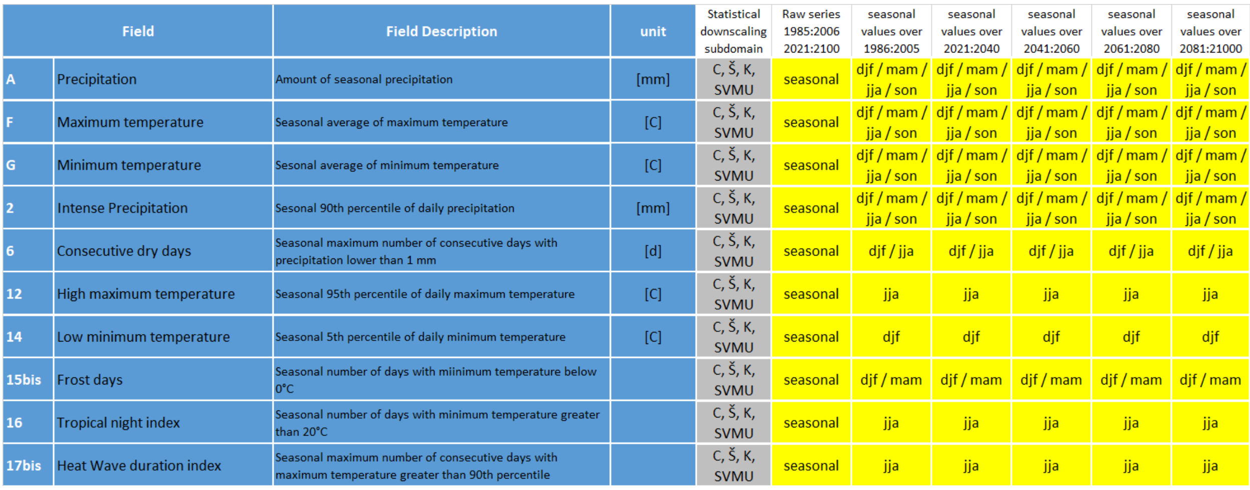

Field		Field Description	unit	Statistical downscaling subdomain	Raw series 1985:2006 2021:2100	seasonal values over 1986:2005	seasonal values over 2021:2040	seasonal values over 2041:2060	seasonal values over 2061:2080	seasonal values over 2081:21000
A	Precipitation	Amount of seasonal precipitation	[mm]	C, Š, K, SVMU	seasonal	djf / mam / jja / son	djf / mam / jja / son	djf / mam / jja / son	djf / mam / jja / son	djf / mam / jja / son
F	Maximum temperature	Seasonal average of maximum temperature	[C]	C, Š, K, SVMU	seasonal	djf / mam / jja / son	djf / mam / jja / son	djf / mam / jja / son	djf / mam / jja / son	djf / mam / jja / son
G	Minimum temperature	Sesonal average of minimum temperature	[C]	C, Š, K, SVMU	seasonal	djf / mam / jja / son	djf / mam / jja / son	djf / mam / jja / son	djf / mam / jja / son	djf / mam / jja / son
2	Intense Precipitation	Sesonal 90th percentile of daily precipitation	[mm]	C, Š, K, SVMU	seasonal	djf / mam / jja / son	djf / mam / jja / son	djf / mam / jja / son	djf / mam / jja / son	djf / mam / jja / son
6	Consecutive dry days	Seasonal maximum number of consecutive days with precipitation lower than 1 mm	[d]	C, Š, K, SVMU	seasonal	djf / jja	djf / jja	djf / jja	djf / jja	djf / jja
12	High maximum temperature	Seasonal 95th percentile of daily maximum temperature	[C]	C, Š, K, SVMU	seasonal	jja	jja	jja	jja	jja
14	Low minimum temperature	Seasonal 5th percentile of daily minimum temperature	[C]	C, Š, K, SVMU	seasonal	djf	djf	djf	djf	djf
15bis	Frost days	Seasonal number of days with miinimum temperature below 0°C		C, Š, K, SVMU	seasonal	djf / mam	djf / mam	djf / mam	djf / mam	djf / mam
16	Tropical night index	Seasonal number of days with minimum temperature greater than 20°C		C, Š, K, SVMU	seasonal	jja	jja	jja	jja	jja
17bis	Heat Wave duration index	Seasonal maximum number of consecutive days with maximum temperature greater than 90th percentile		C, Š, K, SVMU	seasonal	jja	jja	jja	jja	jja

Table 6: List of fields (climate indices), descriptions, domain, periods and type of data availability delivered by statistical downscaling (SD)

5 Future projections as resulting from Dynamical Downscaling over the whole ADRIADAPT domain

In this section we present how regional climate models represent the mean and extreme climate over the ADRIADAPT domain, under different 40y future periods (P1, P2, P3 and P4) compared to the historical period P0 where:

P0 = 1986 - 2005
P1 = 2021-2040
P2 = 2041-2060
P3 = 2061-2080
P4 = 2081-2100

Averages and derived indices shown in this chapter and in chapter 5 are computed over boreal winter (December to February, DJF) and summer (June to August,JJA) seasons, based on daily data (see D3.2.1 and D3.2.2). Results are shown in the same way for all of the parameters considered: the seasonal ensemble averages over the P0 period is shown in the upper panel and the projected ensemble averaged results over the P1 to P4 periods are shown in the lower panels of each figure of the current chapter.

Indices are clustered in two main groups related to temperature and precipitation (subchapters 4.1 and 4.2 respectively).

The considered temperature related indices are averaged temperature (4.1.1), extreme temperature (4.1.2), heat wave duration (4.1.3), tropical nights (4.1.4) and frost days 4.1.5).

The considered precipitation related indices are average precipitation (4.2.1), intense precipitation (4.2.2), extreme precipitation (4.2.3) and consecutive dry days (4.2.4).

5.1 Temperature related indices projections

5.1.1 Averaged temperature

Seasonal averages of temperature differences between P1-P0, P2-P0, P3-P0, P4-P0 are shown in figures 4.1 (winter) and 4.2 (summer) relative to the RCP4.5 scenario and in figures 4.3 (winter) and 4.4 (summer) relative to the RCP8.5 scenario. Following the moderate RCP4.5 scenario, during winter we expect an average temperature increase of about one degree for the middle of the century (P2) and about 1.5 degrees for the end of the century with more pronounced increases expected over land. On the other hand, during summer the increase expected for the middle of the century is of the order of 1.5 degrees and for the end of the century a two degrees increase could be reached over certain portion of land. Following the worst RCP8.5 scenario, consistently with the radiative paths associated to the two scenarios, no huge differences appear for the middle of the century, while for the end of the century (P4), when the two radiative forcing paths substantially diverge, increases of the order of three to four degrees can be expected, with maxima of the order of 4.5 degrees during summer over a substantial portion of land.

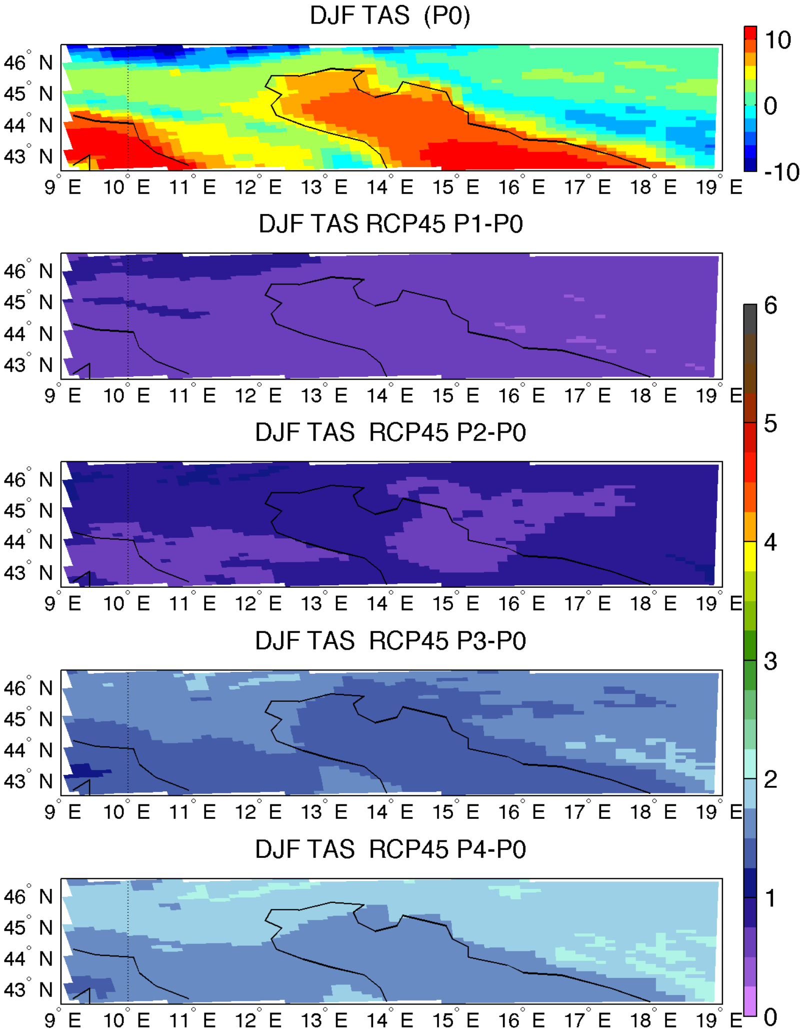

Figure 4-1: Average 2m air Temperature (TAS, units are [°C]) projections for DJF, following RCP4.5 scenario: upper panel shows the ensemble average over the historical 1986:2005 (P0) period. 2nd panel shows the projected ensemble average in 2021:2040 wrt 1986:2005 (P1-P0). 3rd panel shows the projected ensemble average in 2041:2060 wrt 1986:2005 (P2-P0). 4th panel

shows the projected ensemble average in 2061:2080 wrt 1986:2005 (P3-P0). 5th panel shows the projected ensemble average in 2081:2100 wrt 1986:2005 (P4-P0).

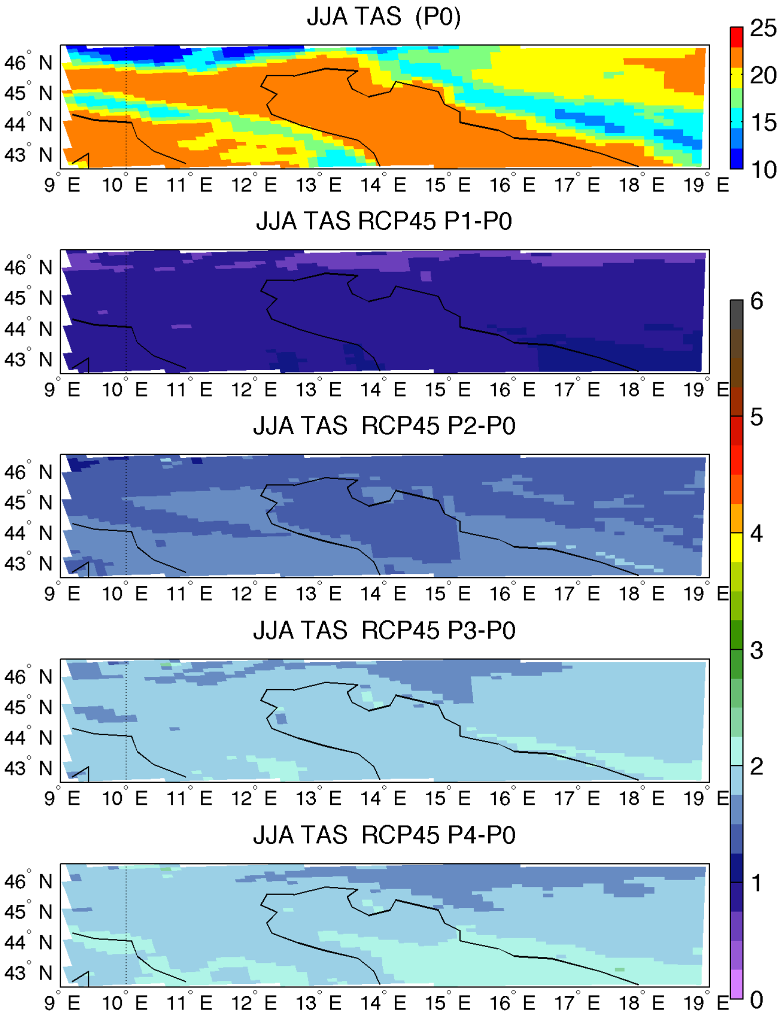

Figure 5-2: Average 2m air Temperature (TAS, units are [ºC]) projections for JJA, following RCP4.5 scenario: upper panel shows the ensemble average over the historical 1986:2005 (P0) period. 2nd panel shows the projected ensemble average in 2021:2040 wrt 1986:2005 (P1-P0). 3rd panel shows the projected ensemble average in 2041:2060 wrt 1986:2005 (P2-P0). 4th panel shows the projected ensemble average in 2061:2080 wrt 1986:2005 (P3-P0). 5th panel shows the projected ensemble average in 2081:2100 wrt 1986:2005 (P4-P0).

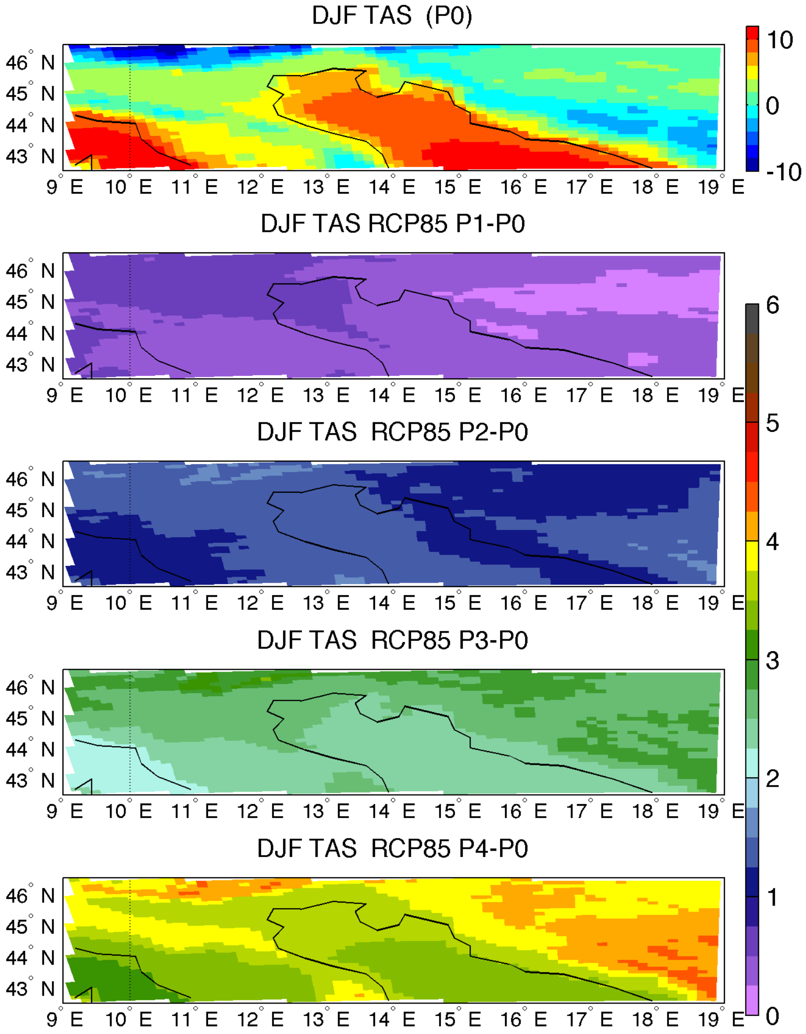

Figure 4-3: Average 2m air Temperature (TAS, units are [°C]) projections for DJF, following RCP8.5 scenario: upper panel shows the ensemble average over the historical 1986:2005 (P0) period. 2nd panel shows the projected ensemble average in 2021:2040 wrt 1986:2005 (P1-P0). 3rd panel shows the projected ensemble average in 2041:2060 wrt 1986:2005 (P2-P0). 4th panel shows the projected ensemble average in 2061:2080 wrt 1986:2005 (P3-P0). 5th panel shows the projected ensemble average in 2081:2100 wrt 1986:2005 (P4-P0). Figure 1

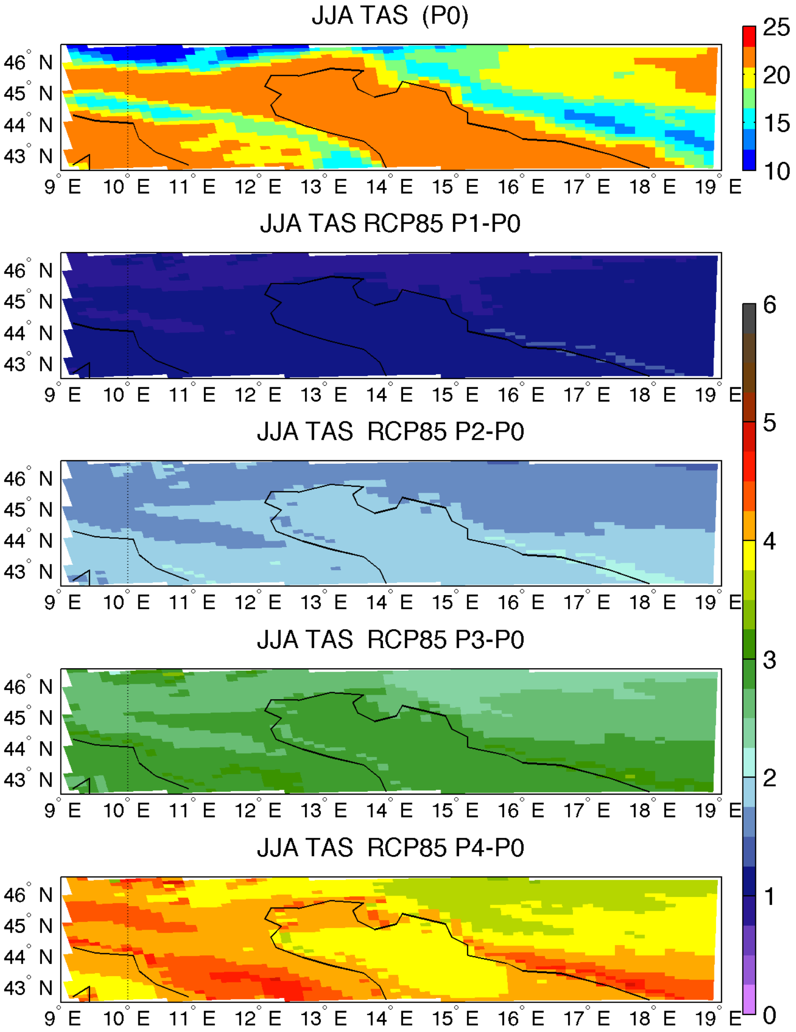

Figure 4-4: Average 2m air Temperature (TAS, units are [°C]) projections for JJA, following RCP8.5 scenario: upper panel shows the ensemble average over the historical 1986:2005 (P0) period. 2nd panel shows the projected ensemble average in 2021:2040 wrt 1986:2005 (P1-P0). 3rd panel shows the projected ensemble average in 2041:2060 wrt 1986:2005 (P2-P0). 4th panel shows the projected ensemble average in 2061:2080 wrt 1986:2005 (P3-P0). 5th panel shows the projected ensemble average in 2081:2100 wrt 1986:2005 (P4-P0).

5.1.2 Extreme temperature

Seasonal averages of extreme temperature differences between P1-P0, P2-P0, P3-P0, P4-P0 are shown in figures 4.5 (winter) and 4.6 (summer) relative to the RCP4.5 scenario and in figures 4.7 (winter) and 4.8 (summer) relative to the RCP8.5 scenario. Following the moderate RCP4.5 scenario, during winter we expect an extreme temperature increase of about one degree for the middle of the century (P2) and about 1.5 degrees for the end of the century with more pronounced increases expected over land. On the other hand, during summer the increase expected for the middle of the century is of the order of 2 degrees and for the end of the century a three degrees increase could be reached over certain portion of land. Following the worst RCP8.5 scenario, consistently with the radiative paths associated to the two scenarios, no huge differences appear for the middle of the century, while for the end of the century (P4), when the two radiative forcing paths substantially diverge, increases of the order of five to six degrees can be expected, with maxima of the order of 6 degrees during summer over a substantial portion of land.

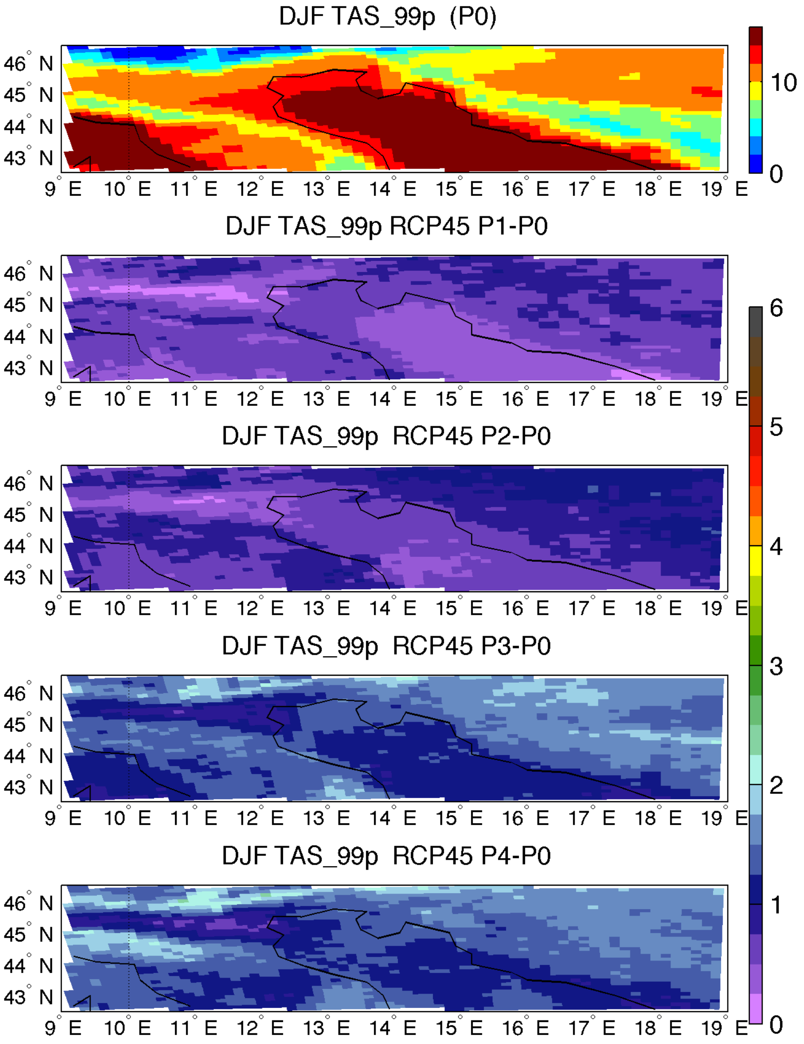

Figure 4-5: 99th percentile of 2m air Temperature (TAS_99p, units are [°C]) projections for DJF, following RCP4.5 scenario: upper panel shows the ensemble average over the historical 1986:2005 (P0) period. 2nd panel shows the projected ensemble average in 2021:2040 wrt 1986:2005 (P1-P0). 3rd panel shows the projected ensemble average in 2041:2060 wrt 1986:2005 (P2-P0). 4th panel shows the projected ensemble average in 2061:2080 wrt 1986:2005 (P3-P0). 5th panel shows the projected ensemble average in 2081:2100 wrt 1986:2005 (P4-P0).

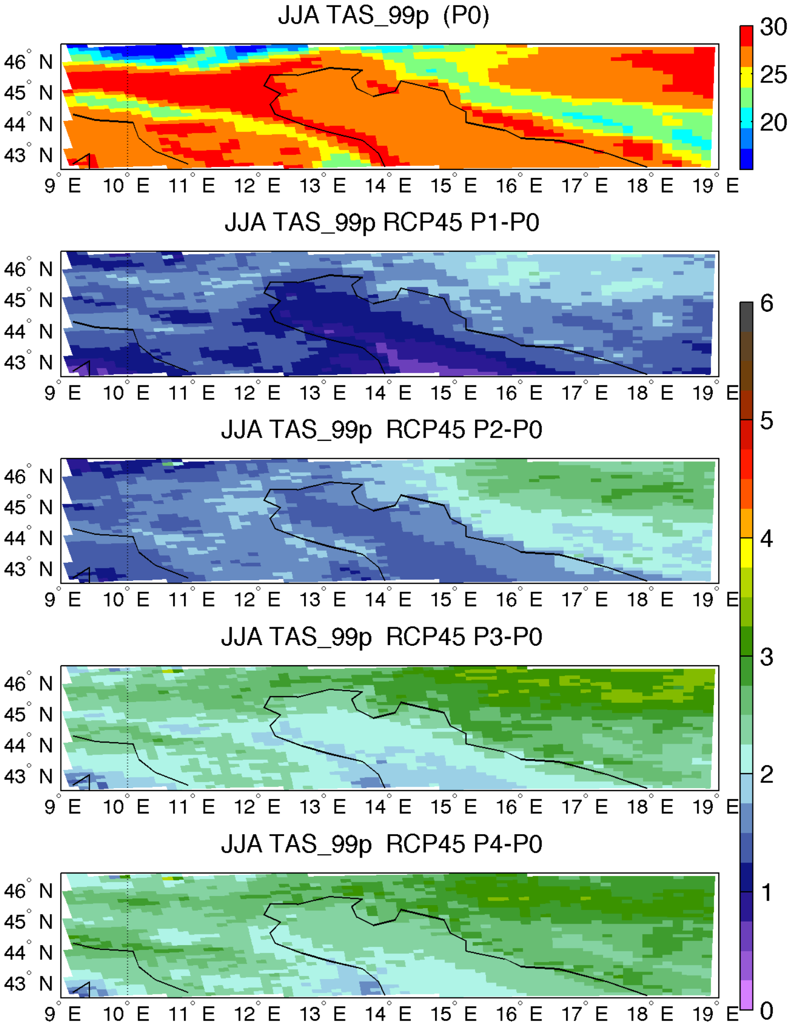

Figure 4-6: 99th percentile of 2m air Temperature (TAS_99p, units are [ºC]) projections for JJA, following RCP4.5 scenario: upper panel shows the ensemble average over the historical 1986:2005 (P0) period. 2nd panel shows the projected ensemble average in 2021:2040 wrt 1986:2005 (P1-P0). 3rd panel shows the projected ensemble average in 2041:2060 wrt 1986:2005 (P2-P0). 4th panel shows the projected ensemble average in 2061:2080 wrt 1986:2005 (P3-P0). 5th panel shows the projected ensemble average in 2081:2100 wrt 1986:2005 (P4-P0).

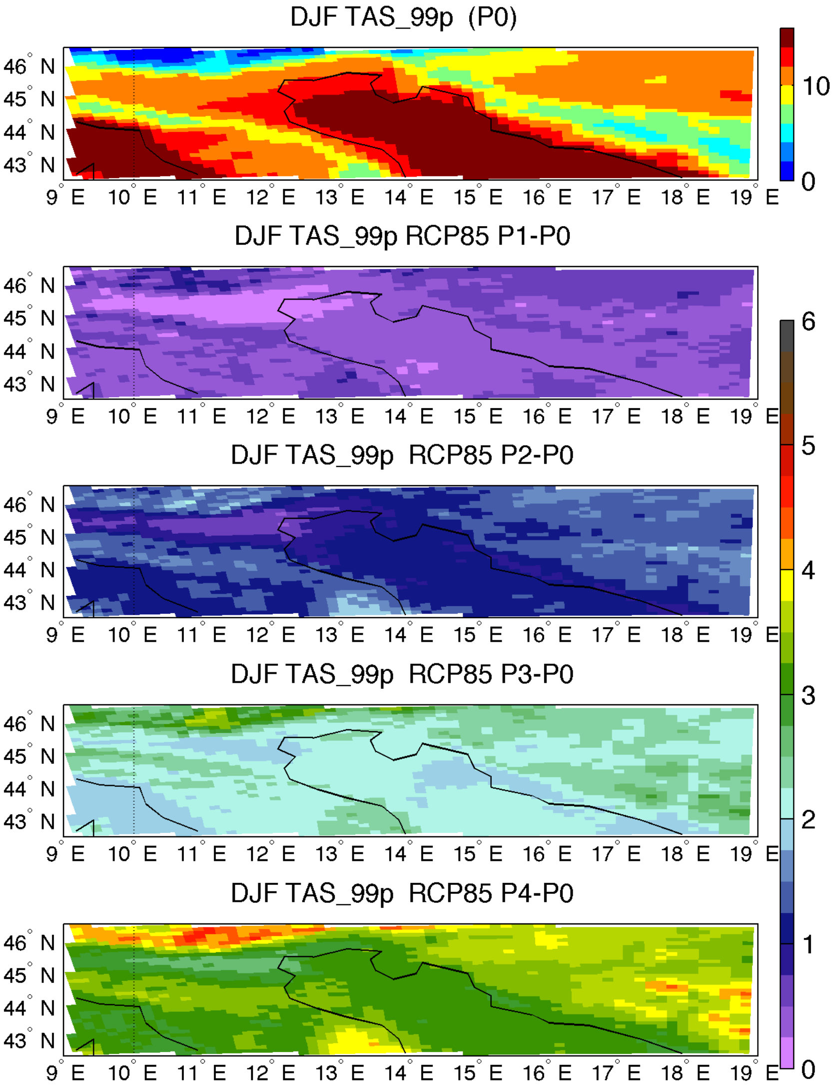

Figure 4-7: 99th percentile of 2m air Temperature (TAS_99p, units are [°C]) projections for DJF, following RCP8.5 scenario: upper panel shows the ensemble average over the historical 1986:2005 (P0) period. 2nd panel shows the projected ensemble average in 2021:2040 wrt 1986:2005 (P1-P0). 3rd panel shows the projected ensemble average in 2041:2060 wrt 1986:2005 (P2-P0). 4th panel shows the projected ensemble average in 2061:2080 wrt 1986:2005 (P3-P0). 5th panel shows the projected ensemble average in 2081:2100 wrt 1986:2005 (P4-P0).

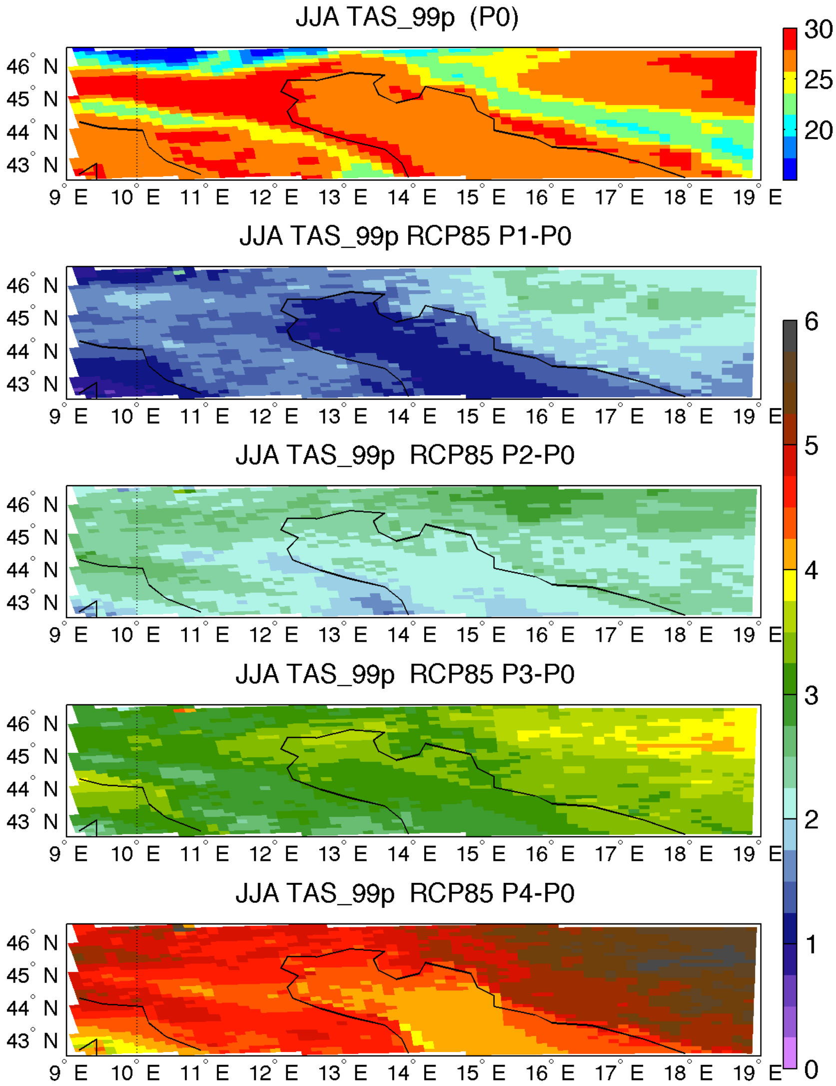

Figure 4-8: 99th percentile of 2m air Temperature (TAS_99p, units are [ºC]) projections for JJA, following RCP8.5 scenario: upper panel shows the ensemble average over the historical 1986:2005 (P0) period. 2nd panel shows the projected ensemble average in 2021:2040 wrt 1986:2005 (P1-P0). 3rd panel shows the projected ensemble average in 2041:2060 wrt 1986:2005 (P2-P0). 4th panel shows the projected ensemble average in 2061:2080 wrt 1986:2005 (P3-P0). 5th panel shows the projected ensemble average in 2081:2100 wrt 1986:2005 (P4-P0).

5.1.3 Heat wave duration

Seasonal averages of heat wave duration (HWDI) in terms of differences between P1-P0, P2-P0, P3-P0, P4-P0 are shown in figures 4.9 (winter) and 4.10 (summer) relative to the RCP4.5 scenario and in figures 4.11 (winter) and 4.12 (summer) relative to the RCP8.5 scenario. The HWDI is defined as the cumulative number of days in the period (~90[days]x20[years]~=a total sample of 1800 days) corresponding to the following conditions: at least 6 consecutive days with maximum daily temperature higher than the averaged (over P0) maximum temperature +5°C. Following the moderate RCP4.5 scenario, during winter we expect an average increase of less than 50 days for the middle of the century (P2) and up to 170 days for the end of the century with more pronounced increases expected over the eastern part of the domain. On the other hand, during summer the increase expected for the middle of the century is of the order of 100 days and for the end of the century a 150 days increase could be reached over most of land, interesting both the eastern and western part of the domain . Following the worst RCP8.5 scenario, consistently with the radiative paths associated to the two scenarios, no huge differences appear for the middle of the century, while for the end of the century (P4), when the two radiative forcing paths substantially diverge, increases up to 300 days interesting also the sea side during summer.

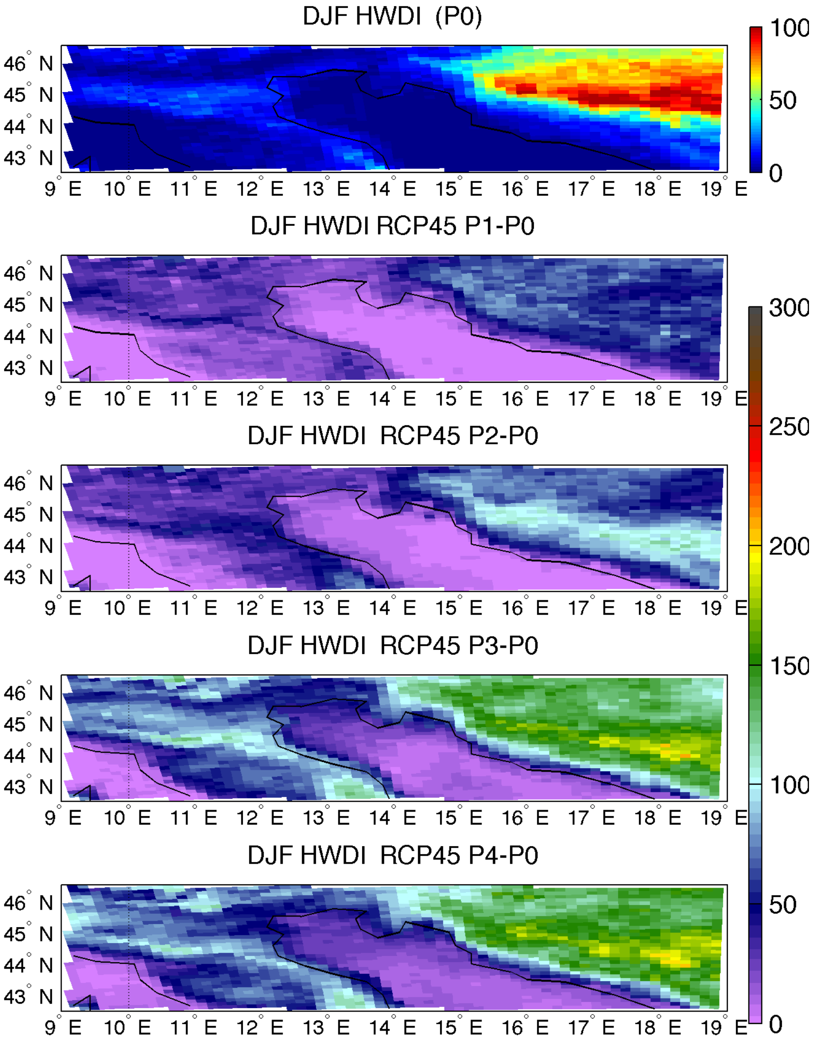

Figure 4-9: Heat Wave duration index (HWDI, units are [days]) projections for DJF, following RCP4.5 scenario: upper panel shows the ensemble average over the historical 1986:2005 (P0) period. 2nd panel shows the projected ensemble average in 2021:2040 wrt 1986:2005 (P1-P0). 3rd panel shows the projected ensemble average in 2041:2060 wrt 1986:2005 (P2-P0). 4th panel shows the projected ensemble average in 2061:2080 wrt 1986:2005 (P3-P0). 5th panel shows the projected ensemble average in 2081:2100 wrt 1986:2005 (P4-P0).

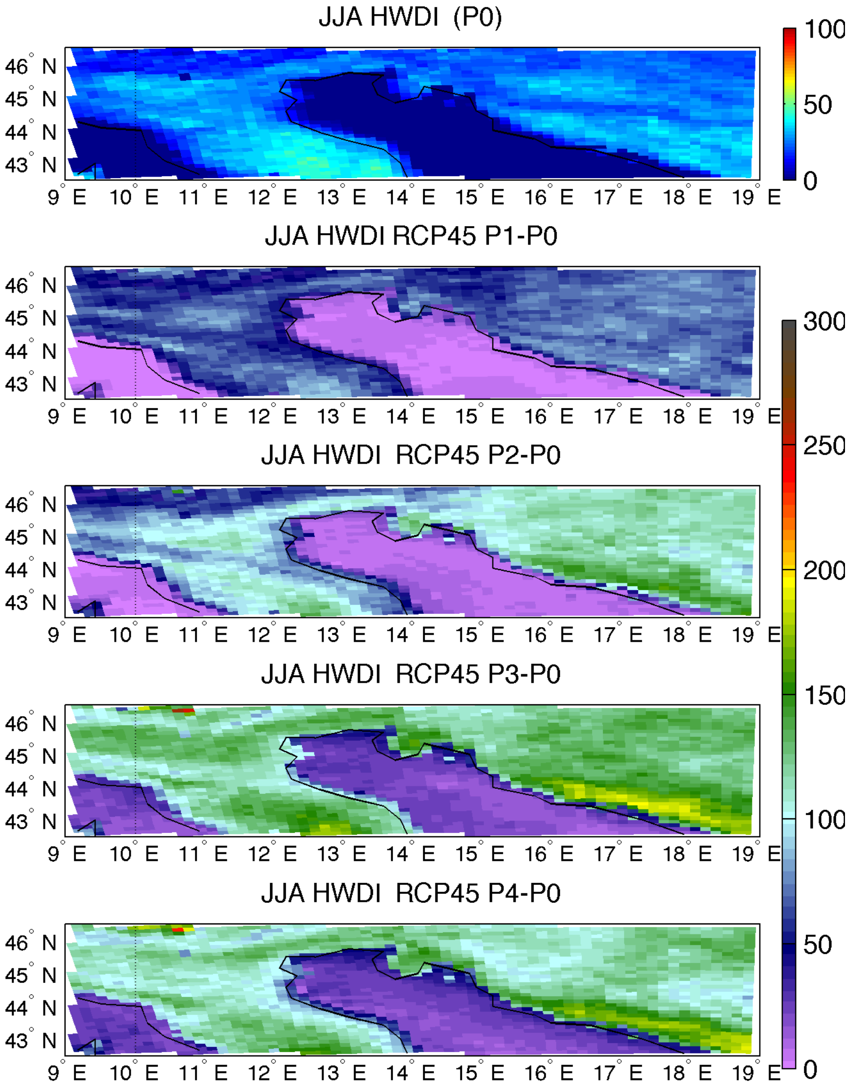

Figure 4-10: Heat Wave duration index (HWDI, units are [days]) projections for JJA, following RCP4.5 scenario: upper panel shows the ensemble average over the historical 1986:2005 (P0) period. 2nd panel shows the projected ensemble average in 2021:2040 wrt 1986:2005 (P1-P0). 3rd panel shows the projected ensemble average in 2041:2060 wrt 1986:2005 (P2-P0). 4th panel shows the projected ensemble average in 2061:2080 wrt 1986:2005 (P3-P0). 5th panel shows the projected ensemble average in 2081:2100 wrt 1986:2005 (P4-P0).

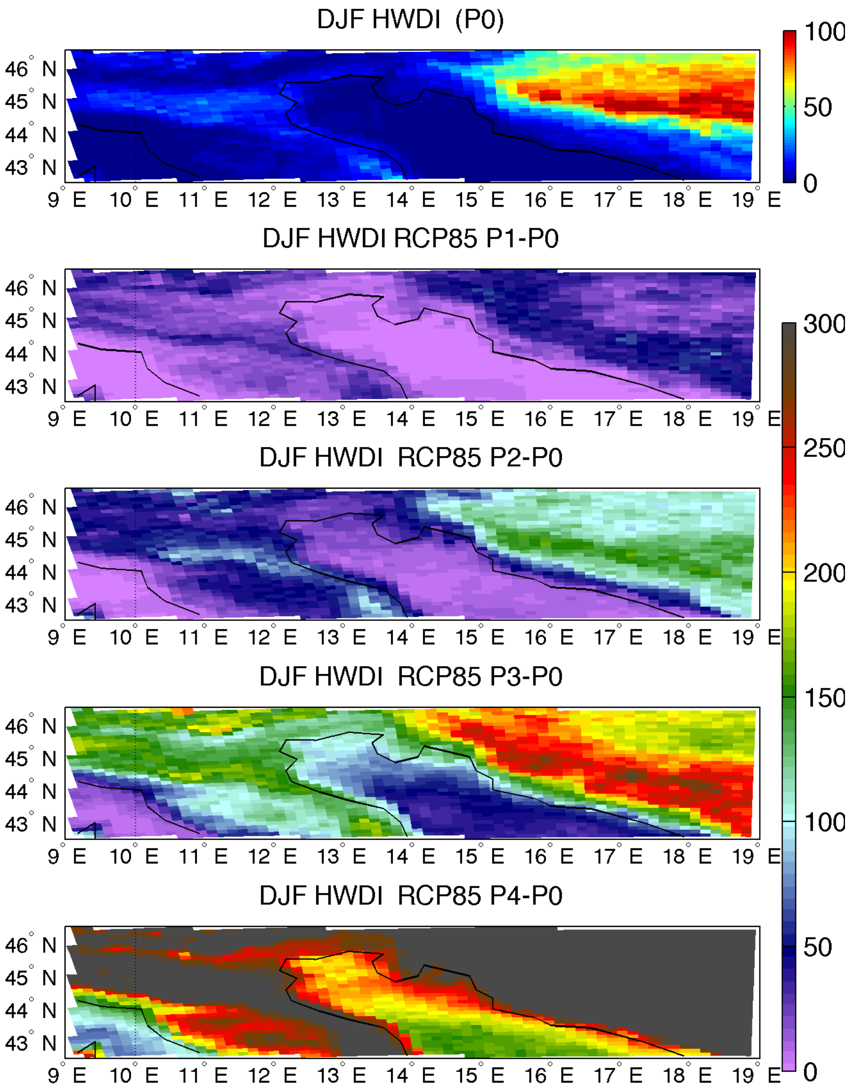

Figure 4-11: Heat Wave duration index (HWDI, units are [days]) projections for DJF, following RCP8.5 scenario: upper panel shows the ensemble average over the historical 1986:2005 (P0) period. 2nd panel shows the projected ensemble average in 2021:2040 wrt 1986:2005 (P1-P0). 3rd panel shows the projected ensemble average in 2041:2060 wrt 1986:2005 (P2-P0). 4th panel shows the projected ensemble average

in 2061:2080 wrt 1986:2005 (P3-P0). 5th panel shows the projected ensemble average in 2081:2100 wrt 1986:2005 (P4-P0).

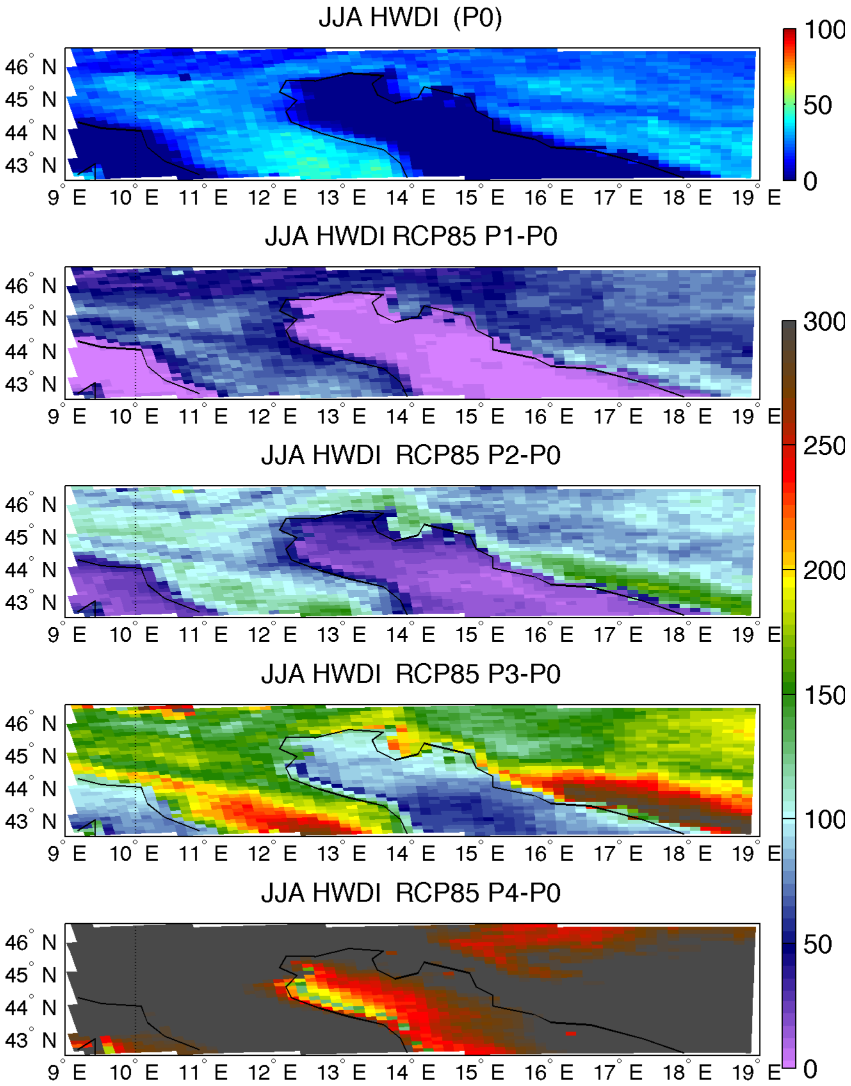

Figure 4-12: Heat Wave duration index (HWDI, units are [days]) projections for JJA, following RCP8.5 scenario: upper panel shows the ensemble average over the historical 1986:2005 (P0) period. 2nd panel shows the projected ensemble average in 2021:2040 wrt 1986:2005 (P1-P0). 3rd panel shows the projected

ensemble average in 2041:2060 wrt 1986:2005 (P2-P0). 4th panel shows the projected ensemble average in 2061:2080 wrt 1986:2005 (P3-P0). 5th panel shows the projected ensemble average in 2081:2100 wrt 1986:2005 (P4-P0).

5.1.4 Tropical nights

Seasonal averages of tropical nights (TR) in terms of differences between P1-P0, P2-P0, P3-P0, P4-P0 are shown in figures 4.13 relative to the RCP4.5 scenario and in figure 4.14 relative to the RCP8.5 scenario for the summer season only (no daily minimum temperature higher than 20°C during winter has been found over P0). The TR is defined as the cumulative number of days in the period (~90[days]x20[years]~=a total sample of 1800 days) corresponding to the following conditions: days in which the minimum daily temperature is higher than 20°C. Following the moderate RCP4.5 scenario, during summer we expect an average increase of up to 300 days for the middle of the century (P2) in both scenarios doubling the historical values. Such increase is expected to increase up to 600 days for the end of the century (P4) with more pronounced increases expected over the plains.

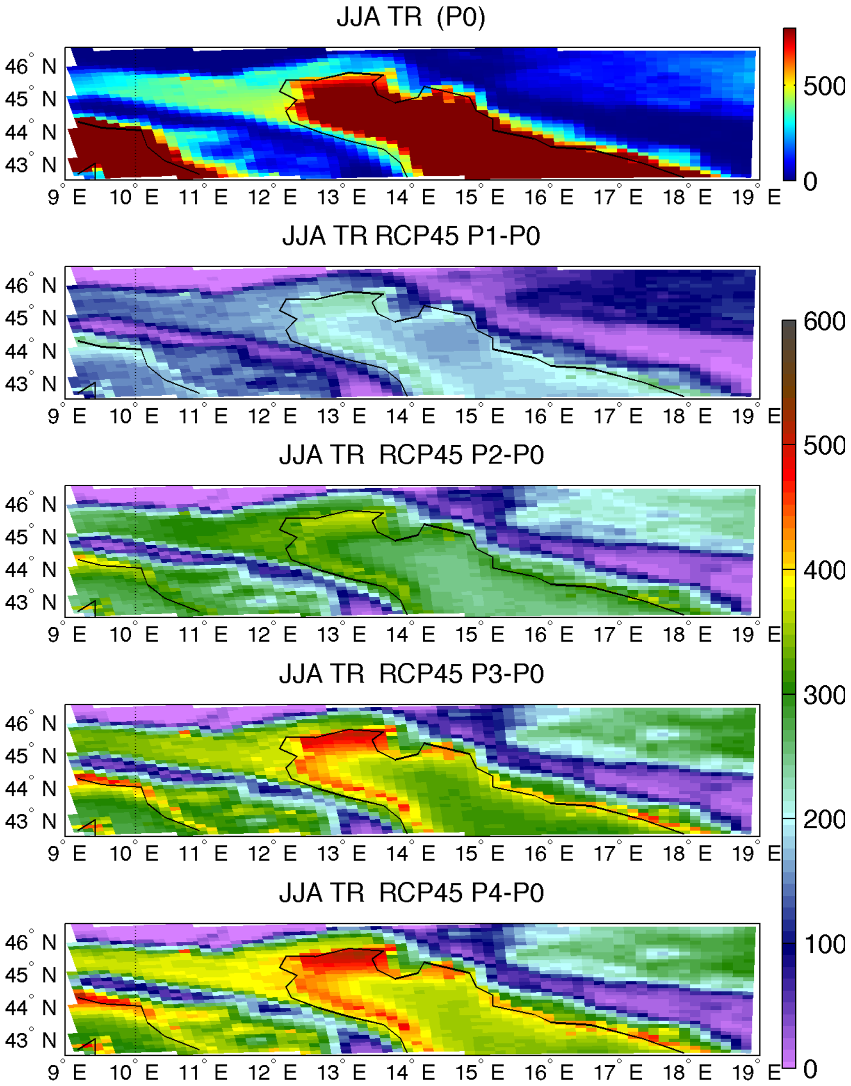

Figure 4-13: Tropical Nights (TR, units are [days]) projections for JJA, following RCP4.5 scenario: upper panel shows the ensemble average over the historical 1986:2005 (P0) period. 2nd panel shows the projected ensemble average in 2021:2040 wrt 1986:2005 (P1-P0). 3rd panel shows the projected ensemble average in 2041:2060 wrt 1986:2005 (P2-P0). 4th panel shows the projected ensemble average in 2061:2080 wrt 1986:2005 (P3-P0). 5th panel shows the projected ensemble average in 2081:2100 wrt 1986:2005 (P4-P0).

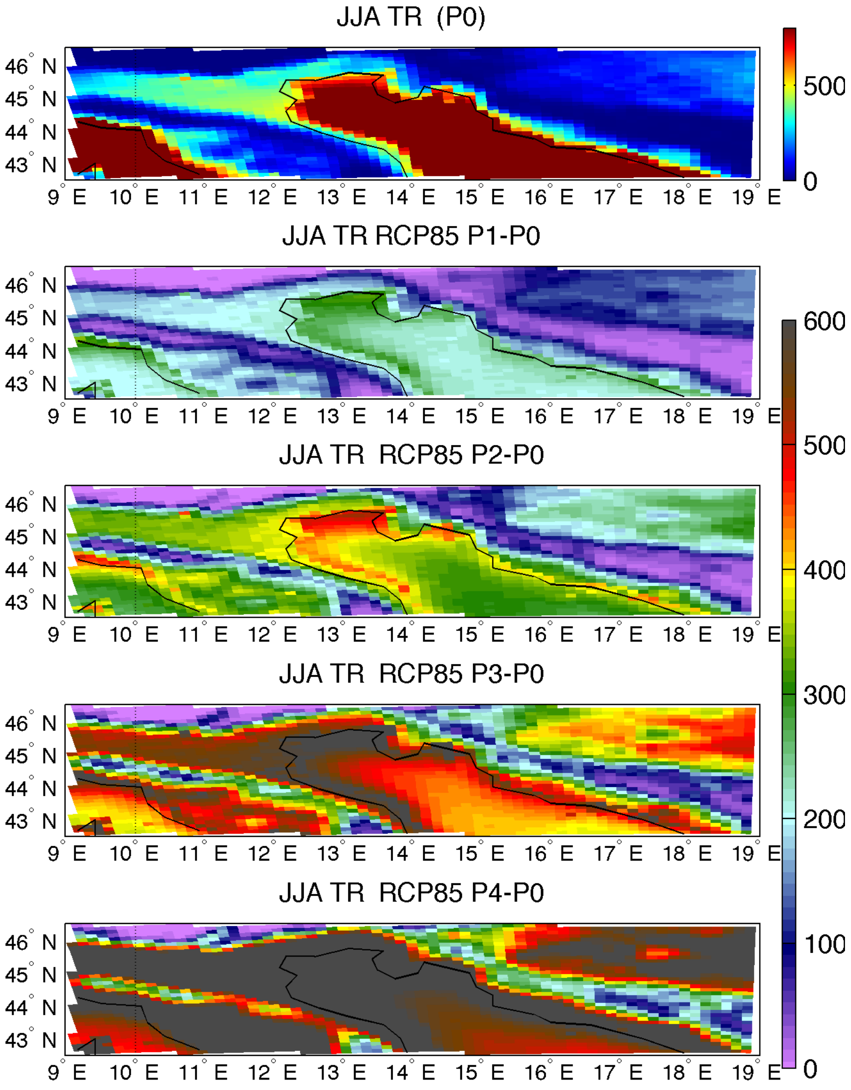

Figure 4-14: Tropical Nights (TR, units are [days]) projections for JJA, following RCP8.5 scenario: upper panel shows the ensemble average over the historical 1986:2005 (P0) period. 2nd panel shows the projected ensemble average in 2021:2040 wrt 1986:2005 (P1-P0). 3rd panel shows the projected ensemble average in 2041:2060 wrt 1986:2005 (P2-P0). 4th panel shows the projected ensemble average in 2061:2080 wrt 1986:2005 (P3-P0). 5th panel shows the projected ensemble average in 2081:2100 wrt 1986:2005 (P4-P0).

5.1.5 Frost days

Seasonal averages of frost days (FD) in terms of differences between P1-P0, P2-P0, P3-P0, P4-P0 are shown in figures 4.15 relative to the RCP4.5 scenario and in figure 4.16 relative to the RCP8.5 scenario for the winter season only (no daily minimum temperature lower than 0°C during summer has been found over P0). The FD is defined as the cumulative number of days in the period (~90[days]x20[years]~=a total sample of 1800 days) corresponding to the following conditions: days in which the minimum daily temperature is lower than 0°C. Following the moderate RCP4.5 scenario, during winter we expect an average decrease of up to 150 days for the middle of the century (P2) corresponding to more than 25% of the historical value in both scenarios. Such decrease is expected to reach 250 and 500 in RCP4.5 and RCP8.5 respectively for the end of the century (P4) with more pronounced decrease expected over the plains where for the RCP8.5 it means that over a consistent portion of the land domain the frost day number will tend to zero.

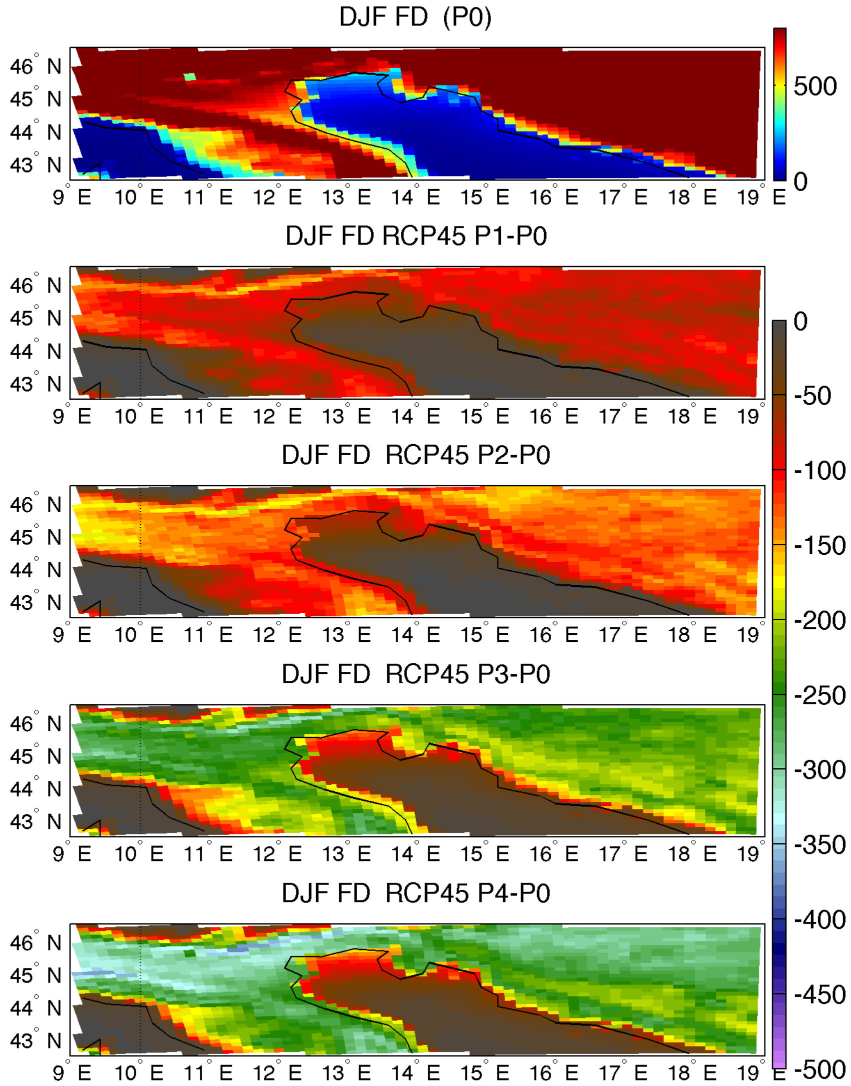

Figure 4-15: Frost Days (FD, units are [°C]) projections for DJF, following RCP4.5 scenario: upper panel shows the ensemble average over the historical 1986:2005 (P0) period. 2nd panel shows the projected ensemble average in 2021:2040 wrt 1986:2005 (P1-P0). 3rd panel shows the projected ensemble average in 2041:2060 wrt 1986:2005 (P2-P0). 4th panel shows the projected ensemble average in 2061:2080 wrt 1986:2005 (P3-P0). 5th panel shows the projected ensemble average in 2081:2100 wrt 1986:2005 (P4-P0).

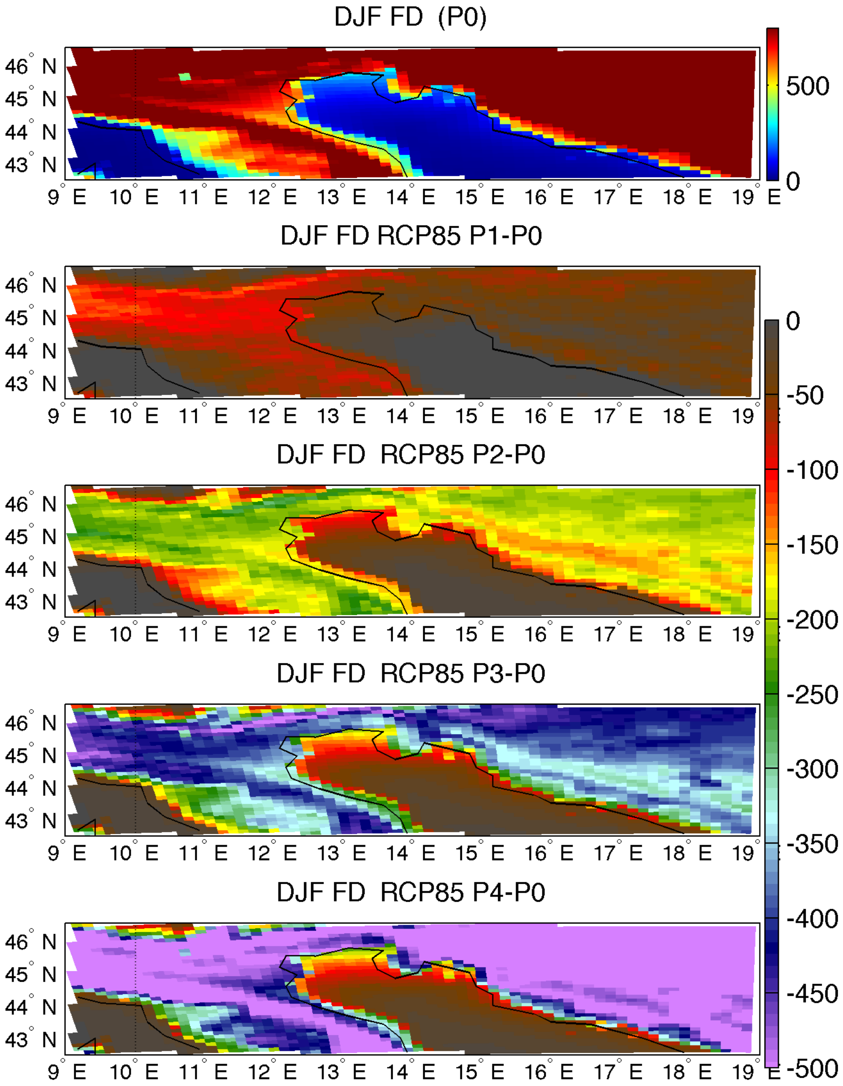

Figure 4-16: Frost Days (FD, units are [°C]) projections for DJF, following RCP8.5 scenario: upper panel shows the ensemble average over the historical 1986:2005 (P0) period. 2nd panel shows the projected ensemble average in 2021:2040 wrt 1986:2005 (P1-P0). 3rd panel shows the projected ensemble average in 2041:2060 wrt 1986:2005 (P2-P0). 4th panel shows the projected ensemble average in 2061:2080 wrt 1986:2005 (P3-P0). 5th panel shows the projected ensemble average in 2081:2100 wrt 1986:2005 (P4-P0)

https://www.italy-croatia.eu/adriadapt

5.2 Precipitation related indices projections

A less clear signal (more spotty and less coherent in space and time), compared to projection of temperature derived indices, is expected in the case of precipitation related indices. For this reason it is important to consider the significance of the shown results especially at the local level. For this reason in the next chapter 5, we also present the statistical significance of the described differences case study by case study and model by model.

5.2.1 Averaged precipitation

Seasonal averages of precipitation differences between P1-P0, P2-P0, P3-P0, P4-P0 are shown in figures 4.17 (winter) and 4.18 (summer) relative to the RCP4.5 scenario and in figures 4.19 (winter) and 4.20 (summer) relative to the RCP8.5 scenario. Following the moderate RCP4.5 scenario, during both winter and summer we do not expect significant differences in terms of precipitation along the whole century. Following the worst RCP8.5 scenario, consistently with the radiative paths associated to the two scenarios, no huge differences appear for the middle of the century, while for the end of the century (P4), when the two radiative forcing paths substantially diverge, increases of the order of one mm/d can be expected during winter over a small portion of the eastern domain , and a decrease of the same magnitude is expected during summer.

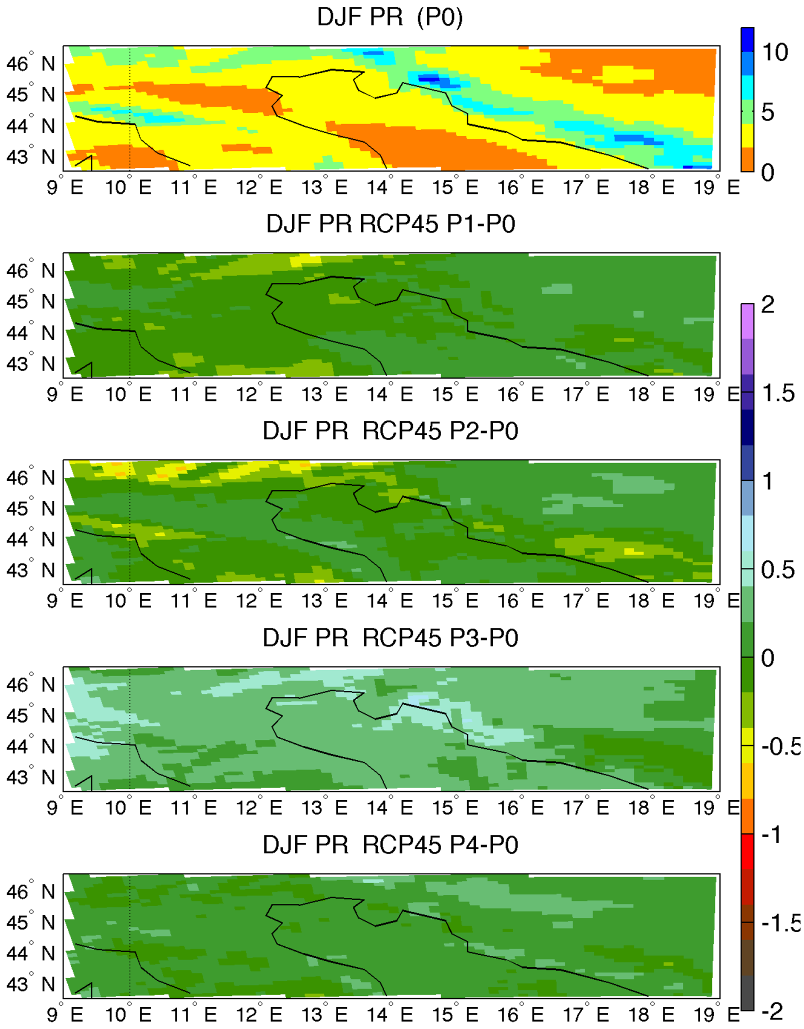

Figure 4-17: Average Precipitation (PR, units are [mm/d]) projections for DJF, following RCP4.5 scenario: upper panel shows the ensemble average over the historical 1986:2005 (P0) period. 2nd panel shows the projected ensemble average in 2021:2040 wrt 1986:2005 (P1-P0). 3rd panel shows the projected ensemble average in 2041:2060 wrt 1986:2005 (P2-P0). 4th panel shows the projected ensemble average in 2061:2080 wrt 1986:2005 (P3-P0). 5th panel shows the projected ensemble average in 2081:2100 wrt 1986:2005 (P4-P0).

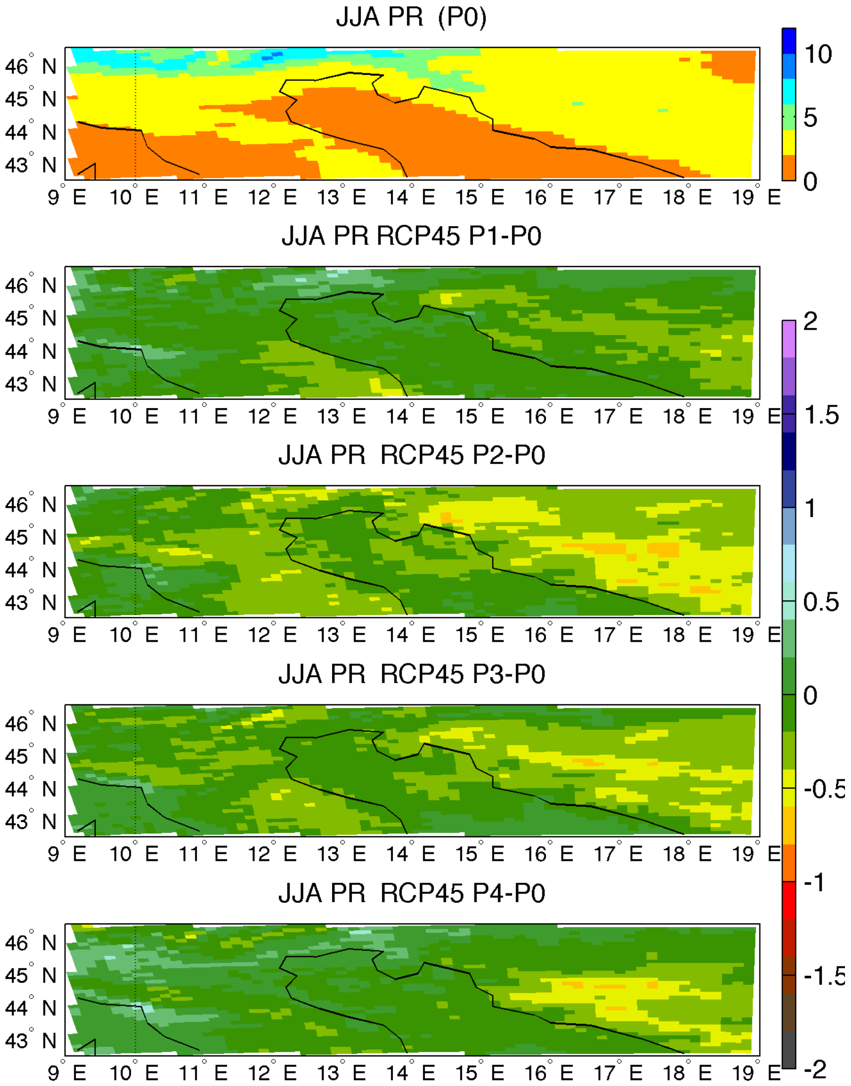

Figure 4-18: Average Precipitation (PR, units are [mm/d]) projections for JJA, following RCP4.5 scenario: upper panel shows the ensemble average over the historical 1986:2005 (P0) period. 2nd panel shows the projected ensemble average in 2021:2040 wrt 1986:2005 (P1-P0). 3rd panel shows the projected ensemble average in 2041:2060 wrt 1986:2005 (P2-P0). 4th panel shows the projected ensemble average in 2061:2080 wrt 1986:2005 (P3-P0). 5th panel shows the projected ensemble average in 2081:2100 wrt 1986:2005 (P4-P0).

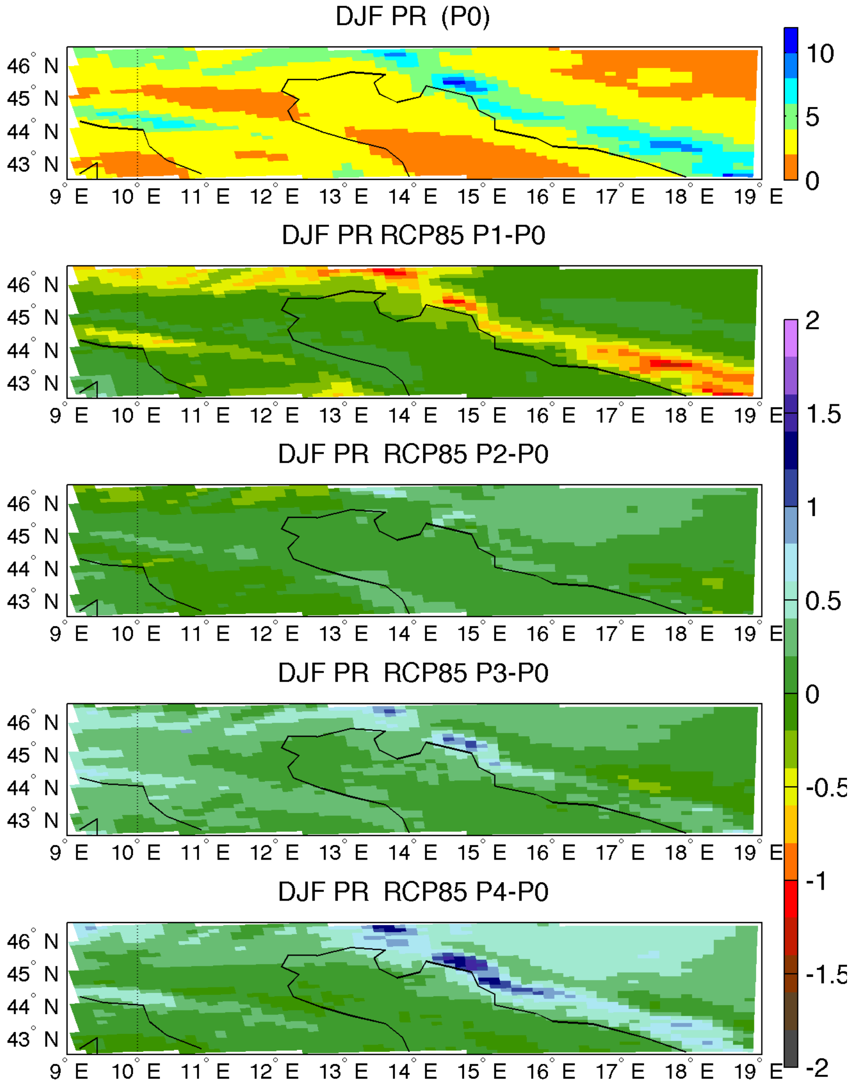

Figure 4-19: Average Precipitation (PR, units are [mm/d]) projections for DJF, following RCP8.5 scenario: upper panel shows the ensemble average over the historical 1986:2005 (P0) period. 2nd panel shows the projected ensemble average in 2021:2040 wrt 1986:2005 (P1-P0). 3rd panel shows the projected ensemble average in 2041:2060 wrt 1986:2005 (P2-P0). 4th panel shows the projected ensemble average in

2061:2080 wrt 1986:2005 (P3-P0). 5th panel shows the projected ensemble average in 2081:2100 wrt 1986:2005 (P4-P0).

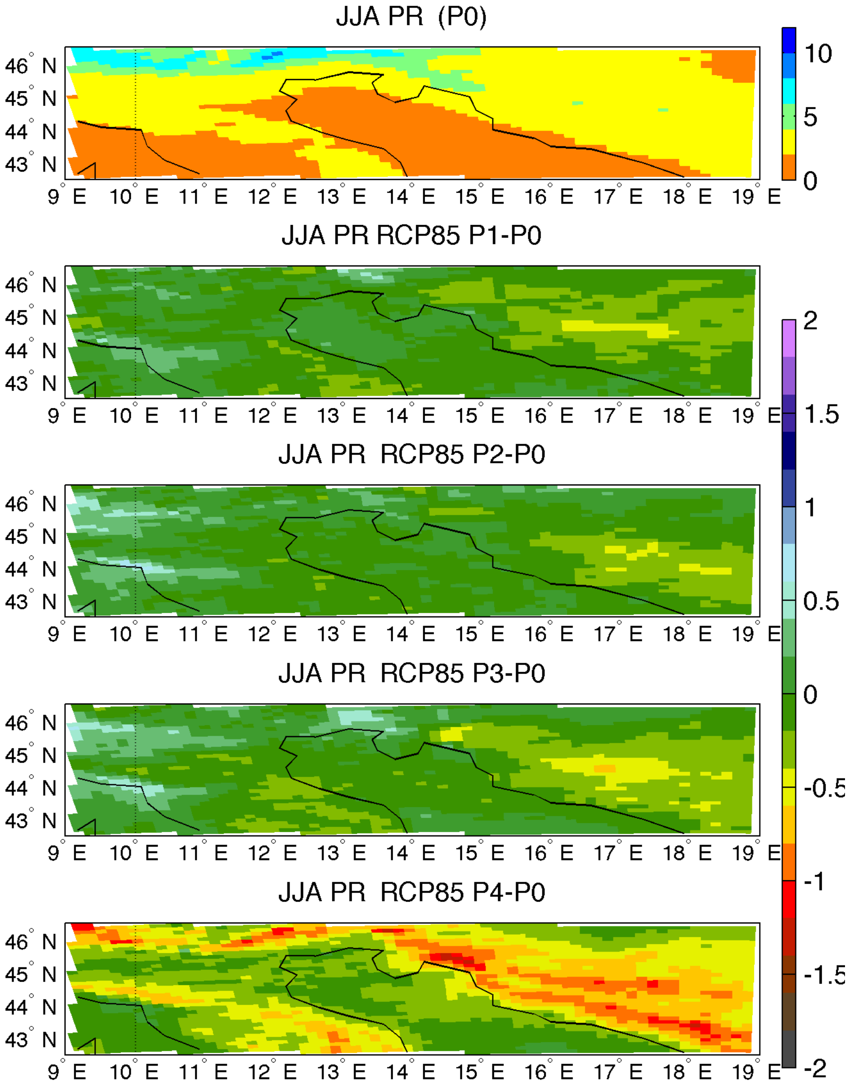

Figure 4-20: Average Precipitation (PR, units are [mm/d]) projections for JJA, following RCP8.5 scenario: upper panel shows the ensemble average over the historical 1986:2005 (P0) period. 2nd panel shows the projected ensemble average in 2021:2040 wrt 1986:2005 (P1-P0). 3rd panel shows the projected ensemble

average in 2041:2060 wrt 1986:2005 (P2-P0). 4th panel shows the projected ensemble average in 2061:2080 wrt 1986:2005 (P3-P0). 5th panel shows the projected ensemble average in 2081:2100 wrt 1986:2005 (P4-P0).

5.2.2 Intense precipitation

Seasonal averages of intense precipitation (the 95th percentile of the precipitation distribution within the 90days x 20 years ~=1800 days) differences between P1-P0, P2-P0, P3-P0, P4-P0 are shown in figures 4.21 (winter) and 4.22 (summer) relative to the RCP4.5 scenario and in figures 4.23 (winter) and 4.24 (summer) relative to the RCP8.5 scenario. The suggested changes relative to the first part of the century up to P3, are not coherent in terms of tendencies associate to the radiative path. This is true for both scenarios especially during winter, while during summer a general tendency is to the reduction of the intense precipitation value over most of the domain. For the end of the century instead (P4) the signal is more clear and suggesting an increase up to 4 mm/d over the eastern part of the domain during winter and decrease of the same order of magnitude during summer, resembling average precipitation patterns.

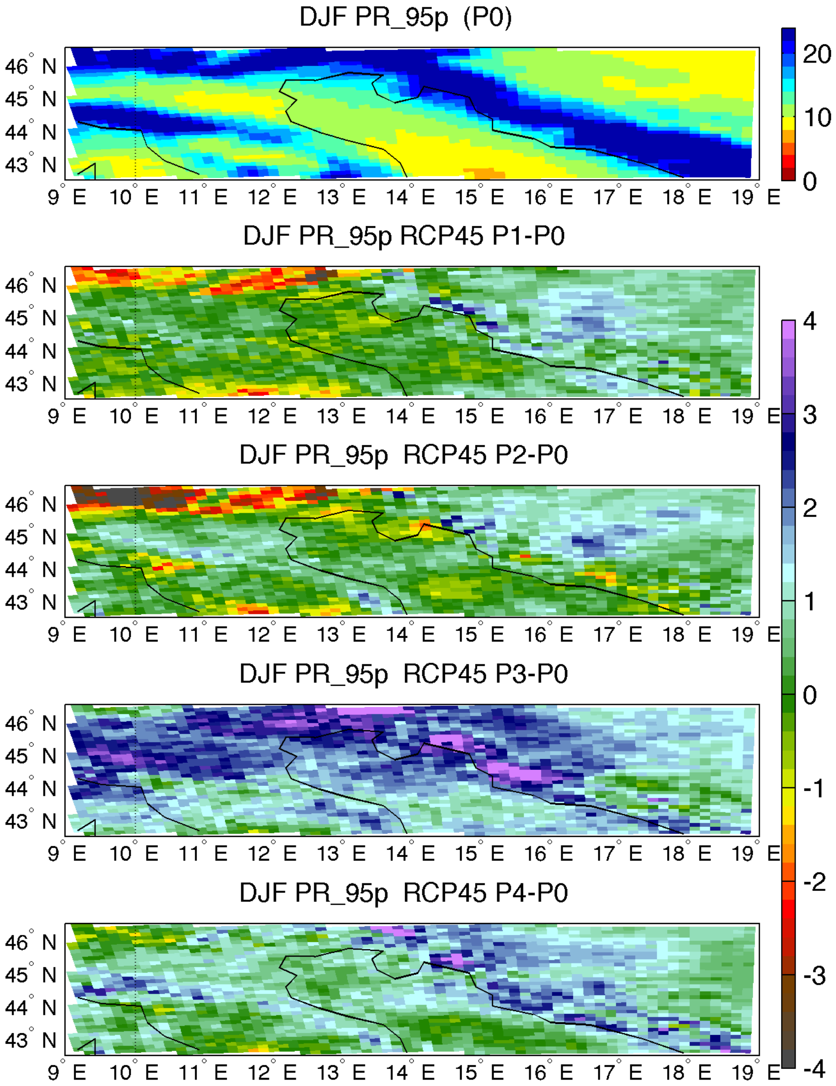

Figure 4-21: Intense Precipitation (PR_95p, units are [mm/d]) projections for DJF, following RCP4.5 scenario: upper panel shows the ensemble average over the historical 1986:2005 (P0) period. 2nd panel shows the projected ensemble average in 2021:2040 wrt 1986:2005 (P1-P0). 3rd panel shows the projected ensemble average in 2041:2060 wrt 1986:2005 (P2-P0). 4th panel shows the projected ensemble average in 2061:2080 wrt 1986:2005 (P3-P0). 5th panel shows the projected ensemble average in 2081:2100 wrt 1986:2005 (P4-P0).

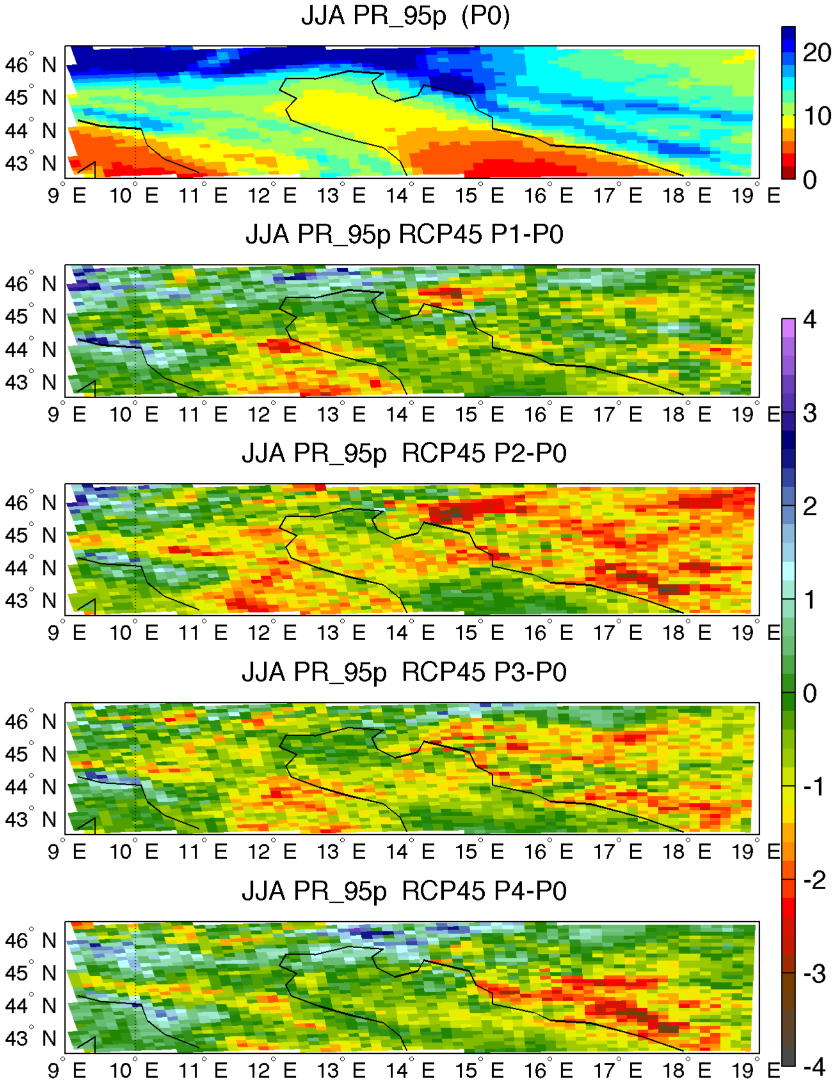

Figure 4-22: Intense Precipitation (PR_95p, units are [mm/d]) projections for JJA, following RCP4.5 scenario: upper panel shows the ensemble average over the historical 1986:2005 (P0) period. 2nd panel shows the projected ensemble average in 2021:2040 wrt 1986:2005 (P1-P0). 3rd panel shows the projected ensemble average in 2041:2060 wrt 1986:2005 (P2-P0). 4th panel shows the projected ensemble average in 2061:2080 wrt 1986:2005 (P3-P0). 5th panel shows the projected ensemble average in 2081:2100 wrt 1986:2005 (P4-P0).

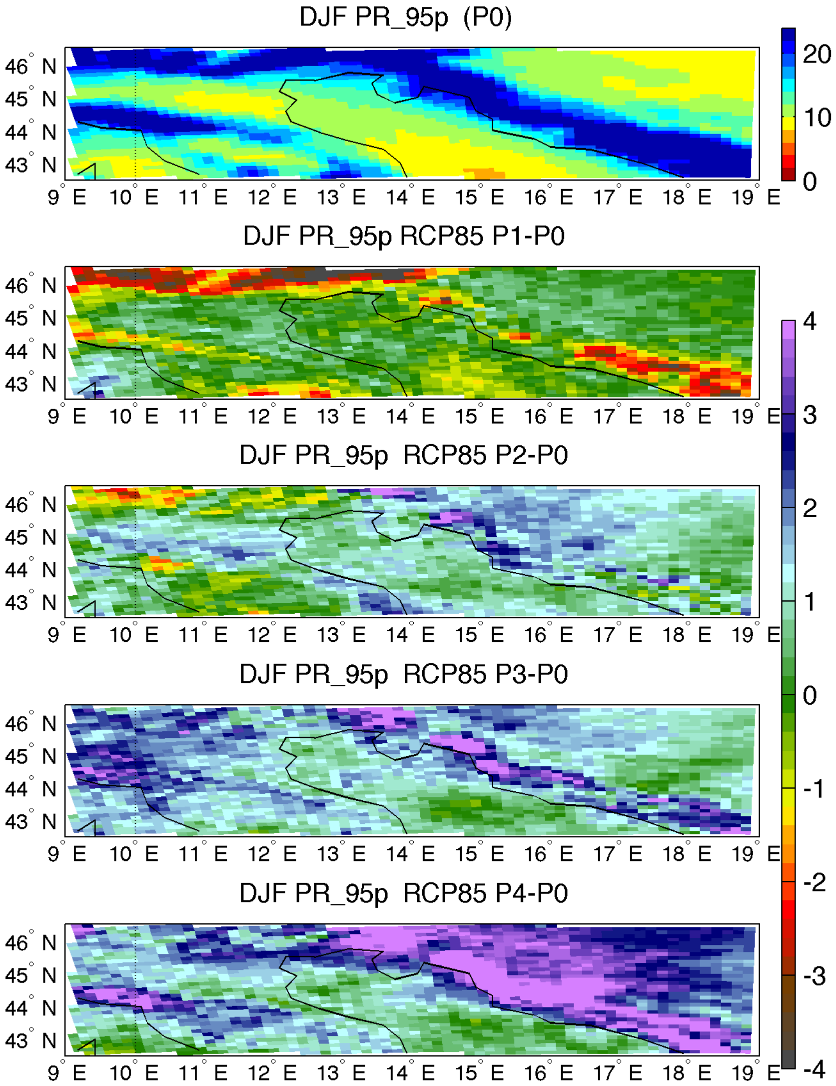

Figure 4-23: Intense Precipitation (PR_95p, units are [mm/d]) projections for DJF, following RCP8.5 scenario: upper panel shows the ensemble average over the historical 1986:2005 (P0) period. 2nd panel shows the projected ensemble average in 2021:2040 wrt 1986:2005 (P1-P0). 3rd panel shows the projected ensemble average in 2041:2060 wrt 1986:2005 (P2-P0). 4th panel shows the projected ensemble average in 2061:2080 wrt 1986:2005 (P3-P0). 5th panel shows the projected ensemble average in 2081:2100 wrt 1986:2005 (P4-P0).

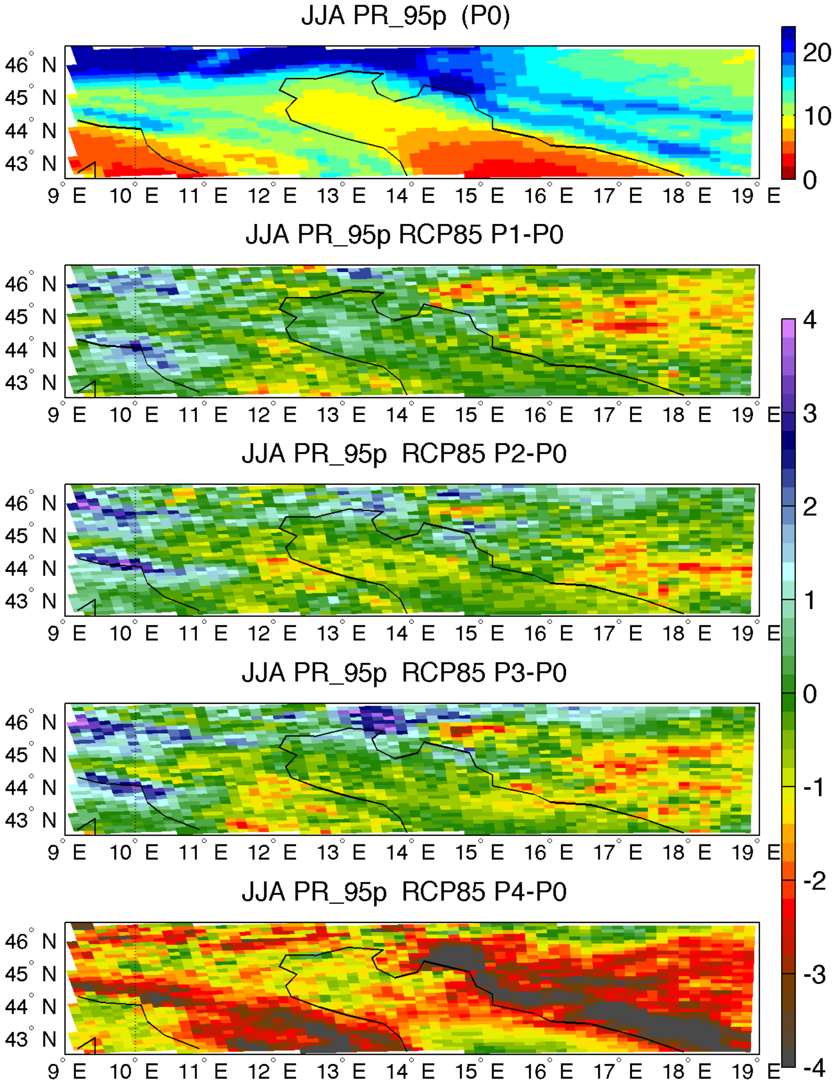

Figure 4-24: Intense Precipitation (PR_95p, units are [mm/d]) projections for JJA, following RCP8.5 scenario: upper panel shows the ensemble average over the historical 1986:2005 (P0) period. 2nd panel shows the projected ensemble average in 2021:2040 wrt 1986:2005 (P1-P0). 3rd panel shows the projected ensemble average in 2041:2060 wrt 1986:2005 (P2-P0). 4th panel shows the projected ensemble average

in 2061:2080 wrt 1986:2005 (P3-P0). 5th panel shows the projected ensemble average in 2081:2100 wrt 1986:2005 (P4-P0).

5.2.3 Extreme precipitation

Seasonal averages of extreme precipitation (the 99th percentile of the precipitation distribution within the 90days x 20 years ~=1800 days) differences between P1-P0, P2-P0, P3-P0, P4-P0 are shown in figures 4.25 (winter) and 4.26 (summer) relative to the RCP4.5 scenario and in figures 4.27 (winter) and 4.28 (summer) relative to the RCP8.5 scenario. The suggested changes relative to the first part of the century up to P3, are not coherent in terms of tendencies associate to the radiative path similarly to what has been found for intense precipitation. This is true for both scenarios especially during winter, while during summer a general tendency is to the reduction of the intense precipitation value over most of the domain. For the end of the century instead (P4) the signal is stronger, suggesting an increase up to 10 mm/d over the eastern part of the domain during winter and a more moderate and spotty decrease during summer.

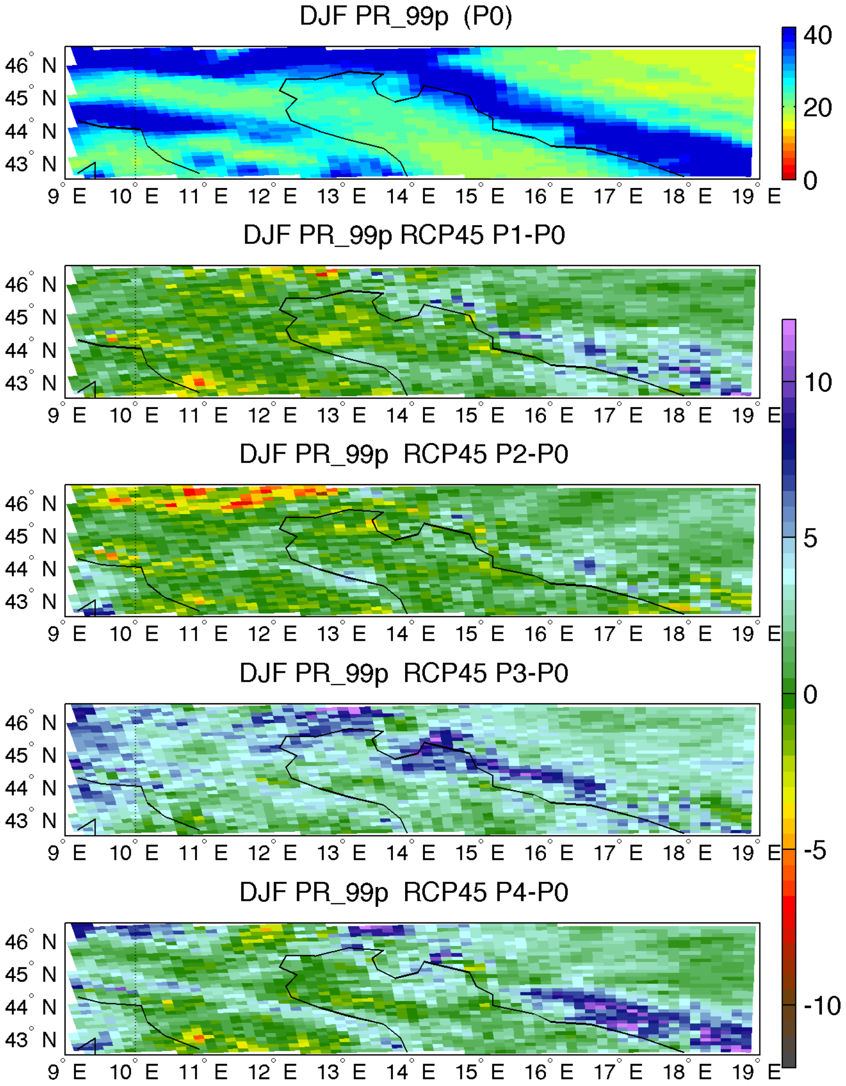

Figure 4-25: Extreme Precipitation (PR_99p, units are [mm/d]) projections for DJF, following RCP4.5 scenario: upper panel shows the ensemble average over the historical 1986:2005 (P0) period. 2nd panel shows the projected ensemble average in 2021:2040 wrt 1986:2005 (P1-P0). 3rd panel shows the projected ensemble average in 2041:2060 wrt 1986:2005 (P2-P0). 4th panel shows the projected ensemble average in 2061:2080 wrt 1986:2005 (P3-P0). 5th panel shows the projected ensemble average in 2081:2100 wrt 1986:2005 (P4-P0)

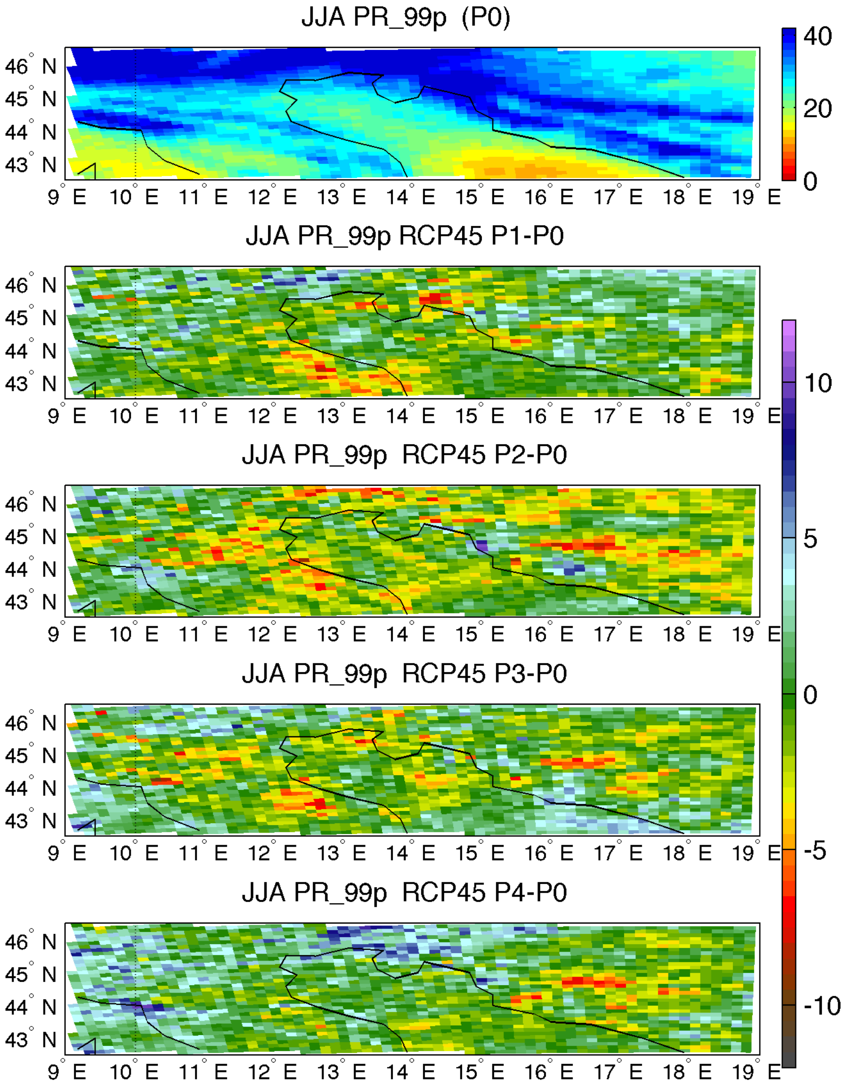

Figure 4-26: Extreme Precipitation (PR_99p, units are [mm/d]) projections for JJA, following RCP4.5 scenario: upper panel shows the ensemble average over the historical 1986:2005 (P0) period. 2nd panel shows the projected ensemble average in 2021:2040 wrt 1986:2005 (P1-P0). 3rd panel shows the projected ensemble average in 2041:2060 wrt 1986:2005 (P2-P0). 4th panel shows the projected ensemble average in 2061:2080 wrt 1986:2005 (P3-P0). 5th panel shows the projected ensemble average in 2081:2100 wrt 1986:2005 (P4-P0)

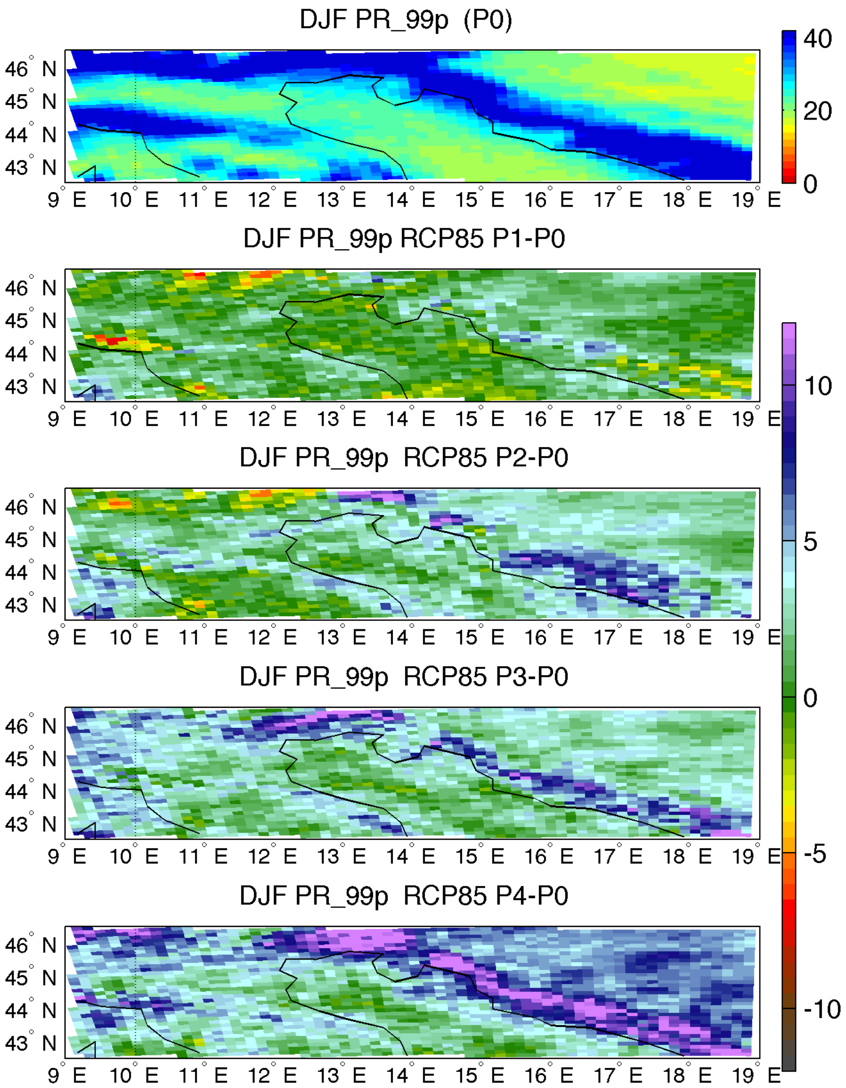

Figure 4-27: Extreme Precipitation (PR_99p, units are [mm/d]) projections for DJF, following RCP8.5 scenario: upper panel shows the ensemble average over the historical 1986:2005 (P0) period. 2nd panel shows the projected ensemble average in 2021:2040 wrt 1986:2005 (P1-P0). 3rd panel shows the projected ensemble average in 2041:2060 wrt 1986:2005 (P2-P0). 4th panel shows the projected ensemble average

in 2061:2080 wrt 1986:2005 (P3-P0). 5th panel shows the projected ensemble average in 2081:2100 wrt 1986:2005 (P4-P0)

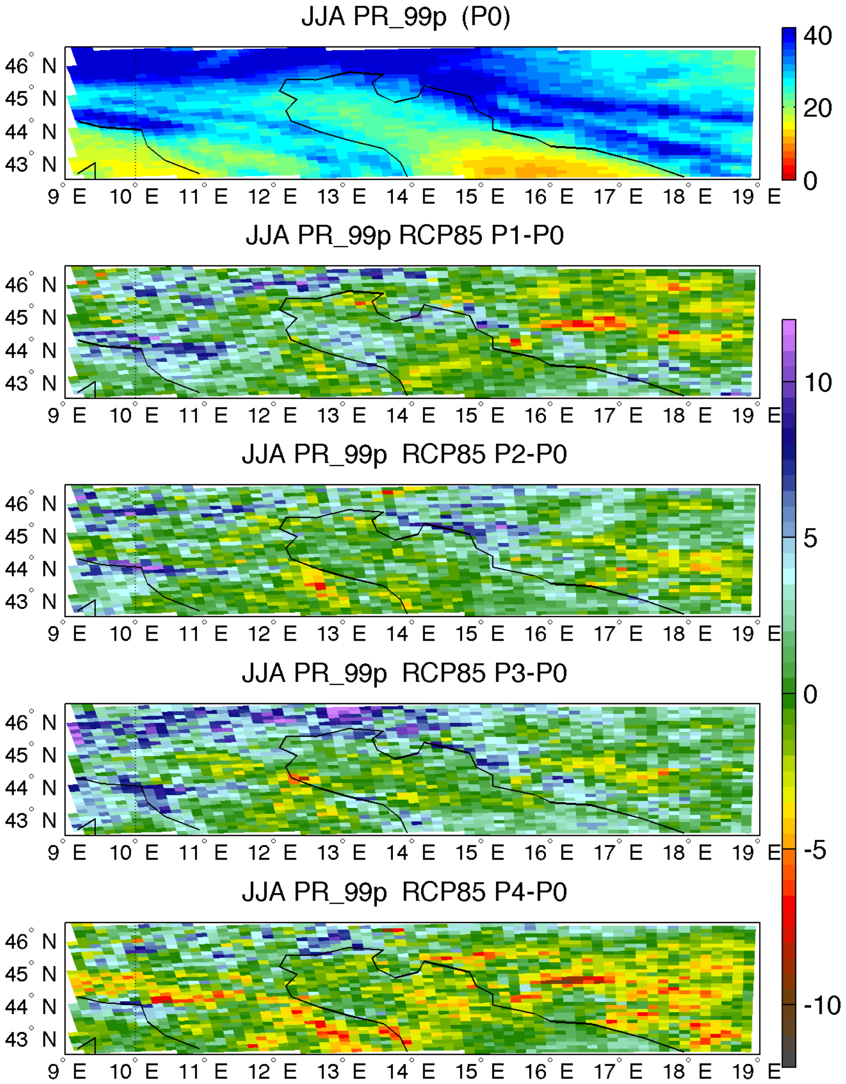

Figure 4-28: Extreme Precipitation (PR_99p, units are [mm/d]) projections for JJA, following RCP8.5 scenario: upper panel shows the ensemble average over the historical 1986:2005 (P0) period. 2nd panel shows the projected ensemble average in 2021:2040 wrt 1986:2005 (P1-P0). 3rd panel shows the projected

ensemble average in 2041:2060 wrt 1986:2005 (P2-P0). 4th panel shows the projected ensemble average in 2061:2080 wrt 1986:2005 (P3-P0). 5th panel shows the projected ensemble average in 2081:2100 wrt 1986:2005 (P4-P0)

5.2.4 Consecutive dry days

Seasonal averages of consecutive dry days (the number of consecutive days in the period with precipitation lower than 1 mm/d) differences between P1-P0, P2-P0, P3-P0, P4-P0 are shown in figures 4.29 (winter) and 4.30 (summer) relative to the RCP4.5 scenario and in figures 4.31 (winter) and 4.32 (summer) relative to the RCP8.5 scenario. The suggested changes relative to the first part of the century up to P3, are not coherent in terms of tendencies associate to the radiative path similarly to what has been found for intense precipitation. This is true for both scenarios especially during winter, while during summer a general tendency to the increase of the number of consecutive dry days is expected. For the end of the century (P4) the summer signal is even stronger, especially for the RCP8.5 scenario, suggesting an increase up to 15 days in the southern part of the domain over both land and sea.

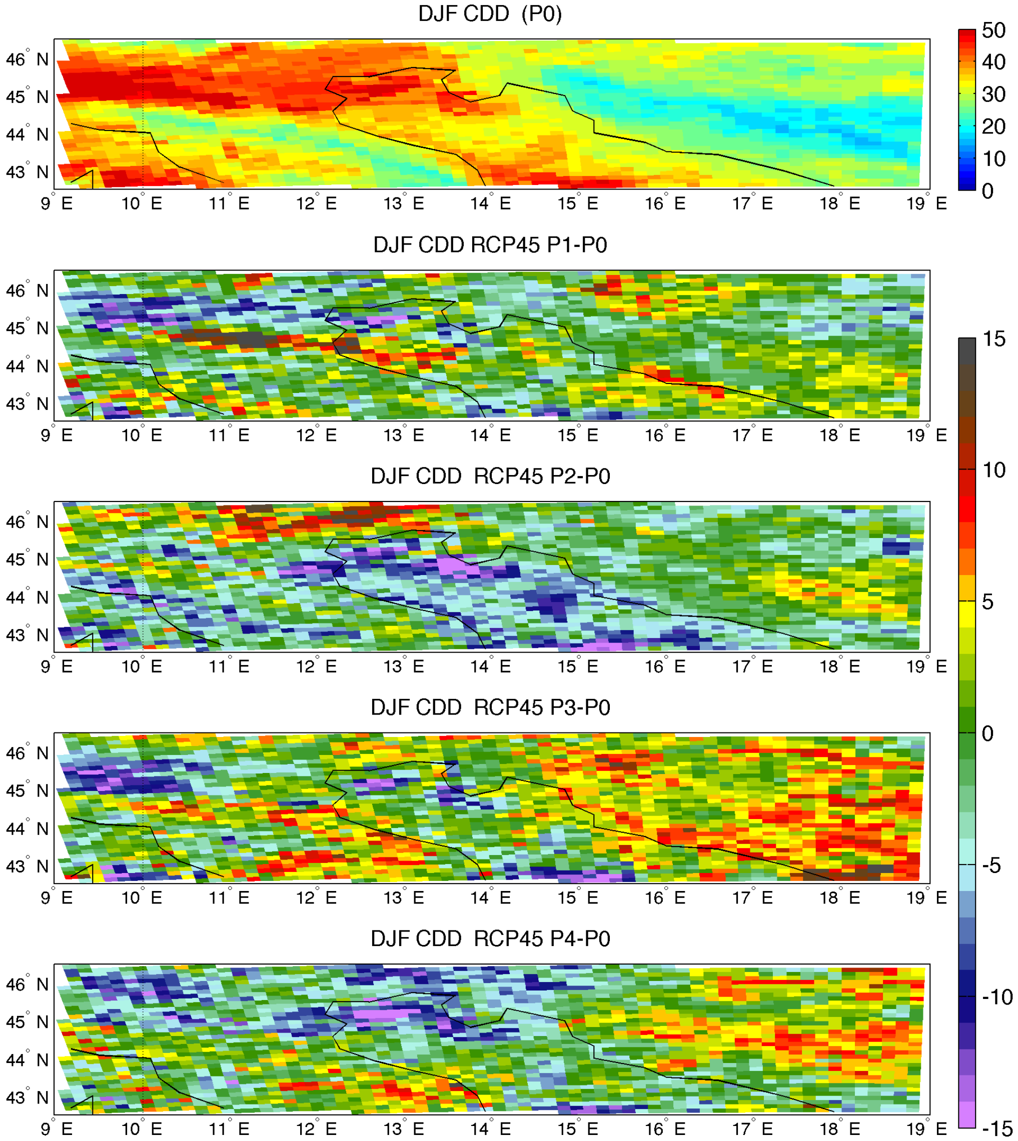

Figure 4-29: Consecutive Dry Days (CDD, units are [days]) projections for DJF, following RCP4.5 scenario: upper panel shows the ensemble average over the historical 1986:2005 (P0) period. 2nd panel shows the projected ensemble average in 2021:2040 wrt 1986:2005 (P1-P0). 3rd panel shows the projected ensemble average in 2041:2060 wrt 1986:2005 (P2-P0). 4th panel shows the projected ensemble average in 2061:2080 wrt 1986:2005 (P3-P0). 5th panel shows the projected ensemble average in 2081:2100 wrt 1986:2005 (P4-P0)

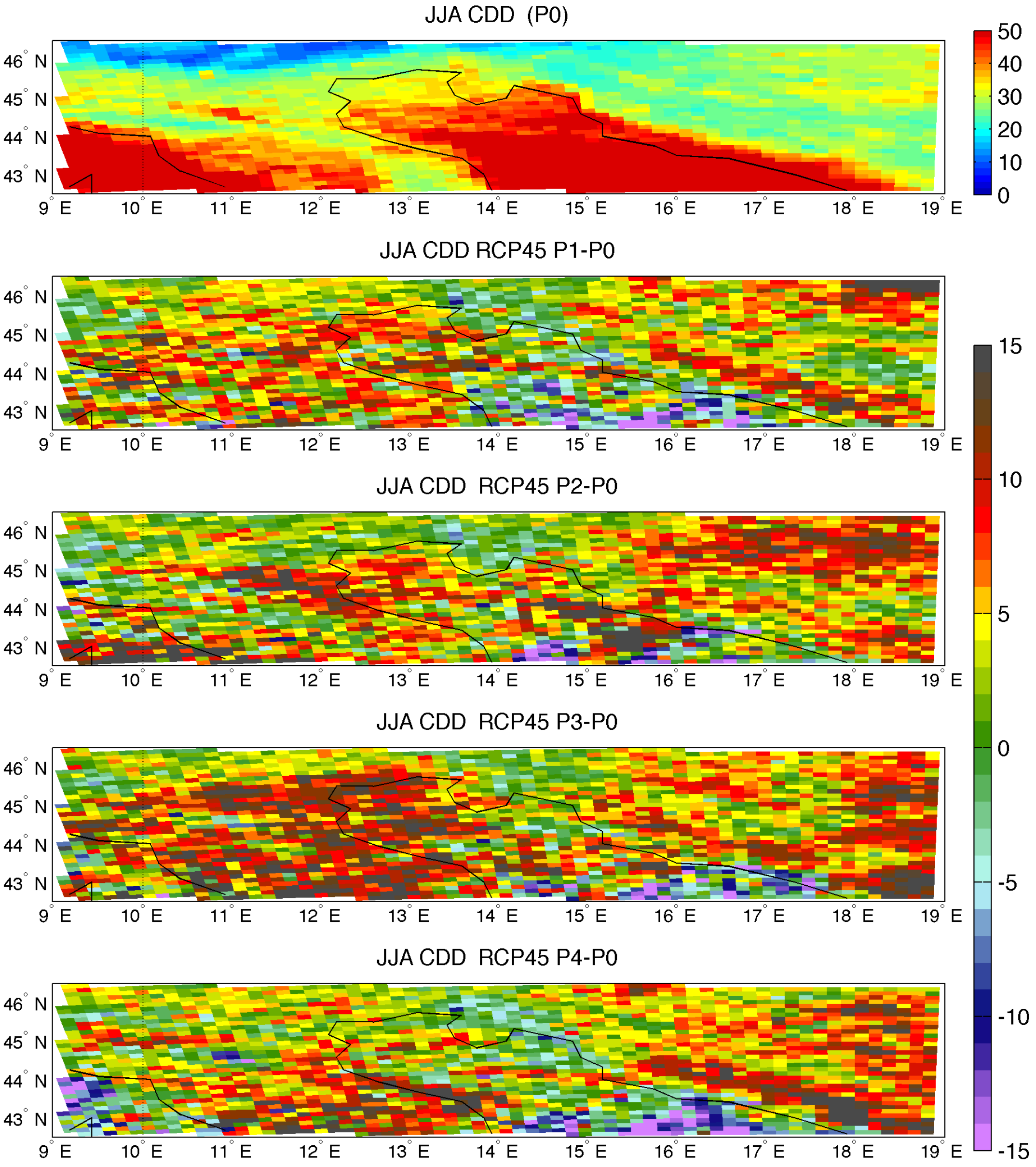

Figure 4-30: Consecutive Dry Days (CDD, units are [days]) projections for JJA, following RCP4.5 scenario: upper panel shows the ensemble average over the historical 1986:2005 (P0) period. 2nd panel shows the projected ensemble average in 2021:2040 wrt 1986:2005 (P1-P0). 3rd panel shows the projected ensemble average in 2041:2060 wrt 1986:2005 (P2-P0). 4th panel shows the projected ensemble average in 2061:2080 wrt 1986:2005 (P3-P0). 5th panel shows the projected ensemble average in 2081:2100 wrt 1986:2005 (P4-P0)

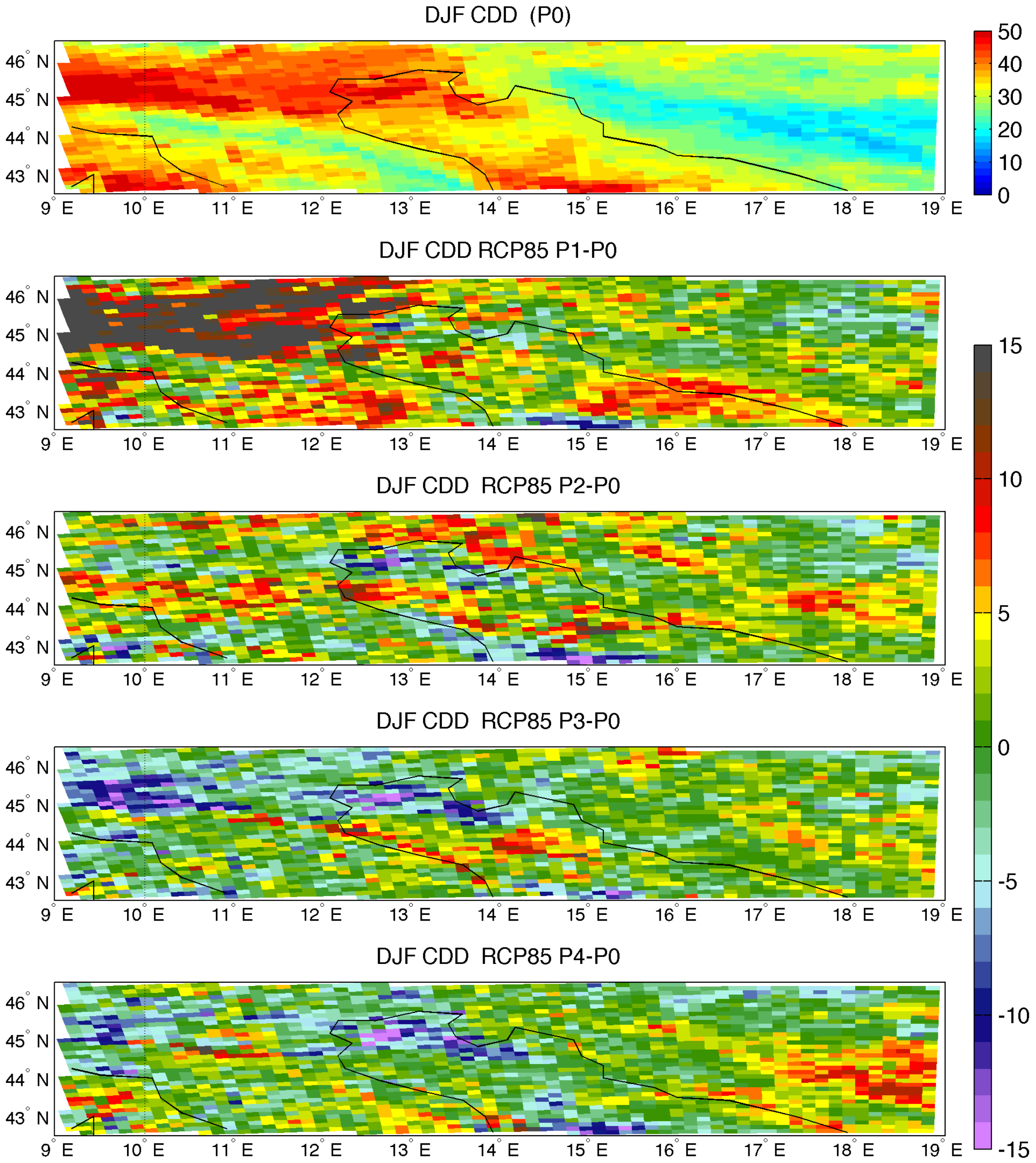

Figure 4-31: Consecutive Dry Days (CDD, units are [days]) projections for DJF, following RCP8.5 scenario: upper panel shows the ensemble average over the historical 1986:2005 (P0) period. 2nd panel shows the projected ensemble average in 2021:2040 wrt 1986:2005 (P1-P0). 3rd panel shows the projected ensemble average in 2041:2060 wrt 1986:2005 (P2-P0). 4th panel shows the projected ensemble average in

2061:2080 wrt 1986:2005 (P3-P0). 5th panel shows the projected ensemble average in 2081:2100 wrt 1986:2005 (P4-P0)

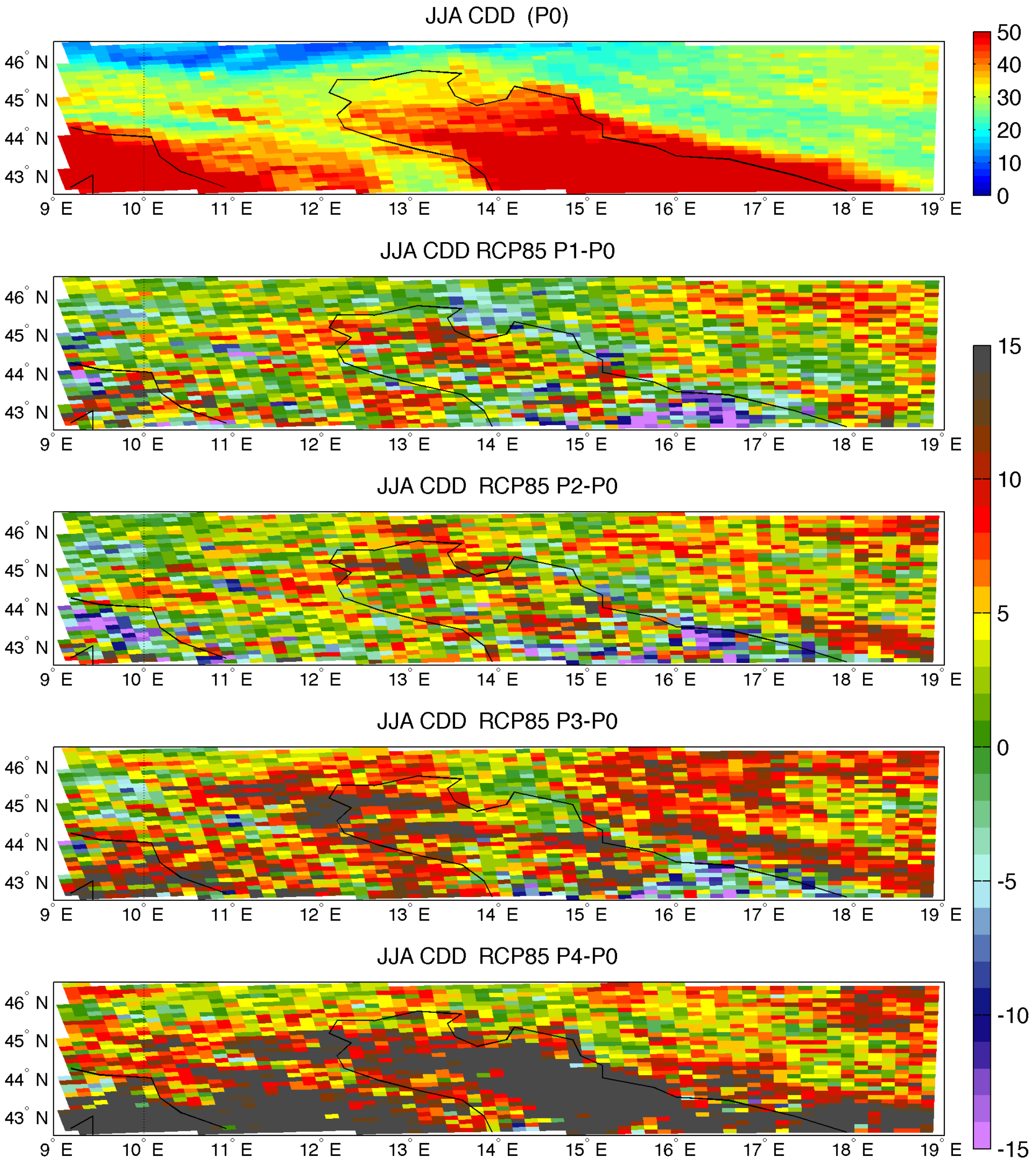

Figure 4-32: Consecutive Dry Days (CDD, units are [days]) projections for JJA, following RCP8.5 scenario: upper panel shows the ensemble average over the historical 1986:2005 (P0) period. 2nd panel shows the projected ensemble average in 2021:2040 wrt 1986:2005 (P1-P0). 3rd panel shows the projected ensemble average in 2041:2060 wrt 1986:2005 (P2-P0). 4th panel shows the projected ensemble average in

2061:2080 wrt 1986:2005 (P3-P0). 5th panel shows the projected ensemble average in 2081:2100 wrt 1986:2005 (P4-P0)

6 Future projections over the case studies

6.1 Case study 1: Knin

6.1.1 Dynamically downscaled results

In this section we present future climate change of temperature and precipitation related indices, surface relative humidity and extra rare humidex projections for Knin. All indices are calculated from the available data set of regional climate models for the grid point that is representing the location of case study Knin. Data set is obtained by bilinear interpolation. All data are presented as follows:

- Climate change diagram of an individual index in seasons and on annual basis for four considered future periods, for two emission scenarios RCP4.5 and RCP8.5. Climate change is calculated as difference between future and reference period (relative difference for precipitation indices and surface relative humidity). Reference period is presented as ensemble mean of available regional climate models (Ref.mean), while climate change is shown for different models as well as for ensemble mean of models (ENSMEAN). Two sample Wilcoxon test is applied to test statistical significance of climate change for individual models (for 95 % confidence level). Significant change is marked by star
- Time series of future anomaly of an individual index for DJF and JJA and for two emission scenarios RCP4.5 and RCP8.5. Anomaly is calculated respect to the reference period and shown for individual models, ensemble mean and 5-year moving average. Mann Kendall trend test is applied to ensemble mean (for 95 % confidence level). Significant trend is marked with star (ns if not significant).

6.1.1.1 *Temperature related indices projections*

6.1.1.1.1 *Averaged 2 meter air temperature*

Averaged temperature change in Knin (Figure 5-1) shows increase in all seasons and on annual scale, for all future periods (exception is in winter for one model realisation). Although each model gives different amplitude of change, in ensemble mean the change is highest during summer and the smallest in winter, for RCP4.5. The temperature increase is more pronounced towards the end of the century when the increase in the ensemble mean is from 1.6 °C in DJF to 2.2 °C in JJA. On annual scale for RCP4.5 temperature increase is for 1.8 °C. The amplitude of temperature change is more pronounced for RCP8.5 scenario, from 3.1 °C in MAM to 4.4 °C in JJA, on annual scale

3.7 °C at the end of 21st century for ensemble mean. The linear trend of temperature anomaly (Figure 5-2) in the future shows increase which is statistically significant for both considered seasons and both scenarios; for DJF ensemble is 0.22 °C / 10 year for RCP4.5 and 0.57 °C / 10 year for RCP8.5; for JJA ensemble is 0.18 °C / 10 year for RCP4.5 and 0.53 °C / 10 year.

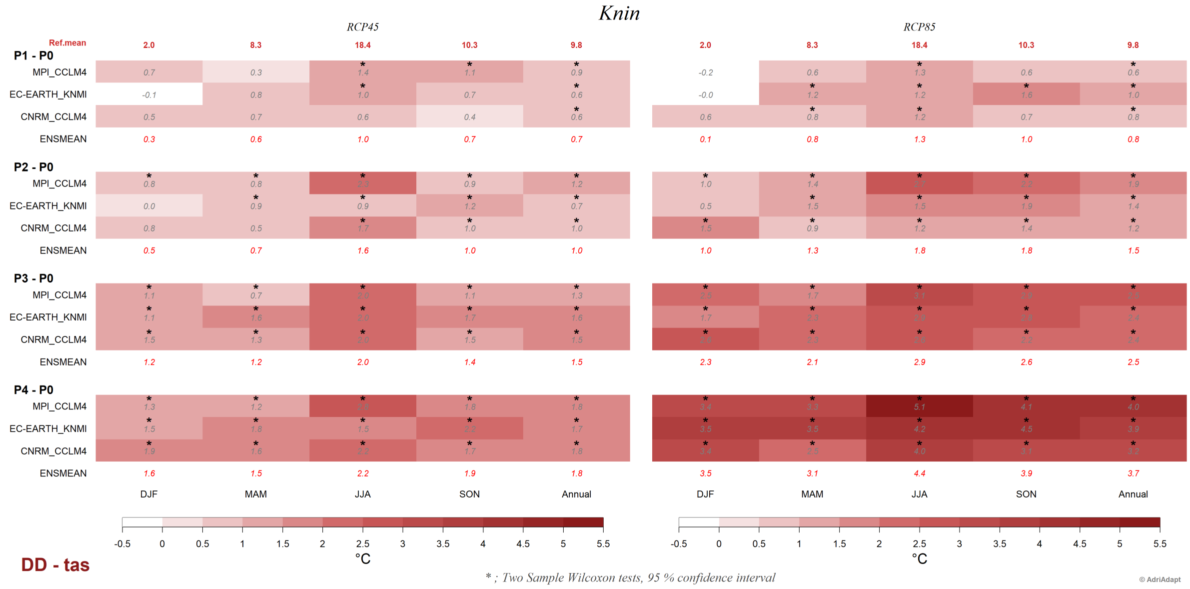

RCP45

	DJF	MAM	JJA	SON	Annual
Ref.mean	2.0	8.3	18.4	10.3	9.8
P1 - P0					
MPI_CCLM4	0.7	0.3	* 1.4	* 1.1	* 0.9
EC-EARTH_KNMI	-0.1	0.8	* 1.0	0.7	* 0.6
CNRM_CCLM4	0.5	0.7	0.6	0.4	* 0.6
ENSMEAN	0.3	0.6	1.0	0.7	0.7
P2 - P0					
MPI_CCLM4	* 0.8	* 0.8	* 2.3	* 0.9	* 1.2
EC-EARTH_KNMI	0.0	* 0.9	* 0.9	* 1.2	* 0.7
CNRM_CCLM4	0.8	0.5	* 1.7	* 1.0	* 1.0
ENSMEAN	0.5	0.7	1.6	1.0	1.0
P3 - P0					
MPI_CCLM4	* 1.1	* 0.7	* 2.0	* 1.1	* 1.3
EC-EARTH_KNMI	* 1.1	* 1.6	* 2.0	* 1.7	* 1.6
CNRM_CCLM4	* 1.5	* 1.3	* 2.0	* 1.5	* 1.5
ENSMEAN	1.2	1.2	2.0	1.4	1.5
P4 - P0					
MPI_CCLM4	* 1.3	* 1.2	* 2.8	* 1.8	* 1.8
EC-EARTH_KNMI	* 1.5	* 1.8	* 1.5	* 2.2	* 1.7
CNRM_CCLM4	* 1.9	* 1.6	* 2.2	* 1.7	* 1.8
ENSMEAN	1.6	1.5	2.2	1.9	1.8

RCP85

	DJF	MAM	JJA	SON	Annual
Ref.mean	2.0	8.3	18.4	10.3	9.8
P1 - P0					
MPI_CCLM4	-0.2	0.6	* 1.3	0.6	* 0.6
EC-EARTH_KNMI	-0.0	* 1.2	* 1.2	* 1.6	* 1.0
CNRM_CCLM4	0.6	* 0.8	* 1.2	0.7	* 0.8
ENSMEAN	0.1	0.8	1.3	1.0	0.8
P2 - P0					
MPI_CCLM4	* 1.0	* 1.4	* 2.7	* 2.2	* 1.9
EC-EARTH_KNMI	0.5	* 1.5	* 1.5	* 1.9	* 1.4
CNRM_CCLM4	* 1.5	* 0.9	* 1.2	* 1.4	* 1.2
ENSMEAN	1.0	1.3	1.8	1.8	1.5
P3 - P0					
MPI_CCLM4	* 2.5	* 1.7	* 3.1	* 2.9	* 2.5
EC-EARTH_KNMI	* 1.7	* 2.3	* 2.9	* 2.8	* 2.4
CNRM_CCLM4	* 2.6	* 2.3	* 2.6	* 2.2	* 2.4
ENSMEAN	2.3	2.1	2.9	2.6	2.5
P4 - P0					
MPI_CCLM4	* 3.4	* 3.3	* 5.1	* 4.1	* 4.0
EC-EARTH_KNMI	* 3.5	* 3.5	* 4.2	* 4.5	* 3.9
CNRM_CCLM4	* 3.4	* 2.5	* 4.0	* 3.1	* 3.2
ENSMEAN	3.5	3.1	4.4	3.9	3.7

** ; Two Sample Wilcoxon tests, 95 % confidence interval*

Figure 5-1: Averaged seasonal and annual 2m air temperature (in °C) obtained by dynamical downscaling for Knin: Ref. mean is 20 year simulated period (1986-2005) for ensemble mean; P1-P0, P2-P0, P3-P0, P4-P0 are changes in the future for following periods P1: 2021-2040, P2: 2041-2060, P3: 2061-2080, P4: 2081-2100. Differences are shown for individual models. Significant change is marked by star. Change is also shown as ensemble mean (ENSMEAN), not tested for significance. Left column is for RCP4.5 scenario and right for RCP8.5 scenario.

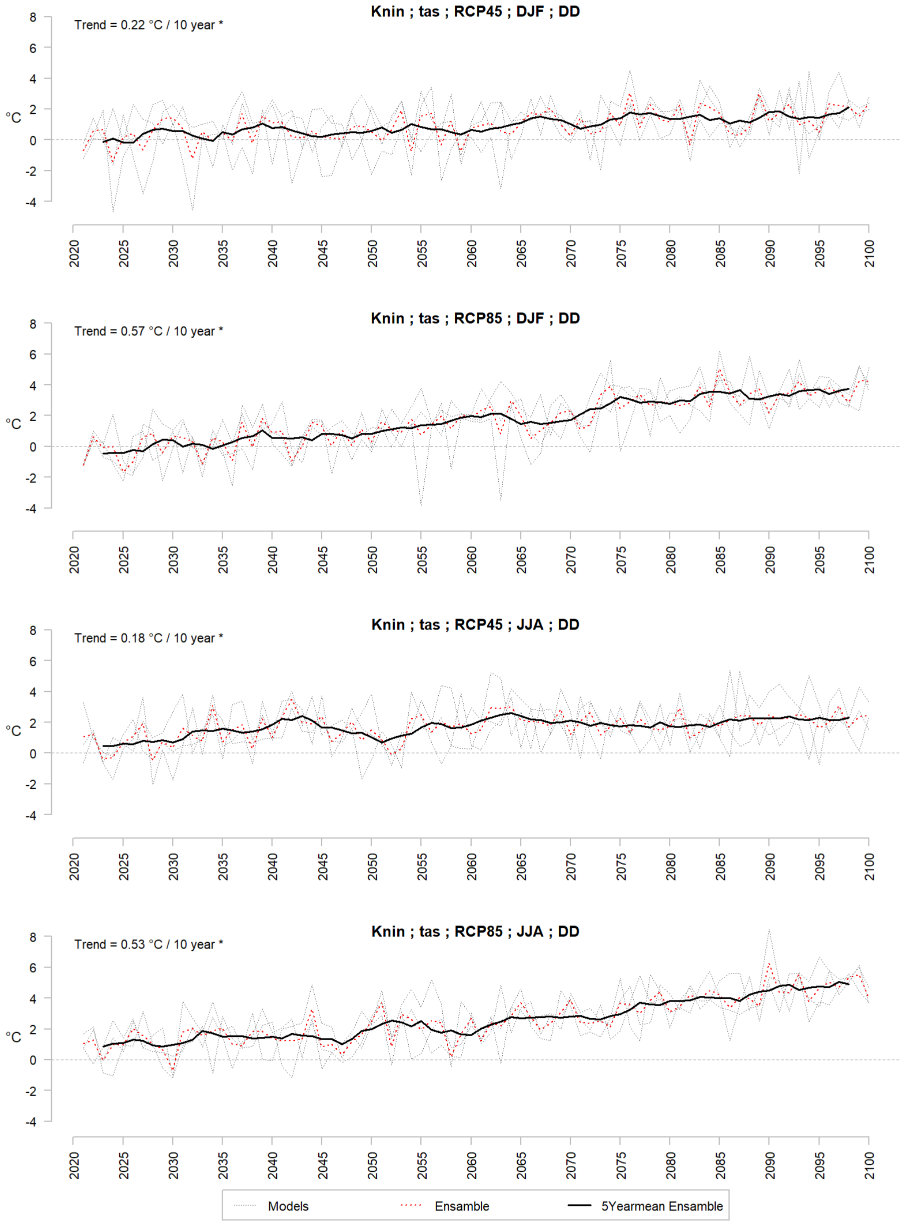

Figure 5-2: Variability of future 2m air temperature anomaly (in °C) in Knin for 2021-2100 obtained by dynamically downscaling for winter (DJF) and summer (JJA) and two RCP scenarios: individual models are in grey, the ensemble mean in red, 5-year moving average in black. Significant trend is marked with star (ns if not significant).

6.1.1.1.2 *Extreme high temperature*

99th percentile of 2m air temperature in Knin is increasing from P1 to P4 future periods with the different amplitudes for each model (Figure 5-3). In ensemble mean at the end of century increase is from 1.2 °C in DJF to 2.7 °C in JJA, 2.7 °C on annual scale for RCP4.5. Amplitude of change is more pronounced for RCP8.5 and is between 3.0 °C in DJF and 5.1 °C in SON, 4.8 °C for annual change at the end of 21st century. Variability of future 99th percentile of 2m air temperature anomaly (Figure 5-4) shows linear trend in change of ensemble mean, 0.19 °C / 10 year in DJF for RCP4.5 and 0.49 °C / 10 year for RCP8.5; 0.17 °C / 10 year in JJA for RCP4.5 and 0.56 °C / 10 year for RCP8.5. All trends are statistically significant.

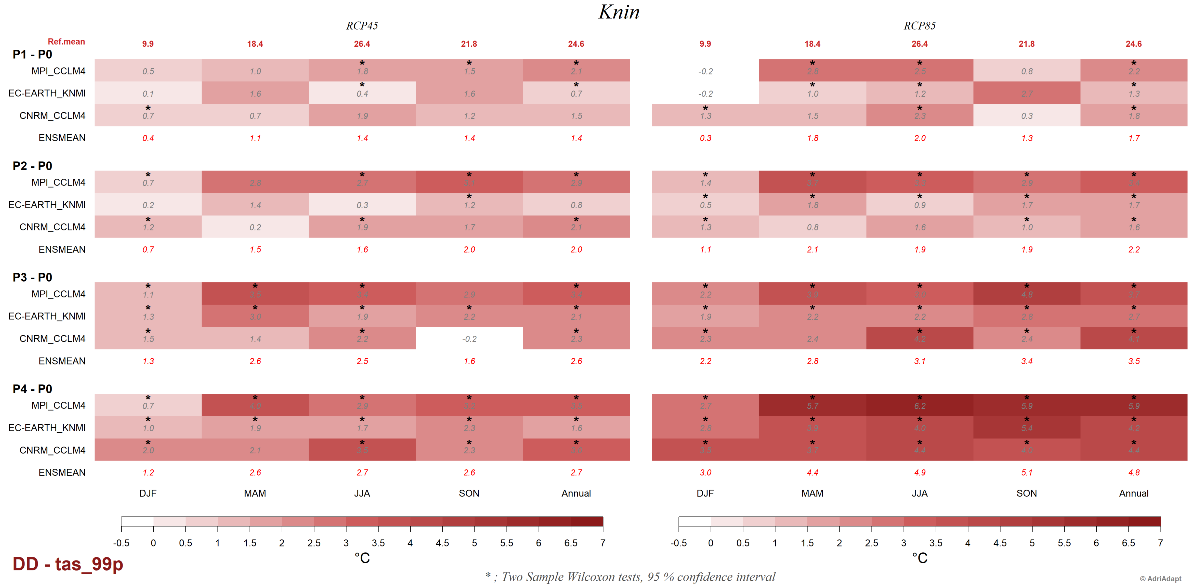

Figure 5-3: Seasonal and annual 99th percentile of 2m air temperature (extreme high temperature, in °C) obtained by dynamical downscaling for Knin: Ref. mean is 20 year simulated period (1986-2005) for ensemble mean; P1-P0, P2-P0, P3-P0, P4-P0 are changes in the future for following periods P1: 2021-2040, P2: 2041-2060, P3: 2061-2080, P4: 2081-2100. Differences are shown for individual models. Significant change is marked by star. Change is also shown as ensemble mean (ENSMEAN), not tested for significance. Left column is for RCP4.5 scenario and right for RCP8.5 scenario.

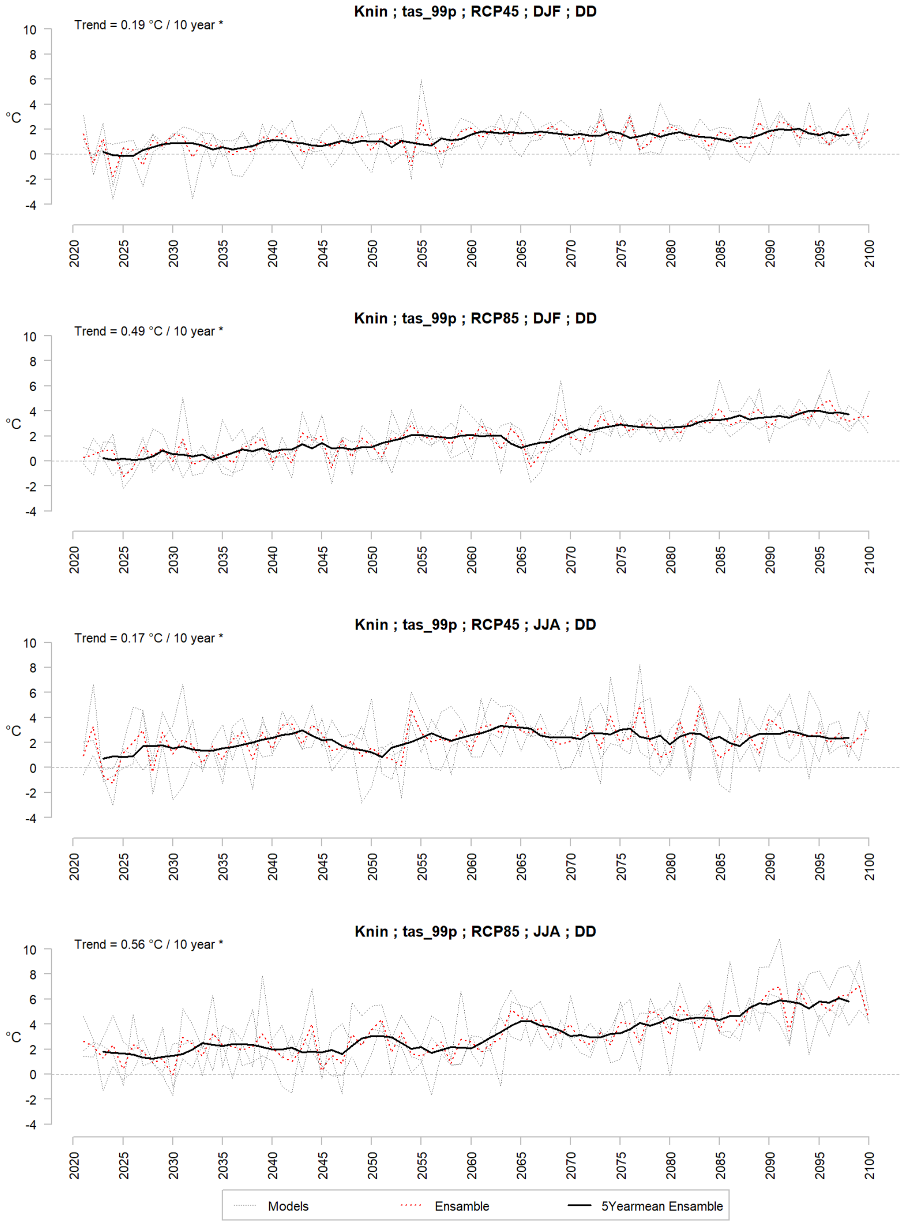

Figure 5-4: Variability of future 99th percentile of 2m air temperature (extreme high temperature) anomaly (in °C) in Knin for 2021-2100 obtained by dynamically downscaling for winter (DJF) and summer (JJA) and two RCP scenarios: individual models are in grey, the ensemble mean in red, 5-year moving average in black. Significant trend is marked with star (ns if not significant).

6.1.1.1.3 *Extreme high maximum temperature*

Future change of 99th percentile of 2m maximum air temperature (Figure 5-5) in Knin is increasing from P1 to P4 periods with the different amplitudes for each model. Although some models show slight decrease for some seasons, in ensemble mean for all periods the change is positive. At the end of century increase is from 1.9 °C in DJF to 3.0 °C in SON; 3.0 °C on annual scale for RCP4.5. Amplitude of change is more pronounced for RCP8.5 and is between 3.7 °C in DJF and 5.4 °C in SON, 5.0 °C for annual change at the end of 21st century. Variability of future 99th percentile of 2m maximum air temperature anomaly (Figure 5-6) shows linear trend in change of ensemble mean, 0.21 °C / 10 year in DJF for RCP4.5 and 0.53 °C / 10 year for RCP8.5; 0.19 °C / 10 year in JJA for RCP4.5 and 0.58 °C / 10 year for RCP8.5. All trends are statistically significant.

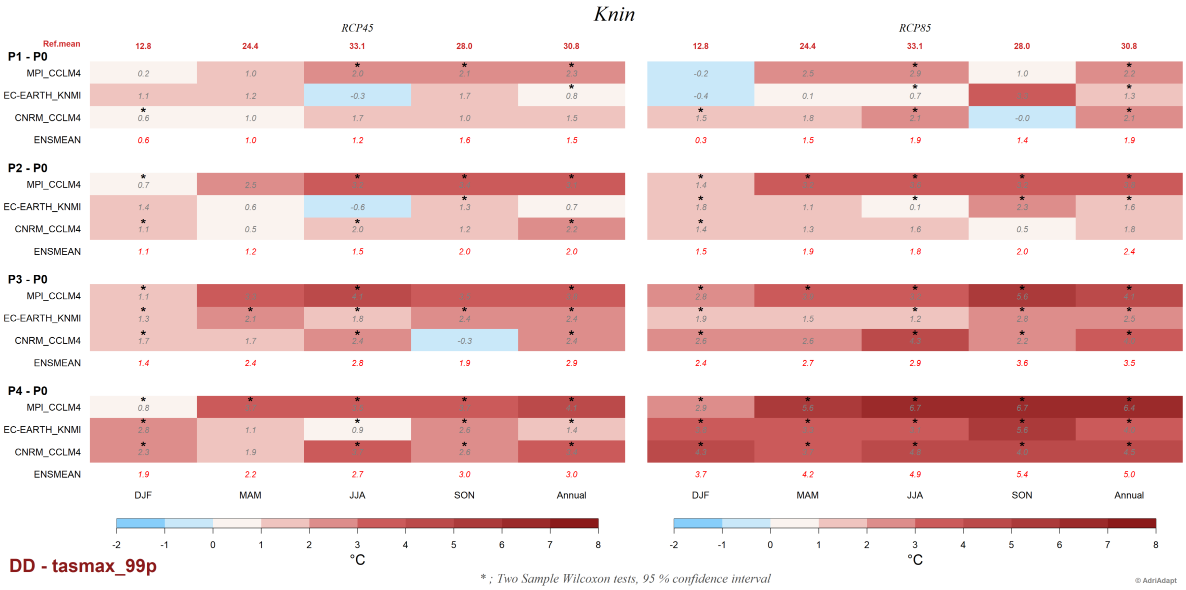

Figure 5-5: Seasonal and annual 99th percentile of 2m maximum air temperature (extreme high maximum temperature, in °C) obtained by dynamical downscaling for Knin: Ref. mean is 20 year simulated period (1986-2005) for ensemble mean; P1-P0, P2-P0, P3-P0, P4-P0 are changes in the future for following periods P1: 2021-2040, P2: 2041-2060, P3: 2061-2080, P4: 2081-2100. Differences are shown for individual models. Significant change is marked by star. Change is also shown as ensemble mean (ENSMEAN), not tested for significance. Left column is for RCP4.5 scenario and right for RCP8.5 scenario.

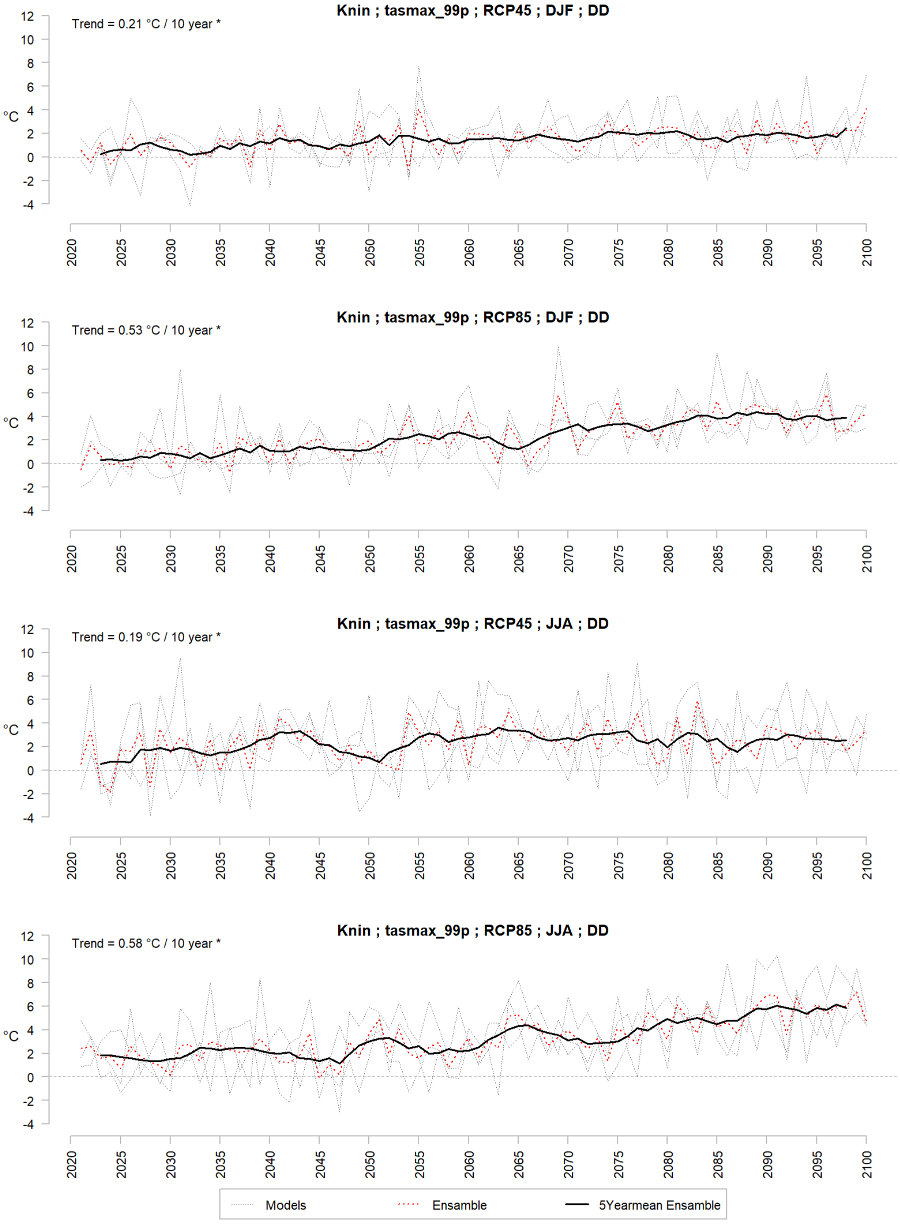

Figure 5-6: Variability of future 99th percentile of 2m maximum air temperature (extreme high maximum temperature) anomaly (in °C) in Knin for 2021-2100 obtained by dynamically downscaling for winter (DJF) and summer (JJA) and two RCP scenarios: individual models are in grey, the ensemble mean in red, 5-year moving average in black. Significant trend is marked with star (ns if not significant).

6.1.1.1.4 *Extreme rare high temperature*

Future change of 99.9th percentile of 2m air temperature (Figure 5-7) in Knin is increasing from P1 to P4 periods with the different amplitudes for each model. Slightly negative change appears for some seasons mostly for EC-EARTH_KNMI model, but the change of ensemble mean is positive for all periods. At the end of century increase is from 1.3 °C in JJA to 2.6 °C in SON, 2.3 °C on annual scale for RCP4.5. Amplitude of change is more pronounced for RCP8.5 and is between 3.6 °C in DJF and 5.3 °C in MAM, 4.4 °C for annual change at the end of 21st century. Variability of future 99.9th percentile of 2m air temperature anomaly (Figure 5-8) shows linear trend in change of ensemble mean, 0.19 °C / 10 year in DJF for RCP4.5 and 0.49 °C / 10 year for RCP8.5; 0.17 °C / 10 year in JJA for RCP4.5 and 0.57 °C / 10 year for RCP8.5. All trends are statistically significant.

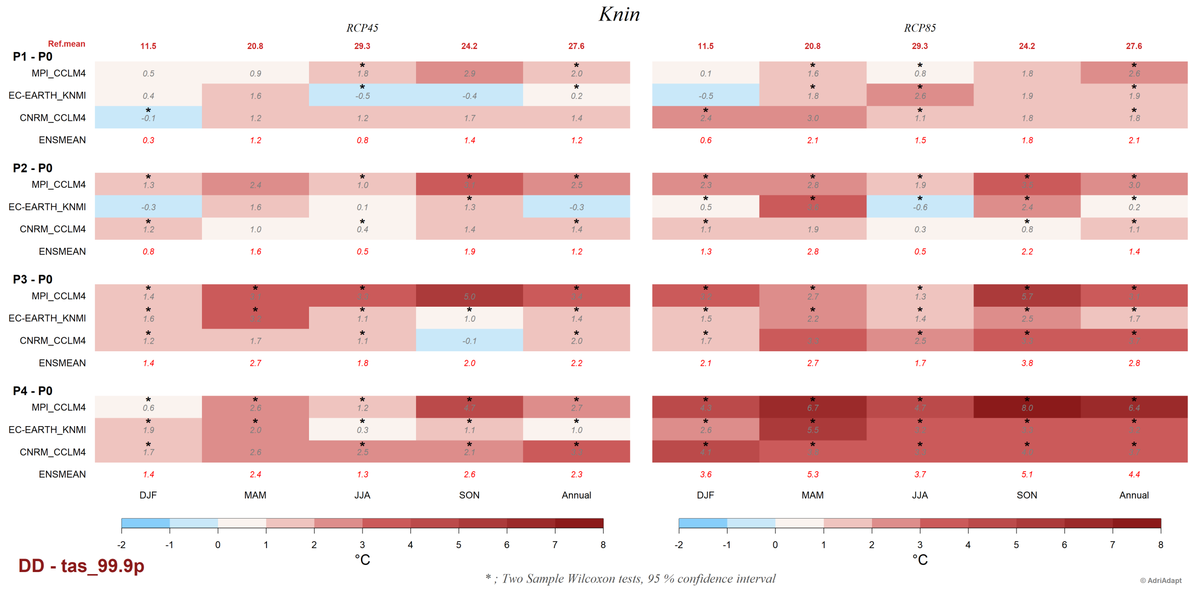

Figure 5-7: Seasonal and annual 99.9th percentile of 2m air temperature (extreme rare high temperature, in °C) obtained by dynamical downscaling for Knin: Ref. mean is 20 year simulated period (1986-2005) for ensemble mean; P1-P0, P2-P0, P3-P0, P4-P0 are changes in the future for following periods P1: 2021-2040, P2: 2041-2060, P3: 2061-2080, P4: 2081-2100. Differences are shown for individual models. Significant change is marked by star. Change is also shown as ensemble mean (ENSMEAN), not tested for significance. Left column is for RCP4.5 scenario and right for RCP8.5 scenario.

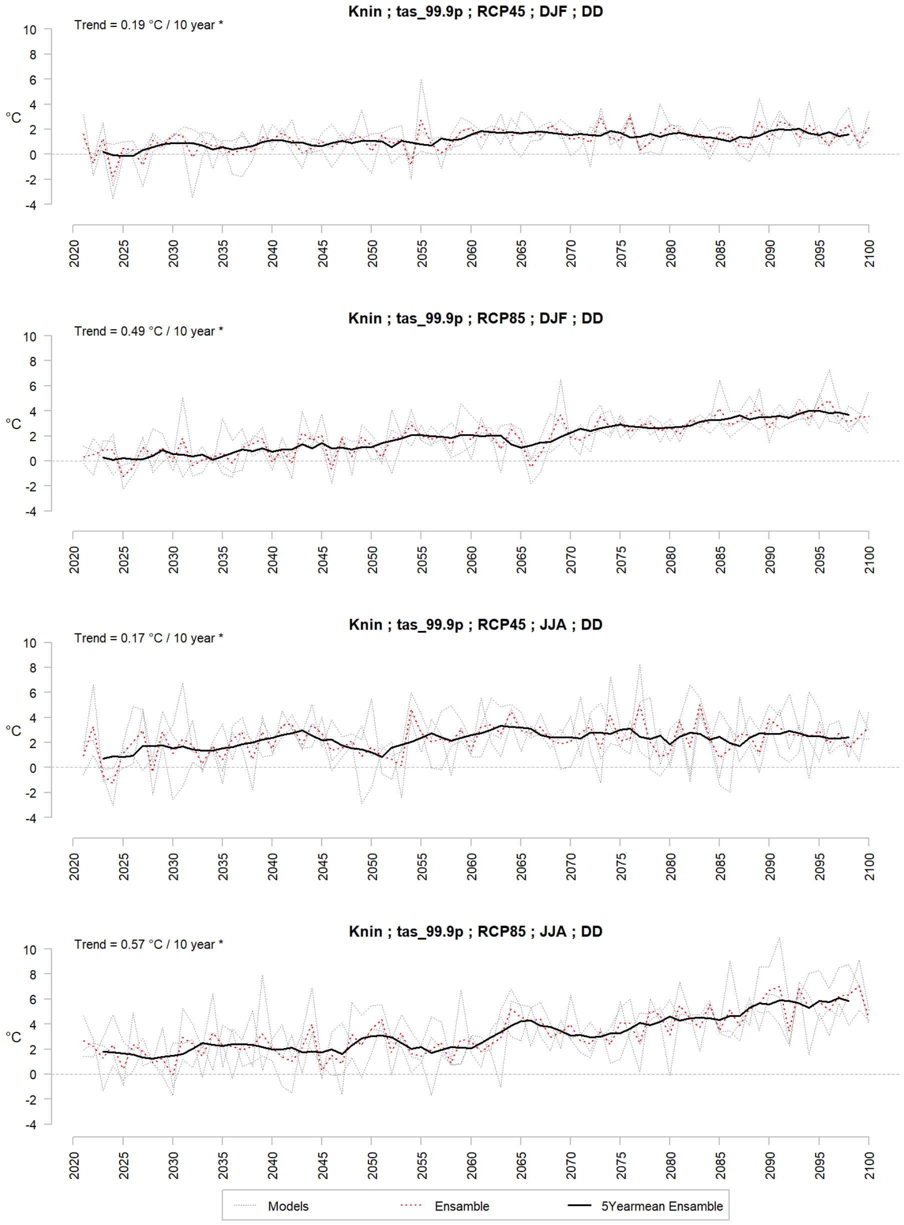

Figure 5-8: Variability of future 99.9th percentile of 2m air temperature (extreme rare high temperature) anomaly (in °C) in Knin for 2021-2100 obtained by dynamically downscaling for winter (DJF) and summer (JJA) and two RCP scenarios: individual models are in grey, the ensemble mean in red, 5-year moving average in black. Significant trend is marked with star (ns if not significant).

6.1.1.1.5 *Extreme rare high maximum temperature*

Future change of 99.9th percentile of 2m maximum air temperature (Figure 5-9) in Knin is changing from P1 to P4 periods with the different amplitudes for each model. Some models show for some time slices negative change, but in general ensemble mean for all seasons and annual change are positive. At the end of 21st century changes are between 1.3 °C in JJA and 3.4 °C in SON, 2.2 °C for annual for RCP4.5 scenario. Amplitude of change is more pronounced for RCP8.5 and is between 2.8 °C in JJA and 5.2 °C in SON, 4.2 °C for annual change at the end of 21st century. Variability of future 99.9th percentile of 2m maximum air temperature anomaly (Figure 5-10) shows linear trend in change of ensemble mean, 0.21 °C / 10 year in DJF for RCP4.5 and 0.53 °C / 10 year for RCP8.5; 0.19 °C / 10 year in JJA for RCP4.5 and 0.58 °C / 10 year for RCP8.5. All trends are statistically significant.

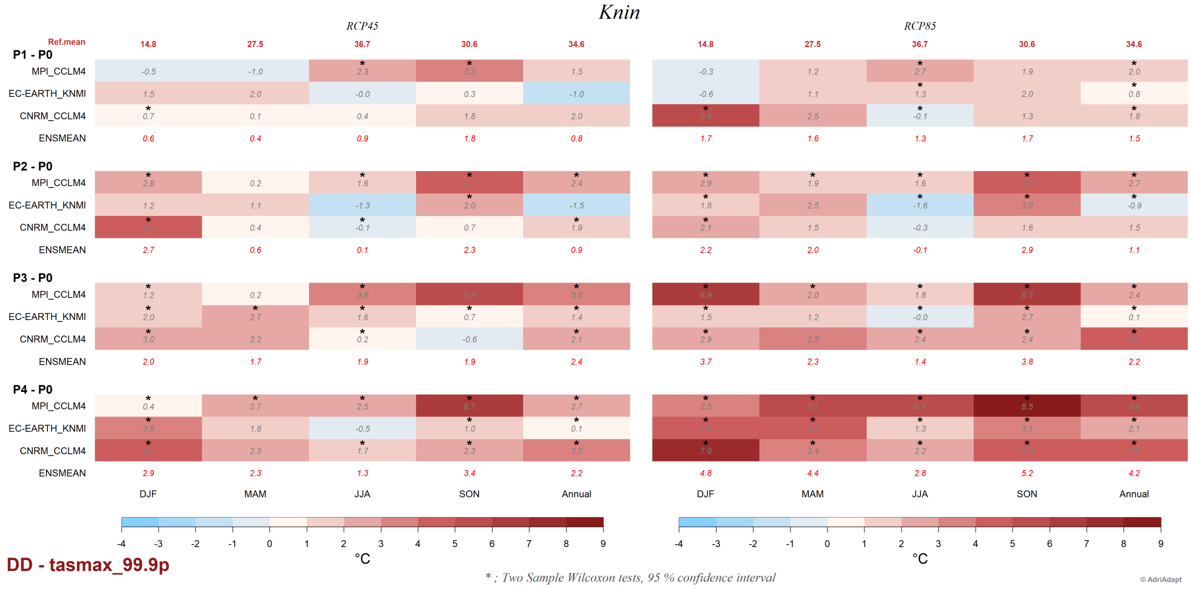

Knin

	RCP45					RCP85				
	DJF	MAM	JJA	SON	Annual	DJF	MAM	JJA	SON	Annual
Ref.mean	14.8	27.5	36.7	30.6	34.6	14.8	27.5	36.7	30.6	34.6
P1 - P0										
MPI_CCLM4	-0.5	-1.0	* 2.3	* 3.3	1.5	-0.3	1.2	* 2.7	1.9	* 2.0
EC-EARTH_KNMI	1.5	2.0	-0.0	0.3	-1.0	-0.6	1.1	* 1.3	2.0	* 0.8
CNRM_CCLM4	* 0.7	0.1	0.4	1.8	2.0	* 5.8	2.5	* -0.1	1.3	* 1.8
ENSMEAN	0.6	0.4	0.9	1.8	0.8	1.7	1.6	1.3	1.7	1.5
P2 - P0										
MPI_CCLM4	* 2.8	0.2	* 1.6	* 4.1	* 2.4	* 2.9	* 1.9	* 1.6	* 4.2	* 2.7
EC-EARTH_KNMI	1.2	1.1	-1.3	* 2.0	-1.5	* 1.8	2.5	* -1.6	* 3.0	* -0.9
CNRM_CCLM4	* 4.1	0.4	* -0.1	0.7	* 1.9	* 2.1	1.5	-0.3	1.6	1.5
ENSMEAN	2.7	0.6	0.1	2.3	0.9	2.2	2.0	-0.1	2.9	1.1
P3 - P0										
MPI_CCLM4	* 1.2	0.2	* 3.8	5.5	* 3.6	* 6.9	* 2.0	* 1.8	* 6.3	* 2.4
EC-EARTH_KNMI	* 2.0	* 2.7	* 1.6	* 0.7	* 1.4	* 1.5	1.2	* -0.0	* 2.7	* 0.1
CNRM_CCLM4	* 3.0	2.2	* 0.2	-0.6	* 2.1	* 2.9	3.5	* 2.4	* 2.4	* 4.3
ENSMEAN	2.0	1.7	1.9	1.9	2.4	3.7	2.3	1.4	3.8	2.2
P4 - P0										
MPI_CCLM4	* 0.4	* 2.7	* 2.5	* 6.7	* 2.7	* 3.5	* 5.1	* 5.1	* 8.5	* 5.8
EC-EARTH_KNMI	* 3.8	1.8	-0.5	* 1.0	* 0.1	* 4.0	* 4.8	* 1.3	* 3.1	* 2.1
CNRM_CCLM4	* 4.4	2.5	* 1.7	* 2.3	* 3.7	* 7.0	* 3.4	* 2.2	* 4.0	* 4.6
ENSMEAN	2.9	2.3	1.3	3.4	2.2	4.8	4.4	2.8	5.2	4.2

* ; Two Sample Wilcoxon tests, 95 % confidence interval

Figure 5-9: Seasonal and annual 99.9th percentile of 2m maximum air temperature (extreme rare high maximum temperature, in °C) obtained by dynamical downscaling for Knin: Ref. mean is 20 year simulated period (1986-2005) for ensemble mean; P1-P0, P2-P0, P3-P0, P4-P0 are changes in the future for following periods P1: 2021-2040, P2: 2041-2060, P3: 2061-2080, P4: 2081-2100. Differences are shown for individual models. Significant change is marked by star. Change is also shown as ensemble mean (ENSMEAN), not tested for significance. Left column is for RCP4.5 scenario and right for RCP8.5 scenario.

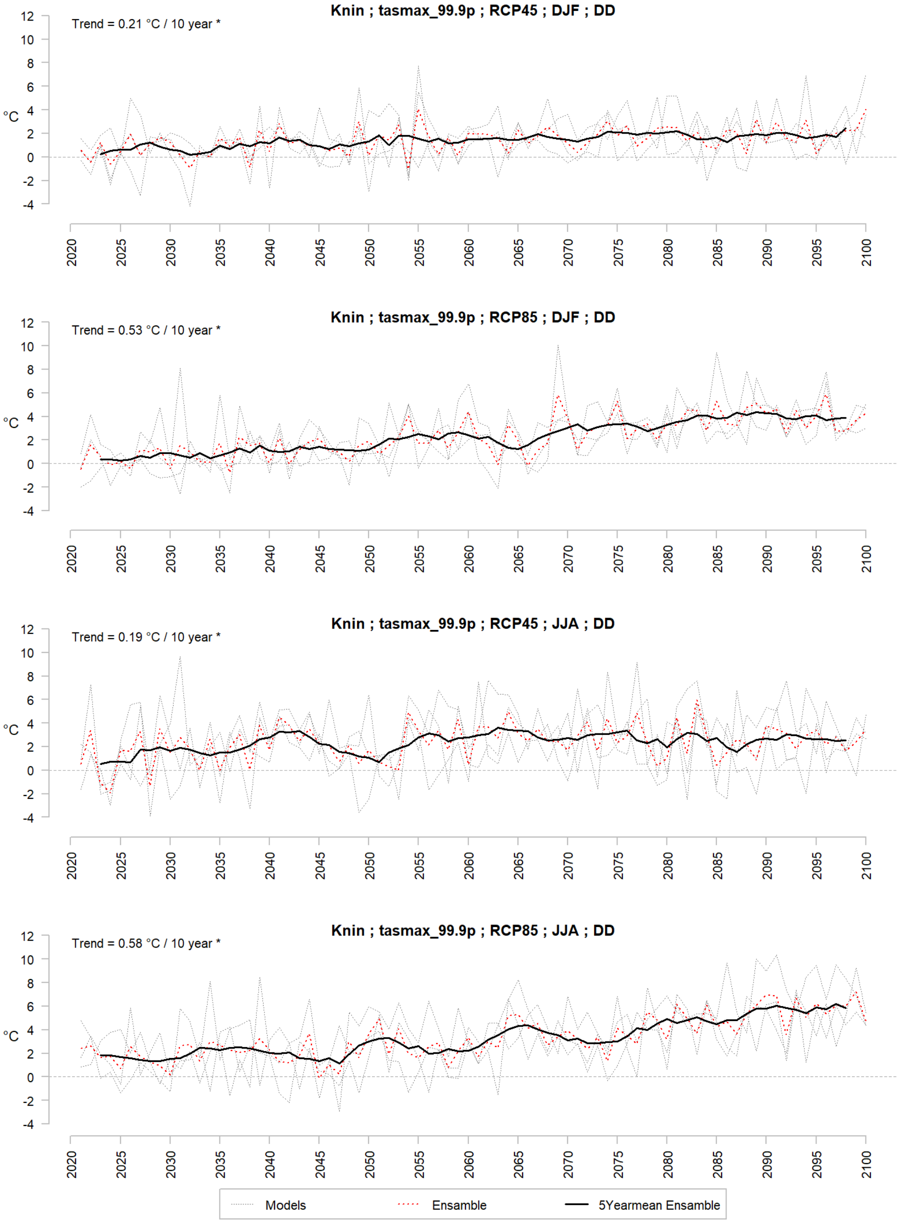

Figure 5-10: Variability of future 99.9th percentile of 2m maximum air temperature (extreme rare high maximum temperature) anomaly (in °C) in Knin for 2021-2100 obtained by dynamically downscaling for winter (DJF) and summer (JJA) and two RCP scenarios: individual models are in grey, the ensemble mean in red, 5-year moving average in black. Significant trend is marked with star (ns if not significant).

6.1.1.2 *Precipitation related indices projections*

6.1.1.2.1 *Averaged precipitation*

Averaged precipitation obtained by dynamical downscaling is expressed in mm/day and its change in the future is shown as relative to the P0 period. Precipitation is much more variable parameter in comparison to the temperature, therefore there is no always unique sign of change through the year as well as from model to model (Figure 5-11). The change in ensemble mean for Knin gives increase of precipitation for winter at the end of century (3.2 % for RCP4.5 and 13.5 % for RCP8.5), decrease of precipitation for other seasons (from -0.9 % in SON to the -9.1 % in JJA for RCP4.5, from -1.9 % for MAM to -29.6 % for JJA for RCP8.5). On the annual scale, decrease of precipitation can be expected, -2.5 % for RCP4.5 and -2.9 % for RCP8.5 scenario. Variability of future precipitation anomaly (Figure 5-12) for ensemble mean in Knin has significant linear trend only for RCP8.5 scenario, with the increase of 3.29 % / 10 year in DJF and decrease of -3.92 % / 10 year in JJA.

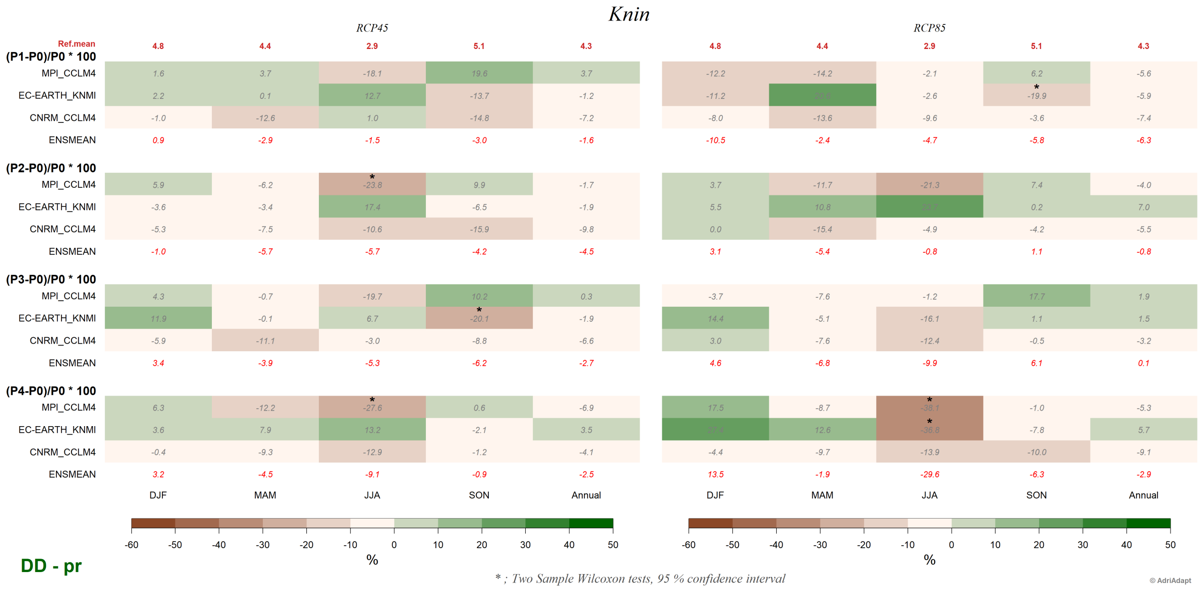

	RCP45					RCP85				
	DJF	MAM	JJA	SON	Annual	DJF	MAM	JJA	SON	Annual
Ref.mean	4.8	4.4	2.9	5.1	4.3	4.8	4.4	2.9	5.1	4.3
(P1-P0)/P0 * 100										
MPI_CCLM4	1.6	3.7	-18.1	19.6	3.7	-12.2	-14.2	-2.1	6.2	-5.6
EC-EARTH_KNMI	2.2	0.1	12.7	-13.7	-1.2	-11.2	20.6	-2.6	* -19.9	-5.9
CNRM_CCLM4	-1.0	-12.6	1.0	-14.8	-7.2	-8.0	-13.6	-9.6	-3.6	-7.4
ENSMEAN	0.9	-2.9	-1.5	-3.0	-1.6	-10.5	-2.4	-4.7	-5.8	-6.3
(P2-P0)/P0 * 100										
MPI_CCLM4	5.9	-6.2	* -23.8	9.9	-1.7	3.7	-11.7	-21.3	7.4	-4.0
EC-EARTH_KNMI	-3.6	-3.4	17.4	-6.5	-1.9	5.5	10.8	23.7	0.2	7.0
CNRM_CCLM4	-5.3	-7.5	-10.6	-15.9	-9.8	0.0	-15.4	-4.9	-4.2	-5.5
ENSMEAN	-1.0	-5.7	-5.7	-4.2	-4.5	3.1	-5.4	-0.8	1.1	-0.8
(P3-P0)/P0 * 100										
MPI_CCLM4	4.3	-0.7	-19.7	10.2	0.3	-3.7	-7.6	-1.2	17.7	1.9
EC-EARTH_KNMI	11.9	-0.1	6.7	* -20.1	-1.9	14.4	-5.1	-16.1	1.1	1.5
CNRM_CCLM4	-5.9	-11.1	-3.0	-8.8	-6.6	3.0	-7.6	-12.4	-0.5	-3.2
ENSMEAN	3.4	-3.9	-5.3	-6.2	-2.7	4.6	-6.8	-9.9	6.1	0.1
(P4-P0)/P0 * 100										
MPI_CCLM4	6.3	-12.2	* -27.6	0.6	-6.9	17.5	-8.7	* -38.1	-1.0	-5.3
EC-EARTH_KNMI	3.6	7.9	13.2	-2.1	3.5	27.4	12.6	* -36.8	-7.8	5.7
CNRM_CCLM4	-0.4	-9.3	-12.9	-1.2	-4.1	-4.4	-9.7	-13.9	-10.0	-9.1
ENSMEAN	3.2	-4.5	-9.1	-0.9	-2.5	13.5	-1.9	-29.6	-6.3	-2.9

* : Two Sample Wilcoxon tests, 95 % confidence interval

Figure 5-11: Averaged seasonal and annual precipitation obtained by dynamical downscaling for Knin: Ref. mean is 20 year simulated period (1986-2005) for ensemble mean in mmday^{-1}; P1-P0, P2-P0, P3-P0, P4-P0 are changes (in %) in the future for following periods P1: 2021-2040, P2: 2041-2060, P3: 2061-2080, P4: 2081-2100. Differences are shown for individual models. Significant change is marked by star. Change is also shown as ensemble mean (ENSMEAN), not tested for significance. Left column is for RCP4.5 scenario and right for RCP8.5 scenario.

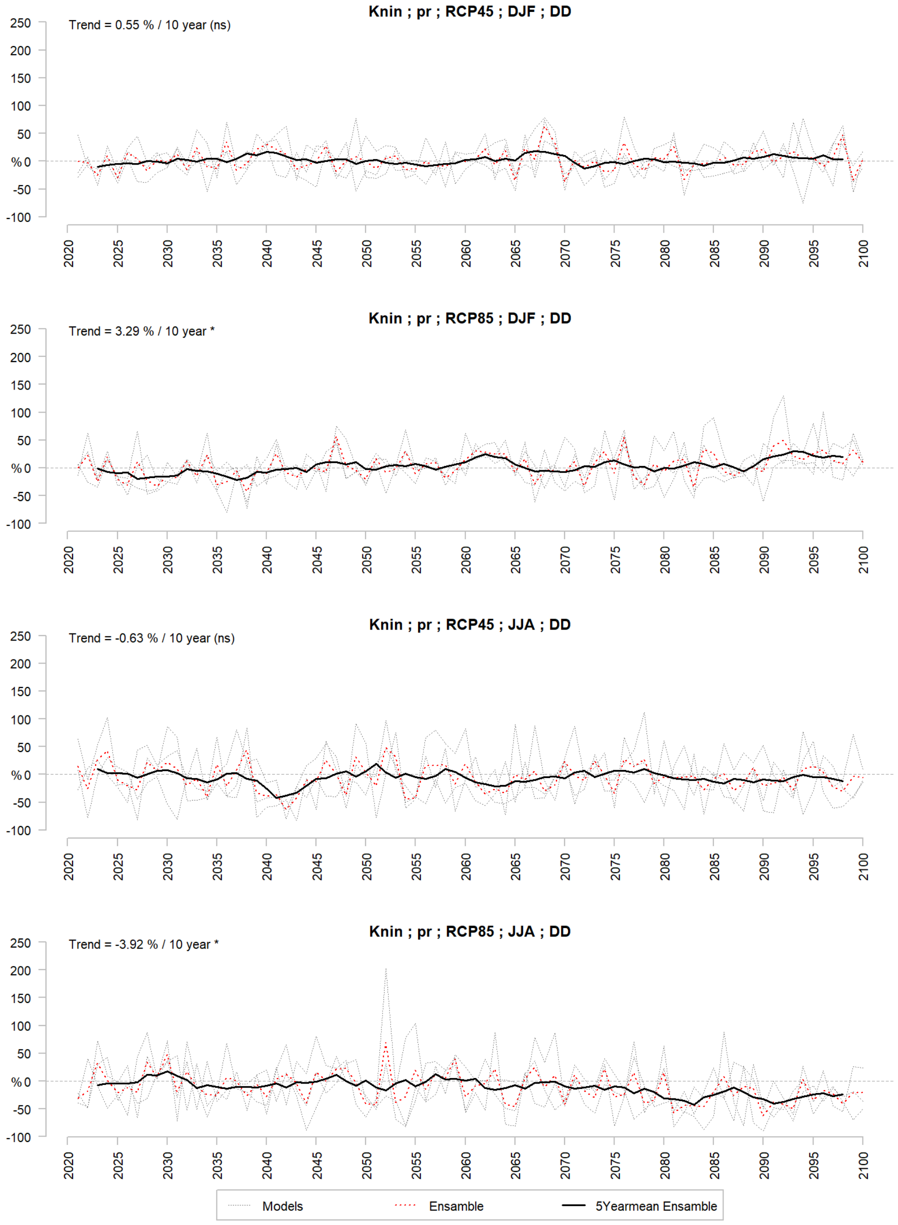

Figure 5-12: Variability of future precipitation anomaly (in %) in Knin for 2021-2100 obtained by dynamically downscaling for winter (DJF) and summer (JJA) and two RCP scenarios: individual models are in grey, the ensemble mean in red, 5-year moving average in black. Significant trend is marked with star (ns if not significant).

6.1.1.2.2 *Intense precipitation*

Intense precipitation (Figure 5-13), defined by 95th percentile of precipitation in Knin, shows for ensemble mean that 95th percentile will increase in all seasons except summer. At the end of century, the increase will be the most pronounced in DJF (7.4 % for RCP4.5, 16.8 % for RCP8.5), while in JJA 95th percentile will decrease for -8.6 % for RCP4.5 and -26.5 % for RCP8.5. On annual scale intense precipitation will increase, 3.3 % for RCP4.5 and 5.7 % for RCP8.5. Variability of future intense precipitation anomaly (Figure 5-14) for ensemble mean in Knin has significant linear trend only for RCP8.5 scenario, with the increase of 3.19 % /10 year in DJF and decrease -3.03 % / 10 year.

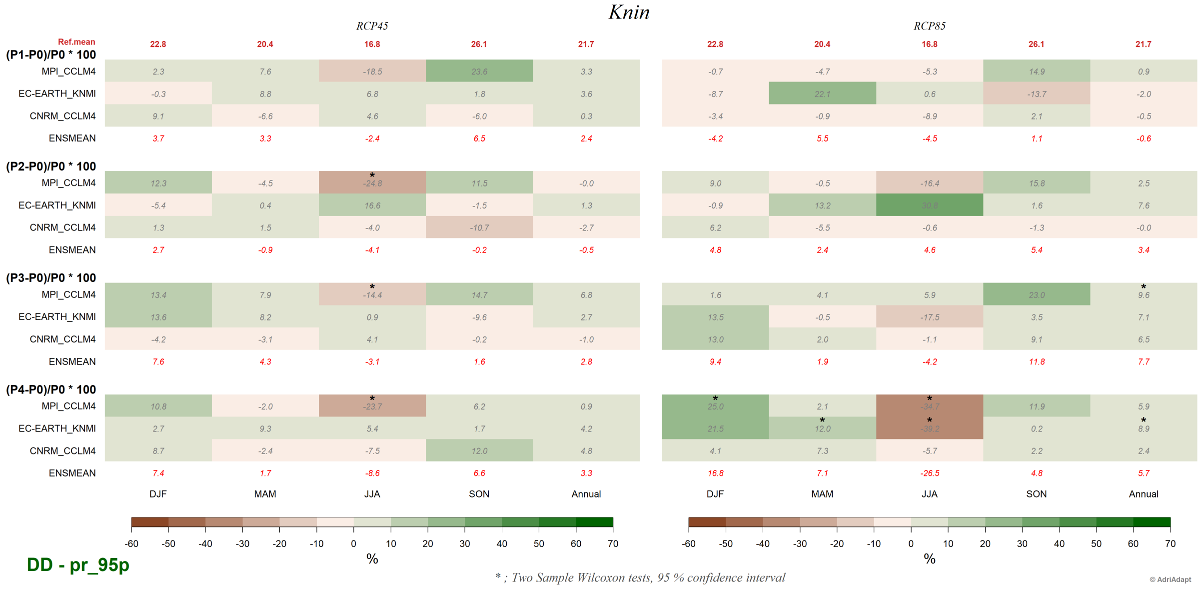

RCP45

	DJF	MAM	JJA	SON	Annual
Ref.mean	22.8	20.4	16.8	26.1	21.7
(P1-P0)/P0 * 100					
MPI_CCLM4	2.3	7.6	-18.5	23.6	3.3
EC-EARTH_KNMI	-0.3	8.8	6.8	1.8	3.6
CNRM_CCLM4	9.1	-6.6	4.6	-6.0	0.3
ENSMEAN	3.7	3.3	-2.4	6.5	2.4
(P2-P0)/P0 * 100					
MPI_CCLM4	12.3	-4.5	* -24.8	11.5	-0.0
EC-EARTH_KNMI	-5.4	0.4	16.6	-1.5	1.3
CNRM_CCLM4	1.3	1.5	-4.0	-10.7	-2.7
ENSMEAN	2.7	-0.9	-4.1	-0.2	-0.5
(P3-P0)/P0 * 100					
MPI_CCLM4	13.4	7.9	* -14.4	14.7	6.8
EC-EARTH_KNMI	13.6	8.2	0.9	-9.6	2.7
CNRM_CCLM4	-4.2	-3.1	4.1	-0.2	-1.0
ENSMEAN	7.6	4.3	-3.1	1.6	2.8
(P4-P0)/P0 * 100					
MPI_CCLM4	10.8	-2.0	* -23.7	6.2	0.9
EC-EARTH_KNMI	2.7	9.3	5.4	1.7	4.2
CNRM_CCLM4	8.7	-2.4	-7.5	12.0	4.8
ENSMEAN	7.4	1.7	-8.6	6.6	3.3

RCP85

	DJF	MAM	JJA	SON	Annual
Ref.mean	22.8	20.4	16.8	26.1	21.7
(P1-P0)/P0 * 100					
MPI_CCLM4	-0.7	-4.7	-5.3	14.9	0.9
EC-EARTH_KNMI	-8.7	22.1	0.6	-13.7	-2.0
CNRM_CCLM4	-3.4	-0.9	-8.9	2.1	-0.5
ENSMEAN	-4.2	5.5	-4.5	1.1	-0.6
(P2-P0)/P0 * 100					
MPI_CCLM4	9.0	-0.5	-16.4	15.8	2.5
EC-EARTH_KNMI	-0.9	13.2	30.8	1.6	7.6
CNRM_CCLM4	6.2	-5.5	-0.6	-1.3	-0.0
ENSMEAN	4.8	2.4	4.6	5.4	3.4
(P3-P0)/P0 * 100					
MPI_CCLM4	1.6	4.1	5.9	23.0	* 9.6
EC-EARTH_KNMI	13.5	-0.5	-17.5	3.5	7.1
CNRM_CCLM4	13.0	2.0	-1.1	9.1	6.5
ENSMEAN	9.4	1.9	-4.2	11.8	7.7
(P4-P0)/P0 * 100					
MPI_CCLM4	* 25.0	2.1	* -34.7	11.9	5.9
EC-EARTH_KNMI	21.5	* 12.0	* -39.2	0.2	* 8.9
CNRM_CCLM4	4.1	7.3	-5.7	2.2	2.4
ENSMEAN	16.8	7.1	-26.5	4.8	5.7

** ; Two Sample Wilcoxon tests, 95 % confidence interval*

Figure 5-13: Seasonal and annual 95th percentile of precipitation (intense precipitation) obtained by dynamical downscaling for Knin: Ref. mean is 20 year simulated period (1986-2005) for ensemble mean in mmday^{-1}; P1-P0, P2-P0, P3-P0, P4-P0 are changes (in %) in the future for following periods P1: 2021-2040, P2: 2041-2060, P3: 2061-2080, P4: 2081-2100. Differences are shown for individual models. Significant change is marked by star. Change is also shown as ensemble mean (ENSMEAN), not tested for significance. Left column is for RCP4.5 scenario and right for RCP8.5 scenario.

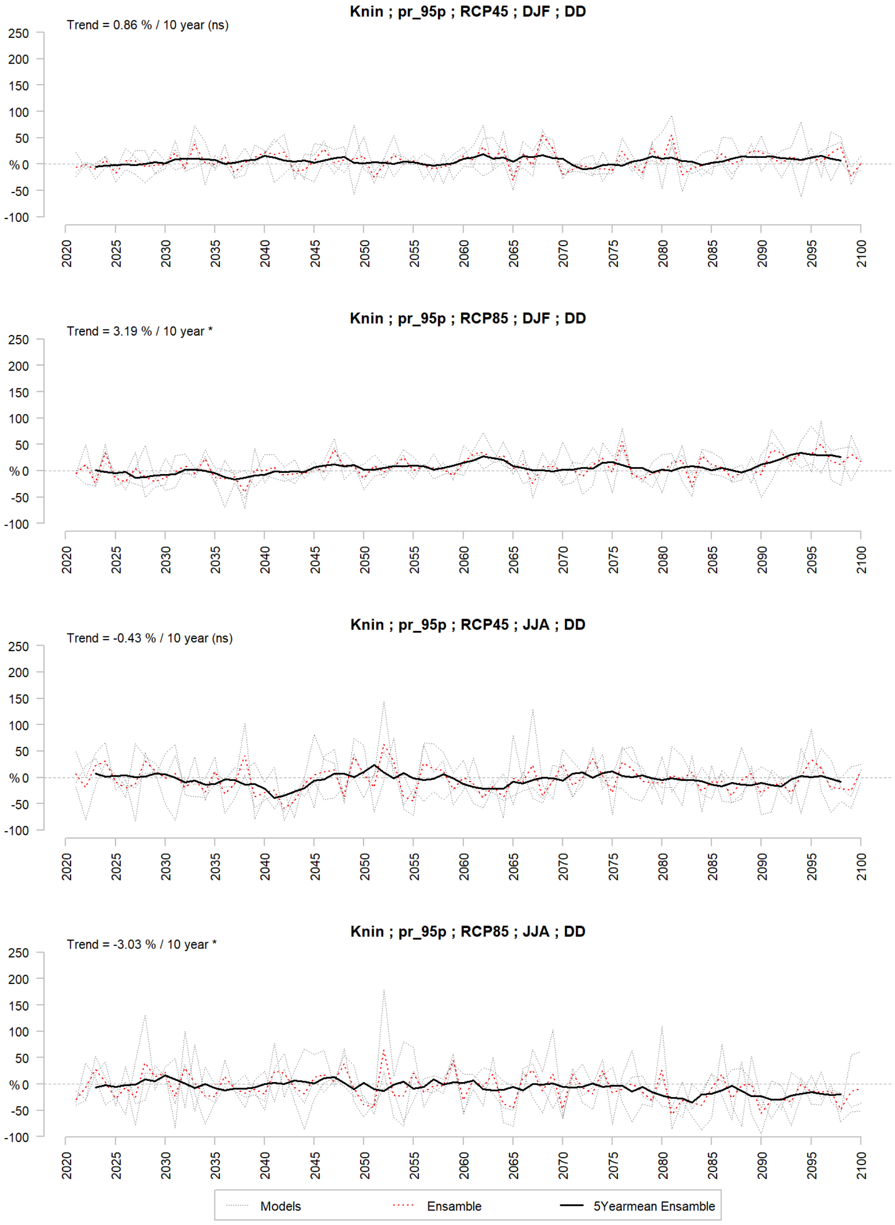

Figure 5-14: Variability of future 95th percentile of precipitation (intense precipitation) anomaly (in %) in Knin for 2021-2100 obtained by dynamically downscaling for winter (DJF) and summer (JJA) and two RCP scenarios: individual models are in grey, the ensemble mean in red, 5-year moving average in black. Significant trend is marked with star (ns if not significant).

6.1.1.2.3 *Extreme precipitation*

Extreme precipitation (Figure 5-15), defined by 99th percentile of precipitation in Knin, shows for ensemble mean increase in all seasons and on annual scale. The increase will change from 2.7 % in MAM to 18.9 % in DJF, 11.9 for annual scale for RCP4.5; between 1.9 % in JJA and 28.9 % in DJF, 18.4 % for annual scale for RCP8.5 at the end of 21st century. The increase of extreme precipitation in all seasons will be present despite different change of average precipitation from season to season, and it shows that extremes will be intensified in the future. Variability of future extreme precipitation anomaly (Figure 5-16) to the end of 21st century for ensemble mean in Knin has significant linear trend only for RCP8.5 scenario in DJF when the extreme precipitation will increase for 3.48 % /10 year.

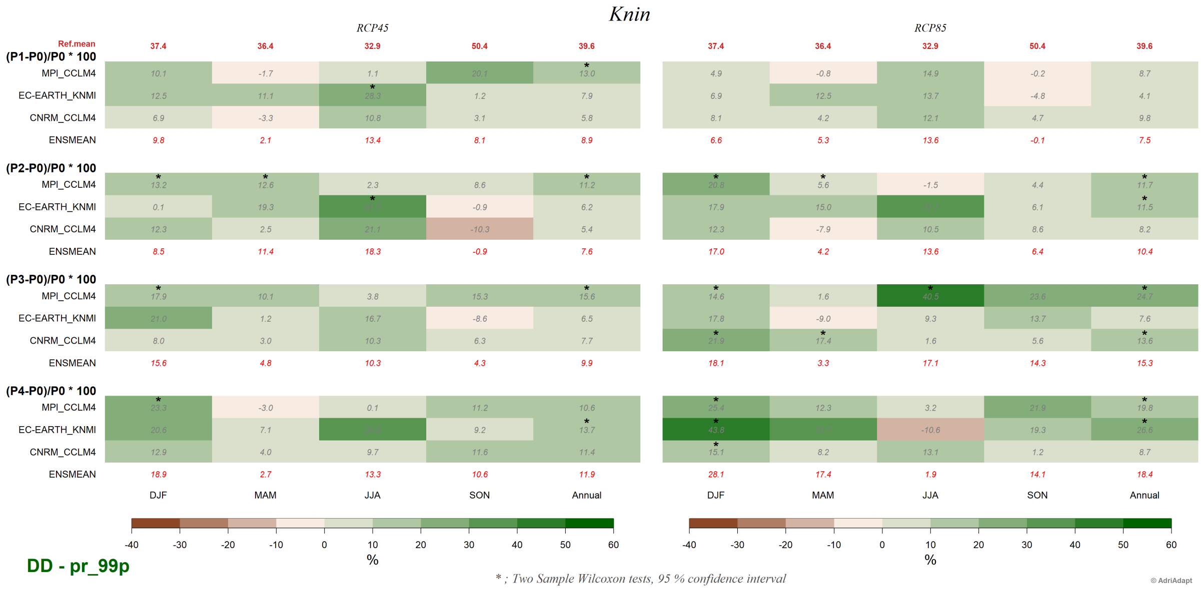

RCP45

	DJF	MAM	JJA	SON	Annual
Ref.mean	37.4	36.4	32.9	50.4	39.6
(P1-P0)/P0 * 100					
MPI_CCLM4	10.1	-1.7	1.1	20.1	* 13.0
EC-EARTH_KNMI	12.5	11.1	* 28.3	1.2	7.9
CNRM_CCLM4	6.9	-3.3	10.8	3.1	5.8
ENSMEAN	9.8	2.1	13.4	8.1	8.9
(P2-P0)/P0 * 100					
MPI_CCLM4	* 13.2	* 12.6	2.3	8.6	* 11.2
EC-EARTH_KNMI	0.1	19.3	* 31.5	-0.9	6.2
CNRM_CCLM4	12.3	2.5	21.1	-10.3	5.4
ENSMEAN	8.5	11.4	18.3	-0.9	7.6
(P3-P0)/P0 * 100					
MPI_CCLM4	* 17.9	10.1	3.8	15.3	* 15.6
EC-EARTH_KNMI	21.0	1.2	16.7	-8.6	6.5
CNRM_CCLM4	8.0	3.0	10.3	6.3	7.7
ENSMEAN	15.6	4.8	10.3	4.3	9.9
(P4-P0)/P0 * 100					
MPI_CCLM4	* 23.3	-3.0	0.1	11.2	10.6
EC-EARTH_KNMI	20.6	7.1	30.0	9.2	* 13.7
CNRM_CCLM4	12.9	4.0	9.7	11.6	11.4
ENSMEAN	18.9	2.7	13.3	10.6	11.9

RCP85

	DJF	MAM	JJA	SON	Annual
Ref.mean	37.4	36.4	32.9	50.4	39.6
(P1-P0)/P0 * 100					
MPI_CCLM4	4.9	-0.8	14.9	-0.2	8.7
EC-EARTH_KNMI	6.9	12.5	13.7	-4.8	4.1
CNRM_CCLM4	8.1	4.2	12.1	4.7	9.8
ENSMEAN	6.6	5.3	13.6	-0.1	7.5
(P2-P0)/P0 * 100					
MPI_CCLM4	* 20.8	* 5.6	-1.5	4.4	* 11.7
EC-EARTH_KNMI	17.9	15.0	31.7	6.1	* 11.5
CNRM_CCLM4	12.3	-7.9	10.5	8.6	8.2
ENSMEAN	17.0	4.2	13.6	6.4	10.4
(P3-P0)/P0 * 100					
MPI_CCLM4	* 14.6	1.6	* 40.5	23.6	* 24.7
EC-EARTH_KNMI	17.8	-9.0	9.3	13.7	7.6
CNRM_CCLM4	* 21.9	* 17.4	1.6	5.6	* 13.6
ENSMEAN	18.1	3.3	17.1	14.3	15.3
(P4-P0)/P0 * 100					
MPI_CCLM4	* 25.4	12.3	3.2	21.9	* 19.8
EC-EARTH_KNMI	* 43.8	31.7	-10.6	19.3	* 26.6
CNRM_CCLM4	* 15.1	8.2	13.1	1.2	8.7
ENSMEAN	28.1	17.4	1.9	14.1	18.4

** ; Two Sample Wilcoxon tests, 95 % confidence interval*

Figure 5-15: Seasonal and annual 99th percentile of precipitation (extreme precipitation) obtained by dynamical downscaling for Knin: Ref. mean is 20 year simulated period (1986-2005) for ensemble mean in mmday^{-1}; P1-P0, P2-P0, P3-P0, P4-P0 are changes (in %) in the future for following periods P1: 2021-2040, P2: 2041-2060, P3: 2061-2080, P4: 2081-2100. Differences are shown for individual models. Significant change is marked by star. Change is also shown as ensemble mean (ENSMEAN), not tested for significance. Left column is for RCP4.5 scenario and right for RCP8.5 scenario.

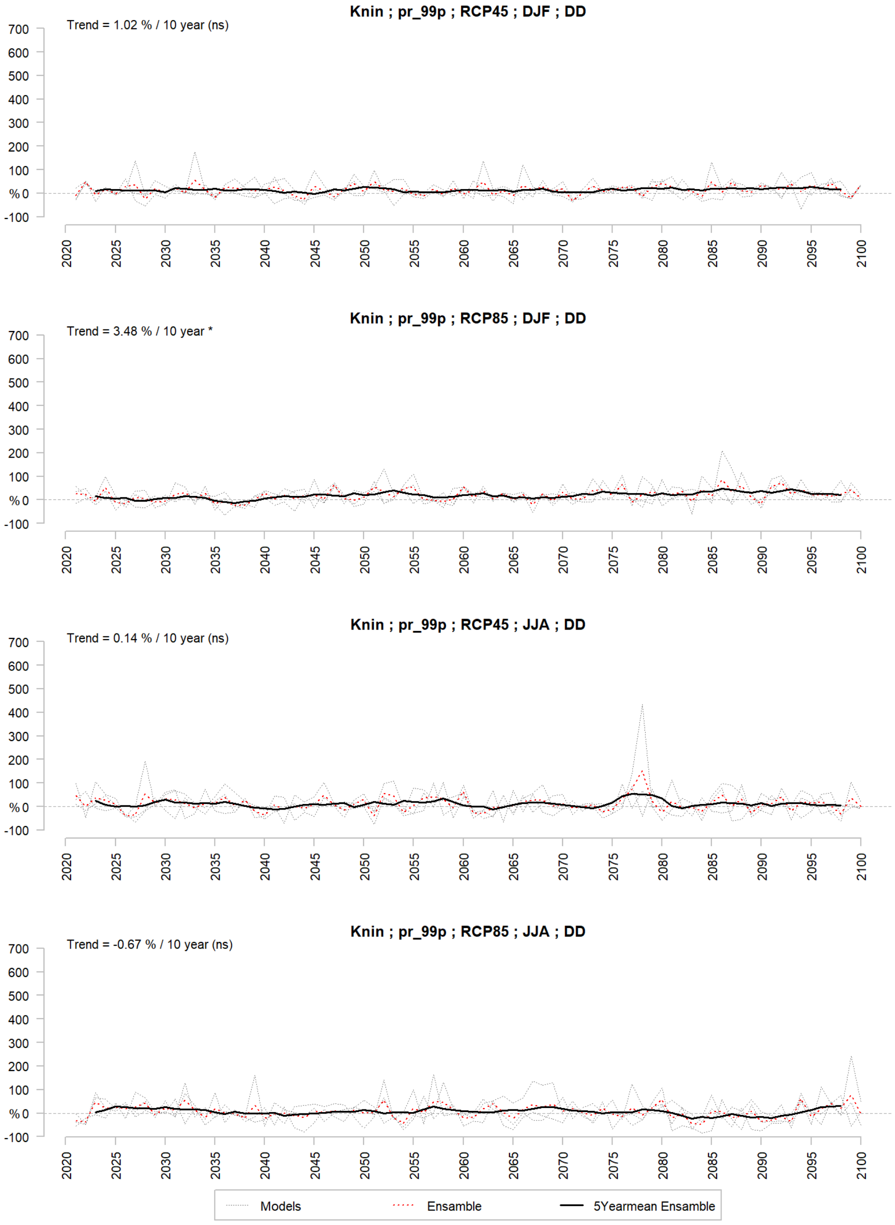

Figure 5-16: Variability of future 99th percentile of precipitation (extreme precipitation) anomaly (in %) in Knin for 2021-2100 obtained by dynamically downscaling for winter (DJF) and summer (JJA) and two RCP scenarios: individual models are in grey, the ensemble mean in red, 5-year moving average in black. Significant trend is marked with star (ns if not significant).

6.1.1.3 *Surface relative humidity projections*

Seasonal and annual change of mean surface relative humidity is shown by two available models realisation (Figure 5-17). Differences in signal change from one to other model clearly indicate the need to use multiple model for the final conclusion about the change in relative humidity. Ensemble mean of surface relative humidity change in Knin shows slightly increase at the end of 21st century (between 0.2 % in MAM and 2.1 % in JJA, 0.9 on annual scale for RCP4.5). The worst case scenario RCP8.5 gives increase of surface relative humidity between 0.4 % in SON and 1.3 % in JJA, decrease -1.3 % in JJA and increase 0.4 % on annual scale. Variability of future surface relative humidity anomaly (Figure 5-18) do not show significant linear trend in either DJF or JJA for any of the considered RCP scenarios.

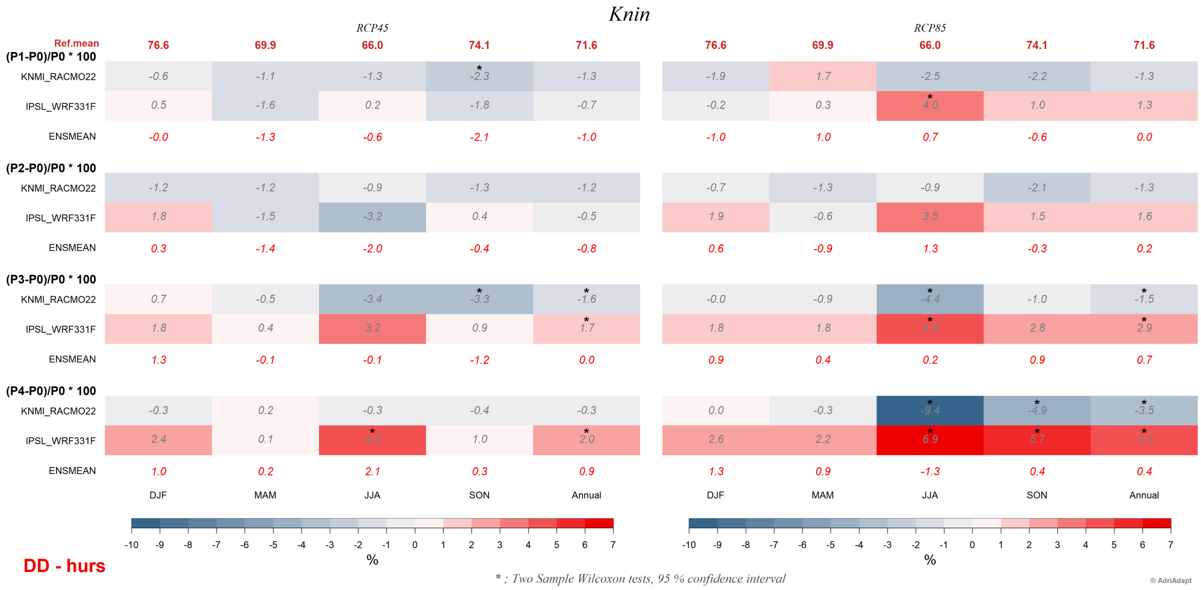

Knin

	RCP45					RCP85				
	DJF	MAM	JJA	SON	Annual	DJF	MAM	JJA	SON	Annual
Ref.mean	**76.6**	**69.9**	**66.0**	**74.1**	**71.6**	**76.6**	**69.9**	**66.0**	**74.1**	**71.6**
(P1-P0)/P0 * 100										
KNMI_RACMO22	-0.6	-1.1	-1.3	* -2.3	-1.3	-1.9	1.7	-2.5	-2.2	-1.3
IPSL_WRF331F	0.5	-1.6	0.2	-1.8	-0.7	-0.2	0.3	* 4.0	1.0	1.3
ENSMEAN	-0.0	-1.3	-0.6	-2.1	-1.0	-1.0	1.0	0.7	-0.6	0.0
(P2-P0)/P0 * 100										
KNMI_RACMO22	-1.2	-1.2	-0.9	-1.3	-1.2	-0.7	-1.3	-0.9	-2.1	-1.3
IPSL_WRF331F	1.8	-1.5	-3.2	0.4	-0.5	1.9	-0.6	3.5	1.5	1.6
ENSMEAN	0.3	-1.4	-2.0	-0.4	-0.8	0.6	-0.9	1.3	-0.3	0.2
(P3-P0)/P0 * 100										
KNMI_RACMO22	0.7	-0.5	-3.4	* -3.3	* -1.6	-0.0	-0.9	* -4.4	-1.0	* -1.5
IPSL_WRF331F	1.8	0.4	3.2	0.9	* 1.7	1.8	1.8	* 4.8	2.8	* 2.9
ENSMEAN	1.3	-0.1	-0.1	-1.2	0.0	0.9	0.4	0.2	0.9	0.7
(P4-P0)/P0 * 100										
KNMI_RACMO22	-0.3	0.2	-0.3	-0.4	-0.3	0.0	-0.3	* -9.4	* -4.9	* -3.5
IPSL_WRF331F	2.4	0.1	* 4.5	1.0	* 2.0	2.6	2.2	* 6.9	* 5.7	* 4.3
ENSMEAN	1.0	0.2	2.1	0.3	0.9	1.3	0.9	-1.3	0.4	0.4

DD - hurs

** ; Two Sample Wilcoxon tests, 95 % confidence interval*

© AdriAdapt

Figure 5-17: Seasonal and annual mean surface relative humidity (in %) obtained by dynamical downscaling for Knin: Ref. mean is 20 year simulated period (1986-2005); P1-P0, P2-P0, P3-P0, P4-P0 are relative changes in the future for following periods P1: 2021-2040, P2: 2041-2060, P3: 2061-2080, P4: 2081-2100. Differences are shown for individual models. Significant change is marked by star. Change is also shown as ensemble mean (ENSMEAN), not tested for significance. Left column is for RCP4.5 scenario and right for RCP8.5 scenario.

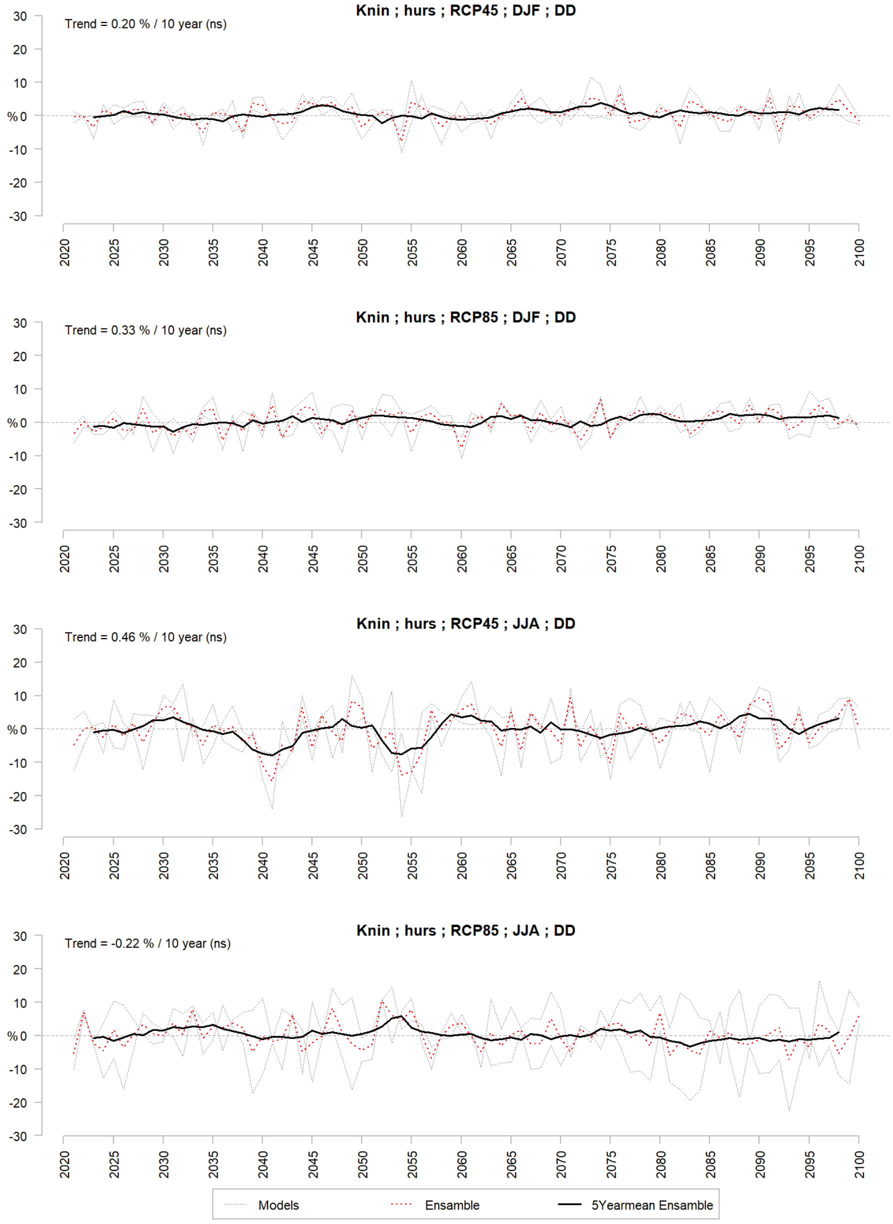

Figure 5-18: Variability of future surface relative humidity anomaly (in %) in Knin for 2021-2100 obtained by dynamically downscaling for winter (DJF) and summer (JJA) and two RCP scenarios: individual models are in grey, the ensemble mean in red, 5-year moving average in black. Significant trend is marked with star (ns if not significant).

https://www.italy-croatia.eu/adriadapt

6.1.1.4 *Extra rare humidex projections*

Extra rare humidex change (defined by 99.9th percentile of humidex) in the future in Knin will slightly increase towards the end of 21st century (Figure 5-19). Ensemble mean will increase between 0.1 in JJA and 2.4 in MAM, 0.9 on annual scale for RCP4.5 scenario. Scenario RCP8.5 gives slightly higher positive amplitudes, from 3.8 in DJF to 6.3 in MAM, 4.4 on annual scale. Variability of future 99.9th percentile of humidex anomaly (Figure 5-20) shows positive linear trend for both seasons and both considered scenarios. It is 0.31 [] / 10 year in DJF for RCP4.5 (0.64 [] /10 year for RCP8.5) and 0.22 [] /10 year in JJA for RCP4.5 (0.79 [] /10 year for RCP8.5). Trends are statistically significant.

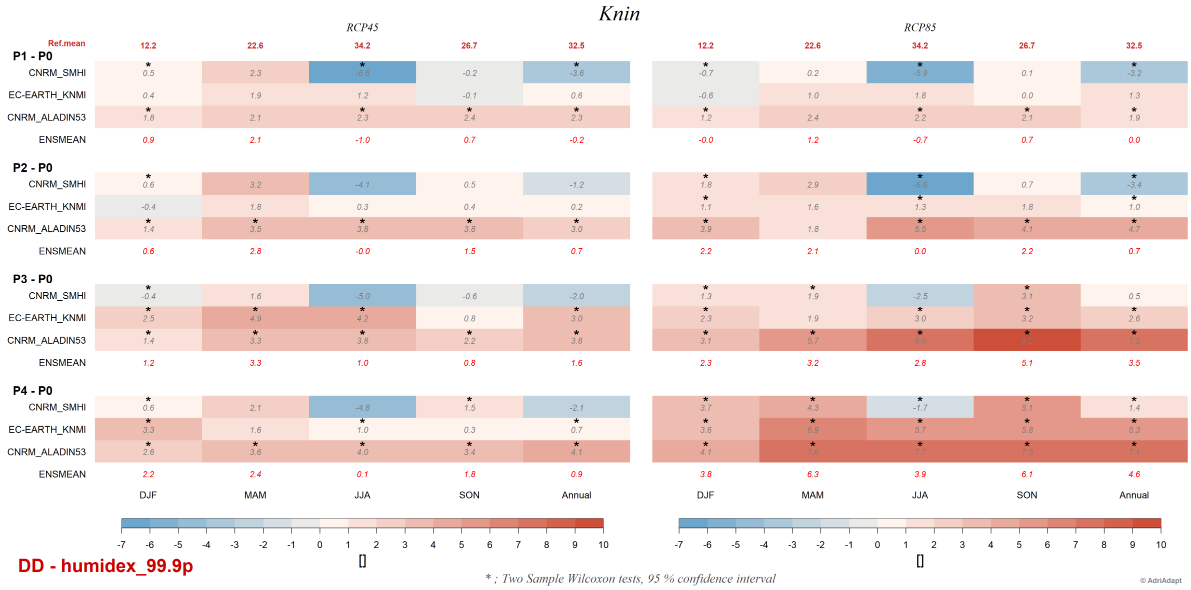

Knin

	RCP45					RCP85				
Ref.mean	12.2	22.6	34.2	26.7	32.5	12.2	22.6	34.2	26.7	32.5
P1 - P0										
CNRM_SMHI	* 0.5	2.3	* -6.6	-0.2	* -3.6	* -0.7	0.2	* -5.9	0.1	* -3.2
EC-EARTH_KNMI	0.4	1.9	1.2	-0.1	0.6	-0.6	1.0	1.8	0.0	1.3
CNRM_ALADIN53	* 1.8	2.1	* 2.3	* 2.4	* 2.3	* 1.2	2.4	* 2.2	* 2.1	* 1.9
ENSMEAN	0.9	2.1	-1.0	0.7	-0.2	-0.0	1.2	-0.7	0.7	0.0
P2 - P0										
CNRM_SMHI	* 0.6	3.2	-4.1	0.5	-1.2	* 1.8	2.9	* -6.6	0.7	* -3.4
EC-EARTH_KNMI	-0.4	1.8	0.3	0.4	0.2	* 1.1	1.6	* 1.3	1.8	* 1.0
CNRM_ALADIN53	* 1.4	* 3.5	* 3.8	* 3.8	* 3.0	* 3.9	1.8	* 5.5	* 4.1	* 4.7
ENSMEAN	0.6	2.8	-0.0	1.5	0.7	2.2	2.1	0.0	2.2	0.7
P3 - P0										
CNRM_SMHI	* -0.4	1.6	-5.0	-0.6	-2.0	* 1.3	* 1.9	-2.5	* 3.1	0.5
EC-EARTH_KNMI	* 2.5	* 4.9	* 4.2	0.8	* 3.0	* 2.3	1.9	* 3.0	* 3.2	* 2.6
CNRM_ALADIN53	* 1.4	* 3.3	* 3.8	* 2.2	* 3.8	* 3.1	* 5.7	* 8.0	* 9.2	* 7.5
ENSMEAN	1.2	3.3	1.0	0.8	1.6	2.3	3.2	2.8	5.1	3.5
P4 - P0										
CNRM_SMHI	* 0.6	2.1	-4.8	* 1.5	-2.1	* 3.7	* 4.3	* -1.7	* 5.1	* 1.4
EC-EARTH_KNMI	* 3.3	1.6	* 1.0	0.3	* 0.7	* 3.6	* 6.9	* 5.7	* 5.8	* 5.3
CNRM_ALADIN53	* 2.6	* 3.6	* 4.0	* 3.4	* 4.1	* 4.1	* 7.6	* 7.7	* 7.5	* 7.1
ENSMEAN	2.2	2.4	0.1	1.8	0.9	3.8	6.3	3.9	6.1	4.6
	DJF	MAM	JJA	SON	Annual	DJF	MAM	JJA	SON	Annual

DD - humidex_99.9p

* ; Two Sample Wilcoxon tests, 95 % confidence interval

© AdriAdapt

Figure 5-19: Seasonal and annual 99.9th percentile of humidex obtained by dynamical downscaling for Knin (in []): Ref. mean is 20 year simulated period (1986-2005); P1-P0, P2-P0, P3-P0, P4-P0 are changes in the future for following periods P1: 2021-2040, P2: 2041-2060, P3: 2061-2080, P4: 2081-2100. Differences are shown for individual models. Significant change is marked by star. Change is also shown as ensemble mean (ENSMEAN), not tested for significance. Left column is for RCP4.5 scenario and right for RCP8.5 scenario.

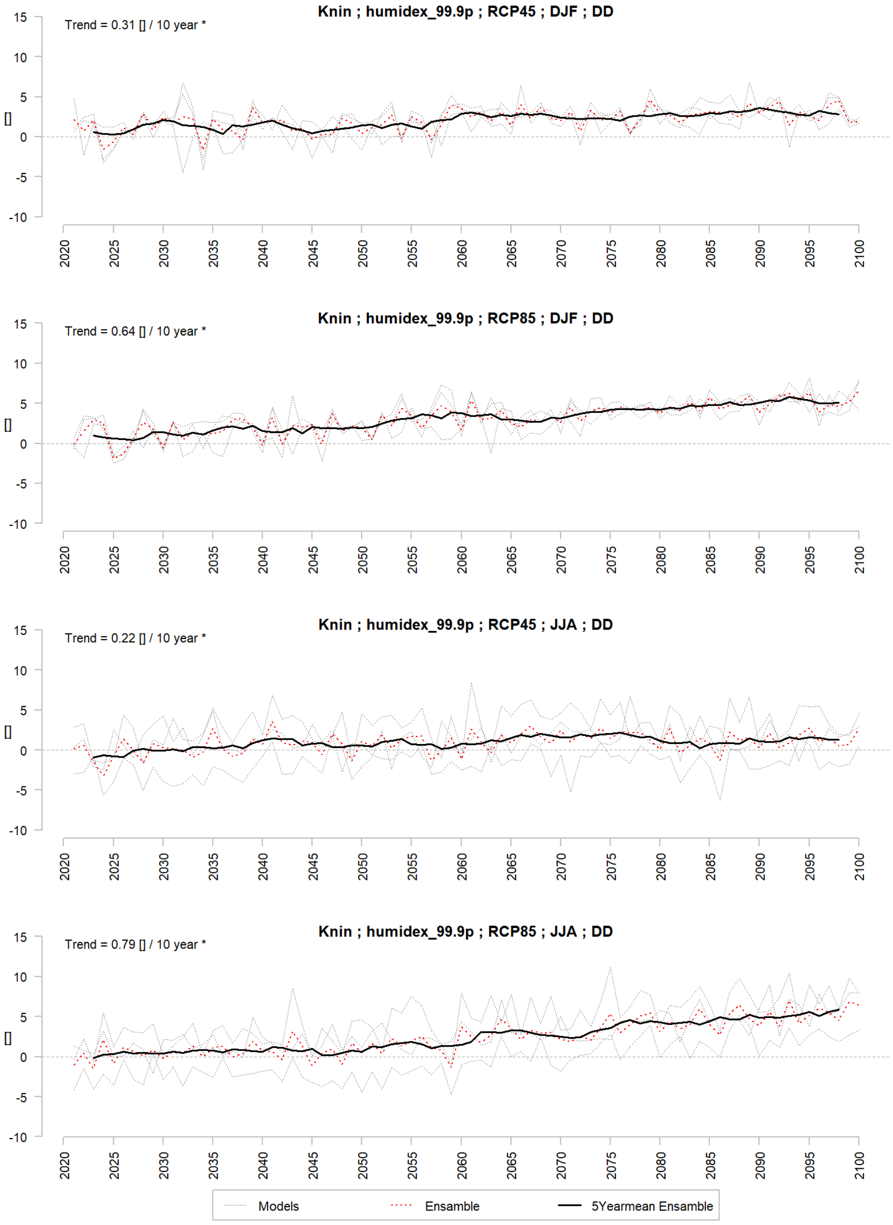

Figure 5-20: Variability of future 99.9th percentile of humidex anomaly (in []) in Knin for 2021-2100 obtained by dynamically downscaling for winter (DJF) and summer (JJA) and two RCP scenarios: individual models are in grey, the ensemble mean in red, 5-year moving average in black. Significant trend is marked with star (ns if not significant).

https://www.italy-croatia.eu/adriadapt

6.1.2 Statistically downscaled results

In this section we present future climate changes of temperature and precipitation related indices for Knin, as result from the statistical downscaling techniques constructed based on the observed local data/observed large scale circulation patterns and, applied then to future large-scale circulation patterns simulated by 4GCMs in the framework of CMIP5 experiments. The coordinates of the grid point are included in table A form Annexes. The results are presented as follow:

- climate change diagram of an individual index for each season and on annual basis for four considered future periods (P1, P2, P3, P4), for two emission scenarios (RCP4.5 and RCP8.5). Climate change is calculated as difference between future (P1, P2, P3, P4) and reference period (P0) for temperature indices and some extreme precipitation indices, and as relative differences (expressed in %) for some precipitation indices. Reference period is 1986-2005, the Ref.mean (obs.) from the diagram (see below) is the climate observed value registered at station take into analysis, while climate changes (P1-P0; P2-P0,P3-P0;P4-P0) are shown for different models (SD_CMCC-CM, SD_CAN-ESM2, SD-MPI, SD_CNRM) as well as for ensemble mean of models (ENSMEAN). The t-Student test is applied to test the statistical significance of future climate (values from P1, or P2, or P3, or P4) with respect to present climate value (value from P0) and the results significant at 95% are marked by a star.
- time series of future anomaly of an individual index for DJF and JJA and for two emission scenarios RCP4.5 and RCP8.5; the anomaly is calculated respect to the reference period and shown for individual models, ensemble mean and 5-year moving average. Mann Kendall trend test is applied to ensemble mean (for 95 % confidence level). Significant trend is marked with star (n.s. if not significant).

6.1.2.1 *Temperature related indices projections*

6.1.2.1.1 *Minimum and maximum air temperature*

Climate change scenarios of minimum and maximum average temperature obtained through statistical downscaling (SDs) technique applied to 4GCMs-CMIP5 experiments, estimate a possible increasing in both minimum and maximum temperature at Knin station, in all seasons and over the four periods: 2021-2040 (P1), 2041-2060 (P2), 2061-2080 (P3), 2081-2100 (P4), with respect to 1986-2005 (reference period).

Figure 5-21 presents the results for minimum average temperature including: the observed reference values, the projected changes by each SDs model and the Ensemble Mean of changes. The simulations show an increase at annual level around 1°C during 2021-2040 period, for both emission scenarios RCP4.5 and RCP8.5. Going to the end of the century the projected increase in annual minimum temperature is around 2°C in the framework of RCP4.5 and around 3.7°C in the framework of RCP8.5. The seasonal projected changes are expected to be more intense during summer and autumn seasons, with a peak of 4.5°C to the end of century. All projected changes in minimum temperature are significant from the statistical point of view.

The long-term variability of seasonal changes of minimum temperature emphasizes a positive trend over 2021-2100, for both emission scenarios. Figure 5-22 presents as an example the tendency in winter and summer minimum temperature (changes) in the framework of RCP4.5 and RCP8.5 emission scenario. The trend coefficients and the significance are also included in the figure. A higher magnitude is expected to occur during summer in the framework of RCP8.5 with a trend coefficient around 0.5°C/10years.

Knin

	RCP4.5					RCP8.5				
	DJF	MAM	JJA	SON	Annual	DJF	MAM	JJA	SON	Annual
Ref. mean (obs)	0,3	7	15,7	8,4	7,9	0,3	7	15,7	8,4	7,9
P1-P0										
SD_CMCC_CM	0,6	★ 0,7	★ 0,5	★ 1,0	★ 0,7	★ 1,4	★ 1,0	★ 0,7	★ 1,3	★ 1,1
SD_MPI_ESM_MR	0,6	★ 0,8	★ 0,7	0,2	★ 0,6	0,2	★ 0,7	★ 1,0	★ 0,6	★ 0,6
SD_CNRM_CM5	0,4	0,4	★ 0,5	★ 0,5	★ 0,5	0,4	0,5	★ 0,7	★ 1,0	★ 0,7
SD_CAN_ESM2	★ 1,3	★ 1,1	★ 2,0	★ 1,7	★ 1,5	★ 1,4	★ 1,0	★ 2,0	★ 1,8	★ 1,6
ENSMEAN	★ 0,7	★ 0,8	★ 0,9	★ 0,9	★ 0,8	★ 0,9	★ 0,8	★ 1,1	★ 1,2	★ 1,0
P2-P0										
SD_CMCC_CM	★ 1,6	★ 1,2	★ 1,4	★ 1,7	★ 1,5	★ 2,1	★ 1,5	★ 1,3	★ 2,4	★ 1,8
SD_MPI_ESM_MR	★ 0,7	★ 1,2	★ 1,2	★ 1,0	★ 1,0	★ 0,9	★ 0,9	★ 1,3	★ 1,3	★ 1,1
SD_CNRM_CM5	0,6	0,5	★ 1,0	★ 1,1	★ 0,8	★ 1,1	★ 0,8	★ 1,1	★ 1,6	★ 1,2
SD_CAN_ESM2	★ 1,7	★ 1,6	★ 2,7	★ 2,2	★ 2,1	★ 1,7	★ 1,7	★ 3,2	★ 2,9	★ 2,4
ENSMEAN	★ 1,2	★ 1,1	★ 1,6	★ 1,5	★ 1,3	★ 1,5	★ 1,2	★ 1,7	★ 2,1	★ 1,6
P3-P0										
SD_CMCC_CM	★ 2,2	★ 1,9	★ 1,7	★ 2,9	★ 2,2	★ 3,0	★ 2,7	★ 3,0	★ 4,0	★ 3,2
SD_MPI_ESM_MR	★ 1,1	★ 1,1	★ 1,2	★ 1,1	★ 1,1	★ 1,7	★ 2,0	★ 2,5	★ 2,3	★ 2,1
SD_CNRM_CM5	★ 1,1	★ 1,1	★ 1,3	★ 1,7	★ 1,3	★ 2,0	★ 1,7	★ 1,8	★ 2,4	★ 2,0
SD_CAN_ESM2	★ 1,9	★ 2,2	★ 2,6	★ 2,6	★ 2,3	★ 3,0	★ 2,9	★ 4,5	★ 4,4	★ 3,7
ENSMEAN	★ 1,6	★ 1,6	★ 1,7	★ 2,1	★ 1,7	★ 2,4	★ 2,3	★ 3,0	★ 3,3	★ 2,7
P4-P0										
SD_CMCC_CM	★ 2,1	★ 2,0	★ 1,8	★ 2,8	★ 2,2	★ 4,7	★ 3,8	★ 4,0	★ 5,3	★ 4,5
SD_MPI_ESM_MR	★ 1,1	★ 1,3	★ 1,6	★ 1,0	★ 1,3	★ 2,3	★ 2,7	★ 3,4	★ 3,4	★ 3,0
SD_CNRM_CM5	★ 1,5	★ 1,4	★ 1,6	★ 1,8	★ 1,6	★ 2,6	★ 2,2	★ 2,7	★ 3,3	★ 2,7
SD_CAN_ESM2	★ 2,1	★ 1,8	★ 3,2	★ 2,9	★ 2,5	★ 3,6	★ 3,6	★ 6,4	★ 5,7	★ 4,8
ENSMEAN	★ 1,7	★ 1,6	★ 2,1	★ 2,1	★ 1,9	★ 3,3	★ 3,1	★ 4,1	★ 4,4	★ 3,7

★ Two Sample Student's T-test, 95 % confidence interval, alternative hypothesis: true difference in means is not equal to 0

Figure 5-21: Seasonal and annual minimum temperature (°C): observed values over reference period (in red), changes projected by statistical downscaling applied to 4GCMs and the Ensemble Mean of changes over the four periods (P1, P2, P3, P4) projected in the framework of RCP4.5 (left) and RCP 8.5 (right). Significant change for each model is marked by star (source Arpae-Simc)

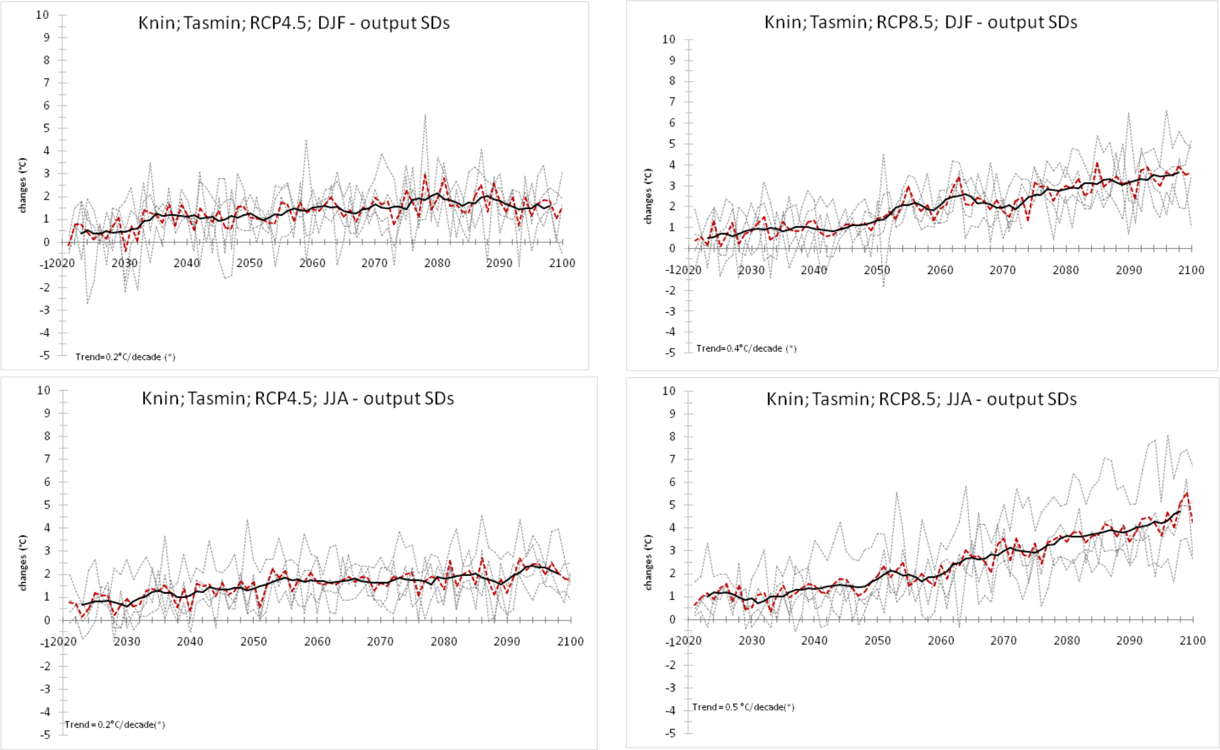

Figure 5-22: Variability of future changes of winter (DJF) and summer (JJA) minimum temperature (°C) projected through SDs applied to 4GCMs (grey lines); the Ensemble Mean (red line) and moving average (black line) - scenario RCP4.5 (left) and RCP8.5 (right), 2021-2100 period. Significant trend is marked with star while n.s. means not significant (source Arpae-Simc).

Similar results are projected for seasonal maximum average temperature that are displayed in figure 5-23, namely an increase during P1, P2, P3, P4 projected by each SDs. This increase is around 1°C at annual level during P1 period, but could reach 2.5°C to the end of century in the framework of RCP4.5. As regards RCP8.5, the annual temperature is projected to increase up to 5°C (see figure 5-23). Seasonally, could be noted that the projected changes are more intense during spring and autumn followed by summer and winter seasons (see figure 5-23).

Comparing the projections of minimum and maximum temperature for Knin it could be observed that those of maximum could be slightly higher than those of maximum temperature.

The long-term variability of changes in maximum temperature for Knin shows positive and significant trends of seasonal maximum temperature (Figure 5-24) with higher magnitude of tendency during summer and RCP8.5 emission scenario (0.5C/decade).

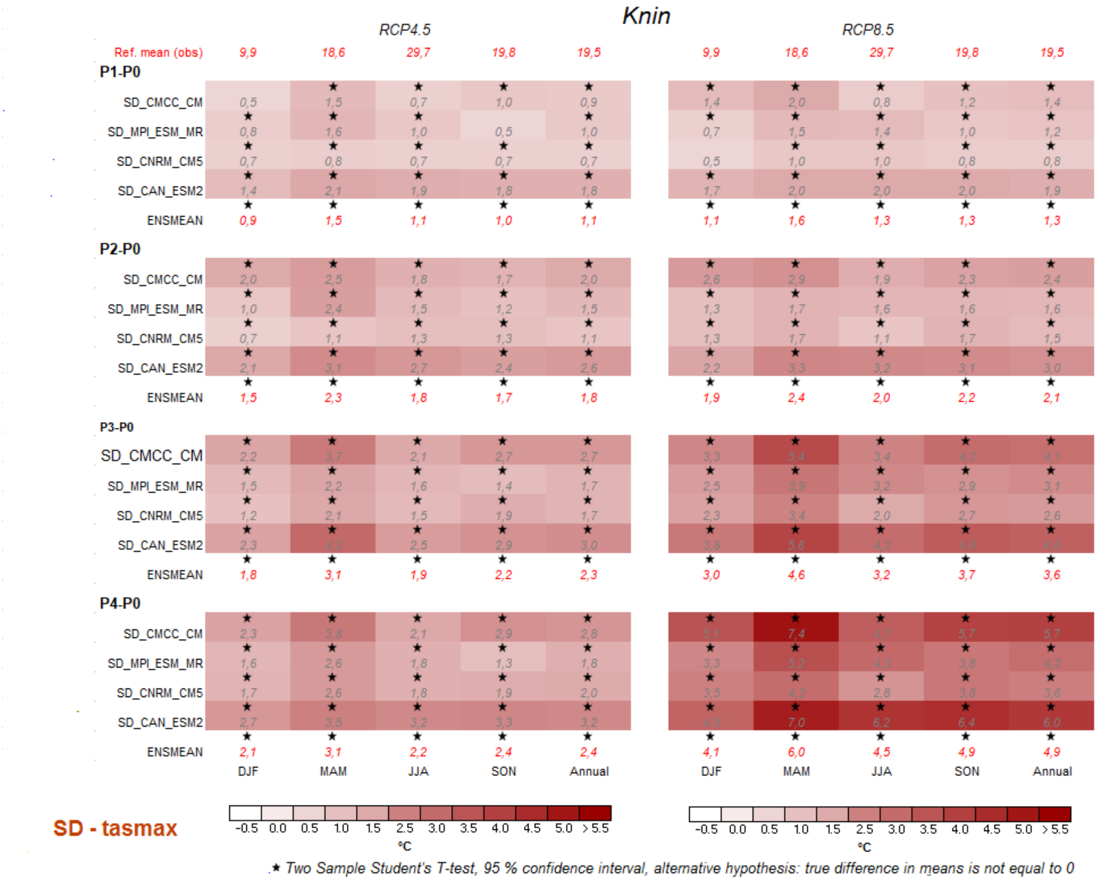

	RCP4.5					RCP8.5				
	DJF	MAM	JJA	SON	Annual	DJF	MAM	JJA	SON	Annual
Ref. mean (obs)	9,9	18,6	29,7	19,8	19,5	9,9	18,6	29,7	19,8	19,5
P1-P0										
SD_CMCC_CM	0,5	★ 1,5	★ 0,7	★ 1,0	★ 0,9	★ 1,4	★ 2,0	★ 0,8	★ 1,2	★ 1,4
SD_MPI_ESM_MR	★ 0,8	★ 1,6	★ 1,0	0,5	★ 1,0	★ 0,7	★ 1,5	★ 1,4	★ 1,0	★ 1,2
SD_CNRM_CM5	★ 0,7	★ 0,8	★ 0,7	★ 0,7	★ 0,7	0,5	★ 1,0	★ 1,0	★ 0,8	★ 0,8
SD_CAN_ESM2	★ 1,4	★ 2,1	★ 1,9	★ 1,8	★ 1,8	★ 1,7	★ 2,0	★ 2,0	★ 2,0	★ 1,9
ENSMEAN	★ 0,9	★ 1,5	★ 1,1	★ 1,0	★ 1,1	★ 1,1	★ 1,6	★ 1,3	★ 1,3	★ 1,3
P2-P0										
SD_CMCC_CM	★ 2,0	★ 2,5	★ 1,8	★ 1,7	★ 2,0	★ 2,6	★ 2,9	★ 1,9	★ 2,3	★ 2,4
SD_MPI_ESM_MR	★ 1,0	★ 2,4	★ 1,5	★ 1,2	★ 1,5	★ 1,3	★ 1,7	★ 1,6	★ 1,6	★ 1,6
SD_CNRM_CM5	★ 0,7	★ 1,1	★ 1,3	★ 1,3	★ 1,1	★ 1,3	★ 1,7	★ 1,1	★ 1,7	★ 1,5
SD_CAN_ESM2	★ 2,1	★ 3,1	★ 2,7	★ 2,4	★ 2,6	★ 2,2	★ 3,3	★ 3,2	★ 3,1	★ 3,0
ENSMEAN	★ 1,5	★ 2,3	★ 1,8	★ 1,7	★ 1,8	★ 1,9	★ 2,4	★ 2,0	★ 2,2	★ 2,1
P3-P0										
SD_CMCC_CM	★ 2,2	★ 3,7	★ 2,1	★ 2,7	★ 2,7	★ 3,3	★ 5,4	★ 3,4	★ 4,2	★ 4,1
SD_MPI_ESM_MR	★ 1,5	★ 2,2	★ 1,6	★ 1,4	★ 1,7	★ 2,5	★ 3,9	★ 3,2	★ 2,9	★ 3,1
SD_CNRM_CM5	★ 1,2	★ 2,1	★ 1,5	★ 1,9	★ 1,7	★ 2,3	★ 3,4	★ 2,0	★ 2,7	★ 2,6
SD_CAN_ESM2	★ 2,3	★ 4,3	★ 2,5	★ 2,9	★ 3,0	★ 3,8	★ 5,6	★ 4,2	★ 4,8	★ 4,6
ENSMEAN	★ 1,8	★ 3,1	★ 1,9	★ 2,2	★ 2,3	★ 3,0	★ 4,6	★ 3,2	★ 3,7	★ 3,6
P4-P0										
SD_CMCC_CM	★ 2,3	★ 3,8	★ 2,1	★ 2,9	★ 2,8	★ 5,1	★ 7,4	★ 4,7	★ 5,7	★ 5,7
SD_MPI_ESM_MR	★ 1,6	★ 2,6	★ 1,8	★ 1,3	★ 1,8	★ 3,3	★ 5,2	★ 4,3	★ 3,8	★ 4,2
SD_CNRM_CM5	★ 1,7	★ 2,6	★ 1,8	★ 1,9	★ 2,0	★ 3,5	★ 4,2	★ 2,8	★ 3,8	★ 3,6
SD_CAN_ESM2	★ 2,7	★ 3,5	★ 3,2	★ 3,3	★ 3,2	★ 4,5	★ 7,0	★ 6,2	★ 6,4	★ 6,0
ENSMEAN	★ 2,1	★ 3,1	★ 2,2	★ 2,4	★ 2,4	★ 4,1	★ 6,0	★ 4,5	★ 4,9	★ 4,9
	DJF	MAM	JJA	SON	Annual	DJF	MAM	JJA	SON	Annual

★ Two Sample Student's T-test, 95 % confidence interval, alternative hypothesis: true difference in means is not equal to 0

Figure 5-23: Seasonal and annual maximum temperature (°C): observed values over reference period (in red), changes projected by statistical downscaling applied to 4GCMs and the Ensemble Mean of changes over the four periods (P1, P2, P3, P4) projected in the framework of RCP4,5 (left) and RCP 8.5 (right). Significant change is marked by star (source Arpae-Simc)

https://www.italy-croatia.eu/adriadapt

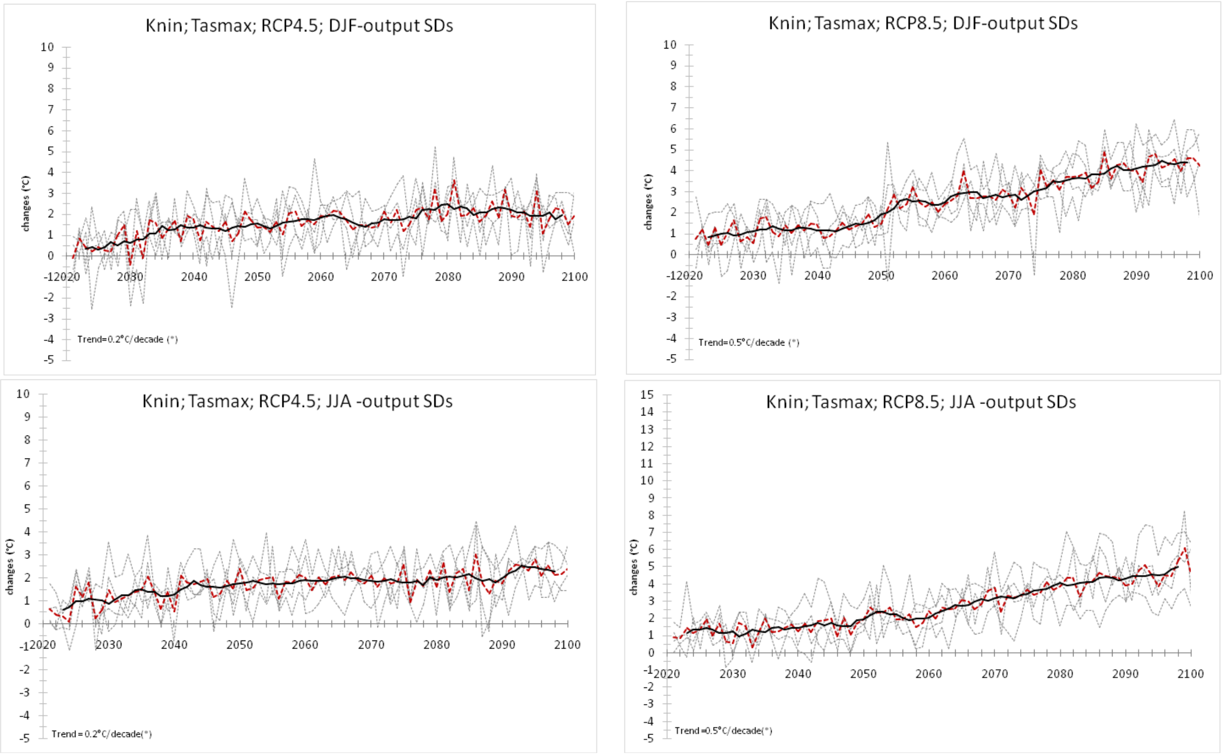

Figure 5-24: Variability of future changes of winter (DJF) and summer (JJA) maximum temperature (°C) projected through SDs applied to 4GCMs (grey lines); the Ensemble Mean (red line) and moving average (black line) - scenario RCP4.5 (left) and RCP8.5 (right), 2021-2100. Significant trend is marked with star while n.s. means not significant (source Arpae-Simc).

6.1.2.1.2 *Extreme temperature*

5th percentile of minimum temperature

The analysis performed on extreme temperature, 5th minimum temperature and 95th maximum temperature reveals important future changes at Knin station. An increase in annual 5th percentile of minimum temperature of 1°C is projected during the first period (2021-2040) and up to 2°C going to the end of century, in the framework of RP4.5 emission scenario. The signal became more intense for RCP8.5 emission scenario and especially during 2061-2080 and 2081-2100 periods, when the annual increases could reach 2.5°C during P3 and 3.5°C during P4 (see figure 5-25). The projected changes are significant at seasonal and annual level, with higher amplitude during spring and autumn (up to 5°C). The long-term variability of changes shows positive trends, both in winter and summer, between 0.2°C and 0.4°C/decade (figure 5-26).

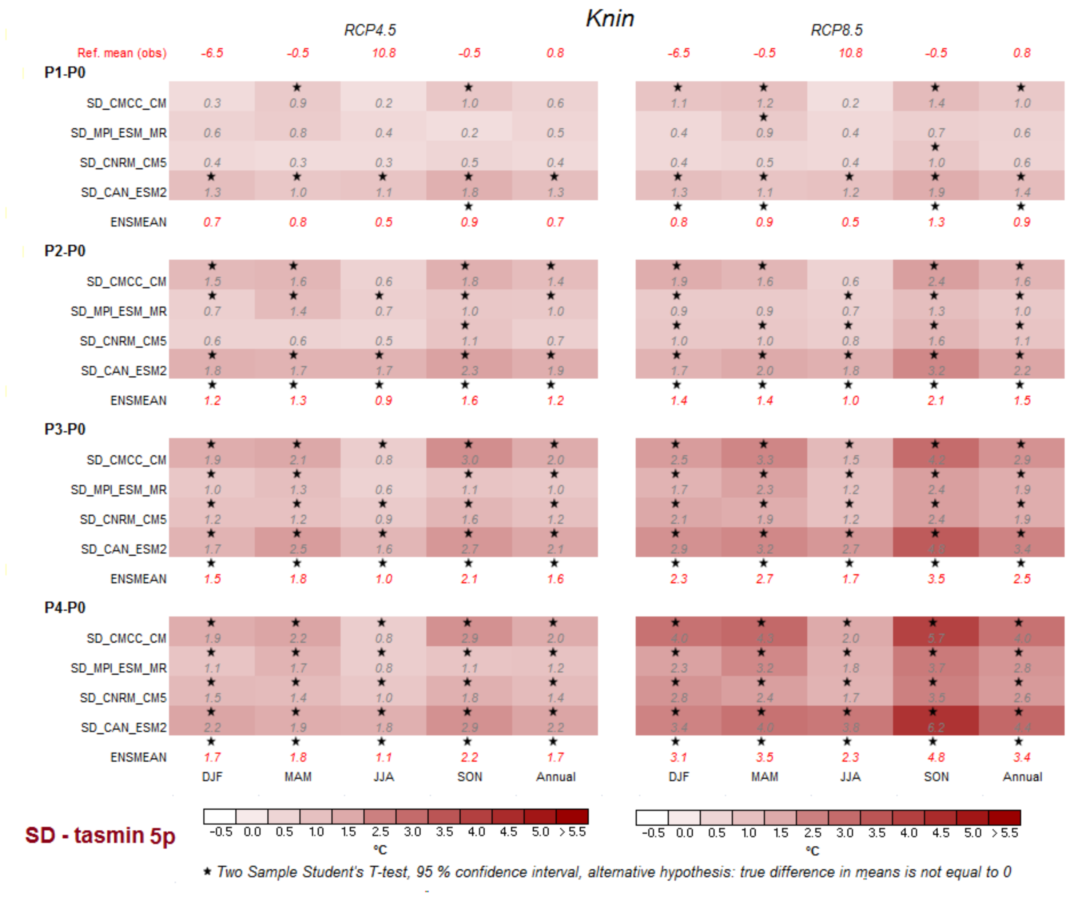

Knin

	RCP4.5					RCP8.5				
	DJF	MAM	JJA	SON	Annual	DJF	MAM	JJA	SON	Annual
Ref. mean (obs)	-6.5	-0.5	10.8	-0.5	0.8	-6.5	-0.5	10.8	-0.5	0.8
P1-P0										
SD_CMCC_CM	0.3	★ 0.9	0.2	★ 1.0	0.6	★ 1.1	★ 1.2	0.2	★ 1.4	★ 1.0
SD_MPI_ESM_MR	0.6	0.8	0.4	0.2	0.5	0.4	★ 0.9	0.4	0.7	0.6
SD_CNRM_CM5	0.4	0.3	0.3	0.5	0.4	0.4	0.5	0.4	★ 1.0	0.6
SD_CAN_ESM2	★ 1.3	★ 1.0	★ 1.1	★ 1.8	★ 1.3	★ 1.3	★ 1.1	★ 1.2	★ 1.9	★ 1.4
ENSMEAN	0.7	0.8	0.5	★ 0.9	0.7	★ 0.8	★ 0.9	0.5	★ 1.3	★ 0.9
P2-P0										
SD_CMCC_CM	★ 1.5	★ 1.6	0.6	★ 1.8	★ 1.4	★ 1.9	★ 1.6	0.6	★ 2.4	★ 1.6
SD_MPI_ESM_MR	★ 0.7	★ 1.4	★ 0.7	★ 1.0	★ 1.0	★ 0.9	0.9	★ 0.7	★ 1.3	★ 1.0
SD_CNRM_CM5	0.6	0.6	0.5	★ 1.1	0.7	★ 1.0	★ 1.0	★ 0.8	★ 1.6	★ 1.1
SD_CAN_ESM2	★ 1.8	★ 1.7	★ 1.7	★ 2.3	★ 1.9	★ 1.7	★ 2.0	★ 1.8	★ 3.2	★ 2.2
ENSMEAN	★ 1.2	★ 1.3	★ 0.9	★ 1.6	★ 1.2	★ 1.4	★ 1.4	★ 1.0	★ 2.1	★ 1.5
P3-P0										
SD_CMCC_CM	★ 1.9	★ 2.1	★ 0.8	★ 3.0	★ 2.0	★ 2.5	★ 3.3	★ 1.5	★ 4.2	★ 2.9
SD_MPI_ESM_MR	★ 1.0	★ 1.3	0.6	★ 1.1	★ 1.0	★ 1.7	★ 2.3	★ 1.2	★ 2.4	★ 1.9
SD_CNRM_CM5	★ 1.2	★ 1.2	★ 0.9	★ 1.6	★ 1.2	★ 2.1	★ 1.9	★ 1.2	★ 2.4	★ 1.9
SD_CAN_ESM2	★ 1.7	★ 2.5	★ 1.6	★ 2.7	★ 2.1	★ 2.9	★ 3.2	★ 2.7	★ 4.8	★ 3.4
ENSMEAN	★ 1.5	★ 1.8	★ 1.0	★ 2.1	★ 1.6	★ 2.3	★ 2.7	★ 1.7	★ 3.5	★ 2.5
P4-P0										
SD_CMCC_CM	★ 1.9	★ 2.2	★ 0.8	★ 2.9	★ 2.0	★ 4.0	★ 4.3	★ 2.0	★ 5.7	★ 4.0
SD_MPI_ESM_MR	★ 1.1	★ 1.7	★ 0.8	★ 1.1	★ 1.2	★ 2.3	★ 3.2	★ 1.8	★ 3.7	★ 2.8
SD_CNRM_CM5	★ 1.5	★ 1.4	★ 1.0	★ 1.8	★ 1.4	★ 2.8	★ 2.4	★ 1.7	★ 3.5	★ 2.6
SD_CAN_ESM2	★ 2.2	★ 1.9	★ 1.8	★ 2.9	★ 2.2	★ 3.4	★ 4.0	★ 3.8	★ 6.2	★ 4.4
ENSMEAN	★ 1.7	★ 1.8	★ 1.1	★ 2.2	★ 1.7	★ 3.1	★ 3.5	★ 2.3	★ 4.8	★ 3.4

★ *Two Sample Student's T-test, 95 % confidence interval, alternative hypothesis: true difference in means is not equal to 0*

https://www.italy-croatia.eu/adriadapt

Figure 5-25: 5th percentile of seasonal and annual minimum temperature: observed values over reference period (in red), changes projected by statistical downscaling applied to 4GCMs and the Ensemble Mean of changes over the four periods (P1, P2,P3,P4) projected in the framework of RCP4.5 (left) and RCP 8.5 (right). Significant change is marked by star (source Arpae-Simc)

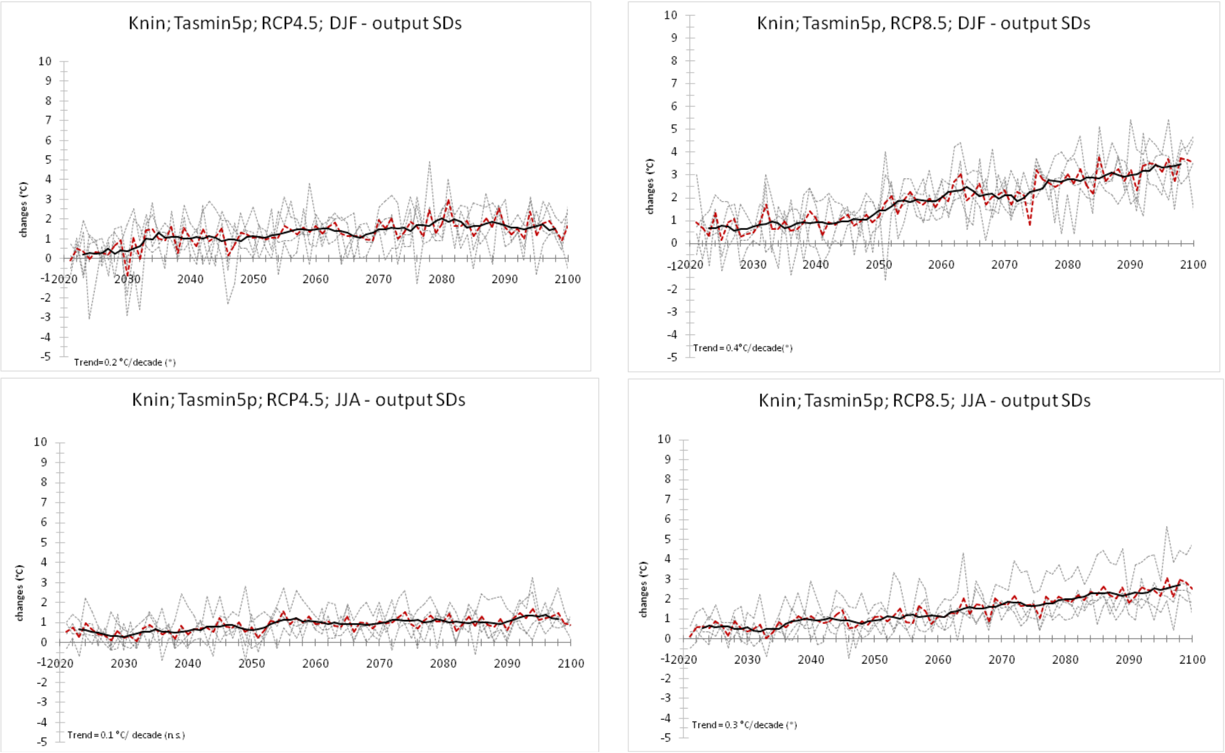

Figure 5-26: Variability of future changes of winter (DJF) and summer (JJA) 5th minimum temperature projected through SDs applied to 4GCMs (grey lines); the Ensemble Mean (red line) and moving average (black line) - scenario RCP4.5 (left) and RCP8.5 (right), 2021-2100 period. Significant trend is marked with star while n.s. means not significant (source Arpae-Simc).

95th percentile of maximum temperature

95th percentile of maximum temperature in Knin is projected to increase from P1 to P4 period, with amplitudes that vary from model to model. The Ensemble Mean shows an increase in annual value of changes up to 1.5°C in the framework of RCP4.5 and up to 3°C in the framework of RCP8.5, going to the end of century (Figure 5-27). A deep analysis on projected changes reveals higher values during spring and autumn with peak of changes around 5°C during 2081-2100 with respect to 1986-2005(RCP8.5).Variability of future changes of 95th percentile of maximum temperature shows positive trend, significant only in the RCP8.5 emission scenario (figure 5-28).

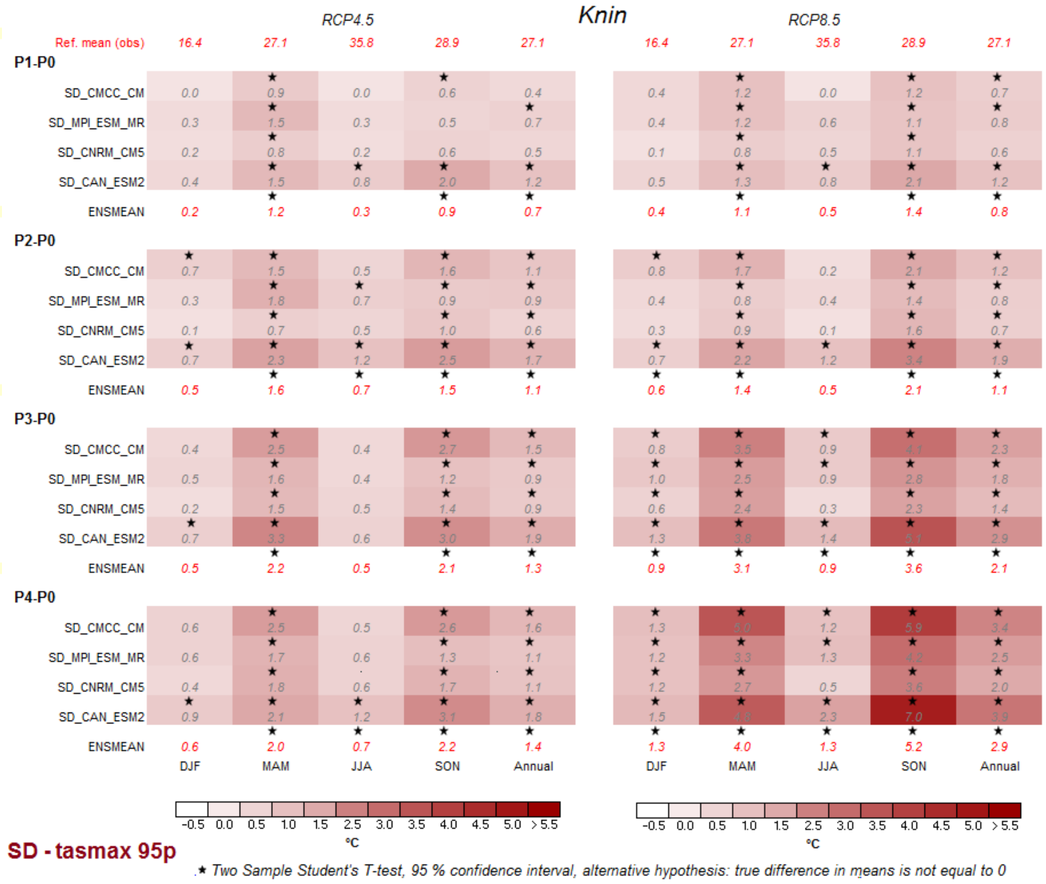

Knin

	RCP4.5					RCP8.5				
	DJF	MAM	JJA	SON	Annual	DJF	MAM	JJA	SON	Annual
Ref. mean (obs)	16.4	27.1	35.8	28.9	27.1	16.4	27.1	35.8	28.9	27.1
P1-P0										
SD_CMCC_CM	0.0	★ 0.9	0.0	★ 0.6	0.4	0.4	★ 1.2	0.0	★ 1.2	★ 0.7
SD_MPI_ESM_MR	0.3	★ 1.5	0.3	0.5	★ 0.7	0.4	★ 1.2	0.6	★ 1.1	★ 0.8
SD_CNRM_CM5	0.2	★ 0.8	0.2	0.6	0.5	0.1	★ 0.8	0.5	★ 1.1	0.6
SD_CAN_ESM2	0.4	★ 1.5	★ 0.8	★ 2.0	★ 1.2	0.5	★ 1.3	★ 0.8	★ 2.1	★ 1.2
ENSMEAN	0.2	★ 1.2	0.3	★ 0.9	★ 0.7	0.4	★ 1.1	0.5	★ 1.4	★ 0.8
P2-P0										
SD_CMCC_CM	★ 0.7	★ 1.5	0.5	★ 1.6	★ 1.1	★ 0.8	★ 1.7	0.2	★ 2.1	★ 1.2
SD_MPI_ESM_MR	0.3	★ 1.8	★ 0.7	★ 0.9	★ 0.9	0.4	★ 0.8	0.4	★ 1.4	★ 0.8
SD_CNRM_CM5	0.1	★ 0.7	0.5	★ 1.0	★ 0.6	0.3	★ 0.9	0.1	★ 1.6	★ 0.7
SD_CAN_ESM2	★ 0.7	★ 2.3	★ 1.2	★ 2.5	★ 1.7	★ 0.7	★ 2.2	★ 1.2	★ 3.4	★ 1.9
ENSMEAN	0.5	★ 1.6	★ 0.7	★ 1.5	★ 1.1	★ 0.6	★ 1.4	0.5	★ 2.1	★ 1.1
P3-P0										
SD_CMCC_CM	0.4	★ 2.5	0.4	★ 2.7	★ 1.5	★ 0.8	★ 3.5	★ 0.9	★ 4.1	★ 2.3
SD_MPI_ESM_MR	0.5	★ 1.6	0.4	★ 1.2	★ 0.9	★ 1.0	★ 2.5	★ 0.9	★ 2.8	★ 1.8
SD_CNRM_CM5	0.2	★ 1.5	0.5	★ 1.4	★ 0.9	★ 0.6	★ 2.4	0.3	★ 2.3	★ 1.4
SD_CAN_ESM2	★ 0.7	★ 3.3	0.6	★ 3.0	★ 1.9	★ 1.3	★ 3.8	★ 1.4	★ 5.1	★ 2.9
ENSMEAN	0.5	★ 2.2	0.5	★ 2.1	★ 1.3	★ 0.9	★ 3.1	★ 0.9	★ 3.6	★ 2.1
P4-P0										
SD_CMCC_CM	0.6	★ 2.5	0.5	★ 2.6	★ 1.6	★ 1.3	★ 5.0	★ 1.2	★ 5.9	★ 3.4
SD_MPI_ESM_MR	0.6	★ 1.7	0.6	★ 1.3	★ 1.1	★ 1.2	★ 3.3	★ 1.3	★ 4.2	★ 2.5
SD_CNRM_CM5	0.4	★ 1.8	0.6	★ 1.7	★ 1.1	★ 1.2	★ 2.7	0.5	★ 3.6	★ 2.0
SD_CAN_ESM2	★ 0.9	★ 2.1	★ 1.2	★ 3.1	★ 1.8	★ 1.5	★ 4.8	★ 2.3	★ 7.0	★ 3.9
ENSMEAN	0.6	★ 2.0	★ 0.7	★ 2.2	★ 1.4	★ 1.3	★ 4.0	★ 1.3	★ 5.2	★ 2.9

★ Two Sample Student's T-test, 95 % confidence interval, alternative hypothesis: true difference in means is not equal to 0

Figure 5-27: 95th percentile of seasonal and annual maximum temperature: observed values over reference period (in red), changes projected by statistical downscaling applied to 4GCMs and the Ensemble Mean of changes over the four periods (P1, P2, P3, P4) projected in the framework of RCP4.5 (left) and RCP 8.5 (right). Significant change is marked by star (source Arpae-Simc)

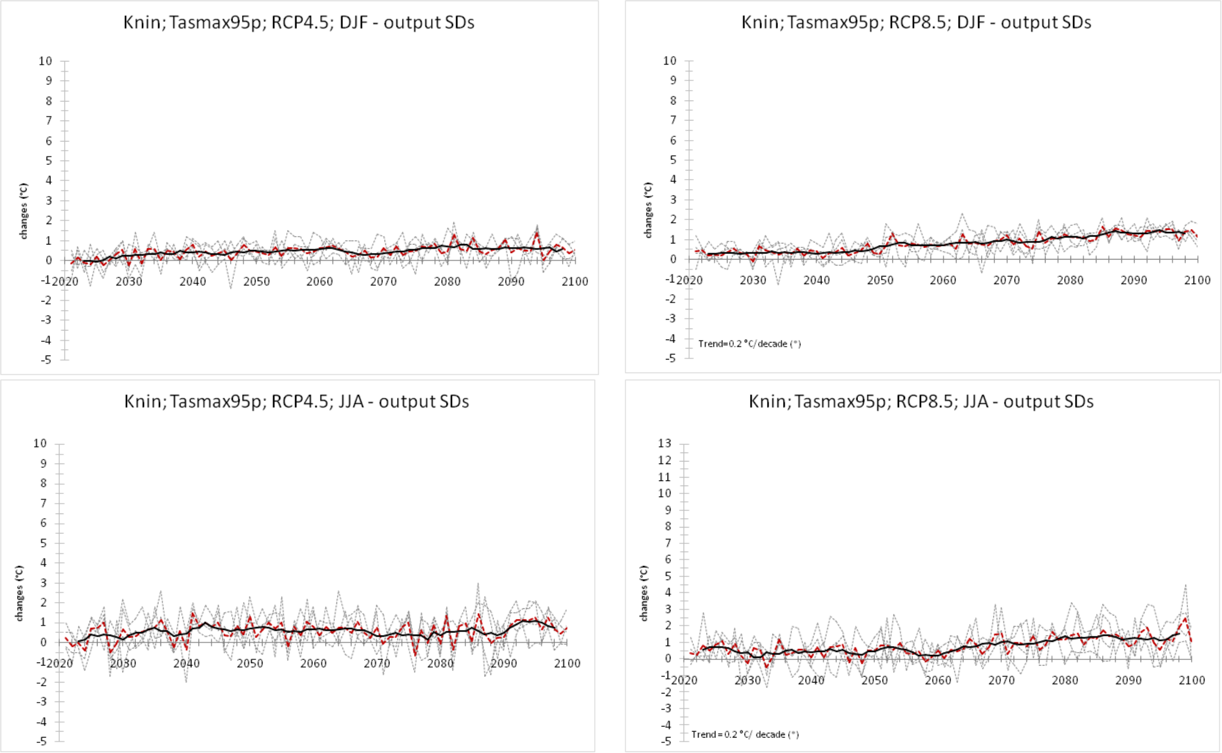

Knin; Tasmax95p; RCP4.5; DJF - output SDs

Knin; Tasmax95p; RCP8.5; DJF - output SDs

Knin; Tasmax95p; RCP4.5; JJA - output SDs

Knin; Tasmax95p; RCP8.5; JJA - output SDs

Figure 5-28: Variability of future changes of winter (DJF) and summer (JJA) 95th percentile of maximum temperature projected through SDs applied to 4GCMs (grey lines); the Ensemble Mean (red line) and moving average (black line) - scenario RCP4.5 (left) and RCP8.5 (right), 2021-2100 period. Significant trend is marked with star while n.s. means not significant (source Arpae-Simc).

6.1.2.1.3 *Heat wave duration*

The projection of the heat wave duration, index defined as the maximum number of consecutive days with maximum temperature greater than 90th percentile, shows an increase during spring and summer. Figure 5-29 includes the projected changes for Knin. As could be observed, for RCP4.5 the projected increase could reach around 16 consecutive days (on spring, during P3 and P4) while in the framework of RCP8.5 could reach 49 consecutive days, both in spring and summer, to the end of century. As regards long term variability of chnges, the trend is positive, more intense in RCP8.5 emission scenario (see figure 5-30).

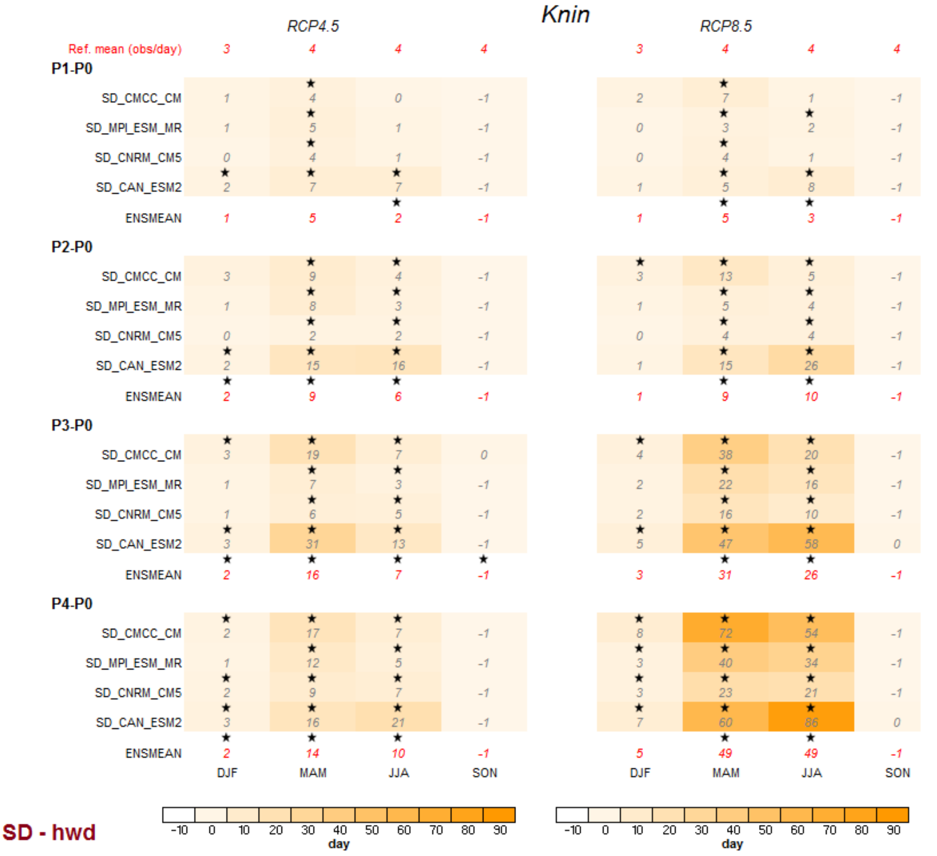

	RCP4.5				RCP8.5			
	DJF	MAM	JJA	SON	DJF	MAM	JJA	SON
Ref. mean (obs/day)	3	4	4	4	3	4	4	4
P1-P0								
SD_CMCC_CM	1	★ 4	0	-1	2	★ 7	1	-1
SD_MPI_ESM_MR	1	★ 5	1	-1	0	★ 3	★ 2	-1
SD_CNRM_CM5	0	★ 4	1	-1	0	★ 4	1	-1
SD_CAN_ESM2	★ 2	★ 7	★ 7	-1	1	★ 5	★ 8	-1
ENSMEAN	1	5	★ 2	-1	1	★ 5	★ 3	-1
P2-P0								
SD_CMCC_CM	3	★ 9	★ 4	-1	★ 3	★ 13	★ 5	-1
SD_MPI_ESM_MR	1	★ 8	★ 3	-1	1	★ 5	★ 4	-1
SD_CNRM_CM5	0	★ 2	★ 2	-1	0	★ 4	★ 4	-1
SD_CAN_ESM2	★ 2	★ 15	★ 16	-1	1	★ 15	★ 26	-1
ENSMEAN	★ 2	★ 9	★ 6	-1	1	★ 9	★ 10	-1
P3-P0								
SD_CMCC_CM	★ 3	★ 19	★ 7	0	★ 4	★ 38	★ 20	-1
SD_MPI_ESM_MR	1	★ 7	★ 3	-1	2	★ 22	★ 16	-1
SD_CNRM_CM5	1	★ 6	★ 5	-1	2	★ 16	★ 10	-1
SD_CAN_ESM2	★ 3	★ 31	★ 13	-1	★ 5	★ 47	★ 58	0
ENSMEAN	★ 2	★ 16	★ 7	★ -1	3	★ 31	★ 26	-1
P4-P0								
SD_CMCC_CM	★ 2	★ 17	★ 7	-1	★ 8	★ 72	★ 54	-1
SD_MPI_ESM_MR	1	★ 12	★ 5	-1	★ 3	★ 40	★ 34	-1
SD_CNRM_CM5	★ 2	★ 9	★ 7	-1	★ 3	★ 23	★ 21	-1
SD_CAN_ESM2	★ 3	★ 16	★ 21	-1	★ 7	★ 60	★ 86	0
ENSMEAN	★ 2	★ 14	★ 10	-1	5	★ 49	★ 49	-1

★ *Two Sample Student's T-test, 95 % confidence interval, alternative hypothesis: true difference in means is not equal to 0*

Figure 5-29: Seasonal heat wave duration: observed values over reference period (in red), changes projected by statistical downscaling applied to 4GCMs and the Ensemble Mean of changes over the four periods (P1, P2, P3, P4) projected in the framework of

RCP4.5 (left) and RCP 8.5(right). Significant change is marked by star (source Arpae-Simc)

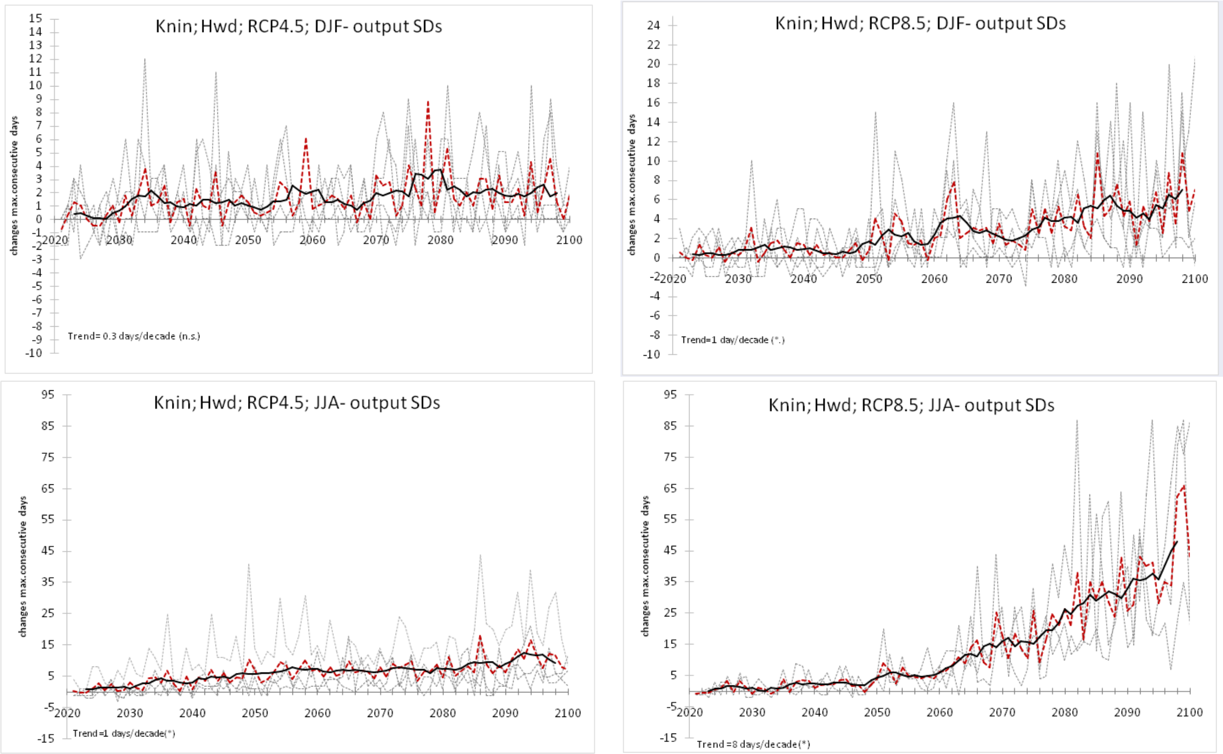

Figure 5-30: Variability of future changes of winter (DJF) and summer (JJA) heat wave duration projected through SDs applied to 4GCMs (grey lines); the Ensemble Mean (red line) and moving average (black line) - scenario RCP4.5 (left) and RCP8.5 (right), 2021-2100 period. Significant trend is marked with star while n.s. means not significant (source Arpae-Simc).

6.1.2.1.4 *Tropical nights*

The projection of the tropical nights, index defined as the number of days with minimum temperature greater than 20°C, shows an increase during the summer season. All SDs models agree with these changes, as could be noted from figure 5-31. The value of changes varies between 30 days during 2021-2040 (RCP4.5) up to 83 days during 2081-2100 (RCP8.5)

Regarding long term variability of changes, the trend is positive and statistically significant (up to 7 days/decade) during 2021-2100 (see figure 5-32).

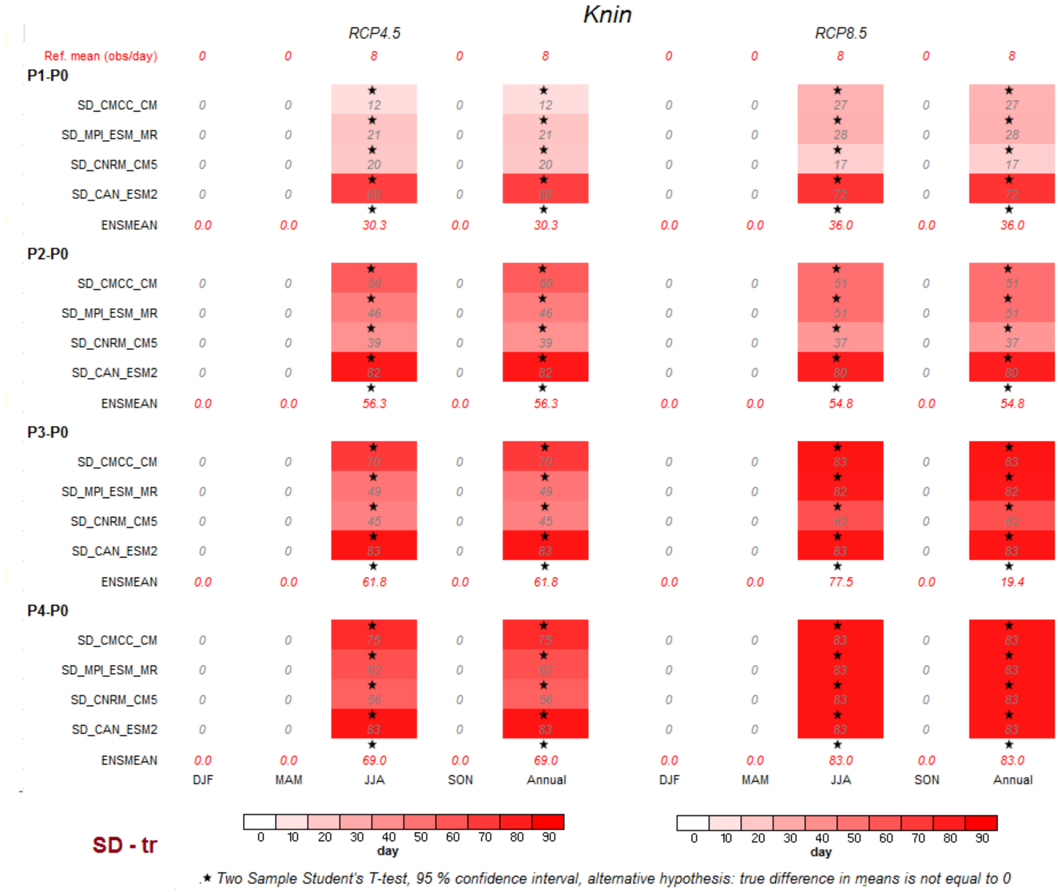

Figure 5-31: Seasonal and annual tropical nights: observed values over reference period (in red), changes projected by statistical downscaling applied to 4GCMs and the Ensemble Mean over the four periods (P1, P2, P3, P4) projected in the framework of

RCP4.5 (left) and RCP 8.5 (right). Significant change is marked by star (source Arpae-Simc).

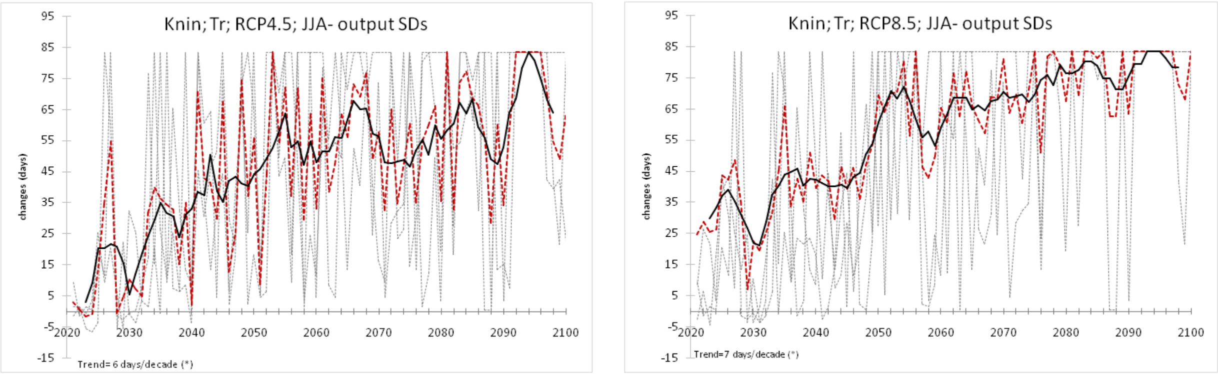

Figure 5-32: Variability of future changes of summer (JJA) tropical nights projected through SDs applied to 4GCMs (grey lines); the Ensemble Mean (red line) and moving average (black line) - scenario RCP4.5 (left) and RCP8.5 (right), 2021-2100 period Significant trend is marked with star while n.s. means not significant (source Arpae-Simc).

6.1.2.1.5 *Frost days*

The future projections of frost days, namely the number of days with minimum temperature lower than 0°C, show a decrease during winter, spring and autumn. All SDs models agree with these changes during all periods, as could be noted from figure 5-33 (significant changes). The signal of changes is higher during winter season, with values of changes in RCP4.5 scenario between -6 days during P1 up to -12 days going to the end of the century. The magnitude of changes is higher for RCP8.5 (see figure 5-33).
Regarding long term variability, the trend is negative (-3days/decade) but statistically significant only for RCP8.5 (see figure 5-34).

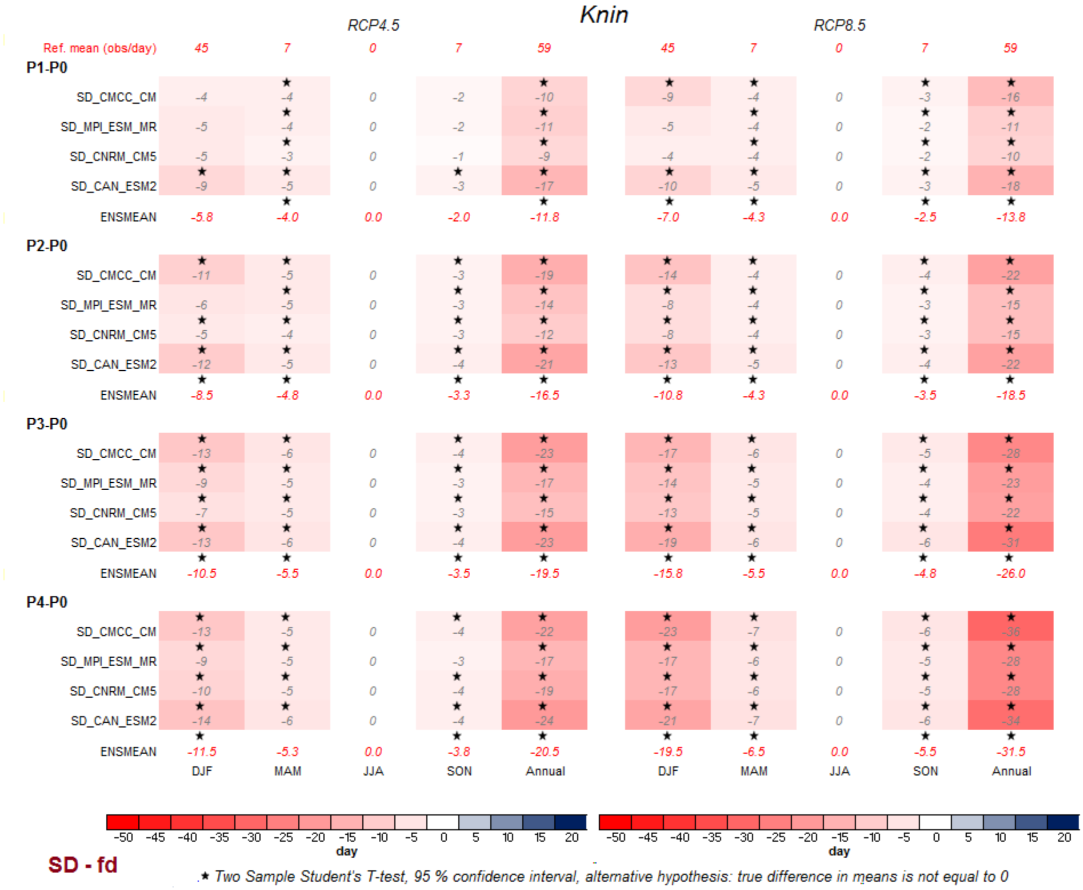

	RCP4.5					RCP8.5				
	DJF	MAM	JJA	SON	Annual	DJF	MAM	JJA	SON	Annual
Ref. mean (obs/day)	45	7	0	7	59	45	7	0	7	59
P1-P0										
SD_CMCC_CM	-4	★ -4	0	-2	★ -10	★ -9	★ -4	0	★ -3	★ -16
SD_MPI_ESM_MR	-5	★ -4	0	-2	★ -11	-5	★ -4	0	★ -2	★ -11
SD_CNRM_CM5	-5	★ -3	0	-1	★ -9	-4	★ -4	0	★ -2	★ -10
SD_CAN_ESM2	★ -9	★ -5	0	★ -3	★ -17	★ -10	★ -5	0	★ -3	★ -18
ENSMEAN	-5.8	★ -4.0	0.0	-2.0	★ -11.8	★ -7.0	★ -4.3	0.0	★ -2.5	★ -13.8
P2-P0										
SD_CMCC_CM	★ -11	★ -5	0	★ -3	★ -19	★ -14	★ -4	0	★ -4	★ -22
SD_MPI_ESM_MR	-6	★ -5	0	★ -3	★ -14	★ -8	★ -4	0	★ -3	★ -15
SD_CNRM_CM5	★ -5	★ -4	0	★ -3	★ -12	★ -8	★ -4	0	★ -3	★ -15
SD_CAN_ESM2	★ -12	★ -5	0	★ -4	★ -21	★ -13	★ -5	0	★ -4	★ -22
ENSMEAN	★ -8.5	★ -4.8	0.0	★ -3.3	★ -16.5	★ -10.8	★ -4.3	0.0	★ -3.5	★ -18.5
P3-P0										
SD_CMCC_CM	★ -13	★ -6	0	★ -4	★ -23	★ -17	★ -6	0	★ -5	★ -28
SD_MPI_ESM_MR	★ -9	★ -5	0	★ -3	★ -17	★ -14	★ -5	0	★ -4	★ -23
SD_CNRM_CM5	★ -7	★ -5	0	★ -3	★ -15	★ -13	★ -5	0	★ -4	★ -22
SD_CAN_ESM2	★ -13	★ -6	0	★ -4	★ -23	★ -19	★ -6	0	★ -6	★ -31
ENSMEAN	★ -10.5	★ -5.5	0.0	★ -3.5	★ -19.5	★ -15.8	★ -5.5	0.0	★ -4.8	★ -26.0
P4-P0										
SD_CMCC_CM	★ -13	★ -5	0	★ -4	★ -22	★ -23	★ -7	0	★ -6	★ -36
SD_MPI_ESM_MR	★ -9	★ -5	0	-3	★ -17	★ -17	★ -6	0	★ -5	★ -28
SD_CNRM_CM5	★ -10	★ -5	0	★ -4	★ -19	★ -17	★ -6	0	★ -5	★ -28
SD_CAN_ESM2	★ -14	★ -6	0	★ -4	★ -24	★ -21	★ -7	0	★ -6	★ -34
ENSMEAN	★ -11.5	-5.3	0.0	★ -3.8	★ -20.5	★ -19.5	★ -6.5	0.0	★ -5.5	★ -31.5

★ Two Sample Student's T-test, 95 % confidence interval, alternative hypothesis: true difference in means is not equal to 0

Figure 5-33: Seasonal and annual frost days: observed values over reference period (in red), changes projected by statistical downscaling applied to 4GCMs and the Ensemble Mean over the four periods (P1, P2, P3, P4) projected in the framework of RCP4,5 (left) and RCP 8.5(right). Significant change is marked by star (source Arpae-Simc).

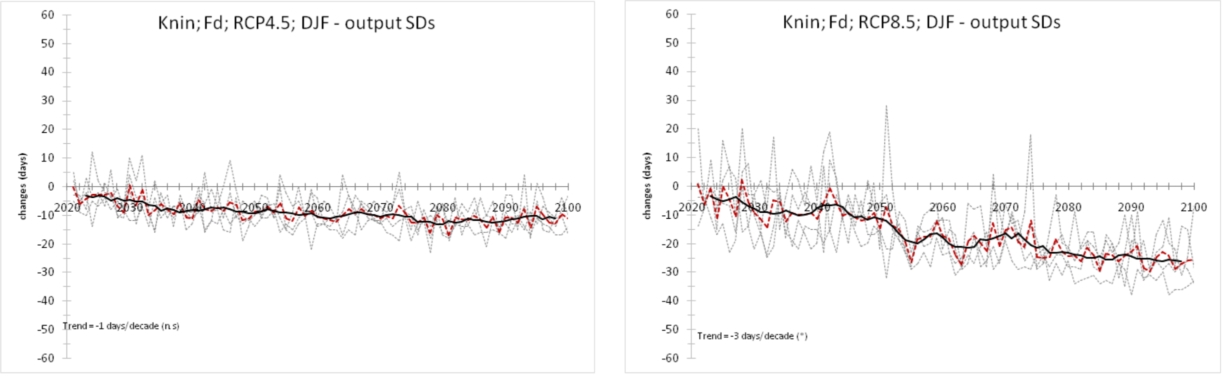

Figure 5-34: Variability of future changes of winter (DJF) frost days projected through SDs applied to 4GCMs (grey lines); the Ensemble Mean (red line) and moving average (black line) - scenario RCP4.5 (left) and RCP8.5 (right), 2021-2100 period. Significant trend is marked with star while n.s. means not significant (source Arpae-Simc).

6.1.2.2 *Precipitation related indices projections*

6.1.2.2.1 *Amount of precipitation*

At annual time scale, a decrease of precipitation can be expected from P1 to P4 up to -20 % for RCP4.5 and -30 % for RCP8.5 scenario (figure 5-35). Precipitation is much more variable parameter in comparison to the temperature, therefore there is no always unique sign of change through the year as well as from model to model. Summarizing the results from the diagram 5-35 and considering only significant results it could be underlie that: an increase of precipitation could occur in winter going to the end of century (up to 23% for RCP8.5) and a decrease of precipitation is projected for other seasons (up to -55% for JJA and SON in the framework of RCP8.5). The long-term variability of future changes in precipitation displayed in figure 5-36 shows: slightly increase in winter and decrease in summer, significant only for RCP8.5

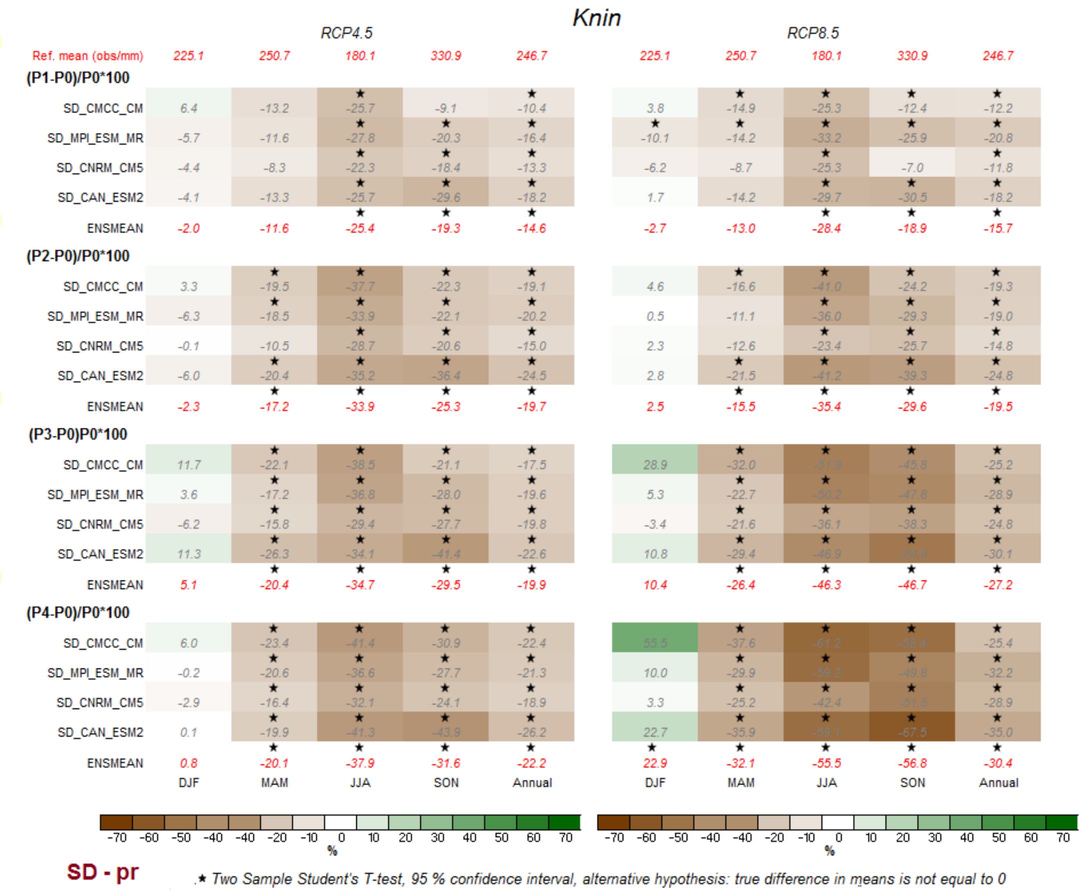

Knin

	RCP4.5					RCP8.5				
	DJF	MAM	JJA	SON	Annual	DJF	MAM	JJA	SON	Annual
Ref. mean (obs/mm)	225.1	250.7	180.1	330.9	246.7	225.1	250.7	180.1	330.9	246.7
(P1-P0)/P0*100										
SD_CMCC_CM	6.4	-13.2	★ -25.7	-9.1	★ -10.4	3.8	★ -14.9	★ -25.3	★ -12.4	★ -12.2
SD_MPI_ESM_MR	-5.7	-11.6	★ -27.8	★ -20.3	★ -16.4	★ -10.1	★ -14.2	★ -33.2	★ -25.9	★ -20.8
SD_CNRM_CM5	-4.4	-8.3	★ -22.3	★ -18.4	★ -13.3	-6.2	-8.7	★ -25.3	-7.0	★ -11.8
SD_CAN_ESM2	-4.1	-13.3	★ -25.7	★ -29.6	★ -18.2	1.7	-14.2	★ -29.7	★ -30.5	★ -18.2
ENSMEAN	-2.0	-11.6	★ -25.4	★ -19.3	★ -14.6	-2.7	-13.0	★ -28.4	★ -18.9	★ -15.7
(P2-P0)/P0*100										
SD_CMCC_CM	3.3	★ -19.5	★ -37.7	★ -22.3	★ -19.1	4.6	★ -16.6	★ -41.0	★ -24.2	★ -19.3
SD_MPI_ESM_MR	-6.3	★ -18.5	★ -33.9	★ -22.1	★ -20.2	0.5	-11.1	★ -36.0	★ -29.3	★ -19.0
SD_CNRM_CM5	-0.1	-10.5	★ -28.7	★ -20.6	★ -15.0	2.3	-12.6	★ -23.4	★ -25.7	★ -14.8
SD_CAN_ESM2	-6.0	★ -20.4	★ -35.2	★ -36.4	★ -24.5	2.8	★ -21.5	★ -41.2	★ -39.3	★ -24.8
ENSMEAN	-2.3	★ -17.2	★ -33.9	★ -25.3	★ -19.7	2.5	★ -15.5	★ -35.4	★ -29.6	★ -19.5
(P3-P0)P0*100										
SD_CMCC_CM	11.7	★ -22.1	★ -38.5	★ -21.1	★ -17.5	28.9	★ -32.0	★ -51.9	★ -45.8	★ -25.2
SD_MPI_ESM_MR	3.6	★ -17.2	★ -36.8	★ -28.0	★ -19.6	5.3	★ -22.7	★ -50.2	★ -47.8	★ -28.9
SD_CNRM_CM5	-6.2	★ -15.8	★ -29.4	★ -27.7	★ -19.8	-3.4	★ -21.6	★ -36.1	★ -38.3	★ -24.8
SD_CAN_ESM2	11.3	★ -26.3	★ -34.1	★ -41.4	★ -22.6	10.8	★ -29.4	★ -46.9	★ -54.8	★ -30.1
ENSMEAN	5.1	★ -20.4	★ -34.7	★ -29.5	★ -19.9	10.4	★ -26.4	★ -46.3	★ -46.7	★ -27.2
(P4-P0)/P0*100										
SD_CMCC_CM	6.0	★ -23.4	★ -41.4	★ -30.9	★ -22.4	55.5	★ -37.6	★ -61.2	★ -58.4	★ -25.4
SD_MPI_ESM_MR	-0.2	★ -20.6	★ -36.6	★ -27.7	★ -21.3	10.0	★ -29.9	★ -59.2	★ -49.8	★ -32.2
SD_CNRM_CM5	-2.9	★ -16.4	★ -32.1	★ -24.1	★ -18.9	3.3	★ -25.2	★ -42.4	★ -51.5	★ -28.9
SD_CAN_ESM2	0.1	★ -19.9	★ -41.3	★ -43.9	★ -26.2	22.7	★ -35.9	★ -59.1	★ -67.5	★ -35.0
ENSMEAN	0.8	★ -20.1	★ -37.9	★ -31.6	★ -22.2	★ 22.9	★ -32.1	★ -55.5	★ -56.8	★ -30.4

SD - pr

★ Two Sample Student's T-test, 95 % confidence interval, alternative hypothesis: true difference in means is not equal to 0

Figure 5-35: Seasonal and annual amount of precipitation: observed values over reference period (in red), changes projected by statistical downscaling applied to 4GCMs and the Ensemble Mean of changes over the four periods (P1, P2, P3, P4) expressed in % ; RCP4.5 (left) and RCP 8.5 (right) scenarios. Significant change is marked by star (source Arpae-Simc)

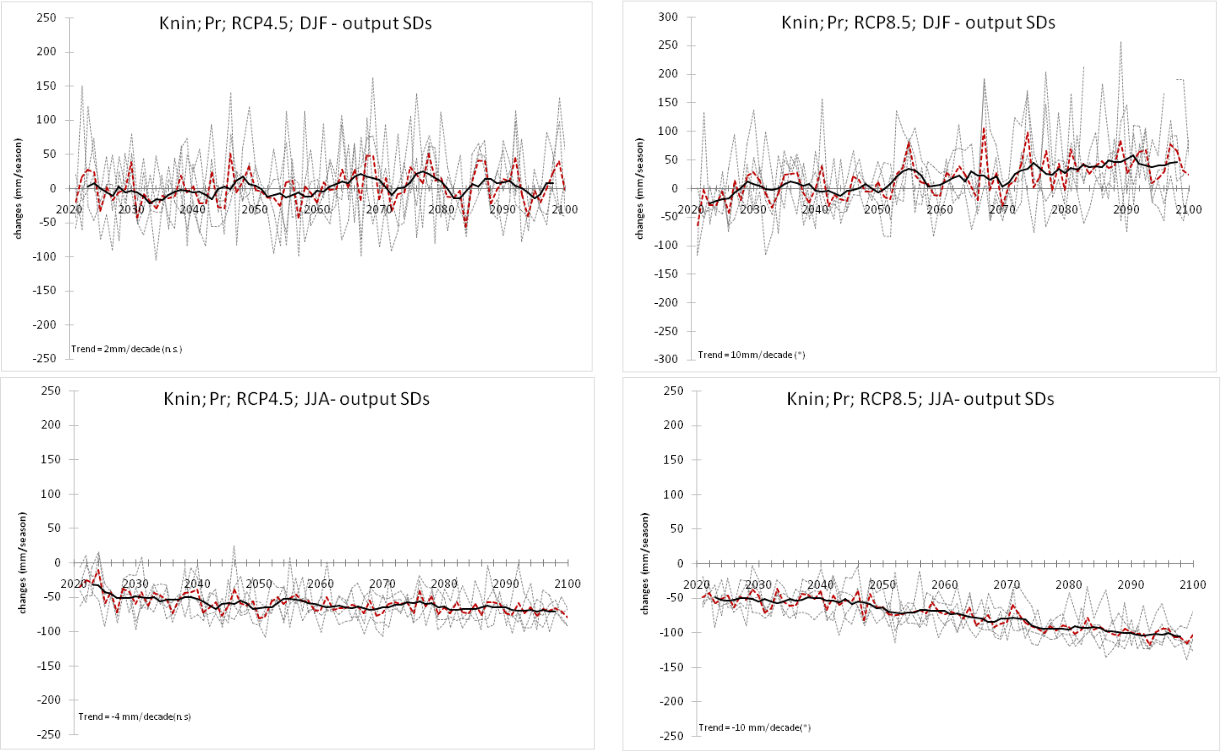

Figure 5-36: Variability of future changes of winter (DJF) and summer (JJA) precipitation (mm/season) projected through SDs applied to 4GCMs (grey lines); the Ensemble Mean (red line) and moving average (black line) - scenario RCP4.5 (left) and RCP8.5 (right), 2021-2100 period. Significant trend is marked with star while n.s. means not significant (source Arpae-Simc).

6.1.2.2.2 *Intense precipitation*

90th percentile of seasonal amount of precipitation

Intense precipitation, defined by 90th percentile of daily precipitation shows for Knin a general slightly decrease at annual level up to -10% going to the end of century ((see figure 5-37)). All SDs model agree with this signal at annual level. At seasonal time scale, a decrease could occur during winter, spring and autumn while an increase is noted during summer especially on P3 and P4 (up to 10%). The signal is statistically significant especially for RCP8.5 in autumn and in winter in the P3 and P4. Long term variability emphasis a negative trend in winter and positive in summer, both of them not statistically significant (figure 5-38).

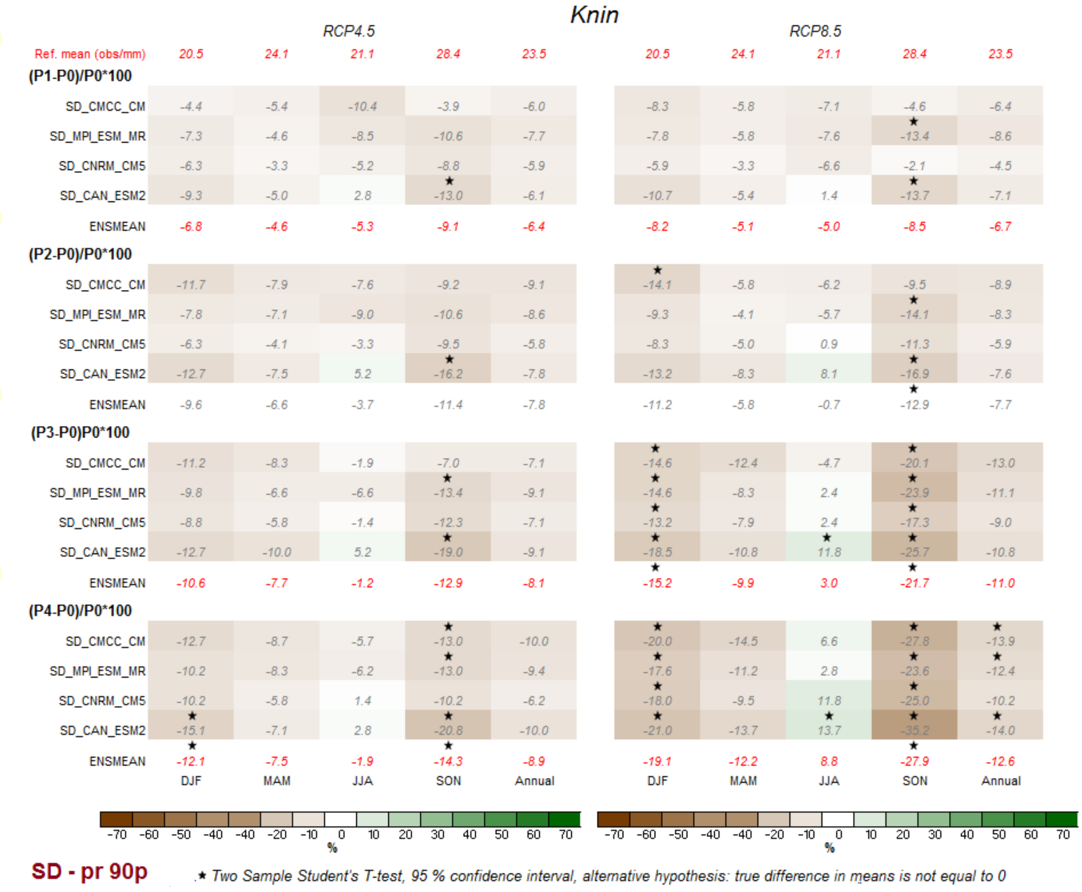

Knin

	RCP4.5					RCP8.5				
Ref. mean (obs/mm)	20.5	24.1	21.1	28.4	23.5	20.5	24.1	21.1	28.4	23.5
(P1-P0)/P0*100										
SD_CMCC_CM	-4.4	-5.4	-10.4	-3.9	-6.0	-8.3	-5.8	-7.1	-4.6	-6.4
SD_MPI_ESM_MR	-7.3	-4.6	-8.5	-10.6	-7.7	-7.8	-5.8	-7.6	★ -13.4	-8.6
SD_CNRM_CM5	-6.3	-3.3	-5.2	-8.8	-5.9	-5.9	-3.3	-6.6	-2.1	-4.5
SD_CAN_ESM2	-9.3	-5.0	2.8	★ -13.0	-6.1	-10.7	-5.4	1.4	★ -13.7	-7.1
ENSMEAN	-6.8	-4.6	-5.3	-9.1	-6.4	-8.2	-5.1	-5.0	-8.5	-6.7
(P2-P0)/P0*100										
SD_CMCC_CM	-11.7	-7.9	-7.6	-9.2	-9.1	★ -14.1	-5.8	-6.2	-9.5	-8.9
SD_MPI_ESM_MR	-7.8	-7.1	-9.0	-10.6	-8.6	-9.3	-4.1	-5.7	★ -14.1	-8.3
SD_CNRM_CM5	-6.3	-4.1	-3.3	-9.5	-5.8	-8.3	-5.0	0.9	-11.3	-5.9
SD_CAN_ESM2	-12.7	-7.5	5.2	★ -16.2	-7.8	-13.2	-8.3	8.1	★ -16.9	-7.6
ENSMEAN	-9.6	-6.6	-3.7	-11.4	-7.8	-11.2	-5.8	-0.7	★ -12.9	-7.7
(P3-P0)P0*100										
SD_CMCC_CM	-11.2	-8.3	-1.9	-7.0	-7.1	★ -14.6	-12.4	-4.7	★ -20.1	-13.0
SD_MPI_ESM_MR	-9.8	-6.6	-6.6	★ -13.4	-9.1	★ -14.6	-8.3	2.4	★ -23.9	-11.1
SD_CNRM_CM5	-8.8	-5.8	-1.4	-12.3	-7.1	★ -13.2	-7.9	2.4	★ -17.3	-9.0
SD_CAN_ESM2	-12.7	-10.0	5.2	★ -19.0	-9.1	★ -18.5	-10.8	★ 11.8	★ -25.7	-10.8
ENSMEAN	-10.6	-7.7	-1.2	-12.9	-8.1	★ -15.2	-9.9	3.0	★ -21.7	-11.0
(P4-P0)/P0*100										
SD_CMCC_CM	-12.7	-8.7	-5.7	★ -13.0	-10.0	★ -20.0	-14.5	6.6	★ -27.8	★ -13.9
SD_MPI_ESM_MR	-10.2	-8.3	-6.2	★ -13.0	-9.4	★ -17.6	-11.2	2.8	★ -23.6	★ -12.4
SD_CNRM_CM5	-10.2	-5.8	1.4	-10.2	-6.2	★ -18.0	-9.5	11.8	★ -25.0	-10.2
SD_CAN_ESM2	★ -15.1	-7.1	2.8	★ -20.8	-10.0	★ -21.0	-13.7	★ 13.7	★ -35.2	★ -14.0
ENSMEAN	★ -12.1	-7.5	-1.9	★ -14.3	-8.9	-19.1	-12.2	8.8	★ -27.9	-12.6
	DJF	MAM	JJA	SON	Annual	DJF	MAM	JJA	SON	Annual

SD - pr 90p

★ *Two Sample Student's T-test, 95 % confidence interval, alternative hypothesis: true difference in means is not equal to 0*

Figure 5-37: Seasonal and annual amount of 90th precipitation: observed values over reference period (in red), changes (%) projected by statistical downscaling applied to 4GCMs and the Ensemble Mean over the four periods (P1, P2 ,P3, P4) projected in the framework of RCP4.5 (left) and RCP 8.5(right). Significant change is marked by star (source Arpae-Simc)

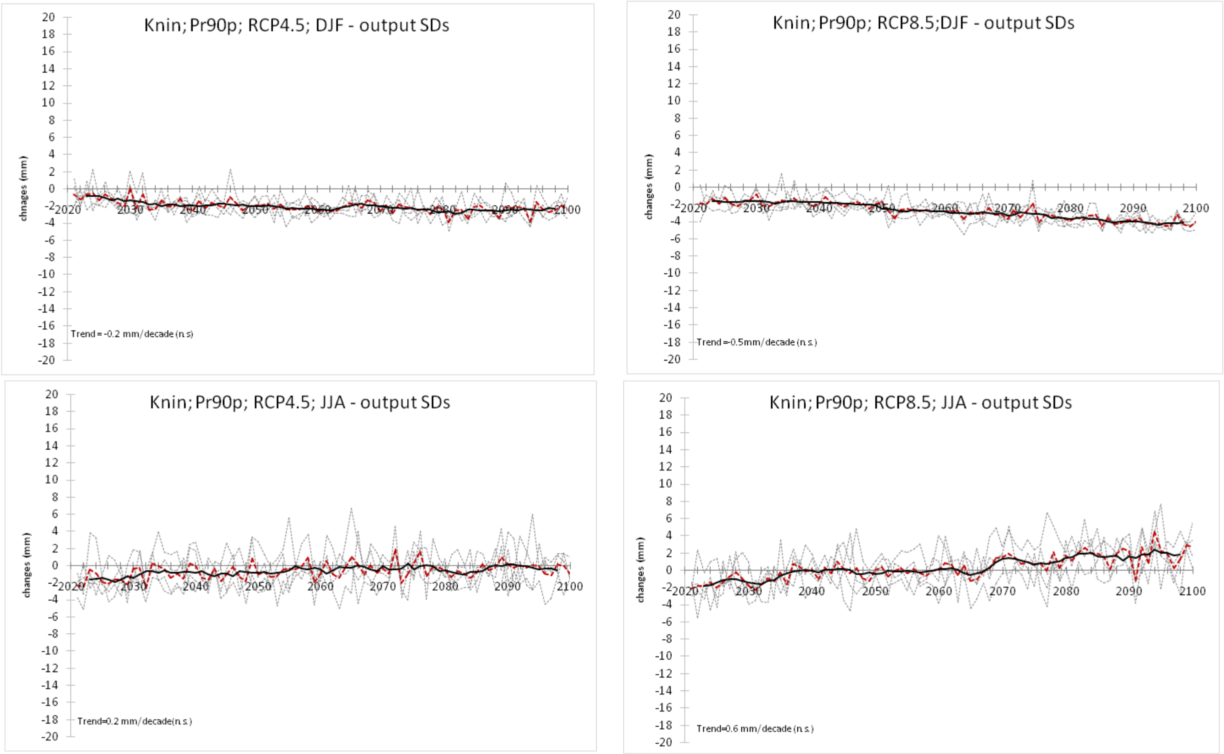

Figure 5-38: Variability of future changes of winter (DJF) and summer (JJA) 90th precipitation projected through SDs applied to 4GCMs (grey lines); the Ensemble Mean (red line) and moving average (black line) - scenario RCP4.5 (left) and RCP8.5 (right), 2021-2100 period. Significant trend is marked with star while n.s. means not significant (source Arpae-Simc).

6.1.2.2.3 *Consecutive dry days*

The consecutive dry days, defined as the maximum number of consecutive days without precipitation shows for Knin an increase during spring, summer and autumn and a decrease during winter. The values of projected changes are significant for RCP8.5, especially during summer and autumn seasons and going to the end of century, when the changes could reach 10 consecutive days (figure 5-39). The long-term variability reveals slightly negative trends during winter and positive during summer up to 1.5 days/decade in RCP8.5 (figure 5-40).

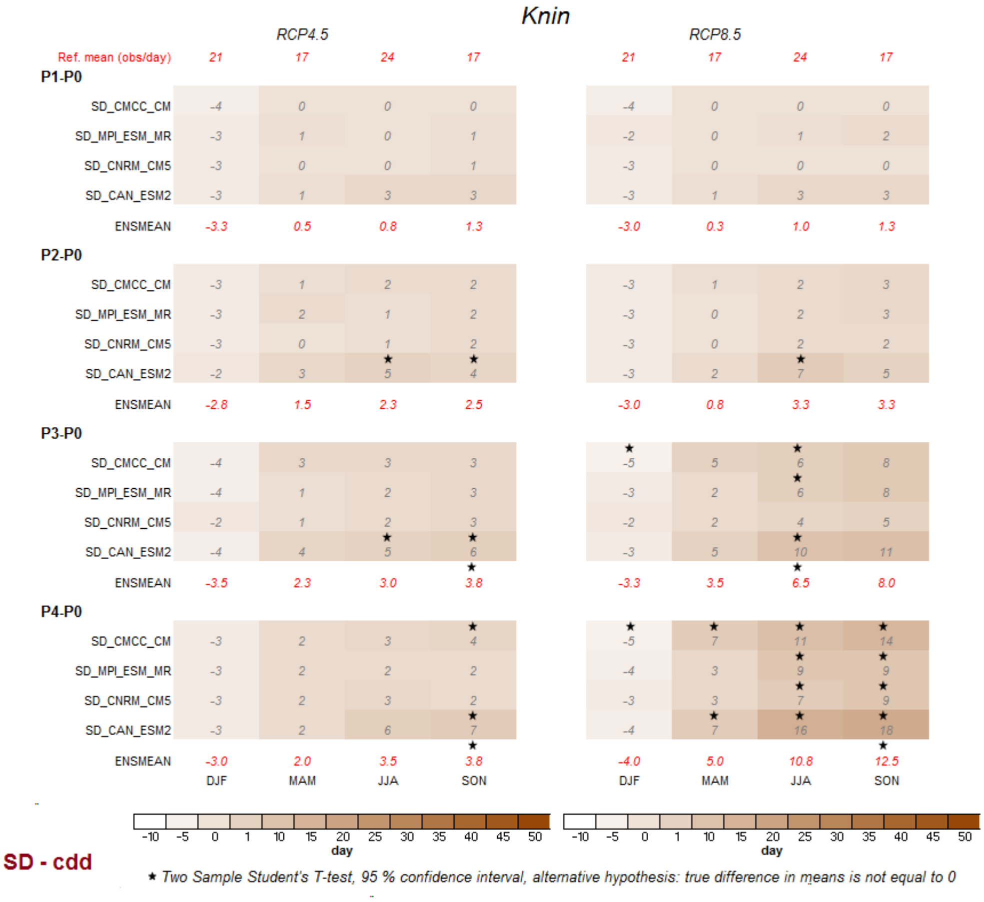

Knin

		RCP4.5				RCP8.5		
Ref. mean (obs/day)	21	17	24	17	21	17	24	17
P1-P0								
SD_CMCC_CM	-4	0	0	0	-4	0	0	0
SD_MPI_ESM_MR	-3	1	0	1	-2	0	1	2
SD_CNRM_CM5	-3	0	0	1	-3	0	0	0
SD_CAN_ESM2	-3	1	3	3	-3	1	3	3
ENSMEAN	-3.3	0.5	0.8	1.3	-3.0	0.3	1.0	1.3
P2-P0								
SD_CMCC_CM	-3	1	2	2	-3	1	2	3
SD_MPI_ESM_MR	-3	2	1	2	-3	0	2	3
SD_CNRM_CM5	-3	0	1	2	-3	0	2	2
SD_CAN_ESM2	-2	3	★ 5	★ 4	-3	2	★ 7	5
ENSMEAN	-2.8	1.5	2.3	2.5	-3.0	0.8	3.3	3.3
P3-P0								
SD_CMCC_CM	-4	3	3	3	★ -5	5	★ 6	8
SD_MPI_ESM_MR	-4	1	2	3	-3	2	★ 6	8
SD_CNRM_CM5	-2	1	2	3	-2	2	4	5
SD_CAN_ESM2	-4	4	★ 5	★ 6	-3	5	★ 10	11
ENSMEAN	-3.5	2.3	3.0	★ 3.8	-3.3	3.5	★ 6.5	8.0
P4-P0								
SD_CMCC_CM	-3	2	3	★ 4	★ -5	★ 7	★ 11	★ 14
SD_MPI_ESM_MR	-3	2	2	2	-4	3	★ 9	★ 9
SD_CNRM_CM5	-3	2	3	2	-3	3	★ 7	★ 9
SD_CAN_ESM2	-3	2	6	★ 7	-4	★ 7	★ 16	★ 18
ENSMEAN	-3.0	2.0	3.5	★ 3.8	-4.0	5.0	10.8	★ 12.5
	DJF	MAM	JJA	SON	DJF	MAM	JJA	SON

★ Two Sample Student's T-test, 95 % confidence interval, alternative hypothesis: true difference in means is not equal to 0

Figure 5-39: Seasonal max. consecutive dry days: observed values over reference period (in red), changes projected by statistical downscaling applied to 4GCMs and the Ensemble Mean over the four periods (P1, P2, P3, P4) projected in the framework of RCP4,5 (left) and RCP 8.5 (right). Significant change is marked by star (source Arpae-Simc)

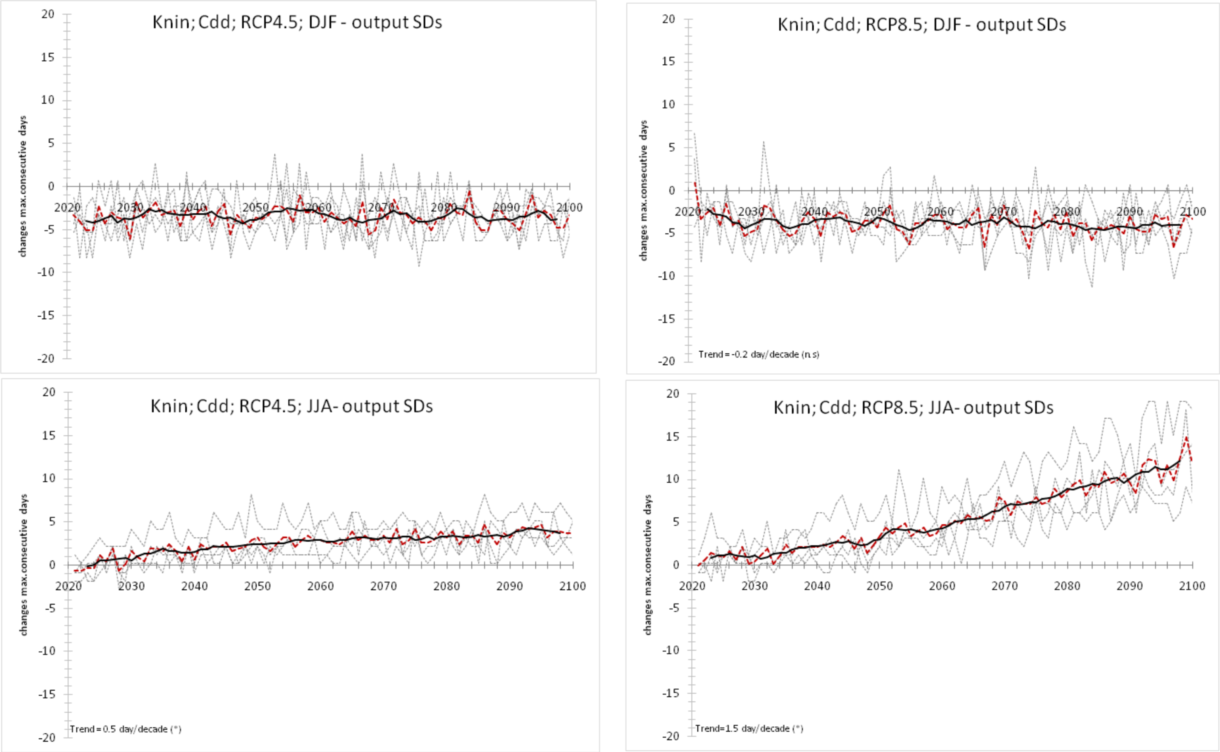

Figure 5-40: Variability of future changes of winter (DJF) and summer (JJA) max. number of consecutive dry days projected through SDs applied to 4GCMs (grey lines); the Ensemble Mean (red line) and moving average (black line) - scenario RCP4.5 (left) and RCP8.5 (right), 2021-2100 period. Significant trend is marked with star while n.s. means not significant (source Arpae-Simc).

6.2 Case study 2: Šibenik

6.2.1 Dynamically downscaled results

In this section we present future climate change of temperature and precipitation related indices, surface relative humidity and extra rare humidex projections for Šibenik. All indices are calculated from the available data set of regional climate models for the grid point that is representing the location of case study Šibenik. Data set is obtained by bilinear interpolation. All data are presented as follows:

- Climate change diagram of an individual index in seasons and on annual basis for four considered future periods, for two emission scenarios RCP4.5 and RCP8.5. Climate change is calculated as difference between future and reference period (relative difference for precipitation indices and surface relative humidity). Reference period is presented as ensemble mean of available regional climate models (Ref.mean), while climate change is shown for different models as well as for ensemble mean of models (ENSMEAN). Two sample Wilcoxon test is applied to test statistical significance of climate change for individual models (for 95 % confidence level). Significant change is marked by star
- Time series of future anomaly of an individual index for DJF and JJA and for two emission scenarios RCP4.5 and RCP8.5. Anomaly is calculated respect to the reference period and shown for individual models, ensemble mean and 5-year moving average. Mann Kendall trend test is applied to ensemble mean (for 95 % confidence level). Significant trend is marked with star (ns if not significant).

6.2.1.1 *Temperature related indices projections*

6.2.1.1.1 *Averaged 2 meter air temperature*

Averaged temperature change (Figure 5-41) in Šibenik shows increase in all seasons and on annual scale, for all future periods (exception is in winter for two models realisations in first two periods). Although each model gives different amplitude of change, in ensemble mean the change is highest during summer and the smallest in winter, for RCP4.5. The temperature increase is more pronounced towards the end of the century when the increase in the ensemble mean is from 1.4 °C in DJF to 2.2 °C in JJA. On annual scale for RCP4.5 temperature increase is for 1.7 °C. The amplitude of temperature change is more pronounced for RCP8.5 scenario, from 3.0 °C in MAM to 4.4 °C in JJA, on annual scale 3.6 °C at the end of 21st century for ensemble mean. The linear trend of temperature anomaly (Figure 5-42) in the future shows increase which is statistically significant for both considered seasons and both scenarios; for DJF ensemble is 0.19 °C

/ 10 year for RCP4.5 and 0.54 °C / 10 year for RCP8.5; for JJA ensemble is 0.18 °C / 10 year for RCP4.5 and 0.52 °C / 10 year.

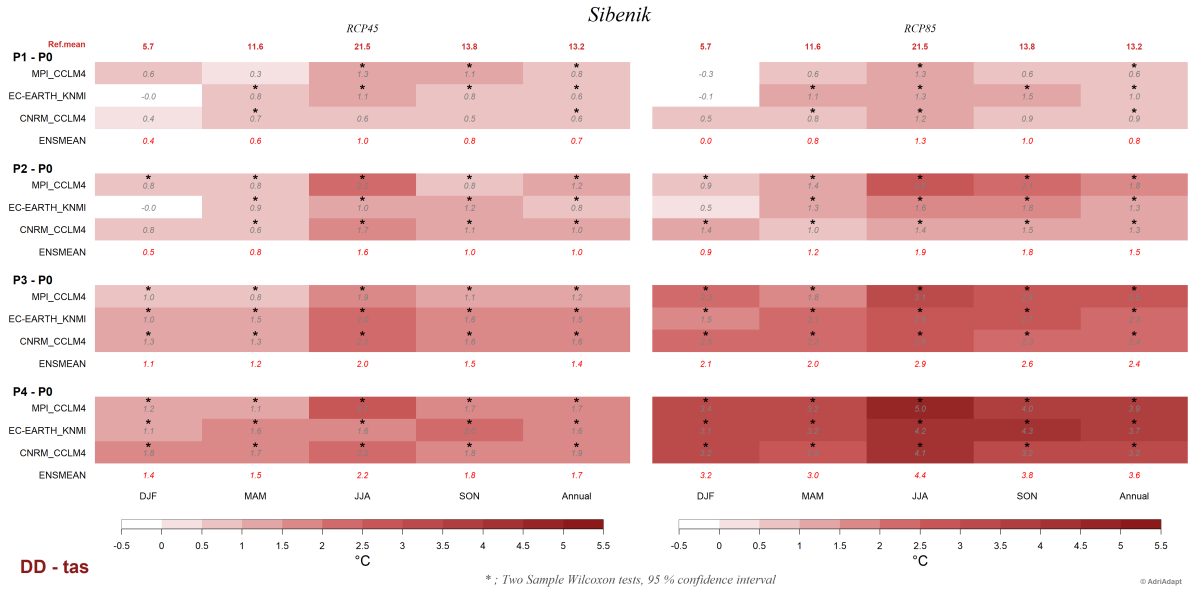

Figure 5-41: Averaged seasonal and annual 2m air temperature (in °C) obtained by dynamical downscaling for Šibenik: Ref. mean is 20 year simulated period (1986-2005) for ensemble mean; P1-P0, P2-P0, P3-P0, P4-P0 are changes in the future for following periods P1: 2021-2040, P2: 2041-2060, P3: 2061-2080, P4: 2081-2100. Differences are shown for individual models. Significant change is marked by star. Change is also shown as ensemble mean (ENSMEAN), not tested for significance. Left column is for RCP4.5 scenario and right for RCP8.5 scenario.

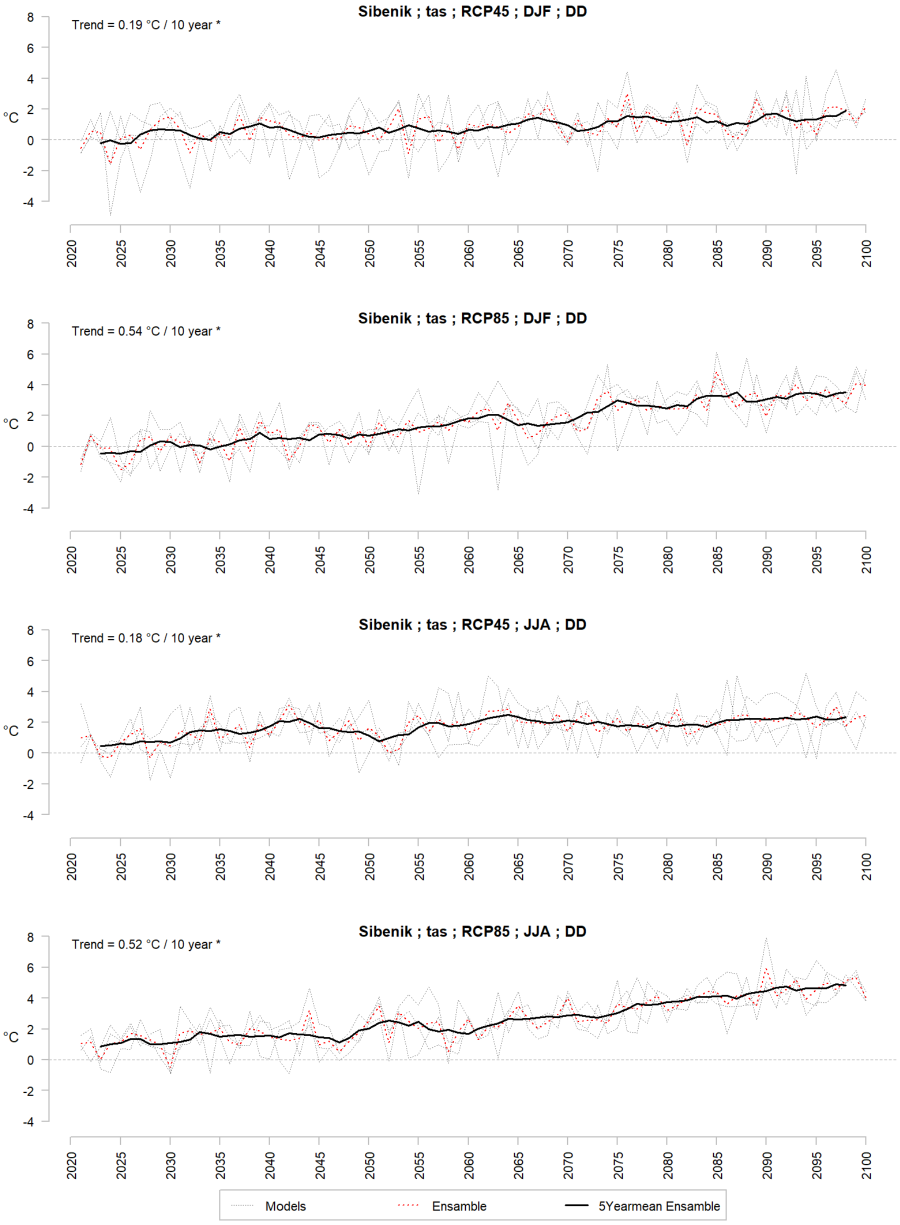

Figure 5-42: Variability of future 2m air temperature anomaly (in °C) in Šibenik for 2021-2100 obtained by dynamically downscaling for winter (DJF) and summer (JJA) and two RCP scenarios: individual models are in grey, the ensemble mean in red, 5-year moving average in black. Significant trend is marked with star (ns if not significant).

6.2.1.1.2 *Extreme high temperature*

99th percentile of 2m air temperature (Figure 5-43) in Šibenik is increasing from P1 to P4 future periods with the different amplitudes for each model. In ensemble mean at the end of century increase is from 1.0 °C in DJF to 2.6 °C in JJA, 2.6 °C on annual scale for RCP4.5. Amplitude of change is more pronounced for RCP8.5 and is between 2.8 °C in DJF and 4.8 °C in SON, 4.7 °C for annual change at the end of 21st century. Variability of future 99th percentile of 2m air temperature anomaly (Figure 5-44) shows linear trend in change of ensemble mean, 0.17 °C / 10 year in DJF for RCP4.5 and 0.45 °C / 10 year for RCP8.5; 0.17 °C / 10 year in JJA for RCP4.5 and 0.54 °C / 10 year for RCP8.5. All trends are statistically significant.

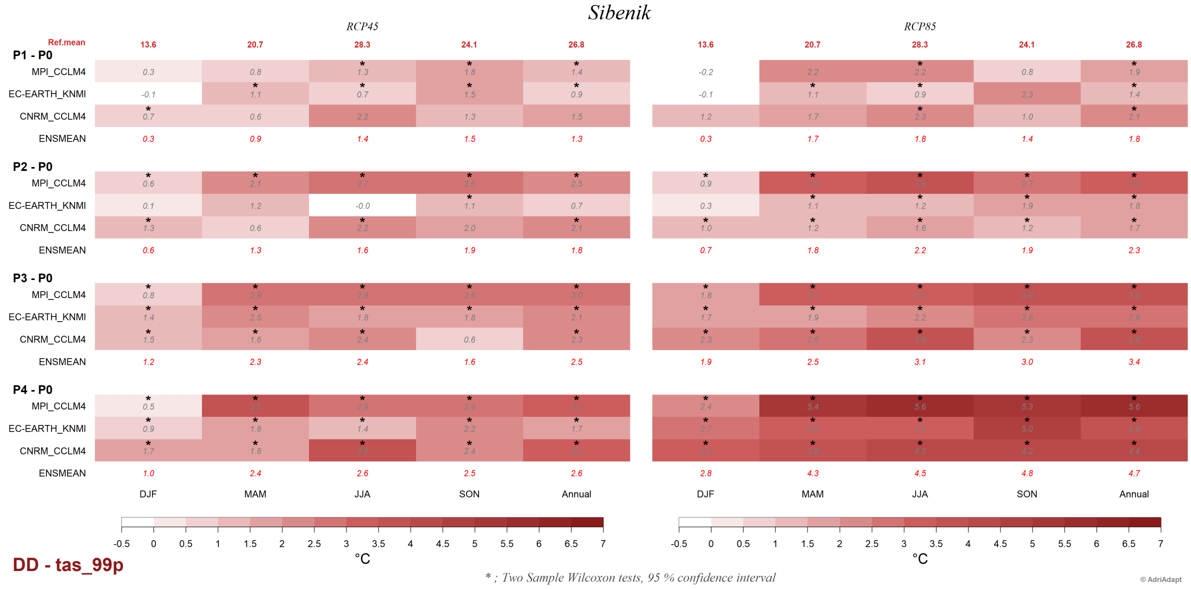

Figure 5-43: Seasonal and annual 99th percentile of 2m air temperature (extreme high temperature, in °C) obtained by dynamical downscaling for Šibenik: Ref. mean is 20 year simulated period (1986-2005) for ensemble mean; P1-P0, P2-P0, P3-P0, P4-P0 are changes in the future for following periods P1: 2021-2040, P2: 2041-2060, P3: 2061-2080, P4: 2081-2100. Differences are shown for individual models. Significant change is marked by star. Change is also shown as ensemble mean (ENSMEAN), not tested for significance. Left column is for RCP4.5 scenario and right for RCP8.5 scenario.

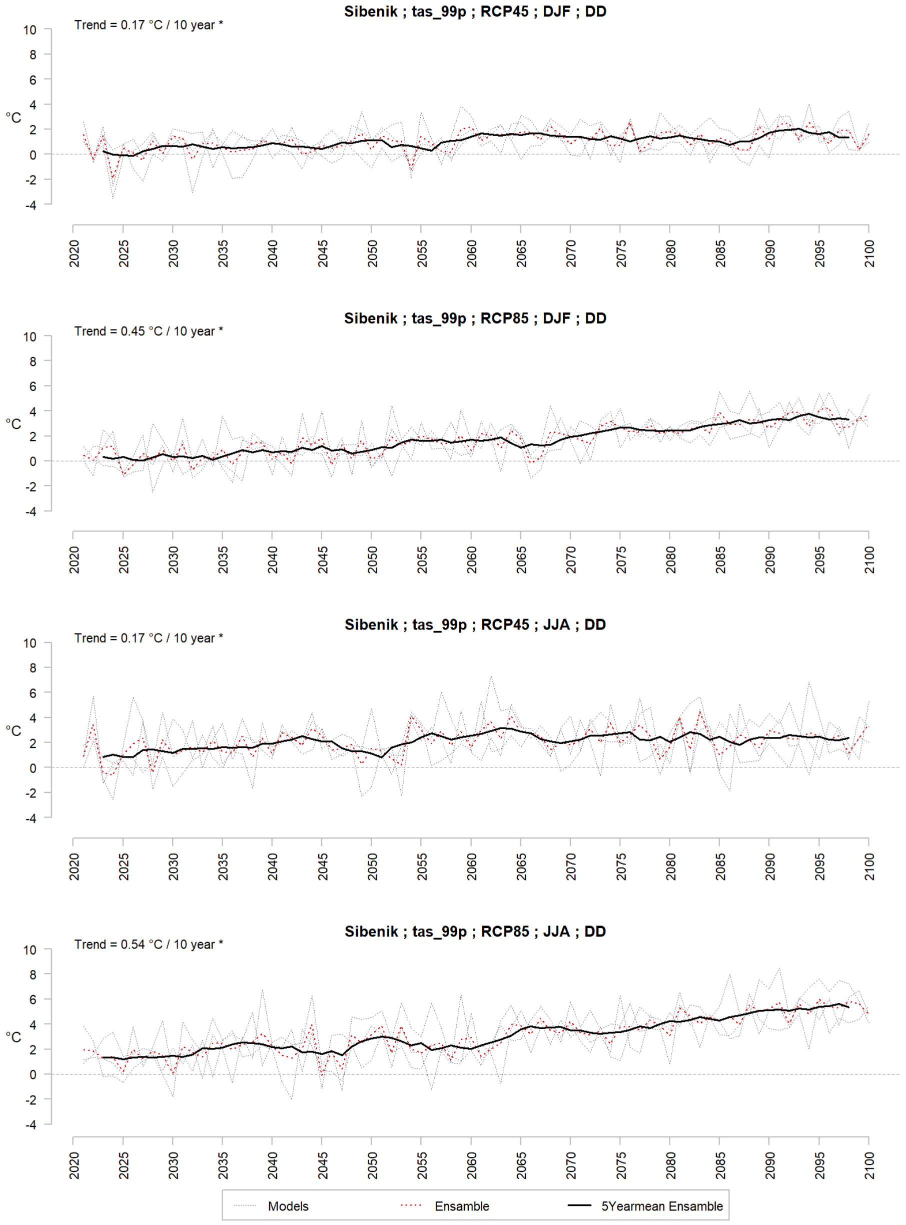

Figure 5-44: Variability of future 99th percentile of 2m air temperature (extreme high temperature) anomaly (in °C) in Šibenik for 2021-2100 obtained by dynamically downscaling for winter (DJF) and summer (JJA) and two RCP scenarios: individual models are in grey, the ensemble mean in red, 5-year moving average in black. Significant trend is marked with star (ns if not significant).

6.2.1.1.3 *Extreme high maximum temperature*

Future change of 99th percentile of 2m maximum air temperature (Figure 5-45) in Šibenik is increasing from P1 to P4 periods with the different amplitudes for each model. Although some models show slight decrease for some seasons, in ensemble mean for all periods the change is positive. At the end of century increase is from 1.1 °C in DJF to 2.8 °C in SON, 2.6 °C on annual scale for RCP4.5. Amplitude of change is more pronounced for RCP8.5 and is between 3.0 °C in DJF and 5.1 °C in SON, 4.7 °C for annual change at the end of 21st century. Variability of future 99th percentile of 2m maximum air temperature anomaly (Figure 5-46) shows linear trend in change of ensemble mean, 0.19 °C / 10 year in DJF for RCP4.5 and 0.48 °C / 10 year for RCP8.5; 0.22 °C / 10 year in JJA for RCP4.5 and 0.50 °C / 10 year for RCP8.5. All trends are statistically significant.

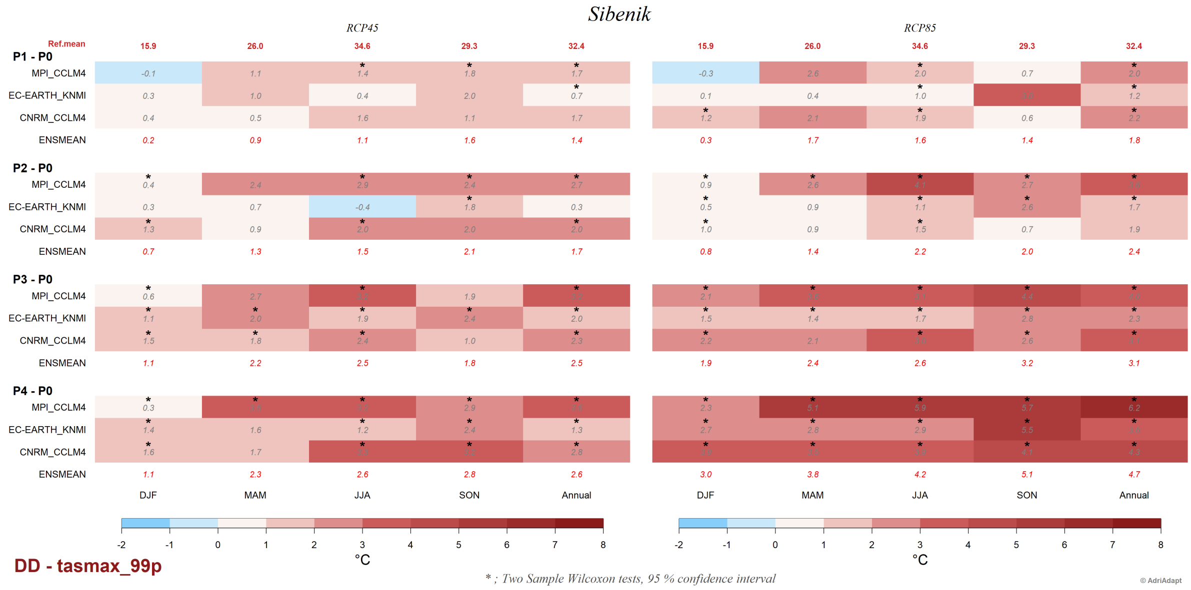

Figure 5-45: Seasonal and annual 99th percentile of 2m maximum air temperature (extreme high maximum temperature, in °C) obtained by dynamical downscaling for Šibenik: Ref. mean is 20 year simulated period (1986-2005) for ensemble mean; P1-P0, P2-P0, P3-P0, P4-P0 are changes in the future for following periods P1: 2021-2040, P2: 2041-2060, P3: 2061-2080, P4: 2081-2100. Differences are shown for individual models. Significant change is marked by star. Change is also shown as ensemble mean (ENSMEAN), not tested for significance. Left column is for RCP4.5 scenario and right for RCP8.5 scenario.

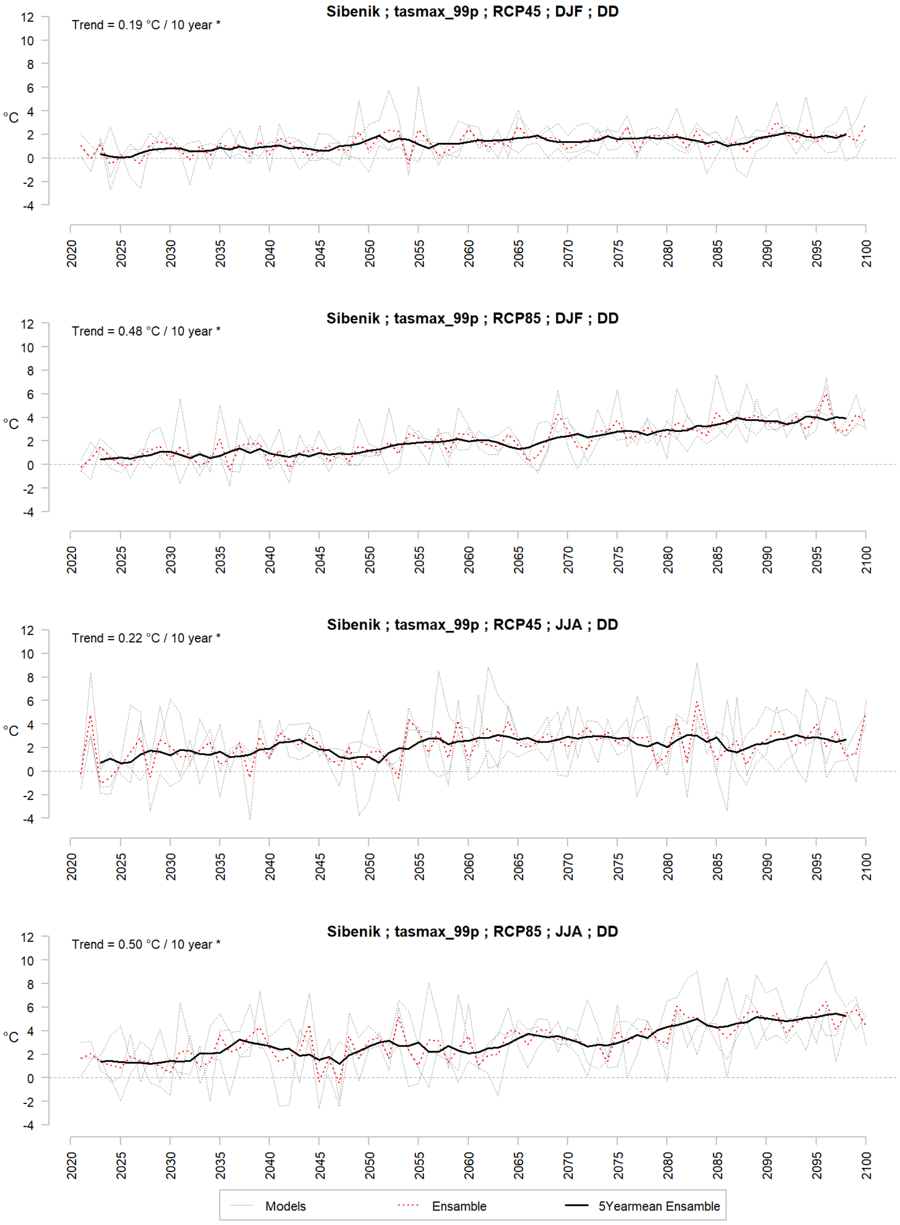

Figure 5-46: Variability of future 99th percentile of 2m maximum air temperature (extreme high maximum temperature) anomaly (in °C) in Šibenik for 2021-2100 obtained by dynamically downscaling for winter (DJF) and summer (JJA) and two RCP scenarios: individual models are in grey, the ensemble mean in red, 5-year moving average in black. Significant trend is marked with star (ns if not significant).

6.2.1.1.4 *Extreme rare high temperature*

Future change of 99.9th percentile of 2m air temperature (Figure 5-47) in Šibenik is increasing from P1 to P4 periods with the different amplitudes for each model. Slightly negative change appears for some seasons and some models in two first periods, but the change of ensemble mean is positive for all periods. At the end of century increase is from 0.9 °C in DJF to 2.5 °C in SON, 2.6 °C on annual scale for RCP4.5. Amplitude of change is more pronounced for RCP8.5 and is between 2.7 °C in DJF and 4.9 °C in SON, 4.5 °C for annual change at the end of 21st century. Variability of future 99.9th percentile of 2m air temperature anomaly (Figure 5-48) shows linear trend in change of ensemble mean, 0.17 °C / 10 year in DJF for RCP4.5 and 0.45 °C / 10 year for RCP8.5; 0.17 °C / 10 year in JJA for RCP4.5 and 0.54 °C / 10 year for RCP8.5. All trends are statistically significant.

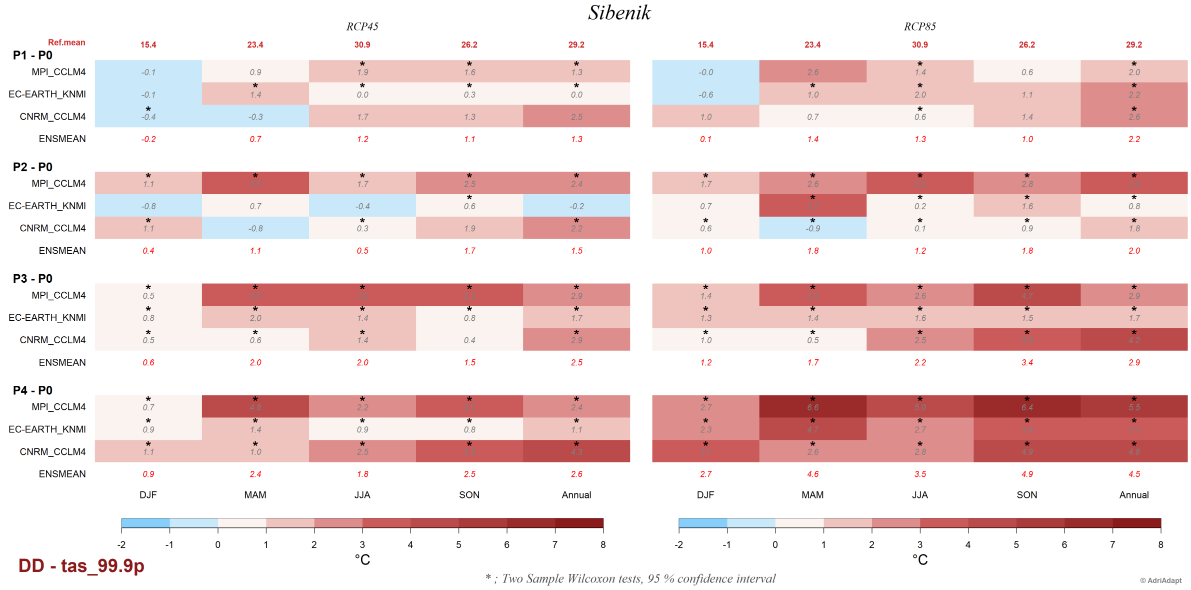

Figure 5-47: Seasonal and annual 99.9th percentile of 2m air temperature (extreme rare high temperature, in °C) obtained by dynamical downscaling for Šibenik: Ref. mean is 20 year simulated period (1986-2005) for ensemble mean; P1-P0, P2-P0, P3-P0, P4-P0 are changes in the future for following periods P1: 2021-2040, P2: 2041-2060, P3: 2061-2080, P4: 2081-2100. Differences are shown for individual models. Significant change is marked by star. Change is also shown as ensemble mean (ENSMEAN), not tested for significance. Left column is for RCP4.5 scenario and right for RCP8.5 scenario.

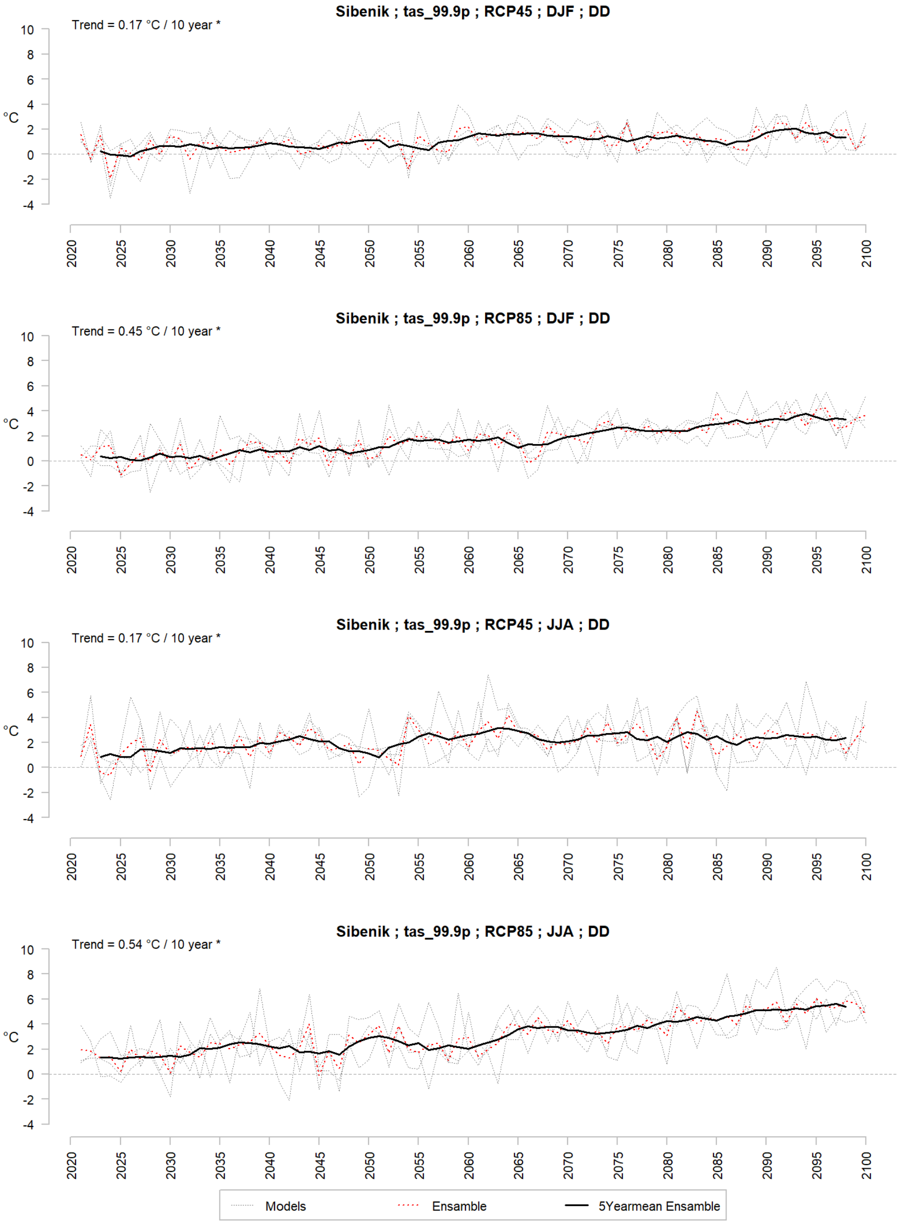

Figure 5-48: Variability of future 99.9th percentile of 2m air temperature (extreme rare high temperature) anomaly (in °C) in Šibenik for 2021-2100 obtained by dynamically downscaling for winter (DJF) and summer (JJA) and two RCP scenarios: individual models are in grey, the ensemble mean in red, 5-year moving average in black. Significant trend is marked with star (ns if not significant).

6.2.1.1.5 *Extreme rare high maximum temperature*

Future change of 99.9th percentile of 2m maximum air temperature (Figure 5-49) in Šibenik is changing from P1 to P4 periods with the different amplitudes for each model. Some models show for some time slices negative change, but in general ensemble mean for all seasons and annual change are positive. At the end of 21st century changes are between 1.9 °C in DJF and 3.6 °C in MAM, 2.7 °C for annual for RCP4.5 scenario. Amplitude of change is more pronounced for RCP8.5 and is between 2.8 °C in JJA and 5.2 °C in SON, 4.4 °C for annual change at the end of 21st century. Variability of future 99.9th percentile of 2m maximum air temperature anomaly (Figure 5-50) shows linear trend in change of ensemble mean, 0.19 °C / 10 year in DJF for RCP4.5 and 0.47 °C / 10 year for RCP8.5; 0.22 °C / 10 year in JJA for RCP4.5 and 0.50 °C / 10 year for RCP8.5. All trends are statistically significant.

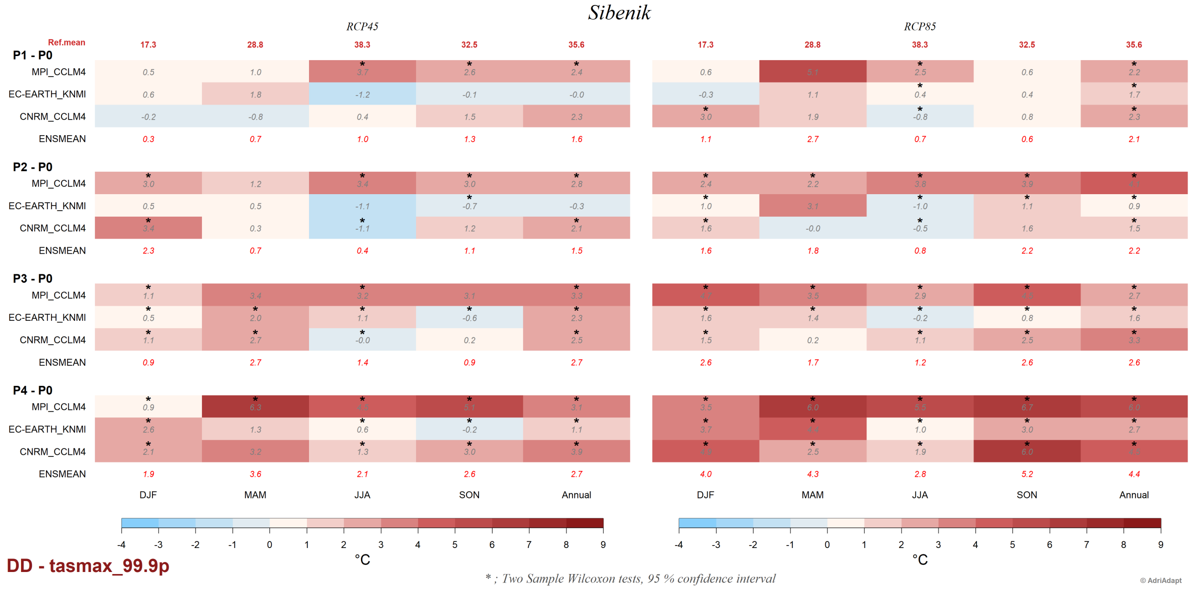

RCP45

	DJF	MAM	JJA	SON	Annual
Ref.mean	17.3	28.8	38.3	32.5	35.6
P1 - P0					
MPI_CCLM4	0.5	1.0	* 3.7	* 2.6	* 2.4
EC-EARTH_KNMI	0.6	1.8	-1.2	-0.1	-0.0
CNRM_CCLM4	-0.2	-0.8	0.4	1.5	2.3
ENSMEAN	0.3	0.7	1.0	1.3	1.6
P2 - P0					
MPI_CCLM4	* 3.0	1.2	* 3.4	* 3.0	* 2.8
EC-EARTH_KNMI	0.5	0.5	-1.1	* -0.7	-0.3
CNRM_CCLM4	* 3.4	0.3	* -1.1	1.2	* 2.1
ENSMEAN	2.3	0.7	0.4	1.1	1.5
P3 - P0					
MPI_CCLM4	* 1.1	3.4	* 3.2	3.1	* 3.3
EC-EARTH_KNMI	* 0.5	* 2.0	* 1.1	* -0.6	* 2.3
CNRM_CCLM4	* 1.1	* 2.7	* -0.0	0.2	* 2.5
ENSMEAN	0.9	2.7	1.4	0.9	2.7
P4 - P0					
MPI_CCLM4	* 0.9	* 6.3	* 4.5	* 5.1	* 3.1
EC-EARTH_KNMI	* 2.6	1.3	* 0.6	* -0.2	* 1.1
CNRM_CCLM4	* 2.1	3.2	* 1.3	* 3.0	* 3.9
ENSMEAN	1.9	3.6	2.1	2.6	2.7

RCP85

	DJF	MAM	JJA	SON	Annual
Ref.mean	17.3	28.8	38.3	32.5	35.6
P1 - P0					
MPI_CCLM4	0.6	5.1	* 2.5	0.6	* 2.2
EC-EARTH_KNMI	-0.3	1.1	* 0.4	0.4	* 1.7
CNRM_CCLM4	* 3.0	1.9	* -0.8	0.8	* 2.3
ENSMEAN	1.1	2.7	0.7	0.6	2.1
P2 - P0					
MPI_CCLM4	* 2.4	* 2.2	* 3.8	* 3.9	* 4.1
EC-EARTH_KNMI	* 1.0	3.1	* -1.0	* 1.1	* 0.9
CNRM_CCLM4	* 1.6	-0.0	* -0.5	1.6	* 1.5
ENSMEAN	1.6	1.8	0.8	2.2	2.2
P3 - P0					
MPI_CCLM4	* 4.7	* 3.5	* 2.9	* 4.5	* 2.7
EC-EARTH_KNMI	* 1.6	* 1.4	* -0.2	* 0.8	* 1.6
CNRM_CCLM4	* 1.5	0.2	* 1.1	* 2.5	* 3.3
ENSMEAN	2.6	1.7	1.2	2.6	2.6
P4 - P0					
MPI_CCLM4	* 3.5	* 6.0	* 5.5	* 6.7	* 6.0
EC-EARTH_KNMI	* 3.7	* 4.4	* 1.0	* 3.0	* 2.7
CNRM_CCLM4	* 4.9	* 2.5	* 1.9	* 6.0	* 4.5
ENSMEAN	4.0	4.3	2.8	5.2	4.4

** ; Two Sample Wilcoxon tests, 95 % confidence interval*

Figure 5-49: Seasonal and annual 99.9th percentile of 2m maximum air temperature (extreme rare high maximum temperature, in °C) obtained by dynamical downscaling for Šibenik: Ref. mean is 20 year simulated period (1986-2005) for ensemble mean; P1-P0, P2-P0, P3-P0, P4-P0 are changes in the future for following periods P1: 2021-2040, P2: 2041-2060, P3: 2061-2080, P4: 2081-2100. Differences are shown for individual models. Significant change is marked by star. Change is also shown as ensemble mean (ENSMEAN), not tested for significance. Left column is for RCP4.5 scenario and right for RCP8.5 scenario.

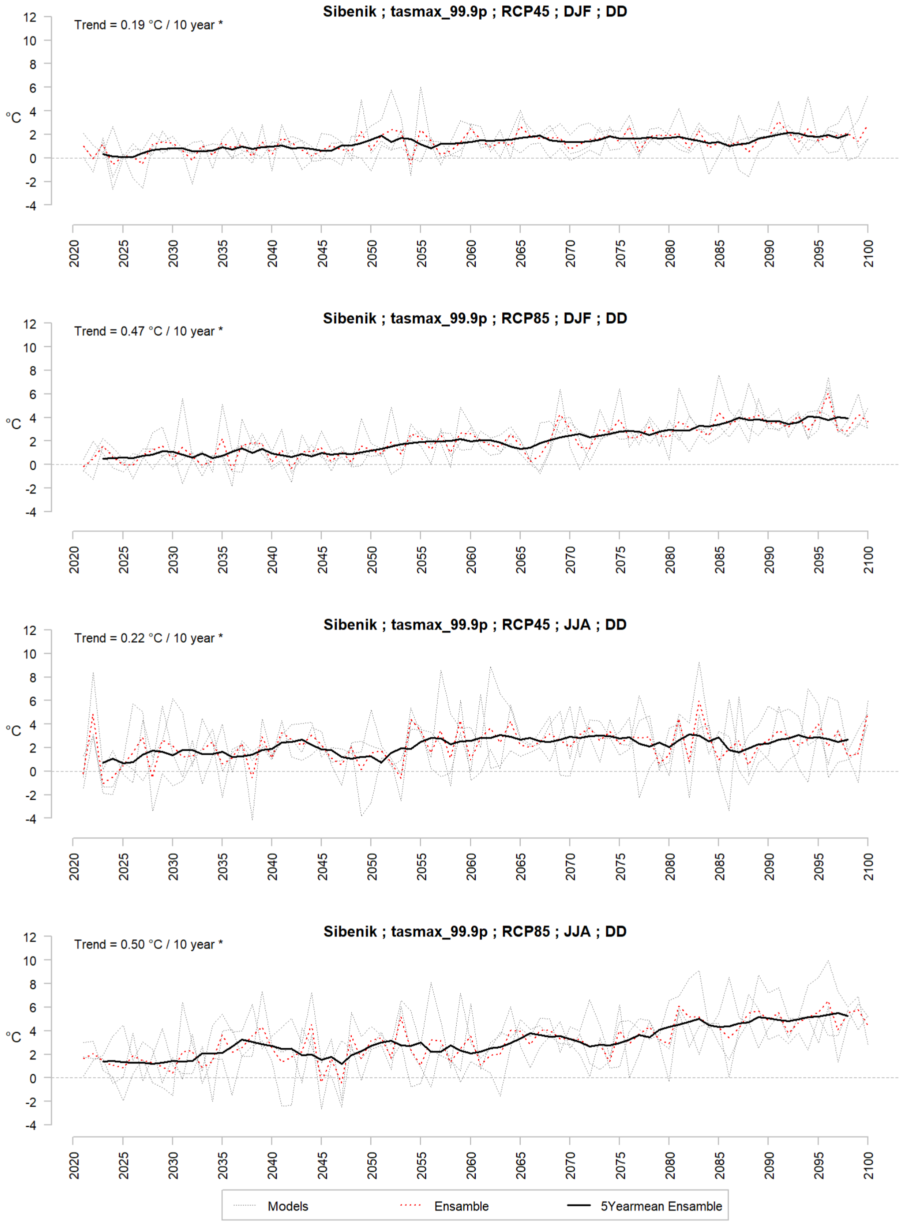

Figure 5-50: Variability of future 99.9th percentile of 2m maximum air temperature (extreme rare high maximum temperature) anomaly (in °C) in Šibenik for 2021-2100 obtained by dynamically downscaling for winter (DJF) and summer (JJA) and two RCP scenarios: individual models are in grey, the ensemble mean in red, 5-year moving average in black. Significant trend is marked with star (ns if not significant).

6.2.1.2 *Precipitation related indices projections*

6.2.1.2.1 *Averaged precipitation*

Averaged precipitation obtained by dynamical downscaling is expressed in mm/day and its change in the future is shown as relative to the P0 period. Precipitation is much more variable parameter in comparison to the temperature, therefore there is no always unique sign of change through the year as well as from model to model. The change in ensemble mean (Figure 5-51) for Šibenik gives increase of precipitation for colder part of the year at the end of century (6.2 % for DJF, 9.1 % for SON) and decrease in the warmer part (-1.8 % in MAM, -7.4 % in JJA) for RCP4.5; on annual scale precipitation will increase for 3.0 %. For scenario RCP8.5, precipitation will decrease in JJA (-22.7 %) and increase in DJF (11.8 %). On annual scale there is almost no change at the end of century. Although variability of future precipitation anomaly (Figure 5-52) for ensemble mean in Šibenik for both scenarios shows increase in precipitation in DJF and decrease of precipitation in JJA, linear trends are not statistically significant.

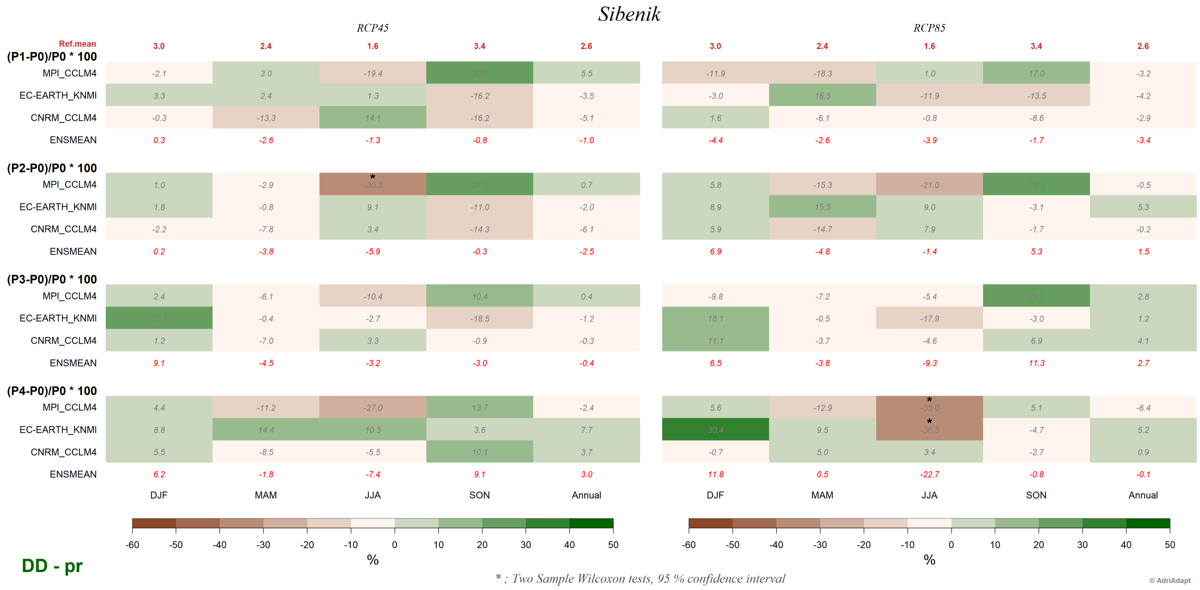

Sibenik

	RCP45					RCP85				
	DJF	MAM	JJA	SON	Annual	DJF	MAM	JJA	SON	Annual
Ref.mean	3.0	2.4	1.6	3.4	2.6	3.0	2.4	1.6	3.4	2.6
(P1-P0)/P0 * 100										
MPI_CCLM4	-2.1	3.0	-19.4	30.0	5.5	-11.9	-18.3	1.0	17.0	-3.2
EC-EARTH_KNMI	3.3	2.4	1.3	-16.2	-3.5	-3.0	16.5	-11.9	-13.5	-4.2
CNRM_CCLM4	-0.3	-13.3	14.1	-16.2	-5.1	1.6	-6.1	-0.8	-8.6	-2.9
ENSMEAN	0.3	-2.6	-1.3	-0.8	-1.0	-4.4	-2.6	-3.9	-1.7	-3.4
(P2-P0)/P0 * 100										
MPI_CCLM4	1.0	-2.9	* -30.3	24.4	0.7	5.8	-15.3	-21.0	20.9	-0.5
EC-EARTH_KNMI	1.8	-0.8	9.1	-11.0	-2.0	8.9	15.5	9.0	-3.1	5.3
CNRM_CCLM4	-2.2	-7.8	3.4	-14.3	-6.1	5.9	-14.7	7.9	-1.7	-0.2
ENSMEAN	0.2	-3.8	-5.9	-0.3	-2.5	6.9	-4.8	-1.4	5.3	1.5
(P3-P0)/P0 * 100										
MPI_CCLM4	2.4	-6.1	-10.4	10.4	0.4	-9.8	-7.2	-5.4	29.9	2.8
EC-EARTH_KNMI	23.7	-0.4	-2.7	-18.5	-1.2	18.1	-0.5	-17.9	-3.0	1.2
CNRM_CCLM4	1.2	-7.0	3.3	-0.9	-0.3	11.1	-3.7	-4.6	6.9	4.1
ENSMEAN	9.1	-4.5	-3.2	-3.0	-0.4	6.5	-3.8	-9.3	11.3	2.7
(P4-P0)/P0 * 100										
MPI_CCLM4	4.4	-11.2	-27.0	13.7	-2.4	5.6	-12.9	* -35.0	5.1	-6.4
EC-EARTH_KNMI	8.8	14.4	10.5	3.6	7.7	30.4	9.5	* -36.5	-4.7	5.2
CNRM_CCLM4	5.5	-8.5	-5.5	10.1	3.7	-0.7	5.0	3.4	-2.7	0.9
ENSMEAN	6.2	-1.8	-7.4	9.1	3.0	11.8	0.5	-22.7	-0.8	-0.1

* : Two Sample Wilcoxon tests, 95 % confidence interval

© AdriAdapt

Figure 5-51: Averaged seasonal and annual precipitation obtained by dynamical downscaling for Šibenik: Ref. mean is 20 year simulated period (1986-2005) for ensemble mean in mmday^{-1}; P1-P0, P2-P0, P3-P0, P4-P0 are changes (in %) in the future for following periods P1: 2021-2040, P2: 2041-2060, P3: 2061-2080, P4: 2081-2100. Differences are shown for individual models. Significant change is marked by star. Change is also shown as ensemble mean (ENSMEAN), not tested for significance. Left column is for RCP4.5 scenario and right for RCP8.5 scenario.

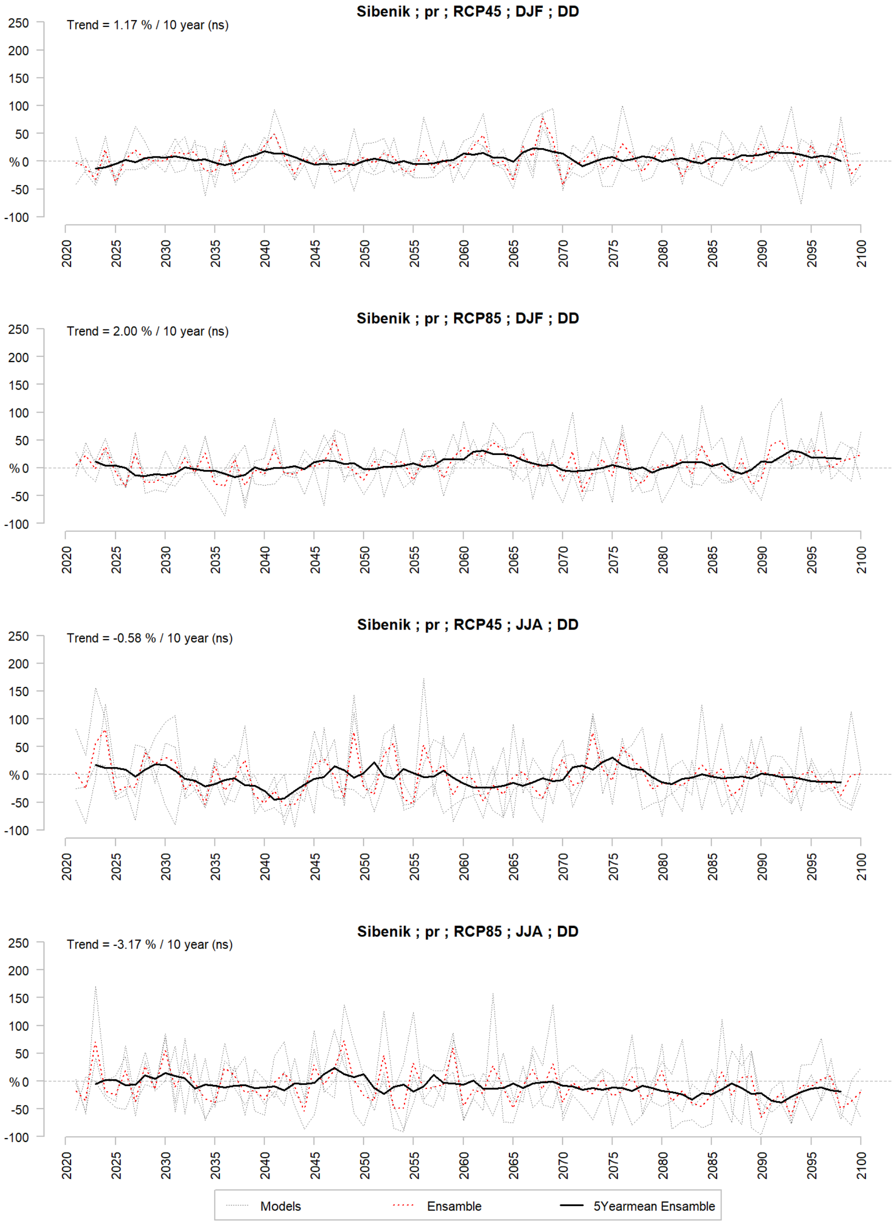

Figure 5-52: Variability of future precipitation anomaly (in %) in Šibenik for 2021-2100 obtained by dynamically downscaling for winter (DJF) and summer (JJA) and two RCP scenarios: individual models are in grey, the ensemble mean in red, 5-year moving average in black. Significant trend is marked with star (ns if not significant).

6.2.1.2.2 *Intense precipitation*

Intense precipitation, defined by 95th percentile of precipitation (Figure 5-53) in Šibenik, shows for ensemble mean that 95th percentile will increase in all seasons except summer. At the end of century, the increase will be the most pronounced in SON for RCP4.5 (18.6 %) and in DJF for RCP8.5 (16.1%), while in JJA 95th percentile will decrease for -1.2 % for RCP4.5 and -24.8 % for RCP8.5. On annual scale intense precipitation will increase, 8.1 % for RCP4.5 and 5.7 % for RCP8.5. Although variability of future intense precipitation anomaly (Figure 5-54) for ensemble mean in Šibenik shows increase in precipitation in DJF for both scenarios, and increase of precipitation in JJA for RCP4.5, but decrease of precipitation in JJA for RCP8.5, linear trend is only statistically significant in DJF for RCP8,5 scenario (2.7 % / 10 year).

Sibenik

	RCP45					RCP85				
	DJF	MAM	JJA	SON	Annual	DJF	MAM	JJA	SON	Annual
Ref.mean	14.9	12.3	9.7	18.2	14.3	14.9	12.3	9.7	18.2	14.3
(P1-P0)/P0 * 100										
MPI_CCLM4	-5.9	5.3	-15.6	28.5	3.8	-4.1	-6.7	11.4	* 23.3	3.4
EC-EARTH_KNMI	12.5	16.6	-2.6	-5.2	3.3	-5.6	16.5	-14.7	-4.4	-2.9
CNRM_CCLM4	12.1	-4.8	12.8	-6.7	0.8	13.2	1.4	-5.1	-5.9	0.2
ENSMEAN	6.2	5.7	-1.8	5.5	2.6	1.2	3.7	-2.8	4.3	0.2
(P2-P0)/P0 * 100										
MPI_CCLM4	-6.6	3.9	-24.0	* 31.0	2.1	0.3	-13.1	-8.6	* 23.1	2.5
EC-EARTH_KNMI	1.2	10.3	7.8	-6.4	0.6	9.5	19.1	10.7	-0.2	6.8
CNRM_CCLM4	11.5	-0.2	-1.7	-5.2	-0.8	14.6	-6.4	-6.3	0.5	-0.4
ENSMEAN	2.0	4.7	-5.9	6.5	0.6	8.1	-0.1	-1.4	7.8	3.0
(P3-P0)/P0 * 100										
MPI_CCLM4	8.8	-0.6	-13.9	15.1	5.7	-8.1	1.6	3.0	* 42.5	6.8
EC-EARTH_KNMI	* 23.6	11.3	2.0	-12.3	4.4	12.4	10.7	-20.1	0.7	5.2
CNRM_CCLM4	14.3	-1.7	9.5	1.3	3.1	20.6	8.0	-2.3	9.8	8.6
ENSMEAN	15.6	3.0	-0.8	1.4	4.4	8.3	6.8	-6.5	17.6	6.9
(P4-P0)/P0 * 100										
MPI_CCLM4	6.6	5.2	-14.0	24.3	7.4	7.7	-2.7	-25.6	22.1	1.5
EC-EARTH_KNMI	11.0	* 21.1	12.7	7.0	10.0	* 21.2	* 8.9	* -49.5	4.7	5.9
CNRM_CCLM4	* 14.6	-1.8	-2.3	* 24.5	6.9	* 19.6	15.0	0.8	4.8	9.7
ENSMEAN	10.7	8.1	-1.2	18.6	8.1	16.1	7.1	-24.8	10.6	5.7

* ; Two Sample Wilcoxon tests, 95 % confidence interval

Figure 5-53: Seasonal and annual 95th percentile of precipitation (intense precipitation) obtained by dynamical downscaling for Šibenik: Ref. mean is 20 year simulated period (1986-2005) for ensemble mean in mmday^{-1}; P1-P0, P2-P0, P3-P0, P4-P0 are changes (in %) in the future for following periods P1: 2021-2040, P2: 2041-2060, P3: 2061-2080, P4: 2081-2100. Differences are shown for individual models. Significant change is marked by star. Change is also shown as ensemble mean (ENSMEAN), not tested for significance. Left column is for RCP4.5 scenario and right for RCP8.5 scenario.

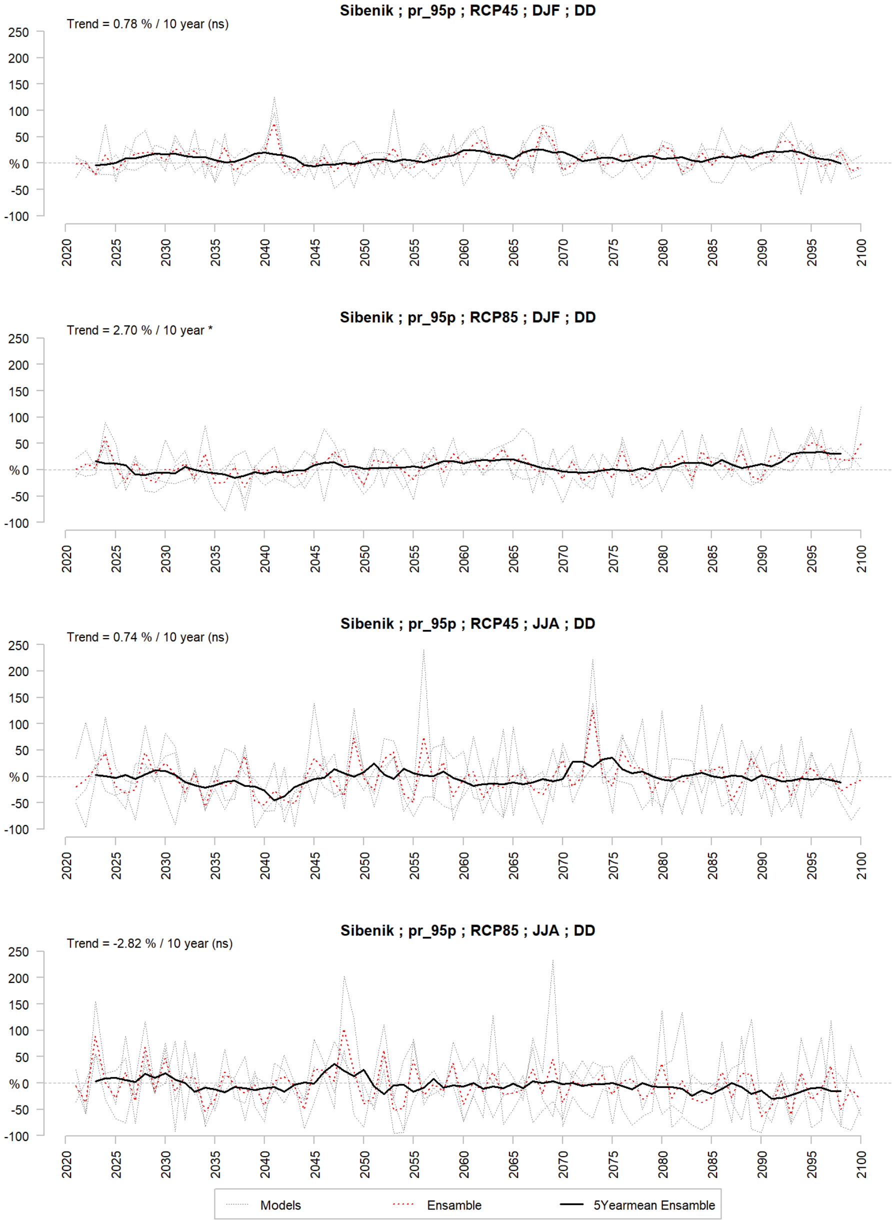

Figure 5-54: Variability of future 95th percentile of precipitation (intense precipitation) anomaly (in %) in Šibenik for 2021-2100 obtained by dynamically downscaling for winter (DJF) and summer (JJA) and two RCP scenarios: individual models are in grey, the ensemble mean in red, 5-year moving average in black. Significant trend is marked with star (ns if not significant).

6.2.1.2.3 *Extreme precipitation*

Extreme precipitation, defined by 99th percentile of precipitation (Figure 5-55) in Šibenik, shows for ensemble mean increase in all seasons (except JJA) and on annual scale. The increase will change from 11.7 % in MAM to 16.0 % in SON, 11.9 % for annual scale for RCP4.5; between 14.1 % in JJA and 30.3 % in DJF, 17.3 % for annual scale for RCP8.5 at the end of 21st century. Decrease of extreme precipitation in JJA will be -5.8 % for RCP4.5 and -2.6 % for RCP8.5 scenario. Variability of future extreme precipitation anomaly (Figure 5-56) to the end of 21st century for ensemble mean in Šibenik has positive trend for DJF, slightly negative for JJA. Only trend in DJF for RCP4.5 is statistically significant (1.84 % / 10 year).

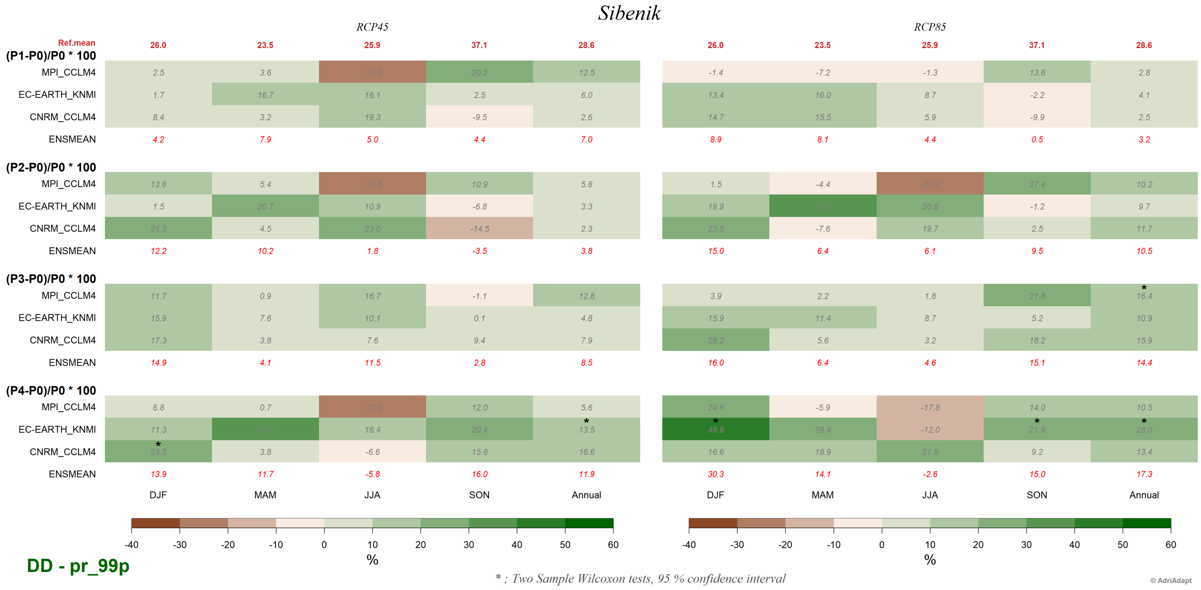

Sibenik

	RCP45					RCP85				
Ref.mean	26.0	23.5	25.9	37.1	28.6	26.0	23.5	25.9	37.1	28.6
(P1-P0)/P0 * 100										
MPI_CCLM4	2.5	3.6	-20.2	20.2	12.5	-1.4	-7.2	-1.3	13.6	2.8
EC-EARTH_KNMI	1.7	16.7	16.1	2.5	6.0	13.4	16.0	8.7	-2.2	4.1
CNRM_CCLM4	8.4	3.2	19.3	-9.5	2.6	14.7	15.5	5.9	-9.9	2.5
ENSMEAN	4.2	7.9	5.0	4.4	7.0	8.9	8.1	4.4	0.5	3.2
(P2-P0)/P0 * 100										
MPI_CCLM4	13.6	5.4	-28.5	10.9	5.8	1.5	-4.4	-22.2	27.4	10.2
EC-EARTH_KNMI	1.5	20.7	10.9	-6.8	3.3	19.9	31.3	20.8	-1.2	9.7
CNRM_CCLM4	21.3	4.5	23.0	-14.5	2.3	23.5	-7.6	19.7	2.5	11.7
ENSMEAN	12.2	10.2	1.8	-3.5	3.8	15.0	6.4	6.1	9.5	10.5
(P3-P0)/P0 * 100										
MPI_CCLM4	11.7	0.9	16.7	-1.1	12.8	3.9	2.2	1.8	21.8	* 16.4
EC-EARTH_KNMI	15.9	7.6	10.1	0.1	4.8	15.9	11.4	8.7	5.2	10.9
CNRM_CCLM4	17.3	3.8	7.6	9.4	7.9	28.2	5.6	3.2	18.2	15.9
ENSMEAN	14.9	4.1	11.5	2.8	8.5	16.0	6.4	4.6	15.1	14.4
(P4-P0)/P0 * 100										
MPI_CCLM4	6.8	0.7	-27.2	12.0	5.6	24.6	-5.9	-17.8	14.0	10.5
EC-EARTH_KNMI	11.3	30.7	16.4	20.4	* 13.5	* 49.8	29.4	-12.0	* 21.9	* 28.0
CNRM_CCLM4	* 23.5	3.8	-6.6	15.8	16.6	16.6	18.9	21.8	9.2	13.4
ENSMEAN	13.9	11.7	-5.8	16.0	11.9	30.3	14.1	-2.6	15.0	17.3
	DJF	MAM	JJA	SON	Annual	DJF	MAM	JJA	SON	Annual

DD - pr_99p

** ; Two Sample Wilcoxon tests, 95 % confidence interval*

Figure 5-55: Seasonal and annual 99th percentile of precipitation (extreme precipitation) obtained by dynamical downscaling for Šibenik: Ref. mean is 20 year simulated period (1986-2005) for ensemble mean in mmday^{-1}; P1-P0, P2-P0, P3-P0, P4-P0 are changes (in %) in the future for following periods P1: 2021-2040, P2: 2041-2060, P3: 2061-2080, P4: 2081-2100. Differences are shown for individual models. Significant change is marked by star. Change is also shown as ensemble mean (ENSMEAN), not tested for significance. Left column is for RCP4.5 scenario and right for RCP8.5 scenario.

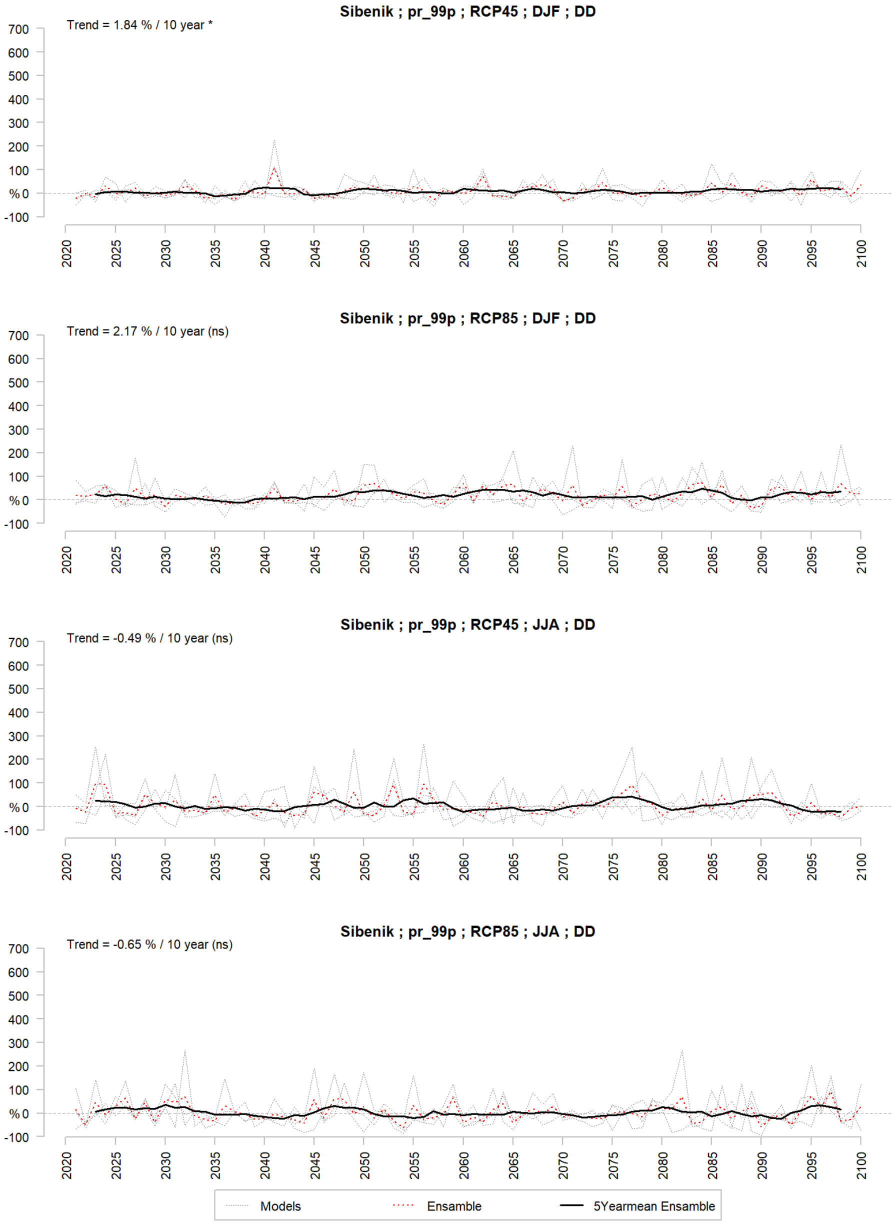

Figure 5-56: Variability of future 99th percentile of precipitation (extreme precipitation) anomaly (in %) in Šibenik for 2021-2100 obtained by dynamically downscaling for winter (DJF) and summer (JJA) and two RCP scenarios: individual models are in grey, the ensemble mean in red, 5-year moving average in black. Significant trend is marked with star (ns if not significant).

6.2.1.3 *Surface relative humidity projections*

Seasonal and annual change of mean surface relative humidity (Figure 5-57) is shown by two available model realisations. Differences in signal change from one to other model clearly indicate the need to use multiple model for the final conclusion about the change in relative humidity. Ensemble mean of surface relative humidity change in Šibenik shows slightly increase at the end of 21st century in all seasons except JJA (between 0.2 % in SON and 1.1 % in DJF, 0.1 % on annual scale for RCP4.5). Surface relative humidity will decrease in JJA for -1 %. The worst case scenario RCP8.5 gives increase of surface relative humidity in MAM for 0.1 % and DJF for 1.5 % and decrease in SON for -1.4 % and in JJA for -6 %. On annual scale surface relative humidity will decrease for -1.4 % at the end of 21st century. Variability of future surface relative humidity anomaly (Figure 5-58) do not show significant linear trend in either DJF or JJA for any of the considered RCP scenarios.

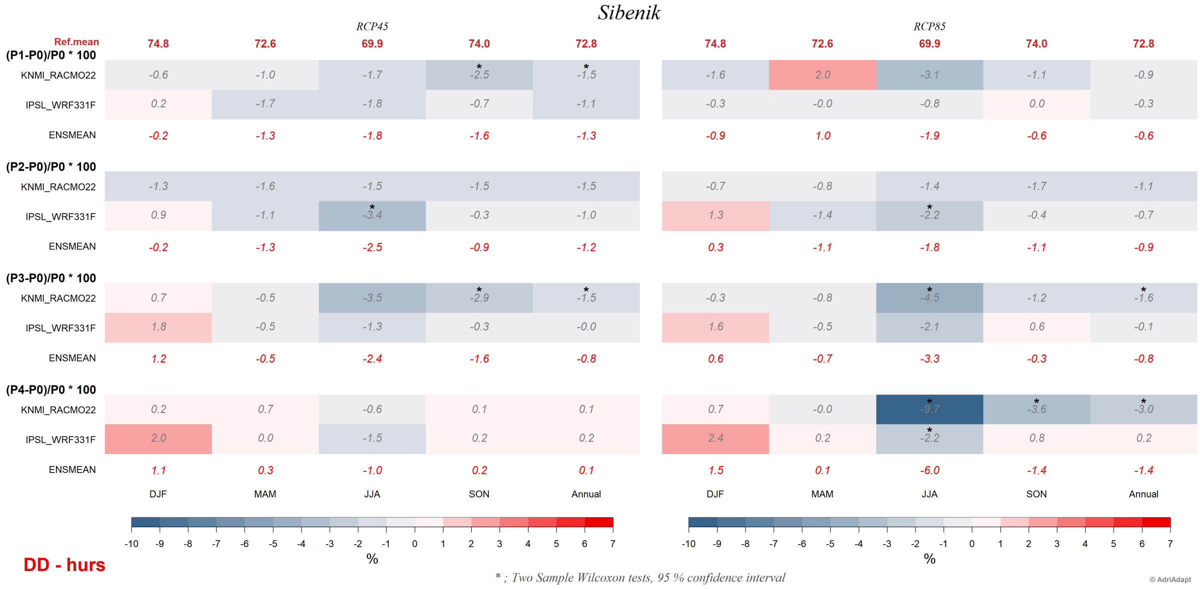

Sibenik

RCP45

	DJF	MAM	JJA	SON	Annual
Ref.mean	74.8	72.6	69.9	74.0	72.8
(P1-P0)/P0 * 100					
KNMI_RACMO22	-0.6	-1.0	-1.7	* -2.5	* -1.5
IPSL_WRF331F	0.2	-1.7	-1.8	-0.7	-1.1
ENSMEAN	-0.2	-1.3	-1.8	-1.6	-1.3
(P2-P0)/P0 * 100					
KNMI_RACMO22	-1.3	-1.6	-1.5	-1.5	-1.5
IPSL_WRF331F	0.9	-1.1	* -3.4	-0.3	-1.0
ENSMEAN	-0.2	-1.3	-2.5	-0.9	-1.2
(P3-P0)/P0 * 100					
KNMI_RACMO22	0.7	-0.5	-3.5	* -2.9	* -1.5
IPSL_WRF331F	1.8	-0.5	-1.3	-0.3	-0.0
ENSMEAN	1.2	-0.5	-2.4	-1.6	-0.8
(P4-P0)/P0 * 100					
KNMI_RACMO22	0.2	0.7	-0.6	0.1	0.1
IPSL_WRF331F	2.0	0.0	-1.5	0.2	0.2
ENSMEAN	1.1	0.3	-1.0	0.2	0.1

RCP85

	DJF	MAM	JJA	SON	Annual
Ref.mean	74.8	72.6	69.9	74.0	72.8
(P1-P0)/P0 * 100					
KNMI_RACMO22	-1.6	2.0	-3.1	-1.1	-0.9
IPSL_WRF331F	-0.3	-0.0	-0.8	0.0	-0.3
ENSMEAN	-0.9	1.0	-1.9	-0.6	-0.6
(P2-P0)/P0 * 100					
KNMI_RACMO22	-0.7	-0.8	-1.4	-1.7	-1.1
IPSL_WRF331F	1.3	-1.4	* -2.2	-0.4	-0.7
ENSMEAN	0.3	-1.1	-1.8	-1.1	-0.9
(P3-P0)/P0 * 100					
KNMI_RACMO22	-0.3	-0.8	* -4.5	-1.2	* -1.6
IPSL_WRF331F	1.6	-0.5	-2.1	0.6	-0.1
ENSMEAN	0.6	-0.7	-3.3	-0.3	-0.8
(P4-P0)/P0 * 100					
KNMI_RACMO22	0.7	-0.0	* -9.7	* -3.6	* -3.0
IPSL_WRF331F	2.4	0.2	* -2.2	0.8	0.2
ENSMEAN	1.5	0.1	-6.0	-1.4	-1.4

DD - hurs

* ; Two Sample Wilcoxon tests, 95 % confidence interval

© AdriAdapt

Figure 5-57: Seasonal and annual mean surface relative humidity (in %) obtained by dynamical downscaling for Šibenik: Ref. mean is 20 year simulated period (1986-2005); P1-P0, P2-P0, P3-P0, P4-P0 are relative changes in the future for following periods P1: 2021-2040, P2: 2041-2060, P3: 2061-2080, P4: 2081-2100. Differences are shown for individual models. Significant change is marked by star. Change is also shown as ensemble mean (ENSMEAN), not tested for significance. Left column is for RCP4.5 scenario and right for RCP8.5 scenario.

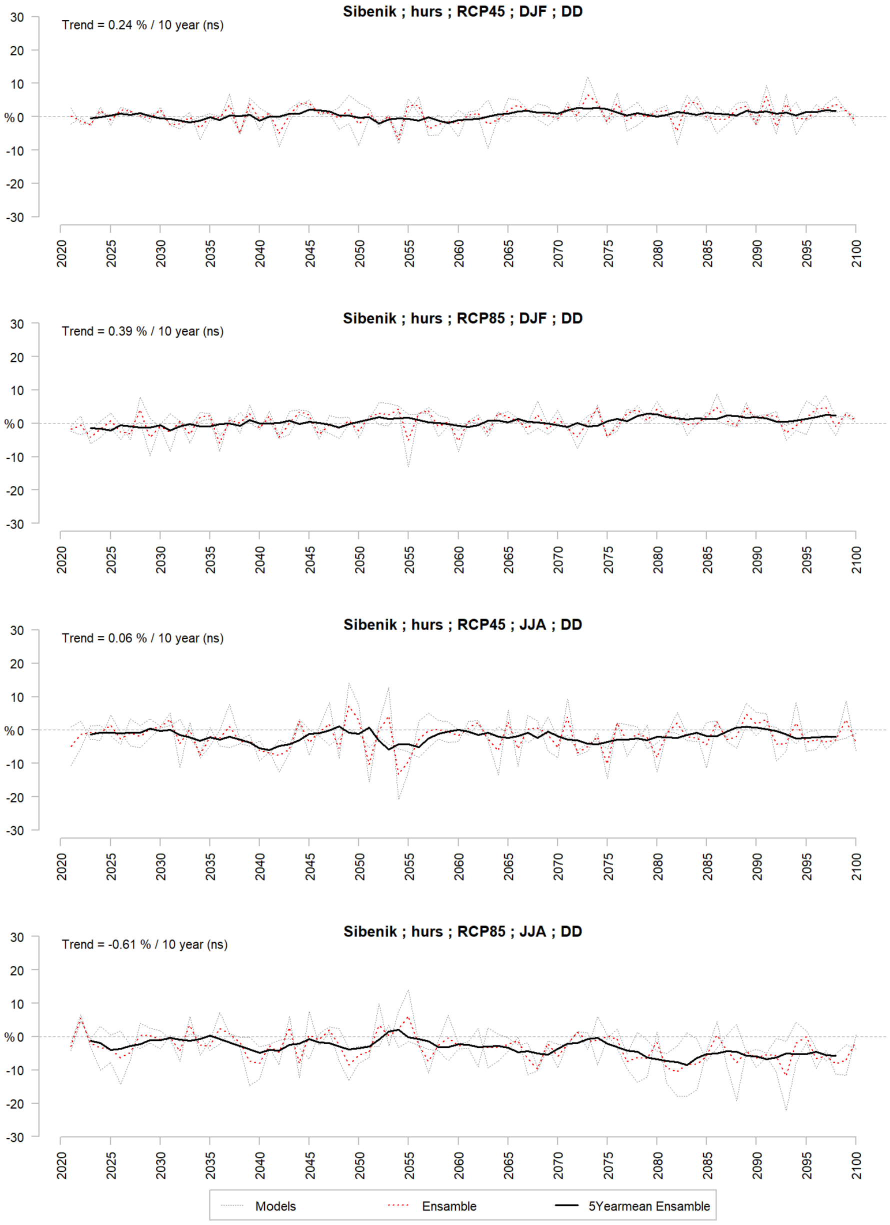

Figure 5-58: Variability of future surface relative humidity anomaly (in %) in Šibenik for 2021-2100 obtained by dynamically downscaling for winter (DJF) and summer (JJA) and two RCP scenarios: individual models are in grey, the ensemble mean in red, 5-year moving average in black. Significant trend is marked with star (ns if not significant).

6.2.1.4 *Extra rare humidex projections*

Extra rare humidex change (defined by 99.9th percentile of humidex) in the future in Šibenik will slightly increase towards the end of 21st century (Figure 5-59). Ensemble mean will increase between 0.8 in JJA and 2.2 in MAM, 1.3 on annual scale for RCP4.5 scenario. Scenario RCP8.5 gives slightly higher positive amplitudes, from 3.9 in JJA to 5.8 in SON, 4.4 on annual scale. Variability of future 99.9th percentile of humidex anomaly (Figure 5-60) shows positive linear trend for both seasons and both considered scenarios. It is 0.30 [] / 10 year in DJF for RCP4.5 (0.64 [] /10 year for RCP8.5) and 0.30 [] /10 year in JJA for RCP4.5 (0.80 [] /10 year for RCP8.5). Trends are statistically significant.

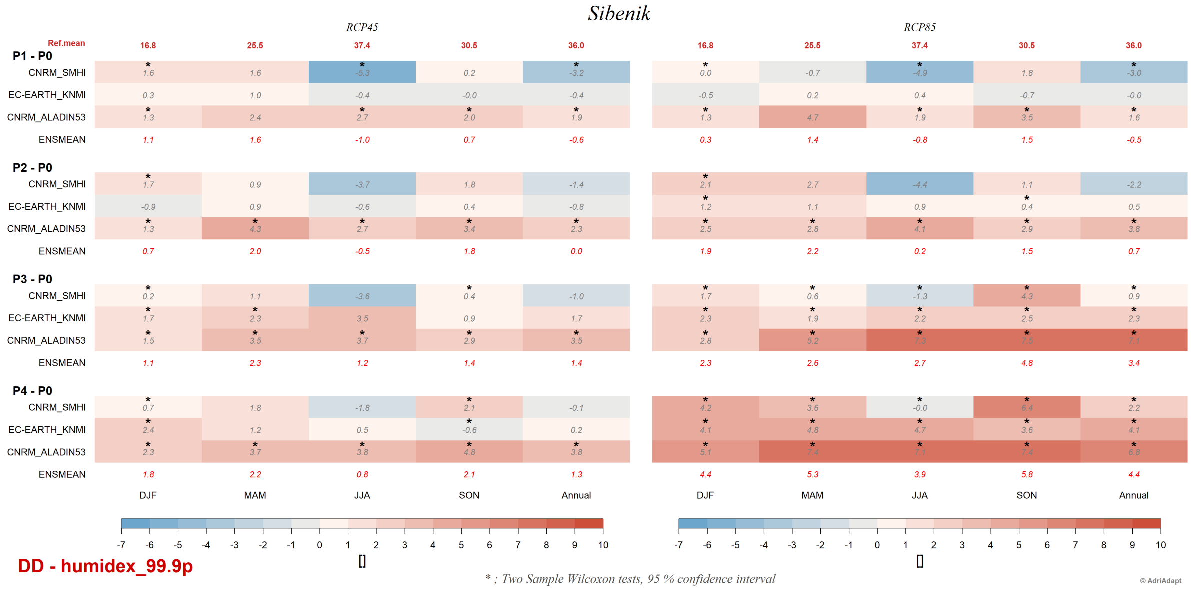

	RCP45					RCP85				
	DJF	MAM	JJA	SON	Annual	DJF	MAM	JJA	SON	Annual
Ref.mean	16.8	25.5	37.4	30.5	36.0	16.8	25.5	37.4	30.5	36.0
P1 - P0										
CNRM_SMHI	* 1.6	1.6	* -5.3	0.2	* -3.2	* 0.0	-0.7	* -4.9	1.8	* -3.0
EC-EARTH_KNMI	0.3	1.0	-0.4	-0.0	-0.4	-0.5	0.2	0.4	-0.7	-0.0
CNRM_ALADIN53	* 1.3	2.4	* 2.7	* 2.0	* 1.9	* 1.3	4.7	* 1.9	* 3.5	* 1.6
ENSMEAN	1.1	1.6	-1.0	0.7	-0.6	0.3	1.4	-0.8	1.5	-0.5
P2 - P0										
CNRM_SMHI	* 1.7	0.9	-3.7	1.8	-1.4	* 2.1	2.7	-4.4	1.1	-2.2
EC-EARTH_KNMI	-0.9	0.9	-0.6	0.4	-0.8	* 1.2	1.1	0.9	* 0.4	0.5
CNRM_ALADIN53	* 1.3	* 4.3	* 2.7	* 3.4	* 2.3	* 2.5	* 2.8	* 4.1	* 2.9	* 3.8
ENSMEAN	0.7	2.0	-0.5	1.8	0.0	1.9	2.2	0.2	1.5	0.7
P3 - P0										
CNRM_SMHI	* 0.2	1.1	-3.6	* 0.4	-1.0	* 1.7	* 0.6	* -1.3	* 4.3	* 0.9
EC-EARTH_KNMI	* 1.7	* 2.3	3.5	0.9	1.7	* 2.3	* 1.9	* 2.2	* 2.5	* 2.3
CNRM_ALADIN53	* 1.5	* 3.5	* 3.7	* 2.9	* 3.5	* 2.8	* 5.2	* 7.3	* 7.5	* 7.1
ENSMEAN	1.1	2.3	1.2	1.4	1.4	2.3	2.6	2.7	4.8	3.4
P4 - P0										
CNRM_SMHI	* 0.7	1.8	-1.8	* 2.1	-0.1	* 4.2	* 3.6	* -0.0	* 6.4	* 2.2
EC-EARTH_KNMI	* 2.4	1.2	0.5	* -0.6	0.2	* 4.1	* 4.8	* 4.7	* 3.6	* 4.1
CNRM_ALADIN53	* 2.3	* 3.7	* 3.8	* 4.8	* 3.8	* 5.1	* 7.4	* 7.1	* 7.4	* 6.8
ENSMEAN	1.8	2.2	0.8	2.1	1.3	4.4	5.3	3.9	5.8	4.4

* ; Two Sample Wilcoxon tests, 95 % confidence interval

Figure 5-59: Seasonal and annual 99.9th percentile of humidex obtained by dynamical downscaling for Šibenik (in []): Ref. mean is 20 year simulated period (1986-2005); P1-P0, P2-P0, P3-P0, P4-P0 are changes in the future for following periods P1: 2021-2040, P2: 2041-2060, P3: 2061-2080, P4: 2081-2100. Differences are shown for individual models. Significant change is marked by star. Change is also shown as ensemble mean (ENSMEAN), not tested for significance. Left column is for RCP4.5 scenario and right for RCP8.5 scenario.

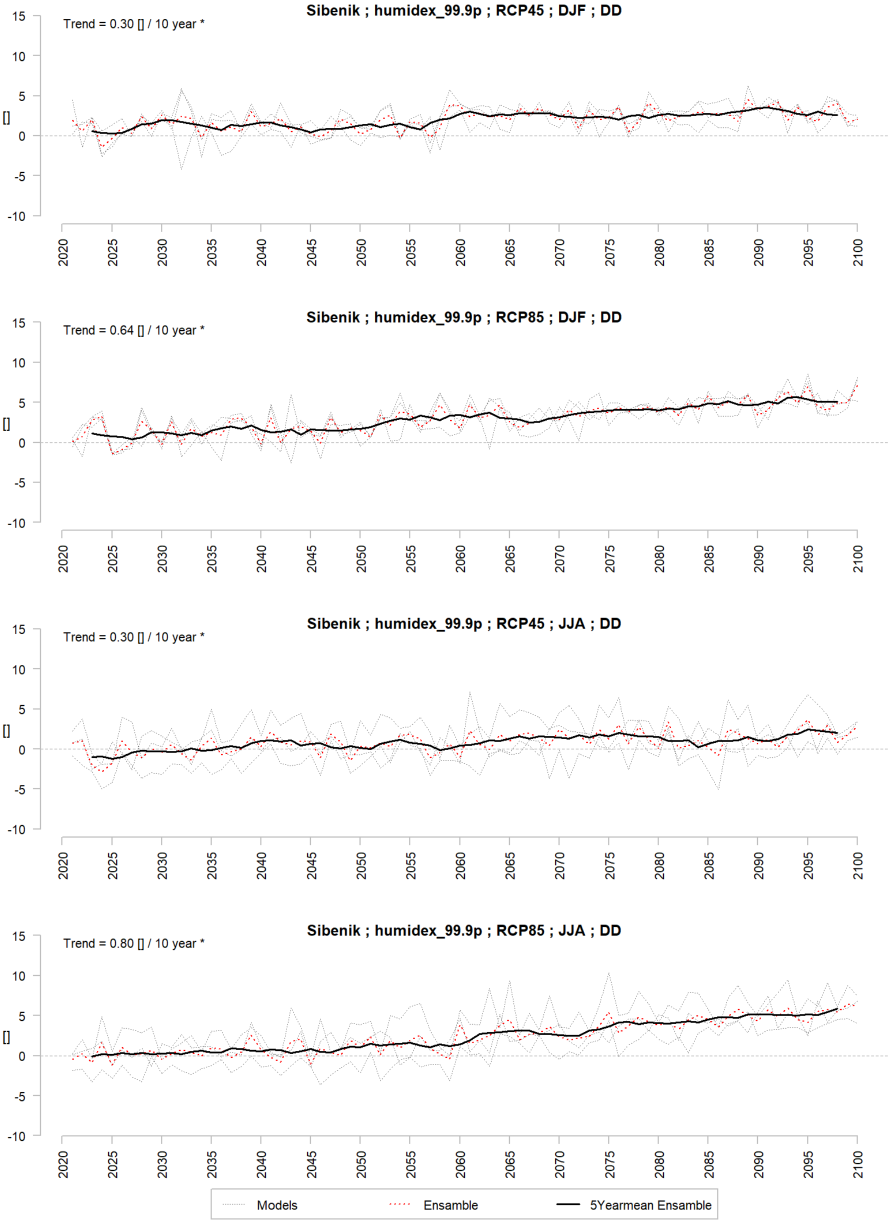

Figure 5-60: Variability of future 99.9th percentile of humidex anomaly (in []) in Šibenik for 2021-2100 obtained by dynamically downscaling for winter (DJF) and summer (JJA) and two RCP scenarios: individual models are in grey, the ensemble mean in red, 5-year moving average in black. Significant trend is marked with star (ns if not significant).

6.2.2 Statistically downscaled results

In this section we present future climate changes of temperature and precipitation related indices for Sibenik, as result from the statistical downscaling techniques constructed based on the observed local data/observed large scale circulation patterns and, applied then to future large-scale circulation patterns simulated by 4GCMs in the framework of CMIP5 experiments. The results are presented as follow:

- climate change diagram of an individual index for each season and on annual basis for four considered future periods (P1, P2, P3, P4), for two emission scenarios (RCP4.5 and RCP8.5). Climate change is calculated as difference between future (P1, P2, P3, P4) and reference period (P0) for temperature indices and some intense precipitation indices, and as relative differences (expressed in %). Reference period is 1986-2005, the Ref. mean (obs.) from the diagram (see below) is the climate observed value registered at station take into analysis, while climate changes (P1-P0; P2-P0,P3-P0;P4-P0) are shown for different models (SD_CMCC-CM, SD_CAN-ESM2, SD-MPI, SD_CNRM) as well as for ensemble mean of models (ENSMEAN). The t-Student test is applied to test the statistical significance of future climate (values from P1, or P2, or P3, or P4) with respect to present climate value (value from P0) and the results significant at 95% are marked by a star.
- time series of future anomaly of an individual index for DJF and JJA and for two emission scenarios RCP4.5 and RCP8.5; the anomaly is calculated respect to the reference period and shown for individual models, ensemble mean and 5-year moving average. Mann Kendall trend test is applied to ensemble mean (for 95 % confidence level). Significant trend is marked with star (n.s. if not significant).

6.2.2.1 *Temperature related indices projections*

6.2.2.1.1 *Seasonal minimum and maximum temperature*

Projected changes of seasonal and annual minimum temperature for Sibenik are shown in figure 5-61, for RCP4.5 and RCP8.5 and over P1, P2, P3, P4 with respect to present climate (P0). Following the moderate RCP4.5 scenario we expect an increase in annual minimum temperature between 1°C during P1 and up to 2°C going to the end of century (P4). The projected increase is higher for RCP8.5, especially for P3 and P4 when the simulations show changes in annual minimum temperature about 4°C. Analysing in details the seasonal projected changes, it could be observed that summer is the season with higher magnitude of changes, up to 3°C for RCP4.5 and up to 5.5°C for RCP8.5(P4 period). Comparing the changes between two emission scenarios it could be observed that starting with P3 the projected changes are higher for RCP8.5 than RCP4.5 (figure 5-61).

The long term variability of projected changes represented in figure 5-62 shows positive and significant trends for winter and summer minimum temperature, more intense for RCP8.5 and especially in summer season, about 0.7°C/decade (figure 5-62).

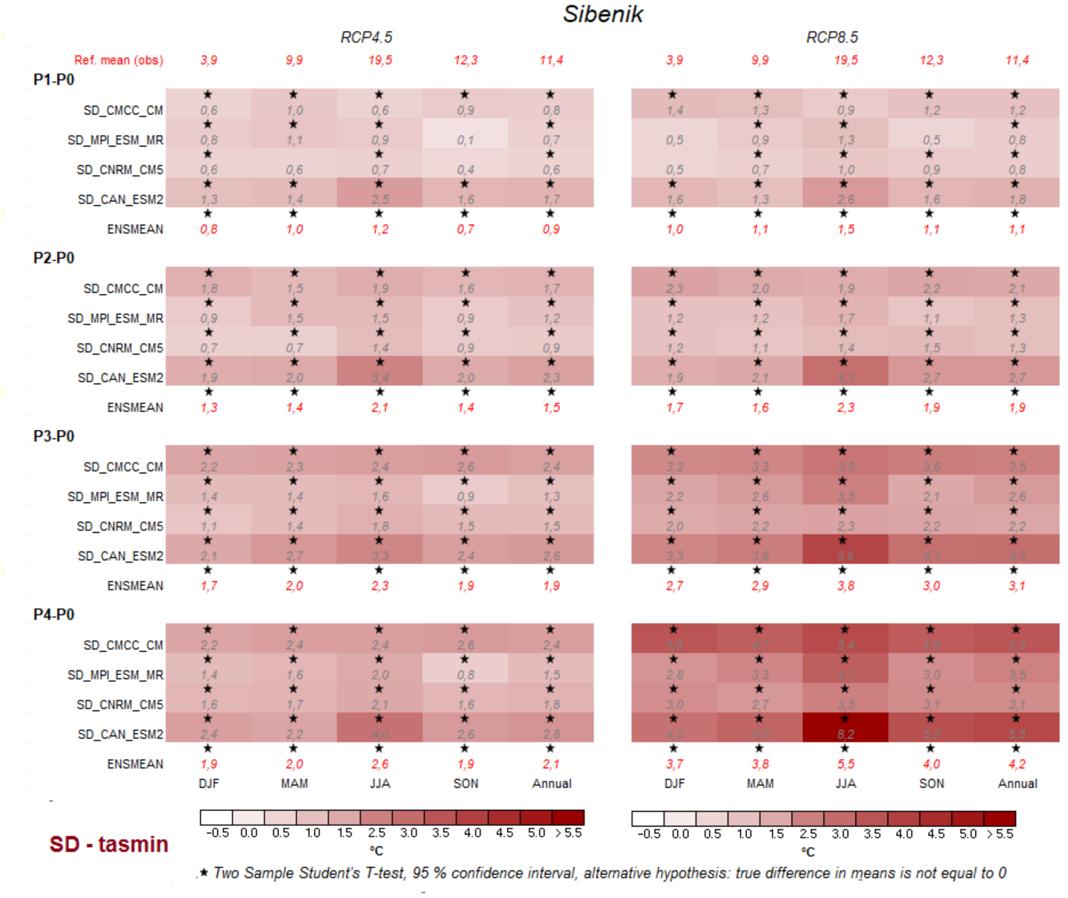

Sibenik

	RCP4.5					RCP8.5				
	DJF	MAM	JJA	SON	Annual	DJF	MAM	JJA	SON	Annual
Ref. mean (obs)	3,9	9,9	19,5	12,3	11,4	3,9	9,9	19,5	12,3	11,4
P1-P0										
SD_CMCC_CM	★ 0,6	★ 1,0	★ 0,6	★ 0,9	★ 0,8	★ 1,4	★ 1,3	★ 0,9	★ 1,2	★ 1,2
SD_MPI_ESM_MR	★ 0,8	★ 1,1	★ 0,9	0,1	★ 0,7	0,5	★ 0,9	★ 1,3	0,5	★ 0,8
SD_CNRM_CM5	★ 0,6	0,6	★ 0,7	0,4	★ 0,6	0,5	★ 0,7	★ 1,0	★ 0,9	★ 0,8
SD_CAN_ESM2	★ 1,3	★ 1,4	★ 2,5	★ 1,6	★ 1,7	★ 1,6	★ 1,3	★ 2,6	★ 1,6	★ 1,8
ENSMEAN	★ 0,8	★ 1,0	★ 1,2	★ 0,7	★ 0,9	★ 1,0	★ 1,1	★ 1,5	★ 1,1	★ 1,1
P2-P0										
SD_CMCC_CM	★ 1,8	★ 1,5	★ 1,9	★ 1,6	★ 1,7	★ 2,3	★ 2,0	★ 1,9	★ 2,2	★ 2,1
SD_MPI_ESM_MR	★ 0,9	★ 1,5	★ 1,5	★ 0,9	★ 1,2	★ 1,2	★ 1,2	★ 1,7	★ 1,1	★ 1,3
SD_CNRM_CM5	★ 0,7	★ 0,7	★ 1,4	★ 0,9	★ 0,9	★ 1,2	★ 1,1	★ 1,4	★ 1,5	★ 1,3
SD_CAN_ESM2	★ 1,9	★ 2,0	★ 3,4	★ 2,0	★ 2,3	★ 1,9	★ 2,1	★ 4,1	★ 2,7	★ 2,7
ENSMEAN	★ 1,3	★ 1,4	★ 2,1	★ 1,4	★ 1,5	★ 1,7	★ 1,6	★ 2,3	★ 1,9	★ 1,9
P3-P0										
SD_CMCC_CM	★ 2,2	★ 2,3	★ 2,4	★ 2,6	★ 2,4	★ 3,2	★ 3,3	★ 3,9	★ 3,6	★ 3,5
SD_MPI_ESM_MR	★ 1,4	★ 1,4	★ 1,6	★ 0,9	★ 1,3	★ 2,2	★ 2,6	★ 3,5	★ 2,1	★ 2,6
SD_CNRM_CM5	★ 1,1	★ 1,4	★ 1,8	★ 1,5	★ 1,5	★ 2,0	★ 2,2	★ 2,3	★ 2,2	★ 2,2
SD_CAN_ESM2	★ 2,1	★ 2,7	★ 3,3	★ 2,4	★ 2,6	★ 3,3	★ 3,6	★ 5,6	★ 4,1	★ 4,2
ENSMEAN	★ 1,7	★ 2,0	★ 2,3	★ 1,9	★ 1,9	★ 2,7	★ 2,9	★ 3,8	★ 3,0	★ 3,1
P4-P0										
SD_CMCC_CM	★ 2,2	★ 2,4	★ 2,4	★ 2,6	★ 2,4	★ 5,0	★ 4,7	★ 5,4	★ 4,8	★ 5,0
SD_MPI_ESM_MR	★ 1,4	★ 1,6	★ 2,0	★ 0,8	★ 1,5	★ 2,8	★ 3,3	★ 4,7	★ 3,0	★ 3,5
SD_CNRM_CM5	★ 1,6	★ 1,7	★ 2,1	★ 1,6	★ 1,8	★ 3,0	★ 2,7	★ 3,5	★ 3,1	★ 3,1
SD_CAN_ESM2	★ 2,4	★ 2,2	★ 4,0	★ 2,6	★ 2,8	★ 4,0	★ 4,5	★ 8,2	★ 5,2	★ 5,5
ENSMEAN	★ 1,9	★ 2,0	★ 2,6	★ 1,9	★ 2,1	★ 3,7	★ 3,8	★ 5,5	★ 4,0	★ 4,2

SD - tasmin

★ *Two Sample Student's T-test, 95 % confidence interval, alternative hypothesis: true difference in means is not equal to 0*

Figure 5-61: Seasonal and annual minimum temperature: observed values over reference period (in red), changes projected by statistical downscaling applied to 4GCMs and the Ensemble Mean of changes over the four periods (P1, P2, P3, P4) projected in the framework of RCP4,5 (left) and RCP 8.5 (right). Significant change is marked by star (source Arpae-Simc).

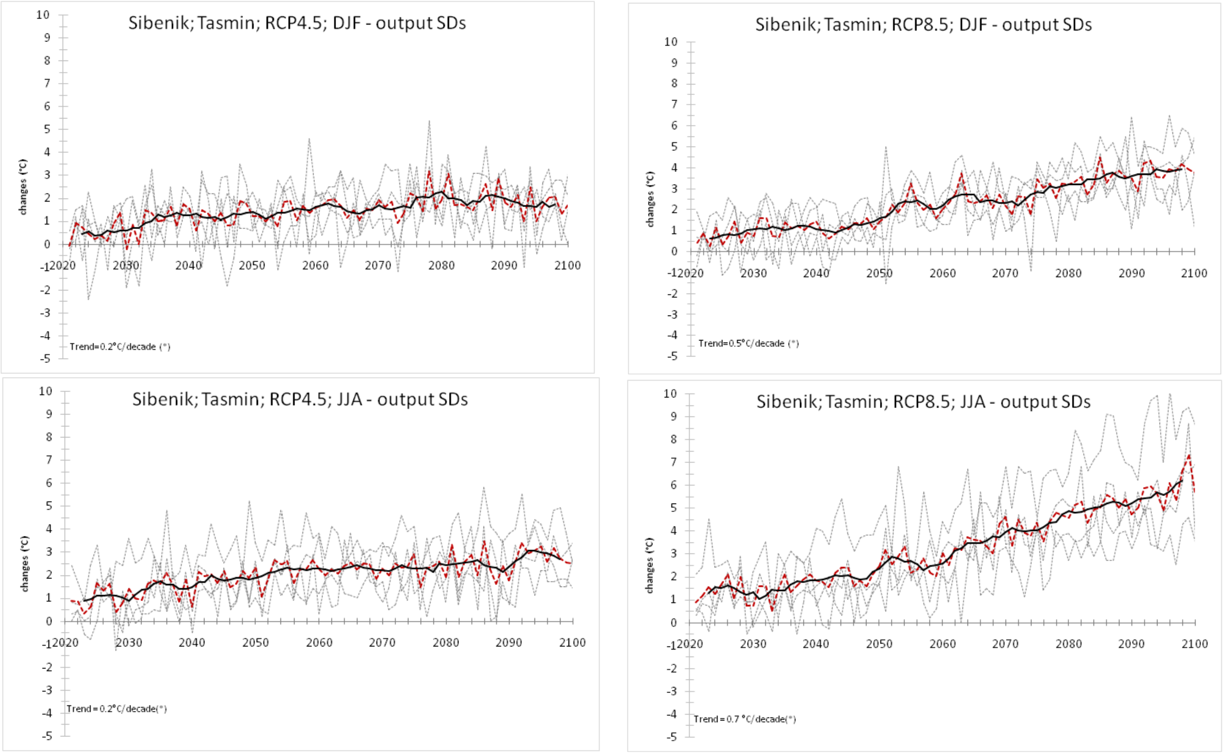

Figure 5-62 Variability of future changes of winter (DJF) and summer (JJA) minimum temperature projected through SDs applied to 4GCMs (grey lines); the Ensemble Mean (red line) and moving average (black line) - scenario RCP4.5 (left) and RCP8.5 (right), 2021-2100 period Significant trend is marked with star while n.s. means not significant (source Arpae-Simc).

Projected changes of seasonal and annual maximum temperature for Sibenik are shown in figure 5-63, for RCP4.5 and RCP8.5 and over P1, P2, P3 and P4 with respect to present climate (P0). Following the moderate RCP4.5 scenario we expect an increase in annual maximum temperature between 1°C during P1 and up to 2°C going to the end of century (P4). The projected increase is higher for RCP8.5, especially for P3 and P4 when the simulations show changes in annual maximum temperature about 3°C and 4°C, respectively. Analysing in details the seasonal projected changes of maximum temperature it could be observed that spring and autumn are seasons with higher magnitude of changes. The magnitude of changes is similar during P1 and P2 periods, up to 2°C for RCP4.5 and RCP8.5, but starting with P3 these became more intense especially for RCP8.5 when peak of 4.5°C is expected during spring and to the end of century. Positive and significant trends are simulated for winter and summer maximum temperature, more intense for RCP8.5 and especially in winter season, about 0.5°C/decade (figure 5-64).

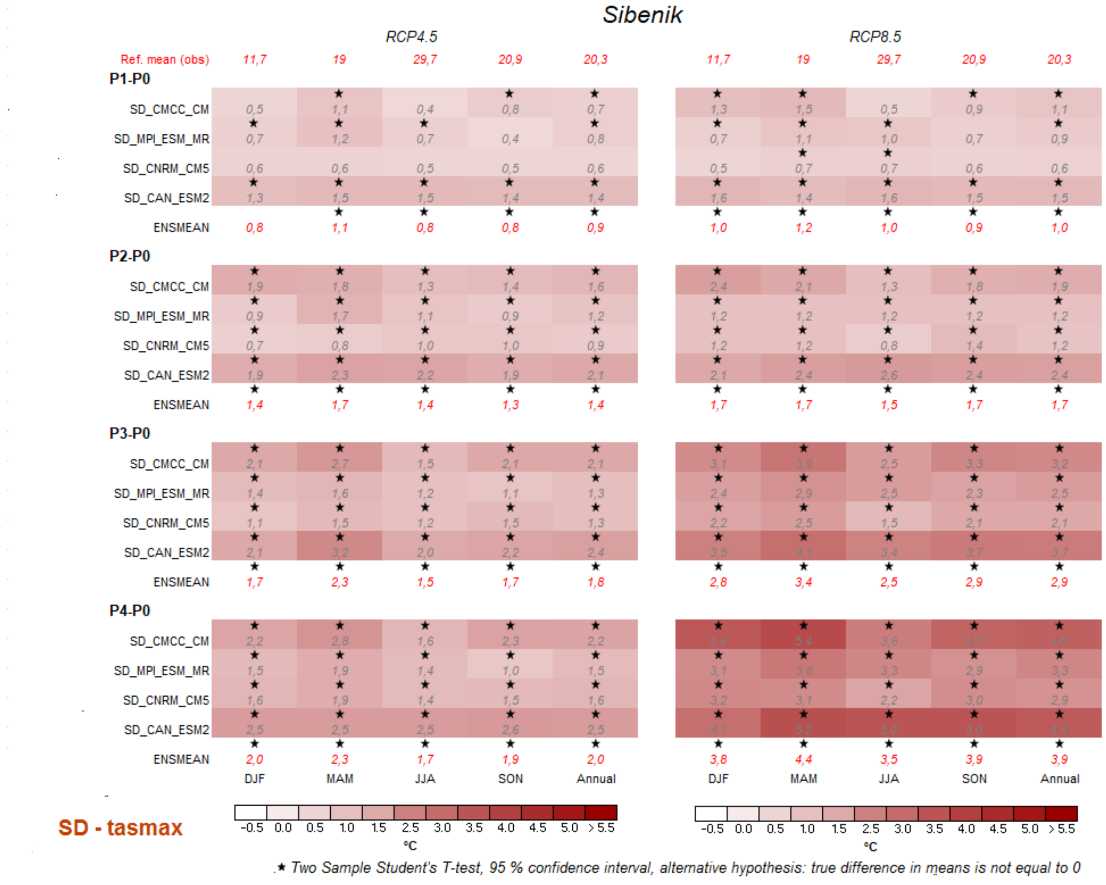

	RCP4.5					RCP8.5				
	DJF	MAM	JJA	SON	Annual	DJF	MAM	JJA	SON	Annual
Ref. mean (obs)	11,7	19	29,7	20,9	20,3	11,7	19	29,7	20,9	20,3
P1-P0										
SD_CMCC_CM	0,5	★ 1,1	0,4	★ 0,8	★ 0,7	★ 1,3	★ 1,5	0,5	★ 0,9	★ 1,1
SD_MPI_ESM_MR	★ 0,7	★ 1,2	★ 0,7	0,4	★ 0,8	★ 0,7	★ 1,1	★ 1,0	0,7	★ 0,9
SD_CNRM_CM5	0,6	0,6	0,5	0,5	0,6	0,5	★ 0,7	★ 0,7	0,6	0,6
SD_CAN_ESM2	★ 1,3	★ 1,5	★ 1,5	★ 1,4	★ 1,4	★ 1,6	★ 1,4	★ 1,6	★ 1,5	★ 1,5
ENSMEAN	0,8	★ 1,1	★ 0,8	★ 0,8	★ 0,9	★ 1,0	★ 1,2	★ 1,0	★ 0,9	★ 1,0
P2-P0										
SD_CMCC_CM	★ 1,9	★ 1,8	★ 1,3	★ 1,4	★ 1,6	★ 2,4	★ 2,1	★ 1,3	★ 1,8	★ 1,9
SD_MPI_ESM_MR	★ 0,9	★ 1,7	★ 1,1	★ 0,9	★ 1,2	★ 1,2	★ 1,2	★ 1,2	★ 1,2	★ 1,2
SD_CNRM_CM5	★ 0,7	★ 0,8	★ 1,0	★ 1,0	★ 0,9	★ 1,2	★ 1,2	★ 0,8	★ 1,4	★ 1,2
SD_CAN_ESM2	★ 1,9	★ 2,3	★ 2,2	★ 1,9	★ 2,1	★ 2,1	★ 2,4	★ 2,6	★ 2,4	★ 2,4
ENSMEAN	★ 1,4	★ 1,7	★ 1,4	★ 1,3	★ 1,4	★ 1,7	★ 1,7	★ 1,5	★ 1,7	★ 1,7
P3-P0										
SD_CMCC_CM	★ 2,1	★ 2,7	★ 1,5	★ 2,1	★ 2,1	★ 3,1	★ 3,9	★ 2,5	★ 3,3	★ 3,2
SD_MPI_ESM_MR	★ 1,4	★ 1,6	★ 1,2	★ 1,1	★ 1,3	★ 2,4	★ 2,9	★ 2,5	★ 2,3	★ 2,5
SD_CNRM_CM5	★ 1,1	★ 1,5	★ 1,2	★ 1,5	★ 1,3	★ 2,2	★ 2,5	★ 1,5	★ 2,1	★ 2,1
SD_CAN_ESM2	★ 2,1	★ 3,2	★ 2,0	★ 2,2	★ 2,4	★ 3,5	★ 4,1	★ 3,4	★ 3,7	★ 3,7
ENSMEAN	★ 1,7	★ 2,3	★ 1,5	★ 1,7	★ 1,8	★ 2,8	★ 3,4	★ 2,5	★ 2,9	★ 2,9
P4-P0										
SD_CMCC_CM	★ 2,2	★ 2,8	★ 1,6	★ 2,3	★ 2,2	★ 4,9	★ 5,4	★ 3,6	★ 4,5	★ 4,6
SD_MPI_ESM_MR	★ 1,5	★ 1,9	★ 1,4	★ 1,0	★ 1,5	★ 3,1	★ 3,8	★ 3,3	★ 2,9	★ 3,3
SD_CNRM_CM5	★ 1,6	★ 1,9	★ 1,4	★ 1,5	★ 1,6	★ 3,2	★ 3,1	★ 2,2	★ 3,0	★ 2,9
SD_CAN_ESM2	★ 2,5	★ 2,5	★ 2,5	★ 2,6	★ 2,5	★ 4,1	★ 5,2	★ 5,0	★ 5,0	★ 4,8
ENSMEAN	★ 2,0	★ 2,3	★ 1,7	★ 1,9	★ 2,0	★ 3,8	★ 4,4	★ 3,5	★ 3,9	★ 3,9

★ *Two Sample Student's T-test, 95 % confidence interval, alternative hypothesis: true difference in means is not equal to 0*

Figure 5-63: Seasonal and annual maximum temperature: observed values over reference period (in red), changes projected by statistical downscaling applied to 4GCMs and the Ensemble Mean of changes over the four periods (P1, P2, P3, P4) projected in the framework of RCP 4.5 (left) and RCP 8.5 (right). Significant change is marked by star (source Arpae-Simc)

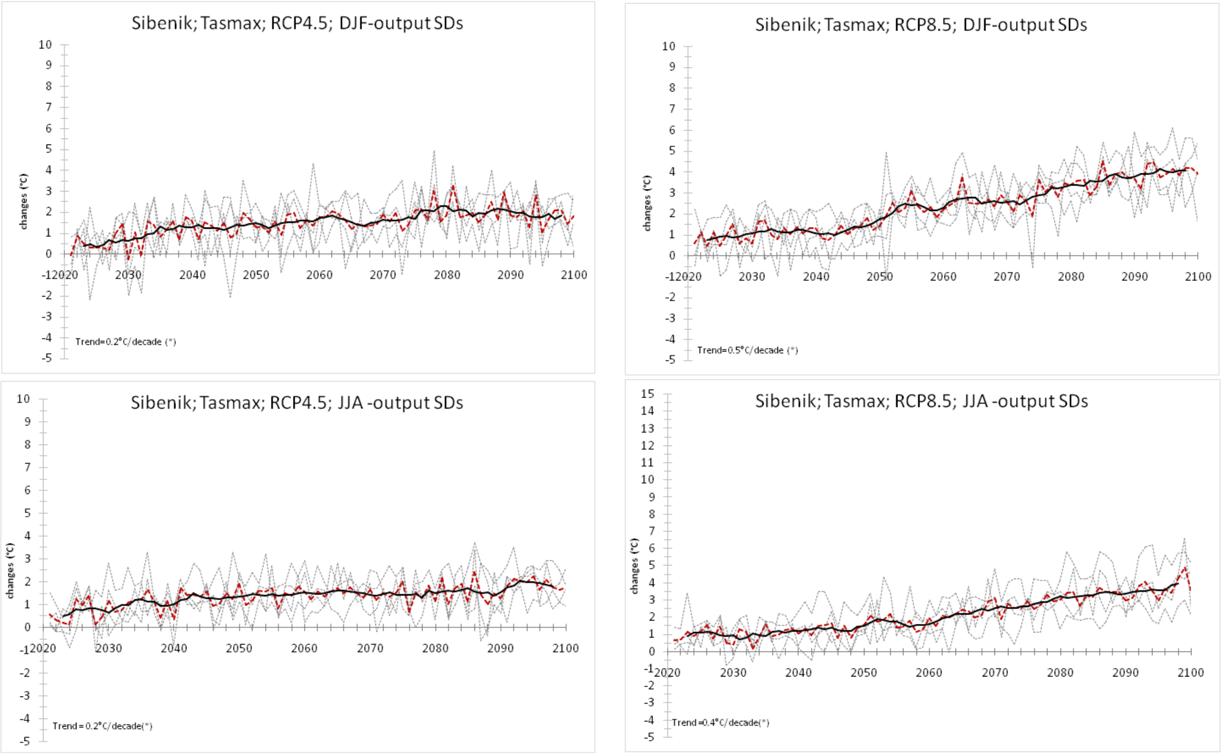

Figure 5-64: Variability of future changes of winter (DJF) and summer (JJA) maximum temperature projected through SDs applied to 4GCMs (grey lines); the Ensemble Mean (red line) and moving average (black line) - scenario RCP4.5 (left) and RCP8.5 (right), 2021-2100 period Significant trend is marked with star while n.s. means not significant (source Arpae-Simc).

6.2.2.1.2 *Extreme temperature*

5th percentile of minimum temperature

The analysis performed on extreme temperature, 5th minimum temperature and 95th maximum temperature reveals important future changes at Sibenik station. An increase in annual 5th percentile of minimum temperature of 1°C is projected during the first period (2021-2040) and up to 2°C going to the end of century, in the framework of RP4.5 emission scenario. The signal became more intense for RCP8.5 emission scenario and especially during 2061-2080 and 2081-2100 periods, when the annual increases could reach 2.5°C during P3 and 3.5°C during P4 (see figure 5-65). At seasonal level, higher amplitude of changes is expected to occur during spring and autumn, about 2.3°C for RCP4.5 and 4.5°C for RCP8.5. The long-term variability of changes shows positive trends, both in winter and summer, statistically significant during winter season and higher for RCP8.5, about 0.6°C/decade (figure 5-66).

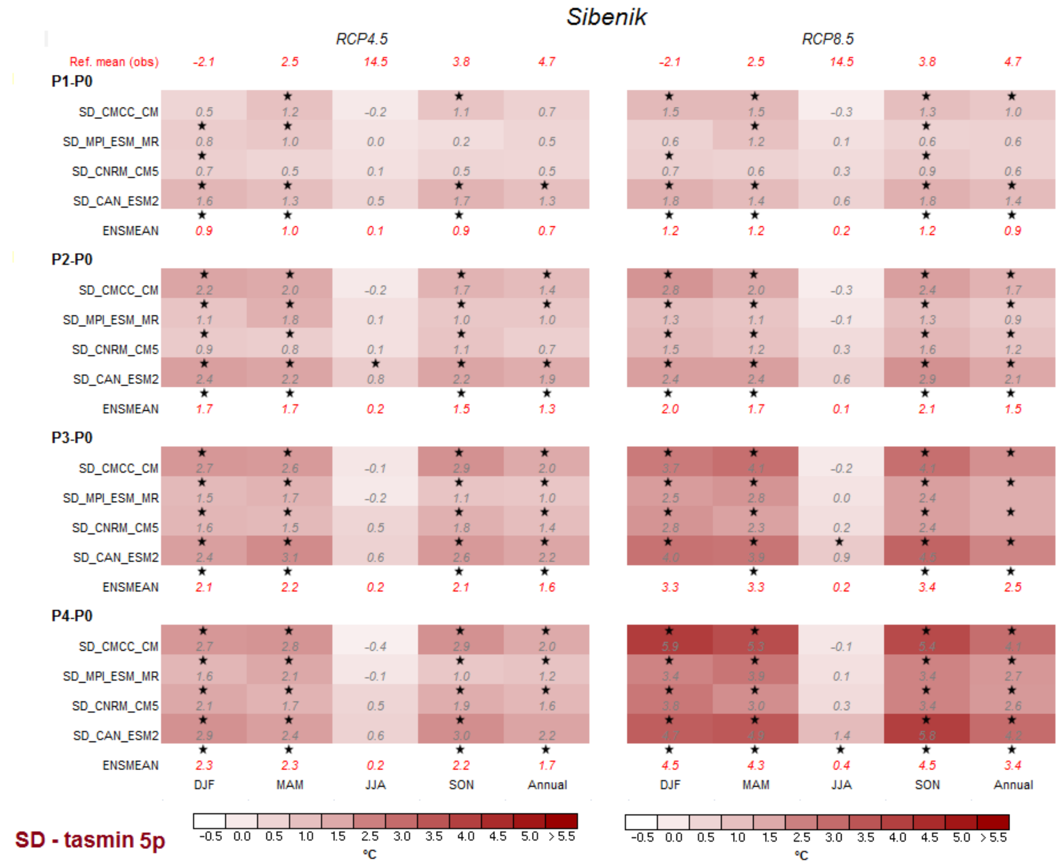

★ Two Sample Student's T-test, 95 % confidence interval, alternative hypothesis: true difference in means is not equal to 0

Figure 5-65: 5th percentile of seasonal and annual minimum temperature: observed values over reference period (in red), changes projected by statistical downscaling applied to 4GCMs and the Ensemble Mean of changes over the four periods (P1, P2, P3, P4) projected in the framework of RCP4.5 (left) and RCP 8.5 (right). Significant change is marked by star (source Arpae-Simc)

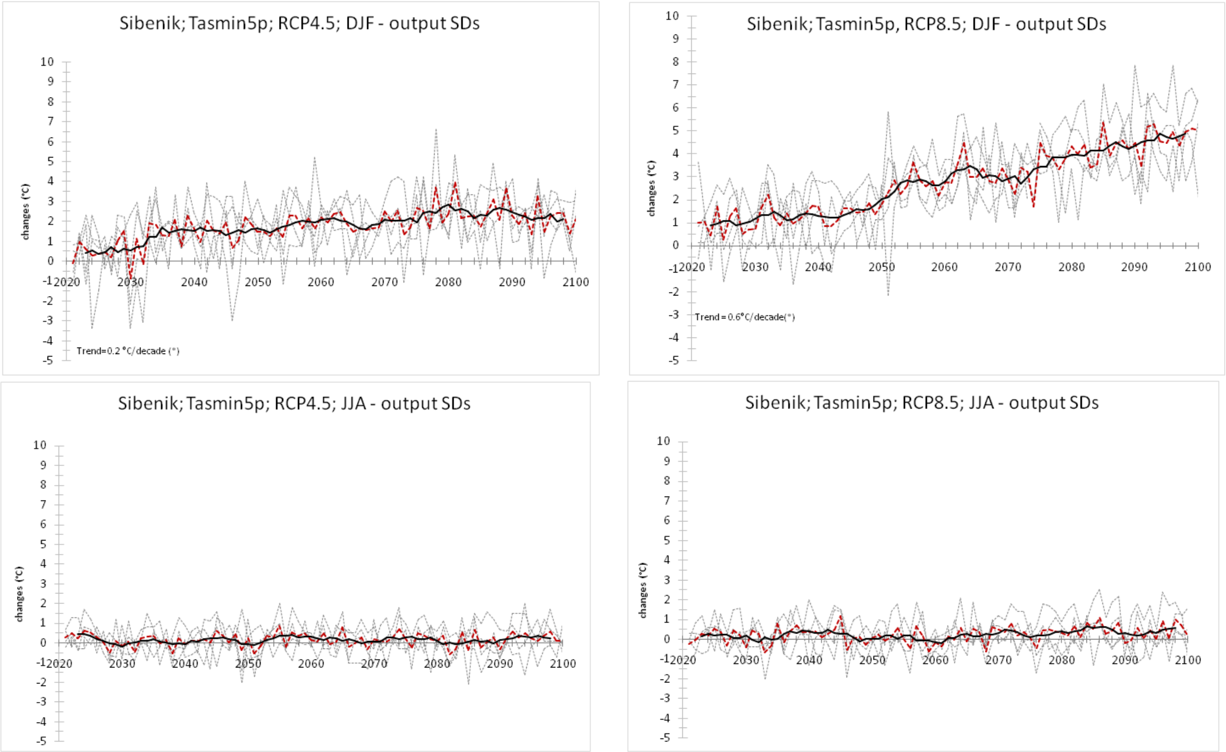

Figure 5-66: Variability of future changes of winter (DJF) and summer (JJA) of 5th minimum temperature projected through SDs applied to 4GCMs (grey lines); the Ensemble Mean (red line) and moving average (black line) - scenario RCP4.5 (left) and RCP8.5 (right), 2021-2100 period Significant trend is marked with star while n.s. means not significant (source Arpae-Simc).

95th percentile of maximum temperature

Future changes of 95th percentile of maximum temperature in Sibenik is projected to increase from P1 to P4 periods, with amplitudes that vary from model to model. The Ensemble Mean shows an increase in annual value of changes up to 1.3°C in the framework of RCP4.5 and up to 2.7°C in the framework of RCP8.5, going to the end of century (Figure 5-67). A deep analysis on projected changes reveals that higher values are expected to occur during spring and autumn with peak of changes around 4°C during 2081-2100 with respect to 1986-2005(RCP8.5)
Long term variability of future changes of 95th percentile of maximum temperature shows positive trend, significant only in the RCP8.5 emission scenario, about 0.2°C/decade (figure 5-68).

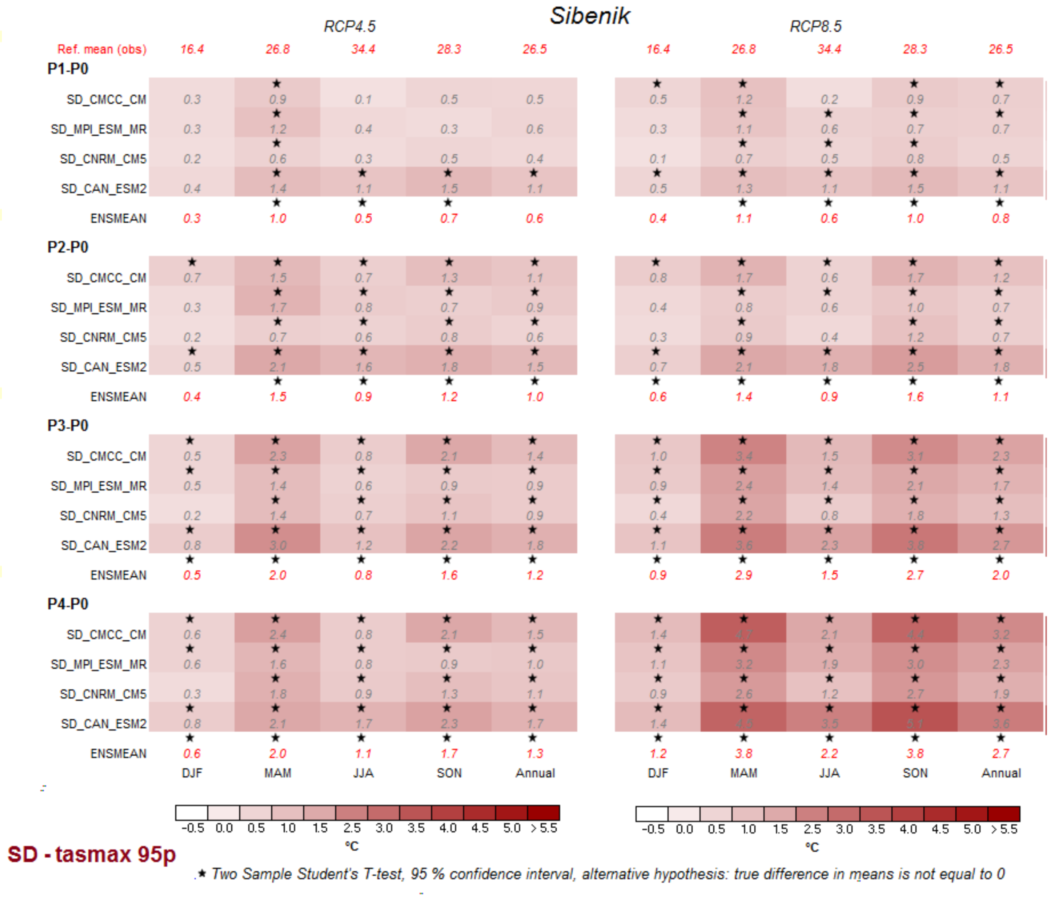

Sibenik

			RCP4.5					RCP8.5		
Ref. mean (obs)	16.4	26.8	34.4	28.3	26.5	16.4	26.8	34.4	28.3	26.5
P1-P0										
SD_CMCC_CM	0.3	★ 0.9	0.1	0.5	0.5	★ 0.5	★ 1.2	0.2	★ 0.9	★ 0.7
SD_MPI_ESM_MR	0.3	★ 1.2	0.4	0.3	0.6	0.3	★ 1.1	★ 0.6	★ 0.7	★ 0.7
SD_CNRM_CM5	0.2	★ 0.6	0.3	0.5	0.4	0.1	★ 0.7	★ 0.5	★ 0.8	0.5
SD_CAN_ESM2	0.4	★ 1.4	★ 1.1	★ 1.5	★ 1.1	★ 0.5	★ 1.3	★ 1.1	★ 1.5	★ 1.1
ENSMEAN	0.3	★ 1.0	★ 0.5	★ 0.7	0.6	0.4	★ 1.1	★ 0.6	★ 1.0	★ 0.8
P2-P0										
SD_CMCC_CM	★ 0.7	★ 1.5	★ 0.7	★ 1.3	★ 1.1	★ 0.8	★ 1.7	★ 0.6	★ 1.7	★ 1.2
SD_MPI_ESM_MR	0.3	★ 1.7	★ 0.8	★ 0.7	★ 0.9	0.4	★ 0.8	★ 0.6	★ 1.0	★ 0.7
SD_CNRM_CM5	0.2	★ 0.7	★ 0.6	★ 0.8	★ 0.6	0.3	★ 0.9	0.4	★ 1.2	★ 0.7
SD_CAN_ESM2	★ 0.5	★ 2.1	★ 1.6	★ 1.8	★ 1.5	★ 0.7	★ 2.1	★ 1.8	★ 2.5	★ 1.8
ENSMEAN	0.4	★ 1.5	★ 0.9	★ 1.2	★ 1.0	★ 0.6	★ 1.4	★ 0.9	★ 1.6	★ 1.1
P3-P0										
SD_CMCC_CM	★ 0.5	★ 2.3	★ 0.8	★ 2.1	★ 1.4	★ 1.0	★ 3.4	★ 1.5	★ 3.1	★ 2.3
SD_MPI_ESM_MR	★ 0.5	★ 1.4	★ 0.6	★ 0.9	★ 0.9	★ 0.9	★ 2.4	★ 1.4	★ 2.1	★ 1.7
SD_CNRM_CM5	0.2	★ 1.4	★ 0.7	★ 1.1	★ 0.9	★ 0.4	★ 2.2	★ 0.8	★ 1.8	★ 1.3
SD_CAN_ESM2	★ 0.8	★ 3.0	★ 1.2	★ 2.2	★ 1.8	★ 1.1	★ 3.6	★ 2.3	★ 3.8	★ 2.7
ENSMEAN	★ 0.5	★ 2.0	★ 0.8	★ 1.6	★ 1.2	★ 0.9	★ 2.9	★ 1.5	★ 2.7	★ 2.0
P4-P0										
SD_CMCC_CM	★ 0.6	★ 2.4	★ 0.8	★ 2.1	★ 1.5	★ 1.4	★ 4.7	★ 2.1	★ 4.4	★ 3.2
SD_MPI_ESM_MR	★ 0.6	★ 1.6	★ 0.8	★ 0.9	★ 1.0	★ 1.1	★ 3.2	★ 1.9	★ 3.0	★ 2.3
SD_CNRM_CM5	0.3	★ 1.8	★ 0.9	★ 1.3	★ 1.1	★ 0.9	★ 2.6	★ 1.2	★ 2.7	★ 1.9
SD_CAN_ESM2	★ 0.8	★ 2.1	★ 1.7	★ 2.3	★ 1.7	★ 1.4	★ 4.5	★ 3.5	★ 5.1	★ 3.6
ENSMEAN	★ 0.6	★ 2.0	★ 1.1	★ 1.7	★ 1.3	★ 1.2	★ 3.8	★ 2.2	★ 3.8	★ 2.7
	DJF	MAM	JJA	SON	Annual	DJF	MAM	JJA	SON	Annual

SD - tasmax 95p

★ Two Sample Student's T-test, 95 % confidence interval, alternative hypothesis: true difference in means is not equal to 0

Figure 5-67: 95th percentile of seasonal and annual maximum temperature: observed values over reference period (in red), changes projected by statistical downscaling applied to 4GCMs and the Ensemble Mean of changes over the four periods (P1, P2, P3 ,P4) projected in the framework of RCP4.5 (left) and RCP 8.5 (right). Significant change is marked by star (source Arpae-Simc)

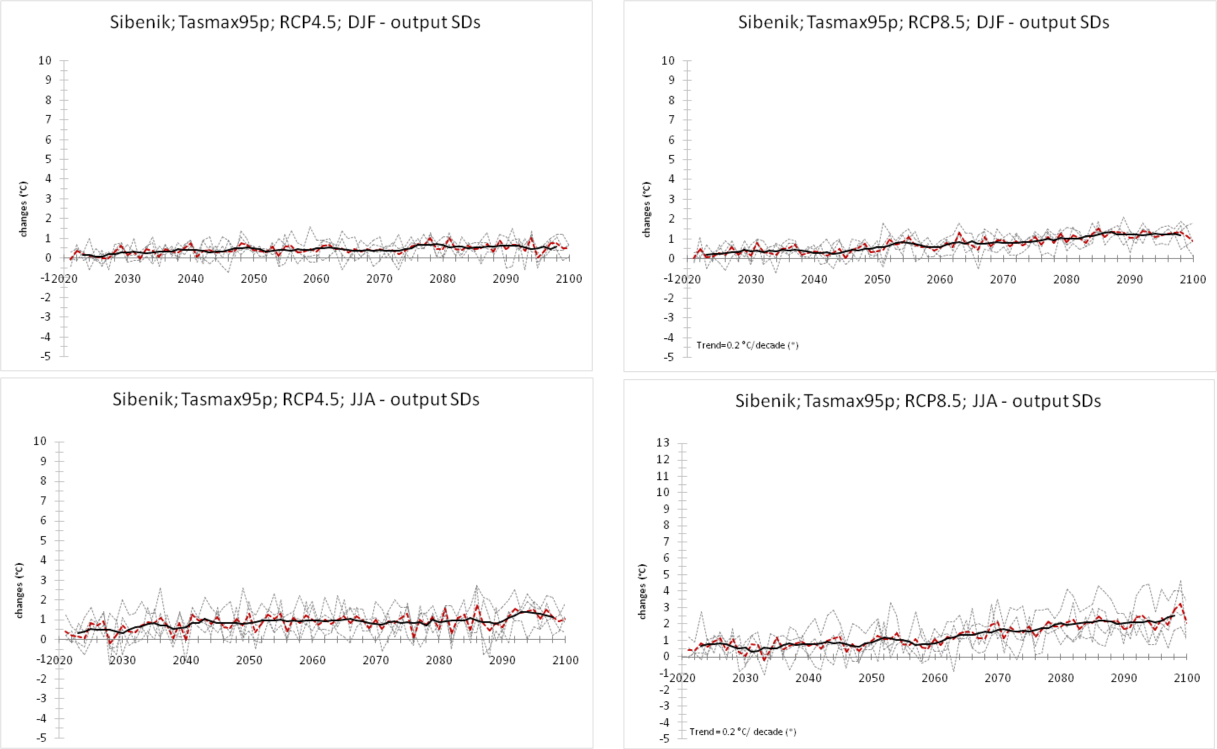

Figure 5-68: Future changes of winter (DJF) and summer (JJA) of 95th percentile of maximum temperature projected through SDs applied to 4GCMs (grey lines); the Ensemble Mean (red line) and moving average (black line) - scenario RCP4.5 (left) and RCP8.5 (right), 2021-2100 period. Significant trend is marked with star while n.s. means not significant (source Arpae-Simc).

6.2.2.1.3 *Heat wave duration*

The projection of the heat wave duration, index defined as the maximum number of consecutive days with maximum temperature greater than 90th daily percentile, shows an increase during spring and summer. Figure 5-69 includes the projected changes for Sibenik. In the framework of RCP4.5, the increase could reach around 20 consecutive days (on spring, during P3 and P4) while in the framework of RCP8.5 could reach 58 consecutive days in spring. As regards summer season, the projected changes is about 11 consecutive days for RCP4.5 andd 38 consecutive days for RCP8.5, going to the end of century. As regards long term variability (see figure 5-70) the trend is positive, statistically significant only during summer

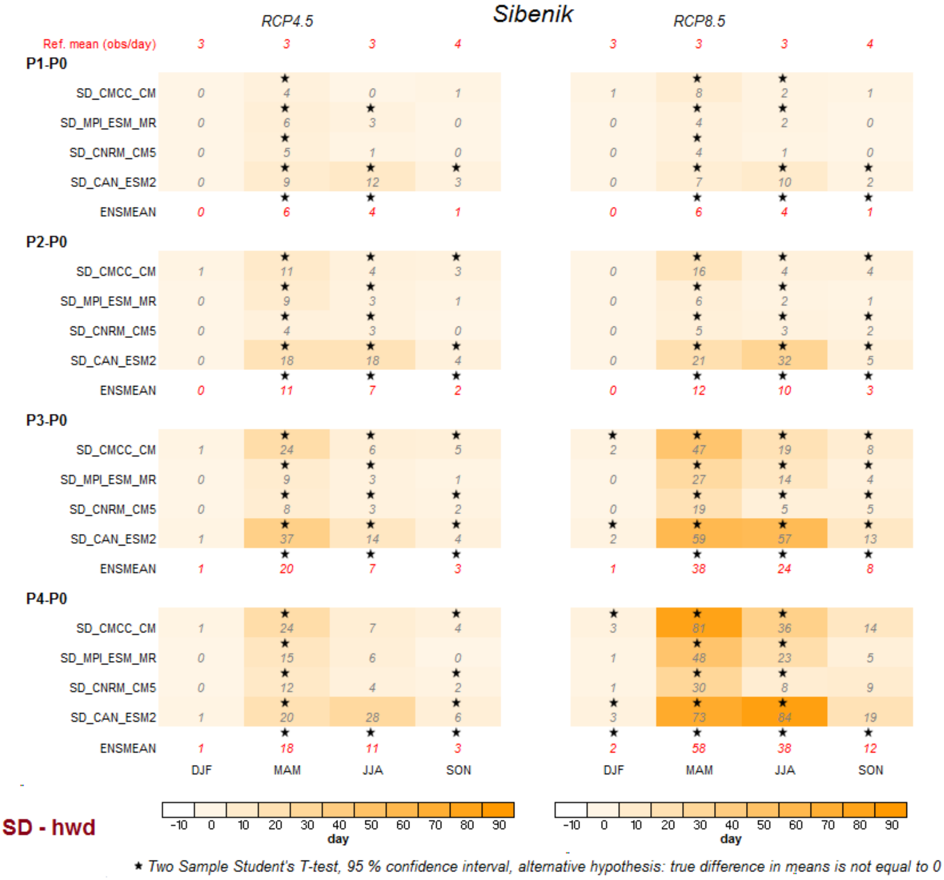

Sibenik

	RCP4.5				RCP8.5			
Ref. mean (obs/day)	3	3	3	4	3	3	3	4
P1-P0								
SD_CMCC_CM	0	★ 4	0	1	1	★ 8	★ 2	1
SD_MPI_ESM_MR	0	★ 6	★ 3	0	0	★ 4	★ 2	0
SD_CNRM_CM5	0	★ 5	1	0	0	★ 4	1	0
SD_CAN_ESM2	0	★ 9	★ 12	★ 3	0	★ 7	★ 10	★ 2
ENSMEAN	0	★ 6	★ 4	1	0	★ 6	★ 4	★ 1
P2-P0								
SD_CMCC_CM	1	★ 11	★ 4	★ 3	0	★ 16	★ 4	★ 4
SD_MPI_ESM_MR	0	★ 9	★ 3	1	0	★ 6	★ 2	1
SD_CNRM_CM5	0	★ 4	★ 3	0	0	★ 5	★ 3	★ 2
SD_CAN_ESM2	0	★ 18	★ 18	★ 4	0	★ 21	★ 32	★ 5
ENSMEAN	0	★ 11	★ 7	★ 2	0	★ 12	★ 10	★ 3
P3-P0								
SD_CMCC_CM	1	★ 24	★ 6	★ 5	★ 2	★ 47	★ 19	★ 8
SD_MPI_ESM_MR	0	★ 9	★ 3	1	0	★ 27	★ 14	★ 4
SD_CNRM_CM5	0	★ 8	★ 3	★ 2	0	★ 19	★ 5	★ 5
SD_CAN_ESM2	1	★ 37	★ 14	★ 4	★ 2	★ 59	★ 57	★ 13
ENSMEAN	1	★ 20	★ 7	★ 3	1	★ 38	★ 24	★ 8
P4-P0								
SD_CMCC_CM	1	★ 24	7	★ 4	★ 3	★ 81	★ 36	14
SD_MPI_ESM_MR	0	★ 15	6	0	1	★ 48	★ 23	5
SD_CNRM_CM5	0	★ 12	4	★ 2	1	★ 30	★ 8	9
SD_CAN_ESM2	1	★ 20	28	★ 6	★ 3	★ 73	★ 84	19
ENSMEAN	1	★ 18	★ 11	★ 3	★ 2	★ 58	★ 38	★ 12
	DJF	MAM	JJA	SON	DJF	MAM	JJA	SON

★ Two Sample Student's T-test, 95 % confidence interval, alternative hypothesis: true difference in means is not equal to 0

Figure 5-69: Seasonal heat wave duration: observed values over reference period (in red), changes projected by statistical downscaling applied to 4GCMs and the Ensemble Mean of changes over the four periods (P1,P2,P3,P4) projected in the framework of

RCP4,5 (left) and RCP 8.5 (right). Significant change is marked by star (source Arpae-Simc)

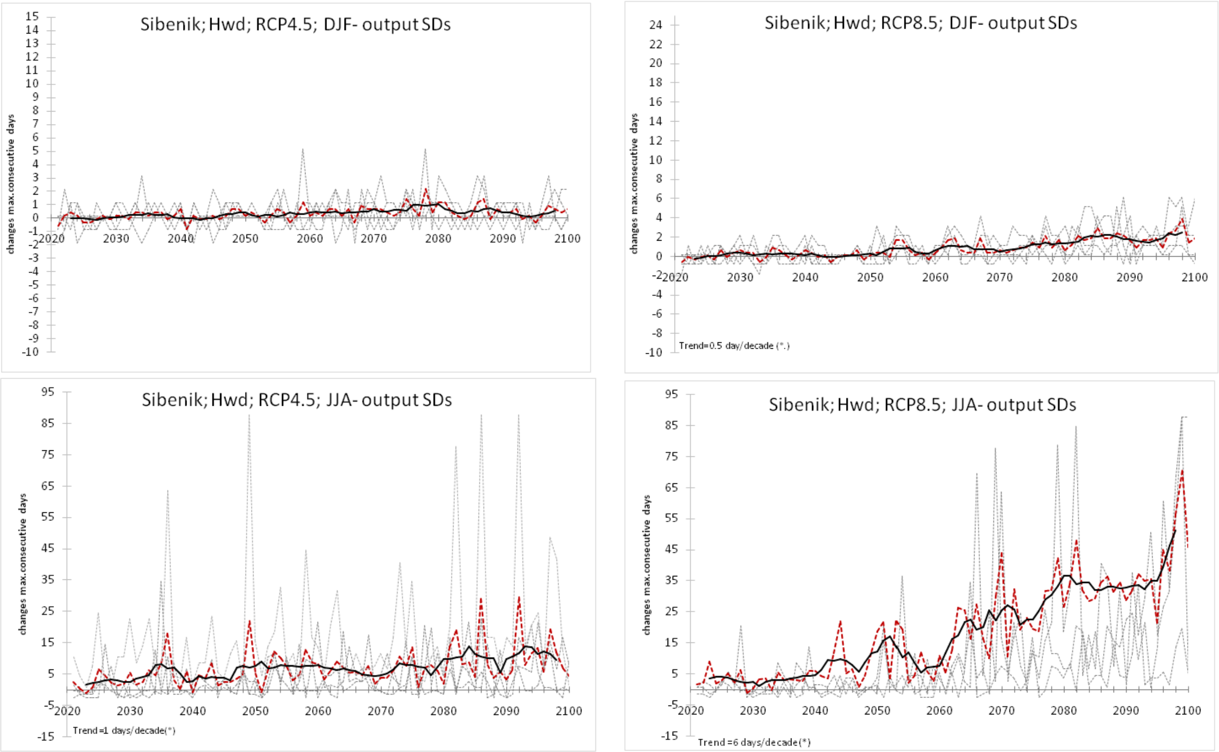

Figure 5-70: Variability of future changes of winter (DJF) and summer (JJA) heat wave duration projected through SDs applied to 4GCMs (grey lines); the Ensemble Mean (red line) and moving average (black line) - scenario RCP4.5 (left) and RCP8.5 (right), 2021-2100 period Significant trend is marked with star while n.s. means not significant (source Arpae-Simc).

6.2.2.1.4 *Tropical nights*

Seasonal changes of tropical nights (tr) in terms of differences between P1-P0, P2-P0, P3-P0, P4-P0 are shown in figures 5-71, relative to the RCP4.5 and RCP8.5 scenarios. The projection of the tropical nights, index defined as the number of days with a minimum temperature greater than 20°C, shows an increase during summer season for both RCPs. All SDs models agree with these changes, as could be noted from figure 5-71. The value of changes varies between 20 to 40 days for RCP4.5 and between 20 to 48 days for RCP8.5 (from P1 to P4). One important signal could be noted also during autumn, when an increase is projected to occur during P3 and P4, up to 11 days.
Regarding long term variability of summer tropical nights, the trend is positive and statistically significant for both RCPs, (up to 4 days/decade) during 2021-2100 (see figure 5-72).

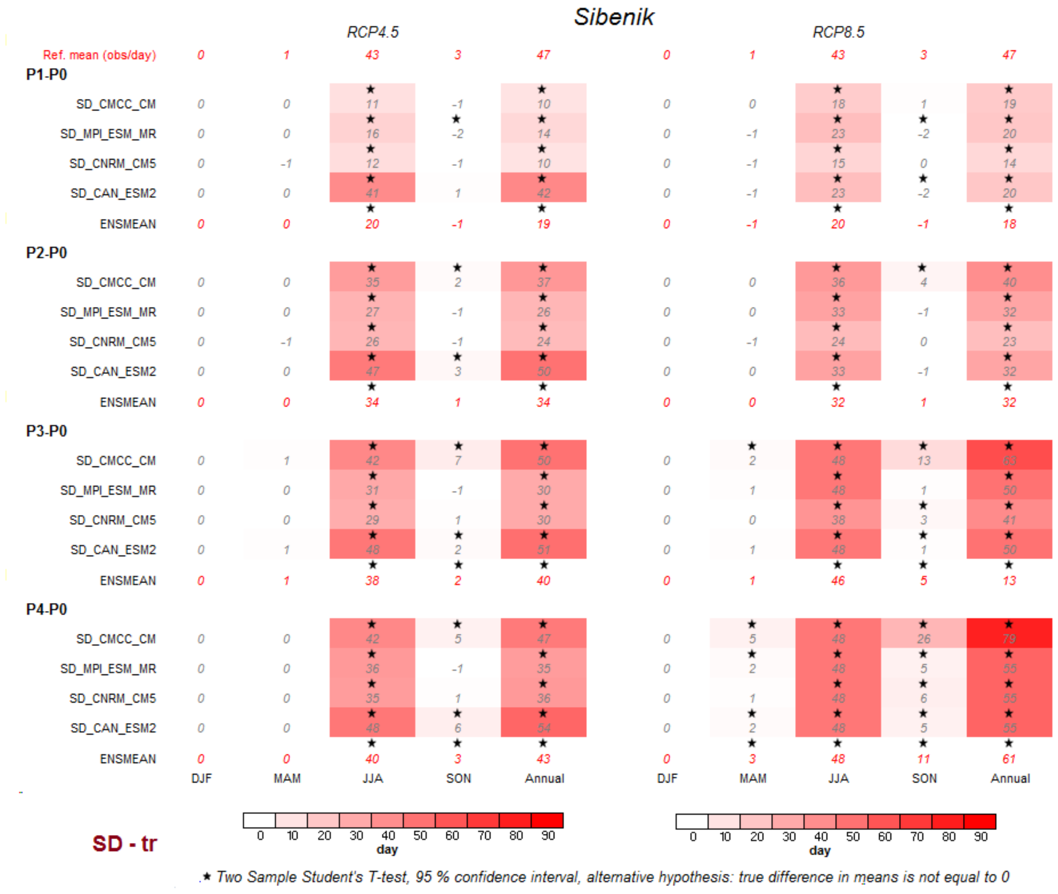

Sibenik

	RCP4.5					RCP8.5				
	DJF	MAM	JJA	SON	Annual	DJF	MAM	JJA	SON	Annual
Ref. mean (obs/day)	0	1	43	3	47	0	1	43	3	47
P1-P0										
SD_CMCC_CM	0	0	★ 11	-1	★ 10	0	0	★ 18	1	★ 19
SD_MPI_ESM_MR	0	0	★ 16	★ -2	★ 14	0	-1	★ 23	★ -2	★ 20
SD_CNRM_CM5	0	-1	★ 12	-1	★ 10	0	-1	★ 15	0	★ 14
SD_CAN_ESM2	0	0	★ 41	1	★ 42	0	-1	★ 23	★ -2	★ 20
ENSMEAN	0	0	★ 20	-1	★ 19	0	-1	★ 20	-1	★ 18
P2-P0										
SD_CMCC_CM	0	0	★ 35	★ 2	★ 37	0	0	★ 36	★ 4	★ 40
SD_MPI_ESM_MR	0	0	★ 27	-1	★ 26	0	0	★ 33	-1	★ 32
SD_CNRM_CM5	0	-1	★ 26	-1	★ 24	0	-1	★ 24	0	★ 23
SD_CAN_ESM2	0	0	★ 47	★ 3	★ 50	0	0	★ 33	-1	★ 32
ENSMEAN	0	0	★ 34	1	★ 34	0	0	★ 32	1	★ 32
P3-P0										
SD_CMCC_CM	0	1	★ 42	★ 7	★ 50	0	★ 2	★ 48	★ 13	★ 63
SD_MPI_ESM_MR	0	0	★ 31	-1	★ 30	0	1	★ 48	1	★ 50
SD_CNRM_CM5	0	0	★ 29	1	★ 30	0	0	★ 38	★ 3	★ 41
SD_CAN_ESM2	0	1	★ 48	★ 2	★ 51	0	1	★ 48	★ 1	★ 50
ENSMEAN	0	1	★ 38	★ 2	★ 40	0	1	★ 46	★ 5	★ 13
P4-P0										
SD_CMCC_CM	0	0	★ 42	★ 5	★ 47	0	★ 5	★ 48	★ 26	★ 79
SD_MPI_ESM_MR	0	0	★ 36	-1	★ 35	0	★ 2	★ 48	★ 5	★ 55
SD_CNRM_CM5	0	0	★ 35	1	★ 36	0	1	★ 48	★ 6	★ 55
SD_CAN_ESM2	0	0	★ 48	★ 6	★ 54	0	★ 2	★ 48	★ 5	★ 55
ENSMEAN	0	0	★ 40	★ 3	★ 43	0	★ 3	★ 48	★ 11	★ 61

SD - tr

★ Two Sample Student's T-test, 95 % confidence interval, alternative hypothesis: true difference in means is not equal to 0

Figure 5-71: Seasonal and annual tropical nights: observed values over reference period (in red), changes projected by statistical downscaling applied to 4GCMs and the Ensemble Mean over the four periods (P1, P2,P3,P4) projected in the framework of RCP4.5 (left) and RCP 8.5 (right). Significant change is marked by star (source Arpae-Simc)

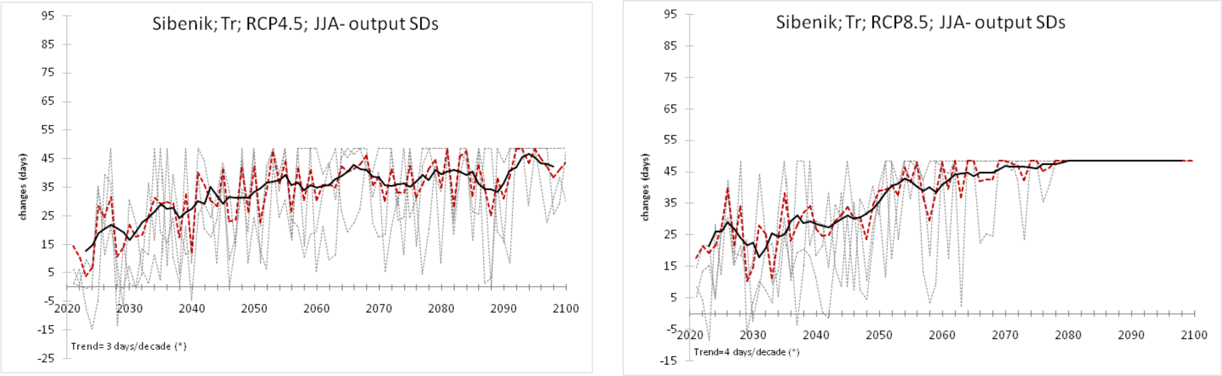

Figure 5-72: Variability of future changes of summer (JJA) tropical nights projected through SDs applied to 4GCMs (grey lines); the Ensemble Mean (red line) and moving average (black line) - scenario RCP4.5 (left) and RCP8.5 (right), 2021-2100 period Significant trend is marked with star while n.s. means not significant (source Arpae-Simc).

6.2.2.1.1 *Frost days*

The future projections of frost days, namely the number of days with minimum temperature lower than 0°C, show a decrease during winter, spring and autumn. All SDs models agree with these changes during all periods, as could be noted from figure 5-73. The signal of changes is higher during winter season, with values of changes in RCP4.5 scenario between -3 days during P1 up to -10 days going to the end of the century. The magnitude of changes is slightly higher for RCP8.5 between -6 to -13 days (see figure 5-73).

Regarding long term variability of changes, the trend is negative but statistically significant only for RCP8.5 (see figure 5-74).

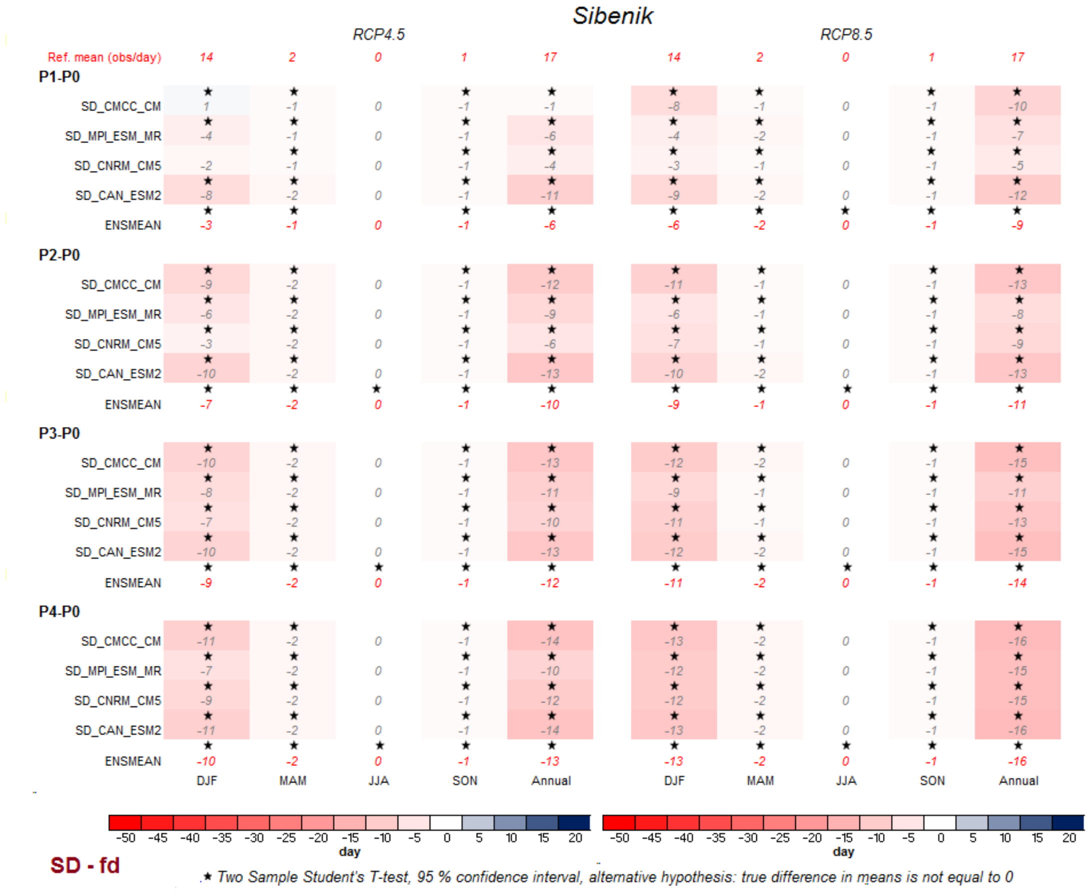

Sibenik

	RCP4.5					RCP8.5				
Ref. mean (obs/day)	14	2	0	1	17	14	2	0	1	17
P1-P0										
SD_CMCC_CM	★ 1	★ -1	0	★ -1	★ -1	★ -8	★ -1	0	★ -1	★ -10
SD_MPI_ESM_MR	★ -4	★ -1	0	★ -1	★ -6	★ -4	★ -2	0	★ -1	★ -7
SD_CNRM_CM5	-2	★ -1	0	★ -1	★ -4	★ -3	★ -1	0	★ -1	★ -5
SD_CAN_ESM2	★ -8	★ -2	0	★ -1	★ -11	★ -9	★ -2	0	★ -1	★ -12
ENSMEAN	★ -3	★ -1	0	★ -1	★ -6	★ -6	★ -2	★ 0	★ -1	★ -9
P2-P0										
SD_CMCC_CM	★ -9	★ -2	0	★ -1	★ -12	★ -11	★ -1	0	★ -1	★ -13
SD_MPI_ESM_MR	★ -6	★ -2	0	★ -1	★ -9	★ -6	★ -1	0	★ -1	★ -8
SD_CNRM_CM5	★ -3	★ -2	0	★ -1	★ -6	★ -7	★ -1	0	★ -1	★ -9
SD_CAN_ESM2	★ -10	★ -2	0	★ -1	★ -13	★ -10	★ -2	0	★ -1	★ -13
ENSMEAN	★ -7	★ -2	★ 0	★ -1	★ -10	★ -9	★ -1	★ 0	★ -1	★ -11
P3-P0										
SD_CMCC_CM	★ -10	★ -2	0	★ -1	★ -13	★ -12	★ -2	0	★ -1	★ -15
SD_MPI_ESM_MR	★ -8	★ -2	0	★ -1	★ -11	★ -9	★ -1	0	★ -1	★ -11
SD_CNRM_CM5	★ -7	★ -2	0	★ -1	★ -10	★ -11	★ -1	0	★ -1	★ -13
SD_CAN_ESM2	★ -10	★ -2	0	★ -1	★ -13	★ -12	★ -2	0	★ -1	★ -15
ENSMEAN	★ -9	★ -2	★ 0	★ -1	★ -12	★ -11	★ -2	★ 0	★ -1	★ -14
P4-P0										
SD_CMCC_CM	★ -11	★ -2	0	★ -1	★ -14	★ -13	★ -2	0	★ -1	★ -16
SD_MPI_ESM_MR	★ -7	★ -2	0	★ -1	★ -10	★ -12	★ -2	0	★ -1	★ -15
SD_CNRM_CM5	★ -9	★ -2	0	★ -1	★ -12	★ -12	★ -2	0	★ -1	★ -15
SD_CAN_ESM2	★ -11	★ -2	0	★ -1	★ -14	★ -13	★ -2	0	★ -1	★ -16
ENSMEAN	★ -10	★ -2	★ 0	★ -1	★ -13	★ -13	★ -2	★ 0	★ -1	★ -16
	DJF	MAM	JJA	SON	Annual	DJF	MAM	JJA	SON	Annual

SD - fd

★ Two Sample Student's T-test, 95 % confidence interval, alternative hypothesis: true difference in means is not equal to 0

Figure 5-73: Seasonal and annual frost days: observed values over reference period (in red), changes projected by statistical downscaling applied to 4GCMs and the Ensemble Mean over the four periods (P1, P2, P3, P4) projected in the framework of RCP4.5 (left) and RCP 8.5 (right). Significant change is marked by star (source Arpae-Simc)

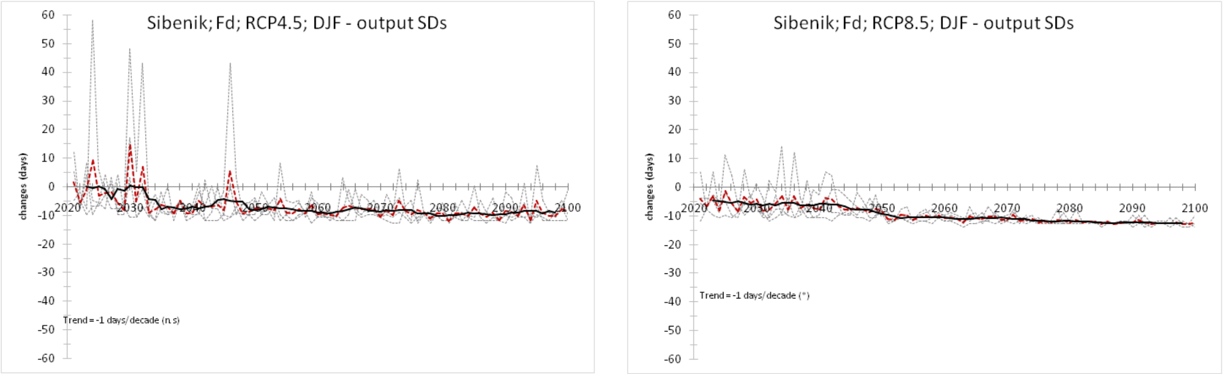

Figure 5-74: Future changes of winter (DJF) frost days projected through SDs applied to 4GCMs (grey lines); the Ensemble Mean (red line) and moving average (black line) - scenario RCP4.5 (left) and RCP8.5 (right), 2021-2100 period. Significant trend is marked with star while n.s. means not significant (source Arpae-Simc).

6.2.2.2 *Precipitation related indices projection*

6.2.2.2.1 *Amount of precipitation*

Precipitation is much more variable parameter in comparison to the temperature, therefore there is no always unique sign of change through the year as well as from model to model. The Ensemble Mean of changes of amount of precipitation presented in figure 5-75 could be summarized as follows:

-at annual level, a decrease of precipitation can be expected to occur starting from P1 going to P4 when is expected a decrease up to -28 % for RCP4.5 and -40 % for RCP8.5 scenario;

-a possible decrease of precipitation during winter in RCP4.5 from P1 to P4 and for RCP8.5 from P1 to P3(not significant) ; some models show an increase for RCP8.5 in the last two periods;

- a decrease of precipitation for other seasons, around to -50% for MAM and SON and -66% for JJA, in the framework of RCP8.5.

The long-term variability of changes in future precipitation over 2021-2100 period shows for Sibenik possible slightly increase in winter and decrease in summer, signals significant only for RCP8.5 (figure 5-76).

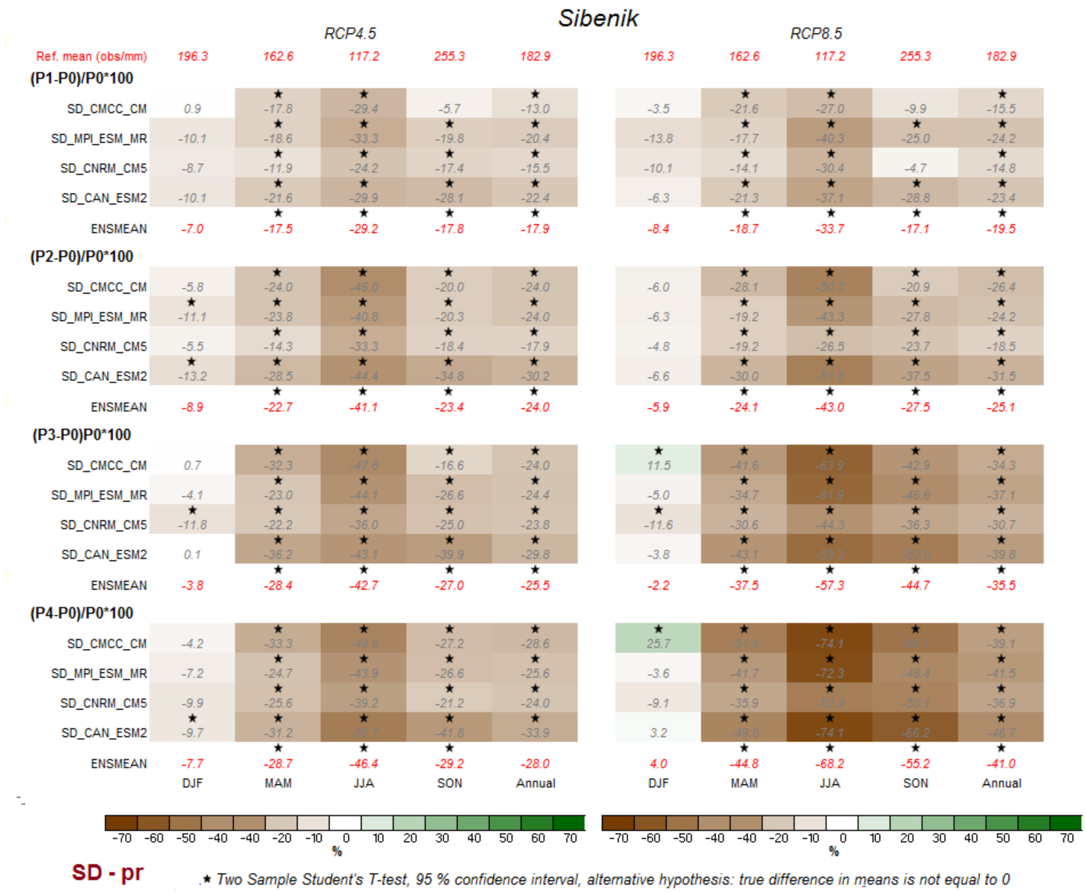

	RCP4.5					RCP8.5				
	DJF	MAM	JJA	SON	Annual	DJF	MAM	JJA	SON	Annual
Ref. mean (obs/mm)	196.3	162.6	117.2	255.3	182.9	196.3	162.6	117.2	255.3	182.9
(P1-P0)/P0*100										
SD_CMCC_CM	0.9	★ -17.8	★ -29.4	-5.7	★ -13.0	-3.5	★ -21.6	★ -27.0	-9.9	★ -15.5
SD_MPI_ESM_MR	-10.1	★ -18.6	★ -33.3	★ -19.8	★ -20.4	-13.8	★ -17.7	★ -40.3	★ -25.0	★ -24.2
SD_CNRM_CM5	-8.7	★ -11.9	★ -24.2	★ -17.4	★ -15.5	-10.1	★ -14.1	★ -30.4	-4.7	★ -14.8
SD_CAN_ESM2	-10.1	★ -21.6	★ -29.9	★ -28.1	★ -22.4	-6.3	★ -21.3	★ -37.1	★ -28.8	★ -23.4
ENSMEAN	-7.0	★ -17.5	★ -29.2	★ -17.8	★ -17.9	-8.4	★ -18.7	★ -33.7	★ -17.1	★ -19.5
(P2-P0)/P0*100										
SD_CMCC_CM	-5.8	★ -24.0	★ -46.0	★ -20.0	★ -24.0	-6.0	★ -28.1	★ -50.7	★ -20.9	★ -26.4
SD_MPI_ESM_MR	★ -11.1	★ -23.8	★ -40.8	★ -20.3	★ -24.0	-6.3	★ -19.2	★ -43.3	★ -27.8	★ -24.2
SD_CNRM_CM5	-5.5	★ -14.3	★ -33.3	★ -18.4	★ -17.9	-4.8	★ -19.2	★ -26.5	★ -23.7	★ -18.5
SD_CAN_ESM2	★ -13.2	★ -28.5	★ -44.4	★ -34.8	★ -30.2	-6.6	★ -30.0	★ -51.8	★ -37.5	★ -31.5
ENSMEAN	-8.9	★ -22.7	★ -41.1	★ -23.4	★ -24.0	-5.9	★ -24.1	★ -43.0	★ -27.5	★ -25.1
(P3-P0)P0*100										
SD_CMCC_CM	0.7	★ -32.3	★ -47.6	★ -16.6	★ -24.0	★ 11.5	★ -41.6	★ -63.9	★ -42.9	★ -34.3
SD_MPI_ESM_MR	-4.1	★ -23.0	★ -44.1	★ -26.6	★ -24.4	-5.0	★ -34.7	★ -61.9	★ -46.6	★ -37.1
SD_CNRM_CM5	★ -11.8	★ -22.2	★ -36.0	★ -25.0	★ -23.8	★ -11.6	★ -30.6	★ -44.3	★ -36.3	★ -30.7
SD_CAN_ESM2	0.1	★ -36.2	★ -43.1	★ -39.9	★ -29.8	-3.8	★ -43.1	★ -59.3	★ -53.0	★ -39.8
ENSMEAN	-3.8	★ -28.4	★ -42.7	★ -27.0	★ -25.5	-2.2	★ -37.5	★ -57.3	★ -44.7	★ -35.5
(P4-P0)/P0*100										
SD_CMCC_CM	-4.2	★ -33.3	★ -49.8	★ -27.2	★ -28.6	★ 25.7	★ -51.8	★ -74.1	★ -56.1	★ -39.1
SD_MPI_ESM_MR	-7.2	★ -24.7	★ -43.9	★ -26.6	★ -25.6	-3.6	★ -41.7	★ -72.3	★ -48.4	★ -41.5
SD_CNRM_CM5	-9.9	★ -25.6	★ -39.2	★ -21.2	★ -24.0	-9.1	★ -35.9	★ -52.4	★ -50.1	★ -36.9
SD_CAN_ESM2	★ -9.7	★ -31.2	★ -52.7	★ -41.8	★ -33.9	3.2	★ -49.8	★ -74.1	★ -66.2	★ -46.7
ENSMEAN	-7.7	★ -28.7	★ -46.4	★ -29.2	-28.0	4.0	★ -44.8	★ -68.2	★ -55.2	★ -41.0

★ Two Sample Student's T-test, 95 % confidence interval, alternative hypothesis: true difference in means is not equal to 0

Figure 5-75: Seasonal and annual amount of precipitation: observed values over reference period (in red), changes projected by statistical downscaling applied to 4GCMs and the Ensemble Mean of changes over the four periods (P1, P2, P3, P4) expressed in % RCP4.5 (left) and RCP 8.5 (right) scenarios. Significant change is marked by star (source Arpae-Simc)

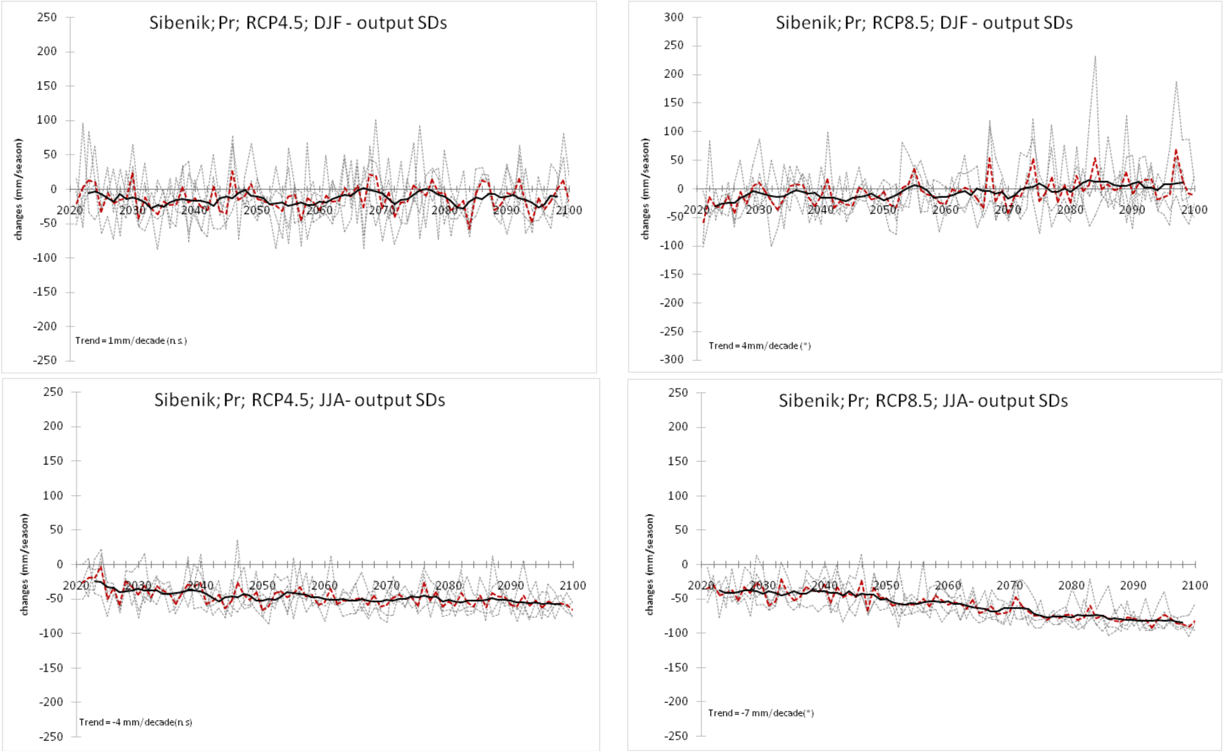

Figure 5-76: Variability of future changes of winter (DJF) and summer (JJA) precipitation projected through SDs applied to 4GCMs (grey lines); the Ensemble Mean (red line) and moving average (black line) - scenario RCP4.5 (left) and RCP8.5 (right), 2021-2100 period. Significant trend is marked with star while n.s. means not significant (source Arpae-Simc).

6.2.2.2.2 *Intense precipitation*

90th percentile of seasonal amount of precipitation

Intense precipitation, defined by 90th percentile of daily precipitation shows for Sibenik:
-significant projected changes during summer season for RCP4.5 and RCP8.5 - all 4 periods- and during winter and autumn over P3 and P4 , both emission scenarios (Figure 5-77).
These changes are referred to a decrease during winter, spring and autumn (between -5 and -22 mm) while an increase is noted during summer up to 20% for RCP4.5 and up to 57 % for RCP8.5 going to end of century.
Long term variability emphasis a negative trend in winter and positive ones in summer statistically significant only for RCP8.5 (figure 5-78).

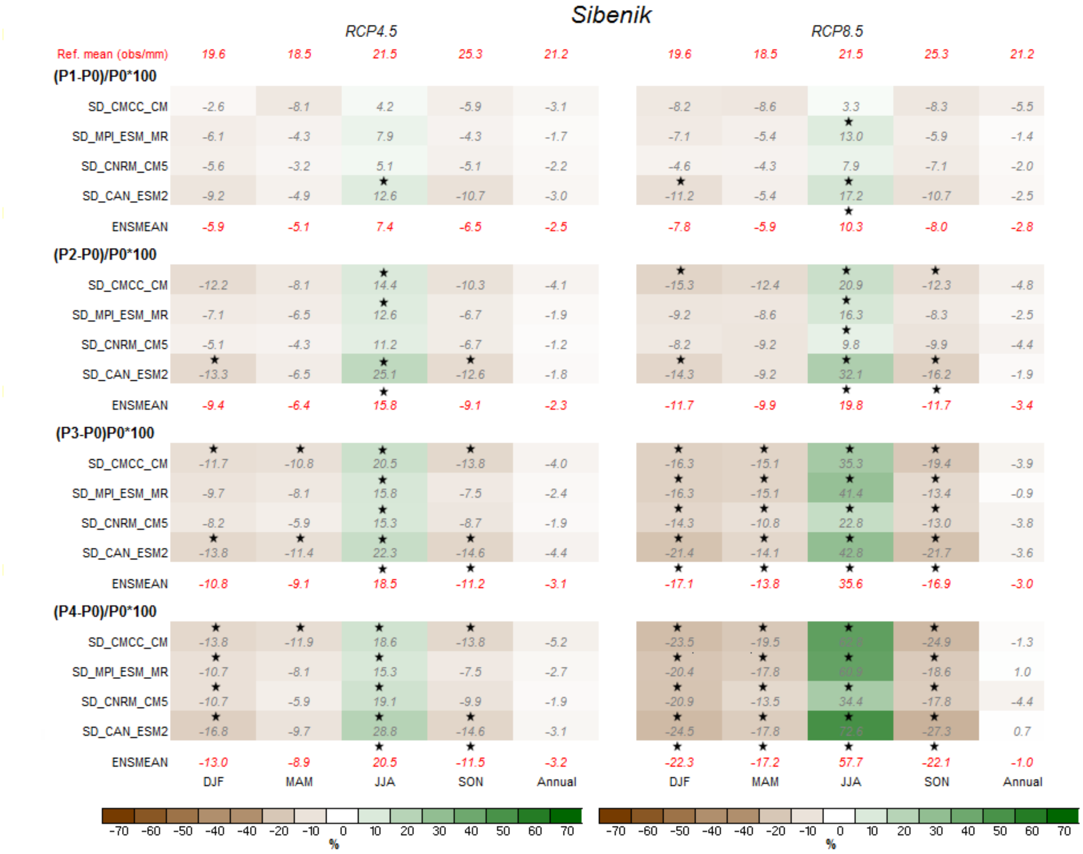

Sibenik

	RCP4.5					RCP8.5				
	DJF	MAM	JJA	SON	Annual	DJF	MAM	JJA	SON	Annual
Ref. mean (obs/mm)	19.6	18.5	21.5	25.3	21.2	19.6	18.5	21.5	25.3	21.2
(P1-P0)/P0*100										
SD_CMCC_CM	-2.6	-8.1	4.2	-5.9	-3.1	-8.2	-8.6	3.3	-8.3	-5.5
SD_MPI_ESM_MR	-6.1	-4.3	7.9	-4.3	-1.7	-7.1	-5.4	★ 13.0	-5.9	-1.4
SD_CNRM_CM5	-5.6	-3.2	5.1	-5.1	-2.2	-4.6	-4.3	7.9	-7.1	-2.0
SD_CAN_ESM2	-9.2	-4.9	★ 12.6	-10.7	-3.0	★ -11.2	-5.4	★ 17.2	-10.7	-2.5
ENSMEAN	-5.9	-5.1	7.4	-6.5	-2.5	-7.8	-5.9	★ 10.3	-8.0	-2.8
(P2-P0)/P0*100										
SD_CMCC_CM	-12.2	-8.1	★ 14.4	-10.3	-4.1	★ -15.3	-12.4	★ 20.9	★ -12.3	-4.8
SD_MPI_ESM_MR	-7.1	-6.5	★ 12.6	-6.7	-1.9	-9.2	-8.6	★ 16.3	-8.3	-2.5
SD_CNRM_CM5	-5.1	-4.3	11.2	-6.7	-1.2	-8.2	-9.2	★ 9.8	-9.9	-4.4
SD_CAN_ESM2	★ -13.3	-6.5	★ 25.1	★ -12.6	-1.8	★ -14.3	-9.2	★ 32.1	★ -16.2	-1.9
ENSMEAN	-9.4	-6.4	★ 15.8	-9.1	-2.3	-11.7	-9.9	★ 19.8	★ -11.7	-3.4
(P3-P0)P0*100										
SD_CMCC_CM	★ -11.7	★ -10.8	★ 20.5	★ -13.8	-4.0	★ -16.3	★ -15.1	★ 35.3	★ -19.4	-3.9
SD_MPI_ESM_MR	-9.7	-8.1	★ 15.8	-7.5	-2.4	★ -16.3	★ -15.1	★ 41.4	★ -13.4	-0.9
SD_CNRM_CM5	-8.2	-5.9	★ 15.3	-8.7	-1.9	★ -14.3	★ -10.8	★ 22.8	★ -13.0	-3.8
SD_CAN_ESM2	★ -13.8	★ -11.4	★ 22.3	★ -14.6	-4.4	★ -21.4	★ -14.1	★ 42.8	★ -21.7	-3.6
ENSMEAN	-10.8	-9.1	★ 18.5	★ -11.2	-3.1	★ -17.1	★ -13.8	★ 35.6	★ -16.9	-3.0
(P4-P0)/P0*100										
SD_CMCC_CM	★ -13.8	★ -11.9	★ 18.6	★ -13.8	-5.2	★ -23.5	★ -19.5	★ 62.8	★ -24.9	-1.3
SD_MPI_ESM_MR	★ -10.7	-8.1	★ 15.3	-7.5	-2.7	★ -20.4	★ -17.8	★ 60.9	★ -18.6	1.0
SD_CNRM_CM5	★ -10.7	-5.9	★ 19.1	-9.9	-1.9	★ -20.9	★ -13.5	★ 34.4	★ -17.8	-4.4
SD_CAN_ESM2	★ -16.8	-9.7	★ 28.8	★ -14.6	-3.1	★ -24.5	★ -17.8	★ 72.6	★ -27.3	0.7
ENSMEAN	-13.0	-8.9	★ 20.5	★ -11.5	-3.2	★ -22.3	★ -17.2	★ 57.7	★ -22.1	-1.0

SD - pr 90p

★ *Two Sample Student's T-test, 95 % confidence interval, alternative hypothesis: true difference in means is not equal to 0*

Figure 5-77: Seasonal and annual amount of 90th precipitation: observed values over reference period (in red), changes projected by statistical downscaling applied to 4GCMs and the Ensemble Mean over the four periods (P1, P2, P3, P4) projected in the framework of RCP4.5 (left) and RCP 8.5 (right). Significant change is marked by star (source Arpae-Simc)

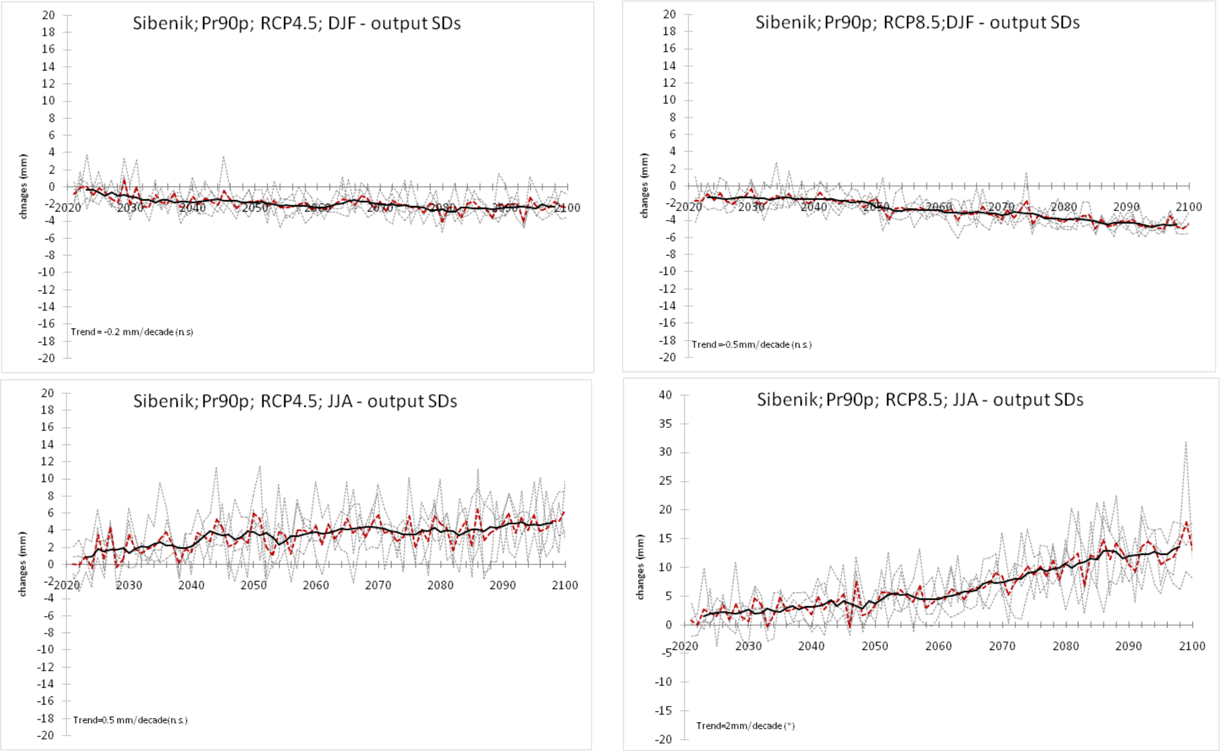

Figure 5-78: Future changes of winter (DJF) and summer (JJA) 90th precipitation projected through SDs applied to 4GCMs (grey lines); the Ensemble Mean (red line) and moving average (black line) - scenario RCP4.5 (left) and RCP8.5 (right), 2021-2100 period. Significant trend is marked with star while n.s. means not significant (source Arpae-Simc).

6.2.2.2.3 *Consecutive dry days*

The consecutive dry days, defined as the maximum number of consecutive days without precipitation shows for Sibenik:
-a decrease during winter and an increase during spring, summer and autumn.
The values of projected changes are in generally significant, with magnitude of changes in summer up to +18 consecutive days for RCP4.5 and +46 consecutive days for RCP8.5 going to P4 (figure 5-79). As regards spring and autumn the diagram shows possible changes about +17 days in spring and +11 days in autumn for the worst emission scenario (RCP8.5).
Winter, is the season when the simulations show possible decrease, around -4 consecutive days.
The long-term variability reveals slightly negative trends during winter, not significant, and positive and statistically significant trends during summer up to 7.5 days/decade in RCP8.5 (figure 5-80).

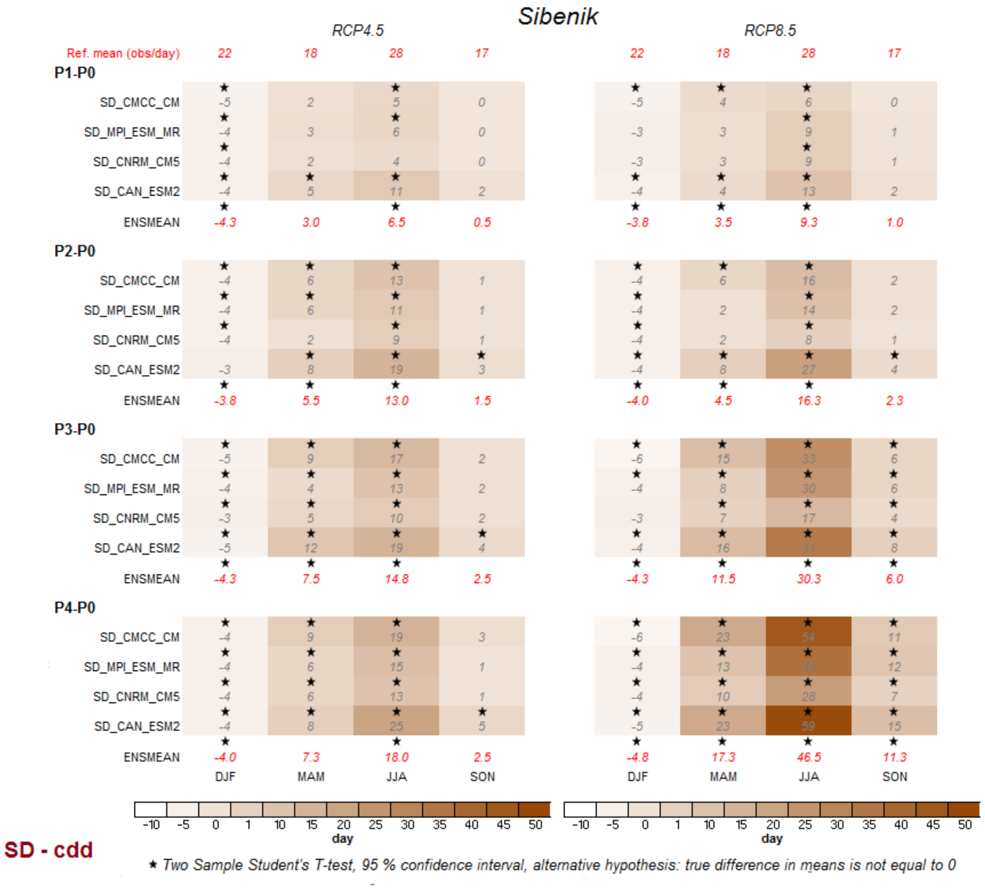

Sibenik

	RCP4.5 DJF	RCP4.5 MAM	RCP4.5 JJA	RCP4.5 SON	RCP8.5 DJF	RCP8.5 MAM	RCP8.5 JJA	RCP8.5 SON
Ref. mean (obs/day)	22	18	28	17	22	18	28	17
P1-P0								
SD_CMCC_CM	★ -5	2	★ 5	0	★ -5	★ 4	★ 6	0
SD_MPI_ESM_MR	★ -4	3	★ 6	0	-3	3	★ 9	1
SD_CNRM_CM5	★ -4	2	4	0	-3	3	★ 9	1
SD_CAN_ESM2	★ -4	★ 5	★ 11	2	★ -4	★ 4	★ 13	2
ENSMEAN	★ -4.3	3.0	★ 6.5	0.5	★ -3.8	★ 3.5	★ 9.3	1.0
P2-P0								
SD_CMCC_CM	★ -4	★ 6	★ 13	1	★ -4	★ 6	★ 16	2
SD_MPI_ESM_MR	★ -4	★ 6	★ 11	1	★ -4	2	★ 14	2
SD_CNRM_CM5	★ -4	2	★ 9	1	★ -4	2	★ 8	1
SD_CAN_ESM2	-3	★ 8	★ 19	★ 3	★ -4	★ 8	★ 27	★ 4
ENSMEAN	★ -3.8	★ 5.5	★ 13.0	1.5	★ -4.0	★ 4.5	★ 16.3	2.3
P3-P0								
SD_CMCC_CM	★ -5	★ 9	★ 17	2	★ -6	★ 15	★ 33	★ 6
SD_MPI_ESM_MR	★ -4	★ 4	★ 13	2	★ -4	★ 8	★ 30	★ 6
SD_CNRM_CM5	★ -3	★ 5	★ 10	2	-3	★ 7	★ 17	★ 4
SD_CAN_ESM2	★ -5	★ 12	★ 19	★ 4	★ -4	★ 16	★ 41	★ 8
ENSMEAN	★ -4.3	★ 7.5	★ 14.8	★ 2.5	★ -4.3	★ 11.5	★ 30.3	★ 6.0
P4-P0								
SD_CMCC_CM	★ -4	★ 9	★ 19	3	★ -6	★ 23	★ 54	★ 11
SD_MPI_ESM_MR	★ -4	★ 6	★ 15	1	★ -4	★ 13	★ 45	★ 12
SD_CNRM_CM5	★ -4	★ 6	★ 13	1	★ -4	★ 10	★ 28	★ 7
SD_CAN_ESM2	★ -4	★ 8	★ 25	★ 5	★ -5	★ 23	★ 59	★ 15
ENSMEAN	★ -4.0	7.3	★ 18.0	2.5	★ -4.8	★ 17.3	★ 46.5	★ 11.3

★ Two Sample Student's T-test, 95 % confidence interval, alternative hypothesis: true difference in means is not equal to 0

Figure 5-79: Seasonal and annual max. consecutive dry days: observed values over reference period (in red), changes projected by statistical downscaling applied to 4GCMs and the Ensemble Mean over the four periods (P1, P2, P3, P4) projected in the framework of RCP4.5 (left) and RCP 8.5 (right). Significant change is marked by star (source Arpae-Simc)

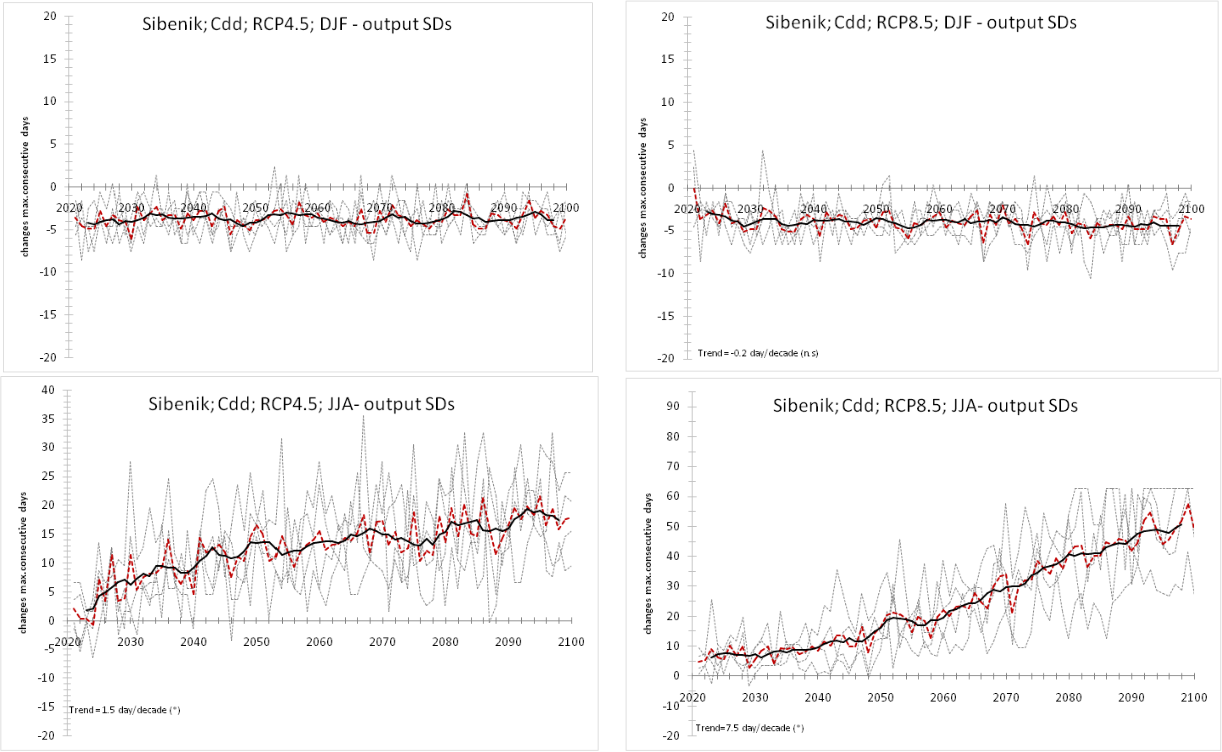

Figure 5-80: Variability of future changes of winter (DJF) and summer (JJA) max. number of consecutive dry days projected through SDs applied to 4GCMs (grey lines); the Ensemble Mean (red line) and moving average (black line) - scenario RCP4.5 (left) and RCP8.5 (right), 2021-2100 period Significant trend is marked with star while n.s. means not significant (source Arpae-Simc).

6.3 Case study 3: Vodice

6.3.1 Dynamically downscaled results

In this section we present future climate change of temperature and precipitation related indices and extra rare humidex projections for Vodice. All indices are calculated from the available data set of regional climate models for the grid point that is representing the location of case study Vodice. Data set is obtained by bilinear interpolation. All data are presented as follows:

- Climate change diagram of an individual index in seasons and on annual basis for four considered future periods, for two emission scenarios RCP4.5 and RCP8.5. Climate change is calculated as difference between future and reference period (relative difference for precipitation indices and surface relative humidity). Reference period is presented as ensemble mean of available regional climate models (Ref.mean), while climate change is shown for different models as well as for ensemble mean of models (ENSMEAN). Two sample Wilcoxon test is applied to test statistical significance of climate change for individual models (for 95 % confidence level). Significant change is marked by star
- Time series of future anomaly of an individual index for DJF and JJA and for two emission scenarios RCP4.5 and RCP8.5. Anomaly is calculated respect to the reference period and shown for individual models, ensemble mean and 5-year moving average. Mann Kendall trend test is applied to ensemble mean (for 95 % confidence level). Significant trend is marked with star (ns if not significant).

6.3.1.1 *Temperature related indices projections*

6.3.1.1.1 *Averaged 2 meter air temperature*

Averaged temperature change in Vodice (Figure 5-81) shows increase in all seasons and on annual scale, for all future periods (exception is in winter for two models realisations in first two periods). Although each model gives different amplitude of change, in ensemble mean the change is highest during summer and the smallest in winter, for RCP4.5. The temperature increase is more pronounced towards the end of the century when the increase in the ensemble mean is from 1.4 °C in DJF to 2.1 °C in JJA. On annual scale for RCP4.5 temperature increase is for 1.7 °C. The amplitude of temperature change is more pronounced for RCP8.5 scenario, from 2.9 °C in MAM to 4.2 °C in JJA, on annual scale 3.5 °C at the end of 21st century for ensemble mean. The linear trend of temperature anomaly (Figure 5-82) in the future shows increase which is statistically significant for both considered seasons and both scenarios; for DJF ensemble is 0.19 °C / 10 year for RCP4.5 and 0.53 °C / 10 year for RCP8.5; for JJA ensemble is 0.18 °C / 10 year for RCP4.5 and 0.49 °C / 10 year.

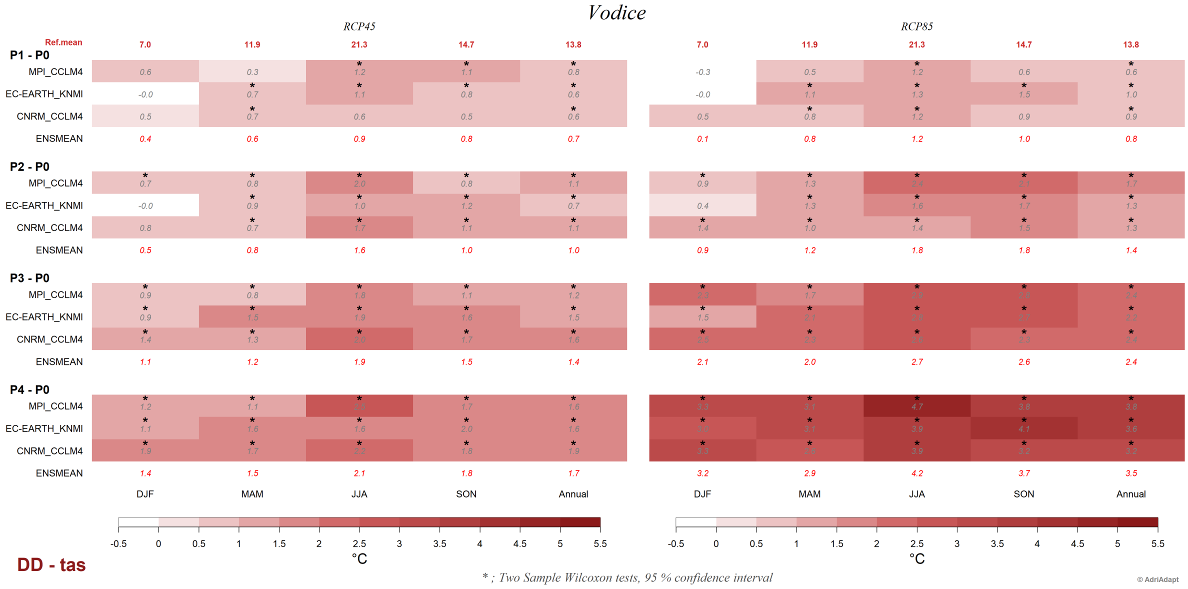

Figure 5-81: Averaged seasonal and annual 2m air temperature (in °C) obtained by dynamical downscaling for Vodice: Ref. mean is 20 year simulated period (1986-2005) for ensemble mean; P1-P0, P2-P0, P3-P0, P4-P0 are changes in the future for following periods P1: 2021-2040, P2: 2041-2060, P3: 2061-2080, P4: 2081-2100. Differences are shown for individual models. Significant change is marked by star. Change is also shown as ensemble mean (ENSMEAN), not tested for significance. Left column is for RCP4.5 scenario and right for RCP8.5 scenario.

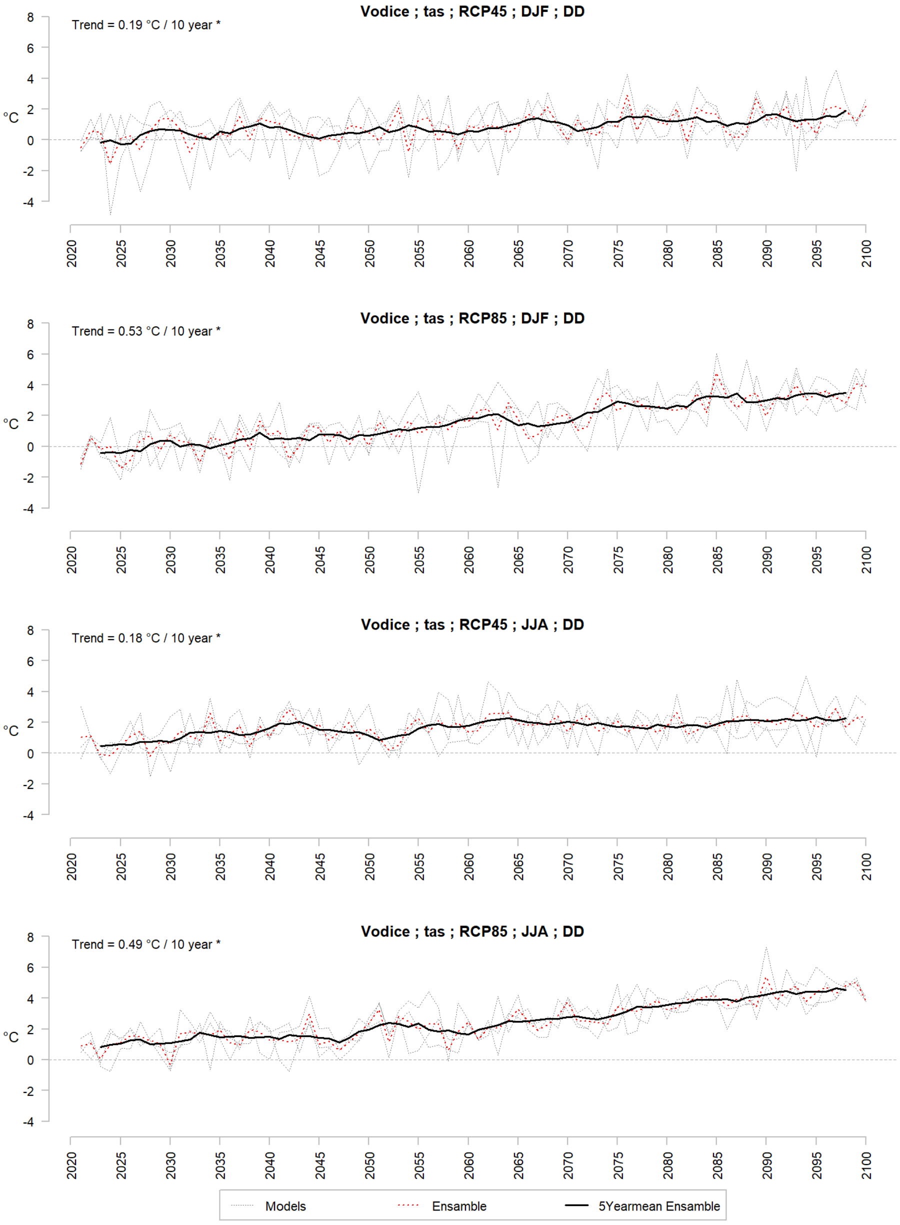

Figure 5-82: Variability of future 2m air temperature anomaly (in °C) in Vodice for 2021-2100 obtained by dynamically downscaling for winter (DJF) and summer (JJA) and two RCP scenarios: individual models are in grey, the ensemble mean in red, 5-year moving average in black. Significant trend is marked with star (ns if not significant).

6.3.1.1.2 *Extreme high temperature*

99th percentile of 2m air temperature (Figure 5-83) in Vodice is increasing from P1 to P4 future periods with the different amplitudes for each model. In ensemble mean at the end of century increase is from 1.0 °C in DJF to 2.6 °C in JJA, 2.5 °C on annual scale for RCP4.5. Amplitude of change is more pronounced for RCP8.5 and is between 2.8 °C in DJF and 4.6 °C in SON, 4.4 °C for annual change at the end of 21st century. Variability of future 99th percentile of 2m air temperature anomaly (Figure 5-84) shows linear trend in change of ensemble mean, 0.15 °C / 10 year in DJF for RCP4.5 and 0.44 °C / 10 year for RCP8.5; 0.17 °C / 10 year in JJA for RCP4.5 and 0.50 °C / 10 year for RCP8.5. All trends are statistically significant.

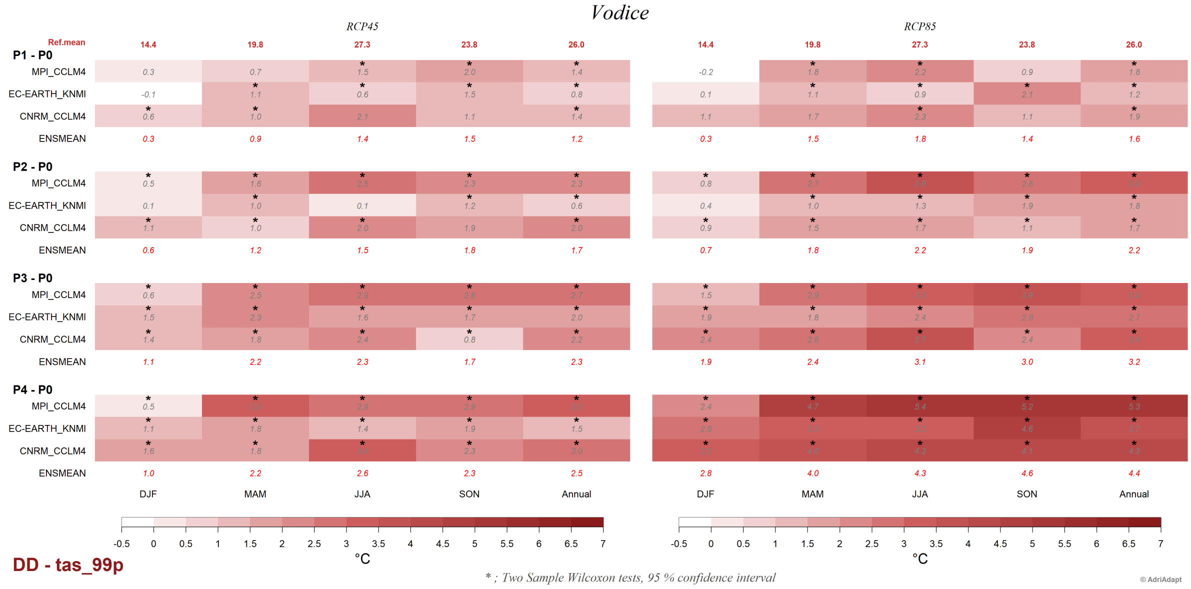

Figure 5-83: Seasonal and annual 99th percentile of 2m air temperature (extreme high temperature, in °C) obtained by dynamical downscaling for Vodice: Ref. mean is 20 year simulated period (1986-2005) for ensemble mean; P1-P0, P2-P0, P3-P0, P4-P0 are changes in the future for following periods P1: 2021-2040, P2: 2041-2060, P3: 2061-2080, P4: 2081-2100. Differences are shown for individual models. Significant change is marked by star. Change is also shown as ensemble mean (ENSMEAN), not tested for significance. Left column is for RCP4.5 scenario and right for RCP8.5 scenario.

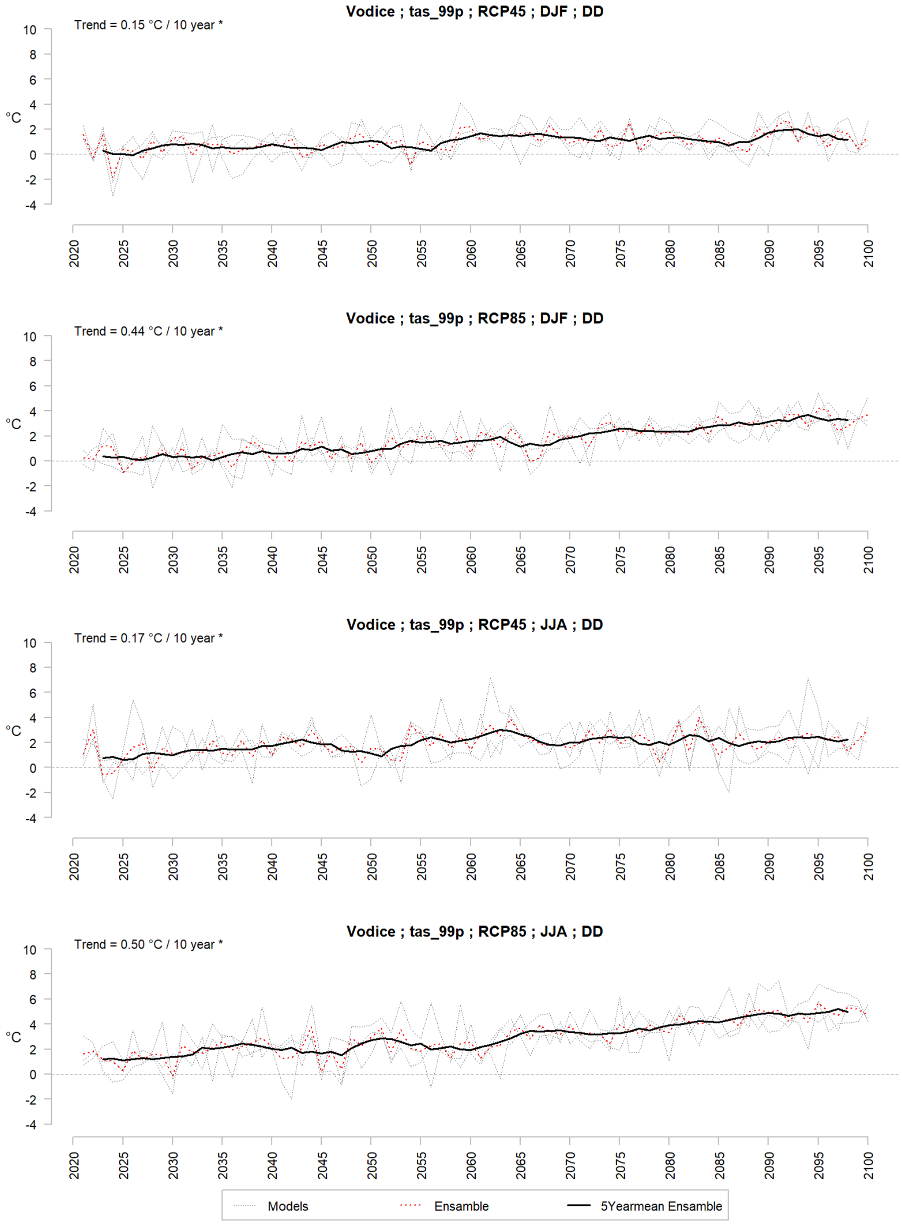

Vodice ; tas_99p ; RCP45 ; DJF ; DD

Vodice ; tas_99p ; RCP85 ; DJF ; DD

Vodice ; tas_99p ; RCP45 ; JJA ; DD

Vodice ; tas_99p ; RCP85 ; JJA ; DD

Figure 5-84: Variability of future 99th percentile of 2m air temperature (extreme high temperature) anomaly (in °C) in Vodice for 2021-2100 obtained by dynamically downscaling for winter (DJF) and summer (JJA) and two RCP scenarios: individual models are in grey, the ensemble mean in red, 5-year moving average in black. Significant trend is marked with star (ns if not significant).

6.3.1.1.3 *Extreme high maximum temperature*

Future change of 99th percentile of 2m maximum air temperature (Figure 5-85) in Vodice is increasing from P1 to P4 periods with the different amplitudes for each model. Ensemble mean of change is positive for all periods. At the end of century increase is from 1.1 °C in DJF to 2.7 °C in JJA and SON, 2.6 °C on annual scale for RCP4.5. Amplitude of change is more pronounced for RCP8.5 and is between 2.9 °C in DJF and 4.9 °C in SON, 4.6 °C for annual change at the end of 21st century. Variability of future 99th percentile of 2m maximum air temperature anomaly (Figure 5-86) shows linear trend in change of ensemble mean, 0.19 °C / 10 year in DJF for RCP4.5 and 0.46 °C / 10 year for RCP8.5; 0.24 °C / 10 year in JJA for RCP4.5 and 0.49 °C / 10 year for RCP8.5. All trends are statistically significant.

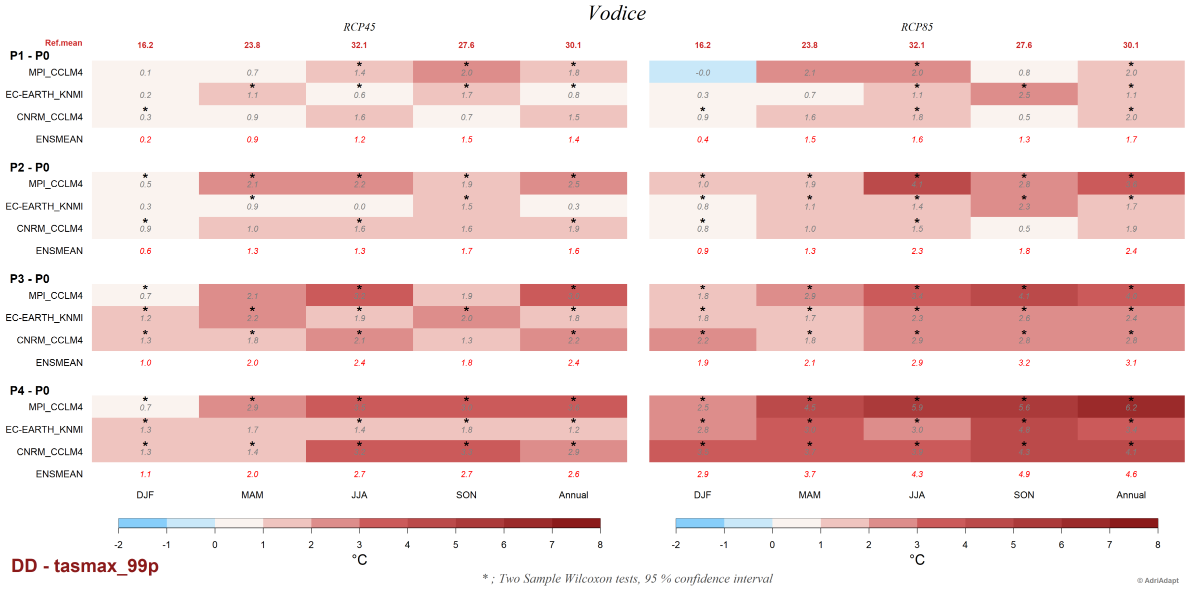

Figure 5-85: Seasonal and annual 99th percentile of 2m maximum air temperature (extreme high maximum temperature, in °C) obtained by dynamical downscaling for Vodice: Ref. mean is 20 year simulated period (1986-2005) for ensemble mean; P1-P0, P2-P0, P3-P0, P4-P0 are changes in the future for following periods P1: 2021-2040, P2: 2041-2060, P3: 2061-2080, P4: 2081-2100. Differences are shown for individual models. Significant change is marked by star. Change is also shown as ensemble mean (ENSMEAN), not tested for significance. Left column is for RCP4.5 scenario and right for RCP8.5 scenario.

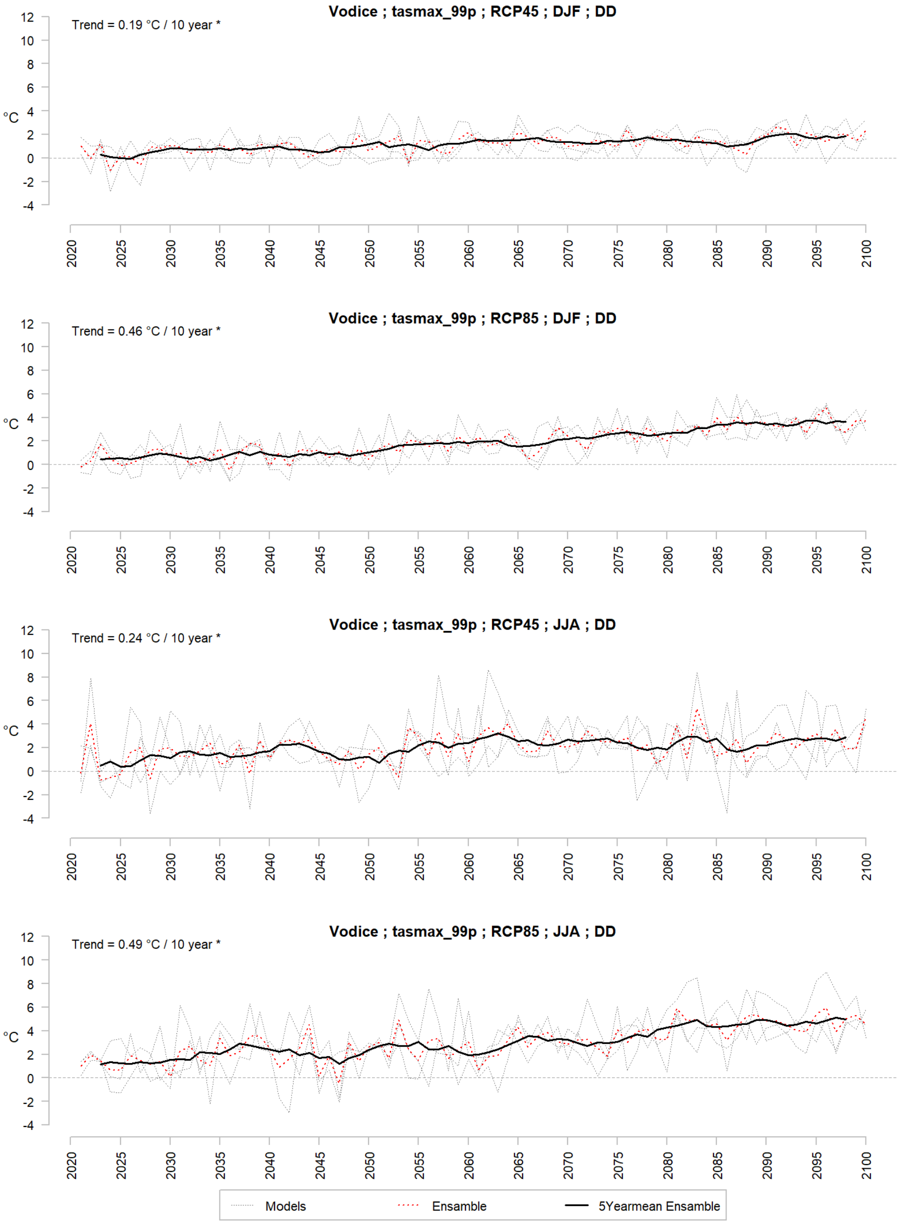

Figure 5-86: Variability of future 99th percentile of 2m maximum air temperature (extreme high maximum temperature) anomaly (in °C) in Vodice for 2021-2100 obtained by dynamically downscaling for winter (DJF) and summer (JJA) and two RCP scenarios: individual models are in grey, the ensemble mean in red, 5-year moving average in black. Significant trend is marked with star (ns if not significant).

6.3.1.1.4 *Extreme rare high temperature*

Future change of 99.9th percentile of 2m air temperature (Figure 5-87) in Vodice is increasing from P1 to P4 periods with the different amplitudes for each model. Slightly negative change appears for some seasons and some models in two first periods, but the change of ensemble mean is positive for all periods (exception is DJF in P1 for RCP4.5). At the end of century increase is from 0.7 °C in DJF to 2.6 °C in MAM, 2.5 °C on annual scale for RCP4.5. Amplitude of change is more pronounced for RCP8.5 and is between 2.4 °C in DJF and 4.9 °C in SON, 4.1 °C for annual change at the end of 21st century. Variability of future 99.9th percentile of 2m air temperature anomaly (Figure 5-88) shows linear trend in change of ensemble mean, 0.15 °C / 10 year in DJF for RCP4.5 and 0.44 °C / 10 year for RCP8.5; 0.17 °C / 10 year in JJA for RCP4.5 and 0.50 °C / 10 year for RCP8.5. All trends are statistically significant.

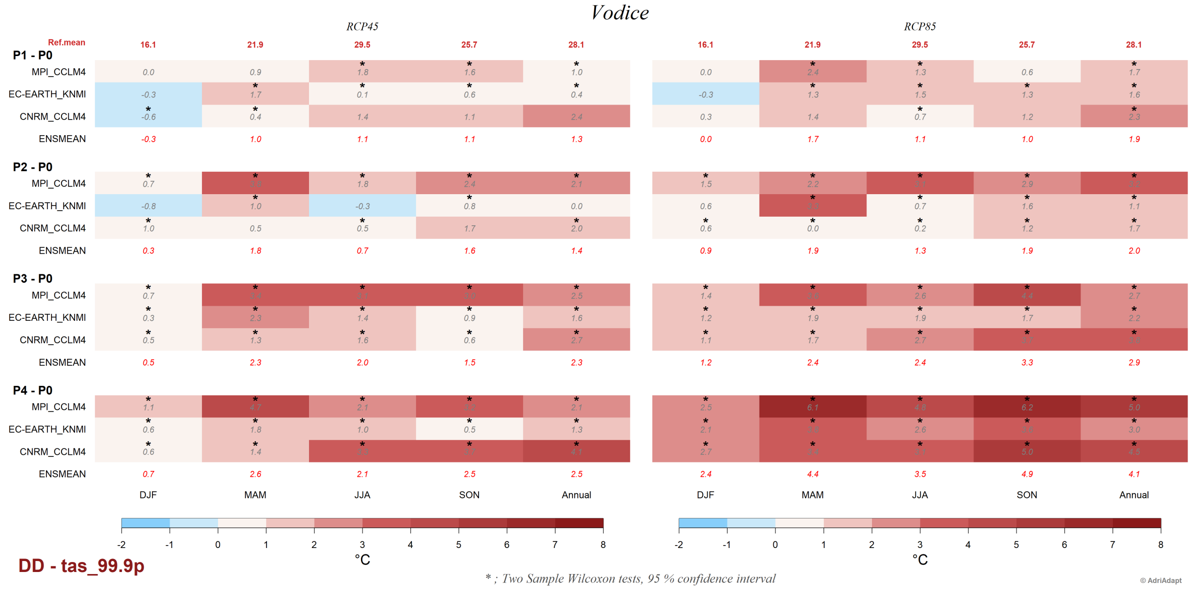

Figure 5-87: Seasonal and annual 99.9th percentile of 2m air temperature (extreme rare high temperature, in °C) obtained by dynamical downscaling for Vodice: Ref. mean is 20 year simulated period (1986-2005) for ensemble mean; P1-P0, P2-P0, P3-P0, P4-P0 are changes in the future for following periods P1: 2021-2040, P2: 2041-2060, P3: 2061-2080, P4: 2081-2100. Differences are shown for individual models. Significant change is marked by star. Change is also shown as ensemble mean (ENSMEAN), not tested for significance. Left column is for RCP4.5 scenario and right for RCP8.5 scenario.

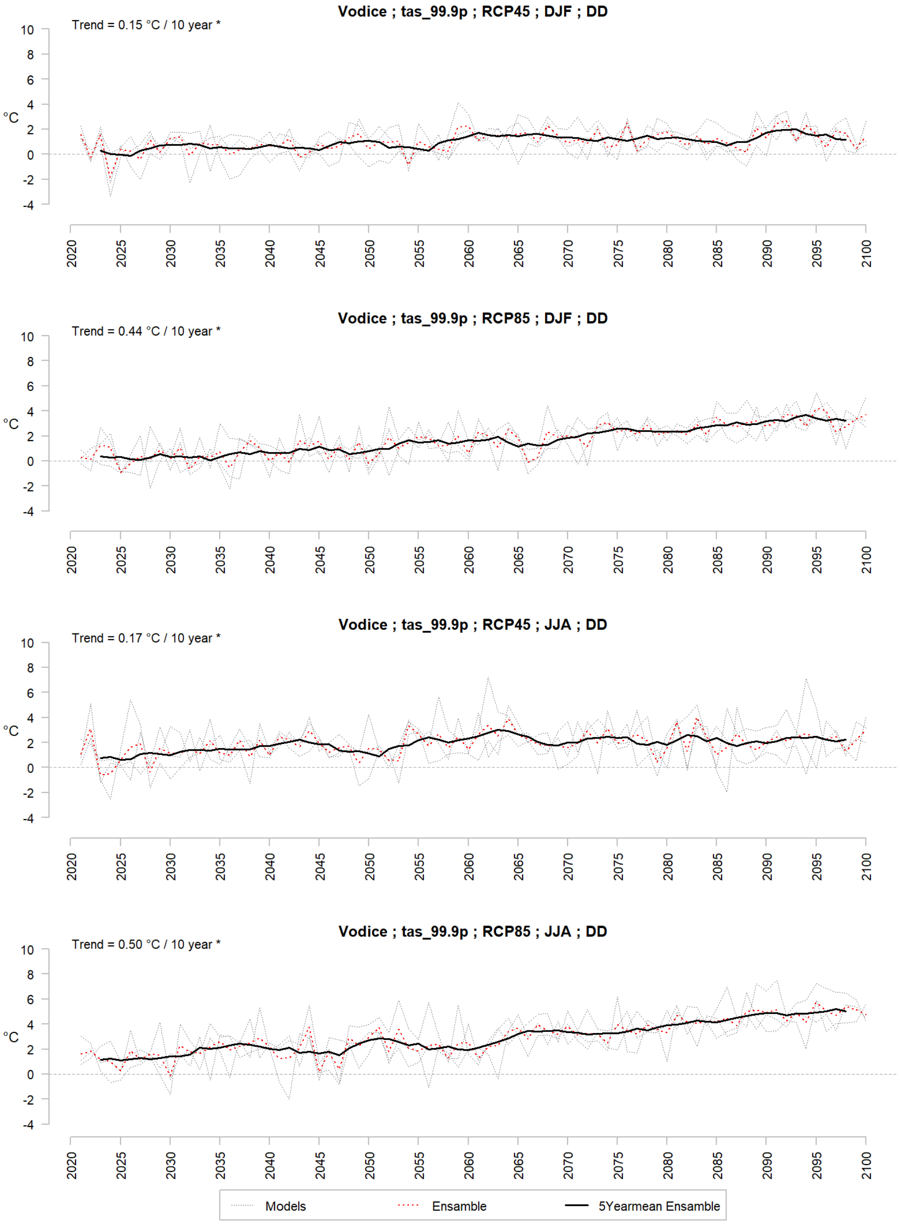

Figure 5-88: Variability of future 99.9th percentile of 2m air temperature (extreme rare high temperature) anomaly (in °C) in Vodice for 2021-2100 obtained by dynamically downscaling for winter (DJF) and summer (JJA) and two RCP scenarios: individual models are in grey, the ensemble mean in red, 5-year moving average in black. Significant trend is marked with star (ns if not significant).

6.3.1.1.5 *Extreme rare high maximum temperature*

Future change of 99.9th percentile of 2m maximum air temperature (Figure 5-89) in Vodice is changing from P1 to P4 periods with the different amplitudes for each model. Some models show for some time slices negative change, but in general ensemble mean for all season and annual change are positive (exception is DJF in P1 for RCP4.5). At the end of 21st century changes are between 1.2 °C in DJF and 3.9 °C in MAM, 2.7 °C for annual for RCP4.5 scenario. Amplitude of change is more pronounced for RCP8.5 and is between 3.0 °C in DJF and 5.7 °C in SON, 4.2 °C for annual change at the end of 21st century. Variability of future 99.9th percentile of 2m maximum air temperature anomaly (Figure 5-90) shows linear trend in change of ensemble mean, 0.19 °C / 10 year in DJF for RCP4.5 and 0.46 °C / 10 year for RCP8.5; 0.24 °C / 10 year in JJA for RCP4.5 and 0.49 °C / 10 year for RCP8.5. All trends are statistically significant.

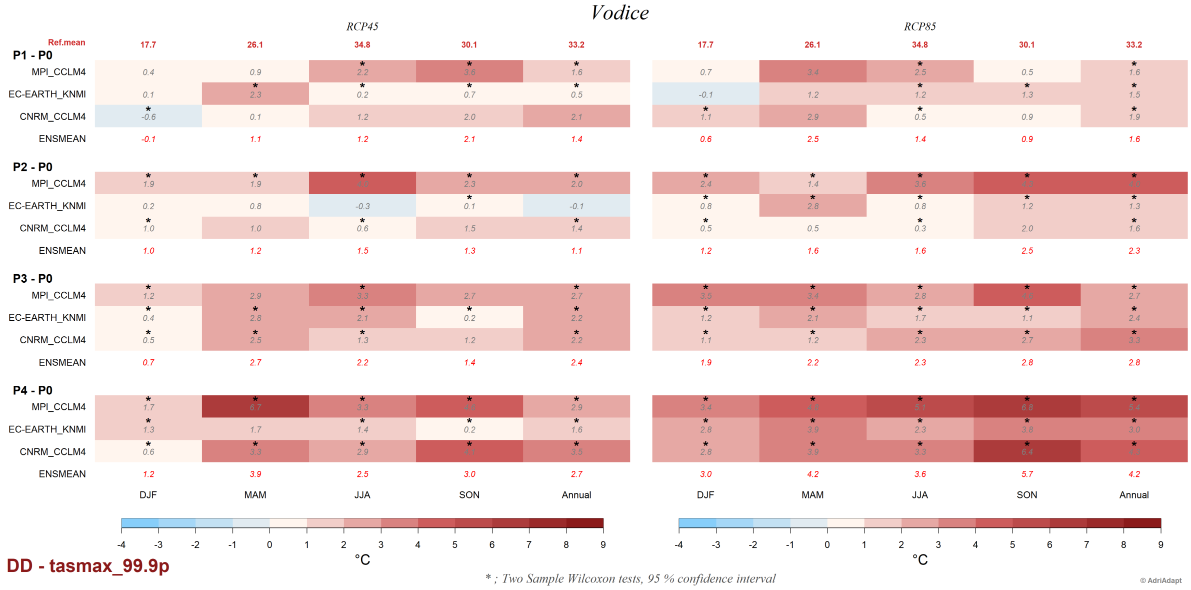

RCP45

	DJF	MAM	JJA	SON	Annual
Ref.mean	17.7	26.1	34.8	30.1	33.2
P1 - P0					
MPI_CCLM4	0.4	0.9	* 2.2	* 3.6	* 1.6
EC-EARTH_KNMI	0.1	* 2.3	* 0.2	* 0.7	* 0.5
CNRM_CCLM4	* -0.6	0.1	1.2	2.0	2.1
ENSMEAN	-0.1	1.1	1.2	2.1	1.4
P2 - P0					
MPI_CCLM4	* 1.9	* 1.9	* 4.0	* 2.3	* 2.0
EC-EARTH_KNMI	0.2	0.8	-0.3	* 0.1	-0.1
CNRM_CCLM4	* 1.0	1.0	* 0.6	1.5	* 1.4
ENSMEAN	1.0	1.2	1.5	1.3	1.1
P3 - P0					
MPI_CCLM4	* 1.2	2.9	* 3.3	2.7	* 2.7
EC-EARTH_KNMI	* 0.4	* 2.8	* 2.1	* 0.2	* 2.2
CNRM_CCLM4	* 0.5	* 2.5	* 1.3	1.2	* 2.2
ENSMEAN	0.7	2.7	2.2	1.4	2.4
P4 - P0					
MPI_CCLM4	* 1.7	* 6.7	* 3.3	* 4.6	* 2.9
EC-EARTH_KNMI	* 1.3	1.7	* 1.4	* 0.2	* 1.6
CNRM_CCLM4	* 0.6	* 3.3	* 2.9	* 4.1	* 3.5
ENSMEAN	1.2	3.9	2.5	3.0	2.7

RCP85

	DJF	MAM	JJA	SON	Annual
Ref.mean	17.7	26.1	34.8	30.1	33.2
P1 - P0					
MPI_CCLM4	0.7	3.4	* 2.5	0.5	* 1.6
EC-EARTH_KNMI	-0.1	1.2	* 1.2	* 1.3	* 1.5
CNRM_CCLM4	* 1.1	2.9	* 0.5	0.9	* 1.9
ENSMEAN	0.6	2.5	1.4	0.9	1.6
P2 - P0					
MPI_CCLM4	* 2.4	* 1.4	* 3.6	* 4.3	* 4.0
EC-EARTH_KNMI	* 0.8	* 2.8	* 0.8	* 1.2	* 1.3
CNRM_CCLM4	* 0.5	0.5	* 0.3	2.0	* 1.6
ENSMEAN	1.2	1.6	1.6	2.5	2.3
P3 - P0					
MPI_CCLM4	* 3.5	* 3.4	* 2.8	* 4.6	* 2.7
EC-EARTH_KNMI	* 1.2	* 2.1	* 1.7	* 1.1	* 2.4
CNRM_CCLM4	* 1.1	* 1.2	* 2.3	* 2.7	* 3.3
ENSMEAN	1.9	2.2	2.3	2.8	2.8
P4 - P0					
MPI_CCLM4	* 3.4	* 4.8	* 5.1	* 6.8	* 5.4
EC-EARTH_KNMI	* 2.8	* 3.9	* 2.3	* 3.8	* 3.0
CNRM_CCLM4	* 2.8	* 3.9	* 3.3	* 6.4	* 4.3
ENSMEAN	3.0	4.2	3.6	5.7	4.2

** ; Two Sample Wilcoxon tests, 95 % confidence interval*

Figure 5-89: Seasonal and annual 99.9th percentile of 2m maximum air temperature (extreme rare high maximum temperature, in °C) obtained by dynamical downscaling for Vodice: Ref. mean is 20 year simulated period (1986-2005) for ensemble mean; P1-P0, P2-P0, P3-P0, P4-P0 are changes in the future for following periods P1: 2021-2040, P2: 2041-2060, P3: 2061-2080, P4: 2081-2100. Differences are shown for individual models. Significant change is marked by star. Change is also shown as ensemble mean (ENSMEAN), not tested for significance. Left column is for RCP4.5 scenario and right for RCP8.5 scenario.

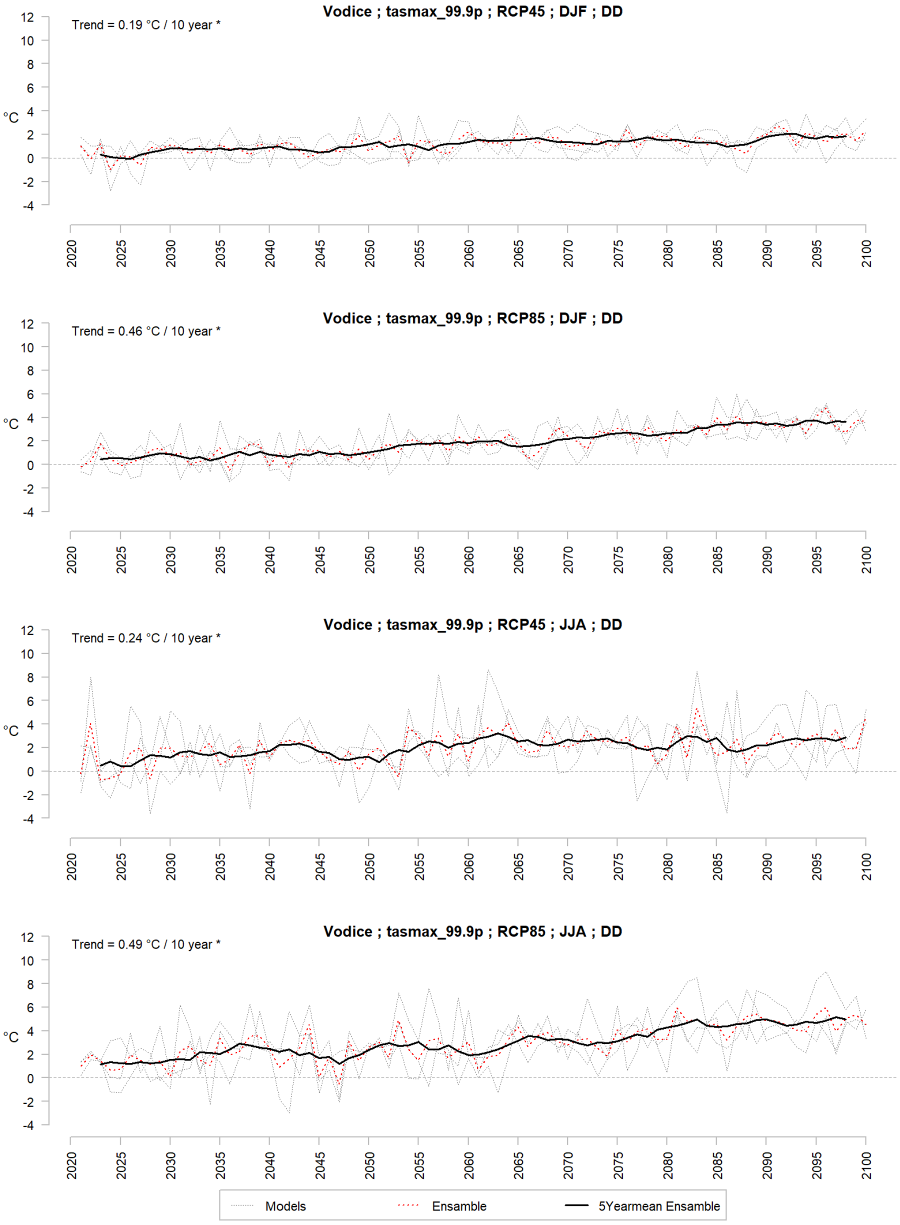

Figure 5-90: Variability of future 99.9th percentile of 2m maximum air temperature (extreme rare high maximum temperature) anomaly (in °C) in Vodice for 2021-2100 obtained by dynamically downscaling for winter (DJF) and summer (JJA) and two RCP scenarios: individual models are in grey, the ensemble mean in red, 5-year moving average in black. Significant trend is marked with star (ns if not significant).

6.3.1.2 *Precipitation related indices projections*

6.3.1.2.1 *Averaged precipitation*

Averaged precipitation obtained by dynamical downscaling is expressed in mm/day and its change in the future is shown as relative to the P0 period. Precipitation is much more variable parameter in comparison to the temperature, therefore there is no always unique sign of change through the year as well as from model to model. The change in ensemble mean (Figure 5-91) for Vodice gives increase of precipitation for colder part of the year at the end of century (7.8 % for DJF, 10.8 % for SON) and decrease in the warmer part (-0.6 % in MAM, -8.4 % in JJA) for RCP4.5; on annual scale precipitation will increase for 4.4 %. For scenario RCP8.5, precipitation will decrease in JJA (-22.9 %) and increase in DJF (13.6 %). On annual scale precipitation will increase for 0.6 % at the end of century. Variability of future precipitation anomaly (Figure 5-92) for ensemble mean in Vodice for both scenarios shows increase in precipitation in DJF and decrease of precipitation in JJA. Linear trend in DJF for RCP8.5 scenario is statistically significant (2.33 % / 10 year).

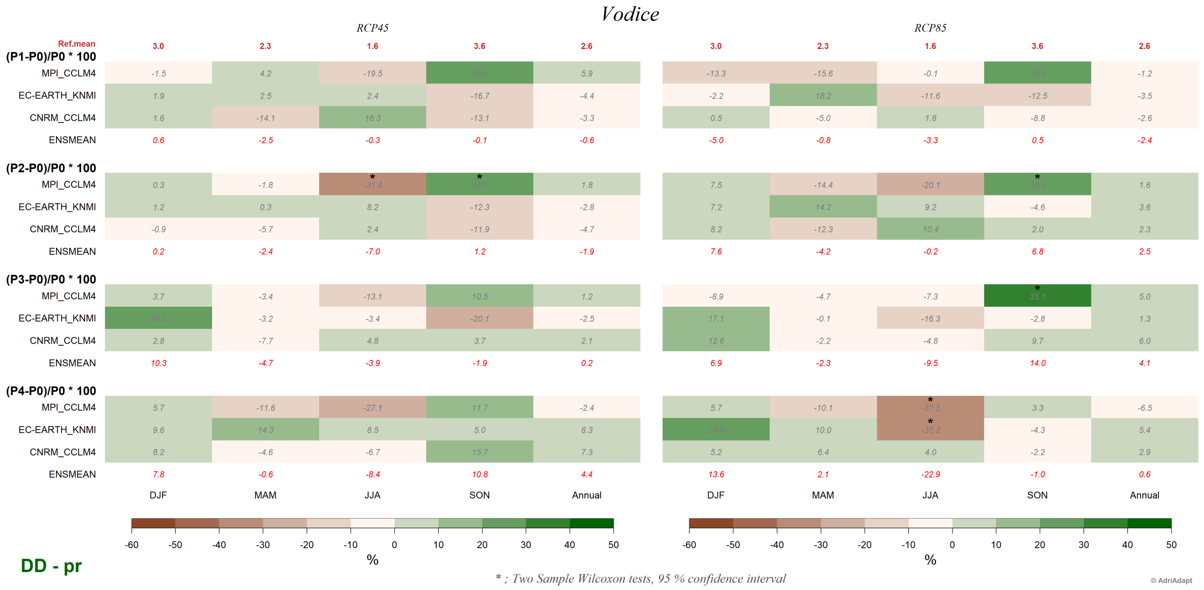

	RCP45					RCP85				
	DJF	MAM	JJA	SON	Annual	DJF	MAM	JJA	SON	Annual
Ref.mean	3.0	2.3	1.6	3.6	2.6	3.0	2.3	1.6	3.6	2.6
(P1-P0)/P0 * 100										
MPI_CCLM4	-1.5	4.2	-19.5	29.5	5.9	-13.3	-15.6	-0.1	22.8	-1.2
EC-EARTH_KNMI	1.9	2.5	2.4	-16.7	-4.4	-2.2	18.2	-11.6	-12.5	-3.5
CNRM_CCLM4	1.6	-14.1	16.3	-13.1	-3.3	0.5	-5.0	1.8	-8.8	-2.6
ENSMEAN	0.6	-2.5	-0.3	-0.1	-0.6	-5.0	-0.8	-3.3	0.5	-2.4
(P2-P0)/P0 * 100										
MPI_CCLM4	0.3	-1.8	* -31.4	* 27.8	1.8	7.5	-14.4	-20.1	* 23.0	1.6
EC-EARTH_KNMI	1.2	0.3	8.2	-12.3	-2.8	7.2	14.2	9.2	-4.6	3.6
CNRM_CCLM4	-0.9	-5.7	2.4	-11.9	-4.7	8.2	-12.3	10.4	2.0	2.3
ENSMEAN	0.2	-2.4	-7.0	1.2	-1.9	7.6	-4.2	-0.2	6.8	2.5
(P3-P0)/P0 * 100										
MPI_CCLM4	3.7	-3.4	-13.1	10.5	1.2	-8.9	-4.7	-7.3	* 35.1	5.0
EC-EARTH_KNMI	24.5	-3.2	-3.4	-20.1	-2.5	17.1	-0.1	-16.3	-2.8	1.3
CNRM_CCLM4	2.8	-7.7	4.8	3.7	2.1	12.6	-2.2	-4.8	9.7	6.0
ENSMEAN	10.3	-4.7	-3.9	-1.9	0.2	6.9	-2.3	-9.5	14.0	4.1
(P4-P0)/P0 * 100										
MPI_CCLM4	5.7	-11.6	-27.1	11.7	-2.4	5.7	-10.1	* -37.5	3.3	-6.5
EC-EARTH_KNMI	9.6	14.3	8.5	5.0	8.3	29.9	10.0	* -35.2	-4.3	5.4
CNRM_CCLM4	8.2	-4.6	-6.7	15.7	7.3	5.2	6.4	4.0	-2.2	2.9
ENSMEAN	7.8	-0.6	-8.4	10.8	4.4	13.6	2.1	-22.9	-1.0	0.6

* : Two Sample Wilcoxon tests, 95 % confidence interval

© AdriAdapt

Figure 5-91: Averaged seasonal and annual precipitation obtained by dynamical downscaling for Vodice: Ref. mean is 20 year simulated period (1986-2005) for ensemble mean in mmday^{-1}; P1-P0, P2-P0, P3-P0, P4-P0 are changes (in %) in the future for following periods P1: 2021-2040, P2: 2041-2060, P3: 2061-2080, P4: 2081-2100. Differences are shown for individual models. Significant change is marked by star. Change is also shown as ensemble mean (ENSMEAN), not tested for significance. Left column is for RCP4.5 scenario and right for RCP8.5 scenario.

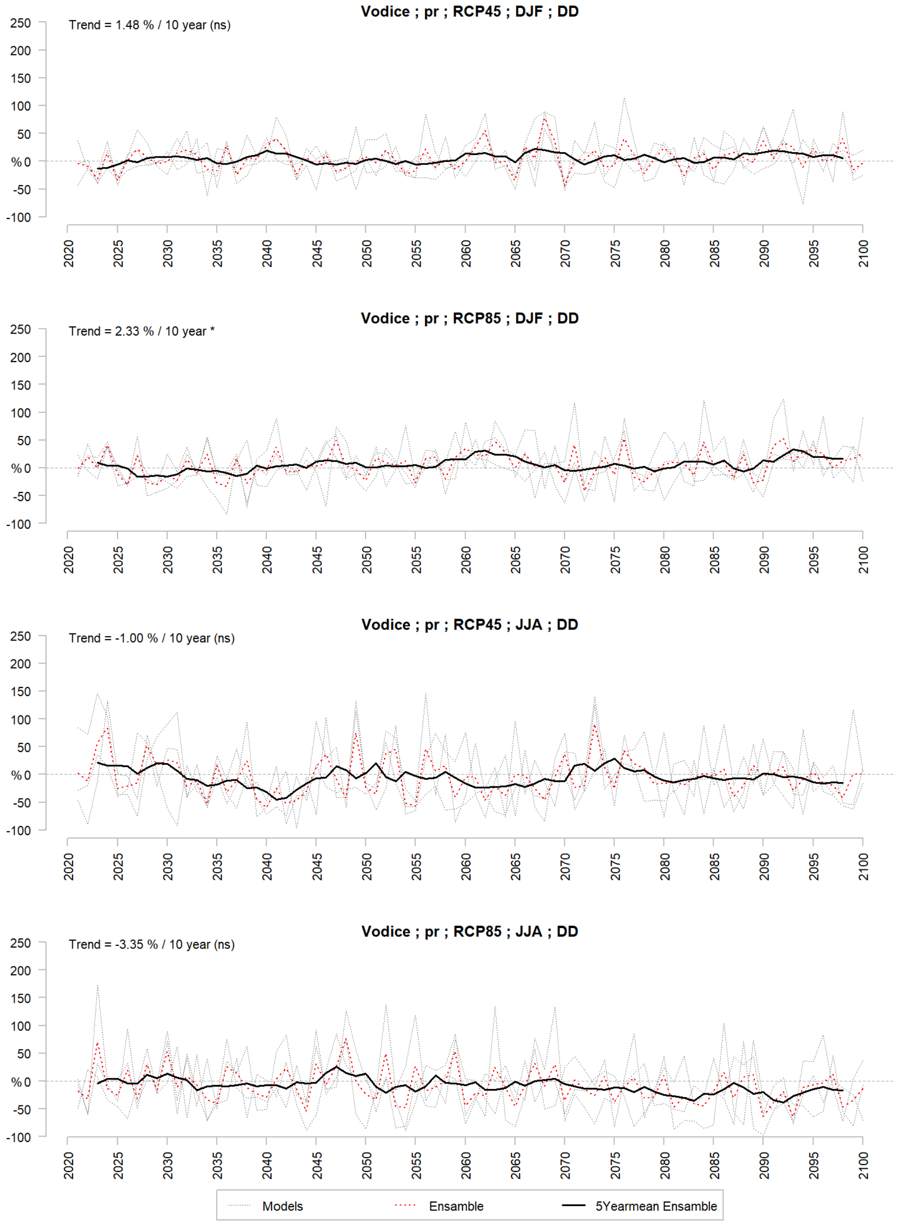

Figure 5-92: Variability of future precipitation anomaly (in %) in Vodice for 2021-2100 obtained by dynamically downscaling for winter (DJF) and summer (JJA) and two RCP scenarios: individual models are in grey, the ensemble mean in red, 5-year moving average in black. Significant trend is marked with star (ns if not significant).

6.3.1.2.2 *Intense precipitation*

Intense precipitation (Figure 5-93), defined by 95th percentile of precipitation in Vodice, shows for ensemble mean that 95th percentile will increase in all seasons except summer. At the end of century, the increase will be the most pronounced in SON for RCP4.5 (19.1 %) and in DJF for RCP8.5 (16.6 %), while in JJA 95th percentile will decrease for -5.5 % for RCP4.5 and -27.2 % for RCP8.5. On annual scale intense precipitation will increase, 8.6 % for RCP4.5 and 5.4 % for RCP8.5. Variability of future intense precipitation anomaly (Figure 5-94) for ensemble mean in Vodice shows increase in precipitation in DJF and decrease of precipitation in JJA for both scenarios. Linear trend is only statistically significant for DJF and RCP8.5 scenario (2.96 % / 10 year).

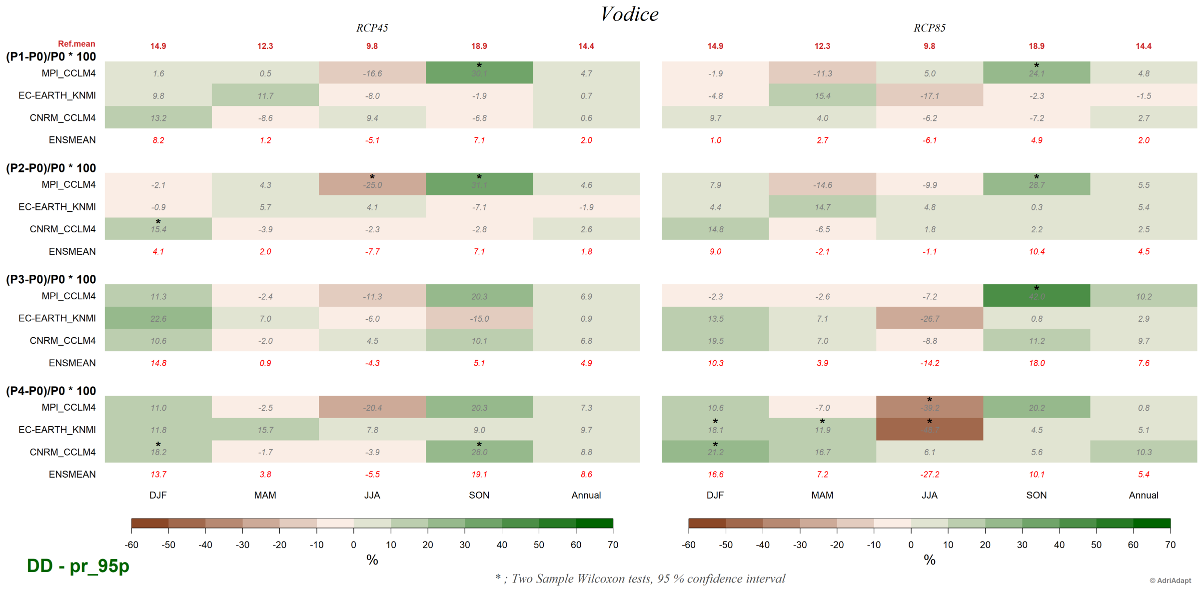

Vodice

	RCP45					RCP85				
	DJF	MAM	JJA	SON	Annual	DJF	MAM	JJA	SON	Annual
Ref.mean	**14.9**	**12.3**	**9.8**	**18.9**	**14.4**	**14.9**	**12.3**	**9.8**	**18.9**	**14.4**
(P1-P0)/P0 * 100										
MPI_CCLM4	1.6	0.5	-16.6	* 30.1	4.7	-1.9	-11.3	5.0	* 24.1	4.8
EC-EARTH_KNMI	9.8	11.7	-8.0	-1.9	0.7	-4.8	15.4	-17.1	-2.3	-1.5
CNRM_CCLM4	13.2	-8.6	9.4	-6.8	0.6	9.7	4.0	-6.2	-7.2	2.7
ENSMEAN	8.2	1.2	-5.1	7.1	2.0	1.0	2.7	-6.1	4.9	2.0
(P2-P0)/P0 * 100										
MPI_CCLM4	-2.1	4.3	* -25.0	* 31.1	4.6	7.9	-14.6	-9.9	* 28.7	5.5
EC-EARTH_KNMI	-0.9	5.7	4.1	-7.1	-1.9	4.4	14.7	4.8	0.3	5.4
CNRM_CCLM4	* 15.4	-3.9	-2.3	-2.8	2.6	14.8	-6.5	1.8	2.2	2.5
ENSMEAN	4.1	2.0	-7.7	7.1	1.8	9.0	-2.1	-1.1	10.4	4.5
(P3-P0)/P0 * 100										
MPI_CCLM4	11.3	-2.4	-11.3	20.3	6.9	-2.3	-2.6	-7.2	* 42.0	10.2
EC-EARTH_KNMI	22.6	7.0	-6.0	-15.0	0.9	13.5	7.1	-26.7	0.8	2.9
CNRM_CCLM4	10.6	-2.0	4.5	10.1	6.8	19.5	7.0	-8.8	11.2	9.7
ENSMEAN	14.8	0.9	-4.3	5.1	4.9	10.3	3.9	-14.2	18.0	7.6
(P4-P0)/P0 * 100										
MPI_CCLM4	11.0	-2.5	-20.4	20.3	7.3	10.6	-7.0	* -39.2	20.2	0.8
EC-EARTH_KNMI	11.8	15.7	7.8	9.0	9.7	* 18.1	* 11.9	* -48.7	4.5	5.1
CNRM_CCLM4	* 18.2	-1.7	-3.9	* 28.0	8.8	* 21.2	16.7	6.1	5.6	10.3
ENSMEAN	13.7	3.8	-5.5	19.1	8.6	16.6	7.2	-27.2	10.1	5.4

DD - pr_95p

** : Two Sample Wilcoxon tests, 95 % confidence interval*

© AdriAdapt

Figure 5-93: Seasonal and annual 95th percentile of precipitation (intense precipitation) obtained by dynamical downscaling for Vodice: Ref. mean is 20 year simulated period (1986-2005) for ensemble mean in mmday^{-1}; P1-P0, P2-P0, P3-P0, P4-P0 are changes (in %) in the future for following periods P1: 2021-2040, P2: 2041-2060, P3: 2061-2080, P4: 2081-2100. Differences are shown for individual models. Significant change is marked by star. Change is also shown as ensemble mean (ENSMEAN), not tested for significance. Left column is for RCP4.5 scenario and right for RCP8.5 scenario.

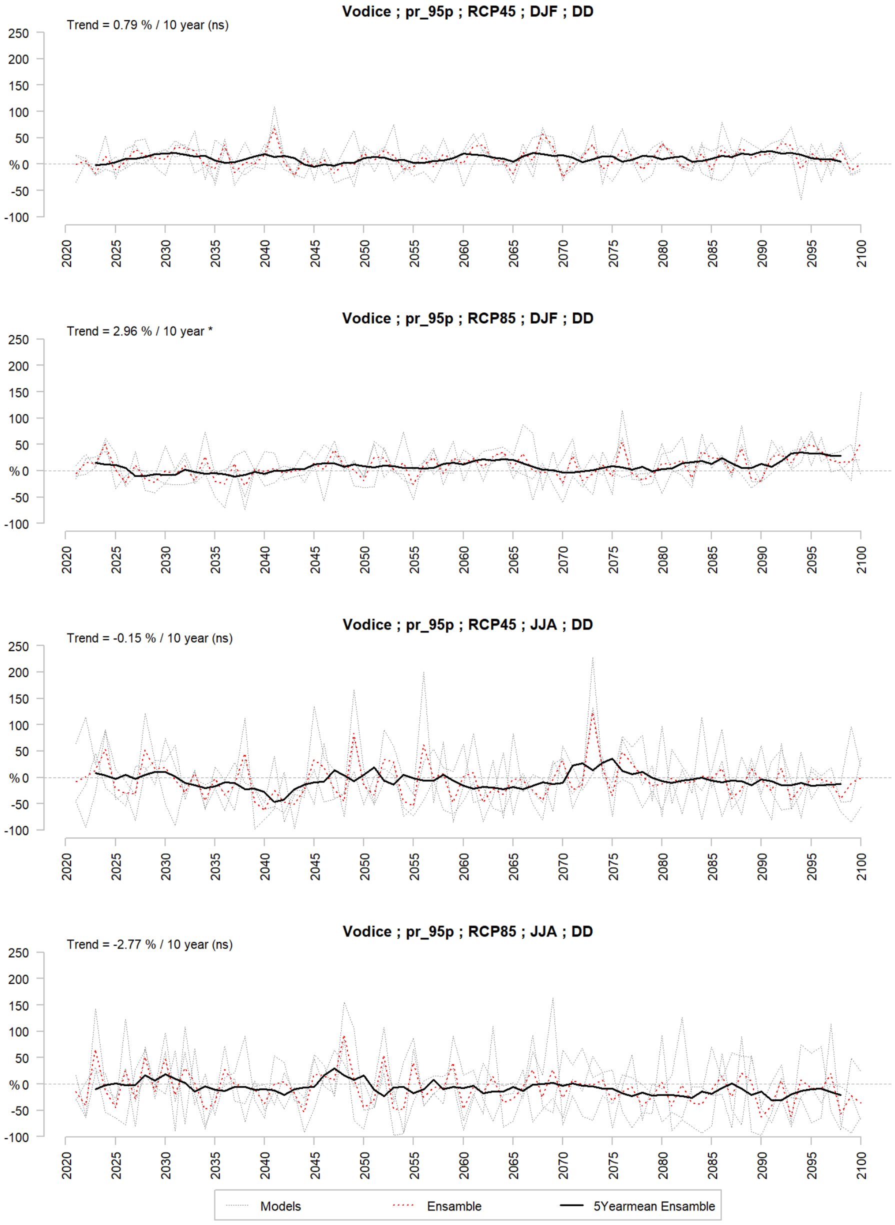

Figure 5-94: Variability of future 95th percentile of precipitation (intense precipitation) anomaly (in %) in Vodice for 2021-2100 obtained by dynamically downscaling for winter (DJF) and summer (JJA) and two RCP scenarios: individual models are in grey, the ensemble mean in red, 5-year moving average in black. Significant trend is marked with star (ns if not significant).

6.3.1.2.3 *Extreme precipitation*

Extreme precipitation (Figure 5-95), defined by 99th percentile of precipitation in Vodice, shows for ensemble mean increase in all seasons (except JJA) and on annual scale. The increase will change from 9.5 % in MAM to 15.9 % in SON, 15.5 % for annual scale for RCP4.5; between 11.3 % in SON and 30.7 % in DJF, 18.0 % for annual scale for RCP8.5 at the end of 21st century. Decrease of extreme precipitation in JJA will be -2.2 % for RCP4.5 and -5.5 % for RCP8.5 scenario. Variability of future extreme precipitation anomaly (Figure 5-96) to the end of 21st century for ensemble mean in Vodice has positive trend for DJF, negative for JJA. Linear trends in DJF are statistically significant for both scenarios (2.88 % / 10 year for RCP4.5 and 2.93 % /10 year for RCP8.5).

	RCP45					RCP85				
	DJF	MAM	JJA	SON	Annual	DJF	MAM	JJA	SON	Annual
Ref.mean	26.3	23.7	25.3	38.0	28.6	26.3	23.7	25.3	38.0	28.6
(P1-P0)/P0 * 100										
MPI_CCLM4	-0.3	5.0	* -20.5	21.4	11.5	-5.4	-4.3	7.3	7.1	2.9
EC-EARTH_KNMI	0.2	21.6	11.3	5.7	7.8	5.2	22.4	-3.2	-1.8	6.4
CNRM_CCLM4	11.5	-7.8	33.5	-7.2	8.5	13.9	5.5	13.3	-11.6	5.1
ENSMEAN	3.8	6.3	8.1	6.6	9.2	4.6	7.9	5.8	-2.1	4.8
(P2-P0)/P0 * 100										
MPI_CCLM4	9.7	3.5	-25.9	10.4	4.2	12.1	-8.4	-8.0	21.3	* 15.3
EC-EARTH_KNMI	0.4	29.4	4.8	-4.5	5.0	12.4	34.1	14.3	-4.5	9.7
CNRM_CCLM4	19.7	0.9	21.5	-11.4	5.7	* 33.2	-2.9	26.9	4.7	* 13.2
ENSMEAN	9.9	11.3	0.1	-1.8	4.9	19.2	7.6	11.1	7.2	12.7
(P3-P0)/P0 * 100										
MPI_CCLM4	4.7	-2.7	17.6	0.0	12.5	3.6	-0.7	3.6	31.8	* 15.6
EC-EARTH_KNMI	15.6	3.7	5.1	2.6	4.4	12.2	19.9	9.8	10.8	* 15.4
CNRM_CCLM4	18.2	-0.4	12.5	10.7	13.1	31.5	6.2	3.1	18.8	* 17.6
ENSMEAN	12.8	0.2	11.8	4.4	10.0	15.8	8.5	5.5	20.5	16.2
(P4-P0)/P0 * 100										
MPI_CCLM4	8.3	-2.6	-13.8	9.5	6.9	14.1	-0.7	-11.8	9.1	7.3
EC-EARTH_KNMI	14.4	29.4	7.7	10.9	* 15.4	* 48.4	27.4	-19.2	* 23.0	* 29.1
CNRM_CCLM4	21.4	1.6	-0.6	* 27.2	* 24.1	29.5	18.2	14.6	2.0	* 17.7
ENSMEAN	14.7	9.5	-2.2	15.9	15.5	30.7	15.0	-5.5	11.3	18.0

Figure 5-95: Seasonal and annual 99th percentile of precipitation (extreme precipitation) obtained by dynamical downscaling for Vodice: Ref. mean is 20 year simulated period (1986-2005) for ensemble mean in mmday^{-1}; P1-P0, P2-P0, P3-P0, P4-P0 are changes (in %) in the future for following periods P1: 2021-2040, P2: 2041-2060, P3: 2061-2080, P4: 2081-2100. Differences are shown for individual models. Significant change is marked by star. Change is also shown as ensemble mean (ENSMEAN), not tested for significance. Left column is for RCP4.5 scenario and right for RCP8.5 scenario.

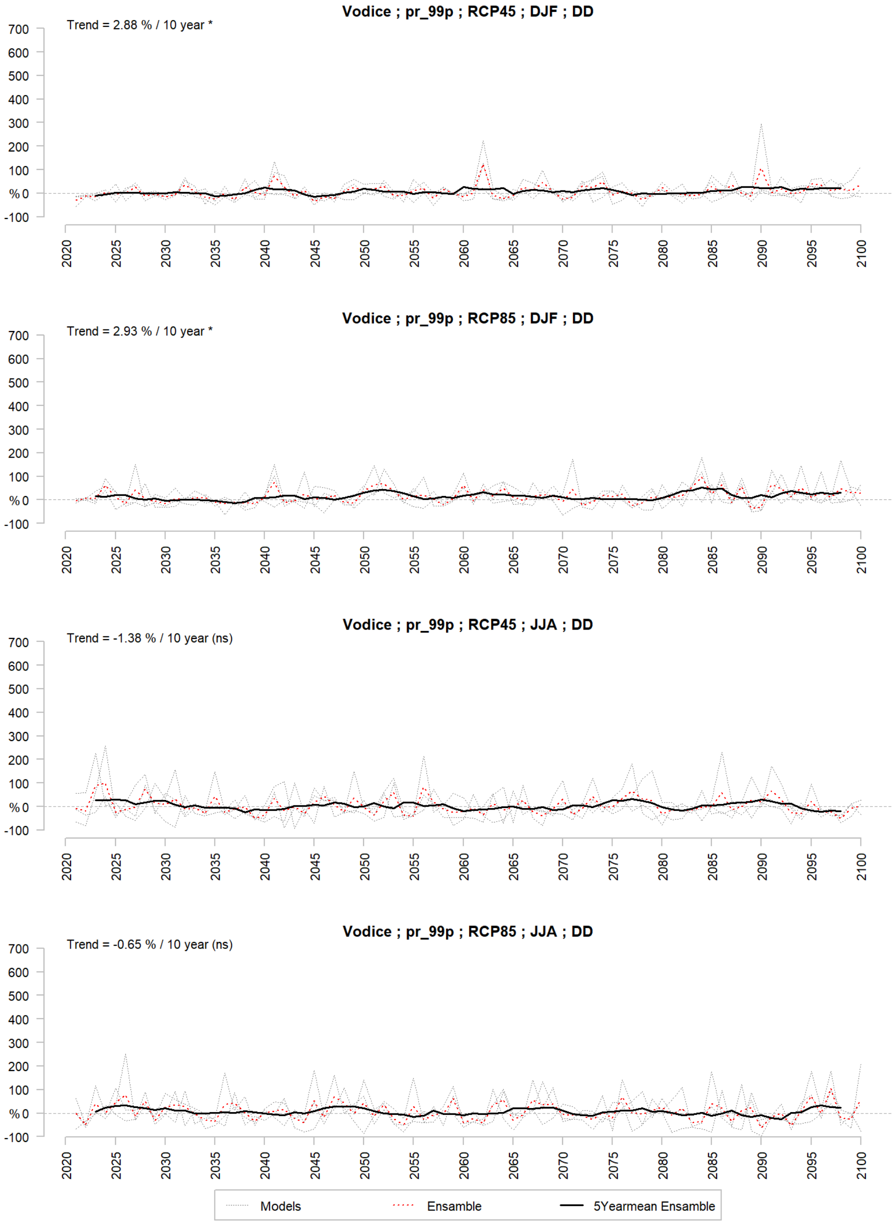

Figure 5-96: Variability of future 99th percentile of precipitation (extreme precipitation) anomaly (in %) in Vodice for 2021-2100 obtained by dynamically downscaling for winter (DJF) and summer (JJA) and two RCP scenarios: individual models are in grey, the ensemble mean in red, 5-year moving average in black. Significant trend is marked with star (ns if not significant).

6.3.1.2.4 *Heavy precipitation index*

Heavy precipitation index (Figure 5-97), defined as number of days with precipitation greater than 10 mm, will change with no unique sign between models in all seasons. In ensemble mean change at the end of century, heavy precipitation index will increase in all seasons (except in JJA, -4.2 %) and on annual scale in the range of 3.4 % in MAM and 17.7 % in DJF; 6.7 for annual scale for RCP4.5 scenario. Worst case scenario RCP8.5 gives increase in MAM (10.0 %) and 21 % in DJF, decrease in SON (-3.7 %) and in JJA (-24.7 %), on annual scale heavy precipitation index will increase for 1.9 % at the end of 21st century. Variability of future heavy precipitation index anomaly (Figure 5-98) to the end of 21st century for ensemble mean in Vodice has positive trend for DJF, negative for JJA. Linear trend in DJF is statistically significant for RCP8.5 scenario (3.04 % / 10 year).

RCP45

	DJF	MAM	JJA	SON	Annual
Ref.mean	8.8	6.4	4.5	11.4	31.2
(P1-P0)/P0 * 100					
MPI_CCLM4	4.0	7.0	-16.7	31.5	9.7
EC-EARTH_KNMI	7.1	18.8	-0.8	-19.9	-4.2
CNRM_CCLM4	16.6	-15.3	12.8	-14.7	-2.5
ENSMEAN	9.2	3.5	-1.6	-1.0	1.0
(P2-P0)/P0 * 100					
MPI_CCLM4	-2.1	-0.7	-31.3	* 28.8	2.2
EC-EARTH_KNMI	3.0	5.1	0.8	-13.8	-4.1
CNRM_CCLM4	6.5	-9.7	-3.7	-5.6	-3.5
ENSMEAN	2.5	-1.8	-11.4	3.1	-1.8
(P3-P0)/P0 * 100					
MPI_CCLM4	9.6	-1.6	-14.2	15.7	5.7
EC-EARTH_KNMI	35.4	8.8	-1.9	* -26.5	-0.5
CNRM_CCLM4	13.2	-7.9	2.2	4.8	2.9
ENSMEAN	19.4	-0.2	-4.6	-2.0	2.7
(P4-P0)/P0 * 100					
MPI_CCLM4	12.6	-9.6	-22.0	15.5	3.8
EC-EARTH_KNMI	16.9	23.7	15.8	-1.3	9.1
CNRM_CCLM4	* 23.5	-3.9	-6.5	10.1	7.4
ENSMEAN	17.7	3.4	-4.2	8.1	6.7

RCP85

	DJF	MAM	JJA	SON	Annual
Ref.mean	8.8	6.4	4.5	11.4	31.2
(P1-P0)/P0 * 100					
MPI_CCLM4	-16.0	-13.6	6.2	* 27.8	1.2
EC-EARTH_KNMI	-3.9	29.2	-11.5	-16.6	-3.6
CNRM_CCLM4	11.9	-1.7	-5.6	-6.3	-0.7
ENSMEAN	-2.7	4.6	-3.6	1.6	-1.1
(P2-P0)/P0 * 100					
MPI_CCLM4	14.9	-22.3	-10.5	21.3	3.6
EC-EARTH_KNMI	7.5	18.0	20.1	-6.6	3.5
CNRM_CCLM4	20.8	-8.0	-0.9	-3.0	1.5
ENSMEAN	14.4	-4.1	2.9	3.9	2.9
(P3-P0)/P0 * 100					
MPI_CCLM4	-9.7	-3.2	-9.7	* 31.0	4.2
EC-EARTH_KNMI	27.1	10.5	-15.7	-11.1	2.3
CNRM_CCLM4	20.1	-0.7	-11.5	2.4	3.4
ENSMEAN	12.5	2.2	-12.3	7.5	3.3
(P4-P0)/P0 * 100					
MPI_CCLM4	7.4	-14.4	* -33.1	4.8	-5.4
EC-EARTH_KNMI	36.6	22.5	* -43.0	-8.8	5.4
CNRM_CCLM4	19.0	21.8	1.9	-7.1	5.6
ENSMEAN	21.0	10.0	-24.7	-3.7	1.9

* ; *Two Sample Wilcoxon tests, 95 % confidence interval*

Figure 5-97: Seasonal and annual heavy precipitation index obtained by dynamical downscaling for Vodice: Ref. mean is 20 year simulated period (1986-2005) for ensemble mean in days; P1-P0, P2-P0, P3-P0, P4-P0 are changes (in %) in the future for following periods P1: 2021-2040, P2: 2041-2060, P3: 2061-2080, P4: 2081-2100. Differences are shown for individual models. Significant change is marked by star. Change is also shown as ensemble mean (ENSMEAN), not tested for significance. Left column is for RCP4.5 scenario and right for RCP8.5 scenario.

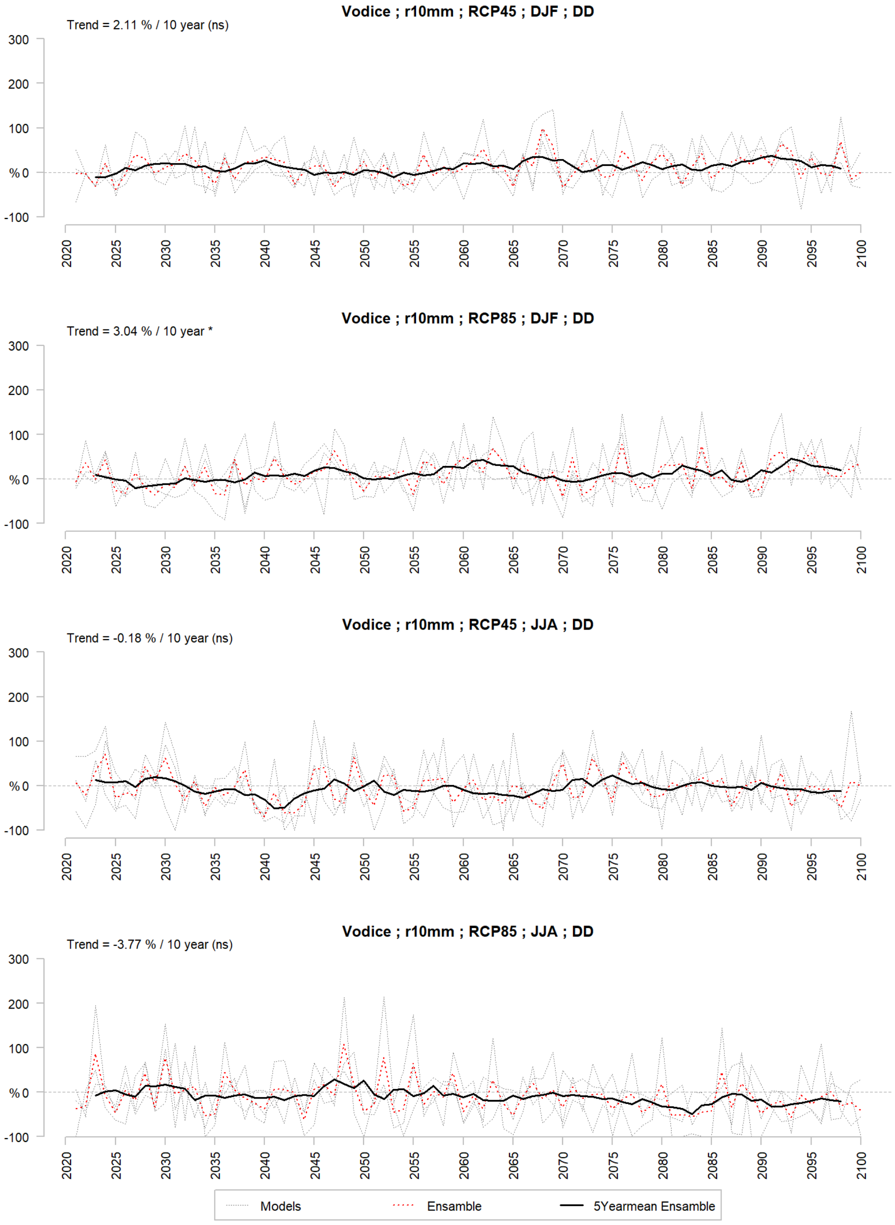

Figure 5-98: Variability of future heavy precipitation index anomaly (in %) in Vodice for 2021-2100 obtained by dynamically downscaling for winter (DJF) and summer (JJA) and two RCP scenarios: individual models are in grey, the ensemble mean in red, 5-year moving average in black. Significant trend is marked with star (ns if not significant).

6.3.1.2.5 *Maximum number of consecutive dry days*

Maximum number of consecutive dry days (Figure 5-99) in Vodice will mostly increase in all periods for most models. The ensemble mean change gives increase in all seasons (except in MAM, -1.5 %) and on annual scale at the end of 21st century for RCP4.5 scenario. Increase will range from 6.5 % in SON to 17.0 % in DJF, 13.3 % on annual scale. For RCP8.5 scenario increase is present in all seasons (from 4.8 % in MAM to 34.1 % in JJA) and on annual scale (27.9 %). Variability of future maximum number of consecutive dry days anomaly (Figure 5-100) to the end of 21st century for ensemble mean in Vodice change a sign of trend in DJF from positive for RCP4.5 into negative for RCP8.5. Both trends are not statistically significant. Variability of future maximum number of consecutive dry days anomaly in JJA is positive for both scenarios, but statistically significant only for RCP8.5 (3.93 % / 10 year).

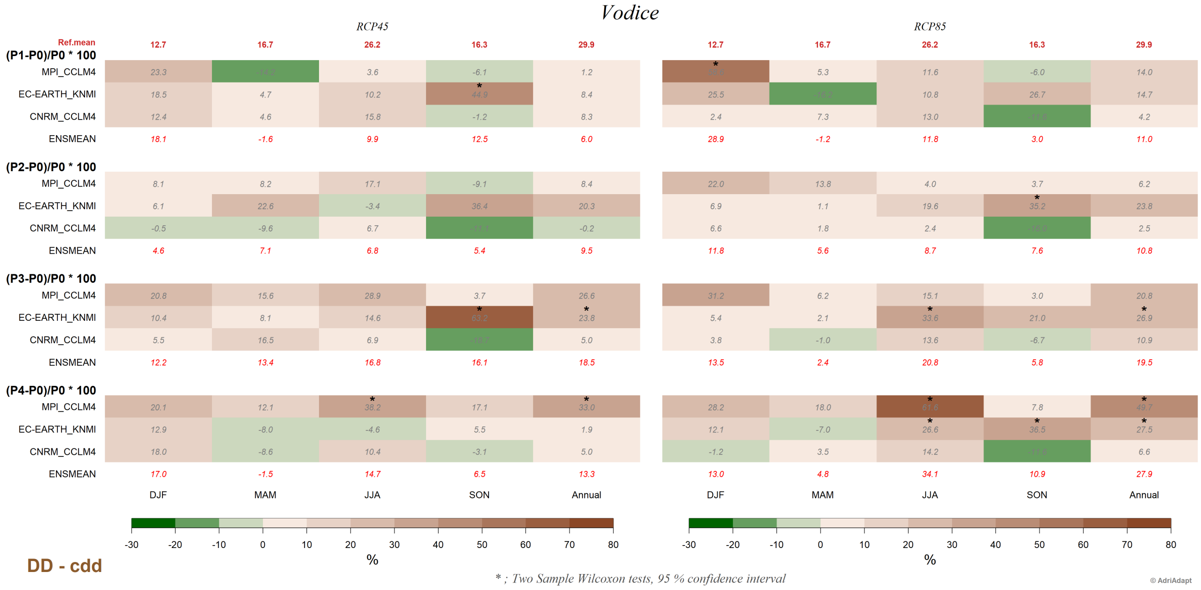

	RCP45					RCP85				
	DJF	MAM	JJA	SON	Annual	DJF	MAM	JJA	SON	Annual
Ref.mean	12.7	16.7	26.2	16.3	29.9	12.7	16.7	26.2	16.3	29.9
(P1-P0)/P0 * 100										
MPI_CCLM4	23.3	-14.2	3.6	-6.1	1.2	* 58.6	5.3	11.6	-6.0	14.0
EC-EARTH_KNMI	18.5	4.7	10.2	* 44.9	8.4	25.5	-16.2	10.8	26.7	14.7
CNRM_CCLM4	12.4	4.6	15.8	-1.2	8.3	2.4	7.3	13.0	-11.6	4.2
ENSMEAN	18.1	-1.6	9.9	12.5	6.0	28.9	-1.2	11.8	3.0	11.0
(P2-P0)/P0 * 100										
MPI_CCLM4	8.1	8.2	17.1	-9.1	8.4	22.0	13.8	4.0	3.7	6.2
EC-EARTH_KNMI	6.1	22.6	-3.4	36.4	20.3	6.9	1.1	19.6	* 35.2	23.8
CNRM_CCLM4	-0.5	-9.6	6.7	-11.1	-0.2	6.6	1.8	2.4	-16.0	2.5
ENSMEAN	4.6	7.1	6.8	5.4	9.5	11.8	5.6	8.7	7.6	10.8
(P3-P0)/P0 * 100										
MPI_CCLM4	20.8	15.6	28.9	3.7	26.6	31.2	6.2	15.1	3.0	20.8
EC-EARTH_KNMI	10.4	8.1	14.6	* 63.2	* 23.8	5.4	2.1	* 33.6	21.0	* 26.9
CNRM_CCLM4	5.5	16.5	6.9	-18.7	5.0	3.8	-1.0	13.6	-6.7	10.9
ENSMEAN	12.2	13.4	16.8	16.1	18.5	13.5	2.4	20.8	5.8	19.5
(P4-P0)/P0 * 100										
MPI_CCLM4	20.1	12.1	* 38.2	17.1	* 33.0	28.2	18.0	* 61.6	7.8	* 49.7
EC-EARTH_KNMI	12.9	-8.0	-4.6	5.5	1.9	12.1	-7.0	* 26.6	* 36.5	* 27.5
CNRM_CCLM4	18.0	-8.6	10.4	-3.1	5.0	-1.2	3.5	14.2	-11.6	6.6
ENSMEAN	17.0	-1.5	14.7	6.5	13.3	13.0	4.8	34.1	10.9	27.9

** ; Two Sample Wilcoxon tests, 95 % confidence interval*

Figure 5-99: Seasonal and annual maximum number of consecutive dry days obtained by dynamical downscaling for Vodice: Ref. mean is 20 year simulated period (1986-2005) for ensemble mean in days; P1-P0, P2-P0, P3-P0, P4-P0 are changes (in %) in the future for following periods P1: 2021-2040, P2: 2041-2060, P3: 2061-2080, P4: 2081-2100. Differences are shown for individual models. Significant change is marked by star. Change is also shown as ensemble mean (ENSMEAN), not tested for significance. Left column is for RCP4.5 scenario and right for RCP8.5 scenario.

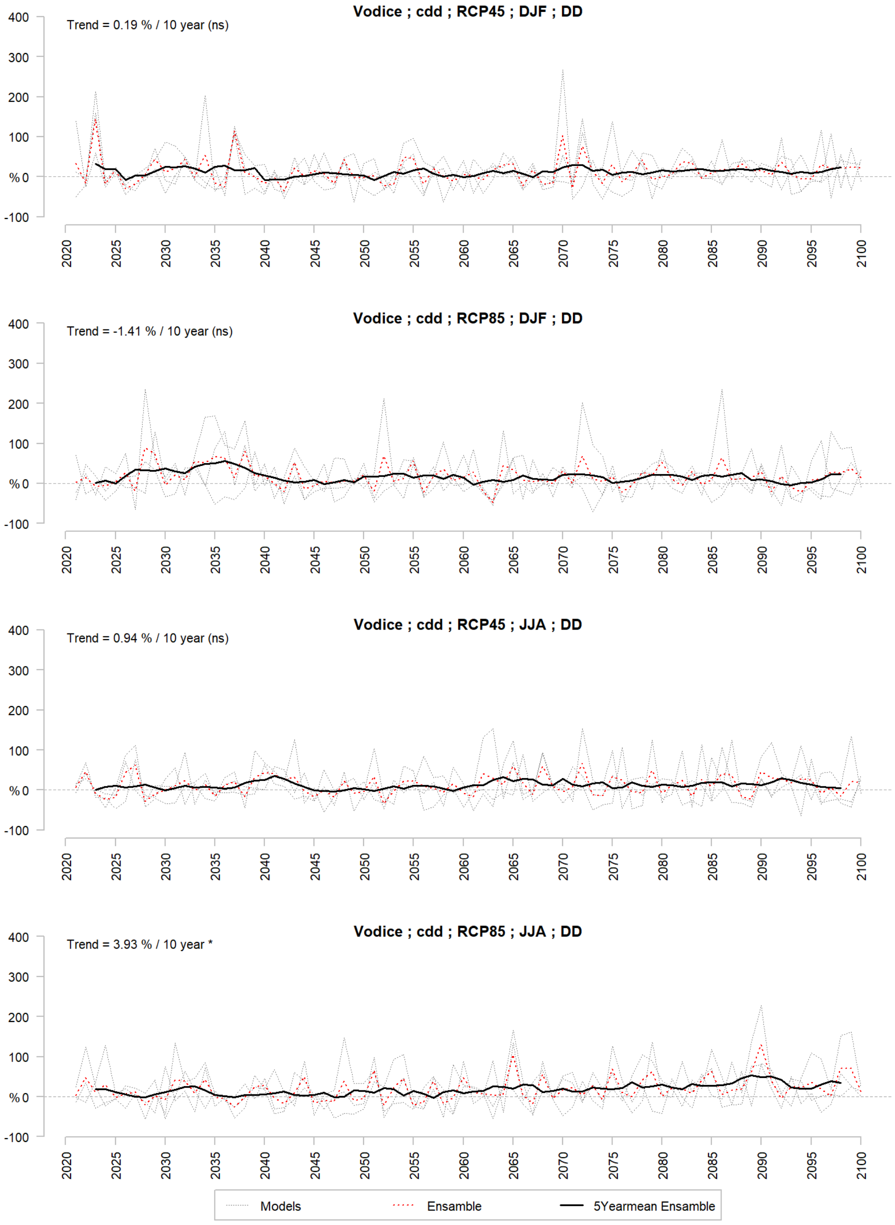

Figure 5-100: Variability of future maximum number of consecutive dry days anomaly (in %) in Vodice for 2021-2100 obtained by dynamically downscaling for winter (DJF) and summer (JJA) and two RCP scenarios: individual models are in grey, the ensemble mean in red, 5-year moving average in black. Significant trend is marked with star (ns if not significant).

6.3.1.3 *Extra rare humidex projections*

Extra rare humidex change (defined by 99.9th percentile of humidex) in the future in Vodice will slightly increase towards the end of 21st century (Figure 5-101). Ensemble mean will increase between 0.8 in JJA and 2.6 in SON, 1.7 on annual scale for RCP4.5 scenario. Scenario RCP8.5 gives slightly higher positive amplitudes, from 3.9 in JJA to 6.3 in SON, 4.7 on annual scale. Variability of future 99.9th percentile of humidex anomaly (Figure 5-102) shows positive linear trend for both seasons and both considered scenarios. It is 0.30 [] / 10 year in DJF for RCP4.5 (0.65 [] /10 year for RCP8.5) and 0.31 [] /10 year in JJA for RCP4.5 (0.80 [] /10 year for RCP8.5). Trends are statistically significant.

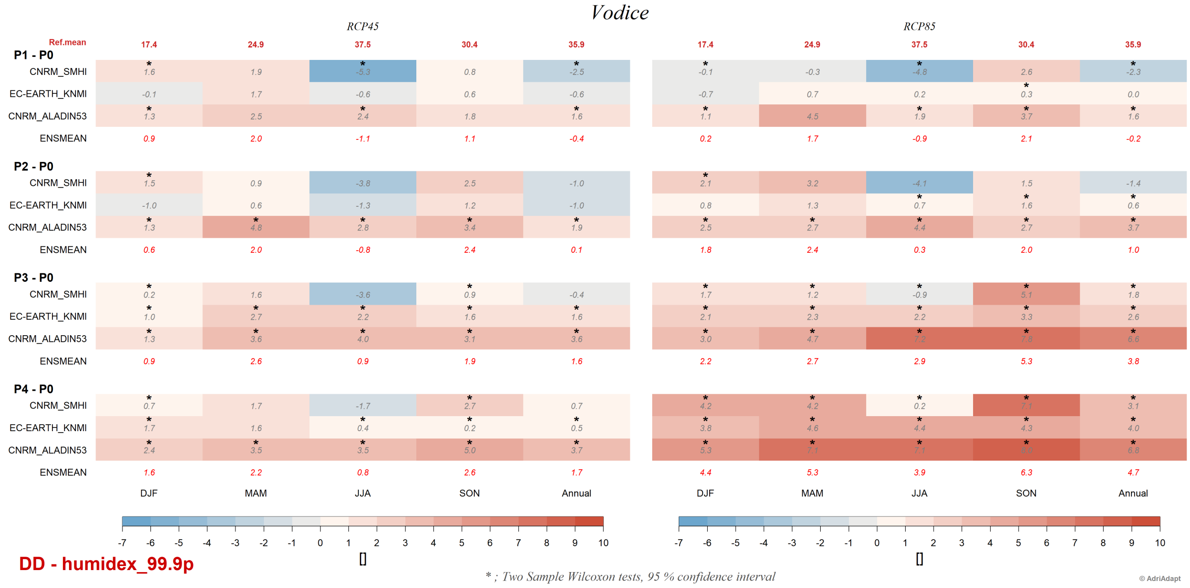

Figure 5-101: Seasonal and annual 99.9th percentile of humidex obtained by dynamical downscaling for Vodice (in []): Ref. mean is 20 year simulated period (1986-2005); P1-P0, P2-P0, P3-P0, P4-P0 are changes in the future for following periods P1: 2021-2040, P2: 2041-2060, P3: 2061-2080, P4: 2081-2100. Differences are shown for individual models. Significant change is marked by star. Change is also shown as ensemble mean (ENSMEAN), not tested for significance. Left column is for RCP4.5 scenario and right for RCP8.5 scenario.

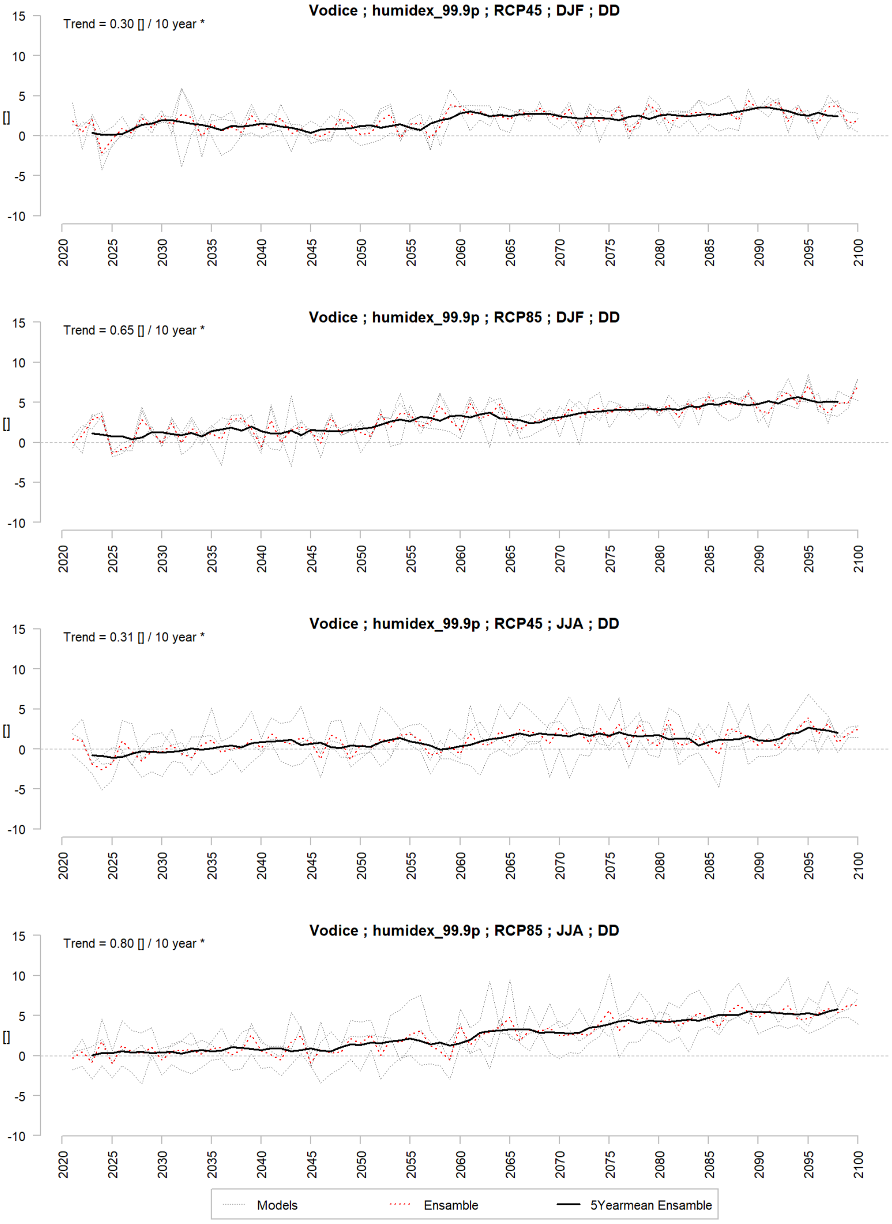

Figure 5-102: Variability of future 99.9th percentile of humidex anomaly (in []) in Vodice for 2021-2100 obtained by dynamically downscaling for winter (DJF) and summer (JJA) and two RCP scenarios: individual models are in grey, the ensemble mean in red, 5-year moving average in black. Significant trend is marked with star (ns if not significant).

6.4 Case study 4: Cervia

6.4.1 Dynamically downscaled results

In this section we present future climate change of temperature and precipitation related indices, extra rare humidex and wind projections for Cervia. All indices are calculated from the available data set of regional climate models for the grid point that is representing the location of case study Cervia. Data set is obtained by bilinear interpolation. All data are presented as follows:

- Climate change diagram of an individual index in seasons and on annual basis for four considered future periods, for two emission scenarios RCP4.5 and RCP8.5. Climate change is calculated as difference between future and reference period (relative difference for precipitation indices, surface relative humidity and wind projections). Reference period is presented as ensemble mean of available regional climate models (Ref.mean), while climate change is shown for different models as well as for ensemble mean of models (ENSMEAN). Two sample Wilcoxon test is applied to test statistical significance of climate change for individual models (for 95 % confidence level). Significant change is marked by star
- Time series of future anomaly of an individual index for DJF and JJA and for two emission scenarios RCP4.5 and RCP8,5. Anomaly is calculated respect to the reference period and shown for individual models, ensemble mean and 5-year moving average. Mann Kendall trend test is applied to ensemble mean (for 95 % confidence level). Significant trend is marked with star (ns if not significant).

6.4.1.1 *Temperature related indices projections*

6.4.1.1.1 *Averaged 2 meter air temperature*

Averaged temperature change (Figure 5-103) in Cervia shows increase in all seasons and on annual scale, for all future periods (exception is in winter for one model realisation in first period). Although each model gives different amplitude of change, in ensemble mean the change is highest during summer or autumn and the smallest in winter, for RCP4.5. The temperature increase is more pronounced towards the end of the century when the increase in the ensemble mean is from 1.5 °C in DJF and MAM to 2.0 °C in JJA. On annual scale for RCP4.5 temperature increase is for 1.7 °C. The amplitude of temperature change is more pronounced for RCP8.5 scenario, from 2.9 °C in MAM to 3.9 °C in JJA and SON, on annual scale 3.6 °C at the end of 21st century for ensemble mean. The linear trend of temperature anomaly (Figure 5-104) in the future shows increase which is statistically significant for both considered seasons and both scenarios; for DJF ensemble is 0.20 °C / 10 year for RCP4.5 and 0.51 °C / 10 year for RCP8.5; for JJA ensemble is 0.17 °C / 10 year for RCP4.5 and 0.46 °C / 10 year.

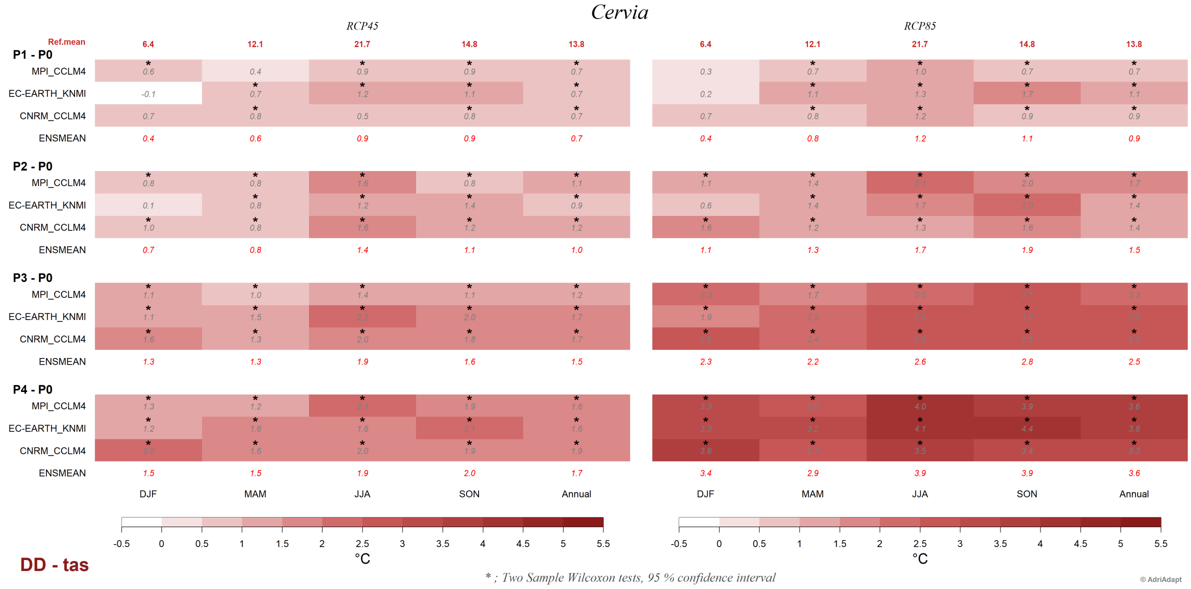

Figure 5-103: Averaged seasonal and annual 2m air temperature (in °C) obtained by dynamical downscaling for Cervia: Ref. mean is 20 year simulated period (1986-2005) for ensemble mean; P1-P0, P2-P0, P3-P0, P4-P0 are changes in the future for following periods P1: 2021-2040, P2: 2041-2060, P3: 2061-2080, P4: 2081-2100. Differences are shown for individual models. Significant change is marked by star. Change is also shown as ensemble mean (ENSMEAN), not tested for significance. Left column is for RCP4.5 scenario and right for RCP8.5 scenario.

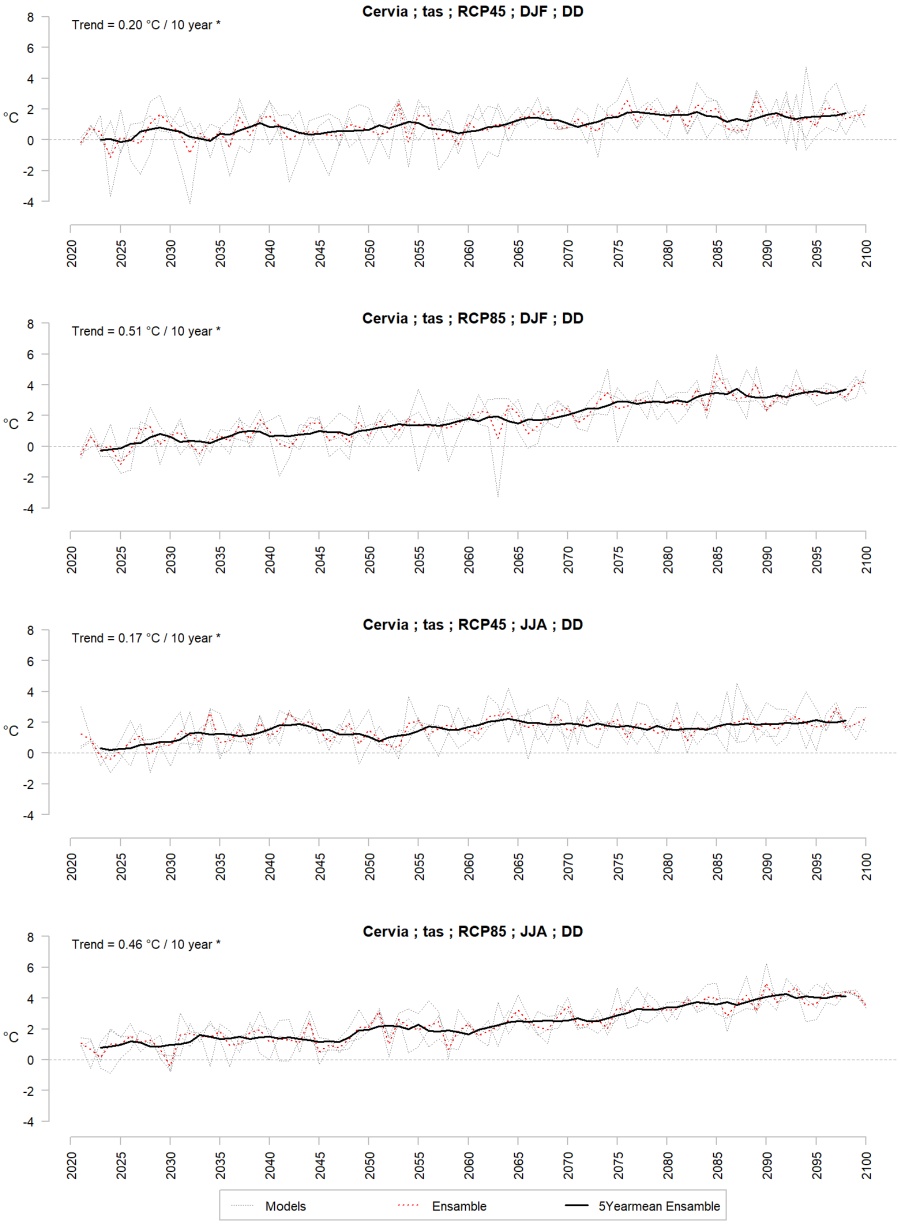

Figure 5-104: Variability of future 2m air temperature anomaly (in °C) in Cervia for 2021-2100 obtained by dynamically downscaling for winter (DJF) and summer (JJA) and two RCP scenarios: individual models are in grey, the ensemble mean in red, 5-year moving average in black. Significant trend is marked with star (ns if not significant).

6.4.1.1.2 *High temperature*

High temperature change (Figure 5-105), defined as 95th percentile of 2m air temperature, in Cervia is increasing from P1 to P4 future periods with the different amplitudes for each model. In ensemble mean at the end of century increase is from 1.5 °C in DJF to 2.5 °C in SON, 2.1 °C on annual scale for RCP4.5. Amplitude of change is more pronounced for RCP8.5 and is between 3.3 °C in DJF and 4.8 °C in SON, 4.3 °C for annual change at the end of 21st century. Variability of future 95th percentile of 2m air temperature anomaly (Figure 5-106) shows linear trend in change of ensemble mean, 0.17 °C / 10 year in DJF for RCP4.5 and 0.47 °C / 10 year for RCP8.5; 0.21 °C / 10 year in JJA for RCP4.5 and 0.51 °C / 10 year for RCP8.5. All trends are statistically significant.

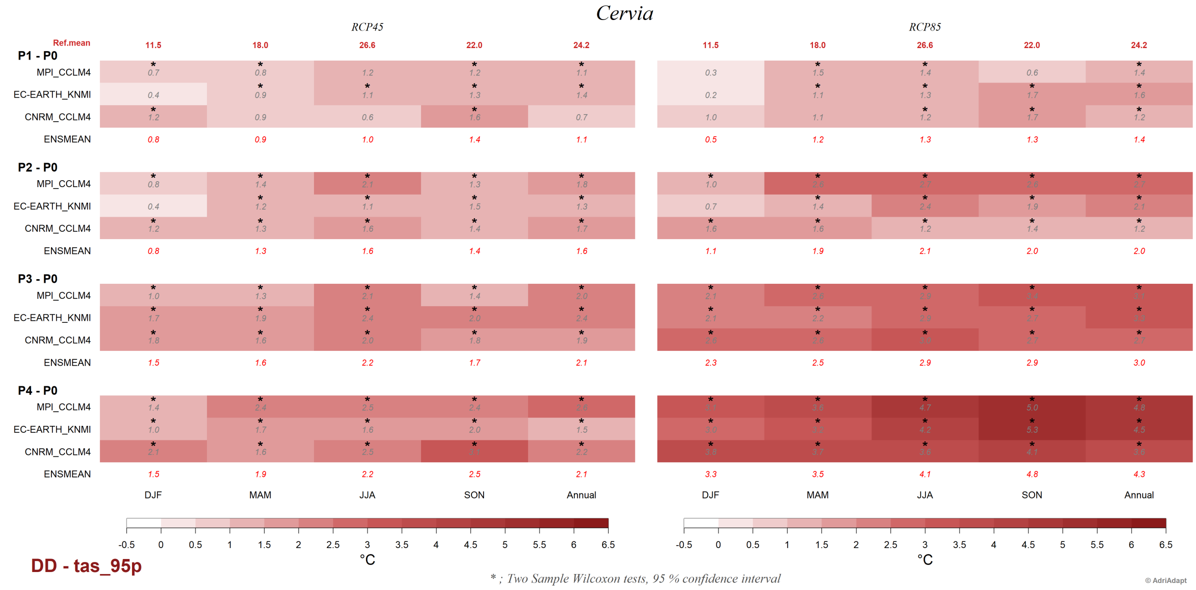

Figure 5-105: Seasonal and annual 95th percentile of 2m air temperature (high temperature, in °C) obtained by dynamical downscaling for Cervia: Ref. mean is 20 year simulated period (1986-2005) for ensemble mean; P1-P0, P2-P0, P3-P0, P4-P0 are changes in the future for following periods P1: 2021-2040, P2: 2041-2060, P3: 2061-2080, P4: 2081-2100. Differences are shown for individual models. Significant change is marked by star. Change is also shown as ensemble mean (ENSMEAN), not tested for significance. Left column is for RCP4.5 scenario and right for RCP8.5 scenario.

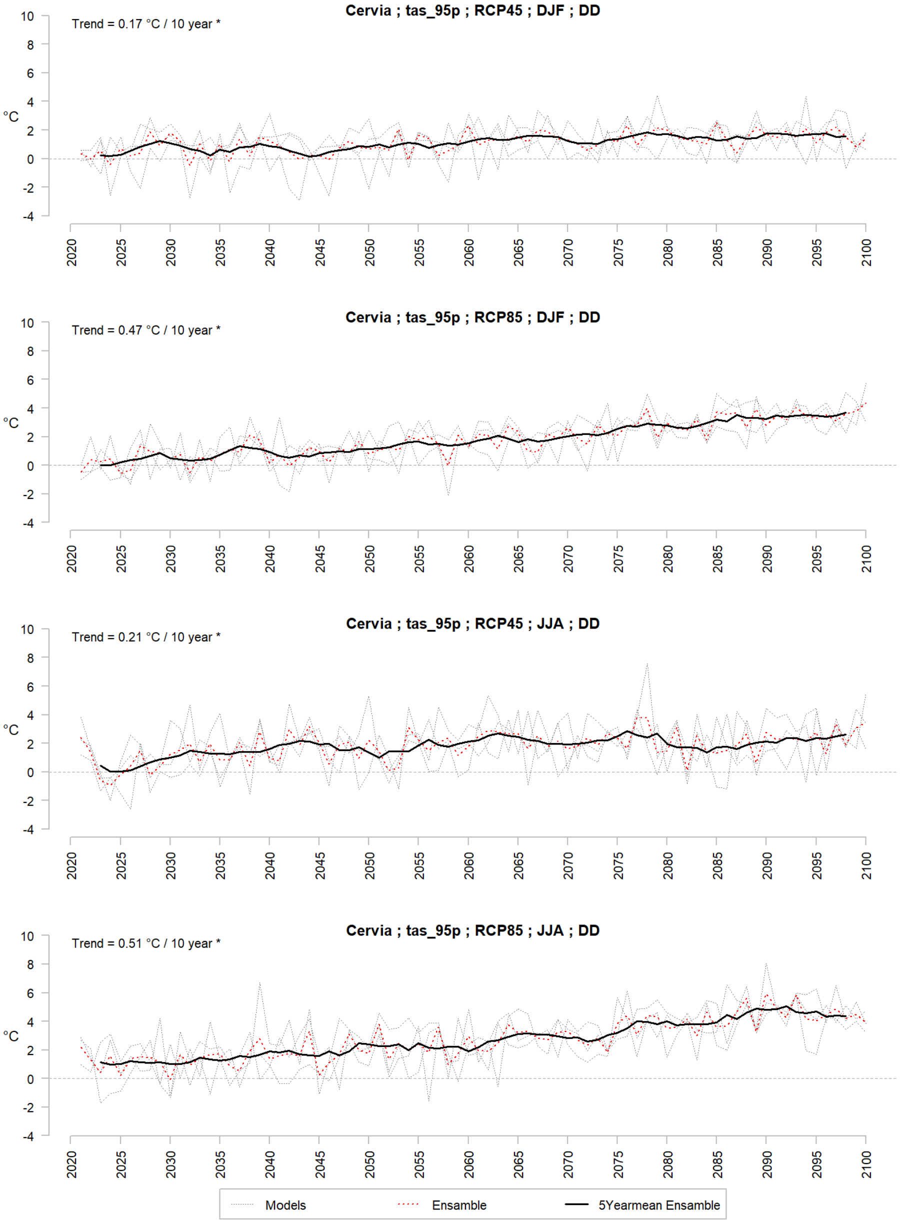

Figure 5-106: Variability of future 95th percentile of 2m air temperature (high temperature) anomaly (in °C) in Cervia for 2021-2100 obtained by dynamically downscaling for winter (DJF) and summer (JJA) and two RCP scenarios: individual models are in grey, the ensemble mean in red, 5-year moving average in black. Significant trend is marked with star (ns if not significant).

6.4.1.1.3 *High maximum temperature*

High maximum temperature change (Figure 5-107), defined as 95th percentile of 2m maximum air temperature, in Cervia is increasing from P1 to P4 future periods with the different amplitudes for each model. In ensemble mean at the end of century increase is from 1.5 °C in DJF to 2.3 °C in SON, 1.8 °C on annual scale for RCP4.5. Amplitude of change is more pronounced for RCP8.5 and is between 3.2 °C in DJF and 4.8 °C in SON, 3.8 °C for annual change at the end of 21st century. Variability of future 95th percentile of 2m maximum air temperature anomaly (Figure 5-108) shows linear trend in change of ensemble mean, 0.18 °C / 10 year in DJF for RCP4.5 and 0.48 °C / 10 year for RCP8.5; 0.23 °C / 10 year in JJA for RCP4.5 and 0.48 °C / 10 year for RCP8.5. All trends are statistically significant.

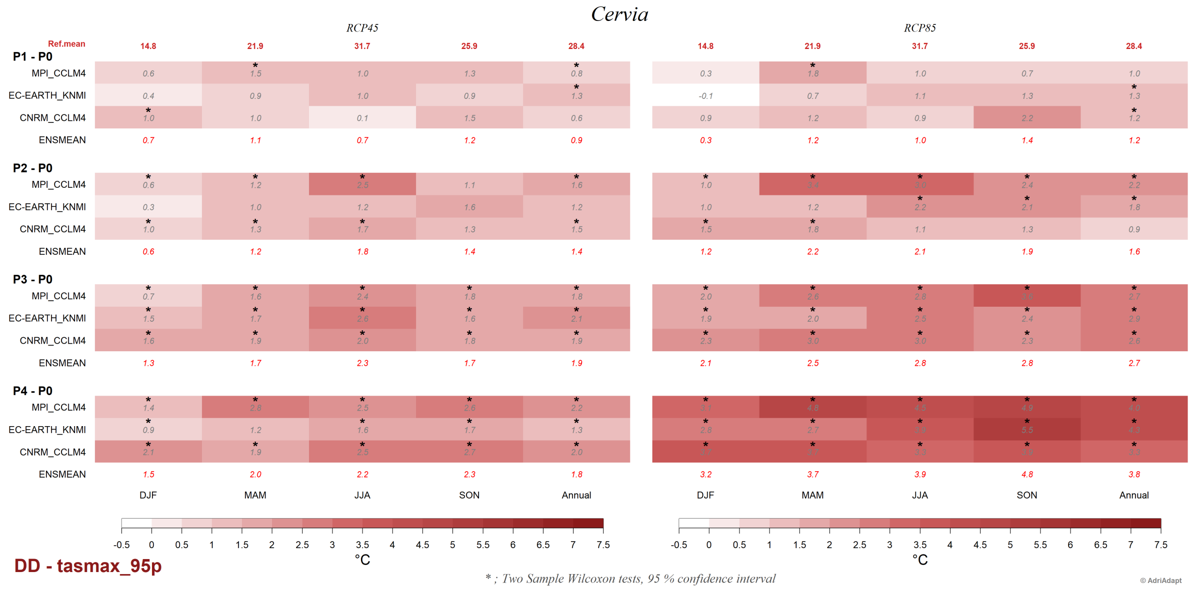

Figure 5-107: Seasonal and annual 95th percentile of 2m maximum air temperature (high maximum temperature, in °C) obtained by dynamical downscaling for Cervia: Ref. mean is 20 year simulated period (1986-2005) for ensemble mean; P1-P0, P2-P0, P3-P0, P4-P0 are changes in the future for following periods P1: 2021-2040, P2: 2041-2060, P3: 2061-2080, P4: 2081-2100. Differences are shown for individual models. Significant change is marked by star. Change is also shown as ensemble mean (ENSMEAN), not tested for significance. Left column is for RCP4.5 scenario and right for RCP8.5 scenario.

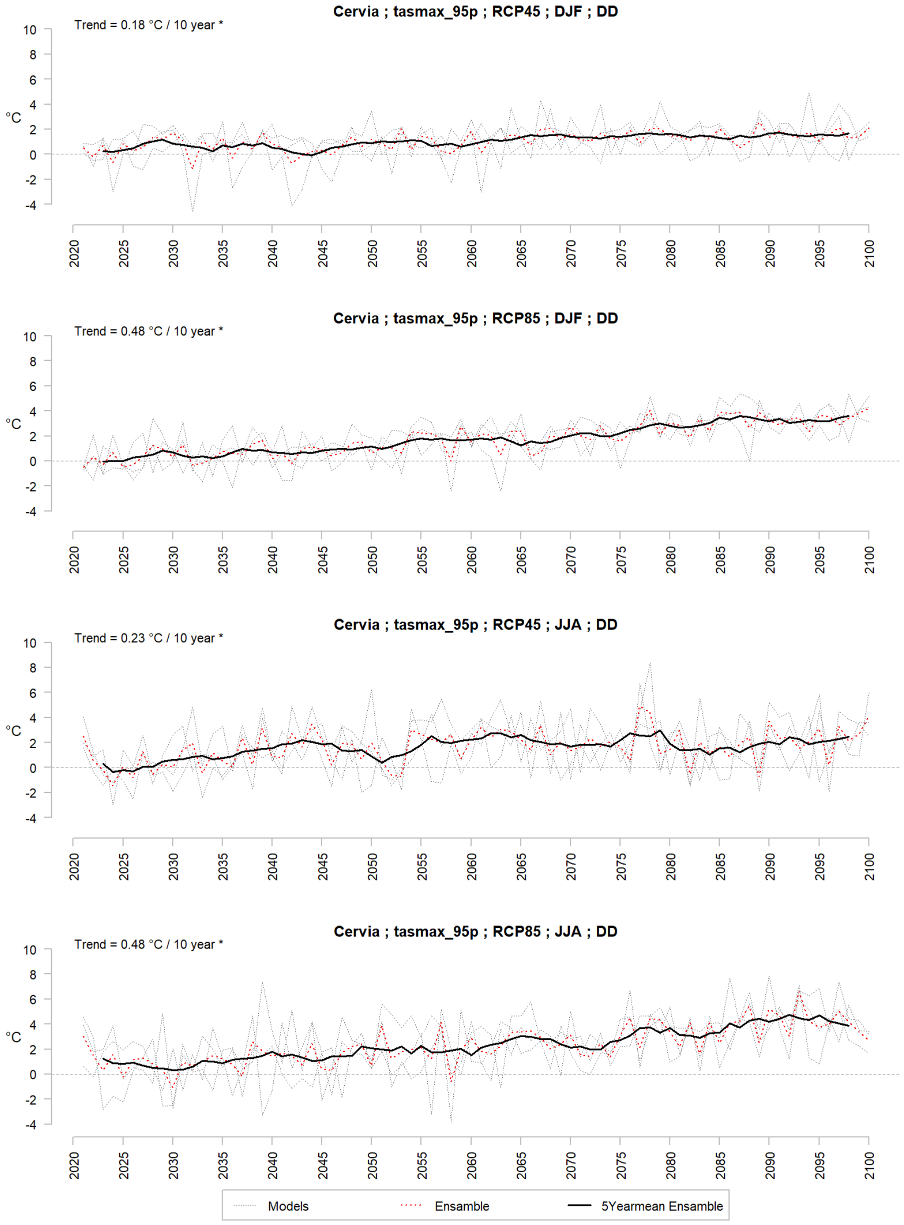

Figure 5-108: Variability of future 95th percentile of 2m maximum air temperature (high maximum temperature) anomaly (in °C) in Cervia for 2021-2100 obtained by dynamically downscaling for winter (DJF) and summer (JJA) and two RCP scenarios: individual models are in grey, the ensemble mean in red, 5-year moving average in black. Significant trend is marked with star (ns if not significant).

6.4.1.1.4 *Extreme high temperature*

99th percentile of 2m air temperature (Figure 5-109) in Cervia is increasing from P1 to P4 future periods with the different amplitudes for each model. In ensemble mean at the end of century increase is from 1.2 °C in DJF to 2.4 °C in MAM, 2.1 °C on annual scale for RCP4.5. Amplitude of change is more pronounced for RCP8.5 and is between 3.1 °C in DJF and 4.8 °C in SON, 4.2 °C for annual change at the end of 21st century. Variability of future 99th percentile of 2m air temperature anomaly (Figure 5-110) shows linear trend in change of ensemble mean, 0.17 °C / 10 year in DJF for RCP4.5 and 0.48 °C / 10 year for RCP8.5; 0.20 °C / 10 year in JJA for RCP4.5 and 0.51 °C / 10 year for RCP8.5. All trends are statistically significant.

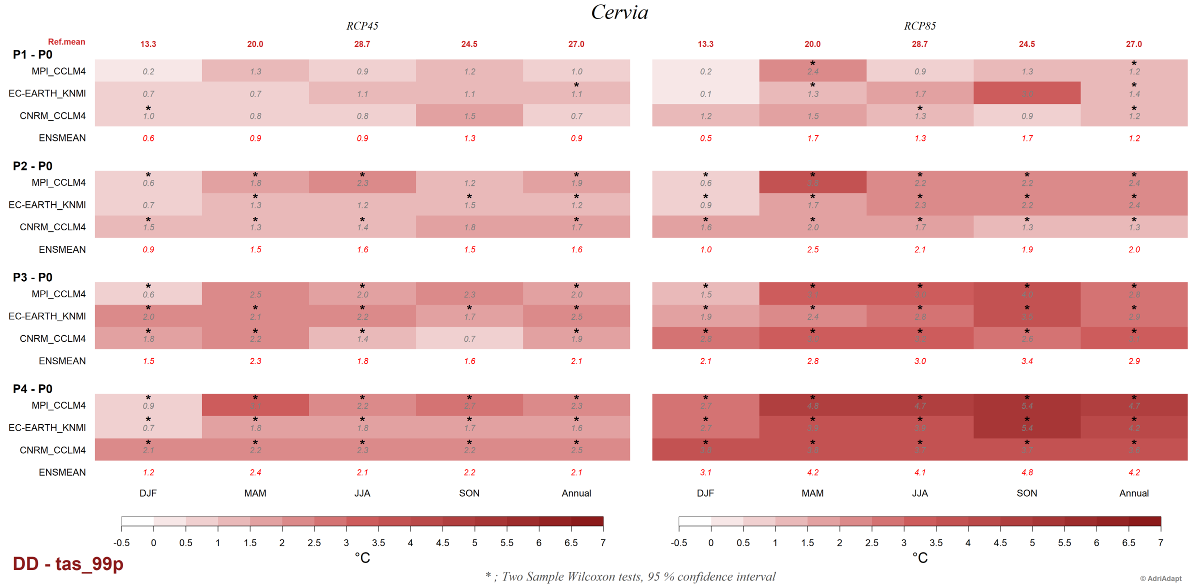

Figure 5-109: Seasonal and annual 99th percentile of 2m air temperature (extreme high temperature, in °C) obtained by dynamical downscaling for Cervia: Ref. mean is 20 year simulated period (1986-2005) for ensemble mean; P1-P0, P2-P0, P3-P0, P4-P0 are changes in the future for following periods P1: 2021-2040, P2: 2041-2060, P3: 2061-2080, P4: 2081-2100. Differences are shown for individual models. Significant change is marked by star. Change is also shown as ensemble mean (ENSMEAN), not tested for significance. Left column is for RCP4.5 scenario and right for RCP8.5 scenario.

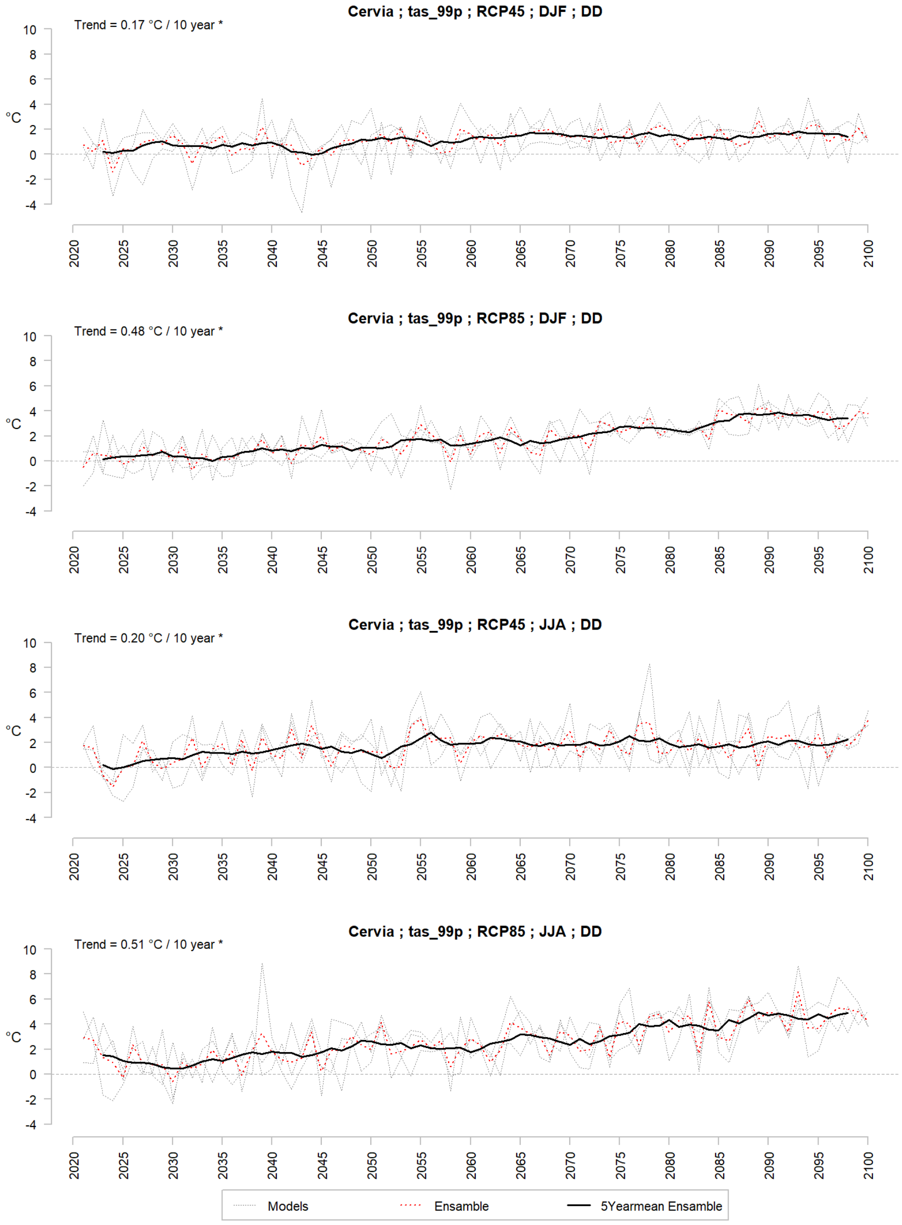

Figure 5-110: Variability of future 99th percentile of 2m air temperature (extreme high temperature) anomaly (in °C) in Cervia for 2021-2100 obtained by dynamically downscaling for winter (DJF) and summer (JJA) and two RCP scenarios: individual models are in grey, the ensemble mean in red, 5-year moving average in black. Significant trend is marked with star (ns if not significant).

6.4.1.1.5 *Extreme high maximum temperature*

Future change of 99th percentile of 2m maximum air temperature (Figure 5-111) in Cervia is increasing from P1 to P4 periods with the different amplitudes for each model (exception is one model in P1 in DJF). Ensemble mean of change is positive for all periods. At the end of century increase is from 1.5 °C in DJF to 2.8 °C in MAM, 2.1 °C on annual scale for RCP4.5. Amplitude of change is more pronounced for RCP8.5 and is between 3.4 °C in DJF and 4.5 °C in SON, 4.0 °C for annual change at the end of 21st century. Variability of future 99th percentile of 2m maximum air temperature anomaly (Figure 5-112) shows linear trend in change of ensemble mean, 0.19 °C / 10 year in DJF for RCP4.5 and 0.48 °C / 10 year for RCP8.5; 0.20 °C / 10 year in JJA for RCP4.5 and 0.57 °C / 10 year for RCP8.5. All trends are statistically significant.

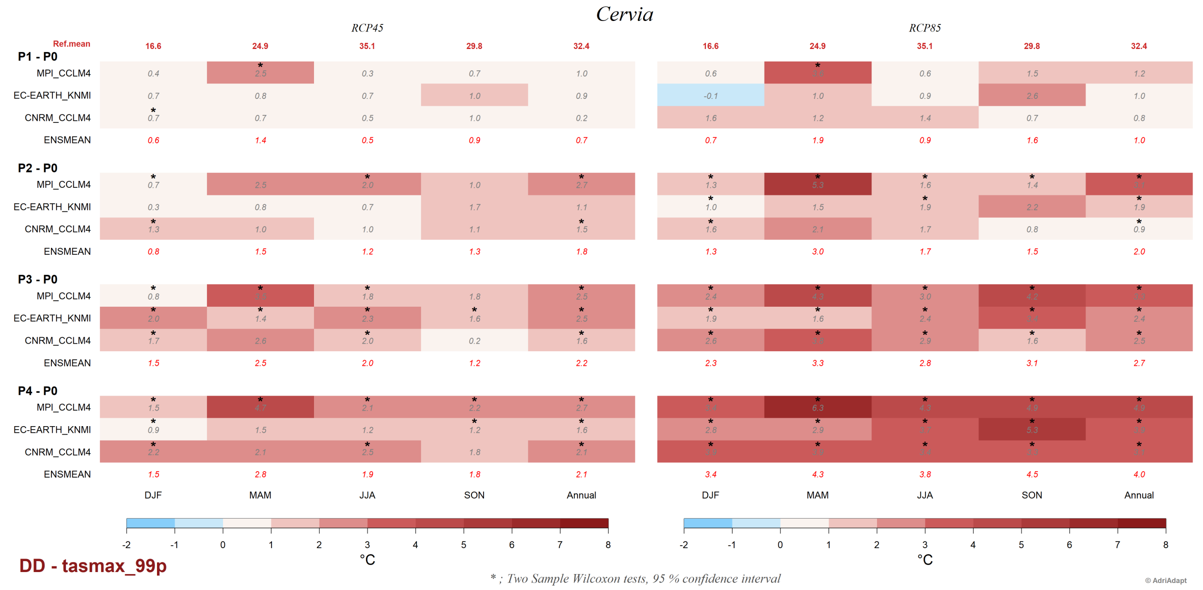

	RCP45					RCP85				
Ref.mean	16.6	24.9	35.1	29.8	32.4	16.6	24.9	35.1	29.8	32.4
P1 - P0										
MPI_CCLM4	0.4	* 2.5	0.3	0.7	1.0	0.6	* 3.6	0.6	1.5	1.2
EC-EARTH_KNMI	0.7	0.8	0.7	1.0	0.9	-0.1	1.0	0.9	2.6	1.0
CNRM_CCLM4	* 0.7	0.7	0.5	1.0	0.2	1.6	1.2	1.4	0.7	0.8
ENSMEAN	0.6	1.4	0.5	0.9	0.7	0.7	1.9	0.9	1.6	1.0
P2 - P0										
MPI_CCLM4	* 0.7	2.5	* 2.0	1.0	* 2.7	* 1.3	* 5.3	* 1.6	* 1.4	* 3.1
EC-EARTH_KNMI	0.3	0.8	0.7	1.7	1.1	* 1.0	1.5	* 1.9	2.2	* 1.9
CNRM_CCLM4	* 1.3	1.0	1.0	1.1	* 1.5	* 1.6	2.1	1.7	0.8	* 0.9
ENSMEAN	0.8	1.5	1.2	1.3	1.8	1.3	3.0	1.7	1.5	2.0
P3 - P0										
MPI_CCLM4	* 0.8	* 3.5	* 1.8	1.8	* 2.5	* 2.4	* 4.3	* 3.0	* 4.2	* 3.3
EC-EARTH_KNMI	* 2.0	* 1.4	* 2.3	* 1.6	* 2.5	* 1.9	* 1.6	* 2.4	* 3.4	* 2.4
CNRM_CCLM4	* 1.7	2.6	* 2.0	0.2	* 1.6	* 2.6	* 3.8	* 2.9	* 1.6	* 2.5
ENSMEAN	1.5	2.5	2.0	1.2	2.2	2.3	3.3	2.8	3.1	2.7
P4 - P0										
MPI_CCLM4	* 1.5	* 4.7	* 2.1	* 2.2	* 2.7	* 3.4	* 6.3	* 4.3	* 4.9	* 4.9
EC-EARTH_KNMI	* 0.9	1.5	1.2	* 1.2	* 1.6	* 2.8	* 2.9	* 3.7	* 5.3	* 3.9
CNRM_CCLM4	* 2.2	2.1	* 2.5	1.8	* 2.1	* 3.9	* 3.9	* 3.4	* 3.3	* 3.1
ENSMEAN	1.5	2.8	1.9	1.8	2.1	3.4	4.3	3.8	4.5	4.0
	DJF	MAM	JJA	SON	Annual	DJF	MAM	JJA	SON	Annual

** ; Two Sample Wilcoxon tests, 95 % confidence interval*

Figure 5-111: Seasonal and annual 99th percentile of 2m maximum air temperature (extreme high maximum temperature, in °C) obtained by dynamical downscaling for Cervia: Ref. mean is 20 year simulated period (1986-2005) for ensemble mean; P1-P0, P2-P0, P3-P0, P4-P0 are changes in the future for following periods P1: 2021-2040, P2: 2041-2060, P3: 2061-2080, P4: 2081-2100. Differences are shown for individual models. Significant change is marked by star. Change is also shown as ensemble mean (ENSMEAN), not tested for significance. Left column is for RCP4.5 scenario and right for RCP8.5 scenario.

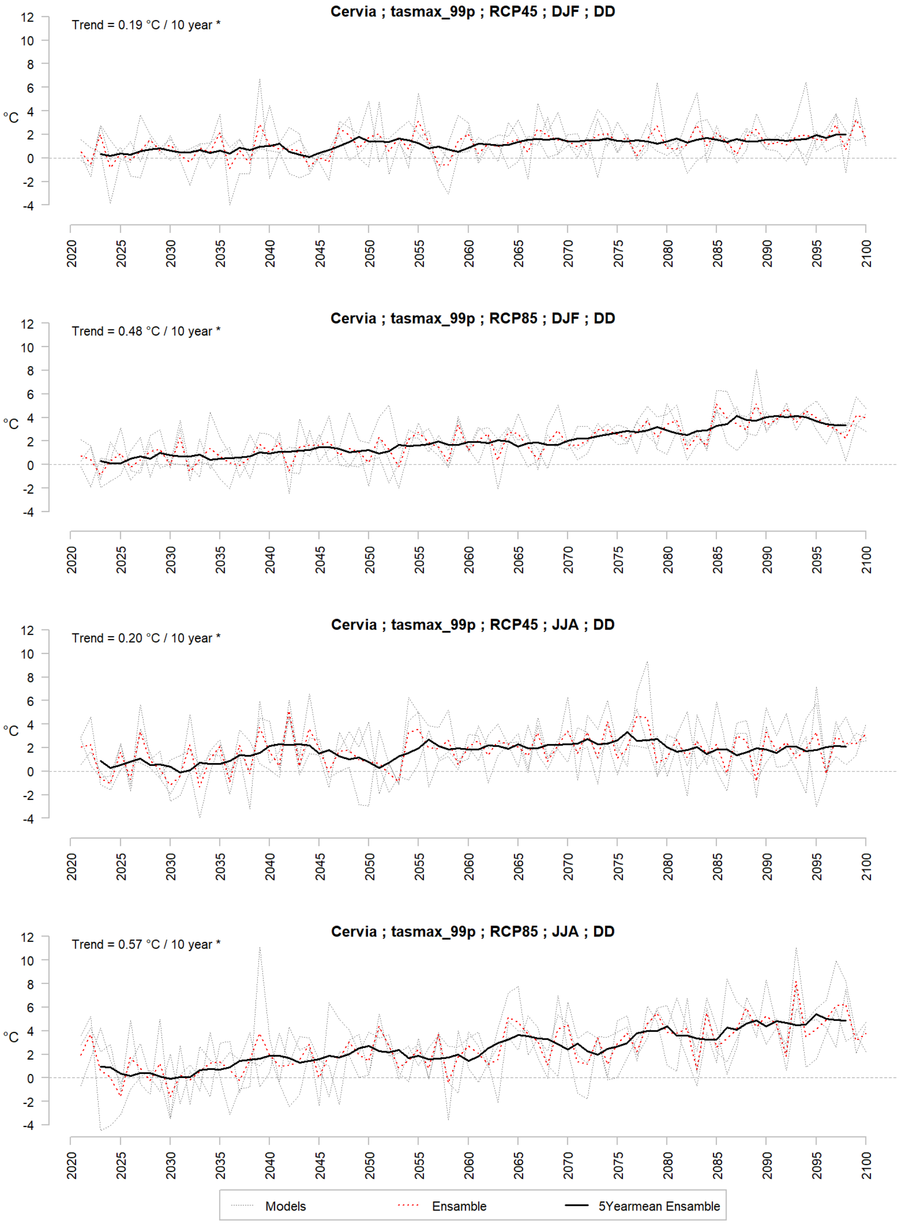

Figure 5-112: Variability of future 99th percentile of 2m maximum air temperature (extreme high maximum temperature) anomaly (in °C) in Cervia for 2021-2100 obtained by dynamically downscaling for winter (DJF) and summer (JJA) and two RCP scenarios: individual models are in grey, the ensemble mean in red, 5-year moving average in black. Significant trend is marked with star (ns if not significant).

6.4.1.1.6 *Extreme rare high temperature*

Future change of 99.9th percentile of 2m air temperature (Figure 5-113) in Cervia is increasing from P1 to P4 periods with the different amplitudes for each model. Slightly negative change appears for some seasons and some models in three first periods, but the change of ensemble mean is positive for all periods. At the end of century increase is from 0.5 °C in DJF to 2.3 °C in MAM, 2.2 °C on annual scale for RCP4.5. Amplitude of change is more pronounced for RCP8.5 and is between 2.4 °C in DJF and 5.0 °C in MAM, 4.1 °C for annual change at the end of 21st century. Variability of future 99.9th percentile of 2m air temperature anomaly (Figure 5-114) shows linear trend in change of ensemble mean, 0.17 °C / 10 year in DJF for RCP4.5 and 0.48 °C / 10 year for RCP8.5; 0.20 °C / 10 year in JJA for RCP4.5 and 0.51 °C / 10 year for RCP8.5. All trends are statistically significant.

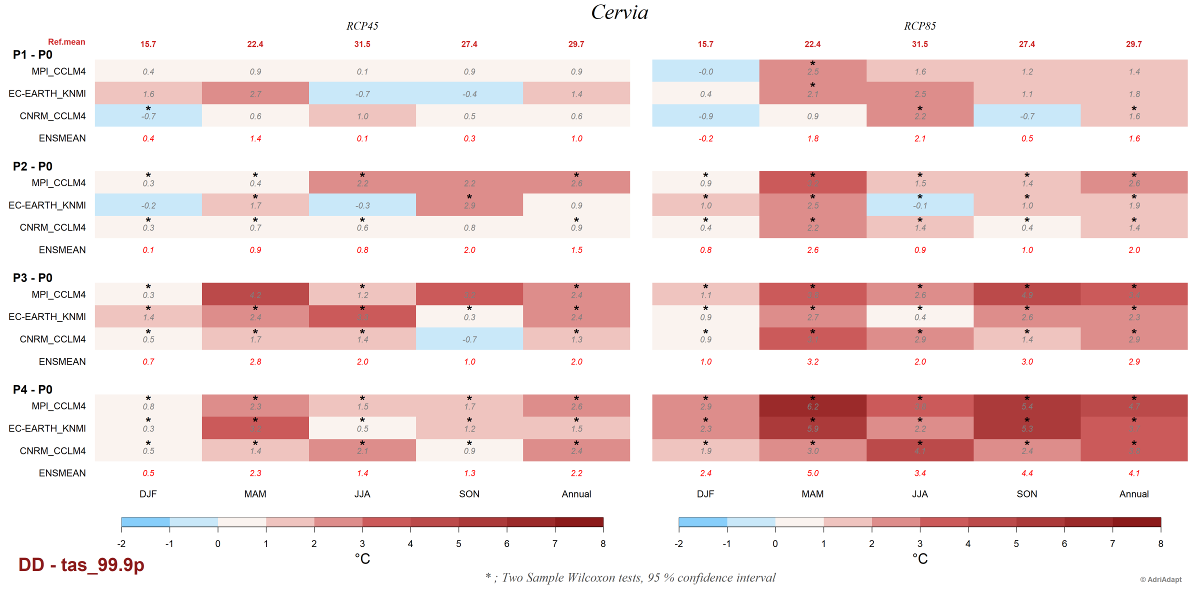

RCP45

	DJF	MAM	JJA	SON	Annual
Ref.mean	15.7	22.4	31.5	27.4	29.7
P1 - P0					
MPI_CCLM4	0.4	0.9	0.1	0.9	0.9
EC-EARTH_KNMI	1.6	2.7	-0.7	-0.4	1.4
CNRM_CCLM4	* -0.7	0.6	1.0	0.5	0.6
ENSMEAN	0.4	1.4	0.1	0.3	1.0
P2 - P0					
MPI_CCLM4	* 0.3	* 0.4	* 2.2	2.2	* 2.6
EC-EARTH_KNMI	-0.2	* 1.7	-0.3	* 2.9	0.9
CNRM_CCLM4	* 0.3	* 0.7	* 0.6	0.8	* 0.9
ENSMEAN	0.1	0.9	0.8	2.0	1.5
P3 - P0					
MPI_CCLM4	* 0.3	4.2	* 1.2	3.2	* 2.4
EC-EARTH_KNMI	* 1.4	* 2.4	* 3.3	* 0.3	* 2.4
CNRM_CCLM4	* 0.5	* 1.7	* 1.4	-0.7	* 1.3
ENSMEAN	0.7	2.8	2.0	1.0	2.0
P4 - P0					
MPI_CCLM4	* 0.8	* 2.3	* 1.5	* 1.7	* 2.6
EC-EARTH_KNMI	* 0.3	* 3.2	* 0.5	* 1.2	* 1.5
CNRM_CCLM4	* 0.5	* 1.4	* 2.1	* 0.9	* 2.4
ENSMEAN	0.5	2.3	1.4	1.3	2.2

RCP85

	DJF	MAM	JJA	SON	Annual
Ref.mean	15.7	22.4	31.5	27.4	29.7
P1 - P0					
MPI_CCLM4	-0.0	* 2.5	1.6	1.2	1.4
EC-EARTH_KNMI	0.4	* 2.1	2.5	1.1	1.8
CNRM_CCLM4	-0.9	0.9	* 2.2	-0.7	* 1.6
ENSMEAN	-0.2	1.8	2.1	0.5	1.6
P2 - P0					
MPI_CCLM4	* 0.9	* 3.2	* 1.5	* 1.4	* 2.6
EC-EARTH_KNMI	* 1.0	* 2.5	* -0.1	* 1.0	* 1.9
CNRM_CCLM4	* 0.4	* 2.2	* 1.4	* 0.4	* 1.4
ENSMEAN	0.8	2.6	0.9	1.0	2.0
P3 - P0					
MPI_CCLM4	* 1.1	* 3.8	* 2.6	* 4.9	* 3.4
EC-EARTH_KNMI	* 0.9	* 2.7	* 0.4	* 2.6	* 2.3
CNRM_CCLM4	* 0.9	* 3.1	* 2.9	* 1.4	* 2.9
ENSMEAN	1.0	3.2	2.0	3.0	2.9
P4 - P0					
MPI_CCLM4	* 2.9	* 6.2	* 3.8	* 5.4	* 4.7
EC-EARTH_KNMI	* 2.3	* 5.9	* 2.2	* 5.3	* 3.7
CNRM_CCLM4	* 1.9	* 3.0	* 4.1	* 2.4	* 3.8
ENSMEAN	2.4	5.0	3.4	4.4	4.1

** ; Two Sample Wilcoxon tests, 95 % confidence interval*

Figure 5-113: Seasonal and annual 99.9th percentile of 2m air temperature (extreme rare high temperature, in °C) obtained by dynamical downscaling for Cervia: Ref. mean is 20 year simulated period (1986-2005) for ensemble mean; P1-P0, P2-P0, P3-P0, P4-P0 are changes in the future for following periods P1: 2021-2040, P2: 2041-2060, P3: 2061-2080, P4: 2081-2100. Differences are shown for individual models. Significant change is marked by star. Change is also shown as ensemble mean (ENSMEAN), not tested for significance. Left column is for RCP4.5 scenario and right for RCP8.5 scenario.

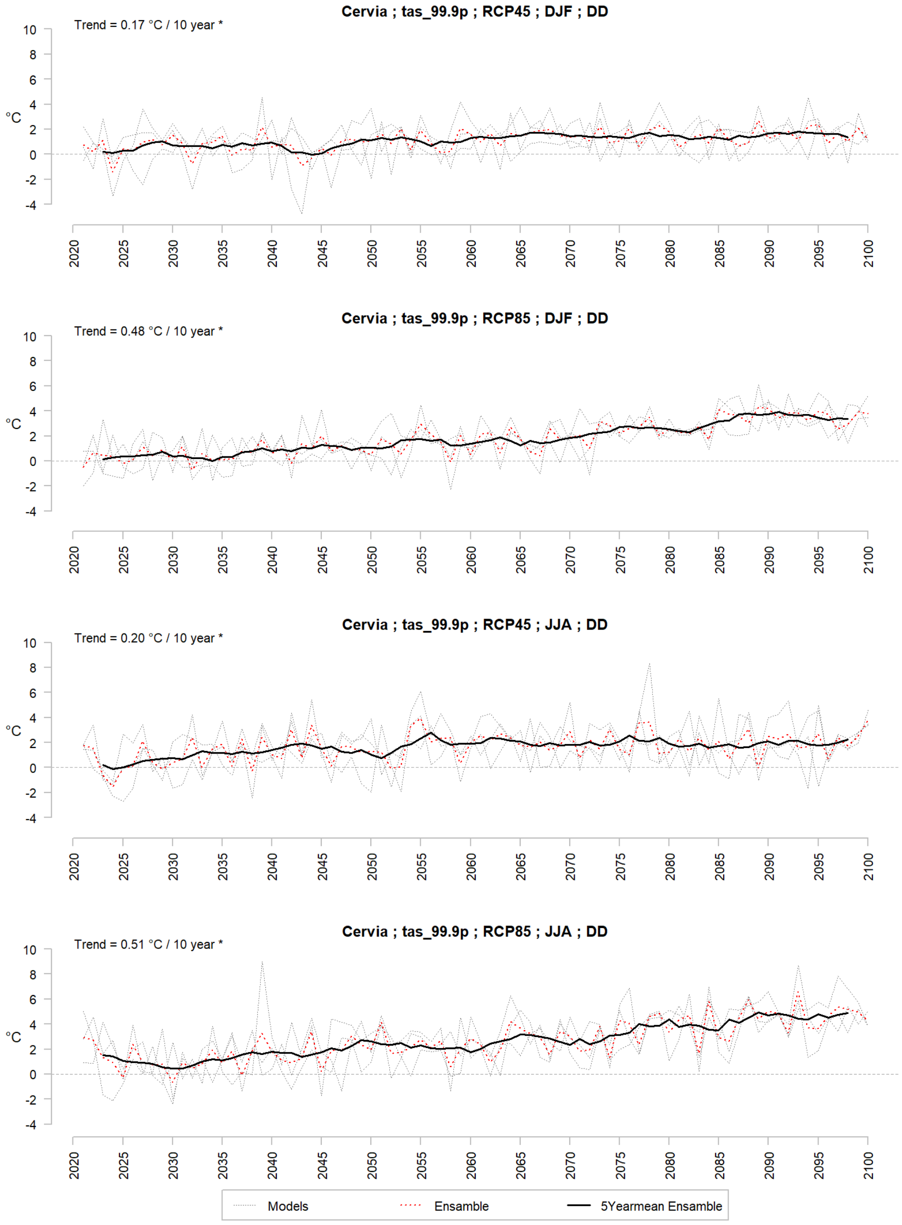

Figure 5-114: Variability of future 99.9th percentile of 2m air temperature (extreme rare high temperature) anomaly (in °C) in Cervia for 2021-2100 obtained by dynamically downscaling for winter (DJF) and summer (JJA) and two RCP scenarios: individual models are in grey, the ensemble mean in red, 5-year moving average in black. Significant trend is marked with star (ns if not significant).

6.4.1.1.7 *Extreme rare high maximum temperature*

Future change of 99.9th percentile of 2m maximum air temperature (Figure 5-115) in Cervia is changing from P1 to P4 periods with the different amplitudes for each model. Some models show for some time slices negative change, but in general ensemble mean for all season and annual change are positive. At the end of 21st century changes are between 1.6 °C in SON and 2.7 °C in MAM, 1.9 °C for annual for RCP4.5 scenario. Amplitude of change is more pronounced for RCP8.5 and is between 3.2 °C in DJF and 5.6 °C in MAM, 4.2 °C for annual change at the end of 21st century. Variability of future 99.9th percentile of 2m maximum air temperature anomaly (Figure 5-116) shows linear trend in change of ensemble mean, 0.19 °C / 10 year in DJF for RCP4.5 and 0.48 °C / 10 year for RCP8.5; 0.20 °C / 10 year in JJA for RCP4.5 and 0.57 °C / 10 year for RCP8.5. All trends are statistically significant.

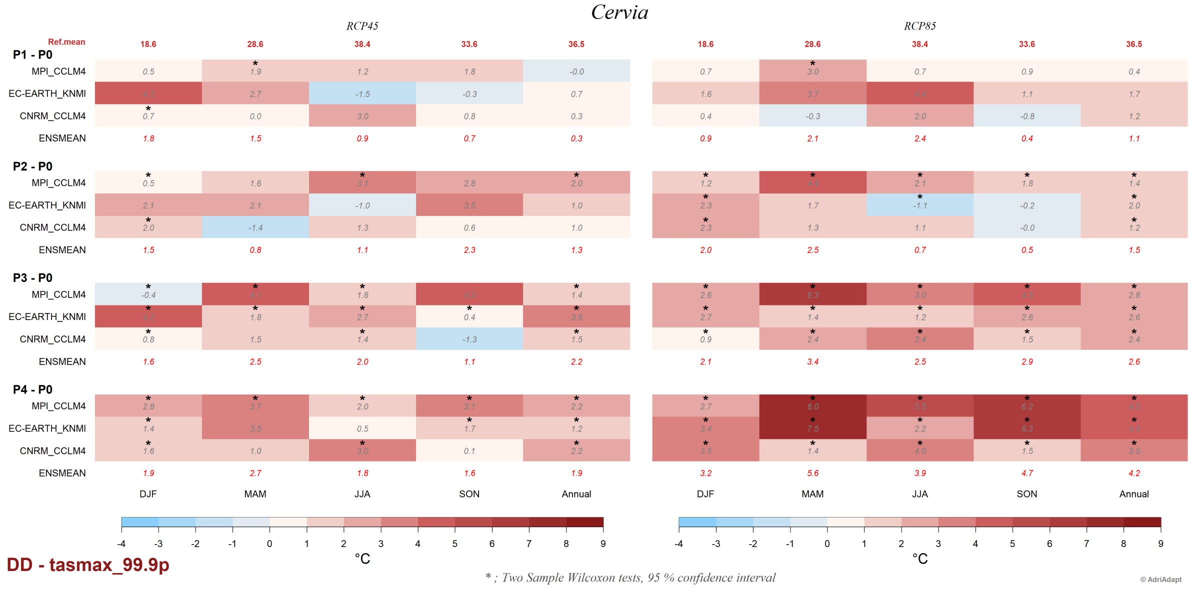

Figure 5-115: Seasonal and annual 99.9th percentile of 2m maximum air temperature (extreme rare high maximum temperature, in °C) obtained by dynamical downscaling for Cervia: Ref. mean is 20 year simulated period (1986-2005) for ensemble mean; P1-P0, P2-P0, P3-P0, P4-P0 are changes in the future for following periods P1: 2021-2040, P2: 2041-2060, P3: 2061-2080, P4: 2081-2100. Differences are shown for individual models. Significant change is marked by star. Change is also shown as ensemble mean (ENSMEAN), not tested for significance. Left column is for RCP4.5 scenario and right for RCP8.5 scenario.

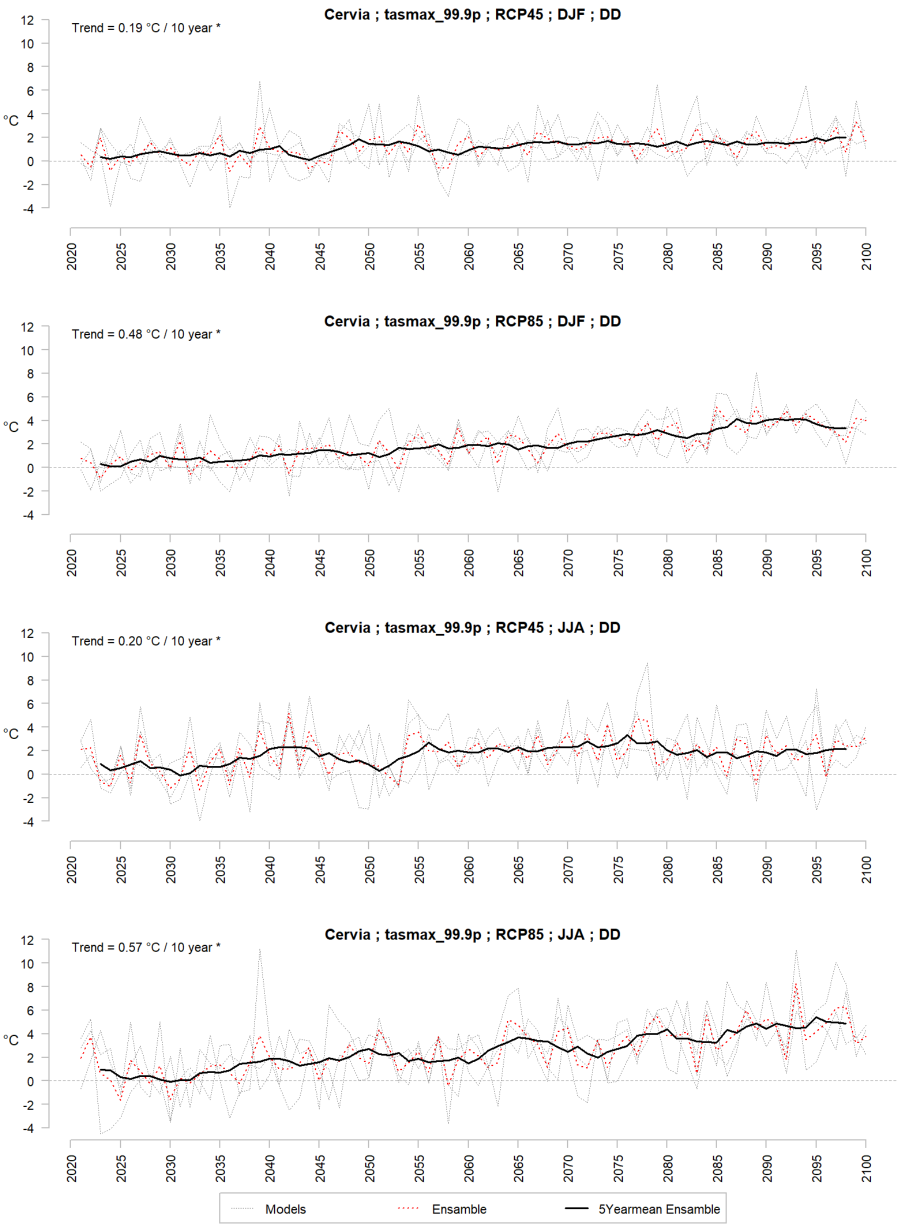

Figure 5-116: Variability of future 99.9th percentile of 2m maximum air temperature (extreme rare high maximum temperature) anomaly (in °C) in Cervia for 2021-2100 obtained by dynamically downscaling for winter (DJF) and summer (JJA) and two RCP scenarios: individual models are in grey, the ensemble mean in red, 5-year moving average in black. Significant trend is marked with star (ns if not significant).

6.4.1.1.8 *Warm spell days index*

Warm spell days index (Figure 5-117) in Cervia shows increase in all seasons and on annual scale, for all future period. Amplitude of change is increasing towards the end of 21st century, for RCP4.5 scenario is between 6.7 days in DJF and 15.2 in JJA; 49.0 days on annual scale. Amplitude of change is more pronounced for RCP8.5 and is between 23.6 days in DJF and 41.7 days in JJA, 137.3 days for annual change at the end of 21st century. Variability of future warm spell days index anomaly (Figure 5-118) shows linear trend in change of ensemble mean, 0.62 days/ 10 year in DJF for RCP4.5 and 3.44 days/ 10 year for RCP8.5; 1.35 days/10 year in JJA for RCP4.5 and 5.55 days/10 year for RCP8.5. All trends are statistically significant.

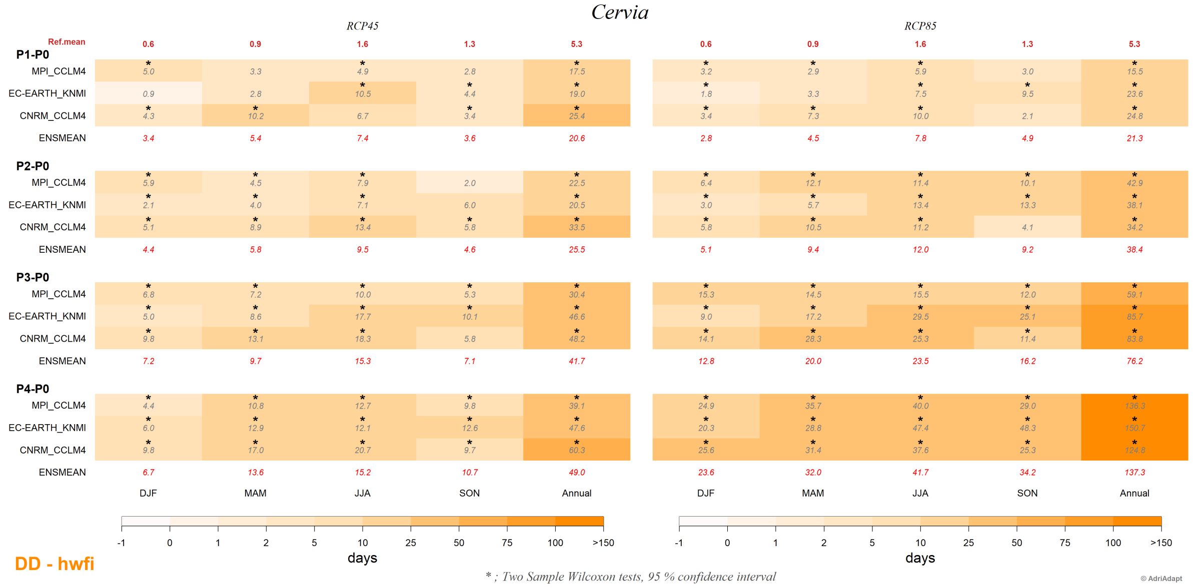

	RCP45					RCP85				
	DJF	MAM	JJA	SON	Annual	DJF	MAM	JJA	SON	Annual
Ref.mean	0.6	0.9	1.6	1.3	5.3	0.6	0.9	1.6	1.3	5.3
P1-P0										
MPI_CCLM4	* 5.0	3.3	* 4.9	2.8	* 17.5	* 3.2	* 2.9	* 5.9	3.0	* 15.5
EC-EARTH_KNMI	0.9	2.8	* 10.5	* 4.4	* 19.0	* 1.8	3.3	* 7.5	* 9.5	* 23.6
CNRM_CCLM4	* 4.3	* 10.2	6.7	* 3.4	* 25.4	* 3.4	* 7.3	* 10.0	2.1	* 24.8
ENSMEAN	3.4	5.4	7.4	3.6	20.6	2.8	4.5	7.8	4.9	21.3
P2-P0										
MPI_CCLM4	* 5.9	* 4.5	* 7.9	2.0	* 22.5	* 6.4	* 12.1	* 11.4	* 10.1	* 42.9
EC-EARTH_KNMI	* 2.1	* 4.0	* 7.1	6.0	* 20.5	* 3.0	* 5.7	* 13.4	* 13.3	* 38.1
CNRM_CCLM4	* 5.1	* 8.9	* 13.4	* 5.8	* 33.5	* 5.8	* 10.5	* 11.2	4.1	* 34.2
ENSMEAN	4.4	5.8	9.5	4.6	25.5	5.1	9.4	12.0	9.2	38.4
P3-P0										
MPI_CCLM4	* 6.8	* 7.2	* 10.0	* 5.3	* 30.4	* 15.3	* 14.5	* 15.5	* 12.0	* 59.1
EC-EARTH_KNMI	* 5.0	* 8.6	* 17.7	* 10.1	* 46.6	* 9.0	* 17.2	* 29.5	* 25.1	* 85.7
CNRM_CCLM4	* 9.8	* 13.1	* 18.3	5.8	* 48.2	* 14.1	* 28.3	* 25.3	* 11.4	* 83.8
ENSMEAN	7.2	9.7	15.3	7.1	41.7	12.8	20.0	23.5	16.2	76.2
P4-P0										
MPI_CCLM4	* 4.4	* 10.8	* 12.7	* 9.8	* 39.1	* 24.9	* 35.7	* 40.0	* 29.0	* 136.3
EC-EARTH_KNMI	* 6.0	* 12.9	* 12.1	* 12.6	* 47.6	* 20.3	* 28.8	* 47.4	* 48.3	* 150.7
CNRM_CCLM4	* 9.8	* 17.0	* 20.7	* 9.7	* 60.3	* 25.6	* 31.4	* 37.6	* 25.3	* 124.8
ENSMEAN	6.7	13.6	15.2	10.7	49.0	23.6	32.0	41.7	34.2	137.3

Figure 5-117: Seasonal and annual warm spell days index (in days) obtained by dynamical downscaling for Cervia: Ref. mean is 20 year simulated period (1986-2005) for ensemble mean; P1-P0, P2-P0, P3-P0, P4-P0 are changes in the future for following periods P1: 2021-2040, P2: 2041-2060, P3: 2061-2080, P4: 2081-2100. Differences are shown for individual models. Significant change is marked by star. Change is also shown as ensemble mean (ENSMEAN), not tested for significance. Left column is for RCP4.5 scenario and right for RCP8.5 scenario.

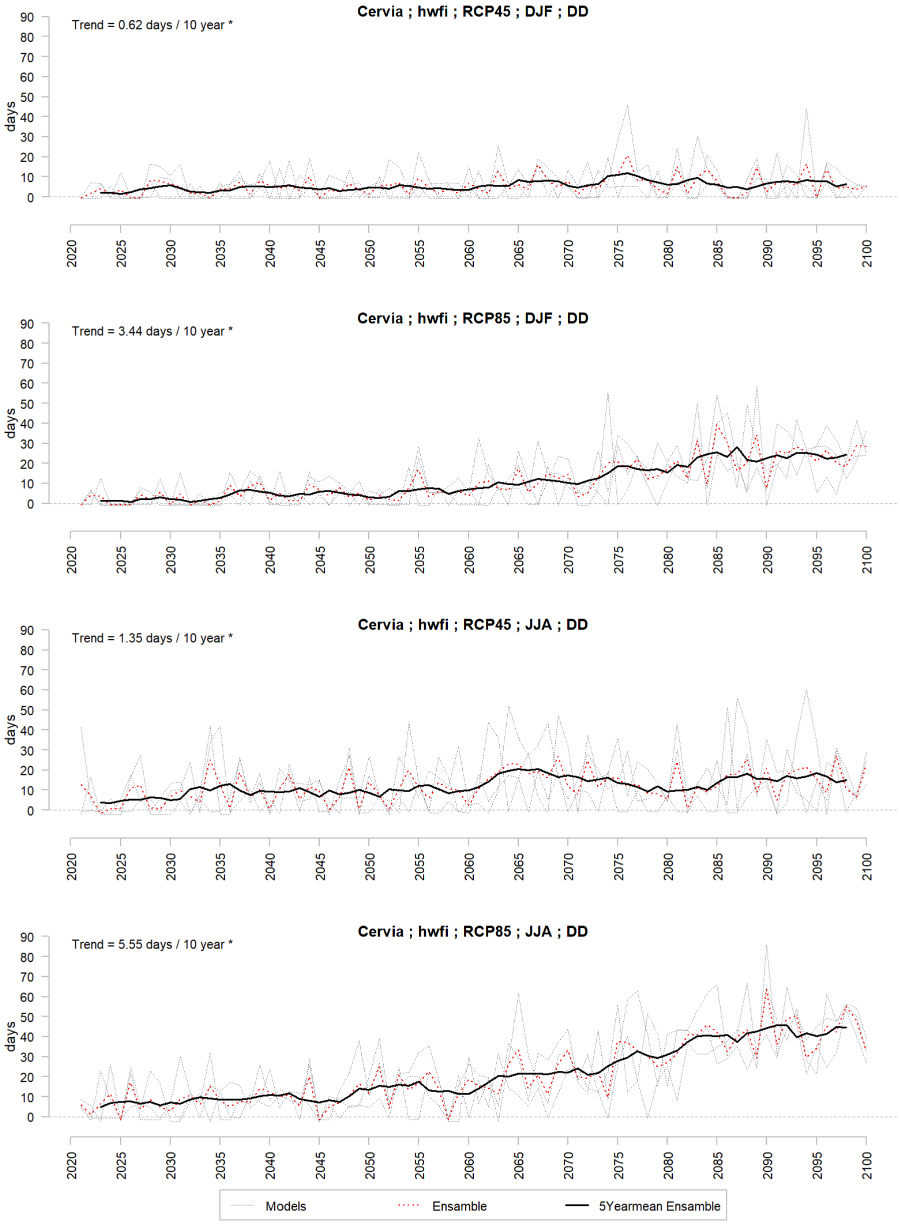

Figure 5-118: Variability of future warm spell days index anomaly in Cervia (in days) for 2021-2100 obtained by dynamically downscaling for winter (DJF) and summer (JJA) and two RCP scenarios: individual models are in grey, the ensemble mean in red, 5-year moving average in black. Significant trend is marked with star (ns if not significant).

6.4.1.1.9 *Heat wave duration index*

Heat wave duration index (Figure 5-119) in Cervia shows increase in all seasons and on annual scale, for all future period (exceptions are small negative change for some models and seasons in first two periods for RCP4.5 scenario). Amplitude of change is increasing towards the end of 21st century, for RCP4.5 scenario ensemble mean change is between 1.2 days in MAM and 2.4 in JJA; 7.4 days on annual scale. Amplitude of change is more pronounced for RCP8.5 and is between 3.6 days in MAM and 13.4 days in SON, 36.0 days for annual change at the end of 21st century. Variability of future heat wave duration index anomaly (Figure 5-120) shows linear trend in change of ensemble mean, 0.31 days/ 10 year in DJF for RCP4.5 and 1.58 days/ 10 year for RCP8.5; 0.29 days/10 year in JJA for RCP4.5 and 1.02 days/10 year for RCP8.5. All trends are statistically significant.

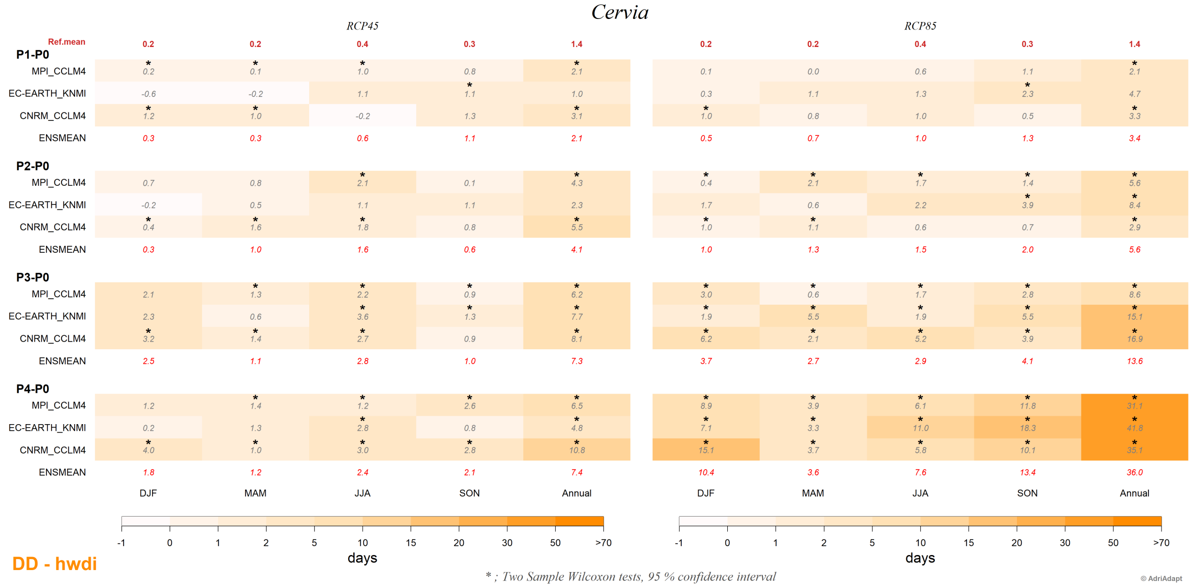

Cervia

	RCP45					RCP85				
	DJF	MAM	JJA	SON	Annual	DJF	MAM	JJA	SON	Annual
Ref.mean	**0.2**	**0.2**	**0.4**	**0.3**	**1.4**	**0.2**	**0.2**	**0.4**	**0.3**	**1.4**
P1-P0										
MPI_CCLM4	* 0.2	* 0.1	* 1.0	0.8	* 2.1	0.1	0.0	0.6	1.1	* 2.1
EC-EARTH_KNMI	-0.6	-0.2	1.1	* 1.1	1.0	0.3	1.1	1.3	* 2.3	4.7
CNRM_CCLM4	* 1.2	* 1.0	-0.2	1.3	* 3.1	* 1.0	0.8	1.0	0.5	* 3.3
ENSMEAN	0.3	0.3	0.6	1.1	2.1	0.5	0.7	1.0	1.3	3.4
P2-P0										
MPI_CCLM4	0.7	0.8	* 2.1	0.1	* 4.3	* 0.4	* 2.1	* 1.7	* 1.4	* 5.6
EC-EARTH_KNMI	-0.2	0.5	1.1	1.1	2.3	1.7	0.6	2.2	* 3.9	* 8.4
CNRM_CCLM4	* 0.4	* 1.6	* 1.8	0.8	* 5.5	* 1.0	* 1.1	0.6	0.7	* 2.9
ENSMEAN	0.3	1.0	1.6	0.6	4.1	1.0	1.3	1.5	2.0	5.6
P3-P0										
MPI_CCLM4	2.1	* 1.3	* 2.2	* 0.9	* 6.2	* 3.0	* 0.6	* 1.7	* 2.8	* 8.6
EC-EARTH_KNMI	2.3	0.6	* 3.6	* 1.3	* 7.7	* 1.9	* 5.5	* 1.9	* 5.5	* 15.1
CNRM_CCLM4	* 3.2	* 1.4	* 2.7	0.9	* 8.1	* 6.2	* 2.1	* 5.2	* 3.9	* 16.9
ENSMEAN	2.5	1.1	2.8	1.0	7.3	3.7	2.7	2.9	4.1	13.6
P4-P0										
MPI_CCLM4	1.2	* 1.4	* 1.2	* 2.6	* 6.5	* 8.9	* 3.9	* 6.1	* 11.8	* 31.1
EC-EARTH_KNMI	0.2	1.3	* 2.8	0.8	* 4.8	* 7.1	* 3.3	* 11.0	* 18.3	* 41.8
CNRM_CCLM4	* 4.0	* 1.0	* 3.0	* 2.8	* 10.8	* 15.1	* 3.7	* 5.8	* 10.1	* 35.1
ENSMEAN	1.8	1.2	2.4	2.1	7.4	10.4	3.6	7.6	13.4	36.0

* ; Two Sample Wilcoxon tests, 95 % confidence interval

© AdriAdapt

Figure 5-119: Seasonal and annual heat wave duration index (in days) obtained by dynamical downscaling for Cervia: Ref. mean is 20 year simulated period (1986-2005) for ensemble mean; P1-P0, P2-P0, P3-P0, P4-P0 are changes in the future for following periods P1: 2021-2040, P2: 2041-2060, P3: 2061-2080, P4: 2081-2100. Differences are shown for individual models. Significant change is marked by star. Change is also shown as ensemble mean (ENSMEAN), not tested for significance. Left column is for RCP4.5 scenario and right for RCP8.5 scenario.

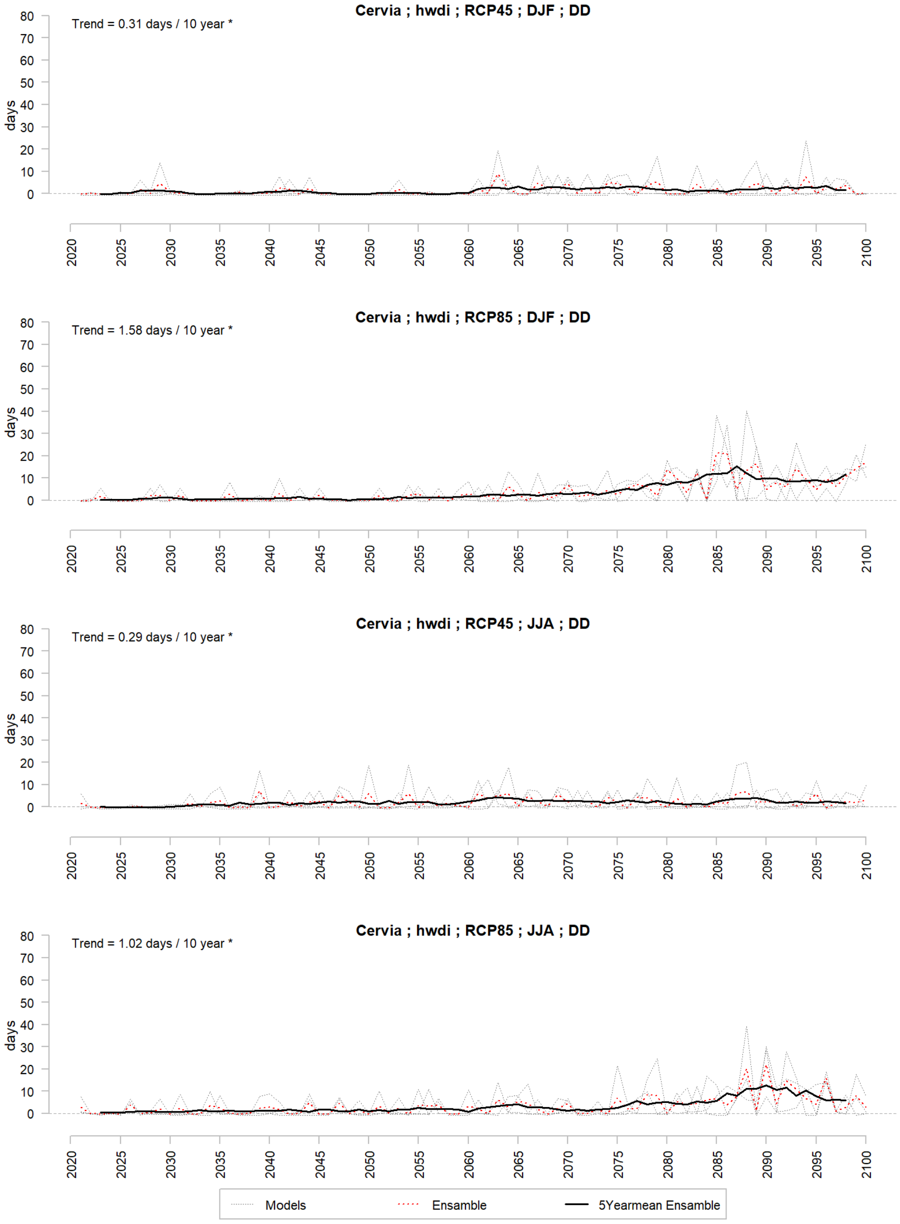

Figure 5-120: Variability of future heat wave duration index anomaly (in days) in Cervia for 2021-2100 obtained by dynamically downscaling for winter (DJF) and summer (JJA) and two RCP scenarios: individual models are in grey, the ensemble mean in red, 5-year moving average in black. Significant trend is marked with star (ns if not significant).

6.4.1.2 *Precipitation related indices projections*

6.4.1.2.1 *Averaged precipitation*

Averaged precipitation obtained by dynamical downscaling is expressed in mm/day and its change in the future is shown as relative to the P0 period (Figure 5-121). Precipitation is much more variable parameter in comparison to the temperature, therefore there is no always unique sign of change through the year as well as from model to model. The change in ensemble mean for Cervia gives increase of precipitation in all seasons except in MAM (-3.0 %). Increase is between 5.6 % in JJA and 8.4 % in SON; 4.1 % on annual scale for RCP4.5 scenario. For scenario RCP8.5, precipitation will decrease in JJA (-12.8 %) and increase in all other seasons (from 2.8 % in DJF to 6.5 % in SON). On annual scale precipitation will almost not change (0.1 %). Variability of future precipitation anomaly (Figure 5-122) for ensemble mean in Cervia changes the sign of trend from positive for RCP4.5 scenario to the negative for RCP8.5 scenario for both seasons. All trends are not statistically significant.

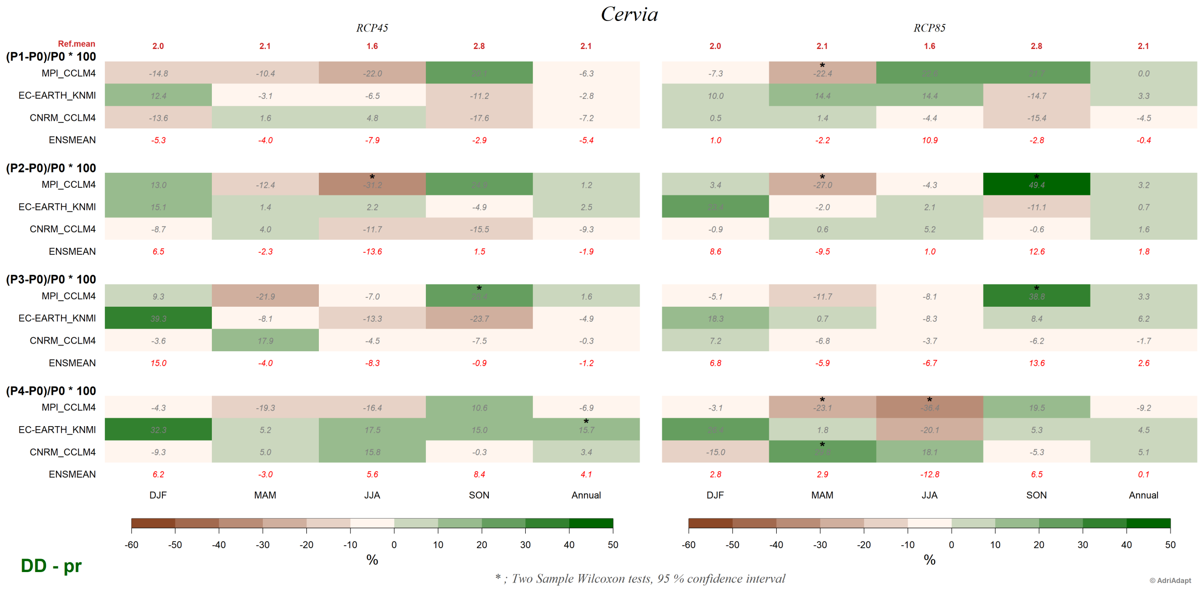

	RCP45					RCP85				
	DJF	MAM	JJA	SON	Annual	DJF	MAM	JJA	SON	Annual
Ref.mean	2.0	2.1	1.6	2.8	2.1	2.0	2.1	1.6	2.8	2.1
(P1-P0)/P0 * 100										
MPI_CCLM4	-14.8	-10.4	-22.0	20.1	-6.3	-7.3	* -22.4	22.6	21.7	0.0
EC-EARTH_KNMI	12.4	-3.1	-6.5	-11.2	-2.8	10.0	14.4	14.4	-14.7	3.3
CNRM_CCLM4	-13.6	1.6	4.8	-17.6	-7.2	0.5	1.4	-4.4	-15.4	-4.5
ENSMEAN	-5.3	-4.0	-7.9	-2.9	-5.4	1.0	-2.2	10.9	-2.8	-0.4
(P2-P0)/P0 * 100										
MPI_CCLM4	13.0	-12.4	* -31.2	24.9	1.2	3.4	* -27.0	-4.3	* 49.4	3.2
EC-EARTH_KNMI	15.1	1.4	2.2	-4.9	2.5	23.4	-2.0	2.1	-11.1	0.7
CNRM_CCLM4	-8.7	4.0	-11.7	-15.5	-9.3	-0.9	0.6	5.2	-0.6	1.6
ENSMEAN	6.5	-2.3	-13.6	1.5	-1.9	8.6	-9.5	1.0	12.6	1.8
(P3-P0)/P0 * 100										
MPI_CCLM4	9.3	-21.9	-7.0	* 28.4	1.6	-5.1	-11.7	-8.1	* 38.8	3.3
EC-EARTH_KNMI	39.3	-8.1	-13.3	-23.7	-4.9	18.3	0.7	-8.3	8.4	6.2
CNRM_CCLM4	-3.6	17.9	-4.5	-7.5	-0.3	7.2	-6.8	-3.7	-6.2	-1.7
ENSMEAN	15.0	-4.0	-8.3	-0.9	-1.2	6.8	-5.9	-6.7	13.6	2.6
(P4-P0)/P0 * 100										
MPI_CCLM4	-4.3	-19.3	-16.4	10.6	-6.9	-3.1	* -23.1	* -36.4	19.5	-9.2
EC-EARTH_KNMI	32.3	5.2	17.5	15.0	* 15.7	26.4	1.8	-20.1	5.3	4.5
CNRM_CCLM4	-9.3	5.0	15.8	-0.3	3.4	-15.0	* 29.8	18.1	-5.3	5.1
ENSMEAN	6.2	-3.0	5.6	8.4	4.1	2.8	2.9	-12.8	6.5	0.1

** : Two Sample Wilcoxon tests, 95 % confidence interval*

Figure 5-121: Averaged seasonal and annual precipitation obtained by dynamical downscaling for Cervia: Ref. mean is 20 year simulated period (1986-2005) for ensemble mean in mmday^{-1}; P1-P0, P2-P0, P3-P0, P4-P0 are changes (in %) in the future for following periods P1: 2021-2040, P2: 2041-2060, P3: 2061-2080, P4: 2081-2100. Differences are shown for individual models. Significant change is marked by star. Change is also shown as ensemble mean (ENSMEAN), not tested for significance. Left column is for RCP4.5 scenario and right for RCP8.5 scenario.

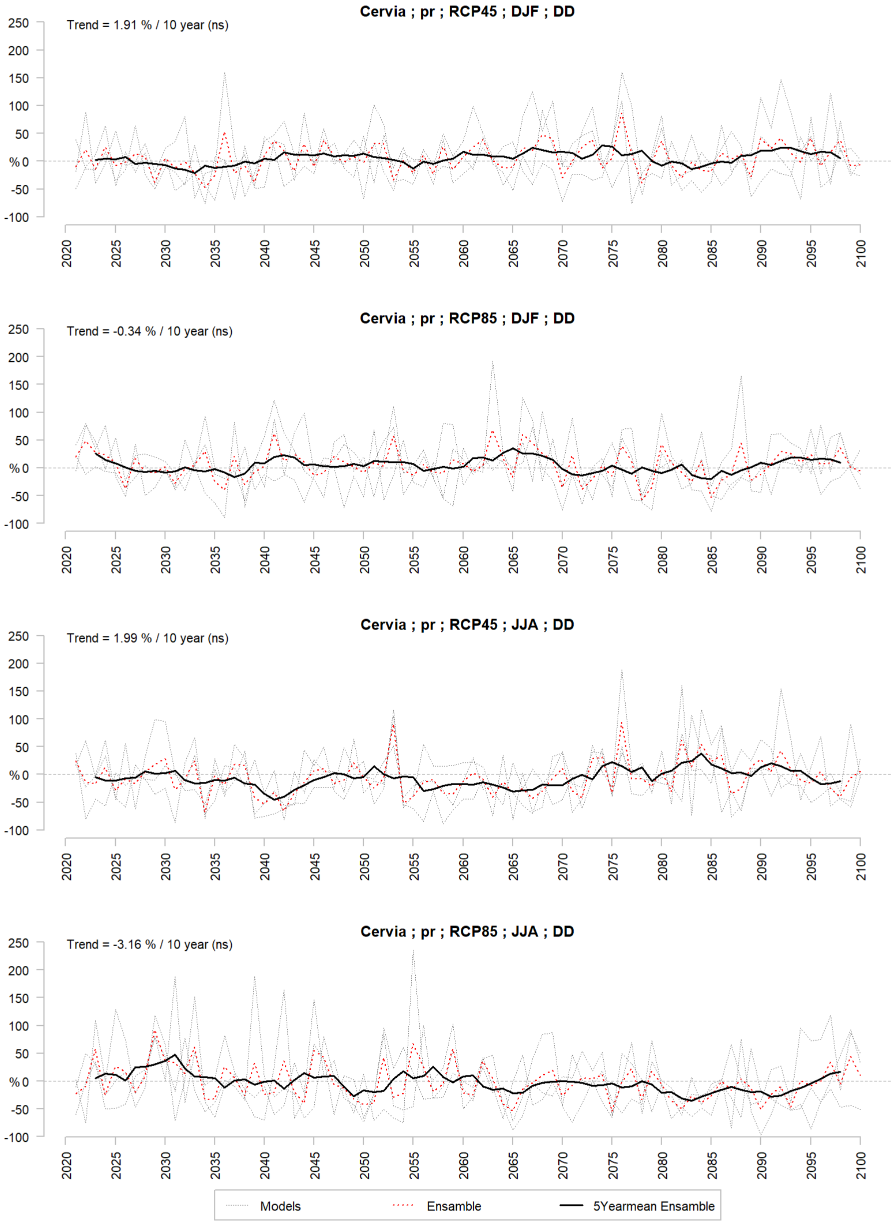

Cervia ; pr ; RCP45 ; DJF ; DD

Trend = 1.91 % / 10 year (ns)

Cervia ; pr ; RCP85 ; DJF ; DD

Trend = -0.34 % / 10 year (ns)

Cervia ; pr ; RCP45 ; JJA ; DD

Trend = 1.99 % / 10 year (ns)

Cervia ; pr ; RCP85 ; JJA ; DD

Trend = -3.16 % / 10 year (ns)

Figure 5-122: Variability of future precipitation anomaly (in %) in Cervia for 2021-2100 obtained by dynamically downscaling for winter (DJF) and summer (JJA) and two RCP scenarios: individual models are in grey, the ensemble mean in red, 5-year moving average in black. Significant trend is marked with star (ns if not significant).

6.4.1.2.2 *Intense precipitation*

Intense precipitation (Figure 5-123), defined by 95th percentile of precipitation in Cervia, show for ensemble mean at the end of 21st century that 95th percentile will increase in DJF and SON (8.6 %) and decrease in MAM (-4.4 %) and JJA (-1.8 %); increase on annual scale (3.1 %) for RCP4.5 scenario. For RCP8.5 increase will be present for all seasons except in JJA (-18.4 %). Increase will be between 4.9 % in MAM and 11.3 % in SON, 2.6 % on annual scale. Variability of future intense precipitation anomaly (Figure 5-124) for ensemble mean in Cervia shows increase in precipitation in DJF for both scenarios, increase in JJA for RCP4.5 and decrease for RCP8.5 scenario. Linear trends are not statistically significant.

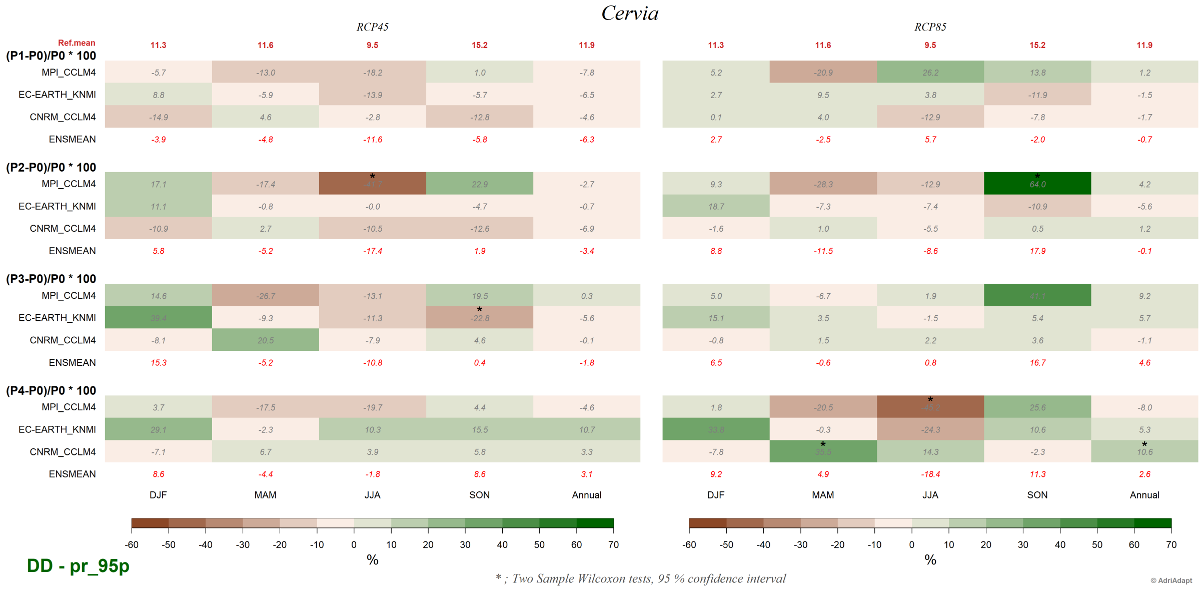

Cervia

	RCP45					RCP85				
	DJF	MAM	JJA	SON	Annual	DJF	MAM	JJA	SON	Annual
Ref.mean	11.3	11.6	9.5	15.2	11.9	11.3	11.6	9.5	15.2	11.9
(P1-P0)/P0 * 100										
MPI_CCLM4	-5.7	-13.0	-18.2	1.0	-7.8	5.2	-20.9	26.2	13.8	1.2
EC-EARTH_KNMI	8.8	-5.9	-13.9	-5.7	-6.5	2.7	9.5	3.8	-11.9	-1.5
CNRM_CCLM4	-14.9	4.6	-2.8	-12.8	-4.6	0.1	4.0	-12.9	-7.8	-1.7
ENSMEAN	-3.9	-4.8	-11.6	-5.8	-6.3	2.7	-2.5	5.7	-2.0	-0.7
(P2-P0)/P0 * 100										
MPI_CCLM4	17.1	-17.4	* -41.7	22.9	-2.7	9.3	-28.3	-12.9	* 64.0	4.2
EC-EARTH_KNMI	11.1	-0.8	-0.0	-4.7	-0.7	18.7	-7.3	-7.4	-10.9	-5.6
CNRM_CCLM4	-10.9	2.7	-10.5	-12.6	-6.9	-1.6	1.0	-5.5	0.5	1.2
ENSMEAN	5.8	-5.2	-17.4	1.9	-3.4	8.8	-11.5	-8.6	17.9	-0.1
(P3-P0)/P0 * 100										
MPI_CCLM4	14.6	-26.7	-13.1	19.5	0.3	5.0	-6.7	1.9	41.1	9.2
EC-EARTH_KNMI	39.4	-9.3	-11.3	* -22.8	-5.6	15.1	3.5	-1.5	5.4	5.7
CNRM_CCLM4	-8.1	20.5	-7.9	4.6	-0.1	-0.8	1.5	2.2	3.6	-1.1
ENSMEAN	15.3	-5.2	-10.8	0.4	-1.8	6.5	-0.6	0.8	16.7	4.6
(P4-P0)/P0 * 100										
MPI_CCLM4	3.7	-17.5	-19.7	4.4	-4.6	1.8	-20.5	* -45.2	25.6	-8.0
EC-EARTH_KNMI	29.1	-2.3	10.3	15.5	10.7	33.8	-0.3	-24.3	10.6	5.3
CNRM_CCLM4	-7.1	6.7	3.9	5.8	3.3	-7.8	* 35.5	14.3	-2.3	* 10.6
ENSMEAN	8.6	-4.4	-1.8	8.6	3.1	9.2	4.9	-18.4	11.3	2.6

* ; Two Sample Wilcoxon tests, 95 % confidence interval

Figure 5-123: Seasonal and annual 95th percentile of precipitation (intense precipitation) obtained by dynamical downscaling for Cervia: Ref. mean is 20 year simulated period (1986-2005) for ensemble mean in mmday^{-1}; P1-P0, P2-P0, P3-P0, P4-P0 are changes (in %) in the future for following periods P1: 2021-2040, P2: 2041-2060, P3: 2061-2080, P4: 2081-2100. Differences are shown for individual models. Significant change is marked by star. Change is also shown as ensemble mean (ENSMEAN), not tested for significance. Left column is for RCP4.5 scenario and right for RCP8.5 scenario.

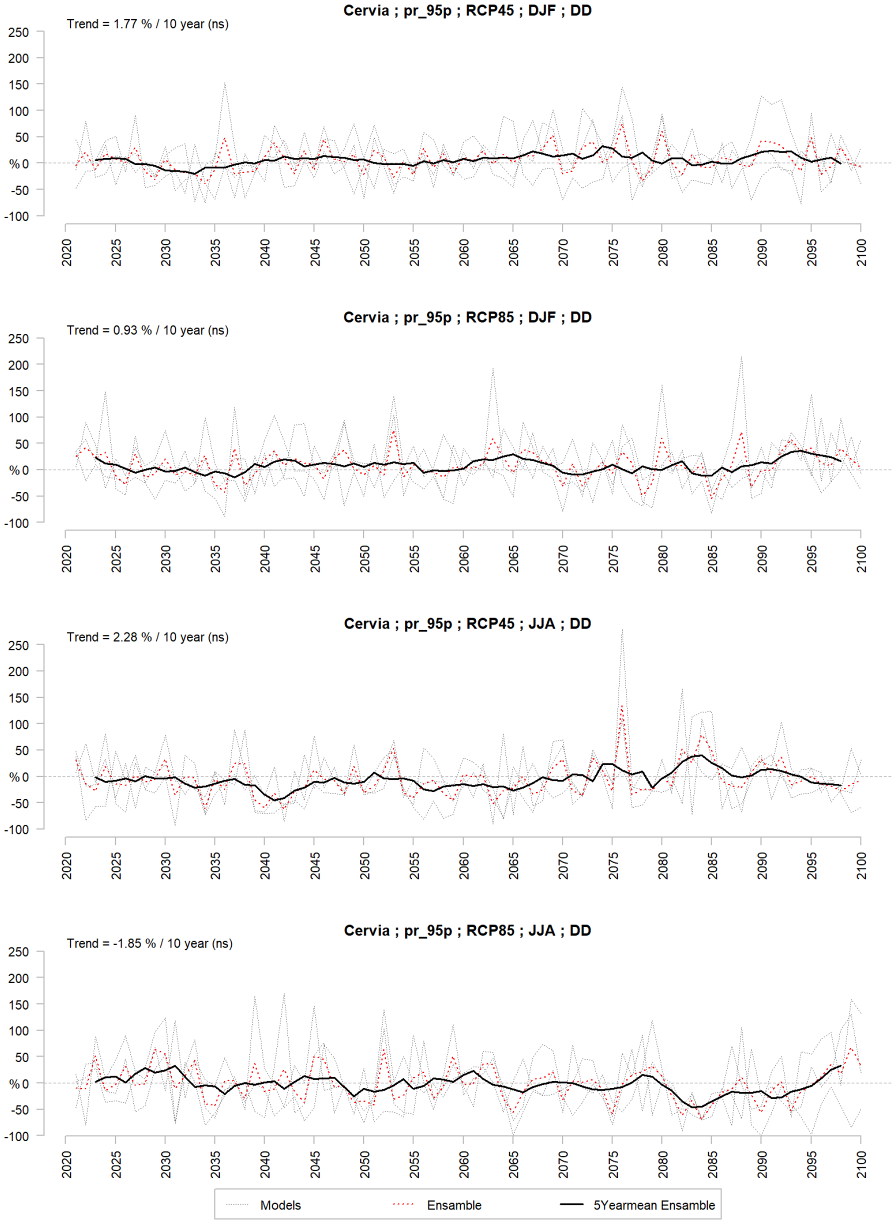

Figure 5-124: Variability of future 95th percentile of precipitation (intense precipitation) anomaly (in %) in Cervia for 2021-2100 obtained by dynamically downscaling for winter (DJF) and summer (JJA) and two RCP scenarios: individual models are in grey, the ensemble mean in red, 5-year moving average in black. Significant trend is marked with star (ns if not significant).

6.4.1.2.3 *Extreme precipitation*

Extreme precipitation (Figure 5-125), defined by 99th percentile of precipitation in Cervia, show for ensemble mean increase in all seasons (except MAM) and on annual scale at the end of 21st century for RCP4.5 scenario. The increase will change from 3.7 % in DJF and SON to 8.9 % in JJA, 2.7 % for annual scale for RCP4.5. For RCP8.5 scenario ensemble mean change is positive for all seasons, between 0.9 % in JJA and 15.3 % in MAM, 11.1 % for annual scale at the end of 21st century. Variability of future extreme precipitation anomaly (Figure 5-126) to the end of 21st century for ensemble mean in Cervia has positive trends for DJF for both scenarios. In JJA variability of future extreme precipitation anomaly has positive trend for RCP4.5 but negative for RCP8.5. All trends are not statistically significant.

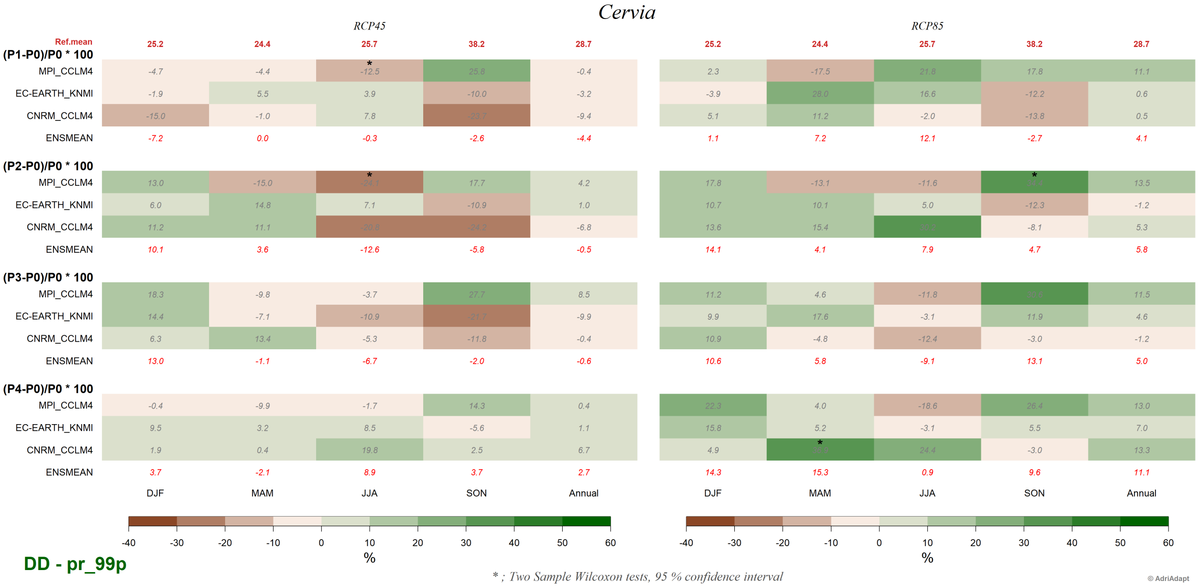

Figure 5-125: Seasonal and annual 99th percentile of precipitation (extreme precipitation) obtained by dynamical downscaling for Cervia: Ref. mean is 20 year simulated period (1986-2005) for ensemble mean in mmday^{-1}; P1-P0, P2-P0, P3-P0, P4-P0 are changes (in %) in the future for following periods P1: 2021-2040, P2: 2041-2060, P3: 2061-2080, P4: 2081-2100. Differences are shown for individual models. Significant change is marked by star. Change is also shown as ensemble mean (ENSMEAN), not tested for significance. Left column is for RCP4.5 scenario and right for RCP8.5 scenario.

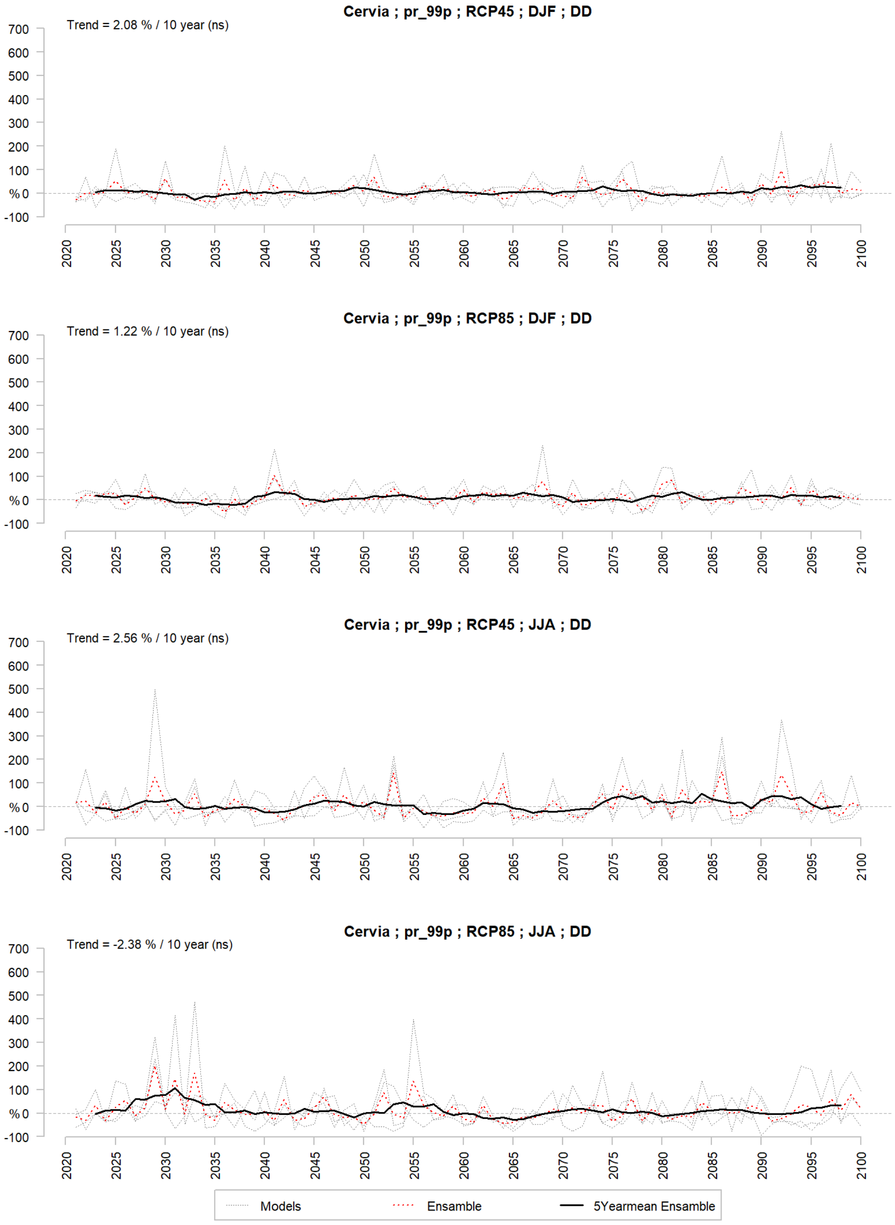

Figure 5-126: Variability of future 99th percentile of precipitation (extreme precipitation) anomaly (in %) in Cervia for 2021-2100 obtained by dynamically downscaling for winter (DJF) and summer (JJA) and two RCP scenarios: individual models are in grey, the ensemble mean in red, 5-year moving average in black. Significant trend is marked with star (ns if not significant).

6.4.1.2.4 *Heavy precipitation index*

Heavy precipitation index (Figure 5-127), defined as number of days with precipitation greater than 10 mm, will change with no unique sign between models in all seasons. In ensemble mean change for Cervia at the end of century, heavy precipitation index will increase in all seasons (except in MAM, -4.1 %) and on annual scale. The change will be in the range of 0.8 % in JJA and 9.7 % in SON; 3.7 for annual scale for RCP4.5 scenario. Worst case scenario RCP8.5 gives decrease in JJA (-18.4 %) and increase in all other seasons and on annual scale (from 8.3 % in SON to 9.2 % in DJF; 2.3 for annual scale). Variability of future heavy precipitation index anomaly (Figure 5-128) to the end of 21st century for ensemble mean in Cervia has positive trend for DJF for both scenarios, positive in JJA for RCP4.5 and negative for RCP8.5 scenario. All trends are not statistically significant.

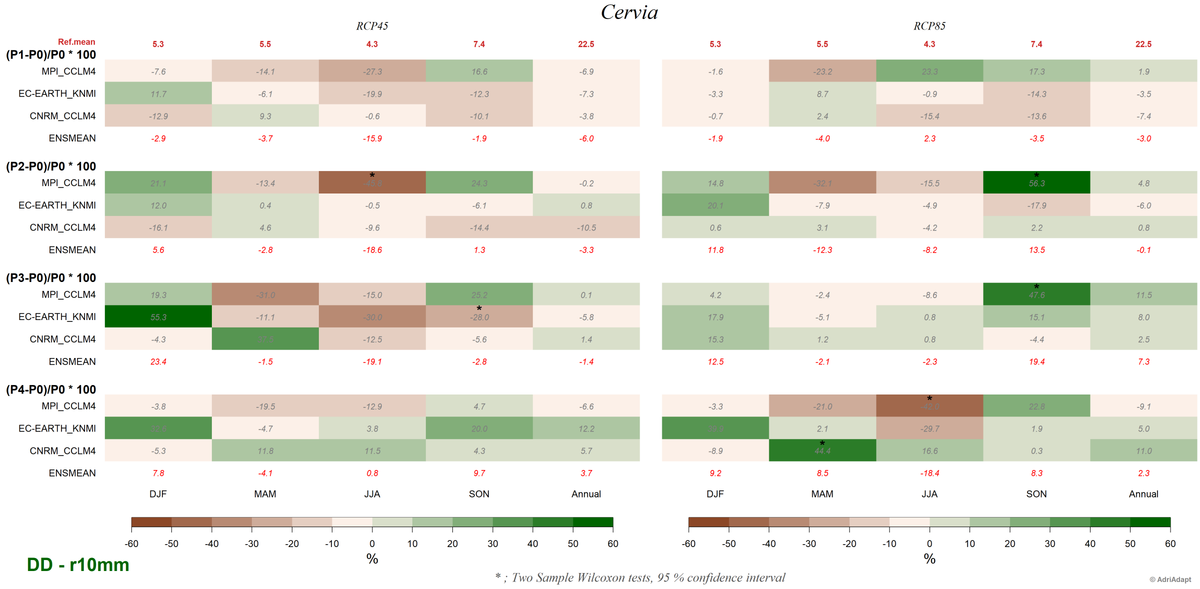

RCP45

	DJF	MAM	JJA	SON	Annual
Ref.mean	5.3	5.5	4.3	7.4	22.5
(P1-P0)/P0 * 100					
MPI_CCLM4	-7.6	-14.1	-27.3	16.6	-6.9
EC-EARTH_KNMI	11.7	-6.1	-19.9	-12.3	-7.3
CNRM_CCLM4	-12.9	9.3	-0.6	-10.1	-3.8
ENSMEAN	-2.9	-3.7	-15.9	-1.9	-6.0
(P2-P0)/P0 * 100					
MPI_CCLM4	21.1	-13.4	* -45.8	24.3	-0.2
EC-EARTH_KNMI	12.0	0.4	-0.5	-6.1	0.8
CNRM_CCLM4	-16.1	4.6	-9.6	-14.4	-10.5
ENSMEAN	5.6	-2.8	-18.6	1.3	-3.3
(P3-P0)/P0 * 100					
MPI_CCLM4	19.3	-31.0	-15.0	25.2	0.1
EC-EARTH_KNMI	55.3	-11.1	-30.0	* -28.0	-5.8
CNRM_CCLM4	-4.3	37.5	-12.5	-5.6	1.4
ENSMEAN	23.4	-1.5	-19.1	-2.8	-1.4
(P4-P0)/P0 * 100					
MPI_CCLM4	-3.8	-19.5	-12.9	4.7	-6.6
EC-EARTH_KNMI	32.6	-4.7	3.8	20.0	12.2
CNRM_CCLM4	-5.3	11.8	11.5	4.3	5.7
ENSMEAN	7.8	-4.1	0.8	9.7	3.7

RCP85

	DJF	MAM	JJA	SON	Annual
Ref.mean	5.3	5.5	4.3	7.4	22.5
(P1-P0)/P0 * 100					
MPI_CCLM4	-1.6	-23.2	23.3	17.3	1.9
EC-EARTH_KNMI	-3.3	8.7	-0.9	-14.3	-3.5
CNRM_CCLM4	-0.7	2.4	-15.4	-13.6	-7.4
ENSMEAN	-1.9	-4.0	2.3	-3.5	-3.0
(P2-P0)/P0 * 100					
MPI_CCLM4	14.8	-32.1	-15.5	* 56.3	4.8
EC-EARTH_KNMI	20.1	-7.9	-4.9	-17.9	-6.0
CNRM_CCLM4	0.6	3.1	-4.2	2.2	0.8
ENSMEAN	11.8	-12.3	-8.2	13.5	-0.1
(P3-P0)/P0 * 100					
MPI_CCLM4	4.2	-2.4	-8.6	* 47.6	11.5
EC-EARTH_KNMI	17.9	-5.1	0.8	15.1	8.0
CNRM_CCLM4	15.3	1.2	0.8	-4.4	2.5
ENSMEAN	12.5	-2.1	-2.3	19.4	7.3
(P4-P0)/P0 * 100					
MPI_CCLM4	-3.3	-21.0	* -42.0	22.8	-9.1
EC-EARTH_KNMI	39.9	2.1	-29.7	1.9	5.0
CNRM_CCLM4	-8.9	* 44.4	16.6	0.3	11.0
ENSMEAN	9.2	8.5	-18.4	8.3	2.3

* ; Two Sample Wilcoxon tests, 95 % confidence interval

Figure 5-127: Seasonal and annual heavy precipitation index obtained by dynamical downscaling for Cervia: Ref. mean is 20 year simulated period (1986-2005) for ensemble mean in days; P1-P0, P2-P0, P3-P0, P4-P0 are changes (in %) in the future for following periods P1: 2021-2040, P2: 2041-2060, P3: 2061-2080, P4: 2081-2100. Differences are shown for individual models. Significant change is marked by star. Change is also shown as ensemble mean (ENSMEAN), not tested for significance. Left column is for RCP4.5 scenario and right for RCP8.5 scenario.

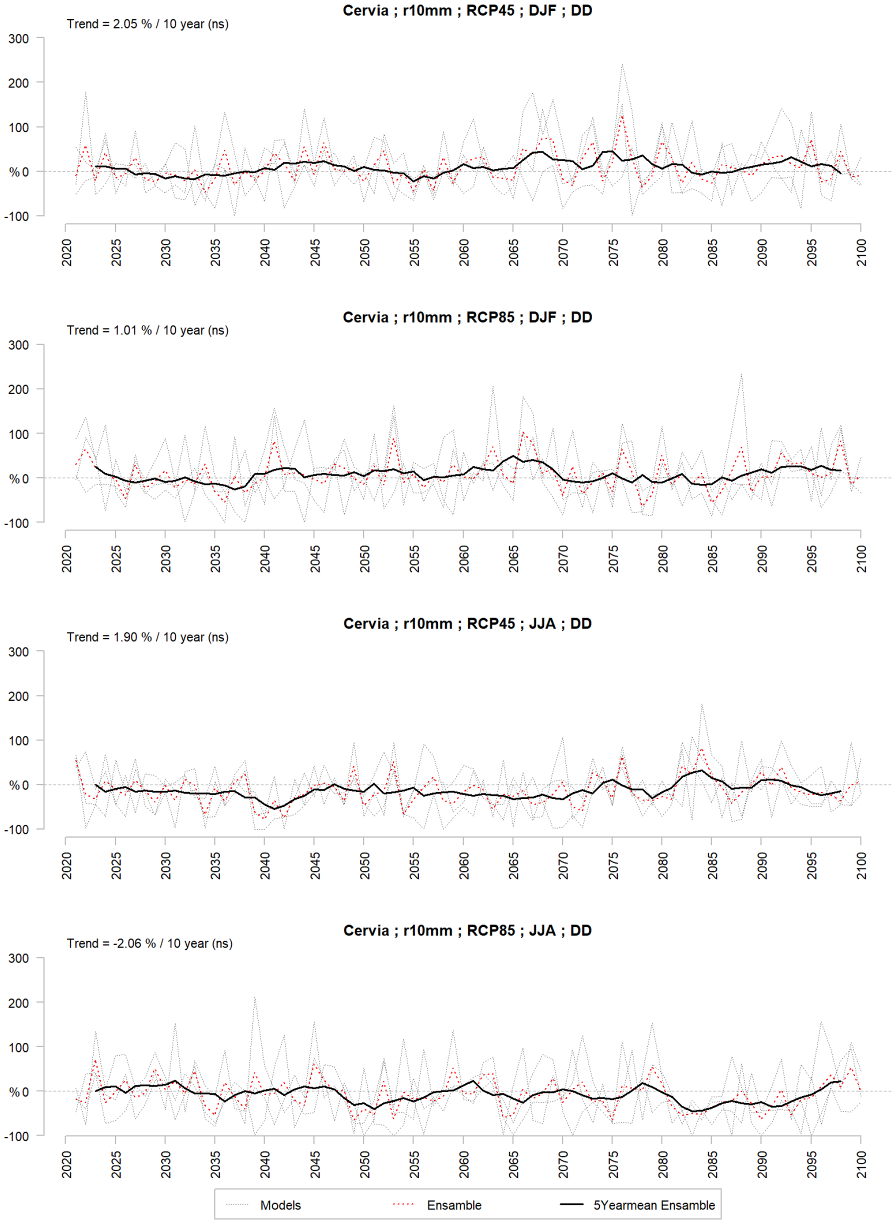

Figure 5-128: Variability of future heavy precipitation index anomaly (in %) in Cervia for 2021-2100 obtained by dynamically downscaling for winter (DJF) and summer (JJA) and two RCP scenarios: individual models are in grey, the ensemble mean in red, 5-year moving average in black. Significant trend is marked with star (ns if not significant).

6.4.1.2.5 *Maximum number of consecutive dry days*

Maximum number of consecutive dry days (Figure 5-129) in Cervia will mostly increase in all periods for most models. The ensemble mean change gives increase in DJF and JJA (9.6, 3.6 % respectively) and decrease in MAM and SON (-1.6, -0.1 % respectively); 7.6 % on annual scale for RCP4.5 scenario at the end of century. For RCP8.5 scenario ensemble mean change gives increase in all seasons and on annual scale by the end of 21st century. The change is between 12.0 % in SON and 17.4 % in DJF, 17.7 % on annual scale. Variability of future maximum number of consecutive dry days anomaly (Figure 5-130) to the end of 21st century for ensemble mean in Cervia has positive trend in DJF for both scenarios, in JJA trend is negative for RCP4.5 and positive for RCP8.5 scenario. All trends are not statistically significant.

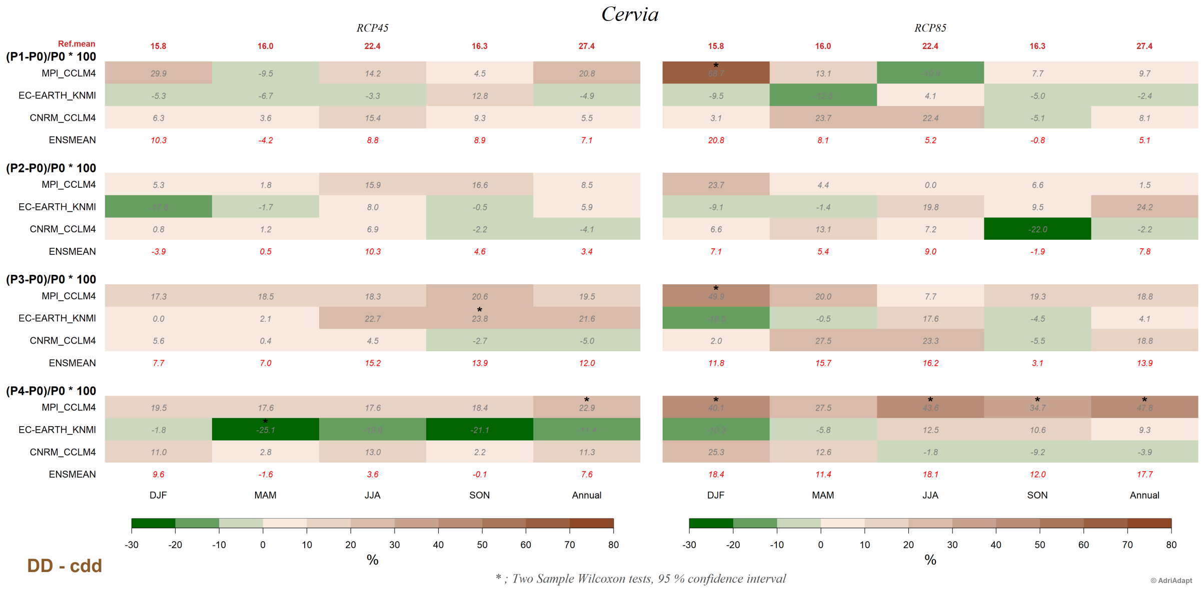

RCP45

	DJF	MAM	JJA	SON	Annual
Ref.mean	15.8	16.0	22.4	16.3	27.4
(P1-P0)/P0 * 100					
MPI_CCLM4	29.9	-9.5	14.2	4.5	20.8
EC-EARTH_KNMI	-5.3	-6.7	-3.3	12.8	-4.9
CNRM_CCLM4	6.3	3.6	15.4	9.3	5.5
ENSMEAN	10.3	-4.2	8.8	8.9	7.1
(P2-P0)/P0 * 100					
MPI_CCLM4	5.3	1.8	15.9	16.6	8.5
EC-EARTH_KNMI	-17.8	-1.7	8.0	-0.5	5.9
CNRM_CCLM4	0.8	1.2	6.9	-2.2	-4.1
ENSMEAN	-3.9	0.5	10.3	4.6	3.4
(P3-P0)/P0 * 100					
MPI_CCLM4	17.3	18.5	18.3	20.6	19.5
EC-EARTH_KNMI	0.0	2.1	22.7	* 23.8	21.6
CNRM_CCLM4	5.6	0.4	4.5	-2.7	-5.0
ENSMEAN	7.7	7.0	15.2	13.9	12.0
(P4-P0)/P0 * 100					
MPI_CCLM4	19.5	17.6	17.6	18.4	* 22.9
EC-EARTH_KNMI	-1.8	* -25.1	-19.8	-21.1	-11.4
CNRM_CCLM4	11.0	2.8	13.0	2.2	11.3
ENSMEAN	9.6	-1.6	3.6	-0.1	7.6

RCP85

	DJF	MAM	JJA	SON	Annual
Ref.mean	15.8	16.0	22.4	16.3	27.4
(P1-P0)/P0 * 100					
MPI_CCLM4	* 68.7	13.1	-10.9	7.7	9.7
EC-EARTH_KNMI	-9.5	-12.5	4.1	-5.0	-2.4
CNRM_CCLM4	3.1	23.7	22.4	-5.1	8.1
ENSMEAN	20.8	8.1	5.2	-0.8	5.1
(P2-P0)/P0 * 100					
MPI_CCLM4	23.7	4.4	0.0	6.6	1.5
EC-EARTH_KNMI	-9.1	-1.4	19.8	9.5	24.2
CNRM_CCLM4	6.6	13.1	7.2	-22.0	-2.2
ENSMEAN	7.1	5.4	9.0	-1.9	7.8
(P3-P0)/P0 * 100					
MPI_CCLM4	* 49.9	20.0	7.7	19.3	18.8
EC-EARTH_KNMI	-16.5	-0.5	17.6	-4.5	4.1
CNRM_CCLM4	2.0	27.5	23.3	-5.5	18.8
ENSMEAN	11.8	15.7	16.2	3.1	13.9
(P4-P0)/P0 * 100					
MPI_CCLM4	* 40.1	27.5	* 43.6	* 34.7	* 47.8
EC-EARTH_KNMI	-10.3	-5.8	12.5	10.6	9.3
CNRM_CCLM4	25.3	12.6	-1.8	-9.2	-3.9
ENSMEAN	18.4	11.4	18.1	12.0	17.7

** ; Two Sample Wilcoxon tests, 95 % confidence interval*

Figure 5-129: Seasonal and annual maximum number of consecutive dry days obtained by dynamical downscaling for Cervia: Ref. mean is 20 year simulated period (1986-2005) for ensemble mean in days; P1-P0, P2-P0, P3-P0, P4-P0 are changes (in %) in the future for following periods P1: 2021-2040, P2: 2041-2060, P3: 2061-2080, P4: 2081-2100. Differences are shown for individual models. Significant change is marked by star. Change is also shown as ensemble mean (ENSMEAN), not tested for significance. Left column is for RCP4.5 scenario and right for RCP8.5 scenario.

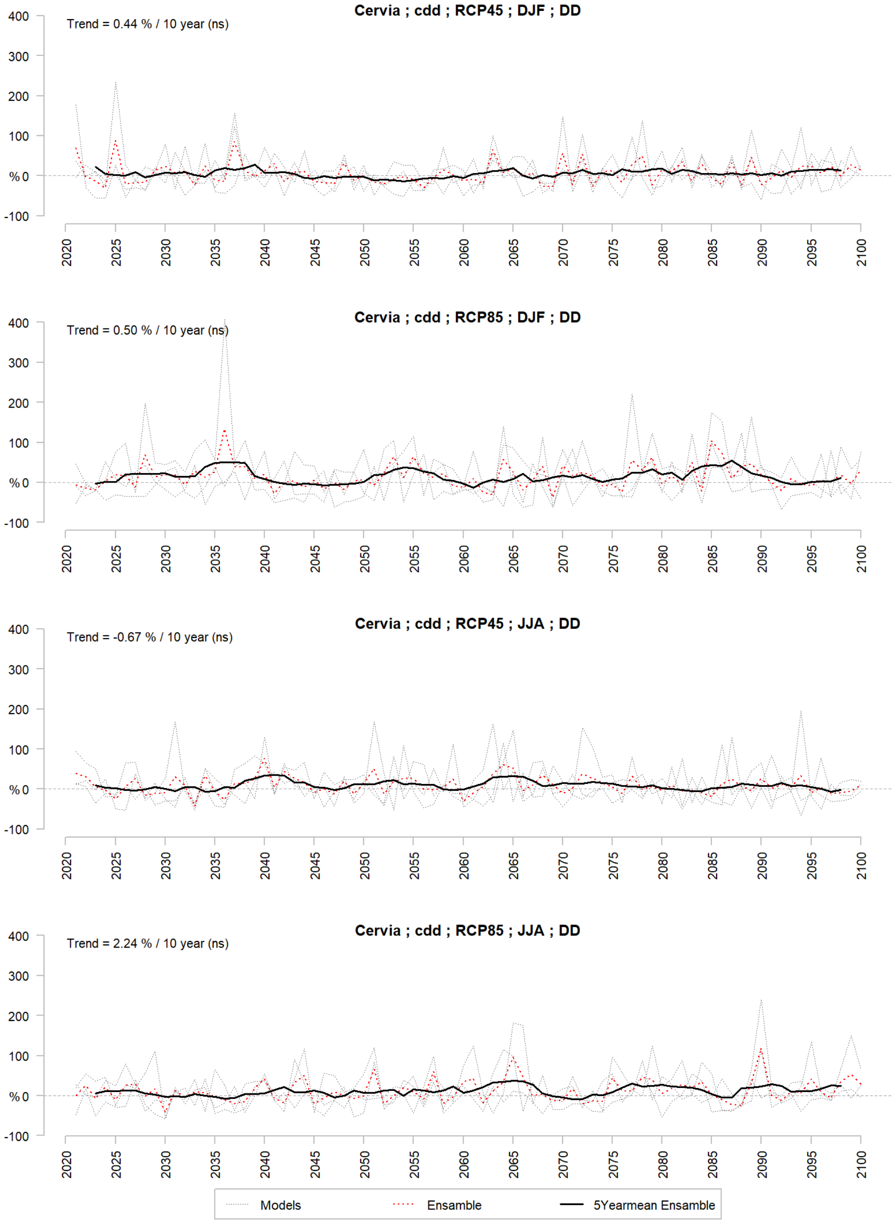

Figure 5-130: Variability of future maximum number of consecutive dry days anomaly (in %) in Cervia for 2021-2100 obtained by dynamically downscaling for winter (DJF) and summer (JJA) and two RCP scenarios: individual models are in grey, the ensemble mean in red, 5-year moving average in black. Significant trend is marked with star (ns if not significant).

6.4.1.3 *Extra rare humidex projections*

Extra rare humidex change (defined by 99.9th percentile of humidex) in the future in Cervia will increase towards the end of 21st century (Figure 5-131). Ensemble mean will increase between 0.8 in SON and 2.0 in MAM, 0.6 on annual scale for RCP4.5 scenario. Only for JJA ensemble mean change will be slightly negative. Scenario RCP8.5 gives higher positive amplitudes, from 3.5 in JJA to 5.0 in MAM and SON, 4.2 on annual scale. Variability of future 99.9th percentile of humidex anomaly (Figure 5-132) shows positive linear trend for both seasons and both considered scenarios. It is 0.28 [] / 10 year in DJF for RCP4.5 (0.65 [] /10 year for RCP8.5) and 0.31 [] /10 year in JJA for RCP4.5 (0.78 [] /10 year for RCP8.5). Trends are statistically significant.

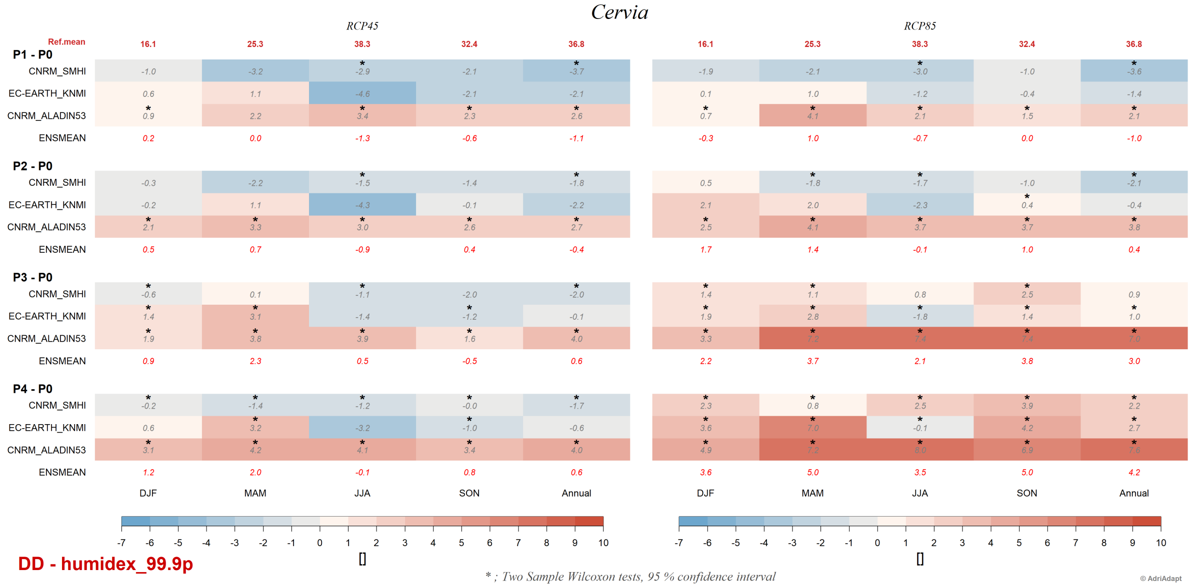

Cervia

	RCP45					RCP85				
Ref.mean	16.1	25.3	38.3	32.4	36.8	16.1	25.3	38.3	32.4	36.8
P1 - P0										
CNRM_SMHI	-1.0	-3.2	* -2.9	-2.1	* -3.7	-1.9	-2.1	* -3.0	-1.0	* -3.6
EC-EARTH_KNMI	0.6	1.1	-4.6	-2.1	-2.1	0.1	1.0	-1.2	-0.4	-1.4
CNRM_ALADIN53	* 0.9	2.2	* 3.4	* 2.3	* 2.6	* 0.7	* 4.1	* 2.1	* 1.5	* 2.1
ENSMEAN	0.2	0.0	-1.3	-0.6	-1.1	-0.3	1.0	-0.7	0.0	-1.0
P2 - P0										
CNRM_SMHI	-0.3	-2.2	* -1.5	-1.4	* -1.8	0.5	* -1.8	* -1.7	-1.0	* -2.1
EC-EARTH_KNMI	-0.2	1.1	-4.3	-0.1	-2.2	2.1	2.0	-2.3	* 0.4	-0.4
CNRM_ALADIN53	* 2.1	* 3.3	* 3.0	* 2.6	* 2.7	* 2.5	* 4.1	* 3.7	* 3.7	* 3.8
ENSMEAN	0.5	0.7	-0.9	0.4	-0.4	1.7	1.4	-0.1	1.0	0.4
P3 - P0										
CNRM_SMHI	* -0.6	0.1	* -1.1	-2.0	* -2.0	* 1.4	* 1.1	0.8	* 2.5	0.9
EC-EARTH_KNMI	* 1.4	* 3.1	-1.4	* -1.2	-0.1	* 1.9	* 2.8	* -1.8	* 1.4	* 1.0
CNRM_ALADIN53	* 1.9	* 3.8	* 3.9	* 1.6	* 4.0	* 3.3	* 7.2	* 7.4	* 7.4	* 7.0
ENSMEAN	0.9	2.3	0.5	-0.5	0.6	2.2	3.7	2.1	3.8	3.0
P4 - P0										
CNRM_SMHI	* -0.2	* -1.4	* -1.2	* -0.0	* -1.7	* 2.3	* 0.8	* 2.5	* 3.9	* 2.2
EC-EARTH_KNMI	0.6	* 3.2	-3.2	* -1.0	-0.6	* 3.6	* 7.0	* -0.1	* 4.2	* 2.7
CNRM_ALADIN53	* 3.1	* 4.2	* 4.1	* 3.4	* 4.0	* 4.9	* 7.2	* 8.0	* 6.9	* 7.6
ENSMEAN	1.2	2.0	-0.1	0.8	0.6	3.6	5.0	3.5	5.0	4.2
	DJF	MAM	JJA	SON	Annual	DJF	MAM	JJA	SON	Annual

* ; Two Sample Wilcoxon tests, 95 % confidence interval

Figure 5-131: Seasonal and annual 99.9th percentile of humidex obtained by dynamical downscaling for Cervia (in []): Ref. mean is 20 year simulated period (1986-2005); P1-P0, P2-P0, P3-P0, P4-P0 are changes in the future for following periods P1: 2021-2040, P2: 2041-2060, P3: 2061-2080, P4: 2081-2100. Differences are shown for individual models. Significant change is marked by star. Change is also shown as ensemble mean (ENSMEAN), not tested for significance. Left column is for RCP4.5 scenario and right for RCP8.5 scenario.

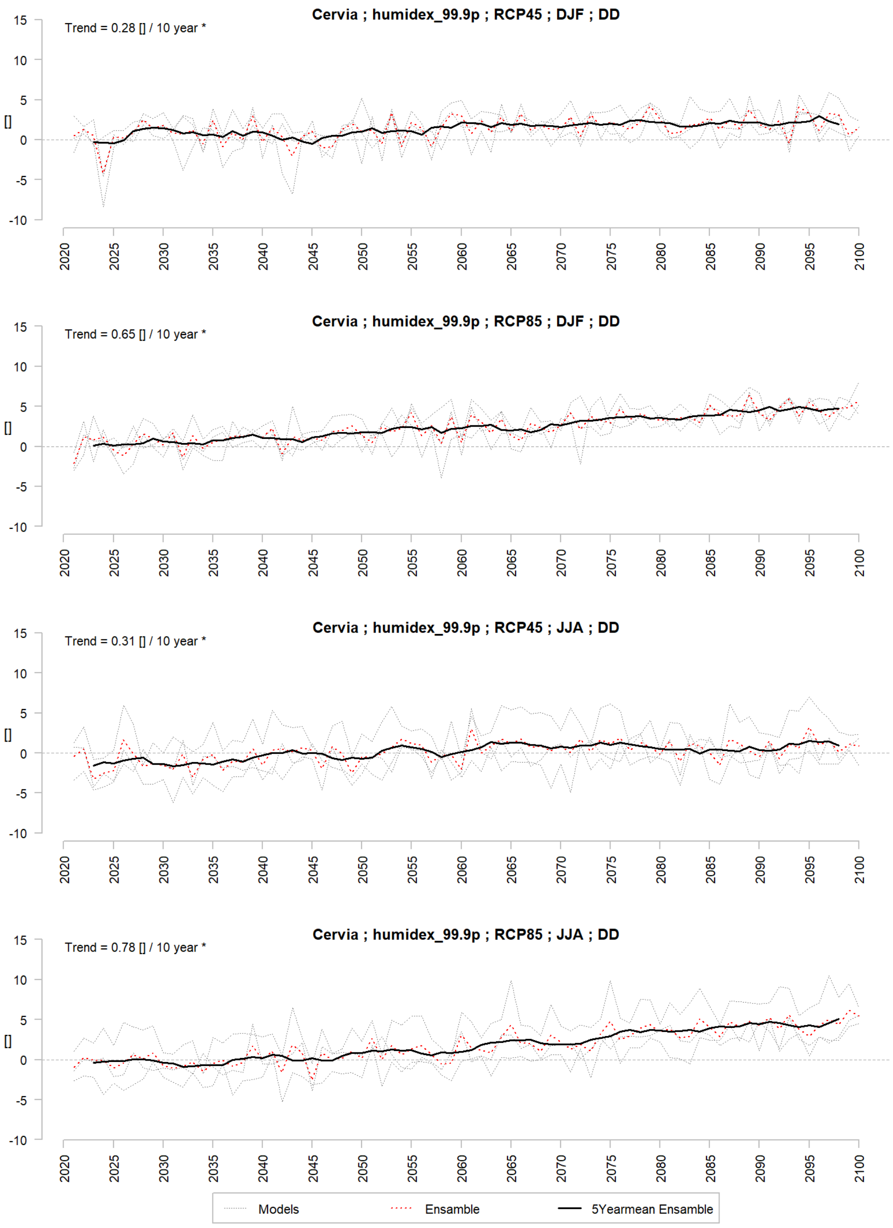

Figure 5-132: Variability of future 99.9th percentile of humidex anomaly (in []) in Cervia for 2021-2100 obtained by dynamically downscaling for winter (DJF) and summer (JJA) and two RCP scenarios: individual models are in grey, the ensemble mean in red, 5-year moving average in black. Significant trend is marked with star (ns if not significant).

6.4.1.4 *Wind projections*

6.4.1.4.1 *Averaged wind module*

The change of wind speed at 10m high (Figure 5-133) is very variable from season to season and from model to model. It is expressed as relative difference to the wind speed in P0 period in percentage. At the end of 21st century wind speed in Cervia will slightly decrease in DJF (-0.3 %) and in JJA (-0.5 %), but will increase in MAM (1 %) and in SON (0.4 %); 0.1 % on annual scale for RCP4.5 scenario. For RCP8.5 scenario wind speed will decrease in all seasons except in JJA (from -1 % in MAM to -2.7 % in DJF), and -1.5 % on annual scale. In JJA wind speed will increase for 0.3 %. Variability of future wind speed at 10m high anomaly (Figure 5-134) shows negative linear trend for both seasons and both considered scenarios. Trend is statistically significant in DJF for RCP8.5 (-0.58 % /10 year).

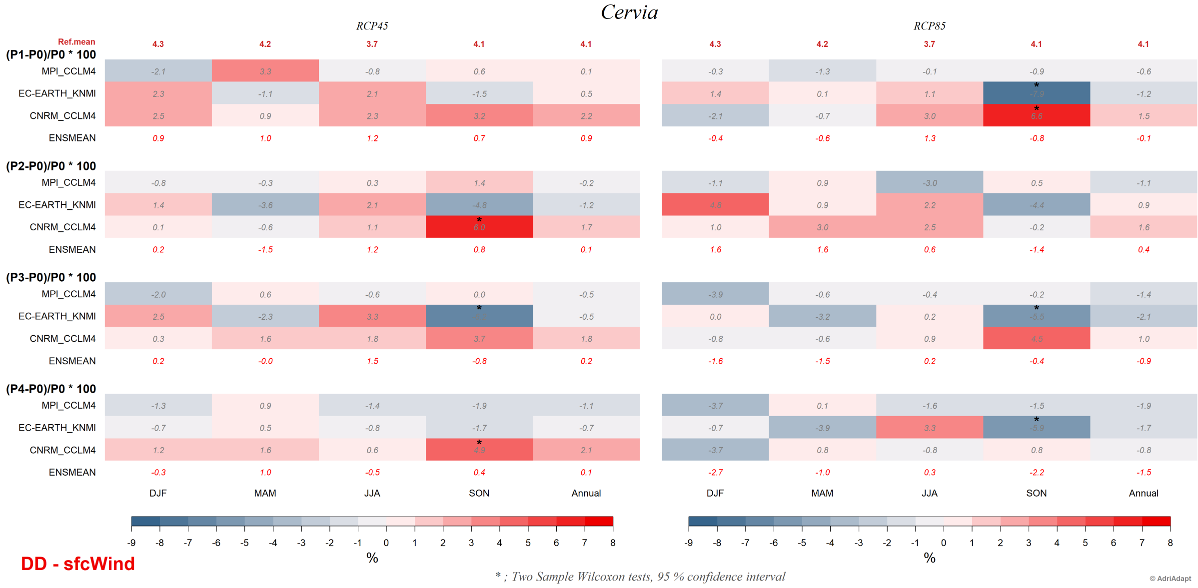

Cervia

	RCP45					RCP85				
	DJF	MAM	JJA	SON	Annual	DJF	MAM	JJA	SON	Annual
Ref.mean	4.3	4.2	3.7	4.1	4.1	4.3	4.2	3.7	4.1	4.1
(P1-P0)/P0 * 100										
MPI_CCLM4	-2.1	3.3	-0.8	0.6	0.1	-0.3	-1.3	-0.1	-0.9	-0.6
EC-EARTH_KNMI	2.3	-1.1	2.1	-1.5	0.5	1.4	0.1	1.1	* -7.9	-1.2
CNRM_CCLM4	2.5	0.9	2.3	3.2	2.2	-2.1	-0.7	3.0	* 6.6	1.5
ENSMEAN	0.9	1.0	1.2	0.7	0.9	-0.4	-0.6	1.3	-0.8	-0.1
(P2-P0)/P0 * 100										
MPI_CCLM4	-0.8	-0.3	0.3	1.4	-0.2	-1.1	0.9	-3.0	0.5	-1.1
EC-EARTH_KNMI	1.4	-3.6	2.1	-4.8	-1.2	4.8	0.9	2.2	-4.4	0.9
CNRM_CCLM4	0.1	-0.6	1.1	* 6.0	1.7	1.0	3.0	2.5	-0.2	1.6
ENSMEAN	0.2	-1.5	1.2	0.8	0.1	1.6	1.6	0.6	-1.4	0.4
(P3-P0)/P0 * 100										
MPI_CCLM4	-2.0	0.6	-0.6	0.0	-0.5	-3.9	-0.6	-0.4	-0.2	-1.4
EC-EARTH_KNMI	2.5	-2.3	3.3	* -6.2	-0.5	0.0	-3.2	0.2	* -5.5	-2.1
CNRM_CCLM4	0.3	1.6	1.8	3.7	1.8	-0.8	-0.6	0.9	4.5	1.0
ENSMEAN	0.2	-0.0	1.5	-0.8	0.2	-1.6	-1.5	0.2	-0.4	-0.9
(P4-P0)/P0 * 100										
MPI_CCLM4	-1.3	0.9	-1.4	-1.9	-1.1	-3.7	0.1	-1.6	-1.5	-1.9
EC-EARTH_KNMI	-0.7	0.5	-0.8	-1.7	-0.7	-0.7	-3.9	3.3	* -5.9	-1.7
CNRM_CCLM4	1.2	1.6	0.6	* 4.9	2.1	-3.7	0.8	-0.8	0.8	-0.8
ENSMEAN	-0.3	1.0	-0.5	0.4	0.1	-2.7	-1.0	0.3	-2.2	-1.5

* ; Two Sample Wilcoxon tests, 95 % confidence interval

© AdriAdapt

Figure 5-133: Averaged seasonal and annual wind module (wind speed at 10m height) obtained by dynamical downscaling for Cervia: Ref. mean is 20 year simulated period (1986-2005) in ms^{-1}; P1-P0, P2-P0, P3-P0, P4-P0 are changes (in %) in the future for following periods P1: 2021-2040, P2: 2041-2060, P3: 2061-2080, P4: 2081-2100. Differences are shown for individual models. Significant change is marked by star. Change is also shown as ensemble mean (ENSMEAN), not tested for significance. Left column is for RCP4.5 scenario and right for RCP8.5 scenario.

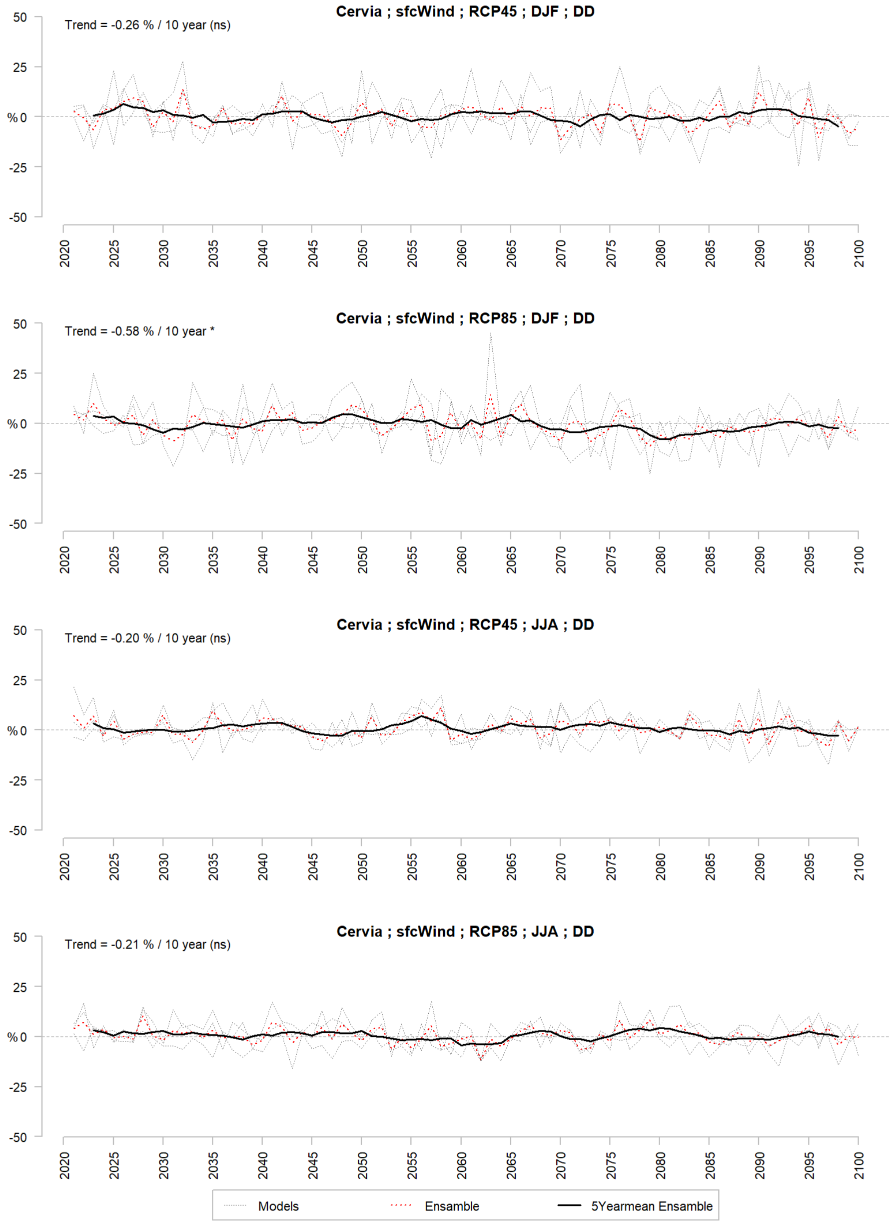

Figure 5-134: Variability of future wind module anomaly (wind speed at 10m height) anomaly (in %) in Cervia for 2021-2100 obtained by dynamically downscaling for winter (DJF) and summer (JJA) and two RCP scenarios: individual models are in grey, the ensemble mean in red, 5-year moving average in black. Significant trend is marked with star (ns if not significant).

6.4.1.4.2 *Maximum wind module*

The change of maximum wind speed at 10m high (Figure 5-135) is very variable from season to season and from model to model. It is expressed as relative difference to the maximum wind speed in P0 period in percentage. At the end of 21st century maximum wind speed in Cervia will slightly decrease in DJF (-0.4 %) and in SON (-0.1 %), but increase in MAM (1.5 %) and in JJA (0.3 %); 0.3 % on annual scale for RCP4.5 scenario. For RCP8.5 scenario wind speed will decrease in DJF and SON (-1.8 %, -1.2 % respectively), increase in MAM (0.6 %) and will not change in JJA. On annual scale maximum wind speed will decrease for -0.7 %. Variability of future maximum wind speed at 10m high anomaly (Figure 5-136) shows negative linear trends to the end of 21st century for both seasons and both considered scenarios. Trends are not statistically significant.

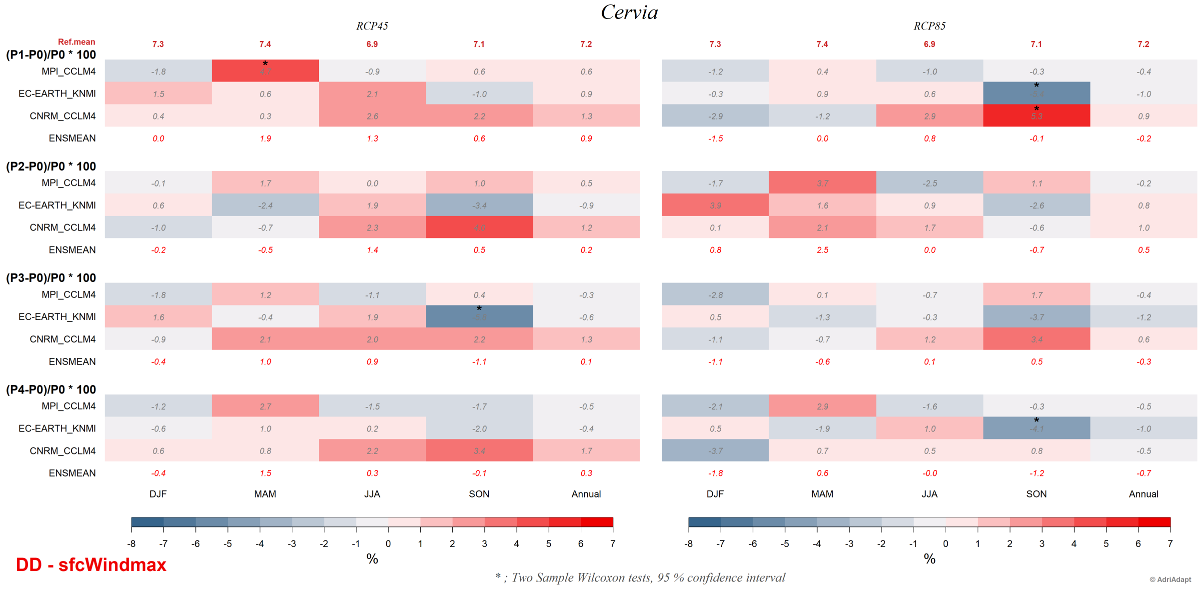

Cervia

	RCP45					RCP85				
	DJF	MAM	JJA	SON	Annual	DJF	MAM	JJA	SON	Annual
Ref.mean	7.3	7.4	6.9	7.1	7.2	7.3	7.4	6.9	7.1	7.2
(P1-P0)/P0 * 100										
MPI_CCLM4	-1.8	* 4.7	-0.9	0.6	0.6	-1.2	0.4	-1.0	-0.3	-0.4
EC-EARTH_KNMI	1.5	0.6	2.1	-1.0	0.9	-0.3	0.9	0.6	* -5.4	-1.0
CNRM_CCLM4	0.4	0.3	2.6	2.2	1.3	-2.9	-1.2	2.9	* 5.3	0.9
ENSMEAN	0.0	1.9	1.3	0.6	0.9	-1.5	0.0	0.8	-0.1	-0.2
(P2-P0)/P0 * 100										
MPI_CCLM4	-0.1	1.7	0.0	1.0	0.5	-1.7	3.7	-2.5	1.1	-0.2
EC-EARTH_KNMI	0.6	-2.4	1.9	-3.4	-0.9	3.9	1.6	0.9	-2.6	0.8
CNRM_CCLM4	-1.0	-0.7	2.3	4.0	1.2	0.1	2.1	1.7	-0.6	1.0
ENSMEAN	-0.2	-0.5	1.4	0.5	0.2	0.8	2.5	0.0	-0.7	0.5
(P3-P0)/P0 * 100										
MPI_CCLM4	-1.8	1.2	-1.1	0.4	-0.3	-2.8	0.1	-0.7	1.7	-0.4
EC-EARTH_KNMI	1.6	-0.4	1.9	* -5.8	-0.6	0.5	-1.3	-0.3	-3.7	-1.2
CNRM_CCLM4	-0.9	2.1	2.0	2.2	1.3	-1.1	-0.7	1.2	3.4	0.6
ENSMEAN	-0.4	1.0	0.9	-1.1	0.1	-1.1	-0.6	0.1	0.5	-0.3
(P4-P0)/P0 * 100										
MPI_CCLM4	-1.2	2.7	-1.5	-1.7	-0.5	-2.1	2.9	-1.6	-0.3	-0.5
EC-EARTH_KNMI	-0.6	1.0	0.2	-2.0	-0.4	0.5	-1.9	1.0	* -4.1	-1.0
CNRM_CCLM4	0.6	0.8	2.2	3.4	1.7	-3.7	0.7	0.5	0.8	-0.5
ENSMEAN	-0.4	1.5	0.3	-0.1	0.3	-1.8	0.6	-0.0	-1.2	-0.7

* ; Two Sample Wilcoxon tests, 95 % confidence interval

Figure 5-135: Seasonal and annual maximum wind module (maximum wind speed at 10m height) obtained by dynamical downscaling for Cervia: Ref. mean is 20 year simulated period (1986-2005) in ms^{-1}; P1-P0, P2-P0, P3-P0, P4-P0 are changes (in %) in the future for following periods P1: 2021-2040, P2: 2041-2060, P3: 2061-2080, P4: 2081-2100. Differences are shown for individual models. Significant change is marked by star. Change is also shown as ensemble mean (ENSMEAN), not tested for significance. Left column is for RCP4.5 scenario and right for RCP8.5 scenario.

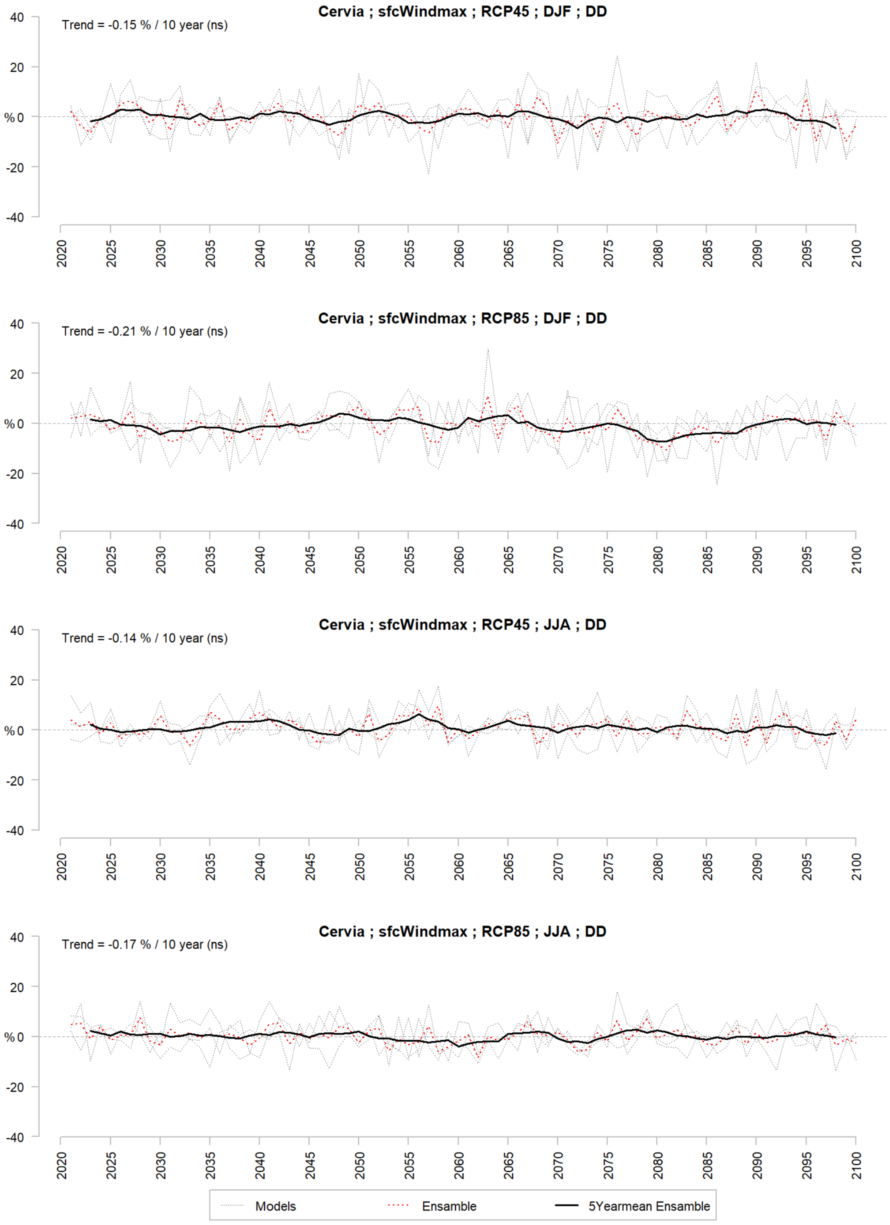

Figure 5-136: Variability of future maximum wind module (maximum wind speed at 10m height) (in %) in Cervia for 2021-2100 obtained by dynamically downscaling for winter (DJF) and summer (JJA) and two RCP scenarios: individual models are in grey, the ensemble mean in red, 5-year moving average in black. Significant trend is marked with star (ns if not significant).

6.4.2 Statistically downscaled results

In this section we present future climate changes of temperature and precipitation related indices for Cervia-Pinarella, as result from the statistical downscaling techniques constructed based on the observed local data/observed large scale circulation patterns and, applied then to future large-scale circulation patterns simulated by 4GCMs in the framework of CMIP5 experiments. The coordinates of the Cervia-Pinarella grid point are included in table A from Annexes. The results are presented as follow:

- climate change diagram of an individual index for each season and on annual basis for four considered future periods (P1, P2, P3, P4), for two emission scenarios (RCP4.5 and RCP8.5). Climate change is calculated as difference between future (P1, P2, P3, P4) and reference period (P0) for temperature indices and some extreme precipitation indices, and as relative differences (expressed in %) for some precipitation indices. Reference period is 1986-2005, the Ref.mean (obs.) from the diagram (see below) is the climate observed value registered at station take into analysis, while climate changes (P1-P0; P2-P0,P3-P0;P4-P0) are shown for different models (SD_CMCC-CM, SD_CAN-ESM2, SD-MPI, SD_CNRM) as well as for ensemble mean of models (ENSMEAN). The t-Student test is applied to test the statistical significance of future climate (values from P1, or P2, or P3, or P4) with respect to present climate value (value from P0) and the results significant at 95% are marked by a star.
- time series of future anomaly of an individual index for DJF and JJA and for two emission scenarios RCP4.5 and RCP8.5; the anomaly is calculated respect to the reference period and shown for individual models, ensemble mean and 5-year moving average. Mann Kendall trend test is applied to ensemble mean (for 95 % confidence level). Significant trend is marked with star (n.s. if not significant).

6.4.2.1 *Temperature related indices projections*

6.4.2.1.1 *Seasonal and annual minimum and maximum temperature*

Projected changes of seasonal and annual minimum temperature for Cervia-Pinarella grid point are shown in figure 5-137, for RCP4.5 and RCP8.5 and over P1, P2, P3 and P4 with respect to present climate (P0). Following the moderate RCP4.5 scenario we expect an increase in annual minimum temperature between 1°C during P1 and up to 2.2°C going to the end of century (P4). The projected increase is higher for RCP8.5, especially for P3 and P4 when the simulations show changes in annual minimum temperature about 3°C for P3 and 4.3°C for P4.

Analysing in details the seasonal projected changes it could be observed that autumn, winter and spring could exhibit changes higher than in summer. During autumn the projected changes could reach 5.6°C at the end of century, while 4°C could be reach in winter and spring in the framework of RCP8.5 (figure 5-137)

During summer the magnitude of change could reach up to 1.8°C for RCP4.5 and up to 3.5°C for RCP8.5 (P4 period).

Long term variability shows positive and significant trends over 2021-2100, both for winter and summer minimum temperature, more intense for RCP8.5 and especially in winter season, about 0.5°C/decade (figure 5-138).

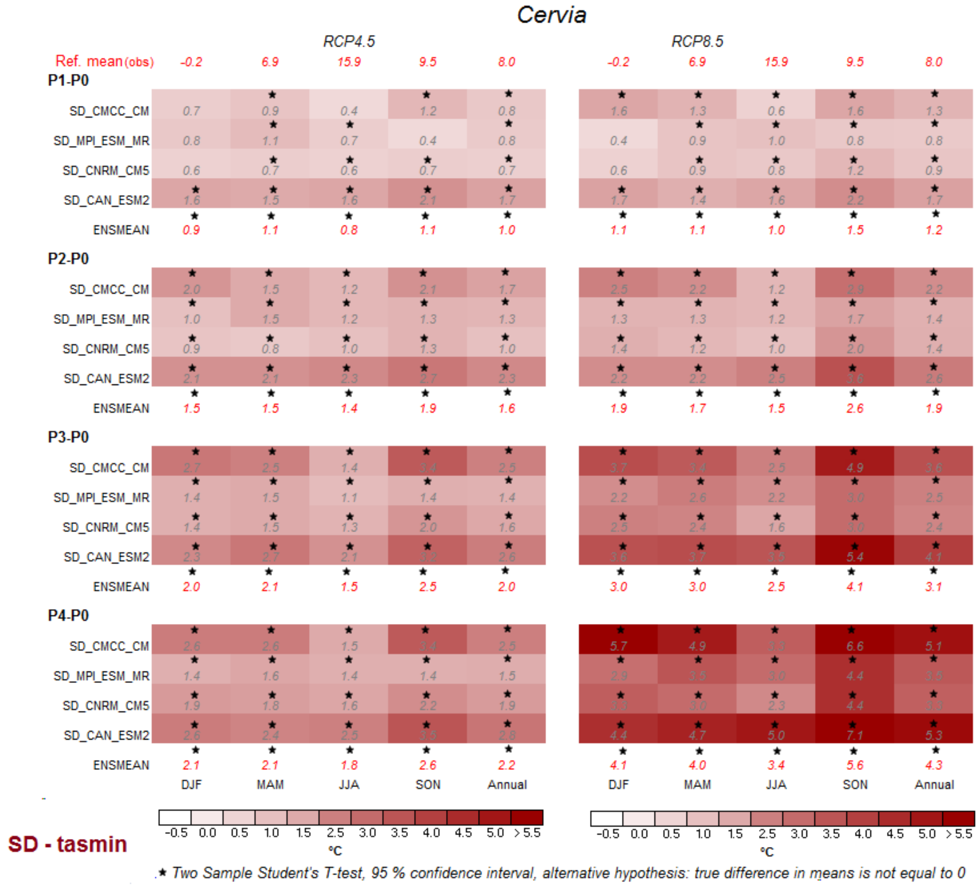

Figure 5-137: Seasonal and annual minimum temperature: observed values over reference period (in red), changes projected by statistical downscaling applied to 4GCMs and the Ensemble Mean of changes over the four periods (P1, P2, P3, P4) projected in the framework of RCP4.5 (left) and RCP 8.5 (right Significant change is marked by star (source Arpae-Simc)

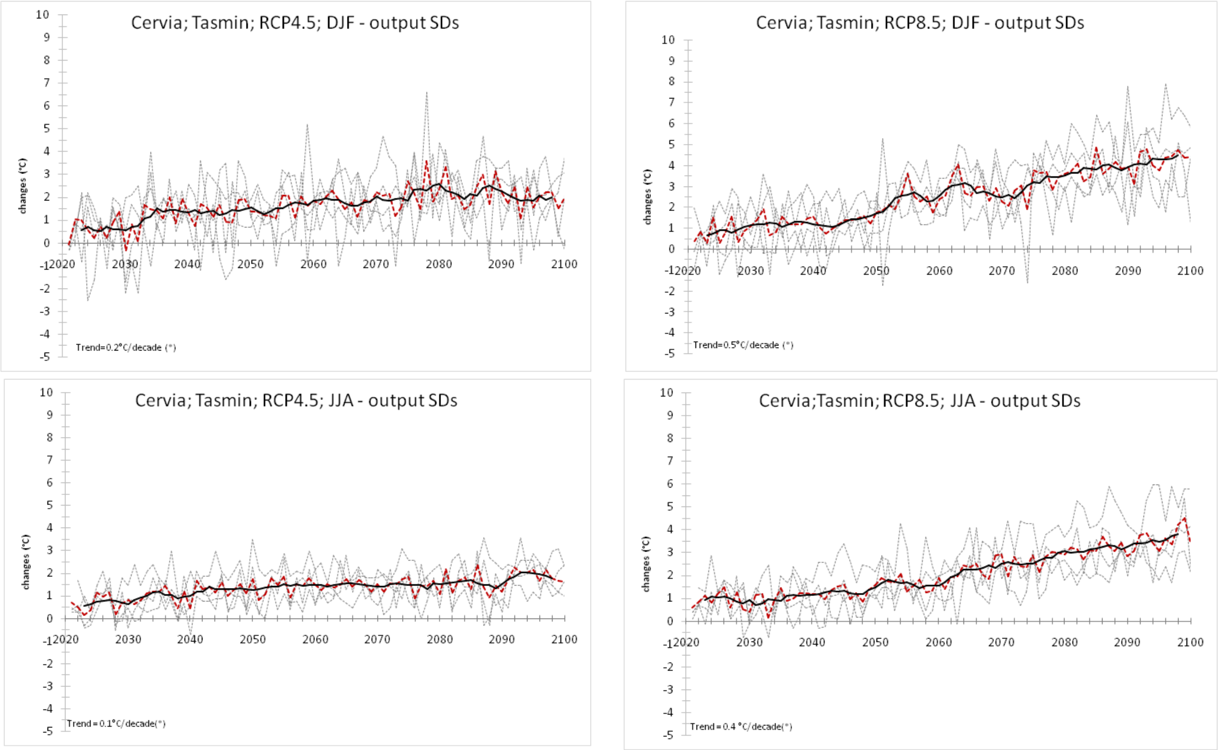

Figure 5-138: Variability of future changes of winter (DJF) and summer (JJA) minimum temperature projected through SDs applied to 4GCMs (grey lines); the Ensemble Mean (red line) and moving average (black line) - scenario RCP4.5 (left) and RCP8.5 (right), 2021-2100 period. Significant trend is marked with star while n.s. means not significant (source Arpae-Simc).

Projected changes of seasonal and annual maximum temperature for Cervia-Pinarella grid point are shown in figure 5-139, for RCP4.5 and RCP8.5 and over P1, P2, P3 and P4 with respect to present climate (P0). Following the moderate RCP4.5 scenario we expect an increase in annual maximum temperature between 1.3°C during P1 and up to 3°C going to the end of century (P4). The projected increase is higher for RCP8.5, especially for P3 and P4 when the simulations show changes in annual maximum temperature about 4.3°C and 5.8°C, respectively.

Analysing in details the seasonal projected changes of maximum temperature it could be observed that during summer the expected changes is very high, about 4.4°C for RCP4.5 and 8.9°C for RCP8.5 , over 2081-2100 (P4). Intense changes could be noted also during spring and autumn for RCP8.5, during P3 and P4 (see figure 5-139)

Positive and significant trends are simulated for winter and summer changes of maximum temperature, more intense for RCP8.5 and especially in summer season, about 1°C/decade over 2021-2100 period (figure 5-140).

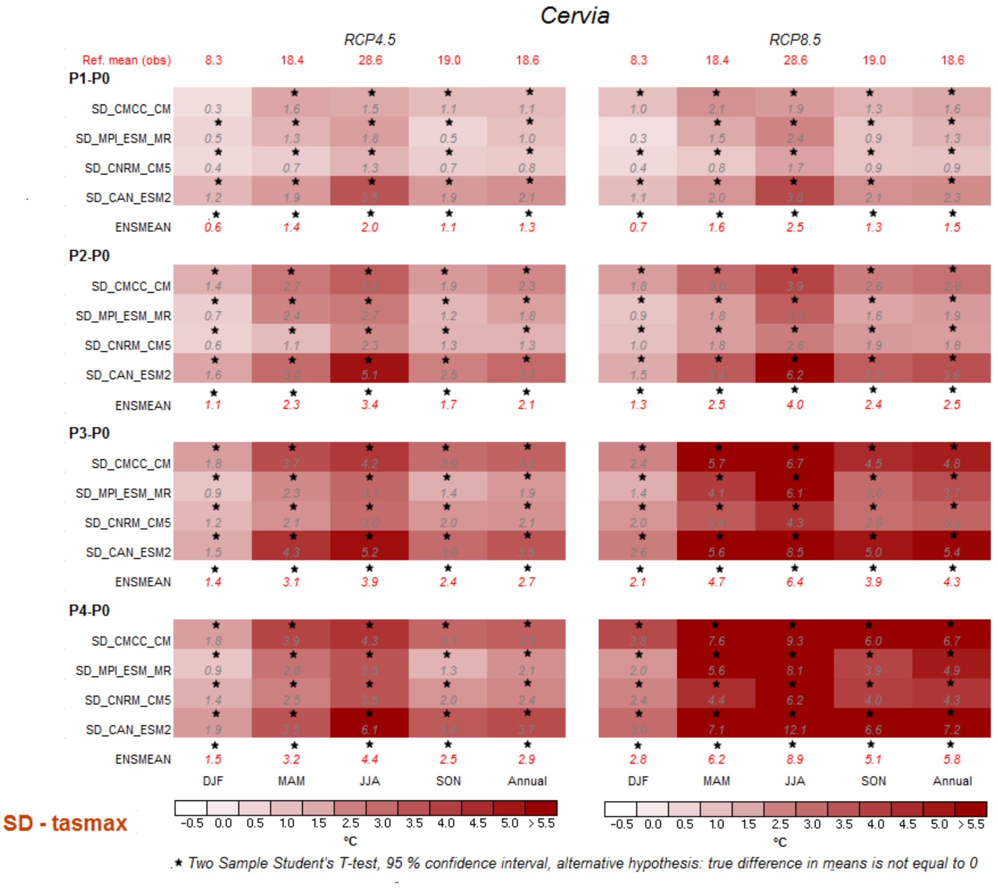

Cervia

	RCP4.5					RCP8.5				
	DJF	MAM	JJA	SON	Annual	DJF	MAM	JJA	SON	Annual
Ref. mean (obs)	8.3	18.4	28.6	19.0	18.6	8.3	18.4	28.6	19.0	18.6
P1-P0										
SD_CMCC_CM	0.3	★ 1.6	★ 1.5	★ 1.1	★ 1.1	★ 1.0	★ 2.1	★ 1.9	★ 1.3	★ 1.6
SD_MPI_ESM_MR	★ 0.5	★ 1.3	★ 1.8	★ 0.5	★ 1.0	0.3	★ 1.5	★ 2.4	★ 0.9	★ 1.3
SD_CNRM_CM5	★ 0.4	★ 0.7	★ 1.3	★ 0.7	★ 0.8	★ 0.4	★ 0.8	★ 1.7	★ 0.9	★ 0.9
SD_CAN_ESM2	★ 1.2	★ 1.9	★ 3.5	★ 1.9	★ 2.1	★ 1.1	★ 2.0	★ 3.8	★ 2.1	★ 2.3
ENSMEAN	★ 0.6	★ 1.4	★ 2.0	★ 1.1	★ 1.3	★ 0.7	★ 1.6	★ 2.5	★ 1.3	★ 1.5
P2-P0										
SD_CMCC_CM	★ 1.4	★ 2.7	★ 3.3	★ 1.9	★ 2.3	★ 1.8	★ 3.0	★ 3.9	★ 2.6	★ 2.8
SD_MPI_ESM_MR	★ 0.7	★ 2.4	★ 2.7	★ 1.2	★ 1.8	★ 0.9	★ 1.8	★ 3.3	★ 1.6	★ 1.9
SD_CNRM_CM5	★ 0.6	★ 1.1	★ 2.3	★ 1.3	★ 1.3	★ 1.0	★ 1.8	★ 2.6	★ 1.9	★ 1.8
SD_CAN_ESM2	★ 1.6	★ 3.0	★ 5.1	★ 2.5	★ 3.1	★ 1.5	★ 3.4	★ 6.2	★ 3.3	★ 3.6
ENSMEAN	★ 1.1	★ 2.3	★ 3.4	★ 1.7	★ 2.1	★ 1.3	★ 2.5	★ 4.0	★ 2.4	★ 2.5
P3-P0										
SD_CMCC_CM	★ 1.8	★ 3.7	★ 4.2	★ 3.0	★ 3.2	★ 2.4	★ 5.7	★ 6.7	★ 4.5	★ 4.8
SD_MPI_ESM_MR	★ 0.9	★ 2.3	★ 3.1	★ 1.4	★ 1.9	★ 1.4	★ 4.1	★ 6.1	★ 3.0	★ 3.7
SD_CNRM_CM5	★ 1.2	★ 2.1	★ 3.0	★ 2.0	★ 2.1	★ 2.0	★ 3.4	★ 4.3	★ 2.9	★ 3.2
SD_CAN_ESM2	★ 1.5	★ 4.3	★ 5.2	★ 3.0	★ 3.5	★ 2.6	★ 5.6	★ 8.5	★ 5.0	★ 5.4
ENSMEAN	★ 1.4	★ 3.1	★ 3.9	★ 2.4	★ 2.7	★ 2.1	★ 4.7	★ 6.4	★ 3.9	★ 4.3
P4-P0										
SD_CMCC_CM	★ 1.8	★ 3.9	★ 4.3	★ 3.1	★ 3.3	★ 3.8	★ 7.6	★ 9.3	★ 6.0	★ 6.7
SD_MPI_ESM_MR	★ 0.9	★ 2.8	★ 3.5	★ 1.3	★ 2.1	★ 2.0	★ 5.6	★ 8.1	★ 3.9	★ 4.9
SD_CNRM_CM5	★ 1.4	★ 2.5	★ 3.5	★ 2.0	★ 2.4	★ 2.4	★ 4.4	★ 6.2	★ 4.0	★ 4.3
SD_CAN_ESM2	★ 1.9	★ 3.5	★ 6.1	★ 3.4	★ 3.7	★ 3.0	★ 7.1	★ 12.1	★ 6.6	★ 7.2
ENSMEAN	★ 1.5	★ 3.2	★ 4.4	★ 2.5	★ 2.9	★ 2.8	★ 6.2	★ 8.9	★ 5.1	★ 5.8

★ Two Sample Student's T-test, 95 % confidence interval, alternative hypothesis: true difference in means is not equal to 0

Figure 5-139: Seasonal and annual maximum temperature: observed values over reference period (in red), changes projected by statistical downscaling applied to 4GCMs and the Ensemble Mean of changes over the four periods (P1, P2, P3, P4) projected in the framework of RCP4.5 (left) and RCP 8.5 (right). Significant change is marked by star (source Arpae-Simc)

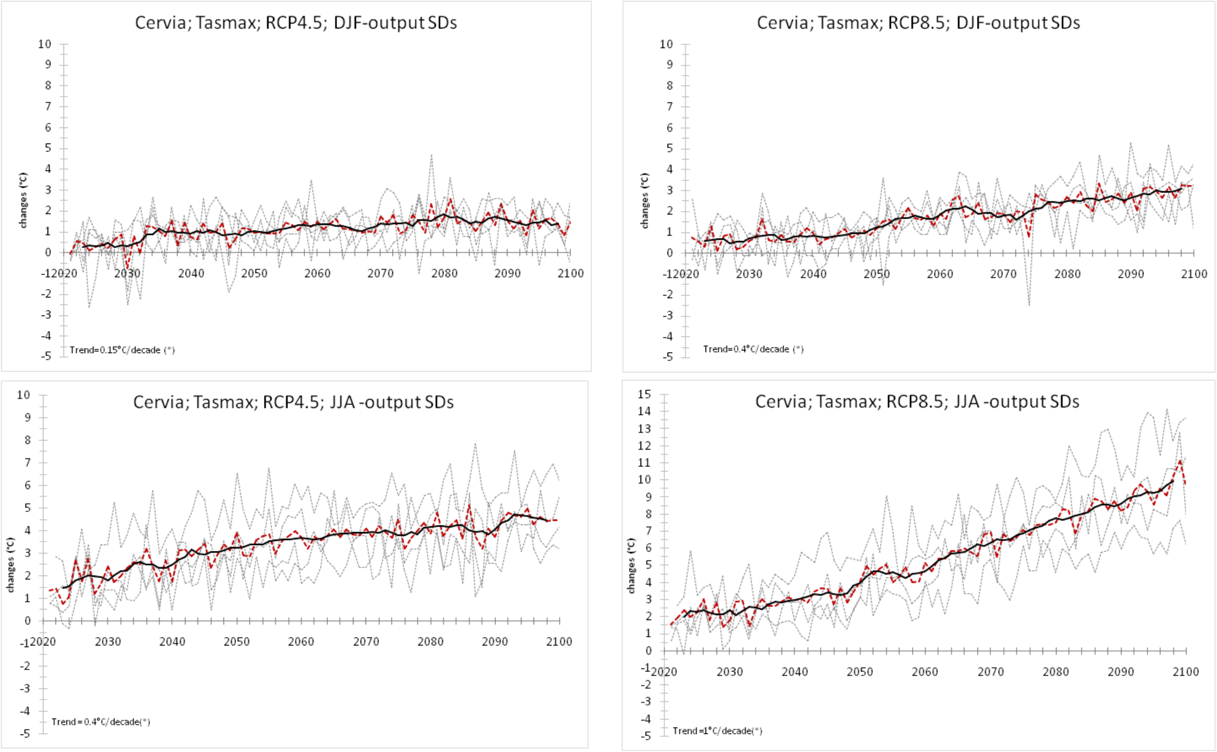

Figure 5-140: Variability of future changes of winter (DJF) and summer (JJA) maximum temperature projected through SDs applied to 4GCMs (grey lines); the Ensemble Mean (red line) and moving average (black line) - scenario RCP4.5 (left) and RCP8.5 (right), 2021-2100 period. Significant trend is marked with star while n.s. means not significant (source Arpae-Simc).

6.4.2.1.2 *Extreme temperature*

5th percentile of minimum temperature

The analysis performed on scenarios of extreme temperature, 5th minimum temperature and 95th maximum temperature reveals important future changes at Cervia-Pinarella grid point. An increase in *annual* 5th percentile of minimum temperature of 1°C is projected during the first period (2021-2040) and up to 2°C going to the end of century, in the framework of RP4.5 emission scenario. The signal became more intense for RCP8.5 emission scenario and especially during 2061-2080 and 2081-2100 periods, when the annual increases could reach 3°C during P3 and 4°C during P4 (see figure 5-141).

The projected changes are significant at seasonal and annual level, with higher amplitude during winter and autumn. The simulations shows in winter changes about 2 °C for RCP4.5 and 4°C for RCP8.5 while in autumn these are about 3 °C for RCP4.5 and 6.7°C for RCP8.5.

The long-term variability shows positive trends, both in winter and summer, statistically significant, but higher during winter season for RCP8.5 (see figure 5-142).

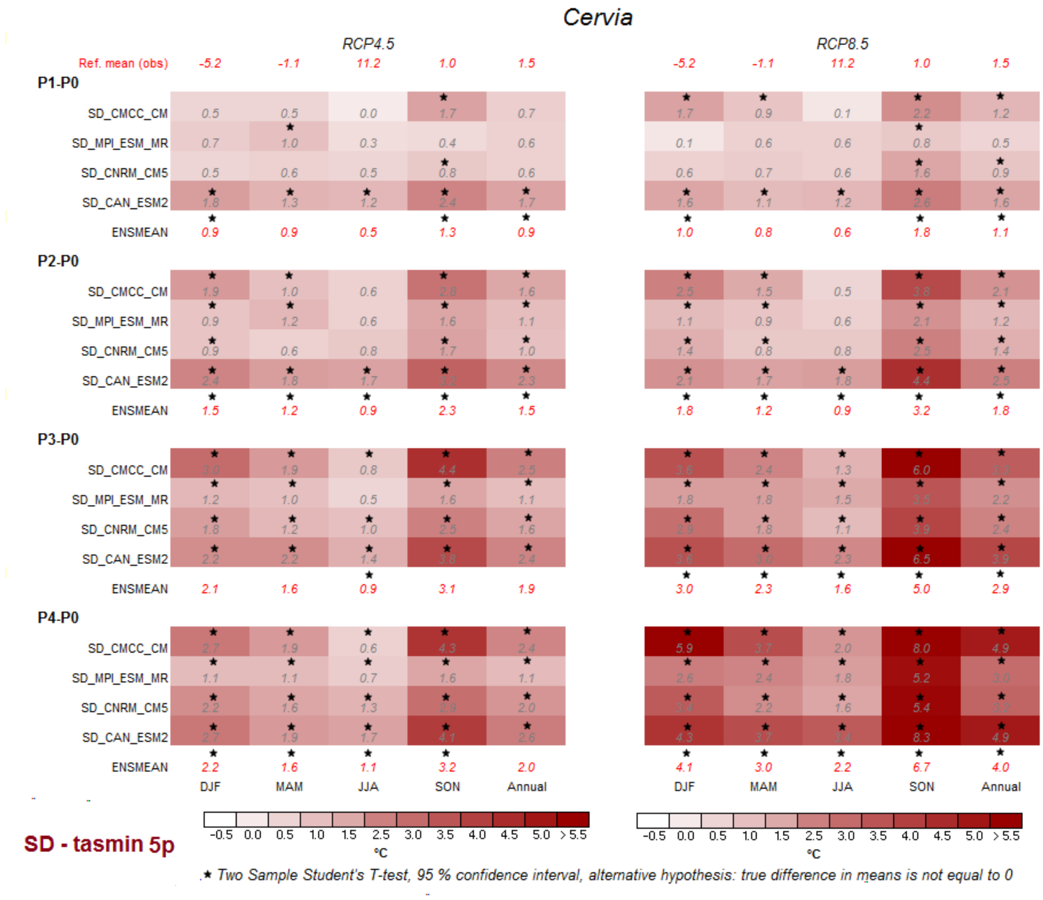

	RCP4.5					RCP8.5				
	DJF	MAM	JJA	SON	Annual	DJF	MAM	JJA	SON	Annual
Ref. mean (obs)	-5.2	-1.1	11.2	1.0	1.5	-5.2	-1.1	11.2	1.0	1.5
P1-P0										
SD_CMCC_CM	0.5	0.5	0.0	★ 1.7	0.7	★ 1.7	★ 0.9	0.1	★ 2.2	★ 1.2
SD_MPI_ESM_MR	0.7	★ 1.0	0.3	0.4	0.6	0.1	0.6	0.6	★ 0.8	0.5
SD_CNRM_CM5	0.5	0.6	0.5	★ 0.8	0.6	0.6	0.7	0.6	★ 1.6	★ 0.9
SD_CAN_ESM2	★ 1.8	★ 1.3	★ 1.2	★ 2.4	★ 1.7	★ 1.6	★ 1.1	★ 1.2	★ 2.6	★ 1.6
ENSMEAN	★ 0.9	0.9	0.5	★ 1.3	★ 0.9	★ 1.0	0.8	0.6	★ 1.8	★ 1.1
P2-P0										
SD_CMCC_CM	★ 1.9	★ 1.0	0.6	★ 2.8	★ 1.6	★ 2.5	★ 1.5	0.5	★ 3.8	★ 2.1
SD_MPI_ESM_MR	★ 0.9	★ 1.2	0.6	★ 1.6	★ 1.1	★ 1.1	★ 0.9	0.6	★ 2.1	★ 1.2
SD_CNRM_CM5	★ 0.9	0.6	0.8	★ 1.7	★ 1.0	★ 1.4	★ 0.8	0.8	★ 2.5	★ 1.4
SD_CAN_ESM2	★ 2.4	★ 1.8	★ 1.7	★ 3.2	★ 2.3	★ 2.1	★ 1.7	★ 1.8	★ 4.4	★ 2.5
ENSMEAN	★ 1.5	★ 1.2	★ 0.9	★ 2.3	★ 1.5	★ 1.8	★ 1.2	★ 0.9	★ 3.2	★ 1.8
P3-P0										
SD_CMCC_CM	★ 3.0	★ 1.9	★ 0.8	★ 4.4	★ 2.5	★ 3.6	★ 2.4	★ 1.3	★ 6.0	★ 3.3
SD_MPI_ESM_MR	★ 1.2	★ 1.0	0.5	★ 1.6	★ 1.1	★ 1.8	★ 1.8	★ 1.5	★ 3.5	★ 2.2
SD_CNRM_CM5	★ 1.8	★ 1.2	★ 1.0	★ 2.5	★ 1.6	★ 2.9	★ 1.8	★ 1.1	★ 3.9	★ 2.4
SD_CAN_ESM2	★ 2.2	★ 2.2	★ 1.4	★ 3.8	★ 2.4	★ 3.6	★ 3.0	★ 2.3	★ 6.5	★ 3.9
ENSMEAN	2.1	1.6	★ 0.9	3.1	1.9	★ 3.0	★ 2.3	★ 1.6	★ 5.0	★ 2.9
P4-P0										
SD_CMCC_CM	★ 2.7	★ 1.9	★ 0.6	★ 4.3	★ 2.4	★ 5.9	★ 3.7	★ 2.0	★ 8.0	★ 4.9
SD_MPI_ESM_MR	★ 1.1	★ 1.1	★ 0.7	★ 1.6	★ 1.1	★ 2.6	★ 2.4	★ 1.8	★ 5.2	★ 3.0
SD_CNRM_CM5	★ 2.2	★ 1.6	★ 1.3	★ 2.9	★ 2.0	★ 3.4	★ 2.2	★ 1.6	★ 5.4	★ 3.2
SD_CAN_ESM2	★ 2.7	★ 1.9	★ 1.7	★ 4.1	★ 2.6	★ 4.3	★ 3.7	★ 3.4	★ 8.3	★ 4.9
ENSMEAN	★ 2.2	★ 1.6	★ 1.1	★ 3.2	2.0	★ 4.1	★ 3.0	★ 2.2	★ 6.7	★ 4.0

SD - tasmin 5p

★ Two Sample Student's T-test, 95 % confidence interval, alternative hypothesis: true difference in means is not equal to 0

Figure 5-141: 5th percentile of seasonal and annual minimum temperature: observed values over reference period (in red), changes projected by statistical downscaling applied to 4GCMs and the Ensemble Mean of changes over the four periods (P1,P2,P3,P4) projected in the framework of RCP4.5 (left) and RCP 8.5 (right). Significant change is marked by star (source Arpae-Simc)

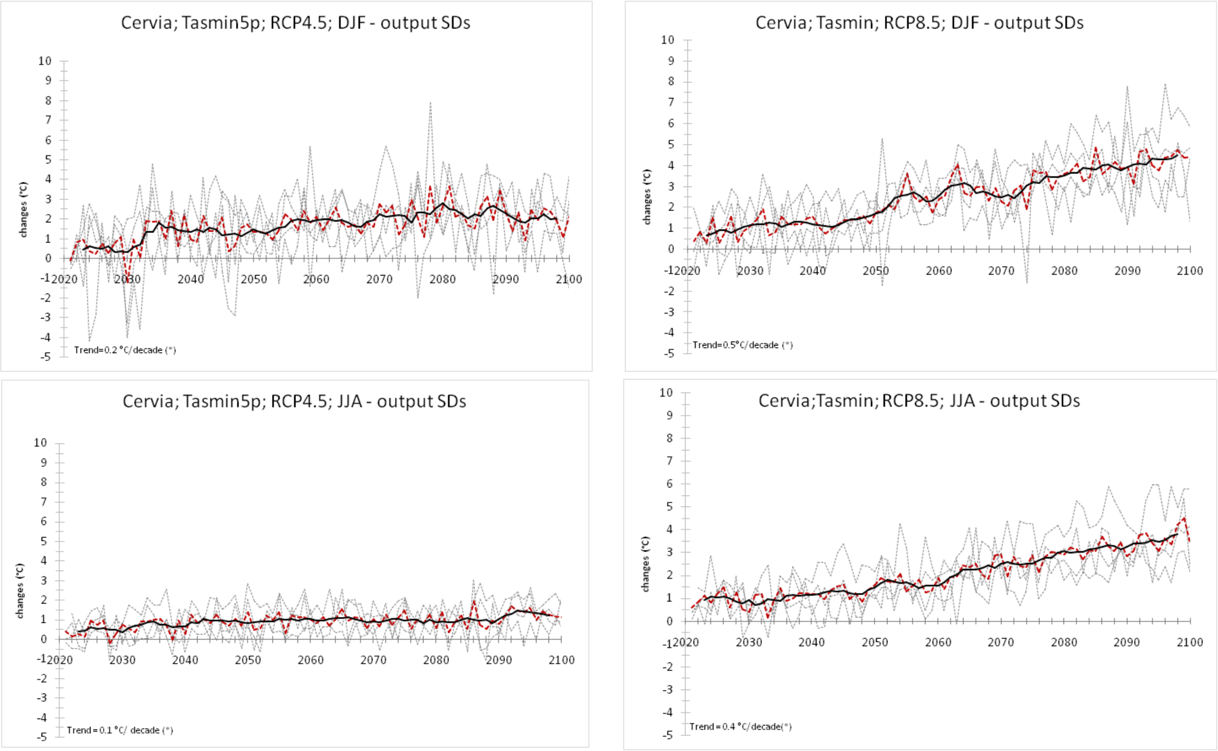

Figure 5-142: Variability of future changes of winter (DJF) and summer (JJA) 5th minimum temperature projected through SDs applied to 4GCMs (grey lines); the Ensemble Mean (red line) and moving average (black line) - scenario RCP4.5 (left) and RCP8.5 (right), 2021-2100 period Significant trend is marked with star while n.s. means not significant (source Arpae-Simc).

95thpercentile of maximum temperature

95th percentile of maximum temperature in Cervia- Pinarella grid point is projected to increase from P1 to P4 periods, with amplitudes that vary from model to model.
The Ensemble Mean shows an increase in annual value of changes between 1.1 and 2.4°C for RCP4.5 and between 1.3°C and 4.9°C in the framework of RCP8.5 from P1 to P4 periods (Figure 5-143). A deep analysis on projected changes reveals that higher values are expected to occur during summer season with peak of changes around 7.5°C during 2081-2100 with respect to 1986-2005 (RCP8.5). In addition, as could be noted the projected changes are similar for P1 and P2 in the framework of RCP4.5 and RCP8.5, but starting with P3 the changes have higher magnitude in RCP8.5.
Variability of future changes of 95th percentile of maximum temperature shows positive and significant trends during winter and summer, with trends coefficients between 0.2 and 0.5°C/decade (see figure5-144).

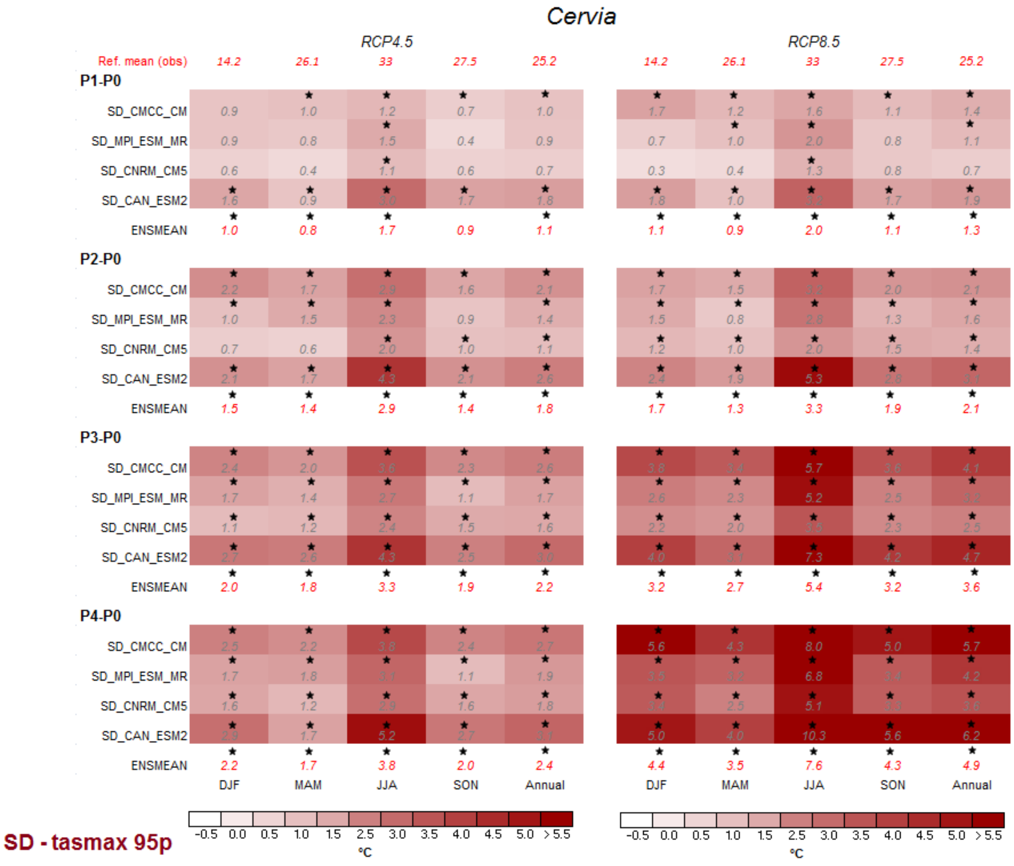

★ Two Sample Student's T-test, 95 % confidence interval, alternative hypothesis: true difference in means is not equal to 0

https://www.italy-croatia.eu/adriadapt

Figure 5-143: 95th percentile of seasonal and annual maximum temperature: observed values over reference period (in red), changes projected by statistical downscaling applied to 4GCMs and the Ensemble Mean of changes over the four periods (P1, P2, P3, P4) projected in the framework of RCP4.5 (left) and RCP 8.5 (right). Significant change is marked by star (source Arpae-Simc)

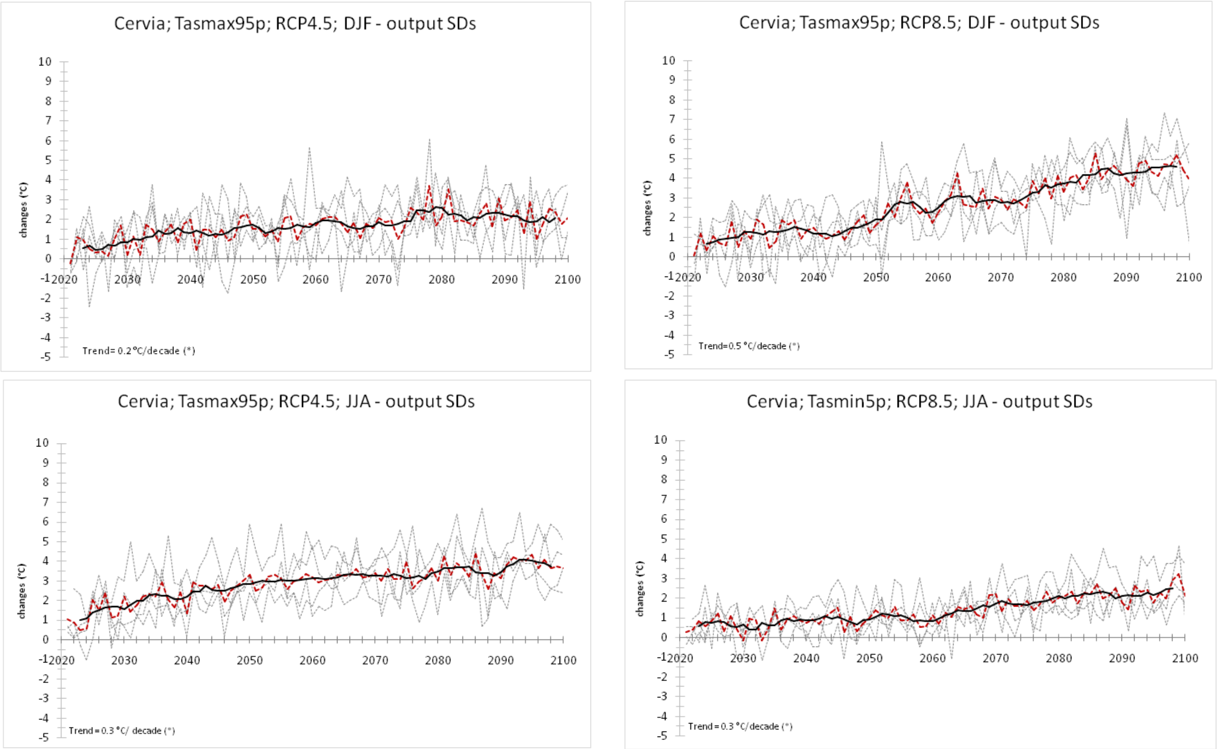

Figure 5-144: Future changes of winter (DJF) and summer (JJA) 95th percentile of maximum temperature projected through SDs applied to 4GCMs (grey lines); the Ensemble Mean (red line) and moving average (black line) - scenario RCP4.5 (left) and RCP8.5 (right), 2021-2100 period Significant trend is marked with star while n.s. means not significant (source Arpae-Simc).

6.4.2.1.3 *Heat wave duration*

The projection of the heat wave duration, index defined as the maximum number of consecutive days with maximum temperature greater than 90th daily percentile, shows an increase during spring and summer. Figure 5-145 includes the projected changes of the index for Cervia-Pinarella.

During spring, the increase could reach 36 consecutive days (P4) in RCP4.5 while in the framework of RCP8.5 could reach 58 consecutive days; in summer the projected changes is up to 63 consecutive days (P4) for RCP4.5 and up to 88 days for RCP8.5 (P4). As regards long term variability (see figure 5-146) the trend is positive during winter and summer, statistically significant during summer and higher especially for RCP8.5 (11 days/decade)

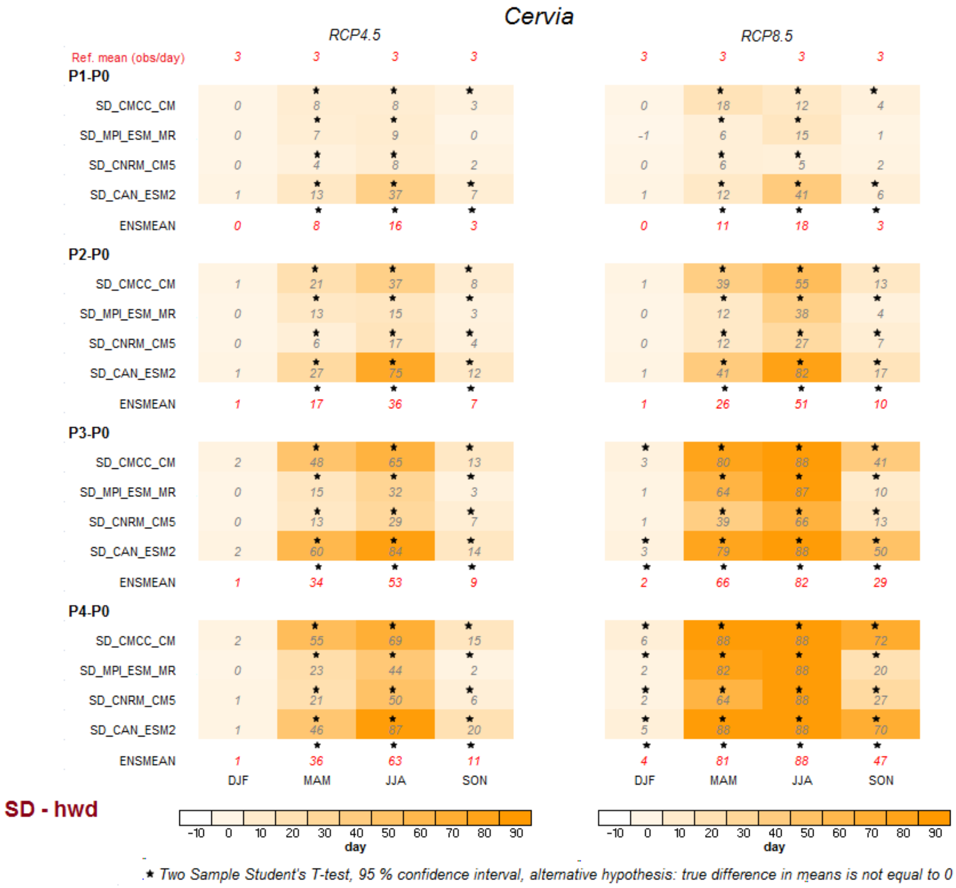

	RCP4.5				RCP8.5			
Ref. mean (obs/day)	3	3	3	3	3	3	3	3
P1-P0								
SD_CMCC_CM	0	★ 8	★ 8	★ 3	0	★ 18	★ 12	★ 4
SD_MPI_ESM_MR	0	★ 7	★ 9	0	-1	★ 6	★ 15	1
SD_CNRM_CM5	0	★ 4	★ 8	2	0	★ 6	★ 5	2
SD_CAN_ESM2	1	★ 13	★ 37	★ 7	1	★ 12	★ 41	★ 6
ENSMEAN	0	★ 8	★ 16	★ 3	0	★ 11	★ 18	★ 3
P2-P0								
SD_CMCC_CM	1	★ 21	★ 37	★ 8	1	★ 39	★ 55	★ 13
SD_MPI_ESM_MR	0	★ 13	★ 15	★ 3	0	★ 12	★ 38	★ 4
SD_CNRM_CM5	0	★ 6	★ 17	★ 4	0	★ 12	★ 27	★ 7
SD_CAN_ESM2	1	★ 27	★ 75	★ 12	1	★ 41	★ 82	★ 17
ENSMEAN	1	★ 17	★ 36	★ 7	1	★ 26	★ 51	★ 10
P3-P0								
SD_CMCC_CM	2	★ 48	★ 65	★ 13	★ 3	★ 80	★ 88	★ 41
SD_MPI_ESM_MR	0	★ 15	★ 32	★ 3	1	★ 64	★ 87	★ 10
SD_CNRM_CM5	0	★ 13	★ 29	★ 7	1	★ 39	★ 66	★ 13
SD_CAN_ESM2	2	★ 60	★ 84	★ 14	★ 3	★ 79	★ 88	★ 50
ENSMEAN	1	★ 34	★ 53	★ 9	★ 2	★ 66	★ 82	★ 29
P4-P0								
SD_CMCC_CM	2	★ 55	★ 69	★ 15	★ 6	★ 88	★ 88	★ 72
SD_MPI_ESM_MR	0	★ 23	★ 44	★ 2	★ 2	★ 82	★ 88	★ 20
SD_CNRM_CM5	1	★ 21	★ 50	★ 6	★ 2	★ 64	★ 88	★ 27
SD_CAN_ESM2	1	★ 46	★ 87	★ 20	★ 5	★ 88	★ 88	★ 70
ENSMEAN	1	★ 36	★ 63	★ 11	★ 4	★ 81	★ 88	★ 47
	DJF	MAM	JJA	SON	DJF	MAM	JJA	SON

★ Two Sample Student's T-test, 95 % confidence interval, alternative hypothesis: true difference in means is not equal to 0

Figure 5-145: Seasonal heat wave duration: observed values over reference period (in red), changes projected by statistical downscaling applied to 4GCMs and the Ensemble Mean of changes over the four periods (P1, P2, P3, P4) projected in the framework of RCP4.5 (left) and RCP 8.5 (right). Significant change is marked by star (source Arpae-Simc)

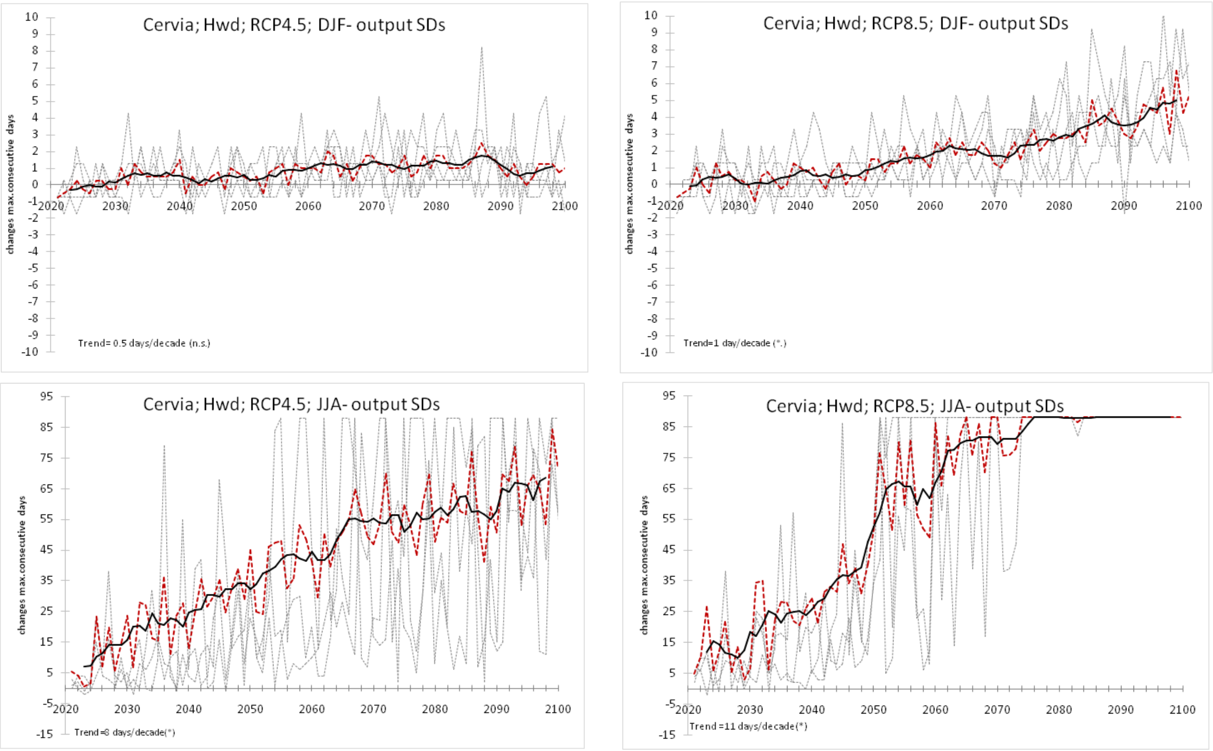

Figure 5-146: Variability of future changes of winter (DJF) and summer (JJA) heat wave duration projected through SDs applied to 4GCMs (grey lines); the Ensemble Mean (red line) and moving average (black line) - scenario RCP4.5 (left) and RCP8.5 (right), 2021-2100 period Significant trend is marked with star while n.s. means not significant (source Arpae-Simc).

6.4.2.1.4 *Tropical nights*

Seasonal changes of tropical nights (tr) in terms of differences between P1-P0, P2-P0, P3-P0, P4-P0 are shown in figures 5-147, relative to the RCP4.5 and RCP8.5 scenarios. The projection of the tropical nights, index defined as the number of days with minimum temperature greater than 20°C, shows an increase during summer season. All SDs models agree with these changes, as could be noted from figure 5-147. The value of changes varies during summer between 10 to 26 days for RCP4.5 and between 10 to 51 days for RC8.5.
Regarding long term variability of the index during summer season, the trend is positive and statistically significant for both RCPs, (up to 7 days/decade), over 2021-2100 (see figure 5-148).

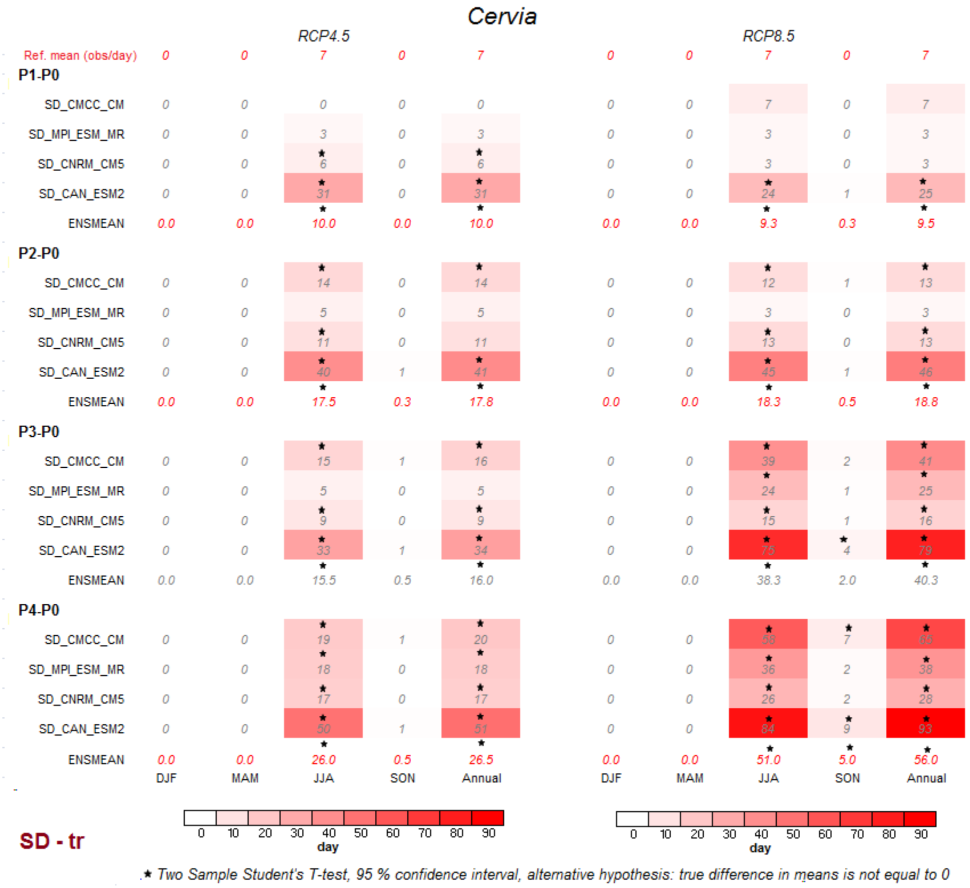

Cervia

	RCP4.5					RCP8.5				
	DJF	MAM	JJA	SON	Annual	DJF	MAM	JJA	SON	Annual
Ref. mean (obs/day)	0	0	7	0	7	0	0	7	0	7
P1-P0										
SD_CMCC_CM	0	0	0	0	0	0	0	7	0	7
SD_MPI_ESM_MR	0	0	3	0	3	0	0	3	0	3
SD_CNRM_CM5	0	0	★ 6	0	★ 6	0	0	3	0	3
SD_CAN_ESM2	0	0	★ 31	0	★ 31	0	0	★ 24	1	★ 25
ENSMEAN	0.0	0.0	★ 10.0	0.0	★ 10.0	0.0	0.0	★ 9.3	0.3	★ 9.5
P2-P0										
SD_CMCC_CM	0	0	★ 14	0	★ 14	0	0	★ 12	1	★ 13
SD_MPI_ESM_MR	0	0	5	0	5	0	0	3	0	3
SD_CNRM_CM5	0	0	★ 11	0	11	0	0	★ 13	0	★ 13
SD_CAN_ESM2	0	0	★ 40	1	★ 41	0	0	★ 45	1	★ 46
ENSMEAN	0.0	0.0	★ 17.5	0.3	★ 17.8	0.0	0.0	★ 18.3	0.5	★ 18.8
P3-P0										
SD_CMCC_CM	0	0	★ 15	1	★ 16	0	0	★ 39	2	★ 41
SD_MPI_ESM_MR	0	0	5	0	5	0	0	★ 24	1	★ 25
SD_CNRM_CM5	0	0	★ 9	0	★ 9	0	0	★ 15	1	★ 16
SD_CAN_ESM2	0	0	★ 33	1	★ 34	0	0	★ 75	★ 4	★ 79
ENSMEAN	0.0	0.0	★ 15.5	0.5	★ 16.0	0.0	0.0	★ 38.3	2.0	★ 40.3
P4-P0										
SD_CMCC_CM	0	0	★ 19	1	★ 20	0	0	★ 58	★ 7	★ 65
SD_MPI_ESM_MR	0	0	★ 18	0	★ 18	0	0	★ 36	2	★ 38
SD_CNRM_CM5	0	0	★ 17	0	★ 17	0	0	★ 26	2	★ 28
SD_CAN_ESM2	0	0	★ 50	1	★ 51	0	0	★ 84	★ 9	★ 93
ENSMEAN	0.0	0.0	★ 26.0	0.5	★ 26.5	0.0	0.0	★ 51.0	★ 5.0	★ 56.0

★ Two Sample Student's T-test, 95 % confidence interval, alternative hypothesis: true difference in means is not equal to 0

Figure 5-147: Seasonal and annual tropical nights: observed values over reference period (in red), changes projected by statistical downscaling applied to 4GCMs and the Ensemble Mean over the four periods (P1, P2, P3, P4) projected in the framework of RCP4.5 (left) and RCP 8.5 (right). Significant change is marked by star (source Arpae-Simc)

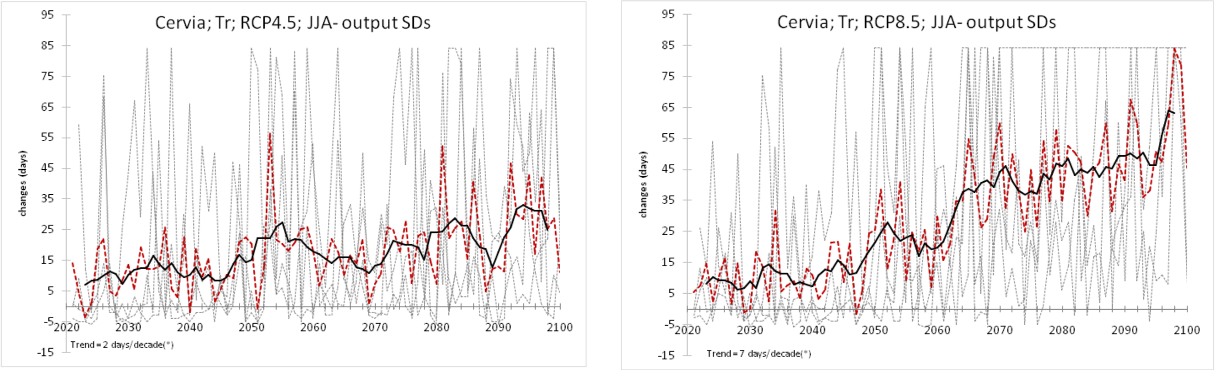

Figure 5-148: Variability of future changes of summer (JJA) tropical nights projected through SDs applied to 4GCMs (grey lines); the Ensemble Mean (red line) and moving average (black line) - scenario RCP4.5 (left) and RCP8.5 (right), 2021-2100 period Significant trend is marked with star while n.s. means not significant (source Arpae-Simc).

6.4.2.1.5 *Frost days*

The future projections of frost days, namely the number of days with minimum temperature lower than 0°C, show for Cervia-Pinarella a decrease during winter, spring and autumn. All SDs models agree with these changes during all periods, as could be noted from figure 5-73. The signal of changes is higher during winter season, when values of change for RCP4.5 scenario is between -10 days during P1 up to -19 days going to the end of the century (P4). The magnitude of changes is higher for RCP8.5 between -11 to -30 days (see figure 5-149). An important signal, statistically significant is expected also during spring and autumn, especially going to the end of century(see figure 5-149)
Regarding long term variability, the trend is negative and statistically significant for both emission scenario, up to -3 days/decade (see figure 5-150).

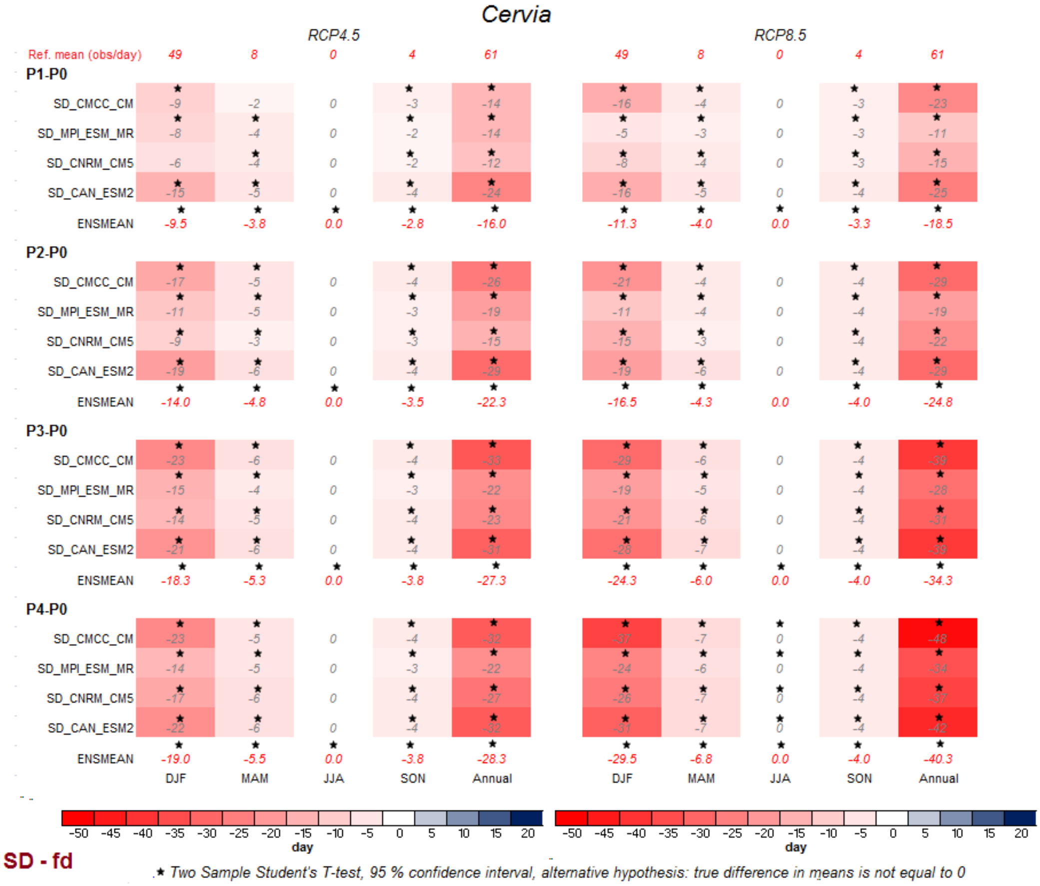

Cervia

	RCP4.5					RCP8.5				
Ref. mean (obs/day)	49	8	0	4	61	49	8	0	4	61
P1-P0										
SD_CMCC_CM	★ -9	-2	0	★ -3	★ -14	★ -16	★ -4	0	★ -3	★ -23
SD_MPI_ESM_MR	★ -8	★ -4	0	★ -2	★ -14	★ -5	★ -3	0	★ -3	★ -11
SD_CNRM_CM5	-6	★ -4	0	★ -2	★ -12	★ -8	★ -4	0	★ -3	★ -15
SD_CAN_ESM2	★ -15	★ -5	0	★ -4	★ -24	★ -16	★ -5	0	★ -4	★ -25
ENSMEAN	★ -9.5	★ -3.8	★ 0.0	★ -2.8	★ -16.0	★ -11.3	★ -4.0	★ 0.0	★ -3.3	★ -18.5
P2-P0										
SD_CMCC_CM	★ -17	★ -5	0	★ -4	★ -26	★ -21	★ -4	0	★ -4	★ -29
SD_MPI_ESM_MR	★ -11	★ -5	0	★ -3	★ -19	★ -11	★ -4	0	★ -4	★ -19
SD_CNRM_CM5	★ -9	★ -3	0	★ -3	★ -15	★ -15	★ -3	0	★ -4	★ -22
SD_CAN_ESM2	★ -19	★ -6	0	★ -4	★ -29	★ -19	★ -6	0	★ -4	★ -29
ENSMEAN	★ -14.0	★ -4.8	★ 0.0	★ -3.5	★ -22.3	★ -16.5	★ -4.3	0.0	★ -4.0	★ -24.8
P3-P0										
SD_CMCC_CM	★ -23	★ -6	0	★ -4	★ -33	★ -29	★ -6	0	★ -4	★ -39
SD_MPI_ESM_MR	★ -15	★ -4	0	★ -3	★ -22	★ -19	★ -5	0	★ -4	★ -28
SD_CNRM_CM5	★ -14	★ -5	0	★ -4	★ -23	★ -21	★ -6	0	★ -4	★ -31
SD_CAN_ESM2	★ -21	★ -6	0	★ -4	★ -31	★ -28	★ -7	0	★ -4	★ -39
ENSMEAN	★ -18.3	★ -5.3	★ 0.0	★ -3.8	★ -27.3	★ -24.3	★ -6.0	★ 0.0	★ -4.0	★ -34.3
P4-P0										
SD_CMCC_CM	★ -23	★ -5	0	★ -4	★ -32	★ -37	★ -7	★ 0	★ -4	★ -48
SD_MPI_ESM_MR	★ -14	★ -5	0	★ -3	★ -22	★ -24	★ -6	★ 0	★ -4	★ -34
SD_CNRM_CM5	★ -17	★ -6	0	★ -4	★ -27	★ -26	★ -7	★ 0	★ -4	★ -37
SD_CAN_ESM2	★ -22	★ -6	0	★ -4	★ -32	★ -31	★ -7	★ 0	★ -4	★ -42
ENSMEAN	★ -19.0	★ -5.5	★ 0.0	★ -3.8	★ -28.3	★ -29.5	★ -6.8	★ 0.0	★ -4.0	★ -40.3
	DJF	MAM	JJA	SON	Annual	DJF	MAM	JJA	SON	Annual

★ Two Sample Student's T-test, 95 % confidence interval, alternative hypothesis: true difference in means is not equal to 0

Figure 5-149: Seasonal and annual frost days: observed values over reference period (in red), changes projected by statistical downscaling applied to 4GCMs and the Ensemble Mean over the four periods (P1, P2, P3, P4) projected in the framework of RCP4.5 (left) and RCP 8.5(right). Significant change is marked by star (source Arpae-Simc)

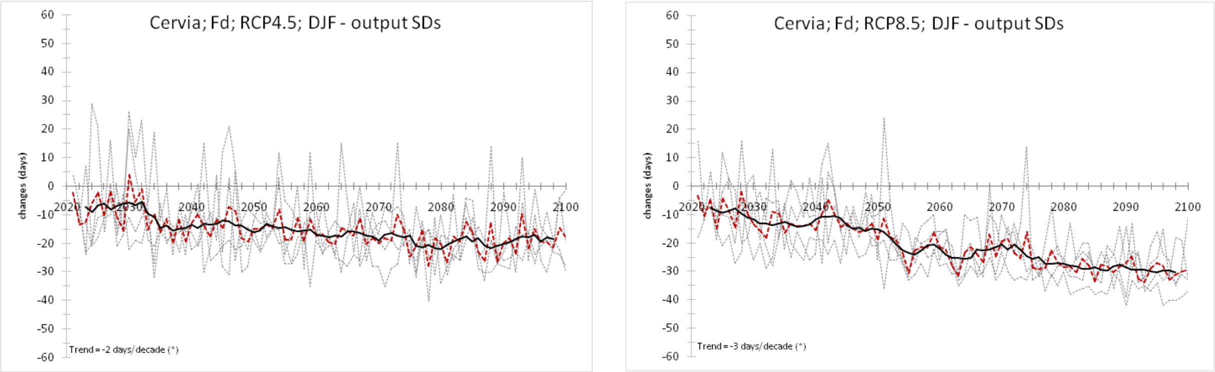

Figure 5-150: Future changes of winter (DJF) frost days projected through SDs applied to 4GCMs (grey lines); the Ensemble Mean (red line) and moving average (black line) - scenario RCP4.5 (left) and RCP8.5 (right), 2021-2100 period Significant trend is marked with star while n.s. means not significant (source Arpae-Simc).

6.4.2.2 *Precipitation related indices projection*

6.4.2.2.1 *Amount of precipitation*

The projected changes for amount of precipitation at Cervia-Pinarella show a general decrease over all period, seasons and for both emission scenarios. Analysing the changes presented in figure 5-151 it could be observed that all SDs agree with this signal and, especially after 2041 the changes are significant for all seasons. Higher decrease is expected to occur during summer, between -29 % (P1) up to -42% (P4) for RCP4.5 and between -32 % (P1) up to -63% (P4) for RCP8.5 (see figure 5-151). Long term variability underlies negative trends during winter and summer, significant only for RCP8.5 scenario (see figure 5-152).

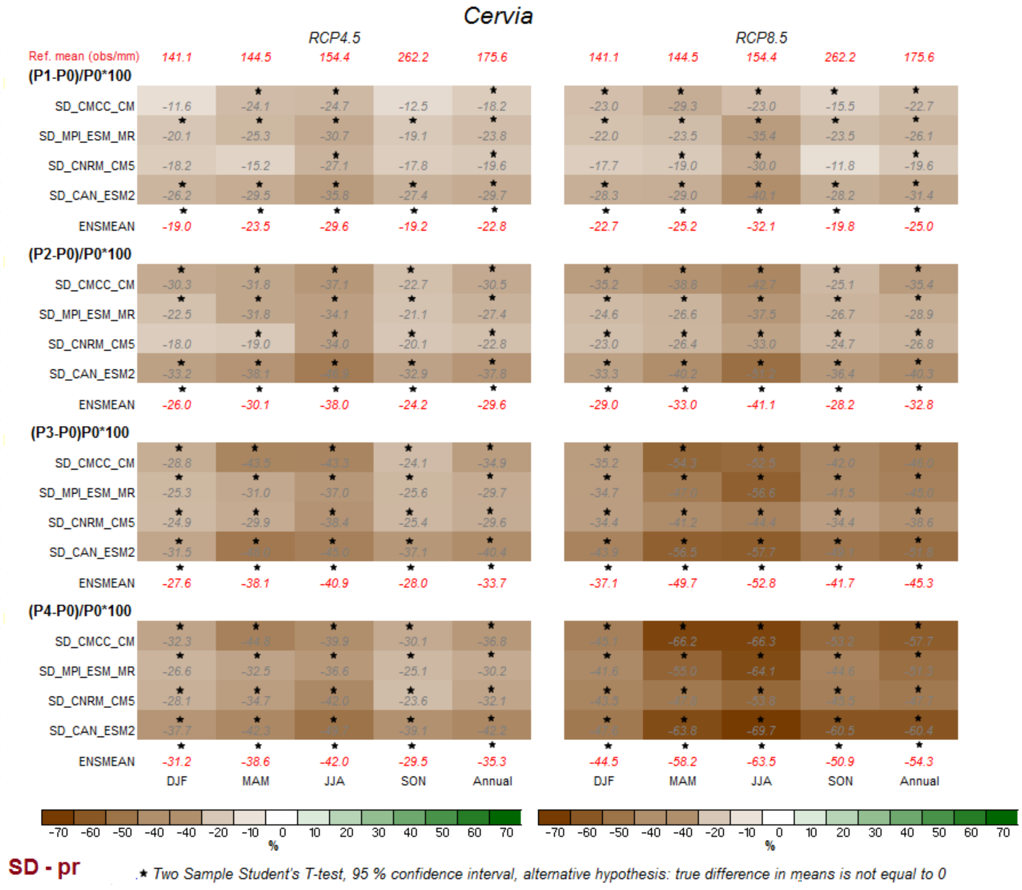

Cervia

	RCP4.5					RCP8.5				
Ref. mean (obs/mm)	141.1	144.5	154.4	262.2	175.6	141.1	144.5	154.4	262.2	175.6
(P1-P0)/P0*100										
SD_CMCC_CM	-11.6	★ -24.1	★ -24.7	-12.5	★ -18.2	★ -23.0	★ -29.3	★ -23.0	★ -15.5	★ -22.7
SD_MPI_ESM_MR	★ -20.1	★ -25.3	★ -30.7	★ -19.1	★ -23.8	★ -22.0	★ -23.5	★ -35.4	★ -23.5	★ -26.1
SD_CNRM_CM5	-18.2	-15.2	★ -27.1	-17.8	★ -19.6	-17.7	★ -19.0	★ -30.0	-11.8	★ -19.6
SD_CAN_ESM2	★ -26.2	★ -29.5	★ -35.8	★ -27.4	★ -29.7	★ -28.3	★ -29.0	★ -40.1	★ -28.2	★ -31.4
ENSMEAN	★ -19.0	★ -23.5	★ -29.6	★ -19.2	★ -22.8	★ -22.7	★ -25.2	★ -32.1	★ -19.8	★ -25.0
(P2-P0)/P0*100										
SD_CMCC_CM	★ -30.3	★ -31.8	★ -37.1	★ -22.7	★ -30.5	★ -35.2	★ -38.8	★ -42.7	★ -25.1	★ -35.4
SD_MPI_ESM_MR	★ -22.5	★ -31.8	★ -34.1	★ -21.1	★ -27.4	★ -24.6	★ -26.6	★ -37.5	★ -26.7	★ -28.9
SD_CNRM_CM5	-18.0	★ -19.0	★ -34.0	★ -20.1	★ -22.8	★ -23.0	★ -26.4	★ -33.0	★ -24.7	★ -26.8
SD_CAN_ESM2	★ -33.2	★ -38.1	★ -46.9	★ -32.9	★ -37.8	★ -33.3	★ -40.2	★ -51.2	★ -36.4	★ -40.3
ENSMEAN	★ -26.0	★ -30.1	★ -38.0	★ -24.2	★ -29.6	★ -29.0	★ -33.0	★ -41.1	★ -28.2	★ -32.8
(P3-P0)P0*100										
SD_CMCC_CM	★ -28.8	★ -43.5	★ -43.3	★ -24.1	★ -34.9	★ -35.2	★ -54.3	★ -52.5	★ -42.0	★ -46.0
SD_MPI_ESM_MR	★ -25.3	★ -31.0	★ -37.0	★ -25.6	★ -29.7	★ -34.7	★ -47.0	★ -56.6	★ -41.5	★ -45.0
SD_CNRM_CM5	★ -24.9	★ -29.9	★ -38.4	★ -25.4	★ -29.6	★ -34.4	★ -41.2	★ -44.4	★ -34.4	★ -38.6
SD_CAN_ESM2	★ -31.5	★ -48.0	★ -45.0	★ -37.1	★ -40.4	★ -43.9	★ -56.5	★ -57.7	★ -49.1	★ -51.8
ENSMEAN	★ -27.6	★ -38.1	★ -40.9	★ -28.0	★ -33.7	★ -37.1	★ -49.7	★ -52.8	★ -41.7	★ -45.3
(P4-P0)/P0*100										
SD_CMCC_CM	★ -32.3	★ -44.8	★ -39.9	★ -30.1	★ -36.8	★ -45.1	★ -66.2	★ -66.3	★ -53.2	★ -57.7
SD_MPI_ESM_MR	★ -26.6	★ -32.5	★ -36.6	★ -25.1	★ -30.2	★ -41.6	★ -55.0	★ -64.1	★ -44.6	★ -51.3
SD_CNRM_CM5	★ -28.1	★ -34.7	★ -42.0	★ -23.6	★ -32.1	★ -43.5	★ -47.8	★ -53.8	★ -45.5	★ -47.7
SD_CAN_ESM2	★ -37.7	★ -42.3	★ -49.7	★ -39.1	★ -42.2	★ -47.6	★ -63.8	★ -69.7	★ -60.5	★ -60.4
ENSMEAN	★ -31.2	★ -38.6	★ -42.0	★ -29.5	★ -35.3	★ -44.5	★ -58.2	★ -63.5	★ -50.9	★ -54.3
	DJF	MAM	JJA	SON	Annual	DJF	MAM	JJA	SON	Annual

SD - pr

★ *Two Sample Student's T-test, 95 % confidence interval, alternative hypothesis: true difference in means is not equal to 0*

Figure 5-151: Seasonal and annual amount of precipitation: observed values over reference period (in red), changes projected by statistical downscaling applied to 4GCMs and the Ensemble Mean of changes over the four periods (P1,P2,P3,P4) expressed in % RCP4.5 (left) and RCP 8.5 (right) scenarios. Significant change is marked by star (source Arpae-Simc)

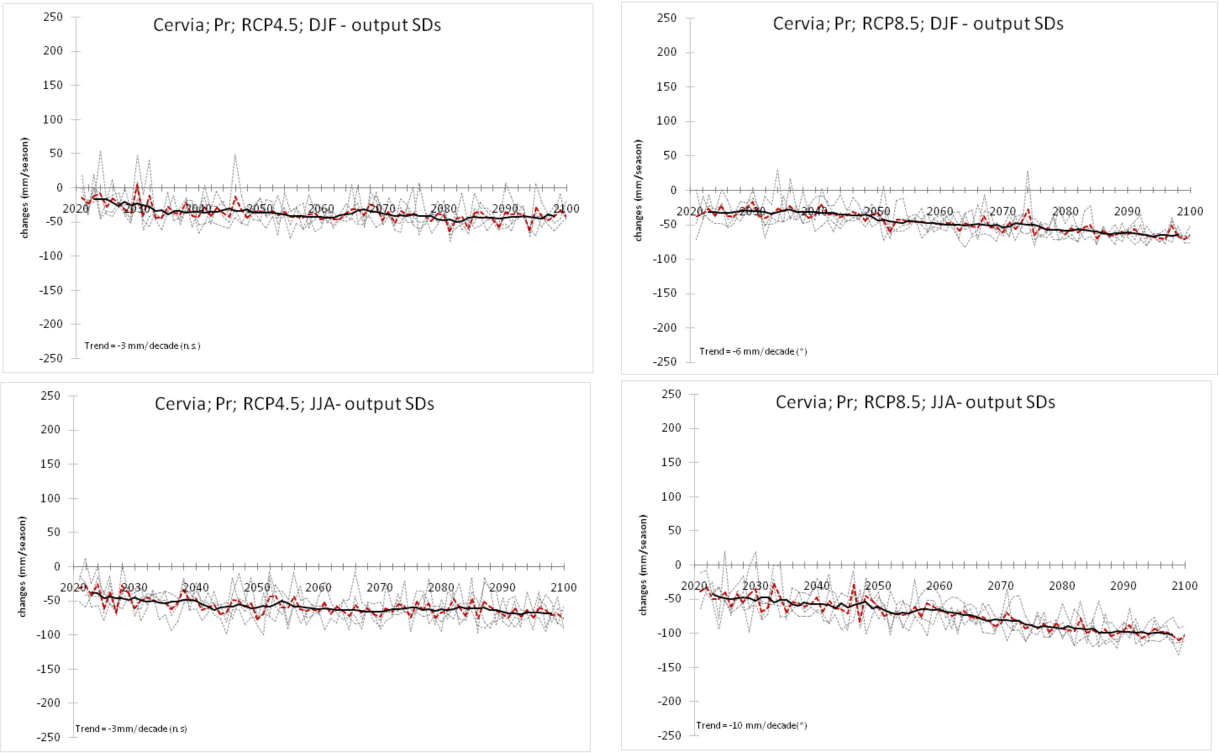

Figure 5-152: Variability of future changes of winter (DJF) and summer (JJA) precipitation projected through SDs applied to 4GCMs (grey lines); the Ensemble Mean (red line) and moving average (black line) - scenario RCP4.5 (left) and RCP8.5 (right), 2021-2100 period Significant trend is marked with star while n.s. means not significant (source Arpae-Simc).

6.4.2.2.2 *Intense precipitation*

90th percentile of seasonal amount of precipitation

Intense precipitation (Figure 5-153), defined by 90th percentile of precipitation in Cervia-Pinarella follow the precipitation patterns, namely a general decrease at annual and seasonal time scale. The annual decrease could reach -20% for RCP4.5 and -33% for RCP8.5. At seasonal level, winter has higher magnitude of decreases, followed by spring and autumn and summer (see figure 5-153). The long-term variability over 2021-2100 show no signal during summer, negative trend only in winter and for RCP8.5(see 5-154).

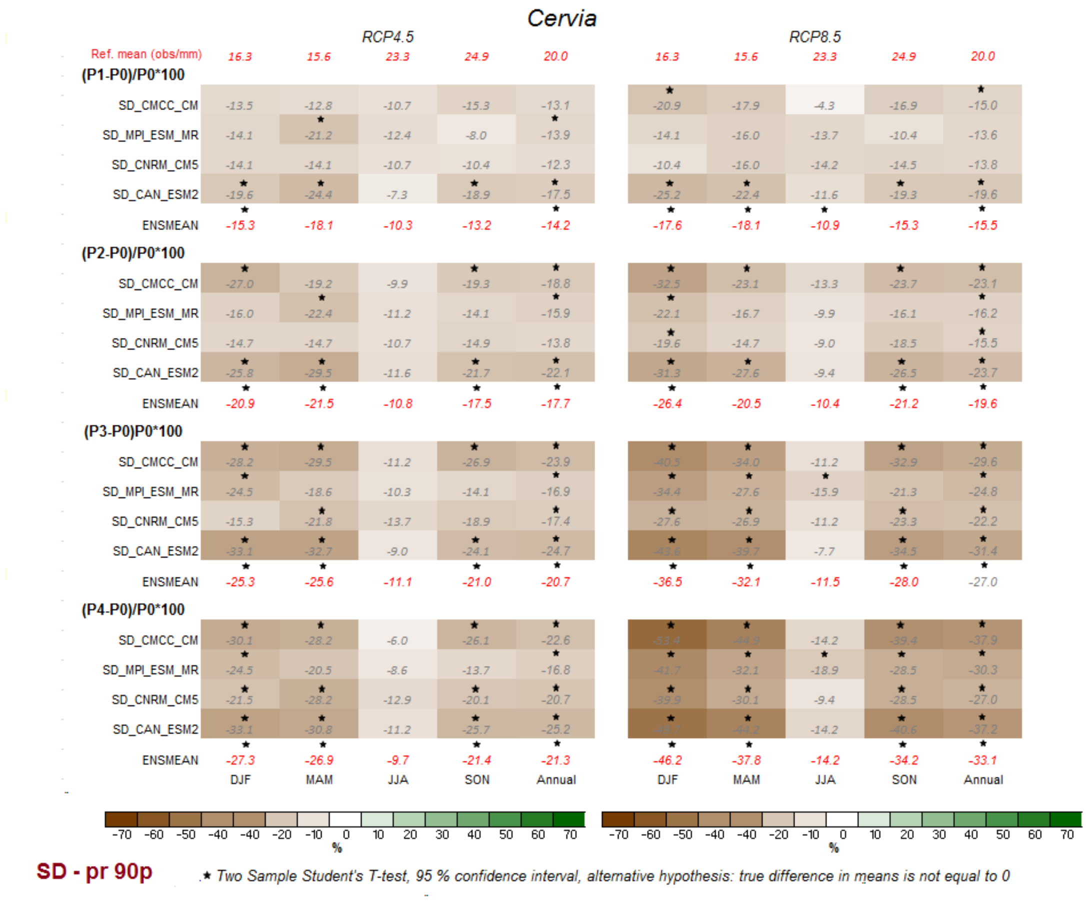

	RCP4.5					RCP8.5				
	DJF	MAM	JJA	SON	Annual	DJF	MAM	JJA	SON	Annual
Ref. mean (obs/mm)	16.3	15.6	23.3	24.9	20.0	16.3	15.6	23.3	24.9	20.0
(P1-P0)/P0*100										
SD_CMCC_CM	-13.5	-12.8	-10.7	-15.3	-13.1	★ -20.9	-17.9	-4.3	-16.9	★ -15.0
SD_MPI_ESM_MR	-14.1	★ -21.2	-12.4	-8.0	★ -13.9	-14.1	-16.0	-13.7	-10.4	-13.6
SD_CNRM_CM5	-14.1	-14.1	-10.7	-10.4	-12.3	-10.4	-16.0	-14.2	-14.5	-13.8
SD_CAN_ESM2	★ -19.6	★ -24.4	-7.3	★ -18.9	★ -17.5	★ -25.2	★ -22.4	-11.6	★ -19.3	★ -19.6
ENSMEAN	★ -15.3	-18.1	-10.3	-13.2	★ -14.2	★ -17.6	★ -18.1	★ -10.9	-15.3	★ -15.5
(P2-P0)/P0*100										
SD_CMCC_CM	★ -27.0	-19.2	-9.9	★ -19.3	★ -18.8	★ -32.5	★ -23.1	-13.3	★ -23.7	★ -23.1
SD_MPI_ESM_MR	-16.0	★ -22.4	-11.2	-14.1	★ -15.9	★ -22.1	-16.7	-9.9	-16.1	★ -16.2
SD_CNRM_CM5	-14.7	-14.7	-10.7	-14.9	-13.8	★ -19.6	-14.7	-9.0	-18.5	★ -15.5
SD_CAN_ESM2	★ -25.8	★ -29.5	-11.6	★ -21.7	★ -22.1	★ -31.3	★ -27.6	-9.4	★ -26.5	★ -23.7
ENSMEAN	★ -20.9	★ -21.5	-10.8	★ -17.5	★ -17.7	★ -26.4	-20.5	-10.4	★ -21.2	★ -19.6
(P3-P0)P0*100										
SD_CMCC_CM	★ -28.2	★ -29.5	-11.2	★ -26.9	★ -23.9	★ -40.5	★ -34.0	-11.2	★ -32.9	★ -29.6
SD_MPI_ESM_MR	★ -24.5	-18.6	-10.3	-14.1	★ -16.9	★ -34.4	★ -27.6	★ -15.9	-21.3	★ -24.8
SD_CNRM_CM5	-15.3	★ -21.8	-13.7	-18.9	★ -17.4	★ -27.6	★ -26.9	-11.2	★ -23.3	★ -22.2
SD_CAN_ESM2	★ -33.1	★ -32.7	-9.0	★ -24.1	★ -24.7	★ -43.6	★ -39.7	-7.7	★ -34.5	★ -31.4
ENSMEAN	★ -25.3	★ -25.6	-11.1	★ -21.0	★ -20.7	★ -36.5	★ -32.1	-11.5	★ -28.0	★ -27.0
(P4-P0)/P0*100										
SD_CMCC_CM	★ -30.1	★ -28.2	-6.0	★ -26.1	★ -22.6	★ -53.4	★ -44.9	-14.2	★ -39.4	★ -37.9
SD_MPI_ESM_MR	★ -24.5	-20.5	-8.6	-13.7	★ -16.8	★ -41.7	★ -32.1	★ -18.9	★ -28.5	★ -30.3
SD_CNRM_CM5	★ -21.5	★ -28.2	-12.9	★ -20.1	★ -20.7	★ -39.9	★ -30.1	-9.4	★ -28.5	★ -27.0
SD_CAN_ESM2	★ -33.1	★ -30.8	-11.2	★ -25.7	★ -25.2	★ -49.7	★ -44.2	-14.2	★ -40.6	★ -37.2
ENSMEAN	★ -27.3	★ -26.9	-9.7	★ -21.4	★ -21.3	★ -46.2	★ -37.8	-14.2	★ -34.2	★ -33.1

★ *Two Sample Student's T-test, 95 % confidence interval, alternative hypothesis: true difference in means is not equal to 0*

Figure 5-153: Seasonal amount of 90th precipitation: observed values over reference period (in red), changes projected by statistical downscaling applied to 4GCMs and the

Ensemble Mean over the four periods (P1, P2, P3, P4) projected in the framework of RCP4.5 (left) and RCP 8.5 (right). Significant change is marked by star (source Arpae-Simc)

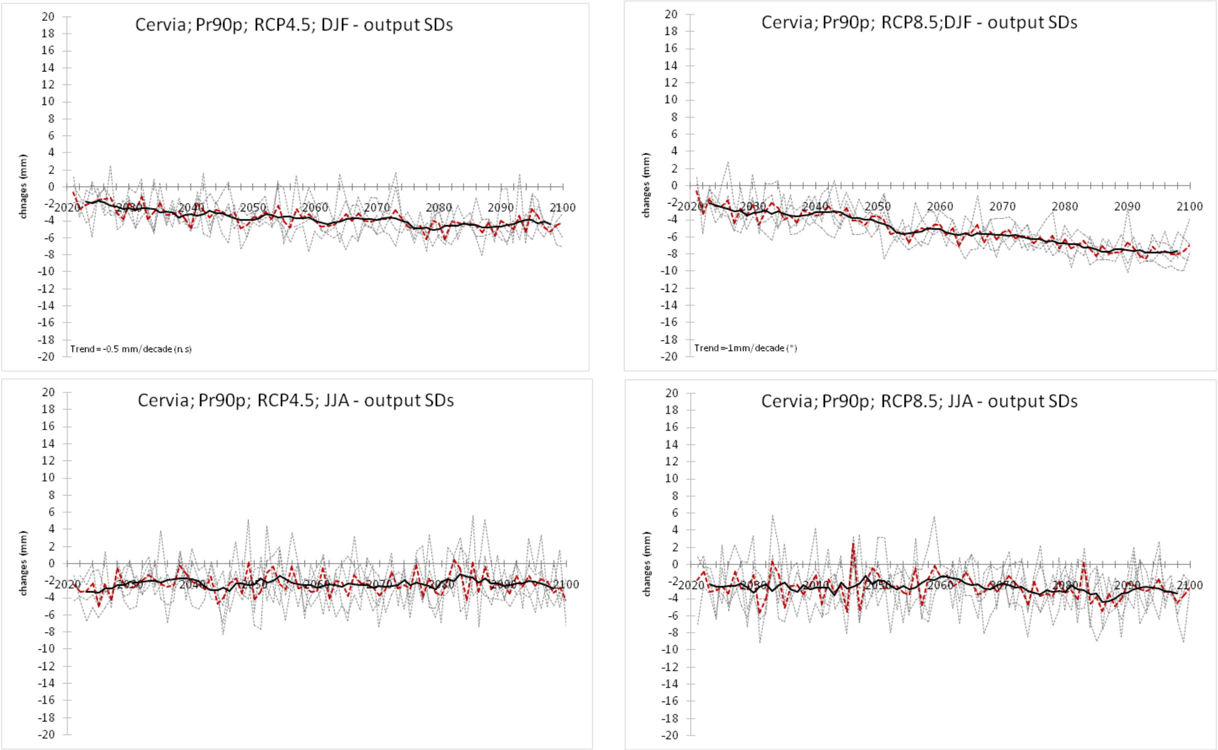

Figure 5-154: Future changes of winter (DJF) and summer (JJA) 90th precipitation projected through SDs applied to 4GCMs (grey lines); the Ensemble Mean (red line) and moving average (black line) - scenario RCP4.5 (left) and RCP8.5 (right), 2021-2100 period Significant trend is marked with star while n.s. means not significant (source Arpae-Simc).

6.4.2.2.3 *Consecutive dry days*

The projected changes of consecutive dry days at Cervia, index defined as the maximum number of consecutive days without precipitation, is presented in figure 5-155. The signal reveals an increase especially during spring and summer (starting from P1 to P4) and, a decrease in winter and autumn. High magnitude of increases is projected in spring, between 5 to 12 for RCP4.5 and between 5 to 30 for RCP8.5.

On the other hand, high magnitude of decreasing is projected in autumn, between -3 to -7 consecutive days. Long term variability presented in figure 5-156 show a positive trend of changes during summer and significant only for RCP8.5 (1.5 days/decade)

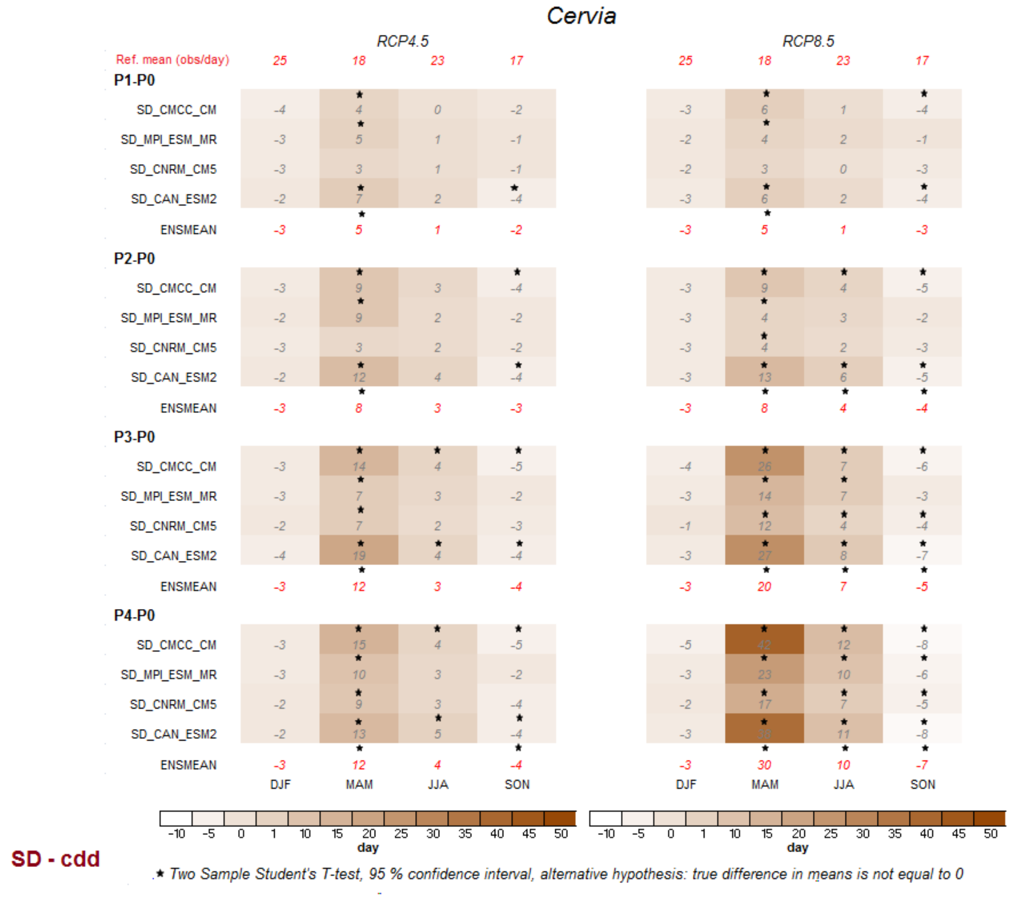

	RCP4.5				RCP8.5			
Ref. mean (obs/day)	25	18	23	17	25	18	23	17
P1-P0								
SD_CMCC_CM	-4	★ 4	0	-2	-3	★ 6	1	★ -4
SD_MPI_ESM_MR	-3	★ 5	1	-1	-2	★ 4	2	-1
SD_CNRM_CM5	-3	3	1	-1	-2	3	0	-3
SD_CAN_ESM2	-2	★ 7	2	★ -4	-3	★ 6	2	★ -4
ENSMEAN	-3	★ 5	1	-2	-3	★ 5	1	-3
P2-P0								
SD_CMCC_CM	-3	★ 9	3	★ -4	-3	★ 9	★ 4	★ -5
SD_MPI_ESM_MR	-2	★ 9	2	-2	-3	★ 4	3	-2
SD_CNRM_CM5	-3	3	2	-2	-3	★ 4	2	-3
SD_CAN_ESM2	-2	★ 12	4	★ -4	-3	★ 13	★ 6	★ -5
ENSMEAN	-3	★ 8	3	-3	-3	★ 8	★ 4	★ -4
P3-P0								
SD_CMCC_CM	-3	★ 14	★ 4	★ -5	-4	★ 26	★ 7	★ -6
SD_MPI_ESM_MR	-3	★ 7	3	-2	-3	★ 14	★ 7	-3
SD_CNRM_CM5	-2	★ 7	2	-3	-1	★ 12	★ 4	★ -4
SD_CAN_ESM2	-4	★ 19	★ 4	★ -4	-3	★ 27	★ 8	★ -7
ENSMEAN	-3	★ 12	3	-4	-3	★ 20	★ 7	★ -5
P4-P0								
SD_CMCC_CM	-3	★ 15	★ 4	★ -5	-5	★ 42	★ 12	★ -8
SD_MPI_ESM_MR	-3	★ 10	3	-2	-3	★ 23	★ 10	★ -6
SD_CNRM_CM5	-2	★ 9	3	-4	-2	★ 17	★ 7	★ -5
SD_CAN_ESM2	-2	★ 13	★ 5	★ -4	-3	★ 38	★ 11	★ -8
ENSMEAN	-3	★ 12	4	★ -4	-3	★ 30	★ 10	★ -7
	DJF	MAM	JJA	SON	DJF	MAM	JJA	SON

★ *Two Sample Student's T-test, 95 % confidence interval, alternative hypothesis: true difference in means is not equal to 0*

Figure 5-155: Seasonal and annual max. consecutive dry days: observed values over reference period (in red), changes projected by statistical downscaling applied to 4GCMs and the Ensemble Mean over the four periods (P1, P2, P3, P4) projected in the framework of RCP4,5 (left) and RCP 8.5 (right). Significant change is marked by star (source Arpae-Simc)

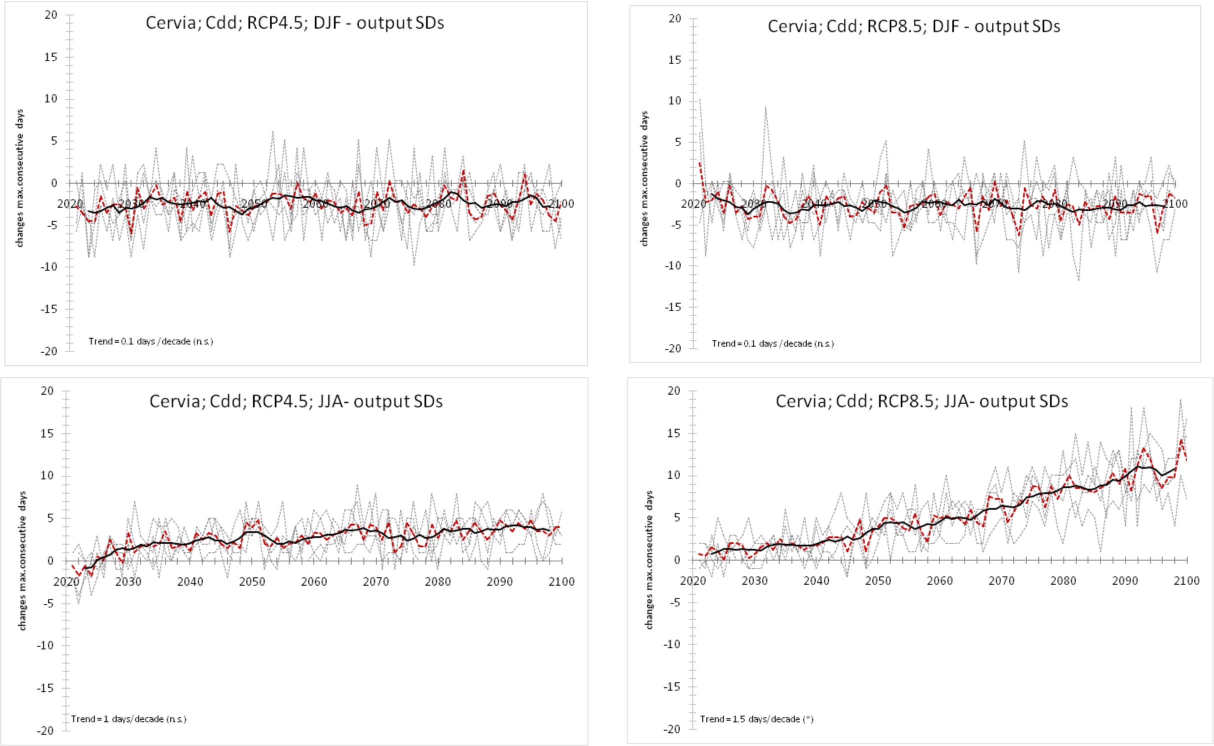

Figure 5-156: Variability of future changes of winter (DJF) and summer (JJA) max. number of consecutive dry days projected through SDs applied to 4GCMs (grey lines); the Ensemble Mean (red line) and moving average (black line) - scenario RCP4.5 (left) and RCP8.5 (right), 2021-2100 period Significant trend is marked with star while n.s. means not significant (source Arpae-Simc).

6.5 Case study 5: Cesena

6.5.1 Dynamically downscaled results

In this section we present future climate change of temperature and precipitation related indices, extra rare humidex and wind projections for Cesena. All indices are calculated from the available data set of regional climate models for the grid point that is representing the location of case study Cesena. Data set is obtained by bilinear interpolation. All data are presented as follows:

- Climate change diagram of an individual index in seasons and on annual basis for four considered future periods, for two emission scenarios RCP4.5 and RCP8.5. Climate change is calculated as difference between future and reference period (relative difference for precipitation indices, surface relative humidity and wind projections). Reference period is presented as ensemble mean of available regional climate models (Ref.mean), while climate change is shown for different models as well as for ensemble mean of models (ENSMEAN). Two sample Wilcoxon test is applied to test statistical significance of climate change for individual models (for 95 % confidence level). Significant change is marked by star
- Time series of future anomaly of an individual index for DJF and JJA and for two emission scenarios RCP4.5 and RCP8,5. Anomaly is calculated respect to the reference period and shown for individual models, ensemble mean and 5-year moving average. Mann Kendall trend test is applied to ensemble mean (for 95 % confidence level). Significant trend is marked with star (ns if not significant).

6.5.1.1 *Temperature related indices projections*

6.5.1.1.1 *Averaged 2 meter air temperature*

Averaged temperature change (Figure 5-157) in Cesena shows increase in all seasons and on annual scale, for all future periods (exception is in winter for one model realisation in first period). Although each model gives different amplitude of change, in ensemble mean the change is highest during summer or autumn and the smallest in winter and spring, for RCP4.5. The temperature increase is more pronounced towards the end of the century when the increase in the ensemble mean is from 1.5 °C in DJF and MAM to 2.0 °C in JJA. On annual scale for RCP4.5 temperature increase is for 1.7 °C. The amplitude of temperature change is more pronounced for RCP8.5 scenario, from 3.0 °C in MAM to 4.2 °C in JJA, on annual scale 3.7 °C at the end of 21st century for ensemble mean. The linear trend of temperature anomaly (Figure 5-158) in the future shows increase which is statistically significant for both considered seasons and both scenarios; for DJF ensemble is 0.20 °C / 10 year for RCP4.5 and 0.54 °C / 10 year for RCP8.5; for JJA ensemble is 0.16 °C / 10 year for RCP4.5 and 0.49 °C / 10 year.

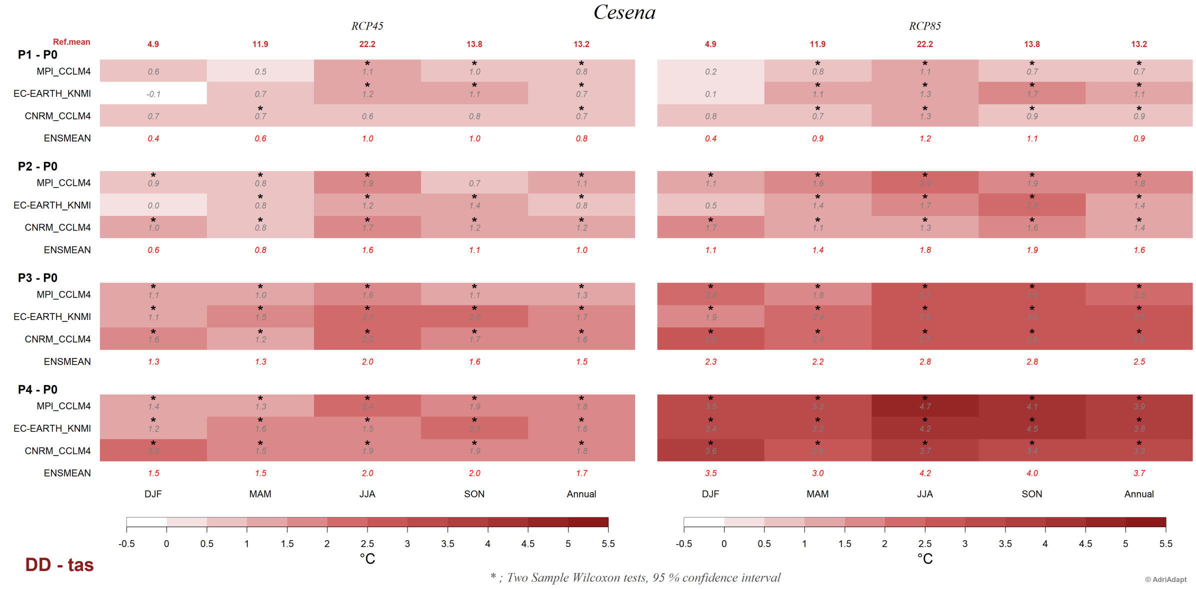

	RCP45					RCP85				
	DJF	MAM	JJA	SON	Annual	DJF	MAM	JJA	SON	Annual
Ref.mean	4.9	11.9	22.2	13.8	13.2	4.9	11.9	22.2	13.8	13.2
P1 - P0										
MPI_CCLM4	0.6	0.5	* 1.1	* 1.0	* 0.8	0.2	* 0.8	* 1.1	* 0.7	* 0.7
EC-EARTH_KNMI	-0.1	0.7	* 1.2	* 1.1	* 0.7	0.1	* 1.1	* 1.3	* 1.7	* 1.1
CNRM_CCLM4	0.7	* 0.7	0.6	0.8	* 0.7	0.8	* 0.7	* 1.3	* 0.9	* 0.9
ENSMEAN	0.4	0.6	1.0	1.0	0.8	0.4	0.9	1.2	1.1	0.9
P2 - P0										
MPI_CCLM4	* 0.9	* 0.8	* 1.9	0.7	* 1.1	* 1.1	* 1.6	* 2.4	* 1.9	* 1.8
EC-EARTH_KNMI	0.0	* 0.8	* 1.2	* 1.4	* 0.8	0.5	* 1.4	* 1.7	* 2.0	* 1.4
CNRM_CCLM4	* 1.0	* 0.8	* 1.7	* 1.2	* 1.2	* 1.7	* 1.1	* 1.3	* 1.6	* 1.4
ENSMEAN	0.6	0.8	1.6	1.1	1.0	1.1	1.4	1.8	1.9	1.6
P3 - P0										
MPI_CCLM4	* 1.1	* 1.0	* 1.6	* 1.1	* 1.3	* 2.4	* 1.8	* 2.7	* 2.9	* 2.5
EC-EARTH_KNMI	* 1.1	* 1.5	* 2.2	* 2.0	* 1.7	* 1.9	* 2.4	* 2.9	* 3.0	* 2.6
CNRM_CCLM4	* 1.6	* 1.2	* 2.0	* 1.7	* 1.6	* 2.6	* 2.4	* 2.7	* 2.6	* 2.6
ENSMEAN	1.3	1.3	2.0	1.6	1.5	2.3	2.2	2.8	2.8	2.5
P4 - P0										
MPI_CCLM4	* 1.4	* 1.3	* 2.4	* 1.9	* 1.8	* 3.5	* 3.3	* 4.7	* 4.1	* 3.9
EC-EARTH_KNMI	* 1.2	* 1.6	* 1.5	* 2.1	* 1.6	* 3.4	* 3.3	* 4.2	* 4.5	* 3.8
CNRM_CCLM4	* 2.0	* 1.5	* 1.9	* 1.9	* 1.8	* 3.6	* 2.6	* 3.7	* 3.4	* 3.3
ENSMEAN	1.5	1.5	2.0	2.0	1.7	3.5	3.0	4.2	4.0	3.7

* ; Two Sample Wilcoxon tests, 95 % confidence interval

Figure 5-157: Averaged seasonal and annual 2m air temperature (in °C) obtained by dynamical downscaling for Cesena: Ref. mean is 20 year simulated period (1986-2005) for ensemble mean; P1-P0, P2-P0, P3-P0, P4-P0 are changes in the future for following periods P1: 2021-2040, P2: 2041-2060, P3: 2061-2080, P4: 2081-2100. Differences are shown for individual models. Significant change is marked by star. Change is also shown as ensemble mean (ENSMEAN), not tested for significance. Left column is for RCP4.5 scenario and right for RCP8.5 scenario.

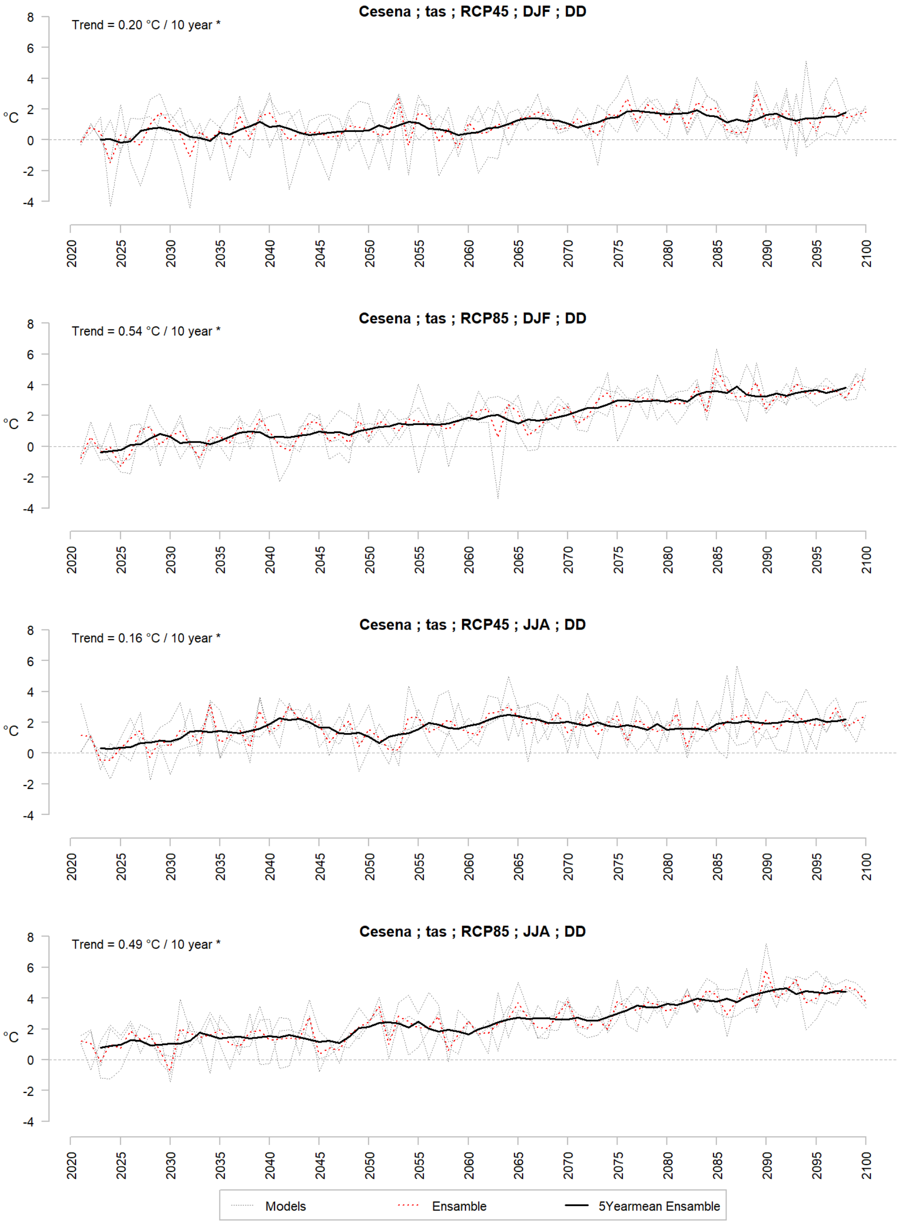

Figure 5-158: Variability of future 2m air temperature anomaly (in °C) in Cesena for 2021-2100 obtained by dynamically downscaling for winter (DJF) and summer (JJA) and two RCP scenarios: individual models are in grey, the ensemble mean in red, 5-year moving average in black. Significant trend is marked with star (ns if not significant).

6.5.1.1.2 *High temperature*

High temperature change (Figure 5-159), defined as 95th percentile of 2m air temperature, in Cesena is increasing from P1 to P4 future periods with the different amplitudes for each model. In ensemble mean at the end of century increase is from 1.5 °C in DJF to 2.8 °C in SON; 2.1 °C on annual scale for RCP4.5. Amplitude of change is more pronounced for RCP8.5 and is between 3.3 °C in DJF and 5.0 °C in SON, 4.6 °C for annual change at the end of 21st century. Variability of future 95th percentile of 2m air temperature anomaly (Figure 5-160) shows linear trend in change of ensemble mean, 0.17 °C / 10 year in DJF for RCP4.5 and 0.51 °C / 10 year for RCP8.5; 0.19 °C / 10 year in JJA for RCP4.5 and 0.56 °C / 10 year for RCP8.5. All trends are statistically significant.

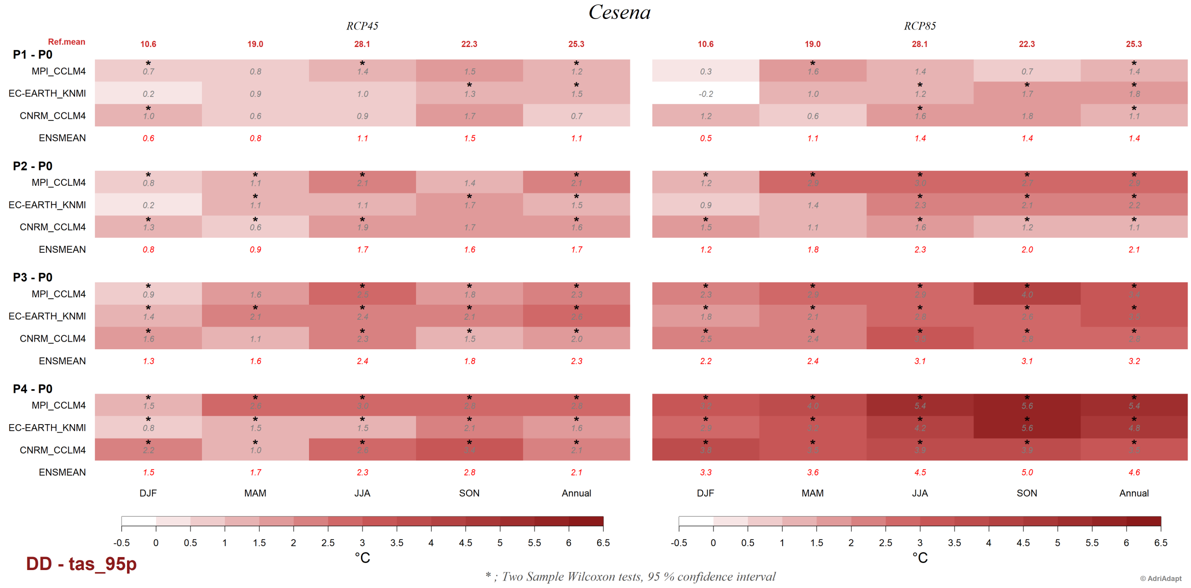

RCP45

	DJF	MAM	JJA	SON	Annual
Ref.mean	10.6	19.0	28.1	22.3	25.3
P1 - P0					
MPI_CCLM4	* 0.7	0.8	* 1.4	1.5	* 1.2
EC-EARTH_KNMI	0.2	0.9	1.0	* 1.3	* 1.5
CNRM_CCLM4	* 1.0	0.6	0.9	1.7	0.7
ENSMEAN	0.6	0.8	1.1	1.5	1.1
P2 - P0					
MPI_CCLM4	* 0.8	* 1.1	* 2.1	1.4	* 2.1
EC-EARTH_KNMI	0.2	* 1.1	1.1	* 1.7	* 1.5
CNRM_CCLM4	* 1.3	* 0.6	* 1.9	1.7	* 1.6
ENSMEAN	0.8	0.9	1.7	1.6	1.7
P3 - P0					
MPI_CCLM4	* 0.9	1.6	* 2.5	* 1.8	* 2.3
EC-EARTH_KNMI	* 1.4	* 2.1	* 2.4	* 2.1	* 2.6
CNRM_CCLM4	* 1.6	1.1	* 2.3	* 1.5	* 2.0
ENSMEAN	1.3	1.6	2.4	1.8	2.3
P4 - P0					
MPI_CCLM4	* 1.5	* 2.6	* 3.0	* 2.8	* 2.8
EC-EARTH_KNMI	* 0.8	* 1.5	* 1.5	* 2.1	* 1.6
CNRM_CCLM4	* 2.2	* 1.0	* 2.6	* 3.4	* 2.1
ENSMEAN	1.5	1.7	2.3	2.8	2.1

RCP85

	DJF	MAM	JJA	SON	Annual
Ref.mean	10.6	19.0	28.1	22.3	25.3
P1 - P0					
MPI_CCLM4	0.3	* 1.6	1.4	0.7	* 1.4
EC-EARTH_KNMI	-0.2	1.0	* 1.2	* 1.7	* 1.8
CNRM_CCLM4	1.2	0.6	* 1.6	1.8	* 1.1
ENSMEAN	0.5	1.1	1.4	1.4	1.4
P2 - P0					
MPI_CCLM4	* 1.2	* 2.9	* 3.0	* 2.7	* 2.9
EC-EARTH_KNMI	0.9	1.4	* 2.3	* 2.1	* 2.2
CNRM_CCLM4	* 1.5	1.1	* 1.6	* 1.2	* 1.1
ENSMEAN	1.2	1.8	2.3	2.0	2.1
P3 - P0					
MPI_CCLM4	* 2.3	* 2.9	* 2.9	* 4.0	* 3.4
EC-EARTH_KNMI	* 1.8	* 2.1	* 2.8	* 2.6	* 3.5
CNRM_CCLM4	* 2.5	* 2.4	* 3.5	* 2.8	* 2.8
ENSMEAN	2.2	2.4	3.1	3.1	3.2
P4 - P0					
MPI_CCLM4	* 3.2	* 4.0	* 5.4	* 5.6	* 5.4
EC-EARTH_KNMI	* 2.9	* 3.2	* 4.2	* 5.6	* 4.8
CNRM_CCLM4	* 3.8	* 3.5	* 3.9	* 3.9	* 3.5
ENSMEAN	3.3	3.6	4.5	5.0	4.6

** ; Two Sample Wilcoxon tests, 95 % confidence interval*

Figure 5-159: Seasonal and annual 95th percentile of 2m air temperature (high temperature, in °C) obtained by dynamical downscaling for Cesena: Ref. mean is 20 year simulated period (1986-2005) for ensemble mean; P1-P0, P2-P0, P3-P0, P4-P0 are changes in the future for following periods P1: 2021-2040, P2: 2041-2060, P3: 2061-2080, P4: 2081-2100. Differences are shown for individual models. Significant change is marked by star. Change is also shown as ensemble mean (ENSMEAN), not tested for significance. Left column is for RCP4.5 scenario and right for RCP8.5 scenario.

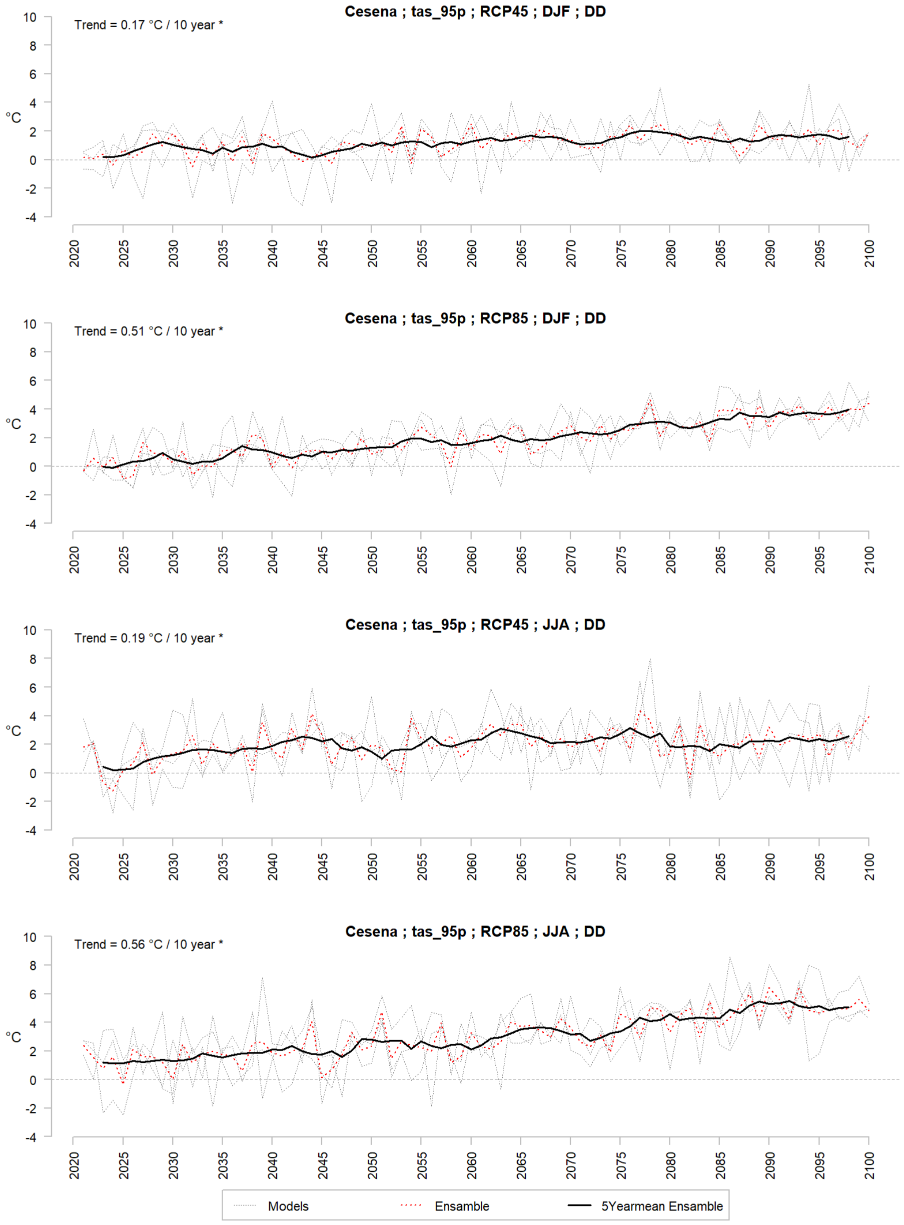

Figure 5-160: Variability of future 95th percentile of 2m air temperature (high temperature) anomaly (in °C) in Cesena for 2021-2100 obtained by dynamically downscaling for winter (DJF) and summer (JJA) and two RCP scenarios: individual models are in grey, the ensemble mean in red, 5-year moving average in black. Significant trend is marked with star (ns if not significant).

6.5.1.1.3 *High maximum temperature*

High maximum temperature change (Figure 5-161), defined as 95th percentile of 2m maximum air temperature, in Cesena is increasing from P1 to P4 future periods with the different amplitudes for each model. In ensemble mean at the end of century increase is from 1.7 °C in DJF to 2.7 °C in SON, 2.1 °C on annual scale for RCP4.5. Amplitude of change is more pronounced for RCP8.5 and is between 3.4 °C in DJF and 5.0 °C in SON, 4.4 °C for annual change at the end of 21st century. Variability of future 95th percentile of 2m maximum air temperature anomaly (Figure 5-162) shows linear trend in change of ensemble mean, 0.17 °C / 10 year in DJF for RCP4.5 and 0.51 °C / 10 year for RCP8.5; 0.19 °C / 10 year in JJA for RCP4.5 and 0.56 °C / 10 year for RCP8.5. All trends are statistically significant.

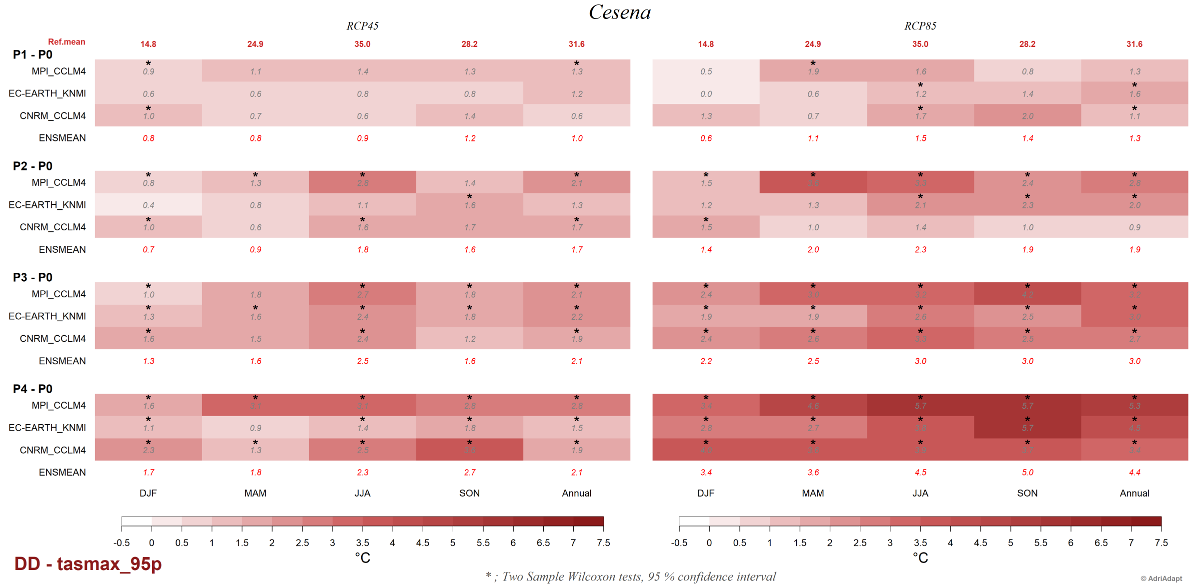

Figure 5-161: Seasonal and annual 95th percentile of 2m maximum air temperature (high maximum temperature, in °C) obtained by dynamical downscaling for Cesena: Ref. mean is 20 year simulated period (1986-2005) for ensemble mean; P1-P0, P2-P0, P3-P0, P4-P0 are changes in the future for following periods P1: 2021-2040, P2: 2041-2060, P3: 2061-2080, P4: 2081-2100. Differences are shown for individual models. Significant change is marked by star. Change is also shown as ensemble mean (ENSMEAN), not tested for significance. Left column is for RCP4.5 scenario and right for RCP8.5 scenario.

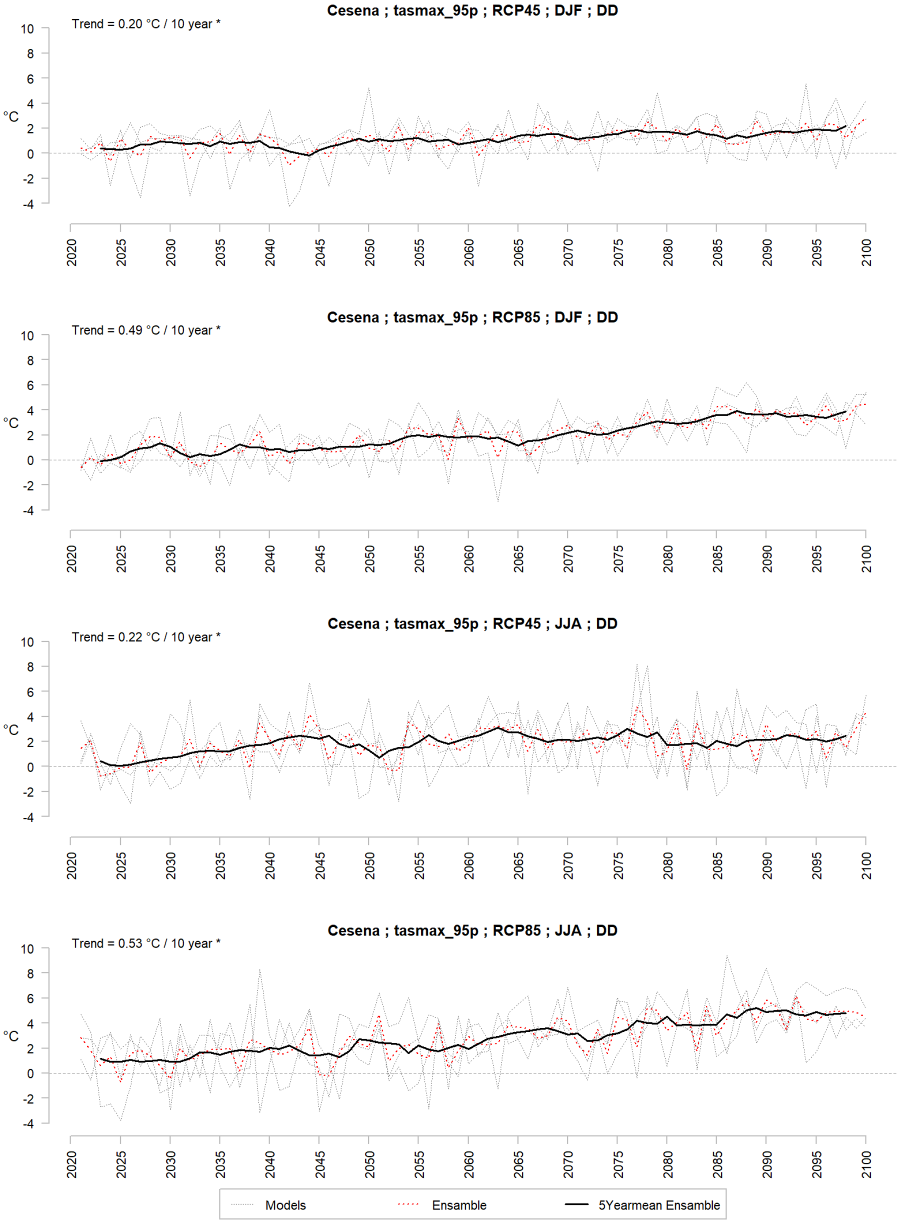

Figure 5-162: Variability of future 95th percentile of 2m maximum air temperature (high maximum temperature) anomaly (in °C) in Cesena for 2021-2100 obtained by dynamically downscaling for winter (DJF) and summer (JJA) and two RCP scenarios: individual models are in grey, the ensemble mean in red, 5-year moving average in black. Significant trend is marked with star (ns if not significant).

6.5.1.1.4 *Extreme high temperature*

99th percentile of 2m air temperature (Figure 5-163) in Cesena is increasing from P1 to P4 future periods with the different amplitudes for each model. In ensemble mean at the end of century increase is from 1.4 °C in DJF to 2.6 °C in SON, 2.4 °C on annual scale for RCP4.5. Amplitude of change is more pronounced for RCP8.5 and is between 3.1 °C in DJF and 5.4 °C in SON, 4.6 °C for annual change at the end of 21st century. Variability of future 99th percentile of 2m air temperature anomaly (Figure 5-164) shows linear trend in change of ensemble mean, 0.18 °C / 10 year in DJF for RCP4.5 and 0.49 °C / 10 year for RCP8.5; 0.20 °C / 10 year in JJA for RCP4.5 and 0.55 °C / 10 year for RCP8.5. All trends are statistically significant.

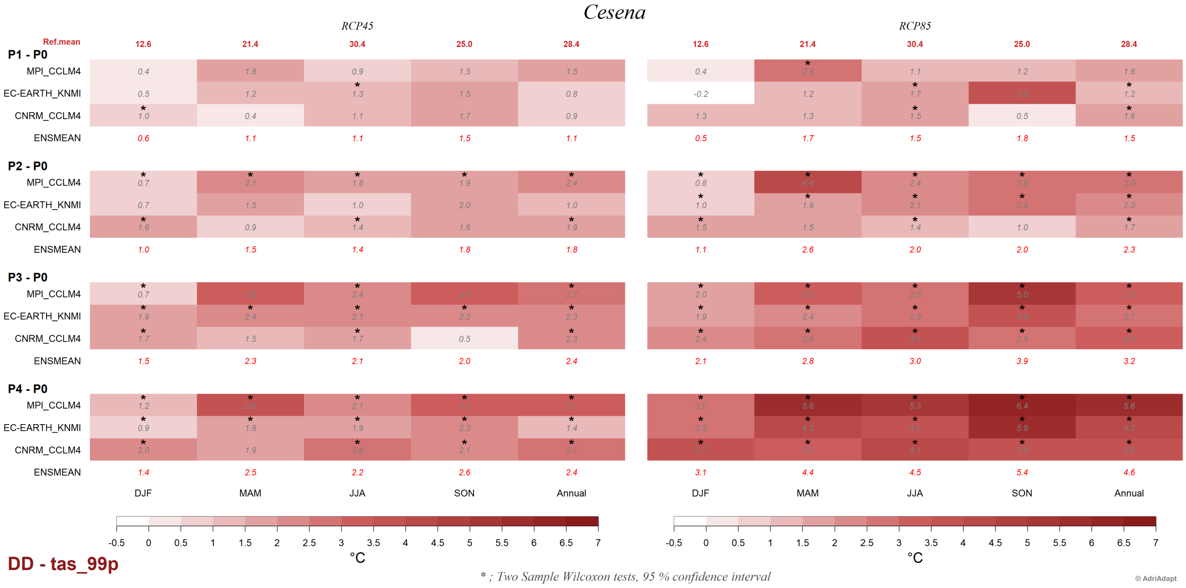

Figure 5-163: Seasonal and annual 99th percentile of 2m air temperature (extreme high temperature, in °C) obtained by dynamical downscaling for Cesena: Ref. mean is 20 year simulated period (1986-2005) for ensemble mean; P1-P0, P2-P0, P3-P0, P4-P0 are changes in the future for following periods P1: 2021-2040, P2: 2041-2060, P3: 2061-2080, P4: 2081-2100. Differences are shown for individual models. Significant change is marked by star. Change is also shown as ensemble mean (ENSMEAN), not tested for significance. Left column is for RCP4.5 scenario and right for RCP8.5 scenario.

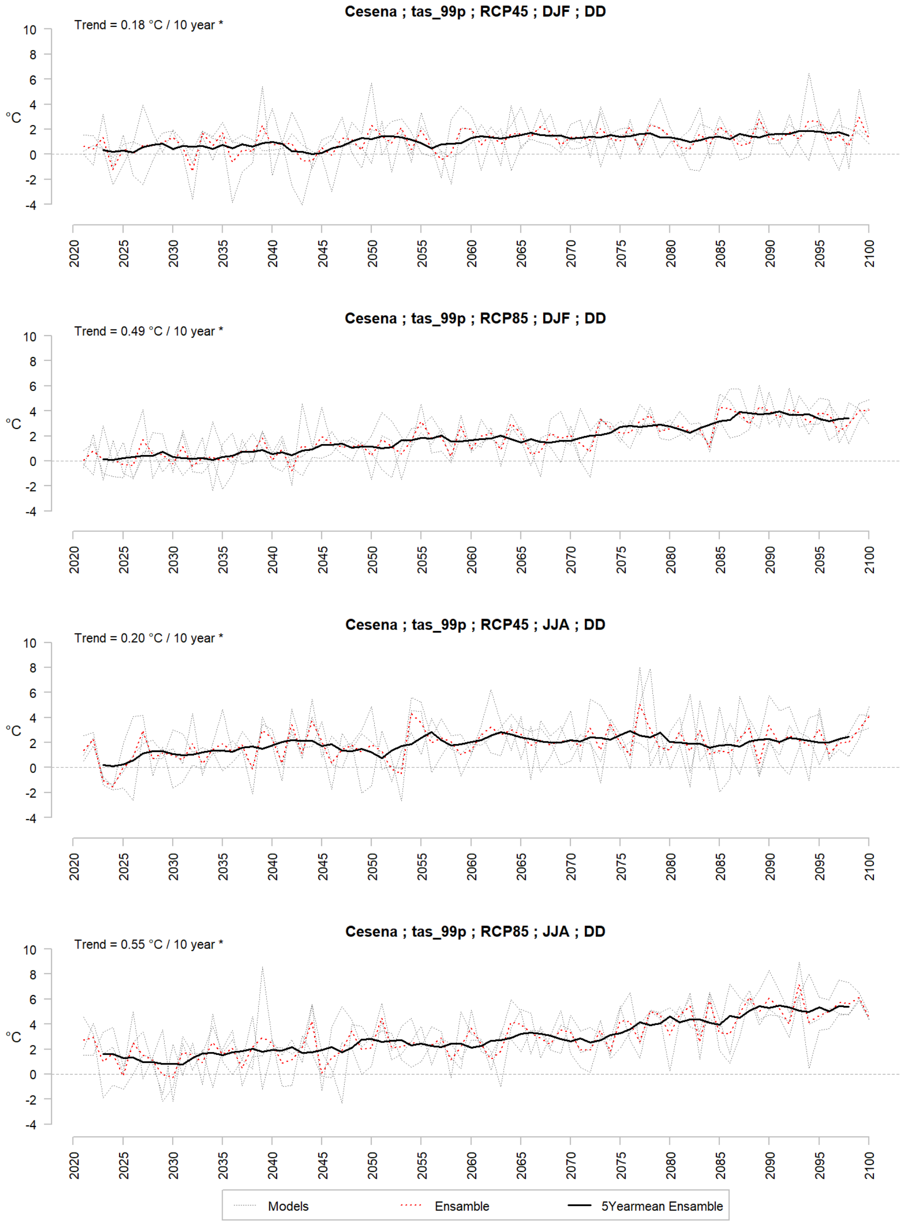

Figure 5-164: Variability of future 99th percentile of 2m air temperature (extreme high temperature) anomaly (in °C) in Cesena for 2021-2100 obtained by dynamically downscaling for winter (DJF) and summer (JJA) and two RCP scenarios: individual models are in grey, the ensemble mean in red, 5-year moving average in black. Significant trend is marked with star (ns if not significant).

6.5.1.1.5 *Extreme high maximum temperature*

Future change of 99th percentile of 2m maximum air temperature (Figure 5-165) in Cesena is changing from P1 to P4 periods with the different amplitudes for each model and mostly increase. Ensemble mean of change is positive for all periods. At the end of century increase is from 1.9 °C in DJF to 2.9 °C in MAM, 2.2 °C on annual scale for RCP4.5. Amplitude of change is more pronounced for RCP8.5 and is between 3.4 °C in DJF and 5.0 °C in SON, 4.3 °C for annual change at the end of 21st century. Variability of future 99th percentile of 2m maximum air temperature anomaly (Figure 5-166) shows linear trend in change of ensemble mean, 0.21 °C / 10 year in DJF for RCP4.5 and 0.51 °C / 10 year for RCP8.5; 0.22 °C / 10 year in JJA for RCP4.5 and 0.60 °C / 10 year for RCP8.5. All trends are statistically significant.

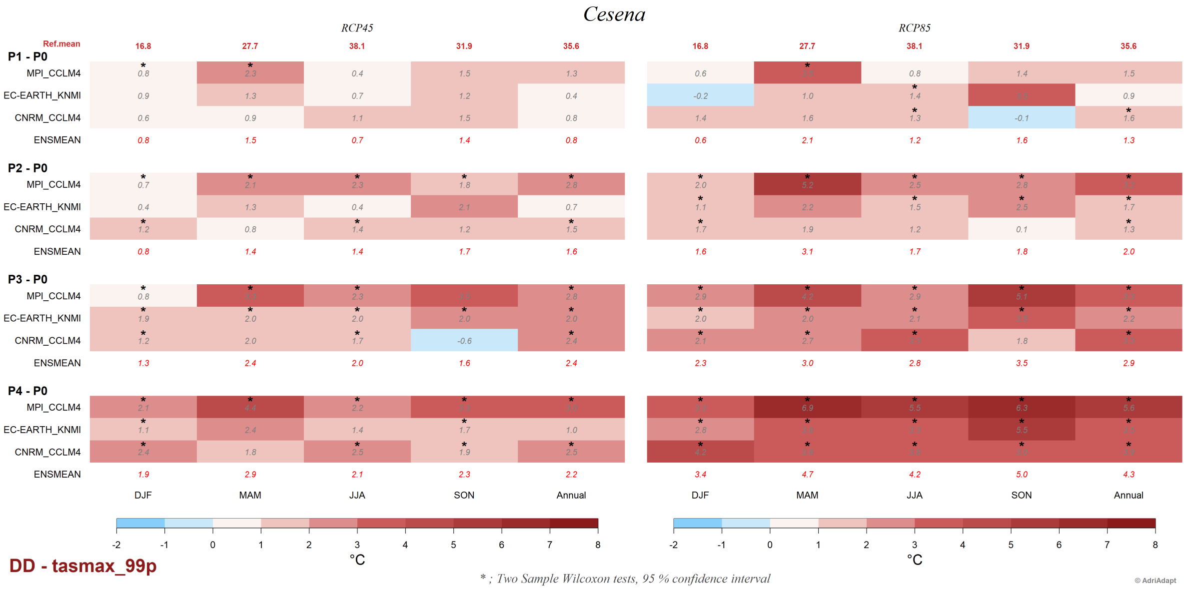

Figure 5-165: Seasonal and annual 99th percentile of 2m maximum air temperature (extreme high maximum temperature, in °C) obtained by dynamical downscaling for Cesena: Ref. mean is 20 year simulated period (1986-2005) for ensemble mean; P1-P0, P2-P0, P3-P0, P4-P0 are changes in the future for following periods P1: 2021-2040, P2: 2041-2060, P3: 2061-2080, P4: 2081-2100. Differences are shown for individual models. Significant change is marked by star. Change is also shown as ensemble mean (ENSMEAN), not tested for significance. Left column is for RCP4.5 scenario and right for RCP8.5 scenario.

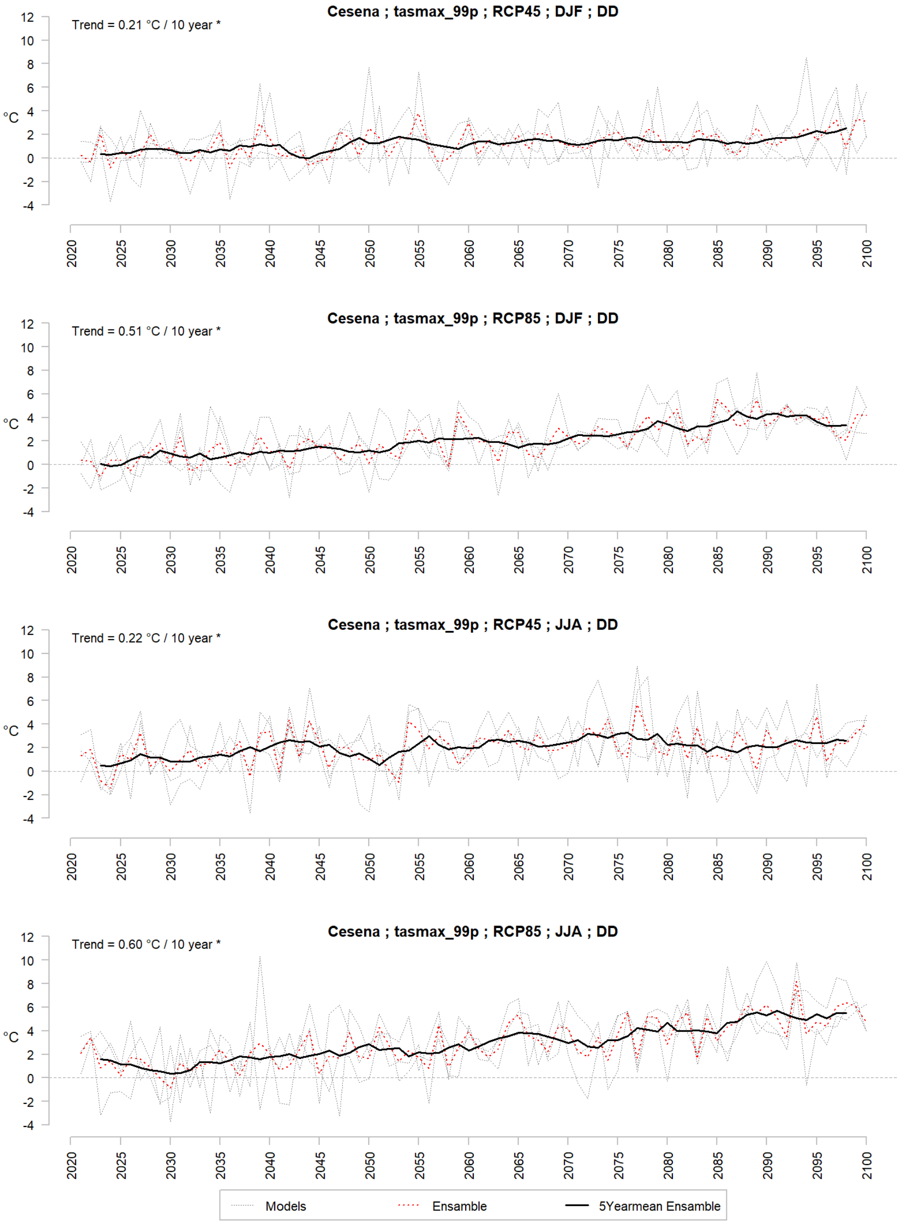

Figure 5-166: Variability of future 99th percentile of 2m maximum air temperature (extreme high maximum temperature) anomaly (in °C) in Cesena for 2021-2100 obtained by dynamically downscaling for winter (DJF) and summer (JJA) and two RCP scenarios: individual models are in grey, the ensemble mean in red, 5-year moving average in black. Significant trend is marked with star (ns if not significant).

6.5.1.1.6 *Extreme rare high temperature*

Future change of 99.9th percentile of 2m air temperature (Figure 5-167) in Cesena is increasing from P1 to P4 periods with the different amplitudes for each model. Slightly negative change appears for some seasons and some models in three first periods, but the change of ensemble mean is positive for all periods. At the end of century increase is from 1.2 °C in SON to 3.4 °C in MAM, 2.2 °C on annual scale for RCP4.5. Amplitude of change is more pronounced for RCP8.5 and is between 2.7 °C in DJF and 5.3 °C in MAM, 4.3 °C for annual change at the end of 21st century. Variability of future 99.9th percentile of 2m air temperature anomaly (Figure 5-168) shows linear trend in change of ensemble mean, 0.18 °C / 10 year in DJF for RCP4.5 and 0.49 °C / 10 year for RCP8.5; 0.20 °C / 10 year in JJA for RCP4.5 and 0.55 °C / 10 year for RCP8.5. All trends are statistically significant.

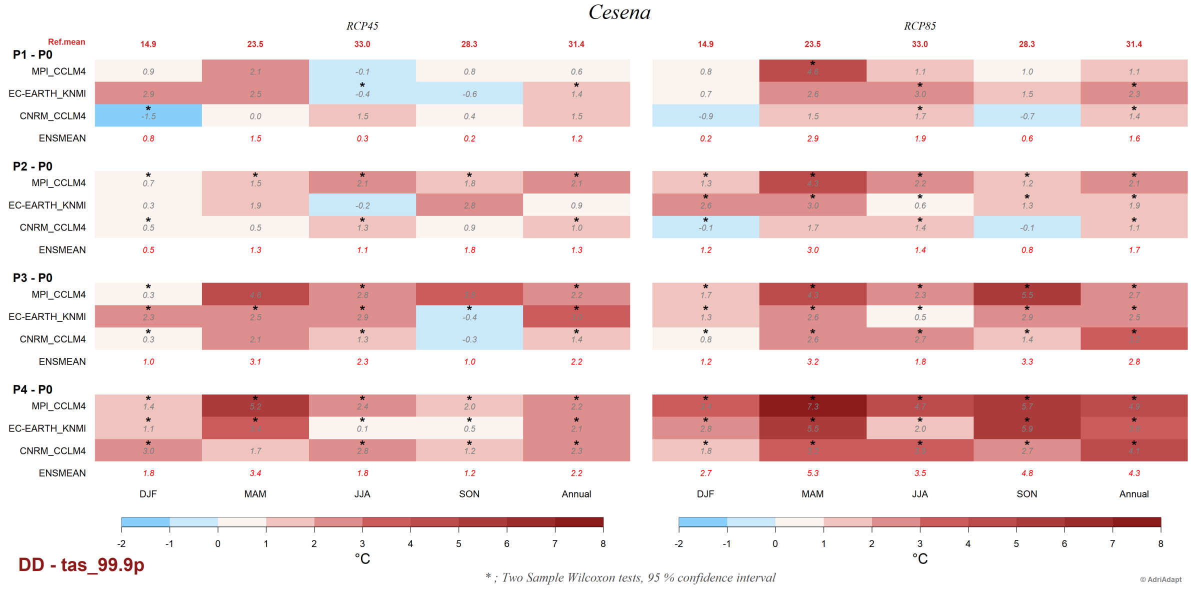

Figure 5-167: Seasonal and annual 99.9th percentile of 2m air temperature (extreme rare high temperature, in °C) obtained by dynamical downscaling for Cesena: Ref. mean is 20 year simulated period (1986-2005) for ensemble mean; P1-P0, P2-P0, P3-P0, P4-P0 are changes in the future for following periods P1: 2021-2040, P2: 2041-2060, P3: 2061-2080, P4: 2081-2100. Differences are shown for individual models. Significant change is marked by star. Change is also shown as ensemble mean (ENSMEAN), not tested for significance. Left column is for RCP4.5 scenario and right for RCP8.5 scenario.

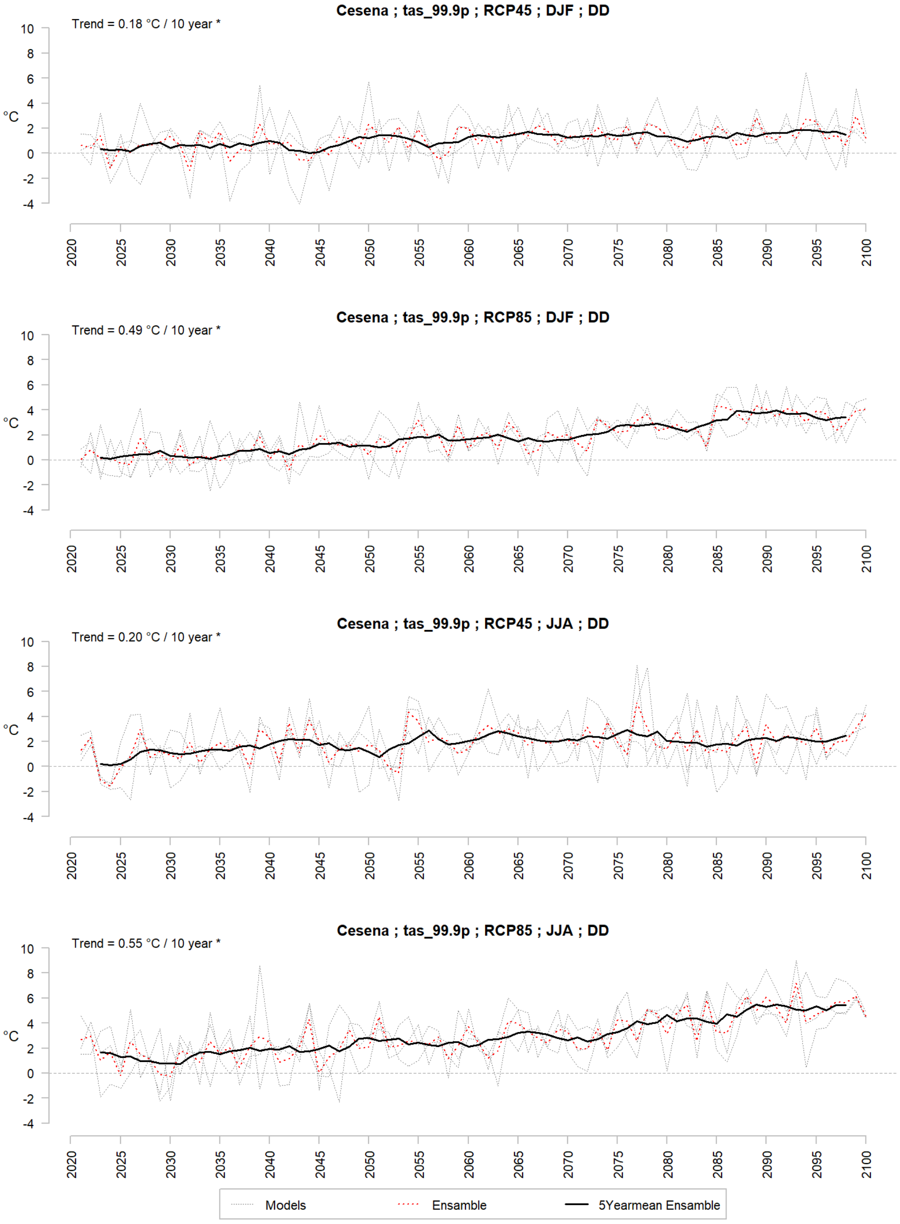

Figure 5-168: Variability of future 99.9th percentile of 2m air temperature (extreme rare high temperature) anomaly (in °C) in Cesena for 2021-2100 obtained by dynamically downscaling for winter (DJF) and summer (JJA) and two RCP scenarios: individual models are in grey, the ensemble mean in red, 5-year moving average in black. Significant trend is marked with star (ns if not significant).

6.5.1.1.7 *Extreme rare high maximum temperature*

Future change of 99.9th percentile of 2m maximum air temperature (Figure 5-169) in Cesena is changing from P1 to P4 periods with the different amplitudes for each model. Some models show for some time slices negative change, but in general ensemble mean for all season and annual change are positive. At the end of 21st century changes are between 1.2 °C in SON and 3.6 °C in MAM, 2.0 °C for annual for RCP4.5 scenario. Amplitude of change is more pronounced for RCP8.5 and is between 3.1 °C in DJF and 6.2 °C in MAM, 4.2 °C for annual change at the end of 21st century. Variability of future 99.9th percentile of 2m maximum air temperature anomaly (Figure 5-170) shows linear trend in change of ensemble mean, 0.21 °C / 10 year in DJF for RCP4.5 and 0.51 °C / 10 year for RCP8.5; 0.22 °C / 10 year in JJA for RCP4.5 and 0.60 °C / 10 year for RCP8.5. All trends are statistically significant.

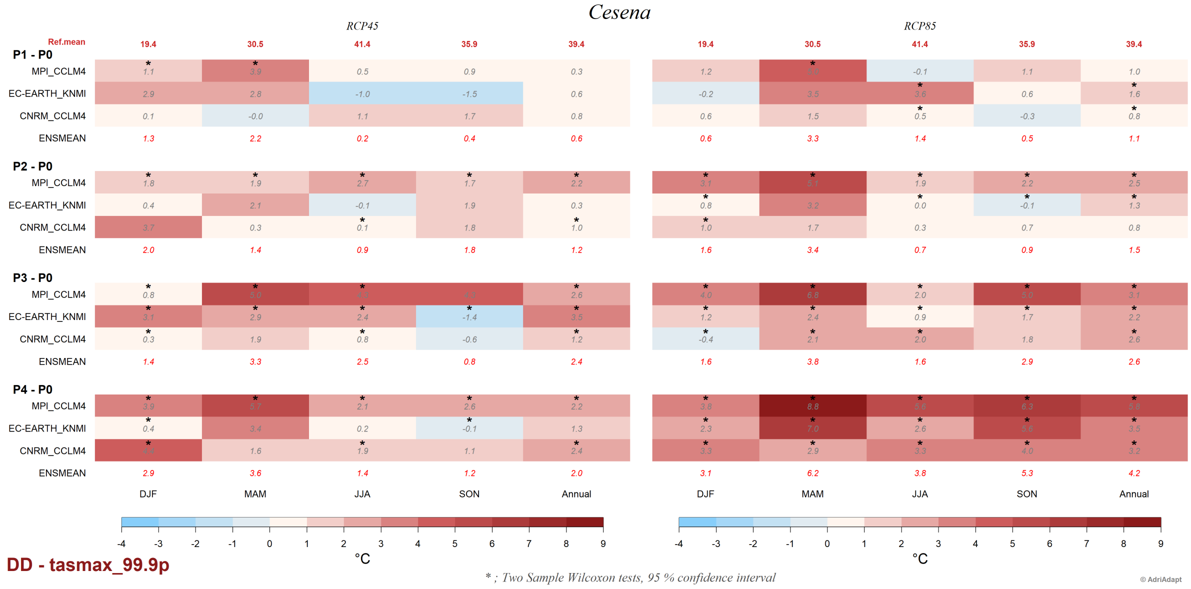

Figure 5-169: Seasonal and annual 99.9th percentile of 2m maximum air temperature (extreme rare high maximum temperature, in °C) obtained by dynamical downscaling for Cesena: Ref. mean is 20 year simulated period (1986-2005) for ensemble mean; P1-P0, P2-P0, P3-P0, P4-P0 are changes in the future for following periods P1: 2021-2040, P2: 2041-2060, P3: 2061-2080, P4: 2081-2100. Differences are shown for individual models. Significant change is marked by star. Change is also shown as ensemble mean (ENSMEAN), not tested for significance. Left column is for RCP4.5 scenario and right for RCP8.5 scenario.

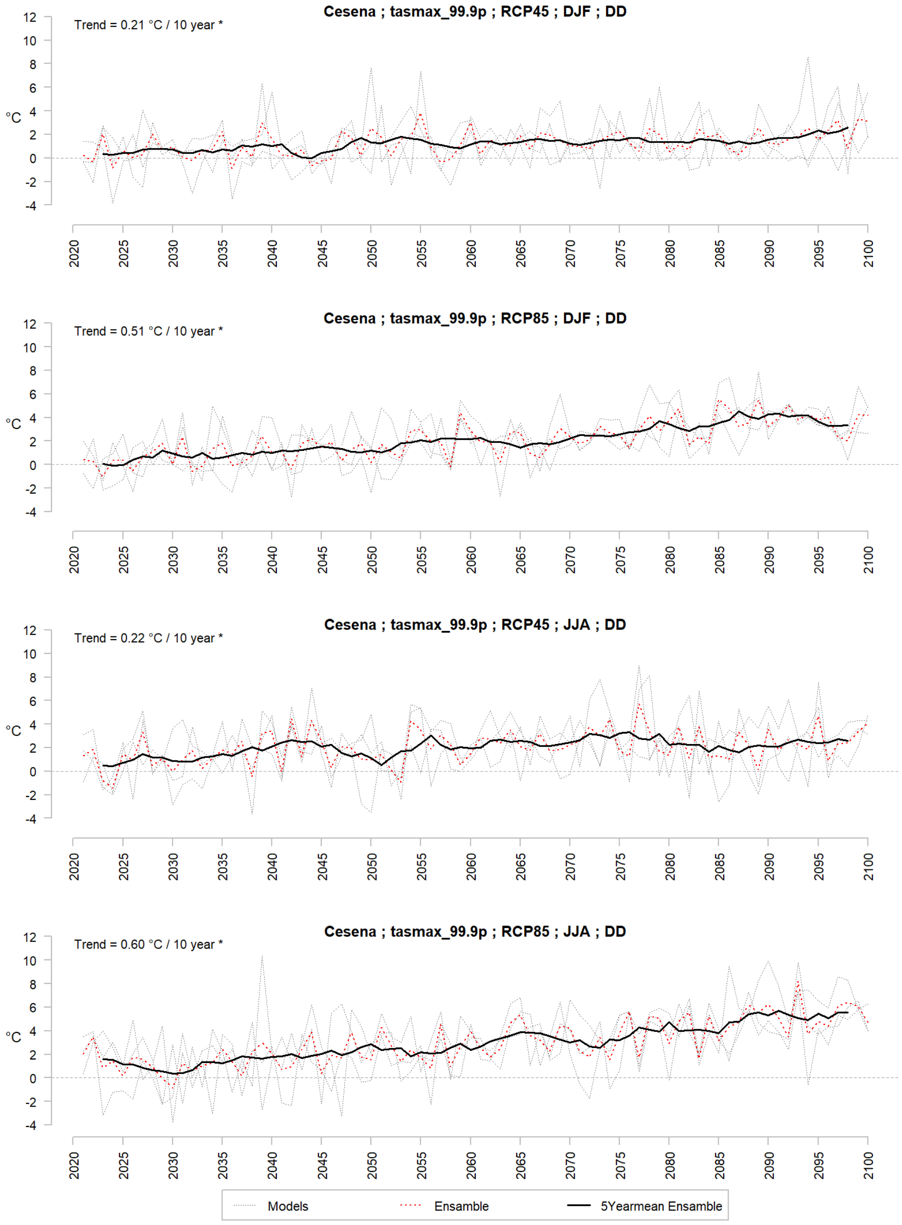

Figure 5-170: Variability of future 99.9th percentile of 2m maximum air temperature (extreme rare high maximum temperature) anomaly (in °C) in Cesena for 2021-2100 obtained by dynamically downscaling for winter (DJF) and summer (JJA) and two RCP scenarios: individual models are in grey, the ensemble mean in red, 5-year moving average in black. Significant trend is marked with star (ns if not significant).

6.5.1.1.8 *Warm spell days index*

Warm spell days index (Figure 5-171) in Cesena shows increase in all seasons and on annual scale, for all future period. Amplitude of change is increasing towards the end of 21st century, for RCP4.5 scenario is between 6.7 days in DJF and 10.5 in JJA; 36.9 days on annual scale. Amplitude of change is more pronounced for RCP8.5 and is between 20.8 days in DJF and 30.5 days in JJA, 104.8 days for annual change at the end of 21st century. Variability of future warm spell days index anomaly (Figure 5-172) shows linear trend in change of ensemble mean, 0.75 days/ 10 year in DJF for RCP4.5 and 3.04 days/ 10 year for RCP8.5; 0.65 days/10 year in JJA for RCP4.5 and 3.78 days/10 year for RCP8.5. All trends are statistically significant.

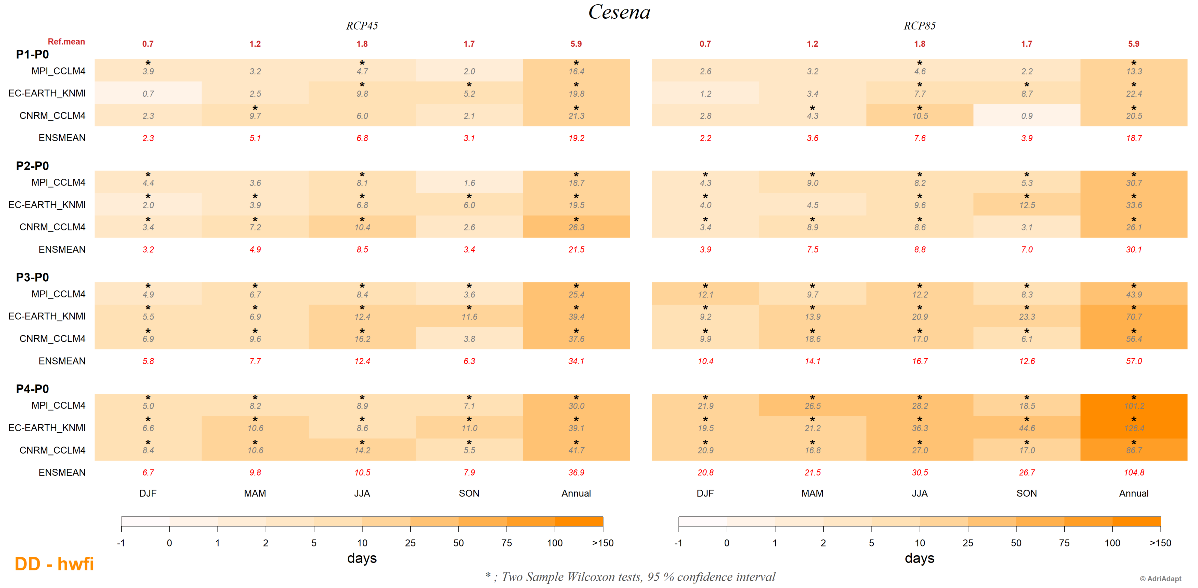

Figure 5-171: Seasonal and annual warm spell days index (in days) obtained by dynamical downscaling for Cesena: Ref. mean is 20 year simulated period (1986-2005) for ensemble mean; P1-P0, P2-P0, P3-P0, P4-P0 are changes in the future for following periods P1: 2021-2040, P2: 2041-2060, P3: 2061-2080, P4: 2081-2100. Differences are shown for individual models. Significant change is marked by star. Change is also shown as ensemble mean (ENSMEAN), not tested for significance. Left column is for RCP4.5 scenario and right for RCP8.5 scenario.

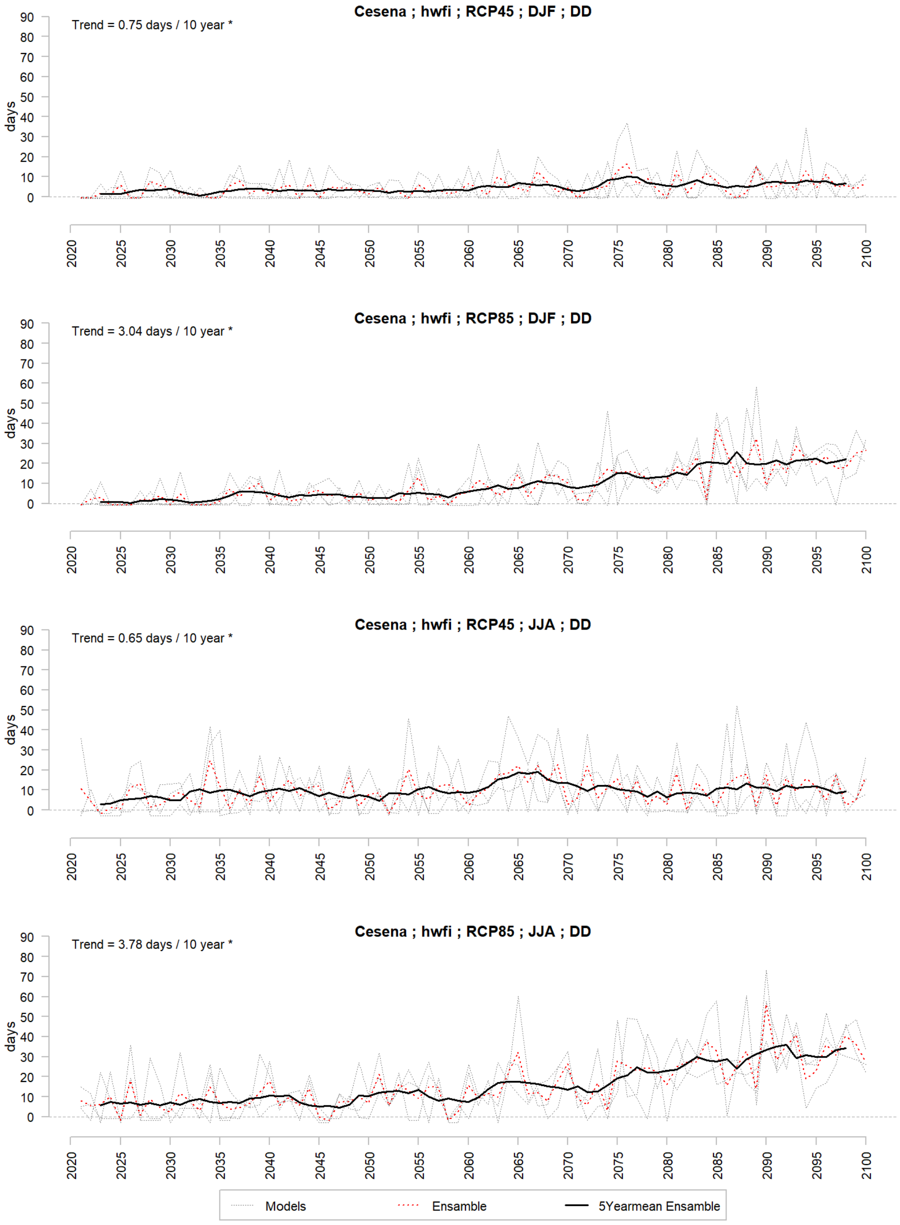

Figure 5-172: Variability of future warm spell days index anomaly in Cesena (in days) for 2021-2100 obtained by dynamically downscaling for winter (DJF) and summer (JJA) and two RCP scenarios: individual models are in grey, the ensemble mean in red, 5-year moving average in black. Significant trend is marked with star (ns if not significant).

6.5.1.1.9 *Heat wave duration index*

Heat wave duration index (Figure 5-173) in Cesena shows increase in all seasons and on annual scale, for all future period (exceptions are small negative changes for one model in DJF in first two periods for RCP4.5 scenario). Amplitude of change is increasing towards the end of 21st century, for RCP4.5 scenario ensemble mean change is between 3.7 days in DJF and 5.2 in SON; 17.4 days on annual scale. Amplitude of change is more pronounced for RCP8.5 and is between 9.8 days in MAM and 16.4 days in SON, 54.5 days for annual change at the end of 21st century. Variability of future heat wave duration index anomaly (Figure 5-174) shows linear trend in change of ensemble mean, 0.49 days/ 10 year in DJF for RCP4.5 and 2.09 days/ 10 year for RCP8.5; 0.33 days/10 year in JJA for RCP4.5 and 1.57 days/10 year for RCP8.5. All trends, except in JJA for RCP4.5, are statistically significant.

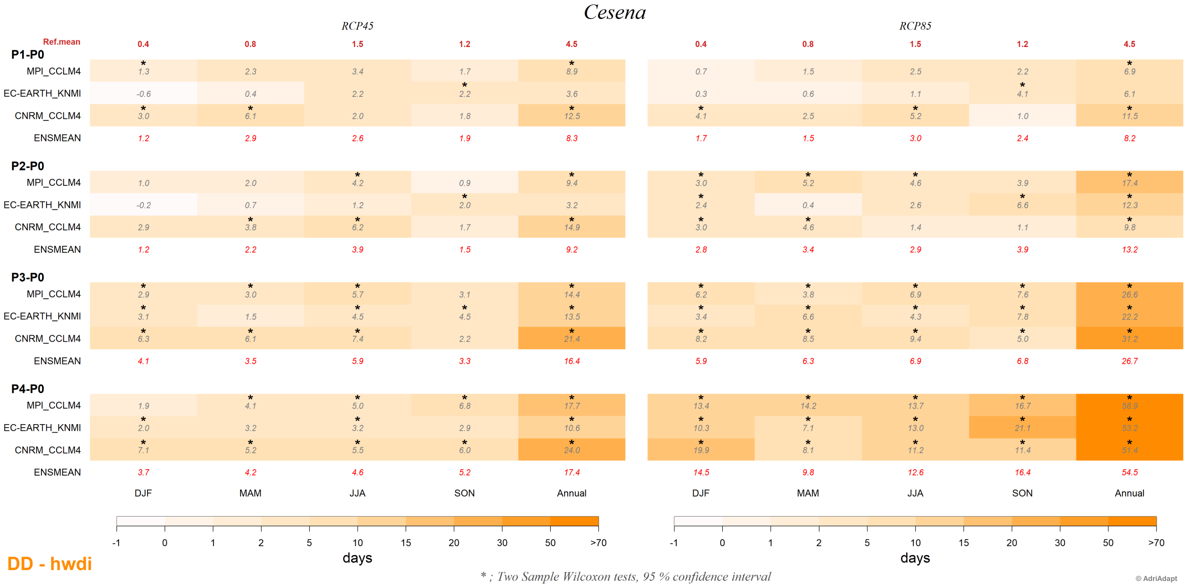

Cesena

	RCP45					RCP85				
	DJF	MAM	JJA	SON	Annual	DJF	MAM	JJA	SON	Annual
Ref.mean	0.4	0.8	1.5	1.2	4.5	0.4	0.8	1.5	1.2	4.5
P1-P0										
MPI_CCLM4	* 1.3	2.3	3.4	1.7	* 8.9	0.7	1.5	2.5	2.2	* 6.9
EC-EARTH_KNMI	-0.6	0.4	2.2	* 2.2	3.6	0.3	0.6	1.1	* 4.1	6.1
CNRM_CCLM4	* 3.0	* 6.1	2.0	1.8	* 12.5	* 4.1	2.5	* 5.2	1.0	* 11.5
ENSMEAN	1.2	2.9	2.6	1.9	8.3	1.7	1.5	3.0	2.4	8.2
P2-P0										
MPI_CCLM4	1.0	2.0	* 4.2	0.9	* 9.4	* 3.0	* 5.2	* 4.6	3.9	* 17.4
EC-EARTH_KNMI	-0.2	0.7	1.2	* 2.0	3.2	* 2.4	0.4	2.6	* 6.6	* 12.3
CNRM_CCLM4	2.9	* 3.8	* 6.2	1.7	* 14.9	* 3.0	* 4.6	1.4	1.1	* 9.8
ENSMEAN	1.2	2.2	3.9	1.5	9.2	2.8	3.4	2.9	3.9	13.2
P3-P0										
MPI_CCLM4	* 2.9	* 3.0	* 5.7	3.1	* 14.4	* 6.2	* 3.8	* 6.9	* 7.6	* 26.6
EC-EARTH_KNMI	* 3.1	1.5	* 4.5	* 4.5	* 13.5	* 3.4	* 6.6	* 4.3	* 7.8	* 22.2
CNRM_CCLM4	* 6.3	* 6.1	* 7.4	2.2	* 21.4	* 8.2	* 8.5	* 9.4	* 5.0	* 31.2
ENSMEAN	4.1	3.5	5.9	3.3	16.4	5.9	6.3	6.9	6.8	26.7
P4-P0										
MPI_CCLM4	1.9	* 4.1	* 5.0	* 6.8	* 17.7	* 13.4	* 14.2	* 13.7	* 16.7	* 58.9
EC-EARTH_KNMI	* 2.0	3.2	* 3.2	2.9	* 10.6	* 10.3	* 7.1	* 13.0	* 21.1	* 53.2
CNRM_CCLM4	* 7.1	* 5.2	* 5.5	* 6.0	* 24.0	* 19.9	* 8.1	* 11.2	* 11.4	* 51.4
ENSMEAN	3.7	4.2	4.6	5.2	17.4	14.5	9.8	12.6	16.4	54.5

* ; Two Sample Wilcoxon tests, 95 % confidence interval

Figure 5-173: Seasonal and annual heat wave duration index (in days) obtained by dynamical downscaling for Cesena: Ref. mean is 20 year simulated period (1986-2005) for ensemble mean; P1-P0, P2-P0, P3-P0, P4-P0 are changes in the future for following periods P1: 2021-2040, P2: 2041-2060, P3: 2061-2080, P4: 2081-2100. Differences are shown for individual models. Significant change is marked by star. Change is also shown as ensemble mean (ENSMEAN), not tested for significance. Left column is for RCP4.5 scenario and right for RCP8.5 scenario.

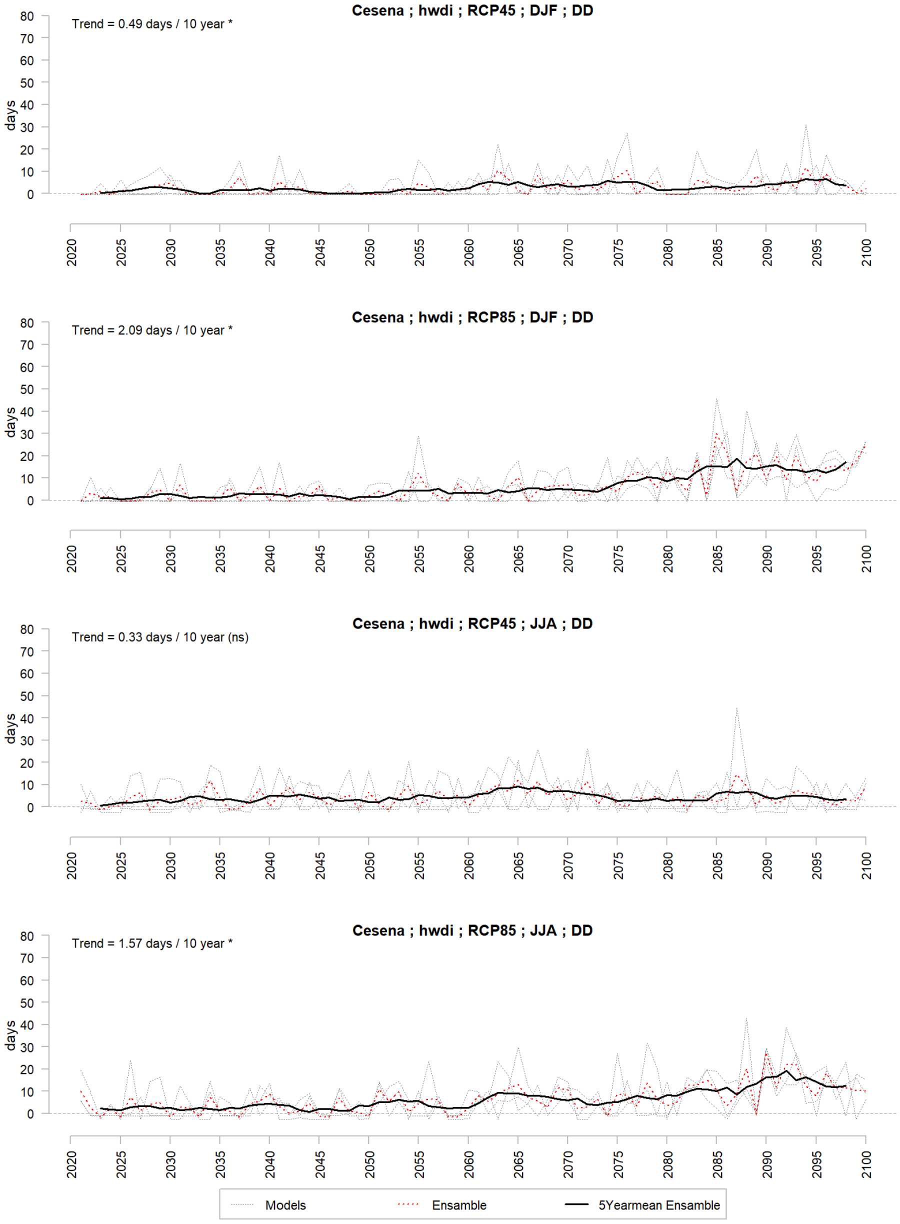

Figure 5-174: Variability of future heat wave duration index anomaly (in days) in Cesena for 2021-2100 obtained by dynamically downscaling for winter (DJF) and summer (JJA) and two RCP scenarios: individual models are in grey, the ensemble mean in red, 5-year moving average in black. Significant trend is marked with star (ns if not significant).

6.5.1.2 *Precipitation related indices projections*

6.5.1.2.1 *Averaged precipitation*

Averaged precipitation obtained by dynamical downscaling is expressed in mm/day and its change in the future is shown as relative to the P0 period (Figure 5-175). Precipitation is much more variable parameter in comparison to the temperature, therefore there is no always unique sign of change through the year as well as from model to model. The change in ensemble mean for Cesena gives increase of precipitation in DJF (5.6 %) and in SON (7.1 %), decrease in JJA (-0.6 %) and no change in MAM; increase on annual scale (2.9 %) at the end of 21st century for RCP4.5 scenario. For scenario RCP8.5, precipitation will decrease in JJA (-18.8 %) and increase in all other seasons (from 0.6 % in DJF to 2.2 % in SON). On annual scale precipitation will decrease (-3.4 %). Variability of future precipitation anomaly (Figure 5-176) for ensemble mean in Cervia change the sign of trend from positive for RCP4.5 scenario to the negative for RCP8.5 scenario for both seasons. All trends are not statistically significant.

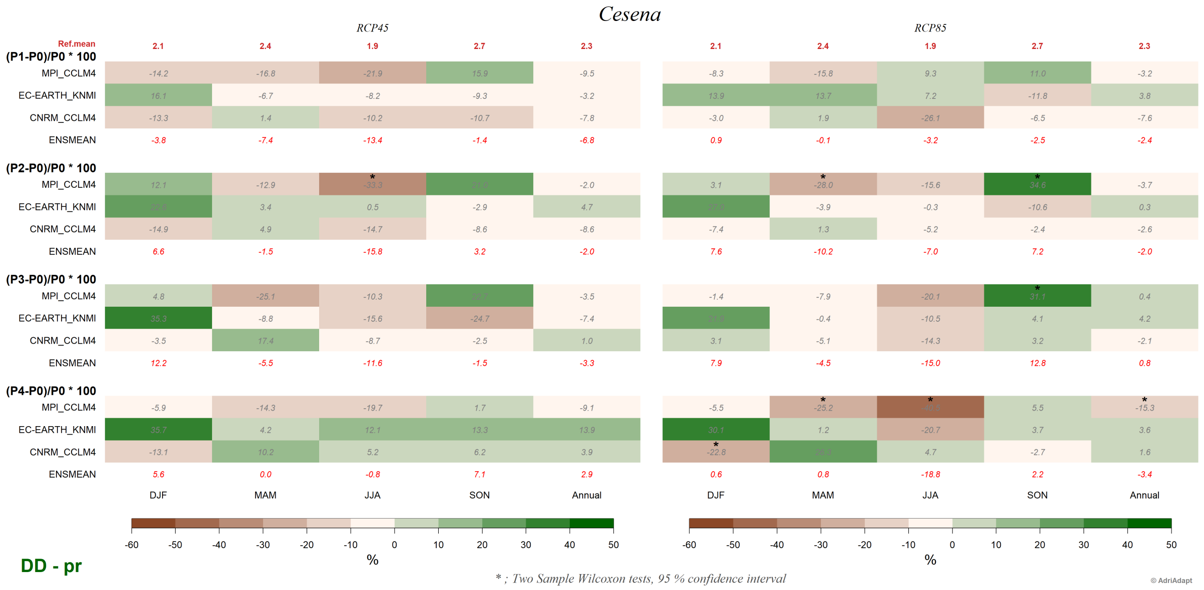

Cesena

RCP45

	DJF	MAM	JJA	SON	Annual
Ref.mean	2.1	2.4	1.9	2.7	2.3
(P1-P0)/P0 * 100					
MPI_CCLM4	-14.2	-16.8	-21.9	15.9	-9.5
EC-EARTH_KNMI	16.1	-6.7	-8.2	-9.3	-3.2
CNRM_CCLM4	-13.3	1.4	-10.2	-10.7	-7.8
ENSMEAN	-3.8	-7.4	-13.4	-1.4	-6.8
(P2-P0)/P0 * 100					
MPI_CCLM4	12.1	-12.9	* -33.3	21.0	-2.0
EC-EARTH_KNMI	22.6	3.4	0.5	-2.9	4.7
CNRM_CCLM4	-14.9	4.9	-14.7	-8.6	-8.6
ENSMEAN	6.6	-1.5	-15.8	3.2	-2.0
(P3-P0)/P0 * 100					
MPI_CCLM4	4.8	-25.1	-10.3	22.7	-3.5
EC-EARTH_KNMI	35.3	-8.8	-15.6	-24.7	-7.4
CNRM_CCLM4	-3.5	17.4	-8.7	-2.5	1.0
ENSMEAN	12.2	-5.5	-11.6	-1.5	-3.3
(P4-P0)/P0 * 100					
MPI_CCLM4	-5.9	-14.3	-19.7	1.7	-9.1
EC-EARTH_KNMI	35.7	4.2	12.1	13.3	13.9
CNRM_CCLM4	-13.1	10.2	5.2	6.2	3.9
ENSMEAN	5.6	0.0	-0.8	7.1	2.9

RCP85

	DJF	MAM	JJA	SON	Annual
Ref.mean	2.1	2.4	1.9	2.7	2.3
(P1-P0)/P0 * 100					
MPI_CCLM4	-8.3	-15.8	9.3	11.0	-3.2
EC-EARTH_KNMI	13.9	13.7	7.2	-11.8	3.8
CNRM_CCLM4	-3.0	1.9	-26.1	-6.5	-7.6
ENSMEAN	0.9	-0.1	-3.2	-2.5	-2.4
(P2-P0)/P0 * 100					
MPI_CCLM4	3.1	* -28.0	-15.6	* 34.6	-3.7
EC-EARTH_KNMI	27.0	-3.9	-0.3	-10.6	0.3
CNRM_CCLM4	-7.4	1.3	-5.2	-2.4	-2.6
ENSMEAN	7.6	-10.2	-7.0	7.2	-2.0
(P3-P0)/P0 * 100					
MPI_CCLM4	-1.4	-7.9	-20.1	* 31.1	0.4
EC-EARTH_KNMI	21.9	-0.4	-10.5	4.1	4.2
CNRM_CCLM4	3.1	-5.1	-14.3	3.2	-2.1
ENSMEAN	7.9	-4.5	-15.0	12.8	0.8
(P4-P0)/P0 * 100					
MPI_CCLM4	-5.5	* -25.2	* -40.5	5.5	* -15.3
EC-EARTH_KNMI	30.1	1.2	-20.7	3.7	3.6
CNRM_CCLM4	* -22.8	26.3	4.7	-2.7	1.6
ENSMEAN	0.6	0.8	-18.8	2.2	-3.4

** ; Two Sample Wilcoxon tests, 95 % confidence interval*

Figure 5-175: Averaged seasonal and annual precipitation obtained by dynamical downscaling for Cesena: Ref. mean is 20 year simulated period (1986-2005) for ensemble mean in mmday^{-1}; P1-P0, P2-P0, P3-P0, P4-P0 are changes (in %) in the future for following periods P1: 2021-2040, P2: 2041-2060, P3: 2061-2080, P4: 2081-2100. Differences are shown for individual models. Significant change is marked by star. Change is also shown as ensemble mean (ENSMEAN), not tested for significance. Left column is for RCP4.5 scenario and right for RCP8.5 scenario.

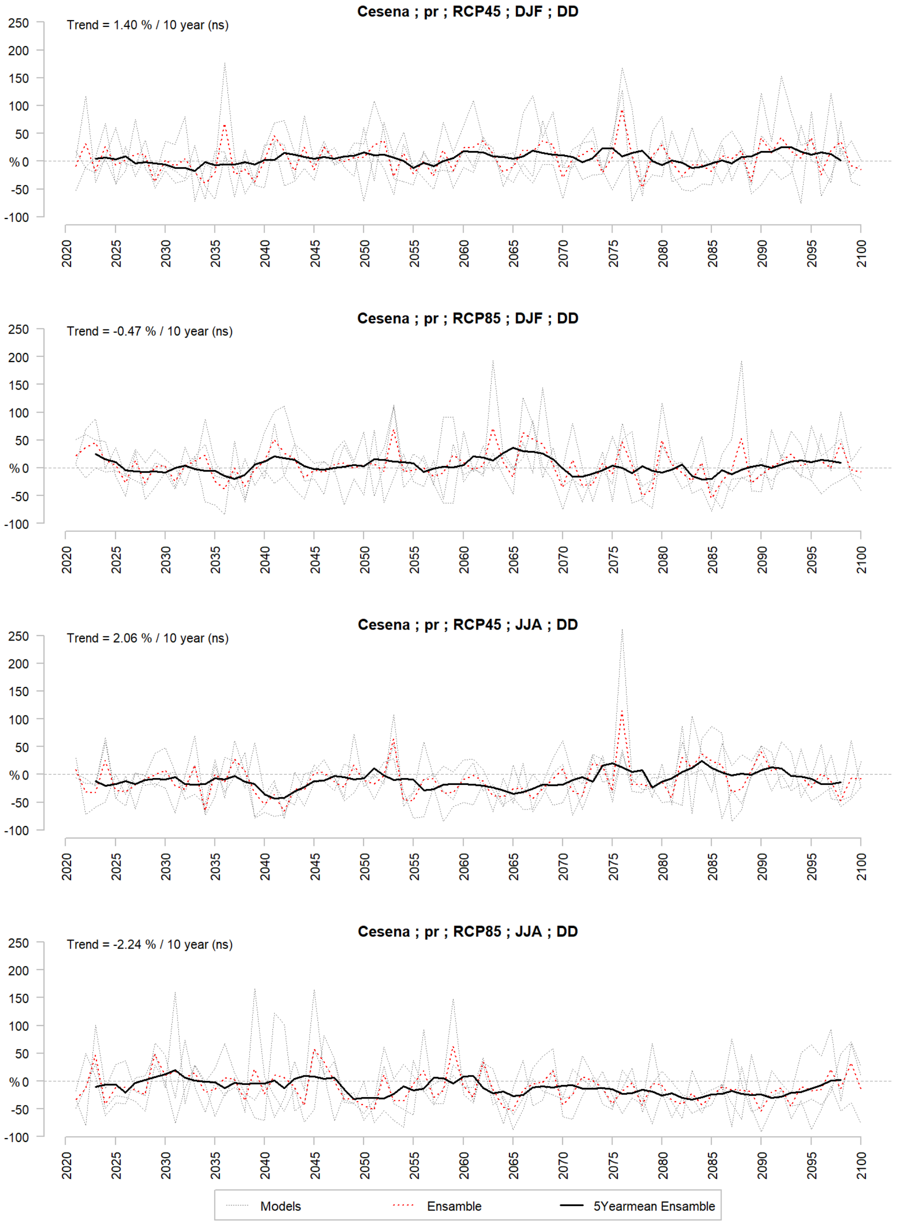

Figure 5-176: Variability of future precipitation anomaly (in %) in Cesena for 2021-2100 obtained by dynamically downscaling for winter (DJF) and summer (JJA) and two RCP scenarios: individual models are in grey, the ensemble mean in red, 5-year moving average in black. Significant trend is marked with star (ns if not significant).

6.5.1.2.2 *Intense precipitation*

Intense precipitation (Figure 5-177), defined by 95th percentile of precipitation in Cesena, shows for ensemble mean at the end of 21st century that 95th percentile will increase in all seasons except in JJA. For RCP4.5 increase will be between 3.1 % in MAM and 12.3 % in DJF; 5.2 % on annual scale, decrease in JJA will be -5.4 %. For RCP8.5 increase will be between 3.7 % in MAM and 12.4 % in SON, 0.8 % on annual scale; decrease in JJA for -22.3 %. Variability of future intense precipitation anomaly (Figure 5-178) for ensemble mean in Cesena shows increase in precipitation in DJF for both scenarios, increase in JJA for RCP4.5 and decrease for RCP8.5 scenario. Linear trends are not statistically significant.

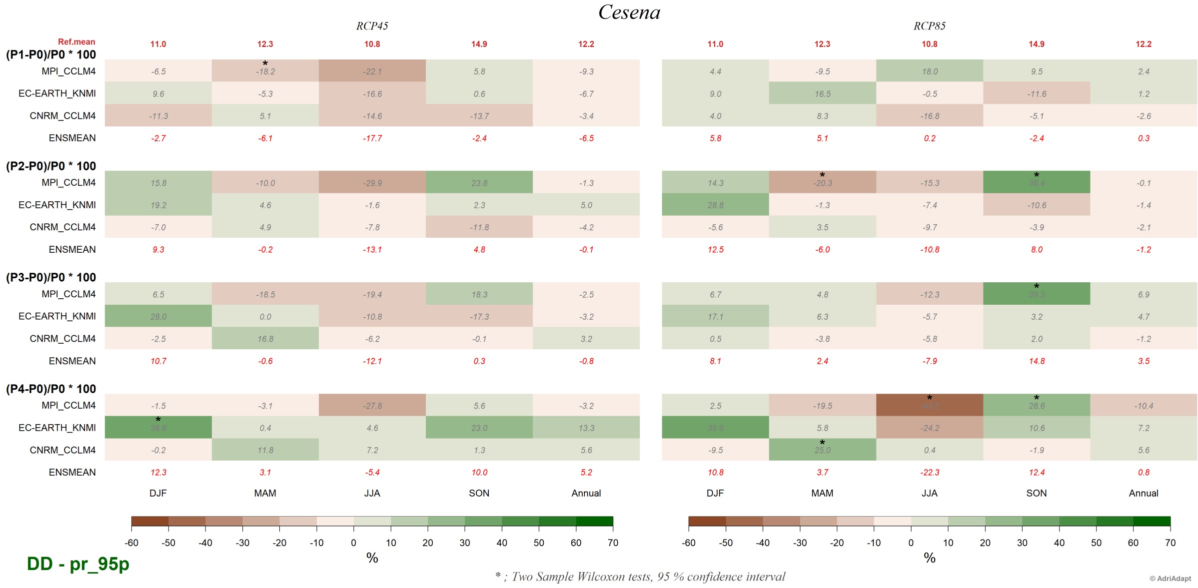

	RCP45					RCP85				
	DJF	MAM	JJA	SON	Annual	DJF	MAM	JJA	SON	Annual
Ref.mean	11.0	12.3	10.8	14.9	12.2	11.0	12.3	10.8	14.9	12.2
(P1-P0)/P0 * 100										
MPI_CCLM4	-6.5	* -18.2	-22.1	5.8	-9.3	4.4	-9.5	18.0	9.5	2.4
EC-EARTH_KNMI	9.6	-5.3	-16.6	0.6	-6.7	9.0	16.5	-0.5	-11.6	1.2
CNRM_CCLM4	-11.3	5.1	-14.6	-13.7	-3.4	4.0	8.3	-16.8	-5.1	-2.6
ENSMEAN	-2.7	-6.1	-17.7	-2.4	-6.5	5.8	5.1	0.2	-2.4	0.3
(P2-P0)/P0 * 100										
MPI_CCLM4	15.8	-10.0	-29.9	23.8	-1.3	14.3	* -20.3	-15.3	* 38.4	-0.1
EC-EARTH_KNMI	19.2	4.6	-1.6	2.3	5.0	28.8	-1.3	-7.4	-10.6	-1.4
CNRM_CCLM4	-7.0	4.9	-7.8	-11.8	-4.2	-5.6	3.5	-9.7	-3.9	-2.1
ENSMEAN	9.3	-0.2	-13.1	4.8	-0.1	12.5	-6.0	-10.8	8.0	-1.2
(P3-P0)/P0 * 100										
MPI_CCLM4	6.5	-18.5	-19.4	18.3	-2.5	6.7	4.8	-12.3	* 39.3	6.9
EC-EARTH_KNMI	28.0	0.0	-10.8	-17.3	-3.2	17.1	6.3	-5.7	3.2	4.7
CNRM_CCLM4	-2.5	16.8	-6.2	-0.1	3.2	0.5	-3.8	-5.8	2.0	-1.2
ENSMEAN	10.7	-0.6	-12.1	0.3	-0.8	8.1	2.4	-7.9	14.8	3.5
(P4-P0)/P0 * 100										
MPI_CCLM4	-1.5	-3.1	-27.8	5.6	-3.2	2.5	-19.5	* -43.2	* 28.6	-10.4
EC-EARTH_KNMI	* 38.6	0.4	4.6	23.0	13.3	39.6	5.8	-24.2	10.6	7.2
CNRM_CCLM4	-0.2	11.8	7.2	1.3	5.6	-9.5	* 25.0	0.4	-1.9	5.6
ENSMEAN	12.3	3.1	-5.4	10.0	5.2	10.8	3.7	-22.3	12.4	0.8

** ; Two Sample Wilcoxon tests, 95 % confidence interval*

Figure 5-177: Seasonal and annual 95th percentile of precipitation (intense precipitation) obtained by dynamical downscaling for Cesena: Ref. mean is 20 year simulated period (1986-2005) for ensemble mean in mmday^{-1}; P1-P0, P2-P0, P3-P0, P4-P0 are changes (in %) in the future for following periods P1: 2021-2040, P2: 2041-2060, P3: 2061-2080, P4: 2081-2100. Differences are shown for individual models. Significant change is marked by star. Change is also shown as ensemble mean (ENSMEAN), not tested for significance. Left column is for RCP4.5 scenario and right for RCP8.5 scenario.

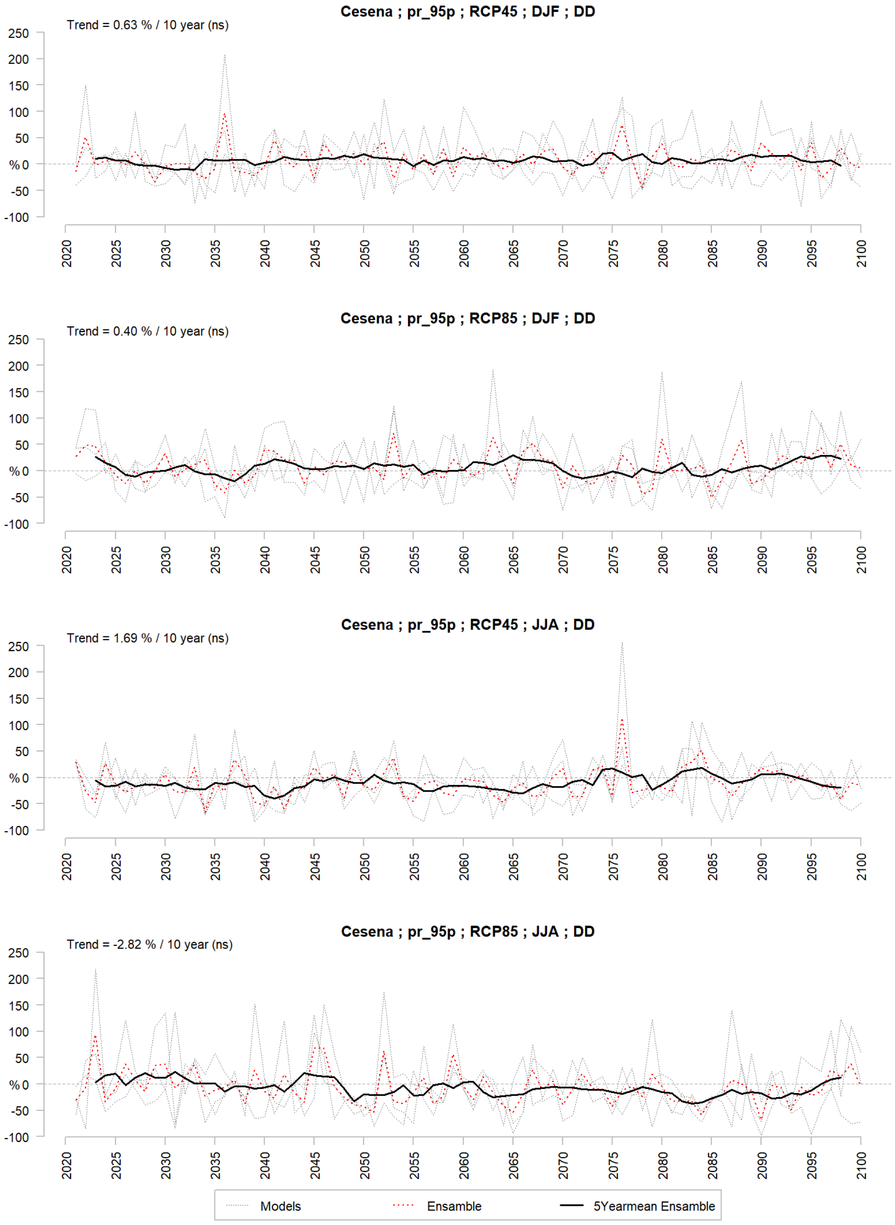

Figure 5-178: Variability of future 95th percentile of precipitation (intense precipitation) anomaly (in %) in Cesena for 2021-2100 obtained by dynamically downscaling for winter (DJF) and summer (JJA) and two RCP scenarios: individual models are in grey, the ensemble mean in red, 5-year moving average in black. Significant trend is marked with star (ns if not significant).

6.5.1.2.3 *Extreme precipitation*

Extreme precipitation (Figure 5-179), defined by 99th percentile of precipitation in Cesena, shows for ensemble mean increase in MAM and SON as well as on annual scale, were there is decrease in DJF and JJA at the end of 21st century for RCP4.5 scenario. The increase will change from 8.7 % in SON to 11.7 % in MAM; 2.6 % for annual scale for RCP4.5. Decrease in DJF will be -2.6 % and in JJA -9.1 %. For RCP8.5 scenario ensemble mean change is positive for all seasons (except in JJA), Increase will be between 2.1 % in DJF and 13.4 % in SON, 7.2 on annual scale. Decrease in JJA will be -8.2 %. Variability of future extreme precipitation anomaly (Figure 5-180) to the end of 21st century for ensemble mean in Cesena has positive trends for DJF for both scenarios. In JJA variability of future extreme precipitation anomaly has positive trend for RCP4.5 but negative for RCP8.5. All trends are not statistically significant.

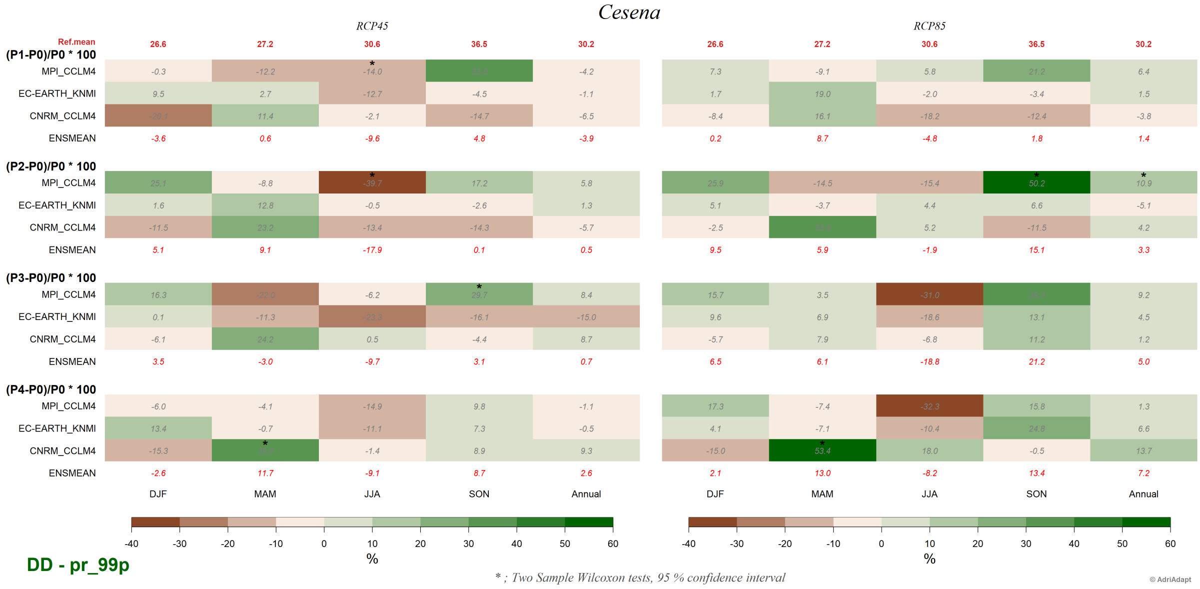

RCP45

	DJF	MAM	JJA	SON	Annual
Ref.mean	26.6	27.2	30.6	36.5	30.2
(P1-P0)/P0 * 100					
MPI_CCLM4	-0.3	-12.2	* -14.0	33.6	-4.2
EC-EARTH_KNMI	9.5	2.7	-12.7	-4.5	-1.1
CNRM_CCLM4	-20.1	11.4	-2.1	-14.7	-6.5
ENSMEAN	-3.6	0.6	-9.6	4.8	-3.9
(P2-P0)/P0 * 100					
MPI_CCLM4	25.1	-8.8	* -39.7	17.2	5.8
EC-EARTH_KNMI	1.6	12.8	-0.5	-2.6	1.3
CNRM_CCLM4	-11.5	23.2	-13.4	-14.3	-5.7
ENSMEAN	5.1	9.1	-17.9	0.1	0.5
(P3-P0)/P0 * 100					
MPI_CCLM4	16.3	-22.0	-6.2	* 29.7	8.4
EC-EARTH_KNMI	0.1	-11.3	-23.3	-16.1	-15.0
CNRM_CCLM4	-6.1	24.2	0.5	-4.4	8.7
ENSMEAN	3.5	-3.0	-9.7	3.1	0.7
(P4-P0)/P0 * 100					
MPI_CCLM4	-6.0	-4.1	-14.9	9.8	-1.1
EC-EARTH_KNMI	13.4	-0.7	-11.1	7.3	-0.5
CNRM_CCLM4	-15.3	* 39.8	-1.4	8.9	9.3
ENSMEAN	-2.6	11.7	-9.1	8.7	2.6

RCP85

	DJF	MAM	JJA	SON	Annual
Ref.mean	26.6	27.2	30.6	36.5	30.2
(P1-P0)/P0 * 100					
MPI_CCLM4	7.3	-9.1	5.8	21.2	6.4
EC-EARTH_KNMI	1.7	19.0	-2.0	-3.4	1.5
CNRM_CCLM4	-8.4	16.1	-18.2	-12.4	-3.8
ENSMEAN	0.2	8.7	-4.8	1.8	1.4
(P2-P0)/P0 * 100					
MPI_CCLM4	25.9	-14.5	-15.4	* 50.2	* 10.9
EC-EARTH_KNMI	5.1	-3.7	4.4	6.6	-5.1
CNRM_CCLM4	-2.5	35.8	5.2	-11.5	4.2
ENSMEAN	9.5	5.9	-1.9	15.1	3.3
(P3-P0)/P0 * 100					
MPI_CCLM4	15.7	3.5	-31.0	39.3	9.2
EC-EARTH_KNMI	9.6	6.9	-18.6	13.1	4.5
CNRM_CCLM4	-5.7	7.9	-6.8	11.2	1.2
ENSMEAN	6.5	6.1	-18.8	21.2	5.0
(P4-P0)/P0 * 100					
MPI_CCLM4	17.3	-7.4	-32.3	15.8	1.3
EC-EARTH_KNMI	4.1	-7.1	-10.4	24.8	6.6
CNRM_CCLM4	-15.0	* 53.4	18.0	-0.5	13.7
ENSMEAN	2.1	13.0	-8.2	13.4	7.2

** ; Two Sample Wilcoxon tests, 95 % confidence interval*

Figure 5-179: Seasonal and annual 99th percentile of precipitation (extreme precipitation) obtained by dynamical downscaling for Cesena: Ref. mean is 20 year simulated period (1986-2005) for ensemble mean in $mmday^{-1}$; P1-P0, P2-P0, P3-P0, P4-P0 are changes (in %) in the future for following periods P1: 2021-2040, P2: 2041-2060, P3: 2061-2080, P4: 2081-2100. Differences are shown for individual models. Significant change is marked by star. Change is also shown as ensemble mean (ENSMEAN), not tested for significance. Left column is for RCP4.5 scenario and right for RCP8.5 scenario.

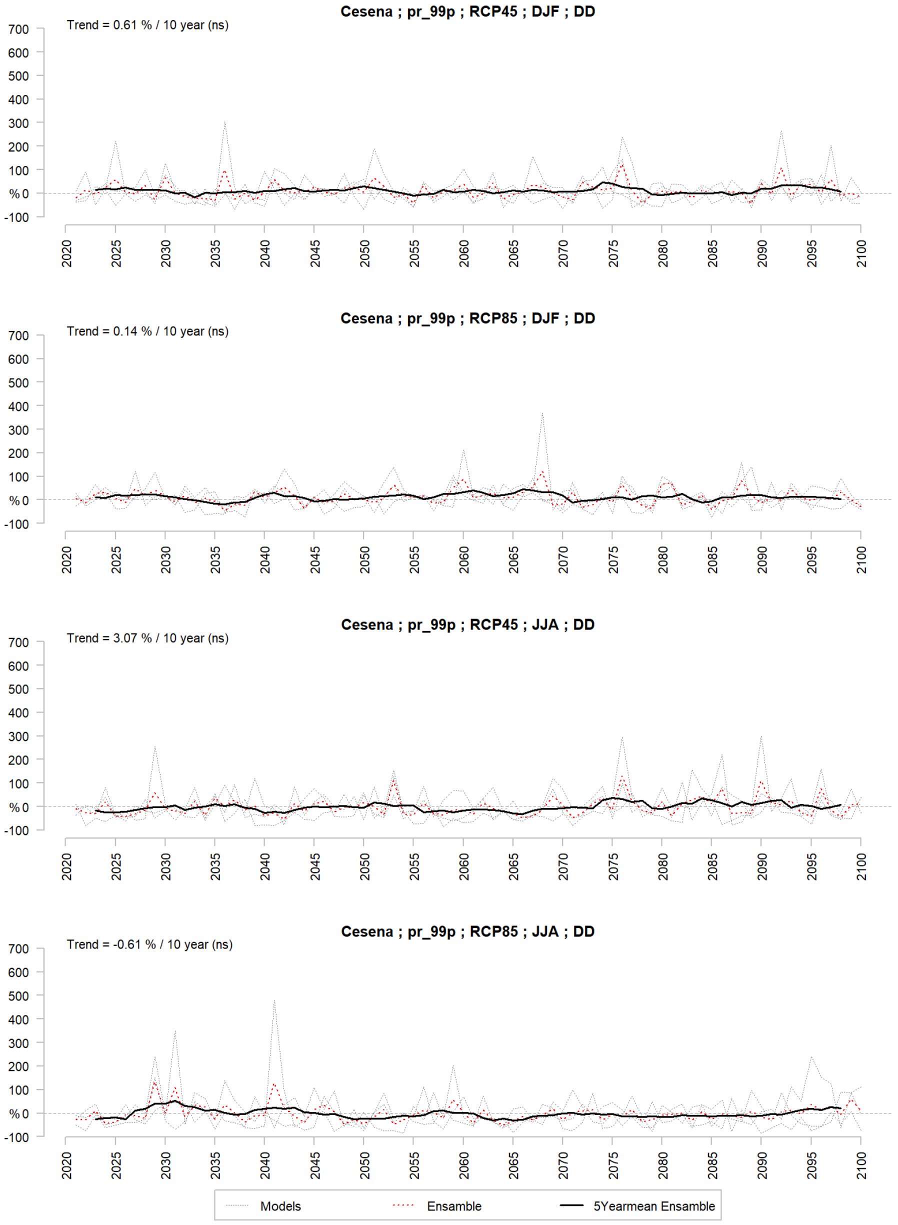

Figure 5-180: Variability of future 99th percentile of precipitation (extreme precipitation) anomaly (in %) in Cesena for 2021-2100 obtained by dynamically downscaling for winter (DJF) and summer (JJA) and two RCP scenarios: individual models are in grey, the ensemble mean in red, 5-year moving average in black. Significant trend is marked with star (ns if not significant).

6.5.1.2.4 *Heavy precipitation index*

Heavy precipitation index (Figure 5-181), defined as number of days with precipitation greater than 10 mm, will change with no unique sign between models in all seasons. In ensemble mean change at the end of century, heavy precipitation index in Cesena will increase in all seasons (except in JJA, -4.5 %) and on annual scale. The change will be in the range of 1.3 % in MMA and 16.8 % in DJF; 6.4 % for annual scale for RCP4.5 scenario. Worst case scenario RCP8.5 gives decrease in JJA (-22.2 %) and increase in all other seasons and on annual scale (from 5.7 % in SON to 12.3 % in DJF; 0.5 for annual scale). Variability of future heavy precipitation index anomaly (Figure 5-182) to the end of 21st century for ensemble mean in Cesena has positive trend for DJF for both scenarios, positive in JJA for RCP4.5 and negative for RCP8.5 scenario. All trends are not statistically significant.

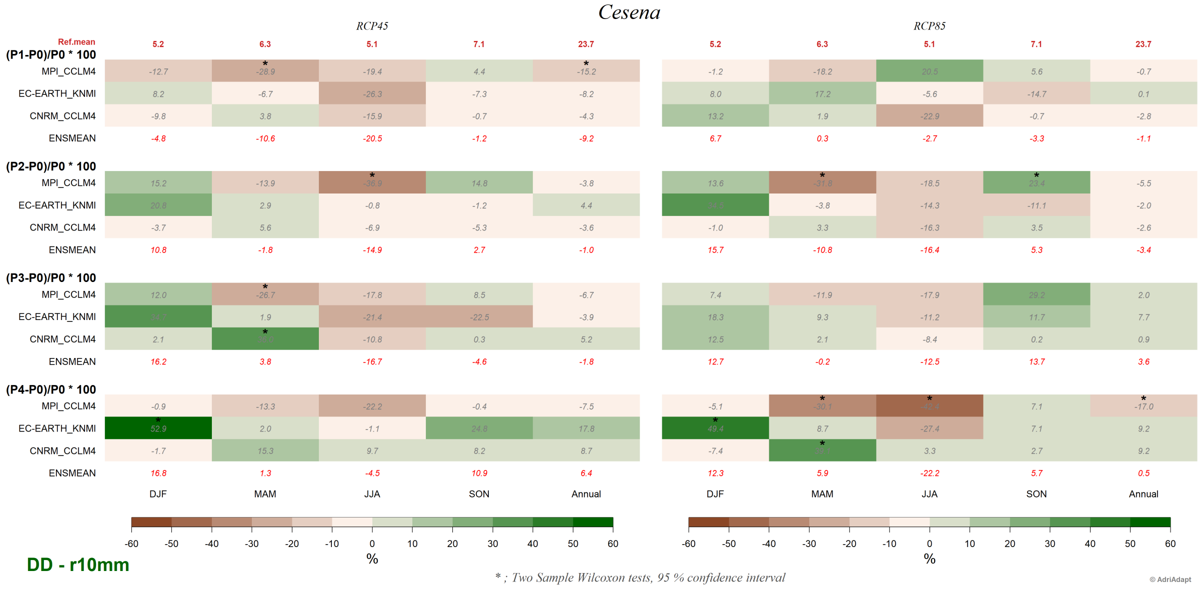

RCP45

	DJF	MAM	JJA	SON	Annual
Ref.mean	5.2	6.3	5.1	7.1	23.7
(P1-P0)/P0 * 100					
MPI_CCLM4	-12.7	* -28.9	-19.4	4.4	* -15.2
EC-EARTH_KNMI	8.2	-6.7	-26.3	-7.3	-8.2
CNRM_CCLM4	-9.8	3.8	-15.9	-0.7	-4.3
ENSMEAN	-4.8	-10.6	-20.5	-1.2	-9.2
(P2-P0)/P0 * 100					
MPI_CCLM4	15.2	-13.9	* -36.9	14.8	-3.8
EC-EARTH_KNMI	20.8	2.9	-0.8	-1.2	4.4
CNRM_CCLM4	-3.7	5.6	-6.9	-5.3	-3.6
ENSMEAN	10.8	-1.8	-14.9	2.7	-1.0
(P3-P0)/P0 * 100					
MPI_CCLM4	12.0	* -26.7	-17.8	8.5	-6.7
EC-EARTH_KNMI	34.7	1.9	-21.4	-22.5	-3.9
CNRM_CCLM4	2.1	* 36.0	-10.8	0.3	5.2
ENSMEAN	16.2	3.8	-16.7	-4.6	-1.8
(P4-P0)/P0 * 100					
MPI_CCLM4	-0.9	-13.3	-22.2	-0.4	-7.5
EC-EARTH_KNMI	* 52.9	2.0	-1.1	24.8	17.8
CNRM_CCLM4	-1.7	15.3	9.7	8.2	8.7
ENSMEAN	16.8	1.3	-4.5	10.9	6.4

RCP85

	DJF	MAM	JJA	SON	Annual
Ref.mean	5.2	6.3	5.1	7.1	23.7
(P1-P0)/P0 * 100					
MPI_CCLM4	-1.2	-18.2	20.5	5.6	-0.7
EC-EARTH_KNMI	8.0	17.2	-5.6	-14.7	0.1
CNRM_CCLM4	13.2	1.9	-22.9	-0.7	-2.8
ENSMEAN	6.7	0.3	-2.7	-3.3	-1.1
(P2-P0)/P0 * 100					
MPI_CCLM4	13.6	* -31.8	-18.5	* 23.4	-5.5
EC-EARTH_KNMI	34.5	-3.8	-14.3	-11.1	-2.0
CNRM_CCLM4	-1.0	3.3	-16.3	3.5	-2.6
ENSMEAN	15.7	-10.8	-16.4	5.3	-3.4
(P3-P0)/P0 * 100					
MPI_CCLM4	7.4	-11.9	-17.9	29.2	2.0
EC-EARTH_KNMI	18.3	9.3	-11.2	11.7	7.7
CNRM_CCLM4	12.5	2.1	-8.4	0.2	0.9
ENSMEAN	12.7	-0.2	-12.5	13.7	3.6
(P4-P0)/P0 * 100					
MPI_CCLM4	-5.1	* -30.1	* -42.4	7.1	* -17.0
EC-EARTH_KNMI	* 49.4	8.7	-27.4	7.1	9.2
CNRM_CCLM4	-7.4	* 39.1	3.3	2.7	9.2
ENSMEAN	12.3	5.9	-22.2	5.7	0.5

* ; Two Sample Wilcoxon tests, 95 % confidence interval

Figure 5-181: Seasonal and annual heavy precipitation index obtained by dynamical downscaling for Cesena: Ref. mean is 20 year simulated period (1986-2005) for ensemble mean in days; P1-P0, P2-P0, P3-P0, P4-P0 are changes (in %) in the future for following periods P1: 2021-2040, P2: 2041-2060, P3: 2061-2080, P4: 2081-2100. Differences are shown for individual models. Significant change is marked by star. Change is also shown as ensemble mean (ENSMEAN), not tested for significance. Left column is for RCP4.5 scenario and right for RCP8.5 scenario.

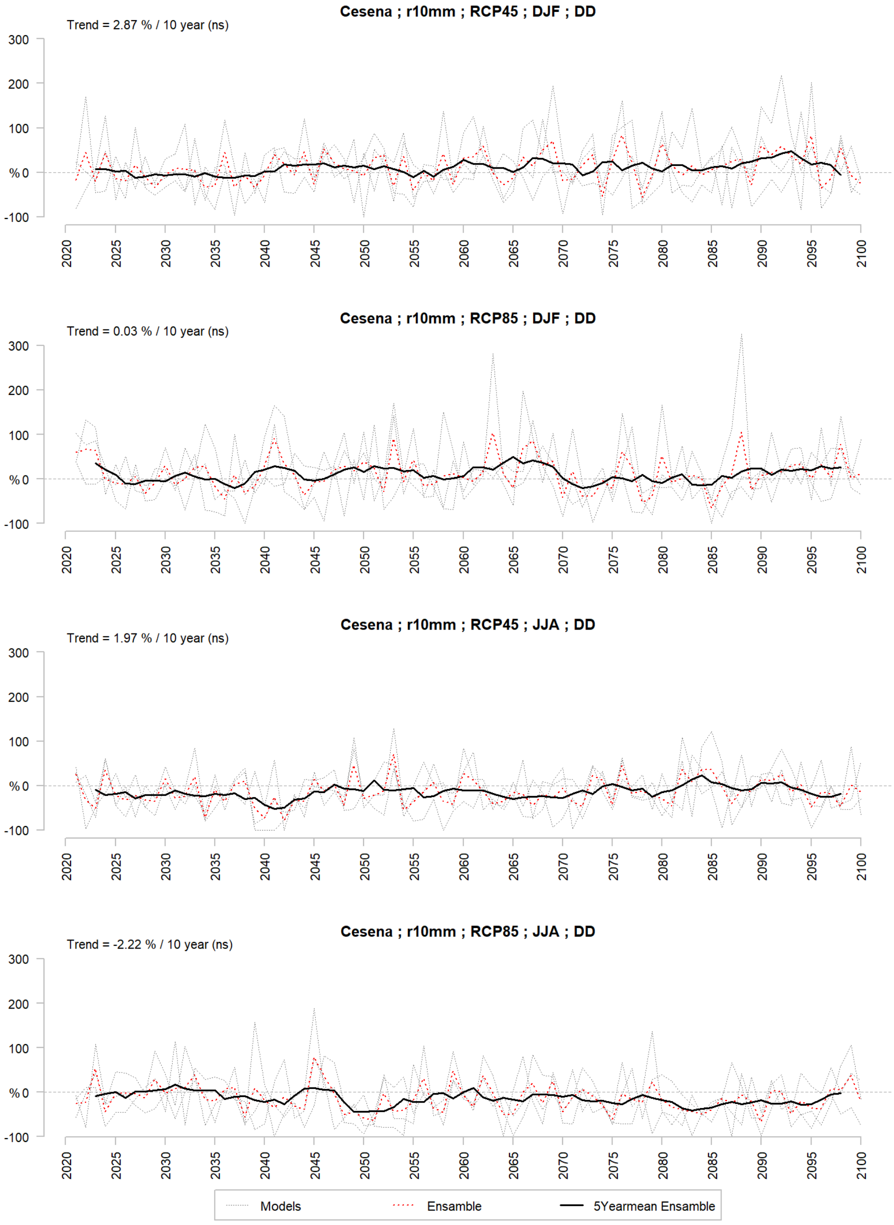

Figure 5-182: Variability of future heavy precipitation index anomaly (in %) in Cesena for 2021-2100 obtained by dynamically downscaling for winter (DJF) and summer (JJA) and two RCP scenarios: individual models are in grey, the ensemble mean in red, 5-year moving average in black. Significant trend is marked with star (ns if not significant).

6.5.1.2.5 *Maximum number of consecutive dry days*

Maximum number of consecutive dry days (Figure 5-183) in Cesena will mostly increase in all periods for most models. The ensemble mean change gives increase in all seasons except in MAM (-0.4 %) at the end of 21st century. Increase will be between 2.4 % in JJA and 5.7 % in DJF; 2.7 % on annual scale for RCP4.5 scenario. For RCP8.5 scenario ensemble mean change gives increase in all seasons and on annual scale by the end of 21st century. The change is between 8.9 % in SON and 19.8 % in DJF, 14.3 % on annual scale. Variability of future maximum number of consecutive dry days anomaly (Figure 5-184) to the end of 21st century for ensemble mean in Cesena has negative trend in both seasons for RCP4.5. The trend is changing sign into positive in both seasons for RCP8.5. All trends are not statistically significant.

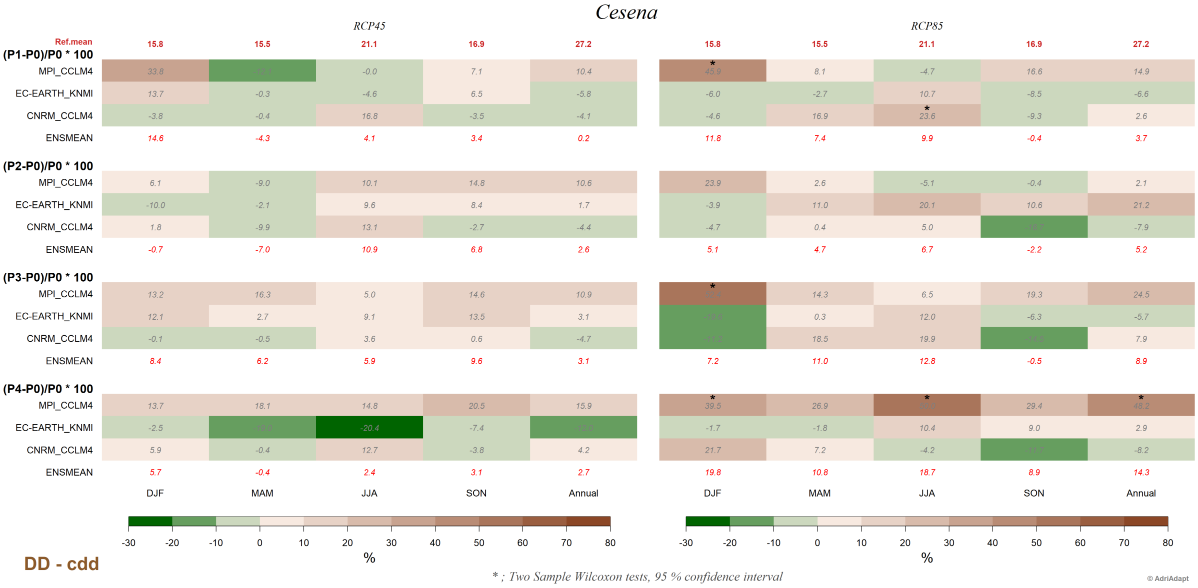

	RCP45					RCP85				
Ref.mean	15.8	15.5	21.1	16.9	27.2	15.8	15.5	21.1	16.9	27.2
(P1-P0)/P0 * 100										
MPI_CCLM4	33.8	-12.1	-0.0	7.1	10.4	* 45.9	8.1	-4.7	16.6	14.9
EC-EARTH_KNMI	13.7	-0.3	-4.6	6.5	-5.8	-6.0	-2.7	10.7	-8.5	-6.6
CNRM_CCLM4	-3.8	-0.4	16.8	-3.5	-4.1	-4.6	16.9	* 23.6	-9.3	2.6
ENSMEAN	14.6	-4.3	4.1	3.4	0.2	11.8	7.4	9.9	-0.4	3.7
(P2-P0)/P0 * 100										
MPI_CCLM4	6.1	-9.0	10.1	14.8	10.6	23.9	2.6	-5.1	-0.4	2.1
EC-EARTH_KNMI	-10.0	-2.1	9.6	8.4	1.7	-3.9	11.0	20.1	10.6	21.2
CNRM_CCLM4	1.8	-9.9	13.1	-2.7	-4.4	-4.7	0.4	5.0	-16.7	-7.9
ENSMEAN	-0.7	-7.0	10.9	6.8	2.6	5.1	4.7	6.7	-2.2	5.2
(P3-P0)/P0 * 100										
MPI_CCLM4	13.2	16.3	5.0	14.6	10.9	* 52.4	14.3	6.5	19.3	24.5
EC-EARTH_KNMI	12.1	2.7	9.1	13.5	3.1	-19.6	0.3	12.0	-6.3	-5.7
CNRM_CCLM4	-0.1	-0.5	3.6	0.6	-4.7	-11.2	18.5	19.9	-14.5	7.9
ENSMEAN	8.4	6.2	5.9	9.6	3.1	7.2	11.0	12.8	-0.5	8.9
(P4-P0)/P0 * 100										
MPI_CCLM4	13.7	18.1	14.8	20.5	15.9	* 39.5	26.9	* 50.0	29.4	* 48.2
EC-EARTH_KNMI	-2.5	-19.0	-20.4	-7.4	-12.0	-1.7	-1.8	10.4	9.0	2.9
CNRM_CCLM4	5.9	-0.4	12.7	-3.8	4.2	21.7	7.2	-4.2	-11.7	-8.2
ENSMEAN	5.7	-0.4	2.4	3.1	2.7	19.8	10.8	18.7	8.9	14.3
	DJF	MAM	JJA	SON	Annual	DJF	MAM	JJA	SON	Annual

* ; Two Sample Wilcoxon tests, 95 % confidence interval

Figure 5-183: Seasonal and annual maximum number of consecutive dry days obtained by dynamical downscaling for Cesena: Ref. mean is 20 year simulated period (1986-2005) for ensemble mean in days; P1-P0, P2-P0, P3-P0, P4-P0 are changes (in %) in the future for following periods P1: 2021-2040, P2: 2041-2060, P3: 2061-2080, P4: 2081-2100. Differences are shown for individual models. Significant change is marked by star. Change is also shown as ensemble mean (ENSMEAN), not tested for significance. Left column is for RCP4.5 scenario and right for RCP8.5 scenario.

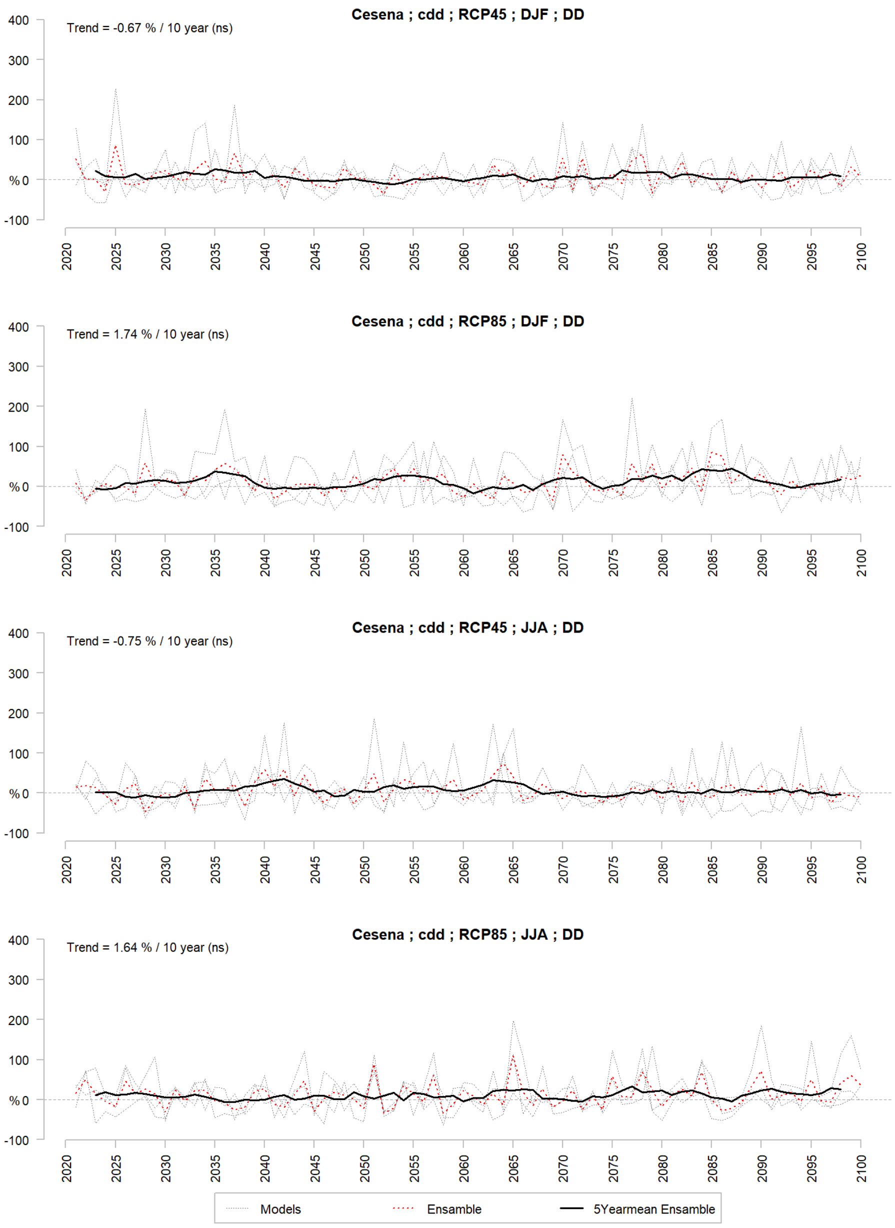

Figure 5-184: Variability of future maximum number of consecutive dry days anomaly (in %) in Cesena for 2021-2100 obtained by dynamically downscaling for winter (DJF) and summer (JJA) and two RCP scenarios: individual models are in grey, the ensemble mean in red, 5-year moving average in black. Significant trend is marked with star (ns if not significant).

6.5.1.3 *Extra rare humidex projections*

Extra rare humidex change (defined by 99.9th percentile of humidex) in the future in Cesena will increase towards the end of 21st century (Figure 5-185). Ensemble mean will increase between 1.3 in SON and 1.9 in MAM, were slight negative change is noticed for JJA (-0.7) and on annual scale (-0.3) for RCP4.5 scenario. Scenario RCP8.5 gives higher positive amplitudes, from 3.1 in JJA to 6.0 in SON, 3.6 on annual scale. Variability of future 99.9th percentile of humidex anomaly (Figure 5-186) shows positive linear trend for both seasons and both considered scenarios. It is 0.31 [] / 10 year in DJF for RCP4.5 (0.63 [] /10 year for RCP8.5) and 0.29 [] /10 year in JJA for RCP4.5 (0.81 [] /10 year for RCP8.5). Trends are statistically significant.

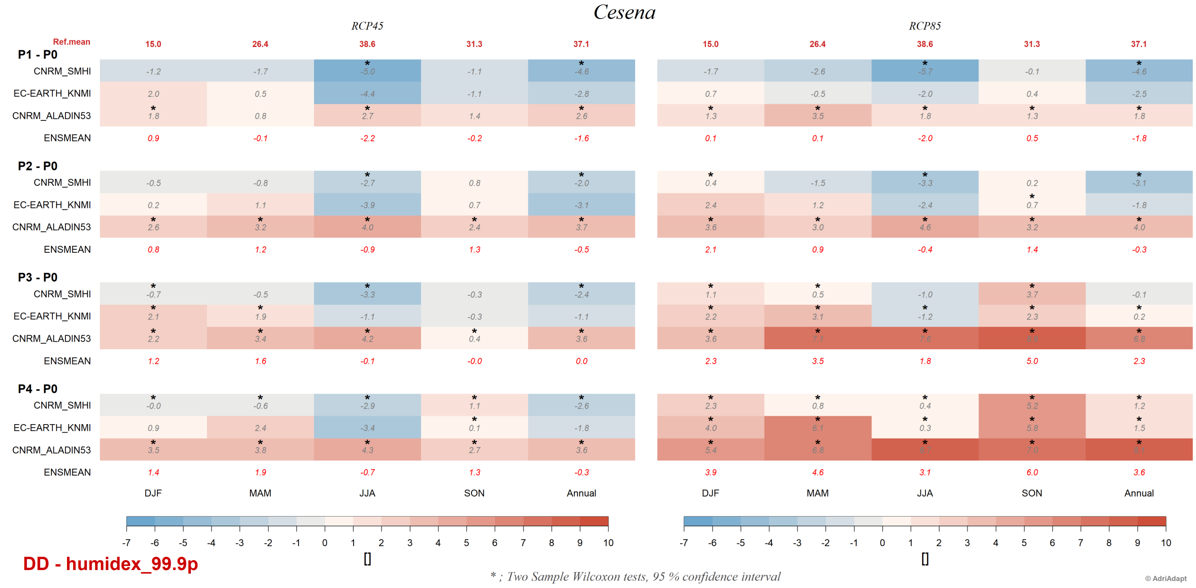

RCP45

	DJF	MAM	JJA	SON	Annual
Ref.mean	15.0	26.4	38.6	31.3	37.1
P1 - P0					
CNRM_SMHI	-1.2	-1.7	* -5.0	-1.1	* -4.6
EC-EARTH_KNMI	2.0	0.5	-4.4	-1.1	-2.8
CNRM_ALADIN53	* 1.8	0.8	* 2.7	1.4	* 2.6
ENSMEAN	0.9	-0.1	-2.2	-0.2	-1.6
P2 - P0					
CNRM_SMHI	-0.5	-0.8	* -2.7	0.8	* -2.0
EC-EARTH_KNMI	0.2	1.1	-3.9	0.7	-3.1
CNRM_ALADIN53	* 2.6	* 3.2	* 4.0	* 2.4	* 3.7
ENSMEAN	0.8	1.2	-0.9	1.3	-0.5
P3 - P0					
CNRM_SMHI	* -0.7	-0.5	* -3.3	-0.3	* -2.4
EC-EARTH_KNMI	* 2.1	* 1.9	-1.1	-0.3	-1.1
CNRM_ALADIN53	* 2.2	* 3.4	* 4.2	* 0.4	* 3.6
ENSMEAN	1.2	1.6	-0.1	-0.0	0.0
P4 - P0					
CNRM_SMHI	* -0.0	* -0.6	* -2.9	* 1.1	* -2.6
EC-EARTH_KNMI	0.9	2.4	-3.4	* 0.1	-1.8
CNRM_ALADIN53	* 3.5	* 3.8	* 4.3	* 2.7	* 3.6
ENSMEAN	1.4	1.9	-0.7	1.3	-0.3

RCP85

	DJF	MAM	JJA	SON	Annual
Ref.mean	15.0	26.4	38.6	31.3	37.1
P1 - P0					
CNRM_SMHI	-1.7	-2.6	* -5.7	-0.1	* -4.6
EC-EARTH_KNMI	0.7	-0.5	-2.0	0.4	-2.5
CNRM_ALADIN53	* 1.3	* 3.5	* 1.8	* 1.3	* 1.8
ENSMEAN	0.1	0.1	-2.0	0.5	-1.8
P2 - P0					
CNRM_SMHI	* 0.4	-1.5	* -3.3	0.2	* -3.1
EC-EARTH_KNMI	2.4	1.2	-2.4	* 0.7	-1.8
CNRM_ALADIN53	* 3.6	* 3.0	* 4.6	* 3.2	* 4.0
ENSMEAN	2.1	0.9	-0.4	1.4	-0.3
P3 - P0					
CNRM_SMHI	* 1.1	* 0.5	-1.0	* 3.7	-0.1
EC-EARTH_KNMI	* 2.2	* 3.1	* -1.2	* 2.3	* 0.2
CNRM_ALADIN53	* 3.6	* 7.1	* 7.6	* 8.9	* 6.8
ENSMEAN	2.3	3.5	1.8	5.0	2.3
P4 - P0					
CNRM_SMHI	* 2.3	* 0.8	* 0.4	* 5.2	* 1.2
EC-EARTH_KNMI	* 4.0	* 6.1	* 0.3	* 5.8	* 1.5
CNRM_ALADIN53	* 5.4	* 6.8	* 8.7	* 7.0	* 8.1
ENSMEAN	3.9	4.6	3.1	6.0	3.6

* ; *Two Sample Wilcoxon tests, 95 % confidence interval*

Figure 5-185: Seasonal and annual 99.9th percentile of humidex obtained by dynamical downscaling for Cesena (in []): Ref. mean is 20 year simulated period (1986-2005); P1-P0, P2-P0, P3-P0, P4-P0 are changes in the future for following periods P1: 2021-2040, P2: 2041-2060, P3: 2061-2080, P4: 2081-2100. Differences are shown for individual models. Significant change is marked by star. Change is also shown as ensemble mean (ENSMEAN), not tested for significance. Left column is for RCP4.5 scenario and right for RCP8.5 scenario.

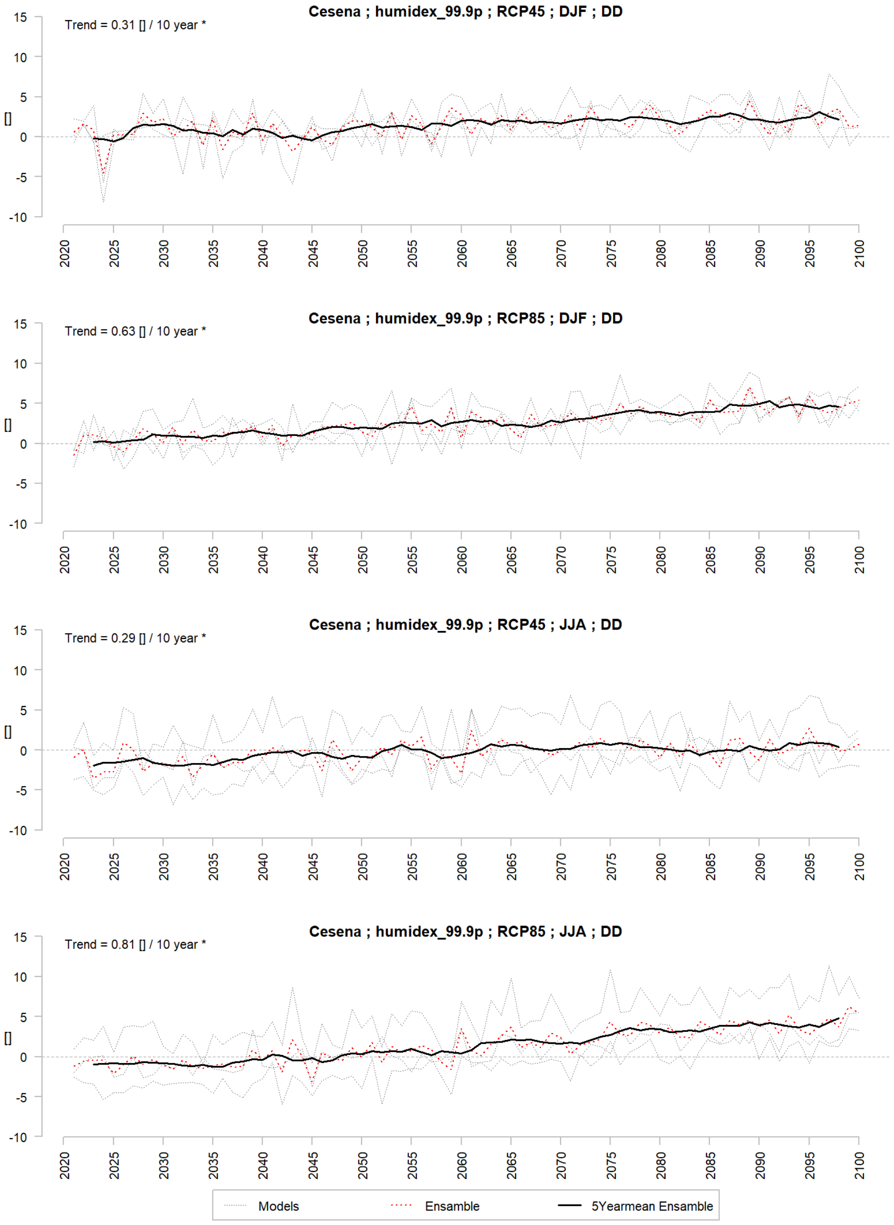

Figure 5-186: Variability of future 99.9th percentile of humidex anomaly (in []) in Cesena for 2021-2100 obtained by dynamically downscaling for winter (DJF) and summer (JJA) and two RCP scenarios: individual models are in grey, the ensemble mean in red, 5-year moving average in black. Significant trend is marked with star (ns if not significant).

6.5.1.4 *Wind projections*

6.5.1.4.1 *Averaged wind module*

The change of wind speed at 10m high (Figure 5-187) is very variable from season to season and from model to model. It is expressed as relative difference to the wind speed in P0 period in percentage. At the end of 21st century wind speed in Cesena will slightly decrease in all seasons except in MAM (0.4 %) and on annual scale. Decrease will be between -0.4 % in DJF and -0.9 % in SON; -0.6 % on annual scale for RCP4.5 scenario. For RCP8.5 scenario wind speed will decrease in all seasons (from -0.7 % in JJA to -2.6 % in SON); -1.4 % on annual scale. Variability of future wind speed at 10m high anomaly (Figure 5-188) shows negative linear trend for both seasons and both considered scenarios. Trends are not statistically significant.

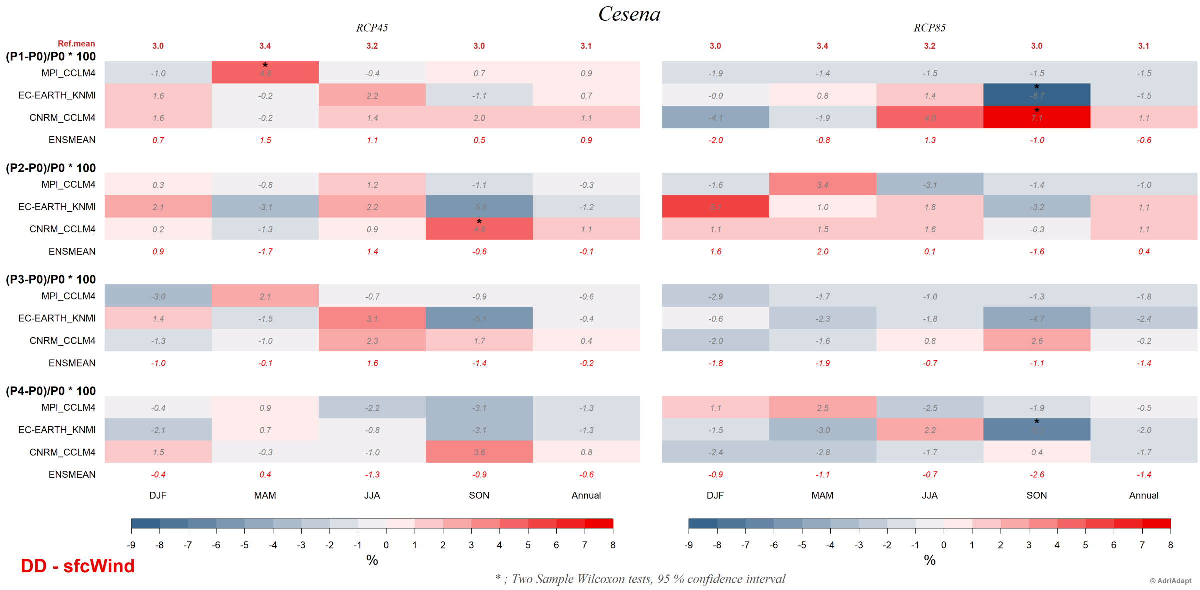

Cesena

	RCP45					RCP85				
	DJF	MAM	JJA	SON	Annual	DJF	MAM	JJA	SON	Annual
Ref.mean	3.0	3.4	3.2	3.0	3.1	3.0	3.4	3.2	3.0	3.1
(P1-P0)/P0 * 100										
MPI_CCLM4	-1.0	* 4.9	-0.4	0.7	0.9	-1.9	-1.4	-1.5	-1.5	-1.5
EC-EARTH_KNMI	1.6	-0.2	2.2	-1.1	0.7	-0.0	0.8	1.4	* -8.7	-1.5
CNRM_CCLM4	1.6	-0.2	1.4	2.0	1.1	-4.1	-1.9	4.0	* 7.1	1.1
ENSMEAN	0.7	1.5	1.1	0.5	0.9	-2.0	-0.8	1.3	-1.0	-0.6
(P2-P0)/P0 * 100										
MPI_CCLM4	0.3	-0.8	1.2	-1.1	-0.3	-1.6	3.4	-3.1	-1.4	-1.0
EC-EARTH_KNMI	2.1	-3.1	2.2	-5.5	-1.2	5.1	1.0	1.8	-3.2	1.1
CNRM_CCLM4	0.2	-1.3	0.9	* 4.8	1.1	1.1	1.5	1.6	-0.3	1.1
ENSMEAN	0.9	-1.7	1.4	-0.6	-0.1	1.6	2.0	0.1	-1.6	0.4
(P3-P0)/P0 * 100										
MPI_CCLM4	-3.0	2.1	-0.7	-0.9	-0.6	-2.9	-1.7	-1.0	-1.3	-1.8
EC-EARTH_KNMI	1.4	-1.5	3.1	-5.1	-0.4	-0.6	-2.3	-1.8	-4.7	-2.4
CNRM_CCLM4	-1.3	-1.0	2.3	1.7	0.4	-2.0	-1.6	0.8	2.6	-0.2
ENSMEAN	-1.0	-0.1	1.6	-1.4	-0.2	-1.8	-1.9	-0.7	-1.1	-1.4
(P4-P0)/P0 * 100										
MPI_CCLM4	-0.4	0.9	-2.2	-3.1	-1.3	1.1	2.5	-2.5	-1.9	-0.5
EC-EARTH_KNMI	-2.1	0.7	-0.8	-3.1	-1.3	-1.5	-3.0	2.2	* -6.3	-2.0
CNRM_CCLM4	1.5	-0.3	-1.0	3.6	0.8	-2.4	-2.8	-1.7	0.4	-1.7
ENSMEAN	-0.4	0.4	-1.3	-0.9	-0.6	-0.9	-1.1	-0.7	-2.6	-1.4

DD - sfcWind

* : Two Sample Wilcoxon tests, 95 % confidence interval

© AdriAdapt

Figure 5-187: Averaged seasonal and annual wind module (wind speed at 10m height) obtained by dynamical downscaling for Cesena: Ref. mean is 20 year simulated period (1986-2005) in ms^{-1}; P1-P0, P2-P0, P3-P0, P4-P0 are changes (in %) in the future for following periods P1: 2021-2040, P2: 2041-2060, P3: 2061-2080, P4: 2081-2100. Differences are shown for individual models. Significant change is marked by star. Change is also shown as ensemble mean (ENSMEAN), not tested for significance. Left column is for RCP4.5 scenario and right for RCP8.5 scenario.

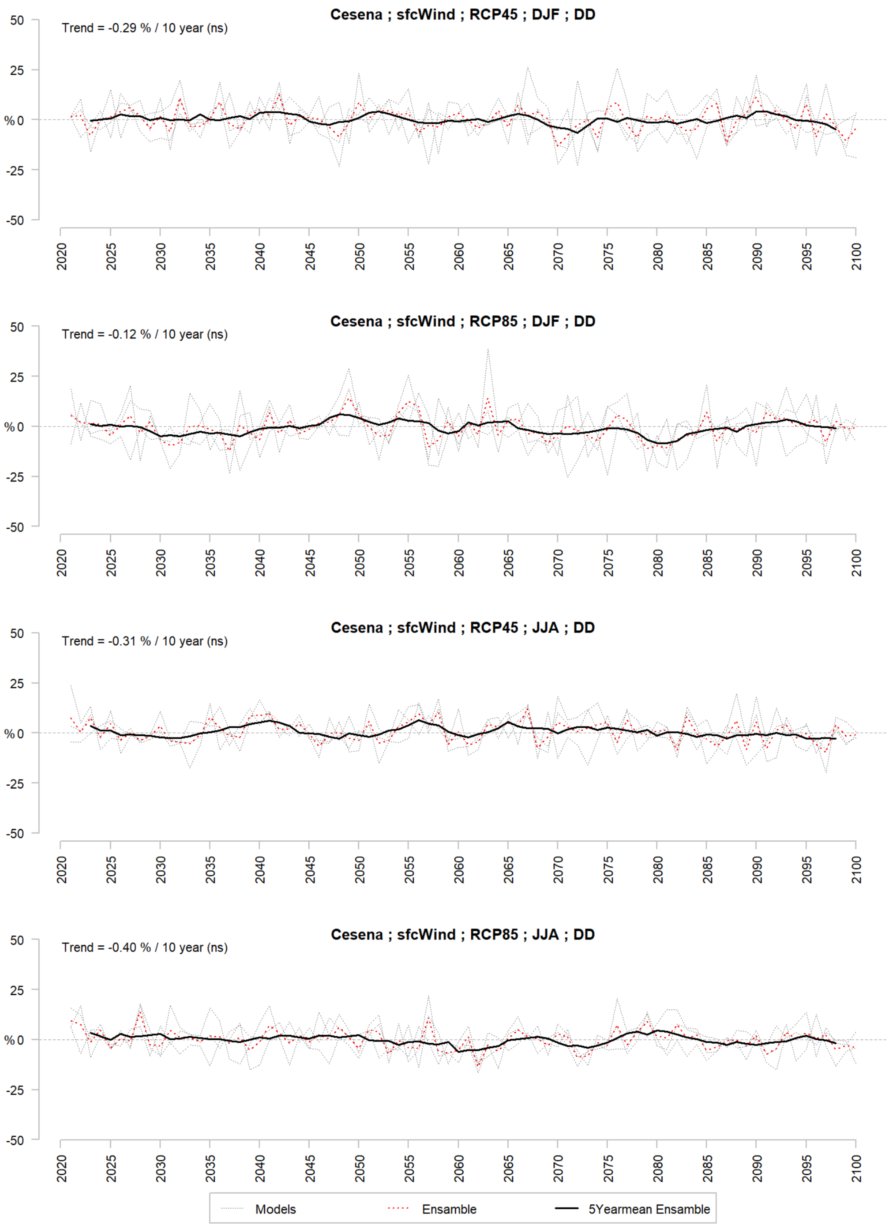

Figure 5-188: Variability of future wind module anomaly (wind speed at 10m height) anomaly (in %) in Cesena for 2021-2100 obtained by dynamically downscaling for winter (DJF) and summer (JJA) and two RCP scenarios: individual models are in grey, the ensemble mean in red, 5-year moving average in black. Significant trend is marked with star (ns if not significant).

6.5.1.4.2 *Maximum wind module*

The change of maximum wind speed at 10m high (Figure 5-189) is very variable from season to season and from model to model. It is expressed as relative difference to the maximum wind speed in P0 period in percentage. At the end of 21st century maximum wind speed in Cesena will slightly decrease in DJF (-0.3 %) and in SON (-0.9 %), but increase in MAM (1.0 %) and in JJA (0.2 %); with no change on annual scale for RCP4.5 scenario. For RCP8.5 scenario wind speed will increase in all seasons except in SON (-1.1 %). Increase will be between 0.1 % in DJF and 0.5 % in MAM. On annual scale there will not be change. Variability of future maximum wind speed at 10m high anomaly (Figure 5-190) shows negative linear trends to the end of 21st century for all trends except in DJF for RCP8.5. Trends are not statistically significant.

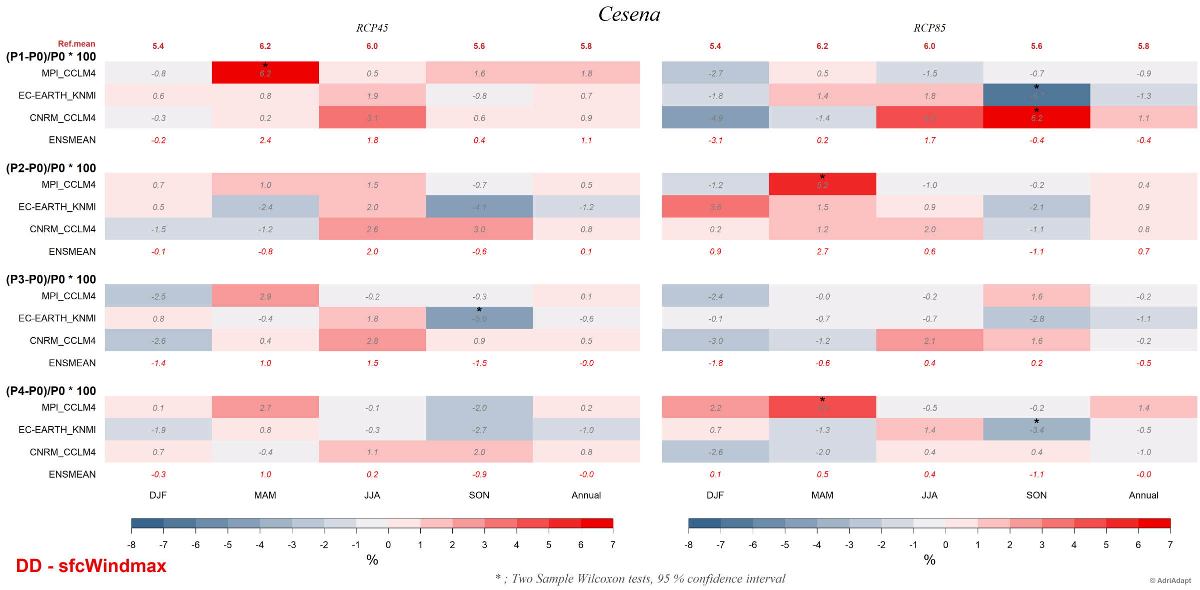

RCP45

	DJF	MAM	JJA	SON	Annual
Ref.mean	5.4	6.2	6.0	5.6	5.8
(P1-P0)/P0 * 100					
MPI_CCLM4	-0.8	* 6.2	0.5	1.6	1.8
EC-EARTH_KNMI	0.6	0.8	1.9	-0.8	0.7
CNRM_CCLM4	-0.3	0.2	3.1	0.6	0.9
ENSMEAN	-0.2	2.4	1.8	0.4	1.1
(P2-P0)/P0 * 100					
MPI_CCLM4	0.7	1.0	1.5	-0.7	0.5
EC-EARTH_KNMI	0.5	-2.4	2.0	-4.1	-1.2
CNRM_CCLM4	-1.5	-1.2	2.6	3.0	0.8
ENSMEAN	-0.1	-0.8	2.0	-0.6	0.1
(P3-P0)/P0 * 100					
MPI_CCLM4	-2.5	2.9	-0.2	-0.3	0.1
EC-EARTH_KNMI	0.8	-0.4	1.8	* -5.0	-0.6
CNRM_CCLM4	-2.6	0.4	2.8	0.9	0.5
ENSMEAN	-1.4	1.0	1.5	-1.5	-0.0
(P4-P0)/P0 * 100					
MPI_CCLM4	0.1	2.7	-0.1	-2.0	0.2
EC-EARTH_KNMI	-1.9	0.8	-0.3	-2.7	-1.0
CNRM_CCLM4	0.7	-0.4	1.1	2.0	0.8
ENSMEAN	-0.3	1.0	0.2	-0.9	-0.0

RCP85

	DJF	MAM	JJA	SON	Annual
Ref.mean	5.4	6.2	6.0	5.6	5.8
(P1-P0)/P0 * 100					
MPI_CCLM4	-2.7	0.5	-1.5	-0.7	-0.9
EC-EARTH_KNMI	-1.8	1.4	1.8	* -6.7	-1.3
CNRM_CCLM4	-4.9	-1.4	4.6	* 6.2	1.1
ENSMEAN	-3.1	0.2	1.7	-0.4	-0.4
(P2-P0)/P0 * 100					
MPI_CCLM4	-1.2	* 5.2	-1.0	-0.2	0.4
EC-EARTH_KNMI	3.6	1.5	0.9	-2.1	0.9
CNRM_CCLM4	0.2	1.2	2.0	-1.1	0.8
ENSMEAN	0.9	2.7	0.6	-1.1	0.7
(P3-P0)/P0 * 100					
MPI_CCLM4	-2.4	-0.0	-0.2	1.6	-0.2
EC-EARTH_KNMI	-0.1	-0.7	-0.7	-2.8	-1.1
CNRM_CCLM4	-3.0	-1.2	2.1	1.6	-0.2
ENSMEAN	-1.8	-0.6	0.4	0.2	-0.5
(P4-P0)/P0 * 100					
MPI_CCLM4	2.2	* 4.9	-0.5	-0.2	1.4
EC-EARTH_KNMI	0.7	-1.3	1.4	* -3.4	-0.5
CNRM_CCLM4	-2.6	-2.0	0.4	0.4	-1.0
ENSMEAN	0.1	0.5	0.4	-1.1	-0.0

** ; Two Sample Wilcoxon tests, 95 % confidence interval*

Figure 5-189: Seasonal and annual maximum wind module (maximum wind speed at 10m height) obtained by dynamical downscaling for Cesena: Ref. mean is 20 year simulated period (1986-2005) in ms^{-1}; P1-P0, P2-P0, P3-P0, P4-P0 are changes (in %) in the future for following periods P1: 2021-2040, P2: 2041-2060, P3: 2061-2080, P4: 2081-2100. Differences are shown for individual models. Significant change is marked by star. Change is also shown as ensemble mean (ENSMEAN), not tested for significance. Left column is for RCP4.5 scenario and right for RCP8.5 scenario.

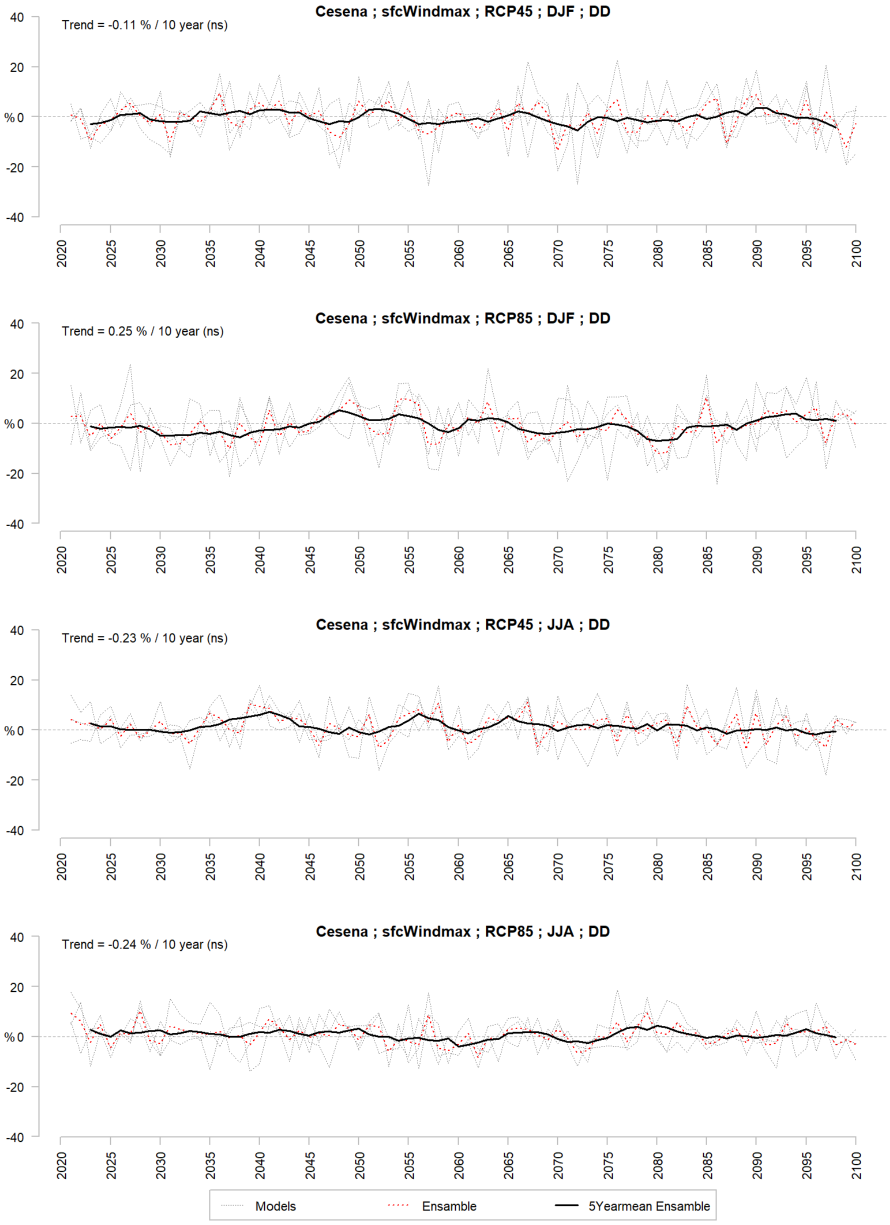

Figure 5-190: Variability of future maximum wind module (maximum wind speed at 10m height) (in %) in Cesena for 2021-2100 obtained by dynamically downscaling for winter (DJF) and summer (JJA) and two RCP scenarios: individual models are in grey, the ensemble mean in red, 5-year moving average in black. Significant trend is marked with star (ns if not significant).

6.5.2 Statistically downscaled results

In this section we present future climate changes of temperature and precipitation related indices for Cesena, as result from the statistical downscaling techniques constructed based on the observed local data/observed large scale circulation patterns and, applied then to future large-scale circulation patterns simulated by 4GCMs in the framework of CMIP5 experiments. The coordinates of the Cesena grid point are included in table A from Annexes. The results are presented as follow:

- climate change diagram of an individual index for each season and on annual basis for four considered future periods (P1, P2, P3, P4), for two emission scenarios (RCP4.5 and RCP8.5). Climate change is calculated as difference between future (P1, P2, P3, P4) and reference period (P0) for temperature indices and some extreme precipitation indices, and as relative differences (expressed in %) for some precipitation indices. Reference period is 1986-2005, the Ref.mean (obs.) from the diagram (see below) is the climate observed value registered at station take into analysis, while climate changes (P1-P0; P2-P0,P3-P0;P4-P0) are shown for different models (SD_CMCC-CM, SD_CAN-ESM2, SD-MPI, SD_CNRM) as well as for ensemble mean of models (ENSMEAN). The t-Student test is applied to test the statistical significance of future climate (values from P1, or P2, or P3, or P4) with respect to present climate value (value from P0) and the results significant at 95% are marked by a star.
- time series of future anomaly of an individual index for DJF and JJA and for two emission scenarios RCP4.5 and RCP8.5; the anomaly is calculated respect to the reference period and shown for individual models, ensemble mean and 5-year moving average. Mann Kendall trend test is applied to ensemble mean (for 95 % confidence level). Significant trend is marked with star (n.s. if not significant)

6.5.2.1 *Temperature related indices projections*

6.5.2.1.1 *Seasonal minimum and maximum temperature*

Projected changes of seasonal and annual minimum temperature for Cesena are shown in figure 5-191, for RCP4.5 and RCP8.5 and over P1, P2, P3 and P4 with respect to present climate (P0). Following the moderate RCP4.5 scenario we expect an increase in annual minimum temperature between 1°C during P1 and up to 2.3°C going to the end of century (P4). The projected increase is higher for RCP8.5, especially for P3 and P4 when the simulations show changes in annual minimum temperature about 3.5°C for P3 and 4.7°C for P4. Analysing in details the seasonal projected changes it could be observed that summer is season with higher magnitude of changes, up to 2.5°C for RCP4.5 and up to 5.1°C for RCP8.5(P4 period). As regards other seasons, the results are significant and higher amplitude especially for RCP8.5 (P3 and P4). Positive and significant trends are simulated for winter and summer minimum temperature, more intense for RCP8.5 and especially in summer season, about 0.6°C/decade (figure 5-192).

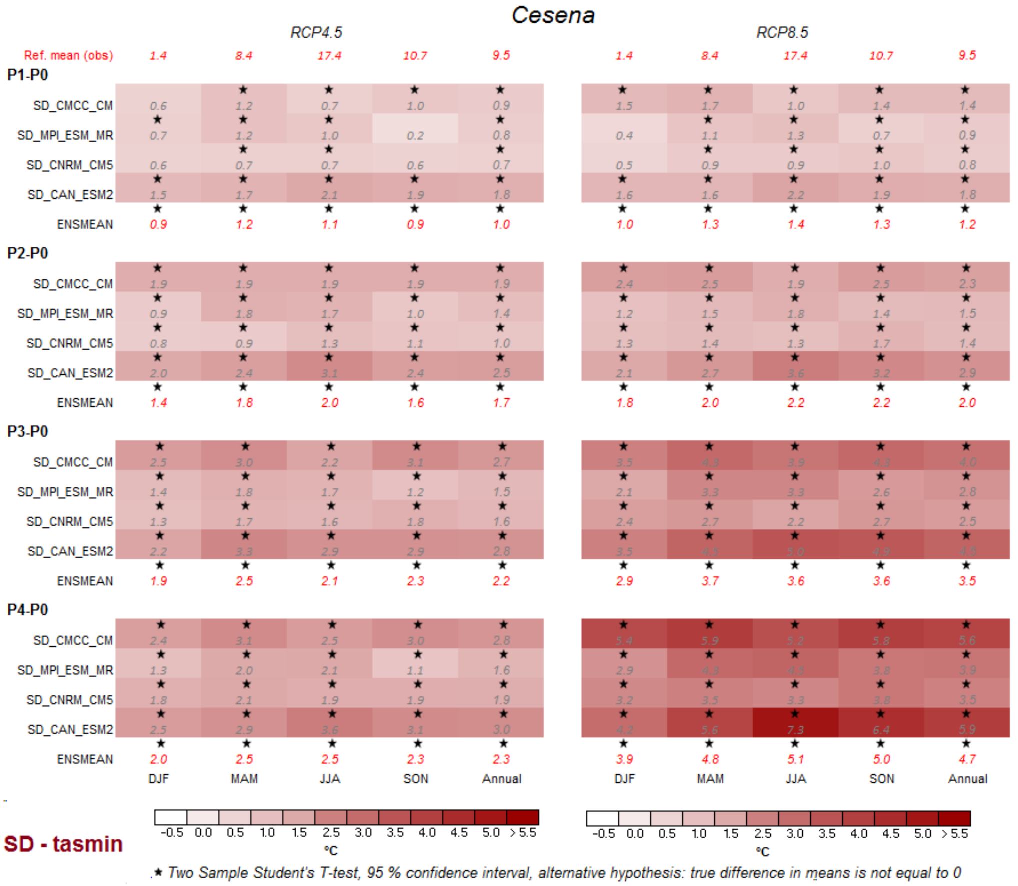

	RCP4.5					RCP8.5				
	DJF	MAM	JJA	SON	Annual	DJF	MAM	JJA	SON	Annual
Ref. mean (obs)	1.4	8.4	17.4	10.7	9.5	1.4	8.4	17.4	10.7	9.5
P1-P0										
SD_CMCC_CM	0.6	★ 1.2	★ 0.7	★ 1.0	★ 0.9	★ 1.5	★ 1.7	★ 1.0	★ 1.4	★ 1.4
SD_MPI_ESM_MR	★ 0.7	★ 1.2	★ 1.0	0.2	★ 0.8	0.4	★ 1.1	★ 1.3	★ 0.7	★ 0.9
SD_CNRM_CM5	0.6	★ 0.7	★ 0.7	0.6	★ 0.7	0.5	★ 0.9	★ 0.9	★ 1.0	★ 0.8
SD_CAN_ESM2	★ 1.5	★ 1.7	★ 2.1	★ 1.9	★ 1.8	★ 1.6	★ 1.6	★ 2.2	★ 1.9	★ 1.8
ENSMEAN	★ 0.9	★ 1.2	★ 1.1	★ 0.9	★ 1.0	★ 1.0	★ 1.3	★ 1.4	★ 1.3	★ 1.2
P2-P0										
SD_CMCC_CM	★ 1.9	★ 1.9	★ 1.9	★ 1.9	★ 1.9	★ 2.4	★ 2.5	★ 1.9	★ 2.5	★ 2.3
SD_MPI_ESM_MR	★ 0.9	★ 1.8	★ 1.7	★ 1.0	★ 1.4	★ 1.2	★ 1.5	★ 1.8	★ 1.4	★ 1.5
SD_CNRM_CM5	★ 0.8	★ 0.9	★ 1.3	★ 1.1	★ 1.0	★ 1.3	★ 1.4	★ 1.3	★ 1.7	★ 1.4
SD_CAN_ESM2	★ 2.0	★ 2.4	★ 3.1	★ 2.4	★ 2.5	★ 2.1	★ 2.7	★ 3.6	★ 3.2	★ 2.9
ENSMEAN	★ 1.4	★ 1.8	★ 2.0	★ 1.6	★ 1.7	★ 1.8	★ 2.0	★ 2.2	★ 2.2	★ 2.0
P3-P0										
SD_CMCC_CM	★ 2.5	★ 3.0	★ 2.2	★ 3.1	★ 2.7	★ 3.5	★ 4.3	★ 3.9	★ 4.3	★ 4.0
SD_MPI_ESM_MR	★ 1.4	★ 1.8	★ 1.7	★ 1.2	★ 1.5	★ 2.1	★ 3.3	★ 3.3	★ 2.6	★ 2.8
SD_CNRM_CM5	★ 1.3	★ 1.7	★ 1.6	★ 1.8	★ 1.6	★ 2.4	★ 2.7	★ 2.2	★ 2.7	★ 2.5
SD_CAN_ESM2	★ 2.2	★ 3.3	★ 2.9	★ 2.9	★ 2.8	★ 3.5	★ 4.5	★ 5.0	★ 4.9	★ 4.5
ENSMEAN	★ 1.9	★ 2.5	★ 2.1	★ 2.3	★ 2.2	★ 2.9	★ 3.7	★ 3.6	★ 3.6	★ 3.5
P4-P0										
SD_CMCC_CM	★ 2.4	★ 3.1	★ 2.5	★ 3.0	★ 2.8	★ 5.4	★ 5.9	★ 5.2	★ 5.8	★ 5.6
SD_MPI_ESM_MR	★ 1.3	★ 2.0	★ 2.1	★ 1.1	★ 1.6	★ 2.9	★ 4.3	★ 4.5	★ 3.8	★ 3.9
SD_CNRM_CM5	★ 1.8	★ 2.1	★ 1.9	★ 1.9	★ 1.9	★ 3.2	★ 3.5	★ 3.3	★ 3.8	★ 3.5
SD_CAN_ESM2	★ 2.5	★ 2.9	★ 3.6	★ 3.1	★ 3.0	★ 4.2	★ 5.6	★ 7.3	★ 6.4	★ 5.9
ENSMEAN	★ 2.0	★ 2.5	★ 2.5	★ 2.3	★ 2.3	★ 3.9	★ 4.8	★ 5.1	★ 5.0	★ 4.7

★ Two Sample Student's T-test, 95 % confidence interval, alternative hypothesis: true difference in means is not equal to 0

Figure 5-191: Seasonal and annual minimum temperature: observed values over reference period (in red), changes projected by statistical downscaling applied to 4GCMs and the Ensemble Mean of changes over the four periods (P1, P2, P3, P4) projected in the framework of RCP4.5 (left) and RCP8.5 (right). Significant change is marked by star (source Arpae-Simc)

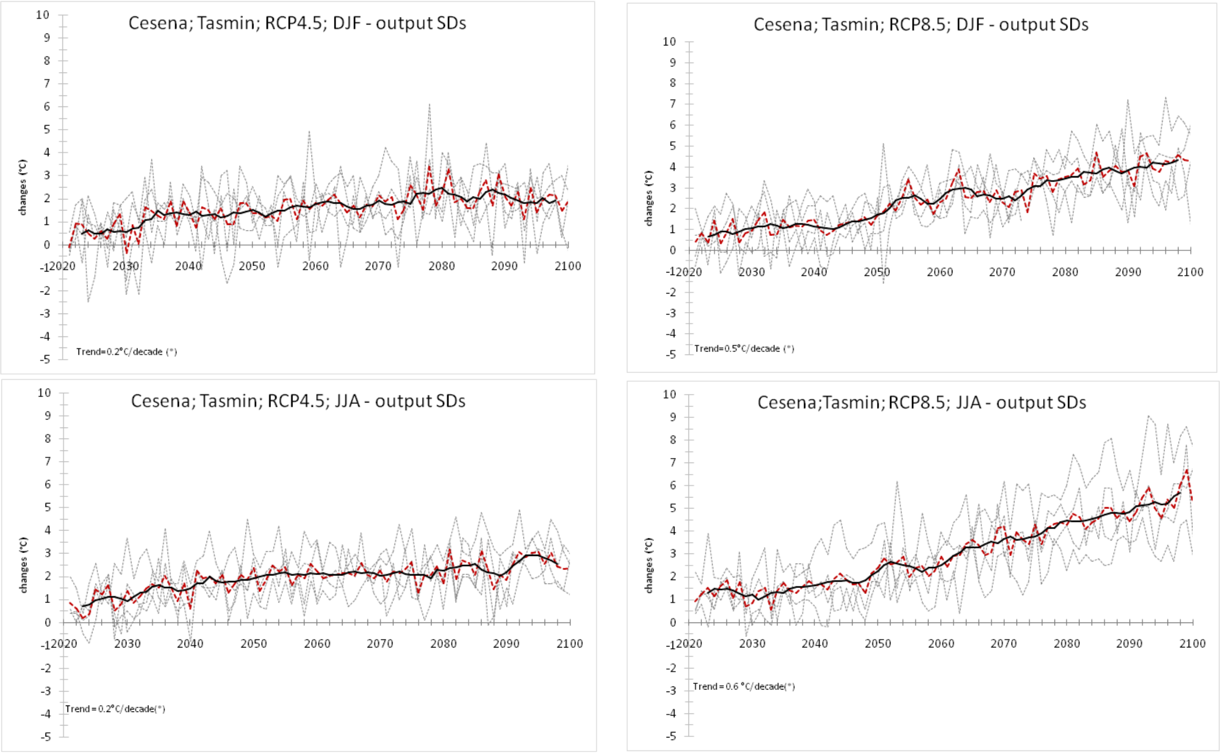

Figure 5-192: Variability of future changes of winter (DJF) and summer (JJA) minimum temperature projected through SDs applied to 4GCMs (grey lines); the Ensemble Mean (red line) and moving average (black line) - scenario RCP4.5 (left) and RCP8.5 (right), 2021-2100 period Significant trend is marked with star while n.s. means not significant (source Arpae-Simc).

Projected changes of seasonal and annual maximum temperature for Cesena are shown in figure 5-193, for RCP4.5 and RCP8.5 and over P1, P2, P3 and P4 with respect to present climate (P0). Following the moderate RCP4.5 scenario we expect an increase in annual maximum temperature between 1.5°C during P1 and up to 3.3°C going to the end of century (P4). The projected increase is higher for RCP8.5, especially for P3 and P4 when the simulations show changes in annual maximum temperature about 4.9°C and 6.6°C, respectively.

Analysing in details the seasonal projected changes of maximum temperature it could be observed that during summer the expected changes is very high, between 5.4°C for RCP4.5 and 11°C for RCP8.5 at the end of century (P4). Considering that the climatological value of summer maximum temperature is 30°C (1985-2006) an increase of 11°C to the end of century for RCP8.5 means values around 41°C. Actually, this value was recently registered over Emilia Romagna, but is very rare, an extreme temperature. The future projections indicate that this could became the climatological value (normal value) for 281-2100.

Positive and significant trends are simulated for winter and summer maximum temperature, more intense for RCP8.5 and especially in summer season, about 1°C/decade over 2021-2100 period (figure 5-194).

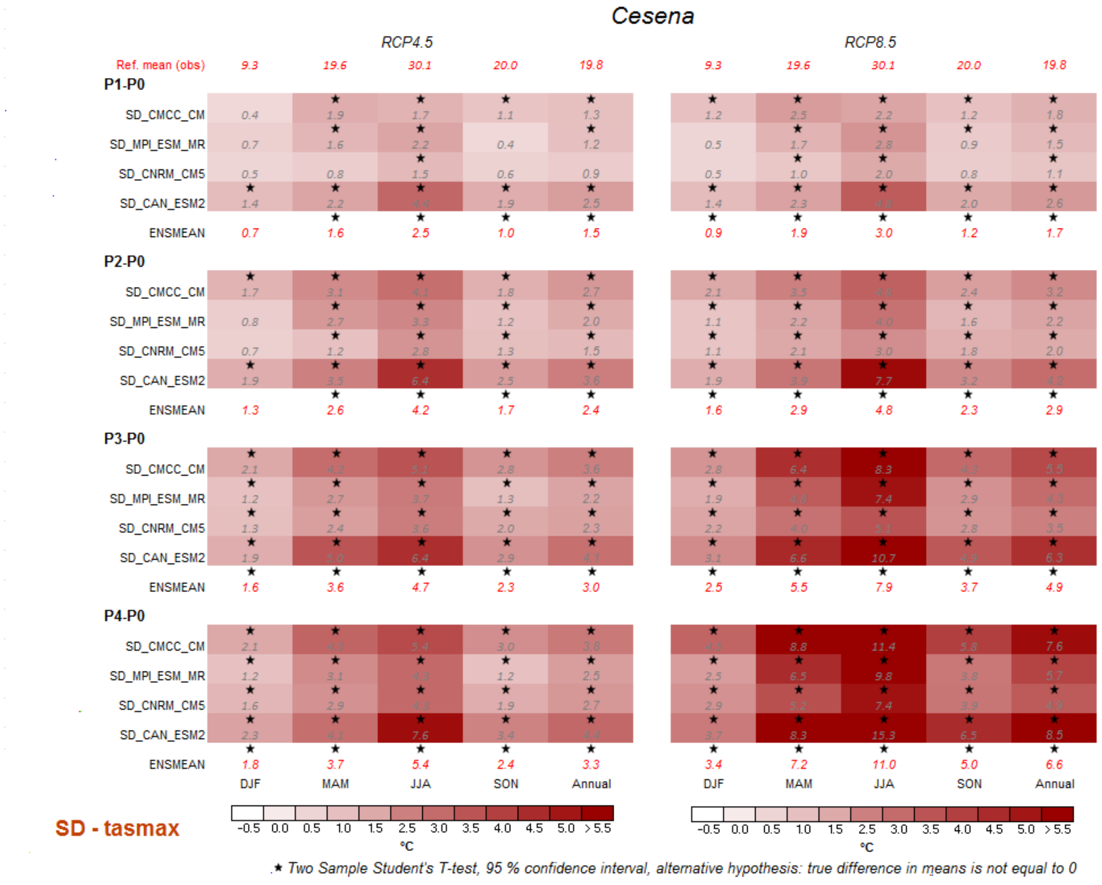

★ Two Sample Student's T-test, 95 % confidence interval, alternative hypothesis: true difference in means is not equal to 0

Figure 5-193: Seasonal and annual maximum temperature: observed values over reference period (in red), changes projected by statistical downscaling applied to 4GCMs and the Ensemble Mean of changes over the four periods (P1, P2, P3, P4) projected in the framework of RCP4.5 (left) and RCP8.5 (right Significant change is marked by star (source Arpae-Simc)

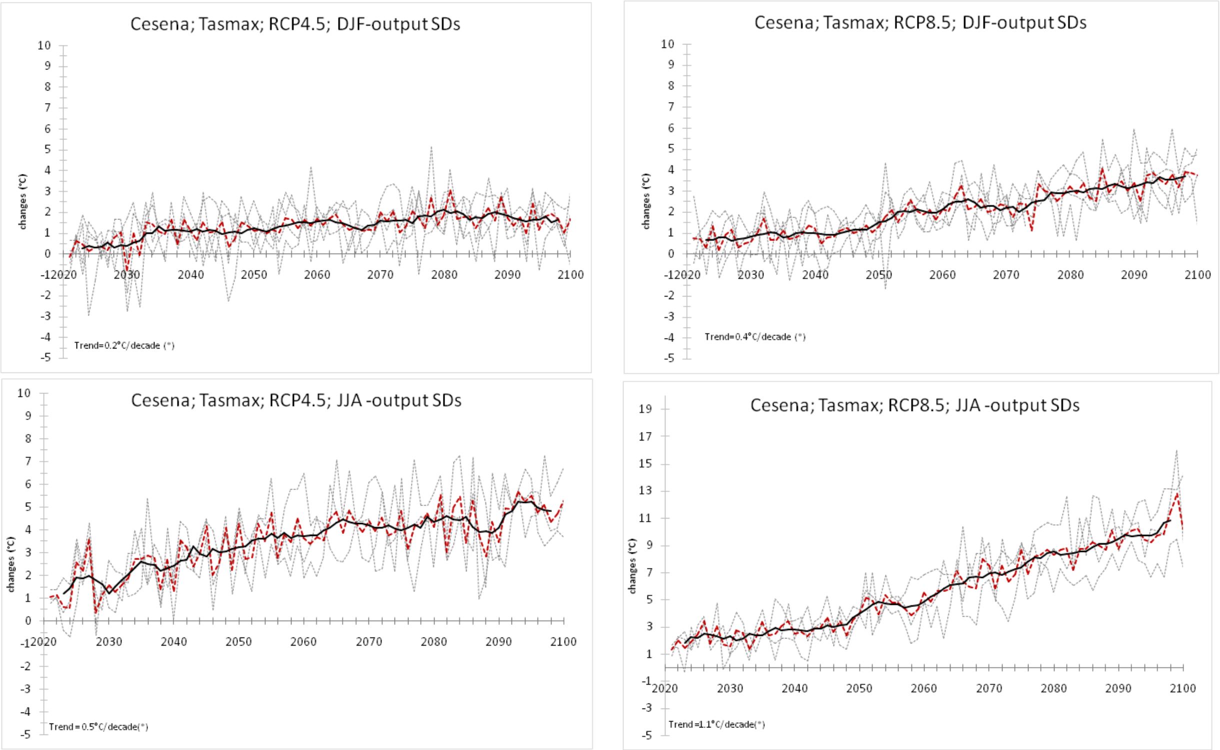

Figure 5-194: Variability of future changes of winter (DJF) and summer (JJA) maximum temperature projected through SDs applied to 4GCMs (grey lines); the Ensemble Mean (red line) and moving average (black line) - scenario RCP4.5 (left) and RCP8.5 (right), 2021-2100 period Significant trend is marked with star while n.s. means not significant (source Arpae-Simc).

6.5.2.1.2 *Extreme temperature*

5th percentile of minimum temperature

The analysis performed on scenarios of extreme temperature, 5th minimum temperature and 95th maximum temperature reveals important future changes at Cesena. An increase in *annual* 5th percentile of minimum temperature of 1°C is projected during the first period (2021-2040) and, up to 2°C going to the end of century, in the framework of RP4.5 emission scenario. The signal became more intense for RCP8.5 emission scenario and especially during 2061-2080 and 2081-2100 periods, when the annual increases could reach 2.6°C during P3 and 3.5°C during P4 (see figure 5-195).

The projected changes are significant at seasonal level, with higher amplitude during autumn, winter and spring. The projected changes in autumn reach 2.8 °C for RCP4.5 and .9°C for RCP8.5 to the end of century, while those of winter and spring could reach 2° °C for RCP4.5 and 3°°C for RCP8.5 The long-term variability shows positive trends, both in winter and summer, statistically significant.(see figure 5-196).

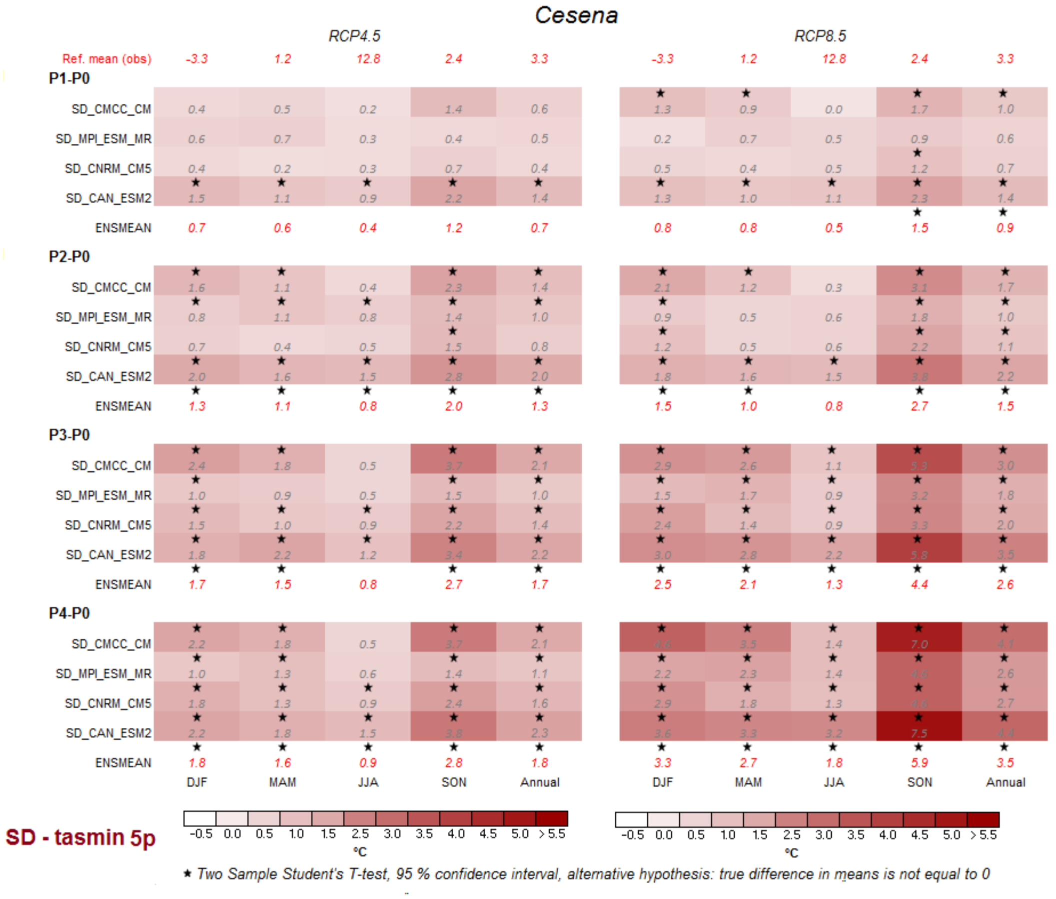

	RCP4.5					RCP8.5				
	DJF	MAM	JJA	SON	Annual	DJF	MAM	JJA	SON	Annual
Ref. mean (obs)	-3.3	1.2	12.8	2.4	3.3	-3.3	1.2	12.8	2.4	3.3
P1-P0										
SD_CMCC_CM	0.4	0.5	0.2	1.4	0.6	★ 1.3	★ 0.9	0.0	★ 1.7	★ 1.0
SD_MPI_ESM_MR	0.6	0.7	0.3	0.4	0.5	0.2	0.7	0.5	0.9	0.6
SD_CNRM_CM5	0.4	0.2	0.3	0.7	0.4	0.5	0.4	0.5	★ 1.2	0.7
SD_CAN_ESM2	★ 1.5	★ 1.1	★ 0.9	★ 2.2	★ 1.4	★ 1.3	★ 1.0	★ 1.1	★ 2.3	★ 1.4
ENSMEAN	0.7	0.6	0.4	1.2	0.7	0.8	0.8	0.5	★ 1.5	★ 0.9
P2-P0										
SD_CMCC_CM	★ 1.6	★ 1.1	0.4	★ 2.3	★ 1.4	★ 2.1	★ 1.2	0.3	★ 3.1	★ 1.7
SD_MPI_ESM_MR	★ 0.8	★ 1.1	★ 0.8	★ 1.4	★ 1.0	★ 0.9	0.5	0.6	★ 1.8	★ 1.0
SD_CNRM_CM5	0.7	0.4	0.5	★ 1.5	0.8	★ 1.2	0.5	0.6	★ 2.2	★ 1.1
SD_CAN_ESM2	★ 2.0	★ 1.6	★ 1.5	★ 2.8	★ 2.0	★ 1.8	★ 1.6	★ 1.5	★ 3.8	★ 2.2
ENSMEAN	★ 1.3	★ 1.1	★ 0.8	★ 2.0	★ 1.3	★ 1.5	★ 1.0	0.8	★ 2.7	★ 1.5
P3-P0										
SD_CMCC_CM	★ 2.4	★ 1.8	0.5	★ 3.7	★ 2.1	★ 2.9	★ 2.6	★ 1.1	★ 5.3	★ 3.0
SD_MPI_ESM_MR	★ 1.0	0.9	0.5	★ 1.5	★ 1.0	★ 1.5	★ 1.7	★ 0.9	★ 3.2	★ 1.8
SD_CNRM_CM5	★ 1.5	★ 1.0	★ 0.9	★ 2.2	★ 1.4	★ 2.4	★ 1.4	★ 0.9	★ 3.3	★ 2.0
SD_CAN_ESM2	★ 1.8	★ 2.2	★ 1.2	★ 3.4	★ 2.2	★ 3.0	★ 2.8	★ 2.2	★ 5.8	★ 3.5
ENSMEAN	★ 1.7	★ 1.5	0.8	★ 2.7	★ 1.7	★ 2.5	★ 2.1	★ 1.3	★ 4.4	★ 2.6
P4-P0										
SD_CMCC_CM	★ 2.2	★ 1.8	0.5	★ 3.7	★ 2.1	★ 4.6	★ 3.5	★ 1.4	★ 7.0	★ 4.1
SD_MPI_ESM_MR	★ 1.0	★ 1.3	0.6	★ 1.4	★ 1.1	★ 2.2	★ 2.3	★ 1.4	★ 4.6	★ 2.6
SD_CNRM_CM5	★ 1.8	★ 1.3	★ 0.9	★ 2.4	★ 1.6	★ 2.9	★ 1.8	★ 1.3	★ 4.6	★ 2.7
SD_CAN_ESM2	★ 2.2	★ 1.8	★ 1.5	★ 3.8	★ 2.3	★ 3.6	★ 3.3	★ 3.2	★ 7.5	★ 4.4
ENSMEAN	★ 1.8	★ 1.6	★ 0.9	★ 2.8	★ 1.8	★ 3.3	★ 2.7	★ 1.8	★ 5.9	★ 3.5

★ *Two Sample Student's T-test, 95 % confidence interval, alternative hypothesis: true difference in means is not equal to 0*

https://www.italy-croatia.eu/adriadapt

Figure 5-195: 5th percentile of seasonal and annual minimum temperature: observed values over reference period (in red), changes projected by statistical downscaling applied to 4GCMs and the Ensemble Mean of changes over the four periods (P1,P2,P3,P4) projected in the framework of RCP4.5 (left) and RCP8.5 (right). Significant change is marked by star (source Arpae-Simc)

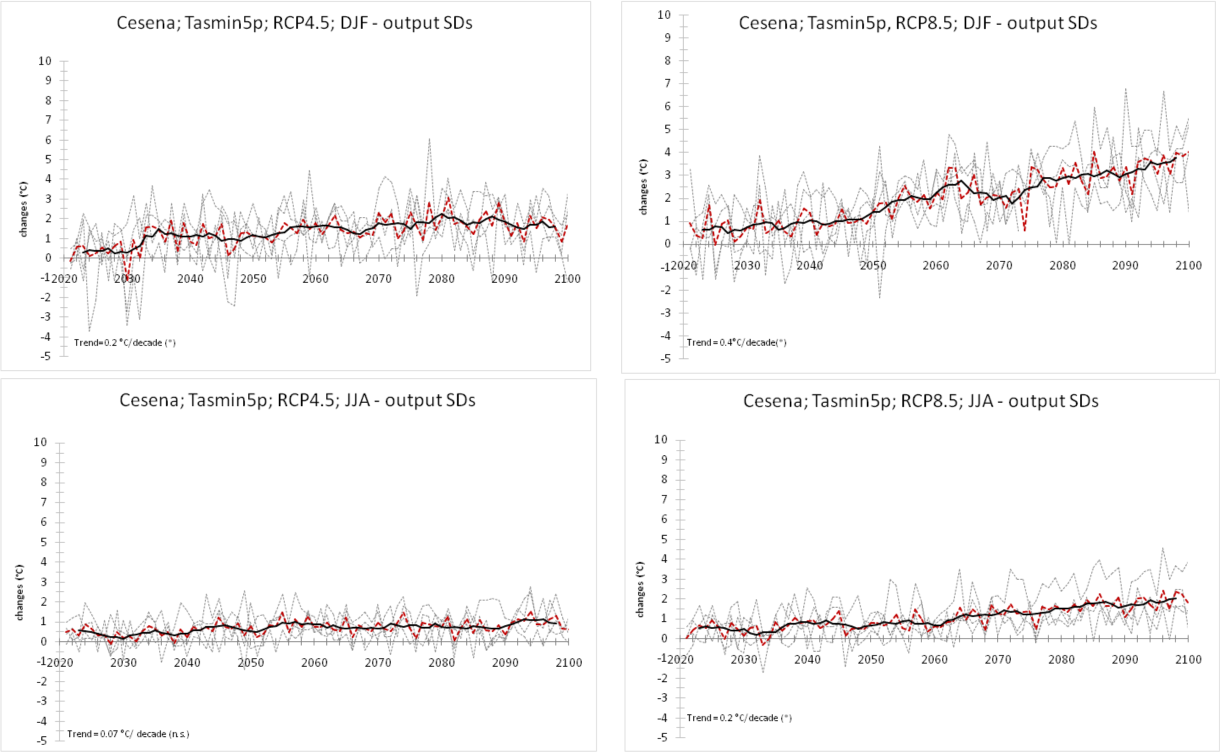

Figure 5-196: Variability of future changes of winter (DJF) and summer (JJA) of 5th minimum temperature through SDs applied to 4GCMs (grey lines); the Ensemble Mean (red line) and moving average (black line) - scenario RCP4.5 (left) and RCP8.5 (right), 2021-2100 period Significant trend is marked with star while n.s. means not significant (source Arpae-Simc).

95th percentile of maximum temperature

Future change of 95th percentile of maximum temperature in Cesena grid point is projected to increase from P1 to P4 periods, with amplitudes that vary from model to model.

The Ensemble Mean shows an increase in annual value of changes between 1.1 and 2.4°C for RCP4.5 and, between 1.3°C and 5°C in the framework of RCP8.5 (Figure 5-197). A deep analysis on projected changes reveals that higher values are expected to occur during summer season with peak of changes for RCP8.5 around 6.6°C during 2081-2100 with respect to 1986-2005. In addition, as could be noted the projected changes are similar for P1 and P2 in the framework of RCP4.5 and RCP8.5, but starting with P3 the changes have higher magnitude in RCP8.5. All the changes are significant form the statistical point of view.

Variability of future changes of 95th percentile of maximum temperature shows positive and significant trends during winter and summer, with trends coefficients between 0.3 and 0.3°C/decade (see figure5-198).

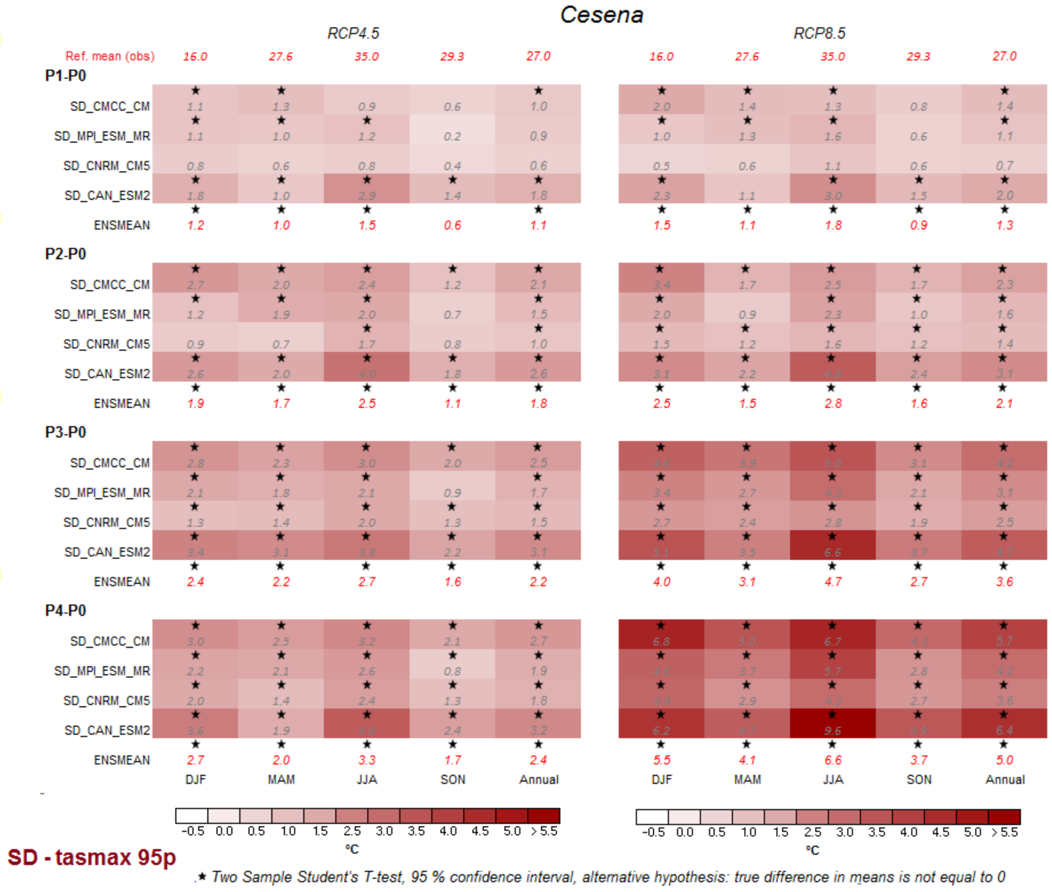

	RCP4.5					RCP8.5				
Ref. mean (obs)	16.0	27.6	35.0	29.3	27.0	16.0	27.6	35.0	29.3	27.0
P1-P0										
SD_CMCC_CM	★ 1.1	★ 1.3	0.9	0.6	★ 1.0	★ 2.0	★ 1.4	★ 1.3	0.8	★ 1.4
SD_MPI_ESM_MR	★ 1.1	★ 1.0	★ 1.2	0.2	0.9	★ 1.0	★ 1.3	★ 1.6	0.6	★ 1.1
SD_CNRM_CM5	0.8	0.6	0.8	0.4	0.6	0.5	0.6	1.1	0.6	0.7
SD_CAN_ESM2	★ 1.8	★ 1.0	★ 2.9	★ 1.4	★ 1.8	★ 2.3	1.1	★ 3.0	★ 1.5	★ 2.0
ENSMEAN	★ 1.2	★ 1.0	★ 1.5	0.6	★ 1.1	★ 1.5	★ 1.1	★ 1.8	★ 0.9	★ 1.3
P2-P0										
SD_CMCC_CM	★ 2.7	★ 2.0	★ 2.4	★ 1.2	★ 2.1	★ 3.4	★ 1.7	★ 2.5	★ 1.7	★ 2.3
SD_MPI_ESM_MR	★ 1.2	★ 1.9	★ 2.0	0.7	★ 1.5	★ 2.0	0.9	★ 2.3	★ 1.0	★ 1.6
SD_CNRM_CM5	0.9	0.7	★ 1.7	0.8	★ 1.0	★ 1.5	★ 1.2	★ 1.6	★ 1.2	★ 1.4
SD_CAN_ESM2	★ 2.6	★ 2.0	★ 4.0	★ 1.8	★ 2.6	★ 3.1	★ 2.2	★ 4.8	★ 2.4	★ 3.1
ENSMEAN	★ 1.9	★ 1.7	★ 2.5	★ 1.1	★ 1.8	★ 2.5	★ 1.5	★ 2.8	★ 1.6	★ 2.1
P3-P0										
SD_CMCC_CM	★ 2.8	★ 2.3	★ 3.0	★ 2.0	★ 2.5	★ 4.6	★ 3.9	★ 5.0	★ 3.1	★ 4.2
SD_MPI_ESM_MR	★ 2.1	★ 1.8	★ 2.1	0.9	★ 1.7	★ 3.4	★ 2.7	★ 4.2	★ 2.1	★ 3.1
SD_CNRM_CM5	★ 1.3	★ 1.4	★ 2.0	★ 1.3	★ 1.5	★ 2.7	★ 2.4	★ 2.8	★ 1.9	★ 2.5
SD_CAN_ESM2	★ 3.4	★ 3.1	★ 3.8	★ 2.2	★ 3.1	★ 5.1	★ 3.5	★ 6.6	★ 3.7	★ 4.7
ENSMEAN	★ 2.4	★ 2.2	★ 2.7	★ 1.6	★ 2.2	★ 4.0	★ 3.1	★ 4.7	★ 2.7	★ 3.6
P4-P0										
SD_CMCC_CM	★ 3.0	★ 2.5	★ 3.2	★ 2.1	★ 2.7	★ 6.8	★ 5.0	★ 6.7	★ 4.3	★ 5.7
SD_MPI_ESM_MR	★ 2.2	★ 2.1	★ 2.6	★ 0.8	★ 1.9	★ 4.6	★ 3.7	★ 5.7	★ 2.8	★ 4.2
SD_CNRM_CM5	★ 2.0	★ 1.4	★ 2.4	★ 1.3	★ 1.8	★ 4.4	★ 2.9	★ 4.2	★ 2.7	★ 3.6
SD_CAN_ESM2	★ 3.6	★ 1.9	★ 4.8	★ 2.4	★ 3.2	★ 6.2	★ 4.7	★ 9.6	★ 4.9	★ 6.4
ENSMEAN	★ 2.7	★ 2.0	★ 3.3	★ 1.7	★ 2.4	★ 5.5	★ 4.1	★ 6.6	★ 3.7	★ 5.0
	DJF	MAM	JJA	SON	Annual	DJF	MAM	JJA	SON	Annual

★ *Two Sample Student's T-test, 95 % confidence interval, alternative hypothesis: true difference in means is not equal to 0*

Figure 5-197: 95th percentile of seasonal and annual maximum temperature: observed values over reference period (in red), changes projected by statistical downscaling applied to 4GCMs and the Ensemble Mean of changes over the four periods (P1, P2, P3, P4) projected in the framework of RCP4.5 (left) and RCP 8.5 (right). Significant change is marked by star (source Arpae-Simc)

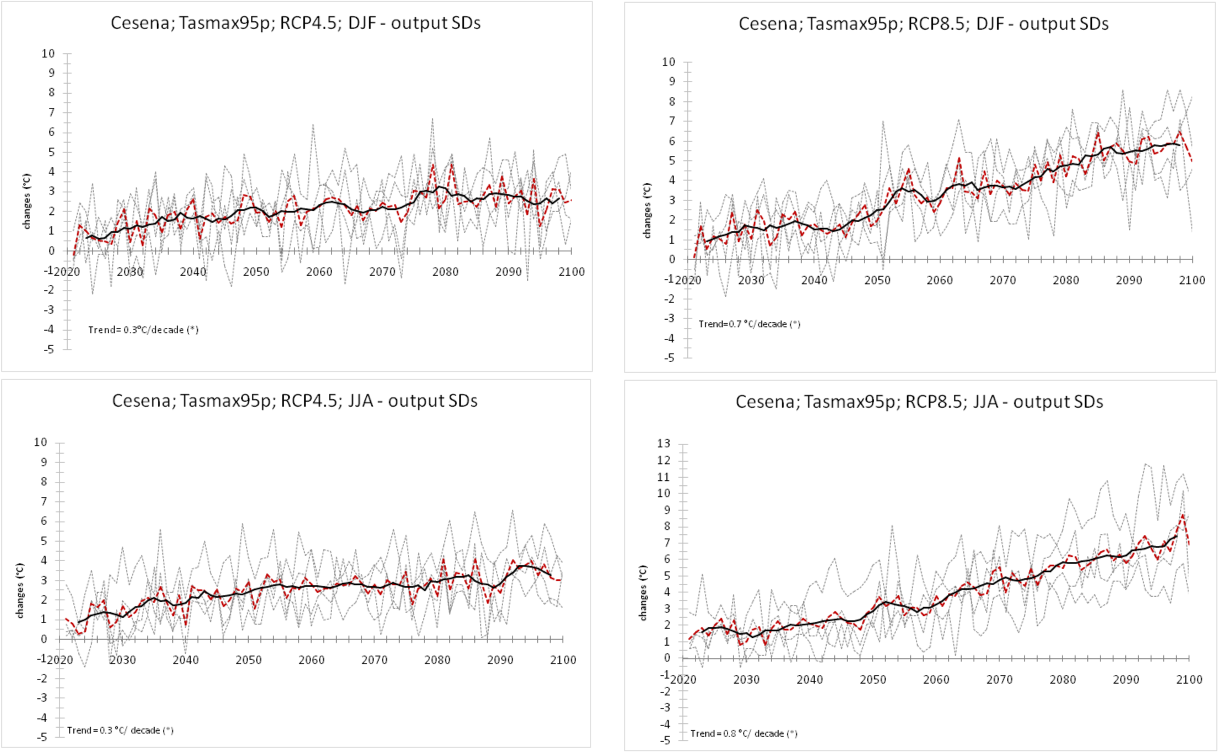

Figure 5-198: Future changes of winter (DJF) and summer (JJA) of 95th percentile of maximum temperature projected through SDs applied to 4GCMs (grey lines); the Ensemble Mean (red line) and moving average (black line) - scenario RCP4.5 (left) and RCP8.5 (right), 2021-2100 period Significant trend is marked with star while n.s. means not significant (source Arpae-Simc).

6.5.2.1.3 *Heat wave duration*

The projection of the heat wave duration, index defined as the maximum number of consecutive days with maximum temperature greater than 90th daily percentile, shows an increase during all seasons and for both RCPs. Figure 5-199 includes the projected changes for Cesena. As could be noted the magnitude is higher during spring followed by summer, autumn and winter.

During spring, the increase could reach 44 consecutive days (P4) in RCP4.5 while in the framework of RCP8.5 could reach 83 consecutive days; in summer the projected changes is up to 24 consecutive days (P4) for RCP4.5 and up to 77 days for RCP8.5 (P4). As regards long term variability (see figure 5-200) the trend is positive during winter and summer, higher in summer especially for RCP8.5 (12 days/decade)

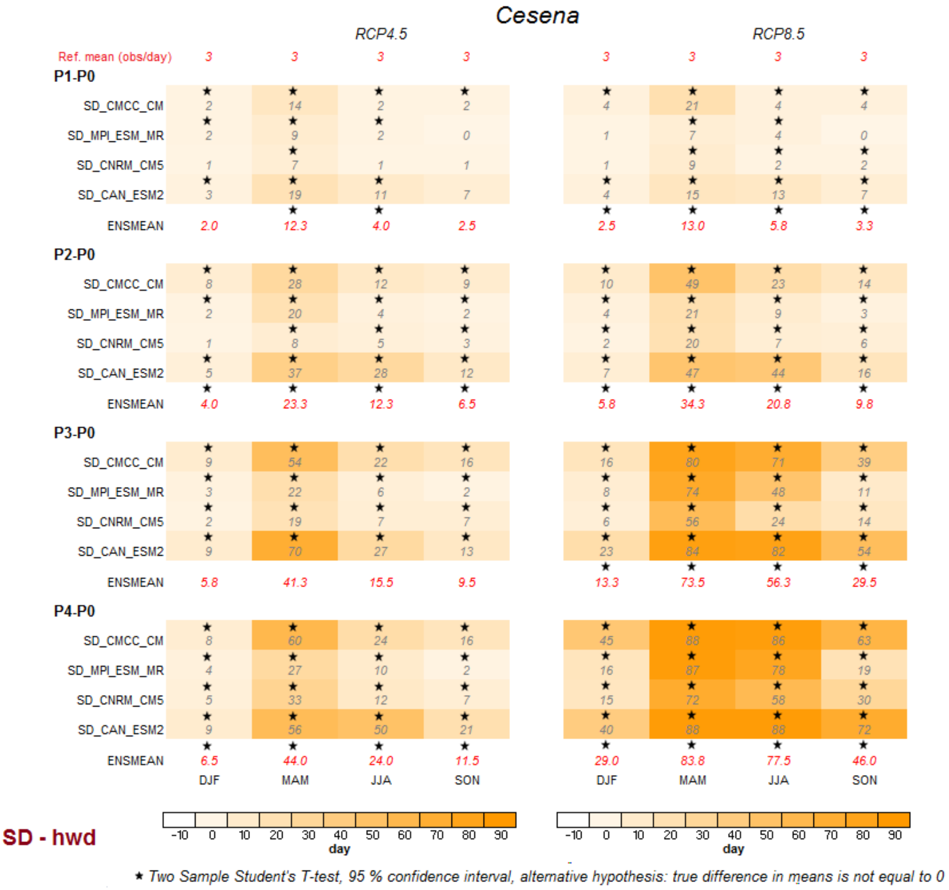

	RCP4.5				RCP8.5			
	DJF	MAM	JJA	SON	DJF	MAM	JJA	SON
Ref. mean (obs/day)	3	3	3	3	3	3	3	3
P1-P0								
SD_CMCC_CM	★ 2	★ 14	★ 2	★ 2	★ 4	★ 21	★ 4	★ 4
SD_MPI_ESM_MR	★ 2	★ 9	★ 2	0	1	★ 7	★ 4	0
SD_CNRM_CM5	1	★ 7	1	1	1	★ 9	★ 2	★ 2
SD_CAN_ESM2	★ 3	★ 19	★ 11	7	★ 4	★ 15	★ 13	★ 7
ENSMEAN	2.0	★ 12.3	★ 4.0	2.5	★ 2.5	★ 13.0	★ 5.8	★ 3.3
P2-P0								
SD_CMCC_CM	★ 8	★ 28	★ 12	★ 9	★ 10	★ 49	★ 23	★ 14
SD_MPI_ESM_MR	★ 2	★ 20	★ 4	★ 2	★ 4	★ 21	★ 9	★ 3
SD_CNRM_CM5	1	★ 8	★ 5	★ 3	★ 2	★ 20	★ 7	★ 6
SD_CAN_ESM2	★ 5	★ 37	★ 28	★ 12	★ 7	★ 47	★ 44	★ 16
ENSMEAN	★ 4.0	★ 23.3	★ 12.3	★ 6.5	★ 5.8	★ 34.3	★ 20.8	★ 9.8
P3-P0								
SD_CMCC_CM	★ 9	★ 54	★ 22	★ 16	★ 16	★ 80	★ 71	★ 39
SD_MPI_ESM_MR	★ 3	★ 22	★ 6	★ 2	★ 8	★ 74	★ 48	★ 11
SD_CNRM_CM5	★ 2	★ 19	★ 7	★ 7	★ 6	★ 56	★ 24	★ 14
SD_CAN_ESM2	★ 9	★ 70	★ 27	★ 13	★ 23	★ 84	★ 82	★ 54
ENSMEAN	5.8	41.3	15.5	9.5	★ 13.3	★ 73.5	★ 56.3	★ 29.5
P4-P0								
SD_CMCC_CM	★ 8	★ 60	★ 24	★ 16	★ 45	★ 88	★ 86	★ 63
SD_MPI_ESM_MR	★ 4	★ 27	★ 10	★ 2	★ 16	★ 87	★ 78	★ 19
SD_CNRM_CM5	★ 5	★ 33	★ 12	★ 7	★ 15	★ 72	★ 58	★ 30
SD_CAN_ESM2	★ 9	★ 56	★ 50	★ 21	★ 40	★ 88	★ 88	★ 72
ENSMEAN	★ 6.5	★ 44.0	★ 24.0	★ 11.5	★ 29.0	★ 83.8	★ 77.5	★ 46.0

★ *Two Sample Student's T-test, 95 % confidence interval, alternative hypothesis: true difference in means is not equal to 0*

https://www.italy-croatia.eu/adriadapt

Figure 5-199: Seasonal and annual heat wave duration: observed values over reference period (in red), changes projected by statistical downscaling applied to 4GCMs and the Ensemble Mean of changes over the four periods (P1,P2,P3,P4) projected in the framework of RCP4.5 (left) and RCP8.5 (right). Significant change is marked by star (source Arpae-Simc)

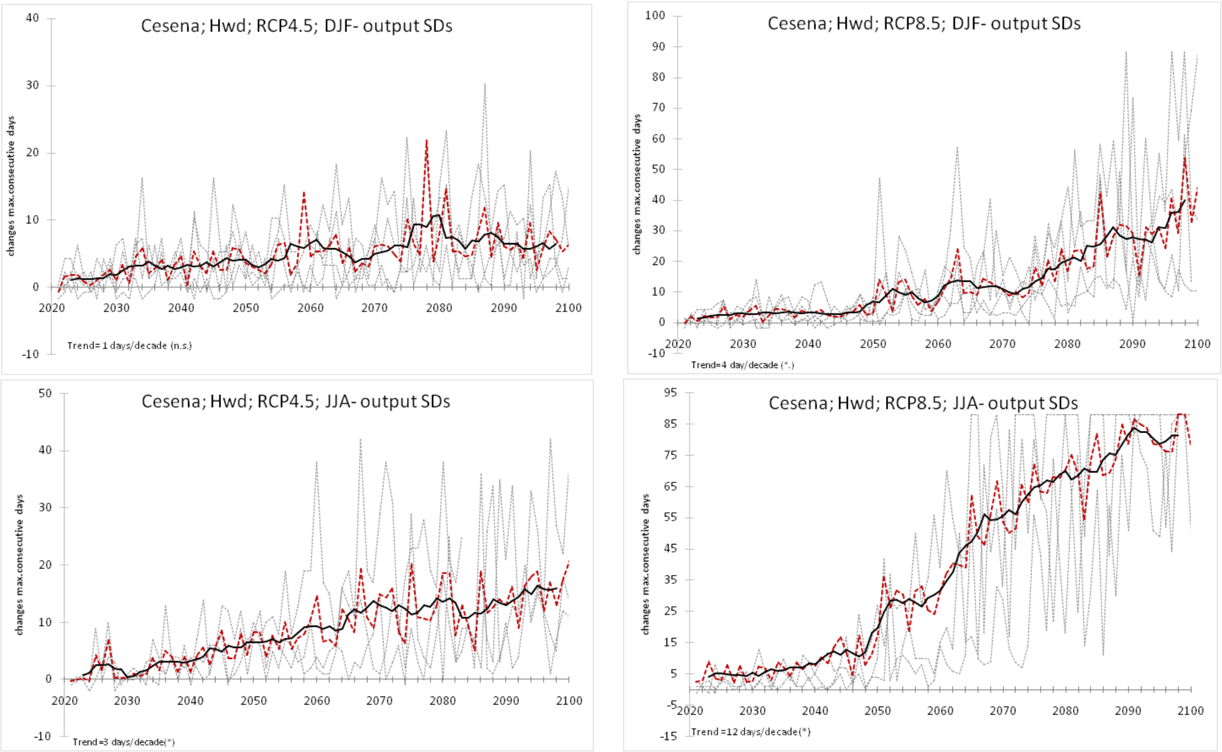

Figure 5-200: Variability of future changes of winter (DJF) and summer (JJA) heat wave duration projected through SDs applied to 4GCMs (grey lines); the Ensemble Mean (red line) and moving average (black line) - scenario RCP4.5 (left) and RCP8.5 (right), 2021-2100 period Significant trend is marked with star while n.s. means not significant (source Arpae-Simc).

6.5.2.1.4 *Tropical nights*

Seasonal changes of tropical nights (tr) in terms of differences between P1-P0, P2-P0, P3-P0, P4-P0 are shown in figures 5-201, relative to the RCP4.5 and RCP8.5 scenarios. The projection of the tropical nights, index defined as the number of days with minimum temperature greater than 20°C, shows an increase during summer season. All SDs models agree with these changes, as could be noted from figure 5-201. The value of changes varies during summer between 19 to 51 days for RCP4.5 and between 22 to 72 days for RC8.5.
Regarding long term variability of the summer index, the trend is positive and statistically significant for both RCPs, (up to 8 days/decade), over 2021-2100 (see figure 5-202).

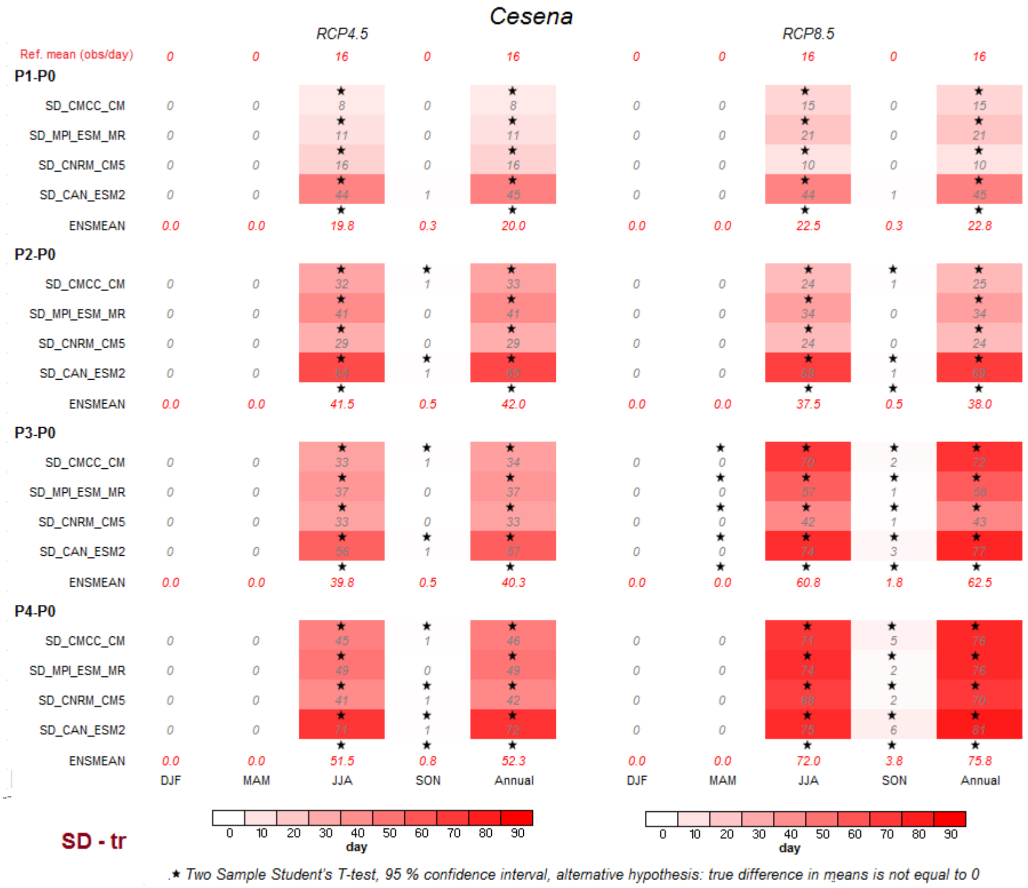

Cesena

	RCP4.5					RCP8.5				
	DJF	MAM	JJA	SON	Annual	DJF	MAM	JJA	SON	Annual
Ref. mean (obs/day)	0	0	16	0	16	0	0	16	0	16
P1-P0										
SD_CMCC_CM	0	0	★ 8	0	★ 8	0	0	★ 15	0	★ 15
SD_MPI_ESM_MR	0	0	★ 11	0	★ 11	0	0	★ 21	0	★ 21
SD_CNRM_CM5	0	0	★ 16	0	★ 16	0	0	★ 10	0	★ 10
SD_CAN_ESM2	0	0	★ 44	1	★ 45	0	0	★ 44	1	★ 45
ENSMEAN	0.0	0.0	★ 19.8	0.3	★ 20.0	0.0	0.0	★ 22.5	0.3	★ 22.8
P2-P0										
SD_CMCC_CM	0	0	★ 32	★ 1	★ 33	0	0	★ 24	★ 1	★ 25
SD_MPI_ESM_MR	0	0	★ 41	0	★ 41	0	0	★ 34	0	★ 34
SD_CNRM_CM5	0	0	★ 29	0	★ 29	0	0	★ 24	0	★ 24
SD_CAN_ESM2	0	0	★ 64	★ 1	★ 65	0	0	★ 68	★ 1	★ 69
ENSMEAN	0.0	0.0	★ 41.5	0.5	★ 42.0	0.0	0.0	★ 37.5	★ 0.5	★ 38.0
P3-P0										
SD_CMCC_CM	0	0	★ 33	★ 1	★ 34	0	★ 0	★ 70	★ 2	★ 72
SD_MPI_ESM_MR	0	0	★ 37	0	★ 37	0	★ 0	★ 57	★ 1	★ 58
SD_CNRM_CM5	0	0	★ 33	0	★ 33	0	★ 0	★ 42	★ 1	★ 43
SD_CAN_ESM2	0	0	★ 56	★ 1	★ 57	0	★ 0	★ 74	★ 3	★ 77
ENSMEAN	0.0	0.0	★ 39.8	0.5	★ 40.3	0.0	★ 0.0	★ 60.8	★ 1.8	★ 62.5
P4-P0										
SD_CMCC_CM	0	0	★ 45	★ 1	★ 46	0	0	★ 71	★ 5	★ 76
SD_MPI_ESM_MR	0	0	★ 49	0	★ 49	0	0	★ 74	★ 2	★ 76
SD_CNRM_CM5	0	0	★ 41	★ 1	★ 42	0	0	★ 68	★ 2	★ 70
SD_CAN_ESM2	0	0	★ 71	★ 1	★ 72	0	0	★ 75	★ 6	★ 81
ENSMEAN	0.0	0.0	★ 51.5	★ 0.8	★ 52.3	0.0	0.0	★ 72.0	★ 3.8	★ 75.8

★ Two Sample Student's T-test, 95 % confidence interval, alternative hypothesis: true difference in means is not equal to 0

Figure 5-201: Seasonal and annual tropical nights: observed values over reference period (in red), changes projected by statistical downscaling applied to 4GCMs and the Ensemble Mean over the four periods (P1, P2,P3,P4) projected in the framework of RCP4.5 (left) and RCP8.5 (right). Significant change is marked by star (source Arpae-Simc)

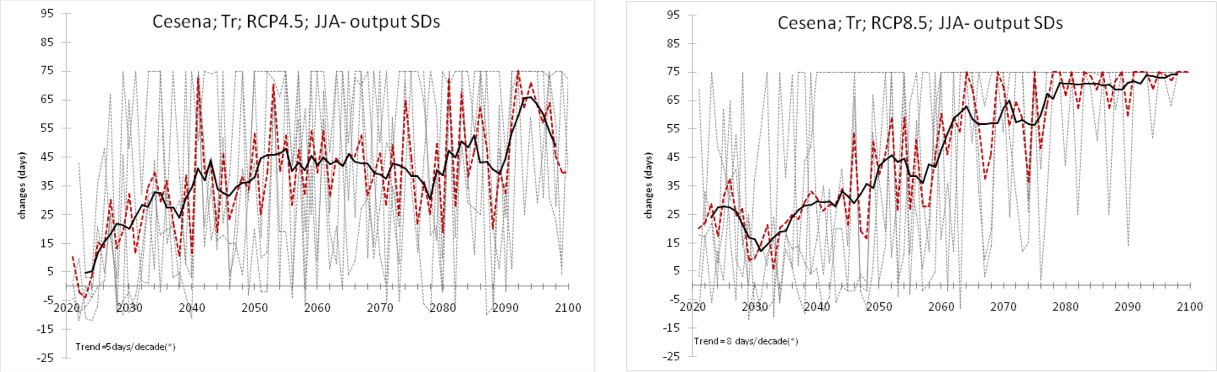

Figure 5-202: Variability of future changes of summer (JJA) tropical nights projected through SDs applied to 4GCMs (grey lines); the Ensemble Mean (red line) and moving average (black line) - scenario RCP4.5 (left) and RCP8.5 (right), 2021-2100 period. Significant trend is marked with star while n.s. means not significant (source Arpae-Simc).

6.5.2.1.5 *Frost days*

The future projections of frost days, namely the number of days with minimum temperature lower than 0°C, show for Cesena a decrease during winter, spring and autumn. All SDs models agree with these changes during all periods, as could be noted from figure 5-203. The signal of changes is higher during winter season, when values of change for RCP4.5 scenario is between -10 days during P1 up to -16 days going to the end of the century (P4). The magnitude of changes is higher for RCP8.5 between -11 to -22 days (see figure 5-149). An important signal, statistically significant is expected also during spring and autumn, especially going to the end of century (see figure 5-203)
Regarding long term variability, the trend is negative and statistically significant or both emission scenario up to -2 days/decade (see figure 5-204).

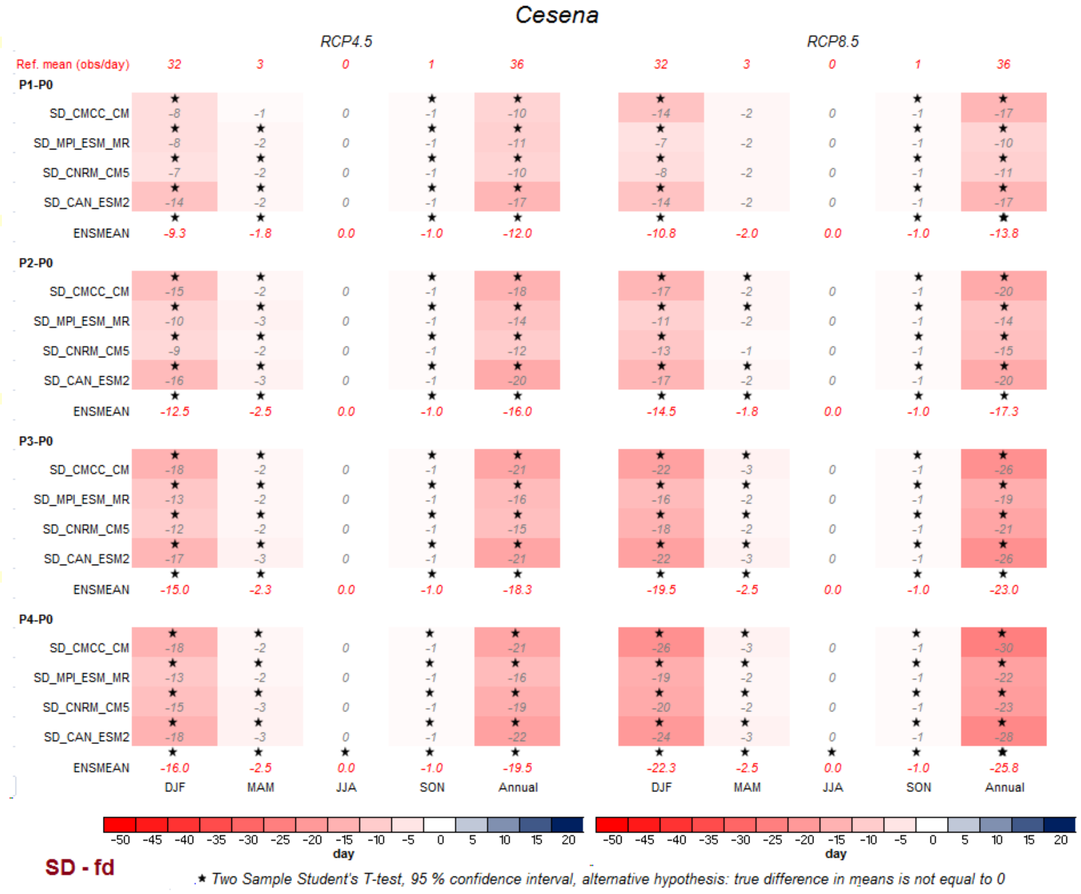

Cesena

	RCP4.5					RCP8.5				
Ref. mean (obs/day)	32	3	0	1	36	32	3	0	1	36
P1-P0										
SD_CMCC_CM	★ -8	-1	0	★ -1	★ -10	★ -14	-2	0	★ -1	★ -17
SD_MPI_ESM_MR	★ -8	★ -2	0	★ -1	★ -11	★ -7	-2	0	★ -1	★ -10
SD_CNRM_CM5	★ -7	★ -2	0	★ -1	★ -10	★ -8	-2	0	★ -1	★ -11
SD_CAN_ESM2	★ -14	★ -2	0	★ -1	★ -17	★ -14	-2	0	★ -1	★ -17
ENSMEAN	★ -9.3	★ -1.8	0.0	★ -1.0	★ -12.0	★ -10.8	-2.0	0.0	★ -1.0	★ -13.8
P2-P0										
SD_CMCC_CM	★ -15	★ -2	0	★ -1	★ -18	★ -17	★ -2	0	★ -1	★ -20
SD_MPI_ESM_MR	★ -10	★ -3	0	★ -1	★ -14	★ -11	★ -2	0	★ -1	★ -14
SD_CNRM_CM5	★ -9	★ -2	0	★ -1	★ -12	★ -13	-1	0	★ -1	★ -15
SD_CAN_ESM2	★ -16	★ -3	0	★ -1	★ -20	★ -17	★ -2	0	★ -1	★ -20
ENSMEAN	★ -12.5	★ -2.5	0.0	★ -1.0	★ -16.0	★ -14.5	★ -1.8	0.0	★ -1.0	★ -17.3
P3-P0										
SD_CMCC_CM	★ -18	★ -2	0	★ -1	★ -21	★ -22	★ -3	0	★ -1	★ -26
SD_MPI_ESM_MR	★ -13	★ -2	0	★ -1	★ -16	★ -16	★ -2	0	★ -1	★ -19
SD_CNRM_CM5	★ -12	★ -2	0	★ -1	★ -15	★ -18	★ -2	0	★ -1	★ -21
SD_CAN_ESM2	★ -17	★ -3	0	★ -1	★ -21	★ -22	★ -3	0	★ -1	★ -26
ENSMEAN	★ -15.0	★ -2.3	0.0	★ -1.0	★ -18.3	★ -19.5	★ -2.5	0.0	★ -1.0	★ -23.0
P4-P0										
SD_CMCC_CM	★ -18	★ -2	0	★ -1	★ -21	★ -26	★ -3	0	★ -1	★ -30
SD_MPI_ESM_MR	★ -13	★ -2	0	★ -1	★ -16	★ -19	★ -2	0	★ -1	★ -22
SD_CNRM_CM5	★ -15	★ -3	0	★ -1	★ -19	★ -20	★ -2	0	★ -1	★ -23
SD_CAN_ESM2	★ -18	★ -3	0	★ -1	★ -22	★ -24	★ -3	0	★ -1	★ -28
ENSMEAN	★ -16.0	★ -2.5	★ 0.0	★ -1.0	★ -19.5	★ -22.3	★ -2.5	★ 0.0	★ -1.0	★ -25.8
	DJF	MAM	JJA	SON	Annual	DJF	MAM	JJA	SON	Annual

★ Two Sample Student's T-test, 95 % confidence interval, alternative hypothesis: true difference in means is not equal to 0

Figure 5-203: Seasonal and annual frost days: observed values over reference period (in red), changes projected by statistical downscaling applied to 4GCMs and the Ensemble Mean over the four periods (P1, P2, P3, P4) projected in the framework of RCP4.5 (left) and RCP 8.5right Significant change is marked by star (source Arpae-Simc)

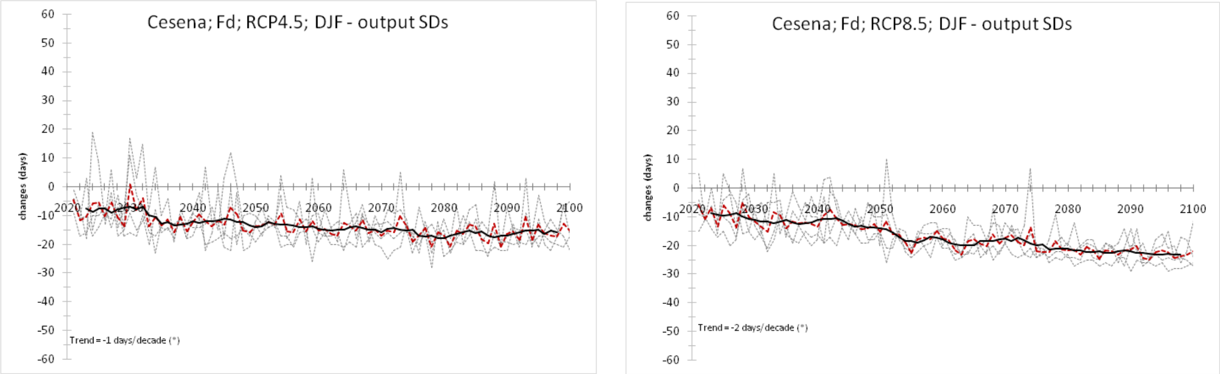

Figure 5-204: Future changes of winter (DJF) frost days projected through SDs applied to 4GCMs (grey lines); the Ensemble Mean (red line) and moving average (black line) - scenario RCP4.5 (left) and RCP8.5 (right), 2021-2100 period Significant trend is marked with star while n.s. means not significant (source Arpae-Simc).

6.5.2.2 *Precipitation related indices projection*

6.5.2.2.1 *Amount of precipitation*

The projected changes for amount of precipitation at Cesena show a general decrease over all period, seasons and for both emission scenarios. Analysing the changes presented in figure 5-205 it could be observed that all SDs agree with this signal and, especially after 2041 the changes projected by each model are significant for all seasons. Higher decrease is expected to occur during summer, between -35 % (P1) up to -48% (P4) for RCP4.5 and between -38 % (P1) up to -69% (P4) for RCP8.5 (see figure 5-205). Long term variability underlies negative trends during winter and summer, significant especially for RCP8.5 scenario (see figure 5-206).

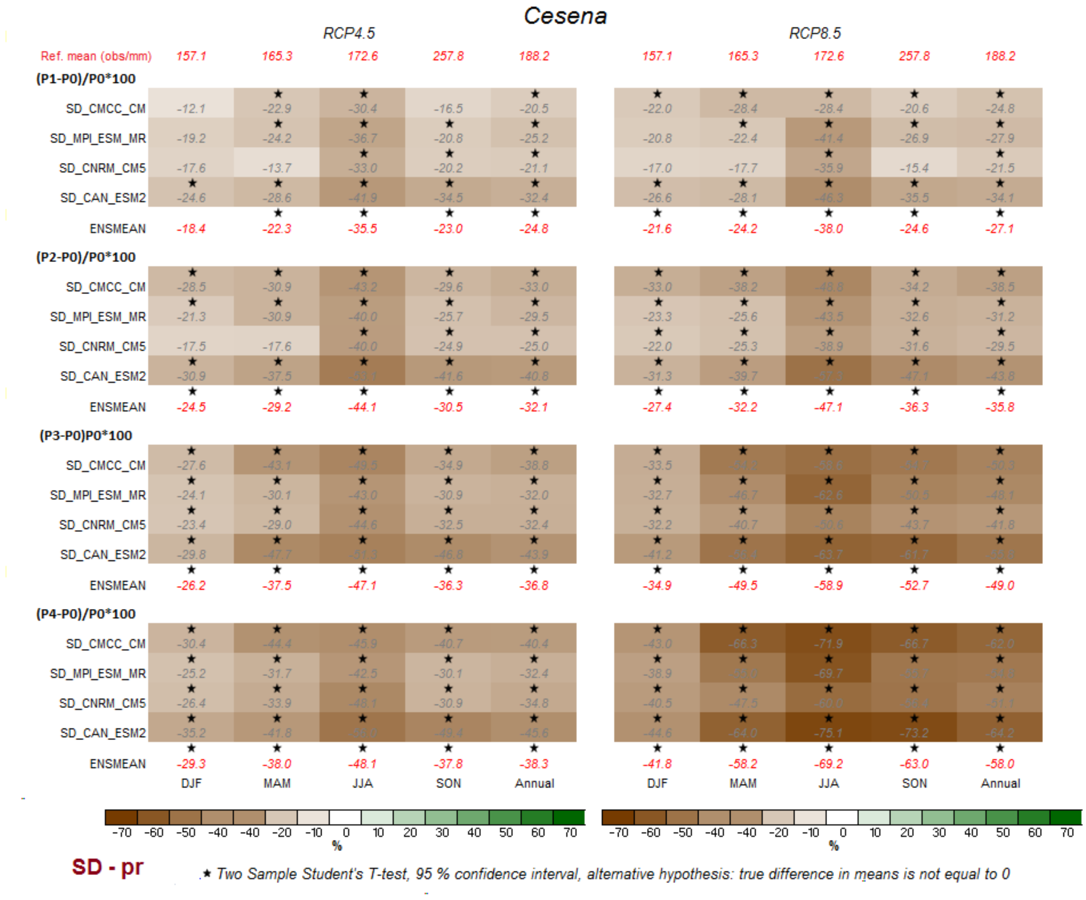

	RCP4.5					RCP8.5				
Ref. mean (obs/mm)	157.1	165.3	172.6	257.8	188.2	157.1	165.3	172.6	257.8	188.2
(P1-P0)/P0*100										
SD_CMCC_CM	-12.1	★ -22.9	★ -30.4	-16.5	★ -20.5	★ -22.0	★ -28.4	★ -28.4	★ -20.6	★ -24.8
SD_MPI_ESM_MR	-19.2	★ -24.2	★ -36.7	★ -20.8	★ -25.2	-20.8	★ -22.4	★ -41.4	★ -26.9	★ -27.9
SD_CNRM_CM5	-17.6	-13.7	★ -33.0	★ -20.2	★ -21.1	-17.0	-17.7	★ -35.9	-15.4	★ -21.5
SD_CAN_ESM2	★ -24.6	★ -28.6	★ -41.9	★ -34.5	★ -32.4	★ -26.6	★ -28.1	★ -46.3	★ -35.5	★ -34.1
ENSMEAN	-18.4	★ -22.3	★ -35.5	★ -23.0	★ -24.8	★ -21.6	★ -24.2	★ -38.0	★ -24.6	★ -27.1
(P2-P0)/P0*100										
SD_CMCC_CM	★ -28.5	★ -30.9	★ -43.2	★ -29.6	★ -33.0	★ -33.0	★ -38.2	★ -48.8	★ -34.2	★ -38.5
SD_MPI_ESM_MR	★ -21.3	★ -30.9	★ -40.0	★ -25.7	★ -29.5	★ -23.3	★ -25.6	★ -43.5	★ -32.6	★ -31.2
SD_CNRM_CM5	-17.5	-17.6	★ -40.0	★ -24.9	★ -25.0	★ -22.0	★ -25.3	★ -38.9	★ -31.6	★ -29.5
SD_CAN_ESM2	★ -30.9	★ -37.5	★ -53.1	★ -41.6	★ -40.8	★ -31.3	★ -39.7	★ -57.3	★ -47.1	★ -43.8
ENSMEAN	★ -24.5	★ -29.2	★ -44.1	★ -30.5	★ -32.1	★ -27.4	★ -32.2	★ -47.1	★ -36.3	★ -35.8
(P3-P0)P0*100										
SD_CMCC_CM	★ -27.6	★ -43.1	★ -49.5	★ -34.9	★ -38.8	★ -33.5	★ -54.2	★ -58.6	★ -54.7	★ -50.3
SD_MPI_ESM_MR	★ -24.1	★ -30.1	★ -43.0	★ -30.9	★ -32.0	★ -32.7	★ -46.7	★ -62.6	★ -50.5	★ -48.1
SD_CNRM_CM5	★ -23.4	★ -29.0	★ -44.6	★ -32.5	★ -32.4	★ -32.2	★ -40.7	★ -50.6	★ -43.7	★ -41.8
SD_CAN_ESM2	★ -29.8	★ -47.7	★ -51.3	★ -46.8	★ -43.9	★ -41.2	★ -56.4	★ -63.7	★ -61.7	★ -55.8
ENSMEAN	★ -26.2	★ -37.5	★ -47.1	★ -36.3	★ -36.8	★ -34.9	★ -49.5	★ -58.9	★ -52.7	★ -49.0
(P4-P0)/P0*100										
SD_CMCC_CM	★ -30.4	★ -44.4	★ -45.9	★ -40.7	★ -40.4	★ -43.0	★ -66.3	★ -71.9	★ -66.7	★ -62.0
SD_MPI_ESM_MR	★ -25.2	★ -31.7	★ -42.5	★ -30.1	★ -32.4	★ -38.9	★ -55.0	★ -69.7	★ -55.7	★ -54.8
SD_CNRM_CM5	★ -26.4	★ -33.9	★ -48.1	★ -30.9	★ -34.8	★ -40.5	★ -47.5	★ -60.0	★ -56.4	★ -51.1
SD_CAN_ESM2	★ -35.2	★ -41.8	★ -56.0	★ -49.4	★ -45.6	★ -44.6	★ -64.0	★ -75.1	★ -73.2	★ -64.2
ENSMEAN	★ -29.3	★ -38.0	★ -48.1	★ -37.8	★ -38.3	★ -41.8	★ -58.2	★ -69.2	★ -63.0	★ -58.0
	DJF	MAM	JJA	SON	Annual	DJF	MAM	JJA	SON	Annual

SD - pr

★ *Two Sample Student's T-test, 95 % confidence interval, alternative hypothesis: true difference in means is not equal to 0*

Figure 5-205: Seasonal and annual amount of precipitation: observed values over reference period (in red), changes projected by statistical downscaling applied to 4GCMs and the Ensemble Mean of changes over the four periods (P1, P2, P3, P4) expressed in % RCP4.5 (left) and RCP 8.5 (right) scenarios. Significant change is marked by star (source Arpae-Simc)

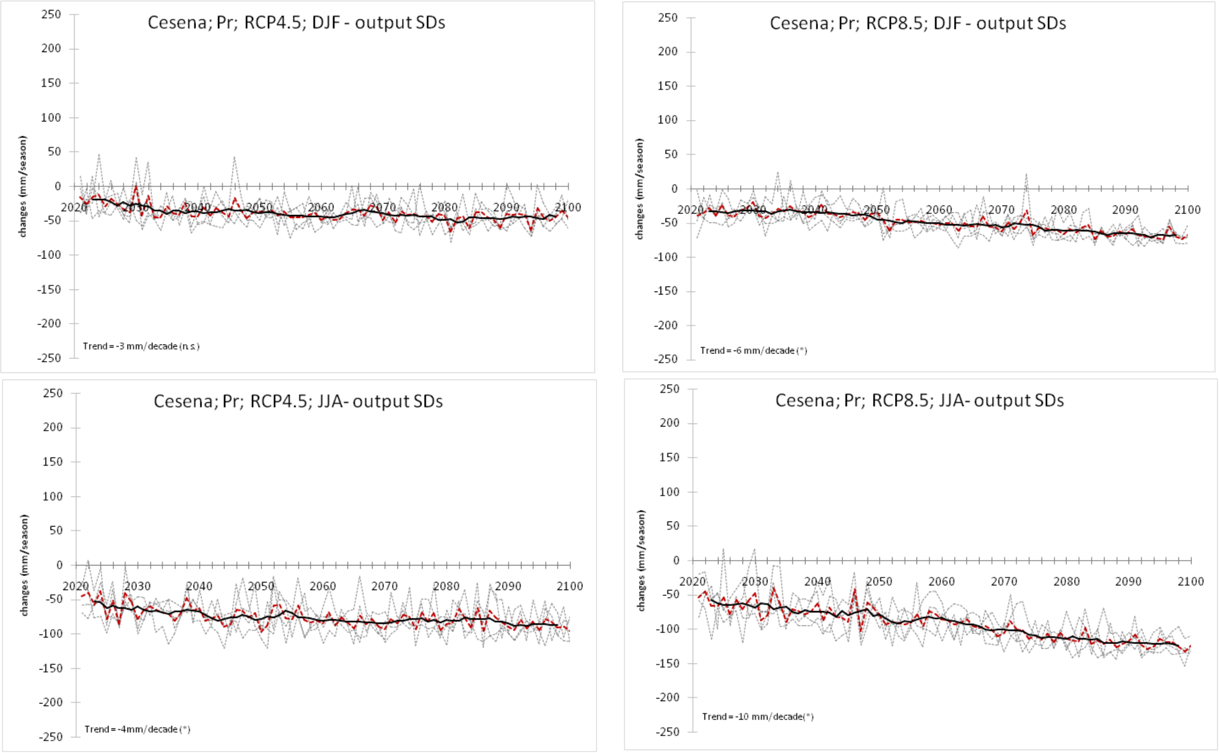

Figure 5-206: Variability of future changes of winter (DJF) and summer (JJA) precipitation through SDs applied to 4GCMs (grey lines); the Ensemble Mean (red line) and moving average (black line) -scenario RCP4.5 (left) and RCP8.5 (right), 2021-2100 period Significant trend is marked with star while n.s. means not significant (source Arpae-Simc).

6.5.2.2.2 *Intense precipitation*

90th percentile of seasonal amount of precipitation

Intense precipitation (Figure 5-207), defined by 90th percentile of precipitation in Cesena- follow the precipitation patterns, namely a general decrease at annual and seasonal time scale. The annual decrease could reach -14% for RCP4.5 and -22% for RCP8.5. At seasonal level, winter has higher magnitude of decreases, followed by autumn, summer and spring (see figure 5-153). The long-term variability over 2021-2100 shows negative and significant trend only in winter and for RCP8.5(see 5-208).

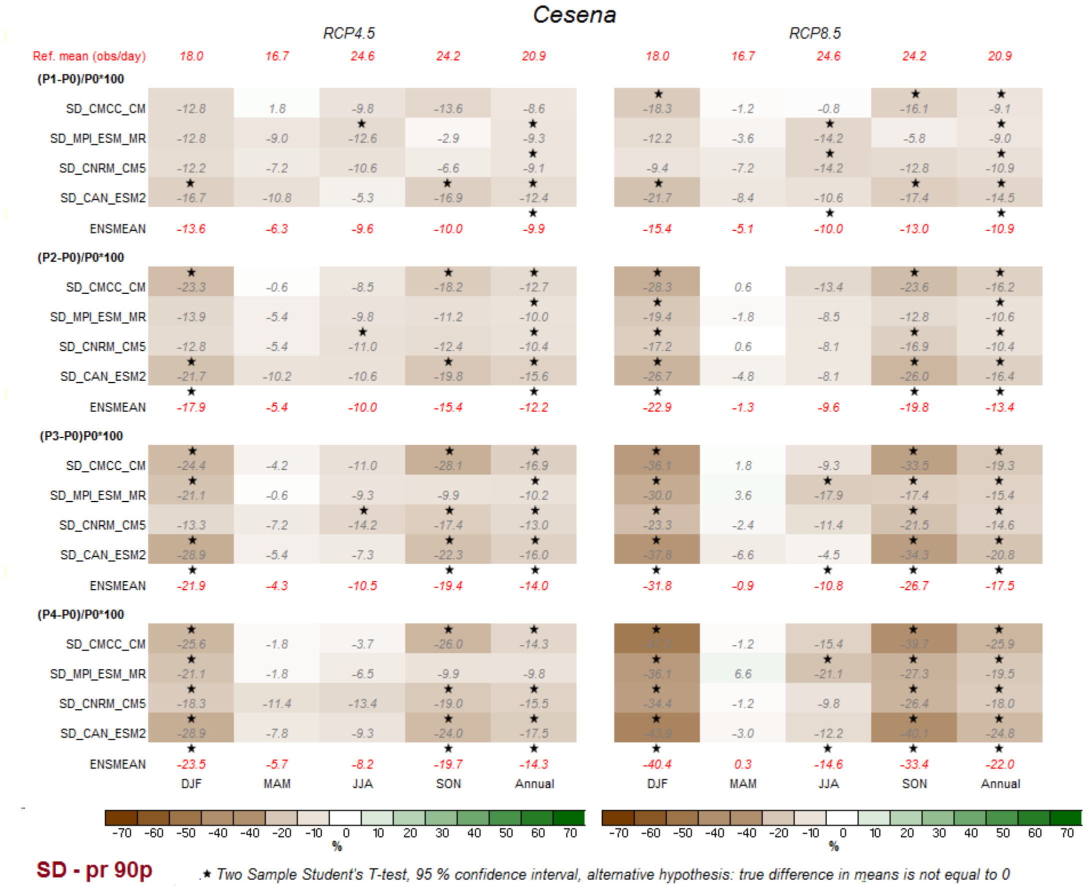

	RCP4.5					RCP8.5				
Ref. mean (obs/day)	18.0	16.7	24.6	24.2	20.9	18.0	16.7	24.6	24.2	20.9
(P1-P0)/P0*100										
SD_CMCC_CM	-12.8	1.8	-9.8	-13.6	-8.6	★ -18.3	-1.2	-0.8	★ -16.1	★ -9.1
SD_MPI_ESM_MR	-12.8	-9.0	★ -12.6	-2.9	★ -9.3	-12.2	-3.6	★ -14.2	-5.8	★ -9.0
SD_CNRM_CM5	-12.2	-7.2	-10.6	-6.6	★ -9.1	-9.4	-7.2	★ -14.2	-12.8	★ -10.9
SD_CAN_ESM2	★ -16.7	-10.8	-5.3	★ -16.9	★ -12.4	★ -21.7	-8.4	-10.6	★ -17.4	★ -14.5
ENSMEAN	-13.6	-6.3	-9.6	-10.0	★ -9.9	-15.4	-5.1	★ -10.0	-13.0	★ -10.9
(P2-P0)/P0*100										
SD_CMCC_CM	★ -23.3	-0.6	-8.5	★ -18.2	★ -12.7	★ -28.3	0.6	-13.4	★ -23.6	★ -16.2
SD_MPI_ESM_MR	-13.9	-5.4	-9.8	-11.2	★ -10.0	★ -19.4	-1.8	-8.5	-12.8	★ -10.6
SD_CNRM_CM5	-12.8	-5.4	★ -11.0	-12.4	★ -10.4	★ -17.2	0.6	-8.1	★ -16.9	★ -10.4
SD_CAN_ESM2	★ -21.7	-10.2	-10.6	★ -19.8	★ -15.6	★ -26.7	-4.8	-8.1	★ -26.0	★ -16.4
ENSMEAN	★ -17.9	-5.4	-10.0	-15.4	★ -12.2	★ -22.9	-1.3	-9.6	★ -19.8	★ -13.4
(P3-P0)P0*100										
SD_CMCC_CM	★ -24.4	-4.2	-11.0	★ -28.1	★ -16.9	★ -36.1	1.8	-9.3	★ -33.5	★ -19.3
SD_MPI_ESM_MR	★ -21.1	-0.6	-9.3	-9.9	★ -10.2	★ -30.0	3.6	★ -17.9	★ -17.4	★ -15.4
SD_CNRM_CM5	-13.3	-7.2	★ -14.2	★ -17.4	★ -13.0	★ -23.3	-2.4	-11.4	★ -21.5	★ -14.6
SD_CAN_ESM2	★ -28.9	-5.4	-7.3	★ -22.3	★ -16.0	★ -37.8	-6.6	-4.5	★ -34.3	★ -20.8
ENSMEAN	★ -21.9	-4.3	-10.5	★ -19.4	★ -14.0	★ -31.8	-0.9	★ -10.8	★ -26.7	★ -17.5
(P4-P0)/P0*100										
SD_CMCC_CM	★ -25.6	-1.8	-3.7	★ -26.0	★ -14.3	★ -47.2	-1.2	-15.4	★ -39.7	★ -25.9
SD_MPI_ESM_MR	★ -21.1	-1.8	-6.5	-9.9	-9.8	★ -36.1	6.6	★ -21.1	★ -27.3	★ -19.5
SD_CNRM_CM5	★ -18.3	-11.4	-13.4	★ -19.0	★ -15.5	★ -34.4	-1.2	-9.8	★ -26.4	★ -18.0
SD_CAN_ESM2	★ -28.9	-7.8	-9.3	★ -24.0	★ -17.5	★ -43.9	-3.0	-12.2	★ -40.1	★ -24.8
ENSMEAN	★ -23.5	-5.7	-8.2	★ -19.7	★ -14.3	★ -40.4	0.3	★ -14.6	★ -33.4	★ -22.0
	DJF	MAM	JJA	SON	Annual	DJF	MAM	JJA	SON	Annual

★ *Two Sample Student's T-test, 95 % confidence interval, alternative hypothesis: true difference in means is not equal to 0*

Figure 5-207: Seasonal and annual amount of 90th precipitation: observed values over reference period (in red), changes projected by statistical downscaling applied to 4GCMs and the Ensemble Mean over the four periods (P1, P2, P3, P4) projected in the framework of RCP4.5 (left) and RCP 8.5 (right). Significant change is marked by star (source Arpae-Simc)

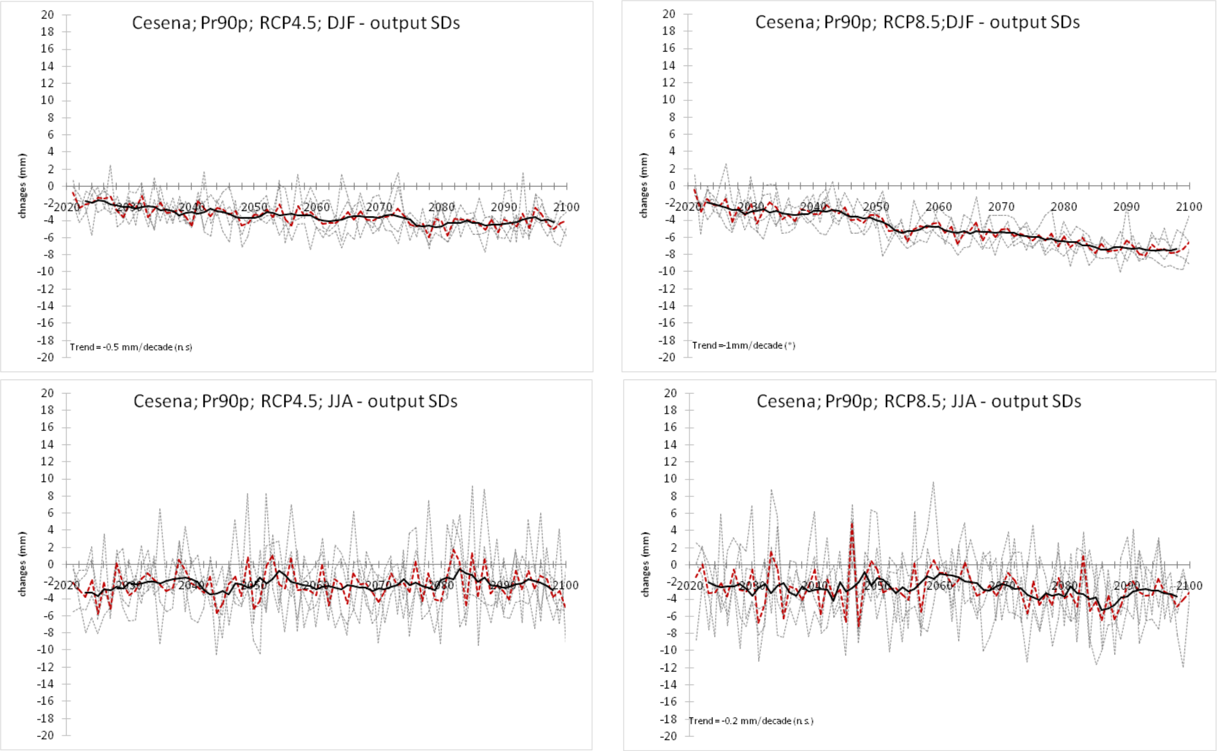

Figure 5-208: Future changes of winter (DJF) and summer (JJA) 90th precipitation projected through SDs applied to 4GCMs (grey lines); the Ensemble Mean (red line) and moving average (black line) - scenario RCP4.5 (left) and RCP8.5 (right), 2021-2100 period Significant trend is marked with star while n.s. means not significant (source Arpae-Simc).

6.5.2.2.3 *Consecutive dry days*

The projected changes of consecutive dry days at Cesena, index defined as the maximum number of consecutive days without precipitation, is presented in figure 5-209. The signal reveals an increase in spring (starting from P1 to P4) and, a decrease in winter and autumn. The magnitude of increase in spring is between 5 to 12 for RCP4.5 and between 5 to 30 for RCP8.5.

Long term variability presented in figure 5-210 (no significant trends is detected)

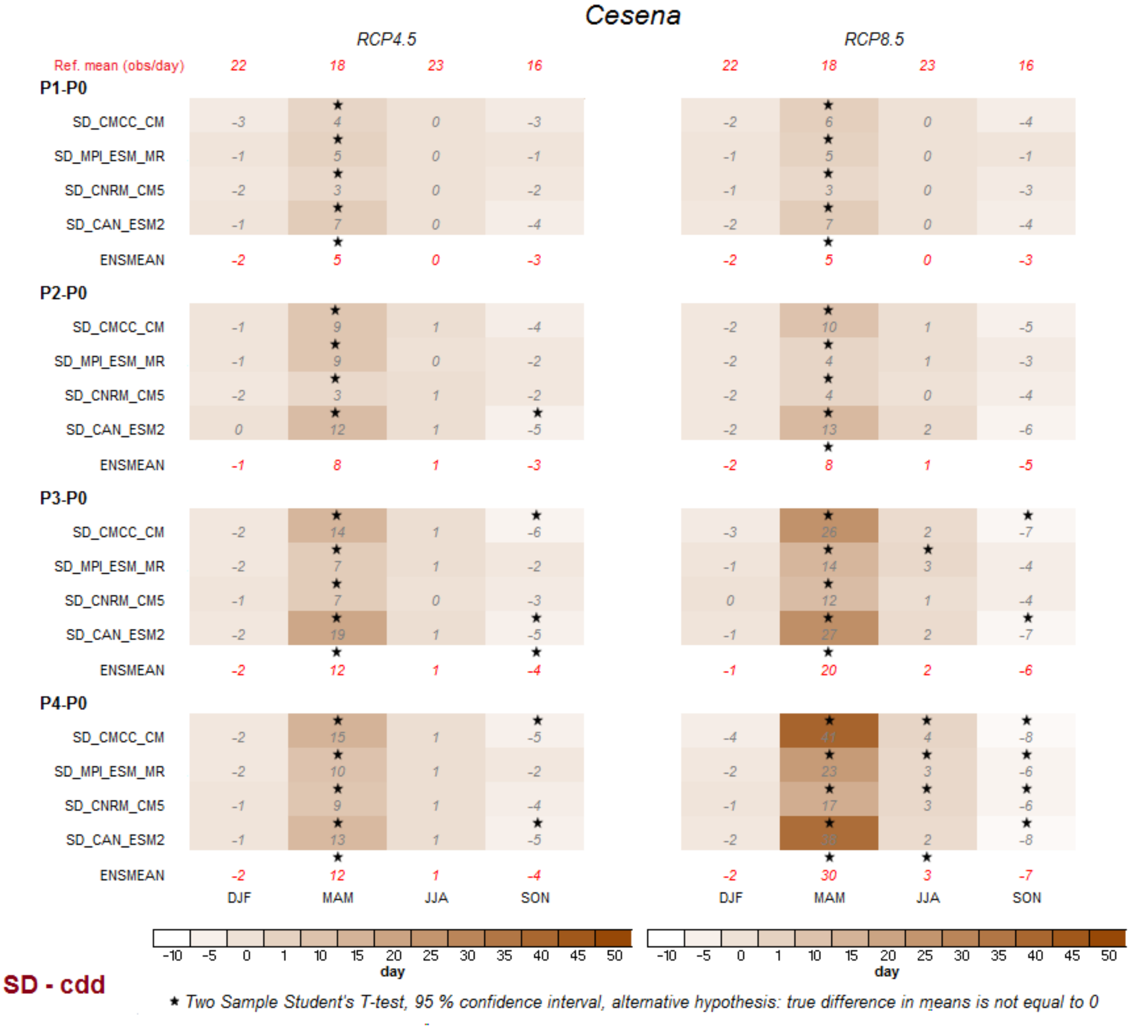

Cesena

	RCP4.5				RCP8.5			
	DJF	MAM	JJA	SON	DJF	MAM	JJA	SON
Ref. mean (obs/day)	22	18	23	16	22	18	23	16
P1-P0								
SD_CMCC_CM	-3	★ 4	0	-3	-2	★ 6	0	-4
SD_MPI_ESM_MR	-1	★ 5	0	-1	-1	★ 5	0	-1
SD_CNRM_CM5	-2	★ 3	0	-2	-1	★ 3	0	-3
SD_CAN_ESM2	-1	★ 7	0	-4	-2	★ 7	0	-4
ENSMEAN	-2	★ 5	0	-3	-2	★ 5	0	-3
P2-P0								
SD_CMCC_CM	-1	★ 9	1	-4	-2	★ 10	1	-5
SD_MPI_ESM_MR	-1	★ 9	0	-2	-2	★ 4	1	-3
SD_CNRM_CM5	-2	★ 3	1	-2	-2	★ 4	0	-4
SD_CAN_ESM2	0	★ 12	1	★ -5	-2	★ 13	2	-6
ENSMEAN	-1	8	1	-3	-2	★ 8	1	-5
P3-P0								
SD_CMCC_CM	-2	★ 14	1	★ -6	-3	★ 26	2	★ -7
SD_MPI_ESM_MR	-2	★ 7	1	-2	-1	★ 14	★ 3	-4
SD_CNRM_CM5	-1	★ 7	0	-3	0	★ 12	1	-4
SD_CAN_ESM2	-2	★ 19	1	★ -5	-1	★ 27	2	★ -7
ENSMEAN	-2	★ 12	1	★ -4	-1	★ 20	2	-6
P4-P0								
SD_CMCC_CM	-2	★ 15	1	★ -5	-4	★ 41	★ 4	★ -8
SD_MPI_ESM_MR	-2	★ 10	1	-2	-2	★ 23	★ 3	★ -6
SD_CNRM_CM5	-1	★ 9	1	-4	-1	★ 17	★ 3	★ -6
SD_CAN_ESM2	-1	★ 13	1	★ -5	-2	★ 38	2	★ -8
ENSMEAN	-2	★ 12	1	-4	-2	★ 30	★ 3	-7

SD - cdd

★ Two Sample Student's T-test, 95 % confidence interval, alternative hypothesis: true difference in means is not equal to 0

Figure 5-209: Seasonal and annual max. consecutive dry days: observed values over reference period (in red), changes projected by statistical downscaling applied to 4GCMs and the Ensemble Mean over the four periods (P1, P2, P3, P4) projected in the framework of RCP4.5 (left) and RCP 8.5 (right). Significant change is marked by star (source Arpae-Simc)

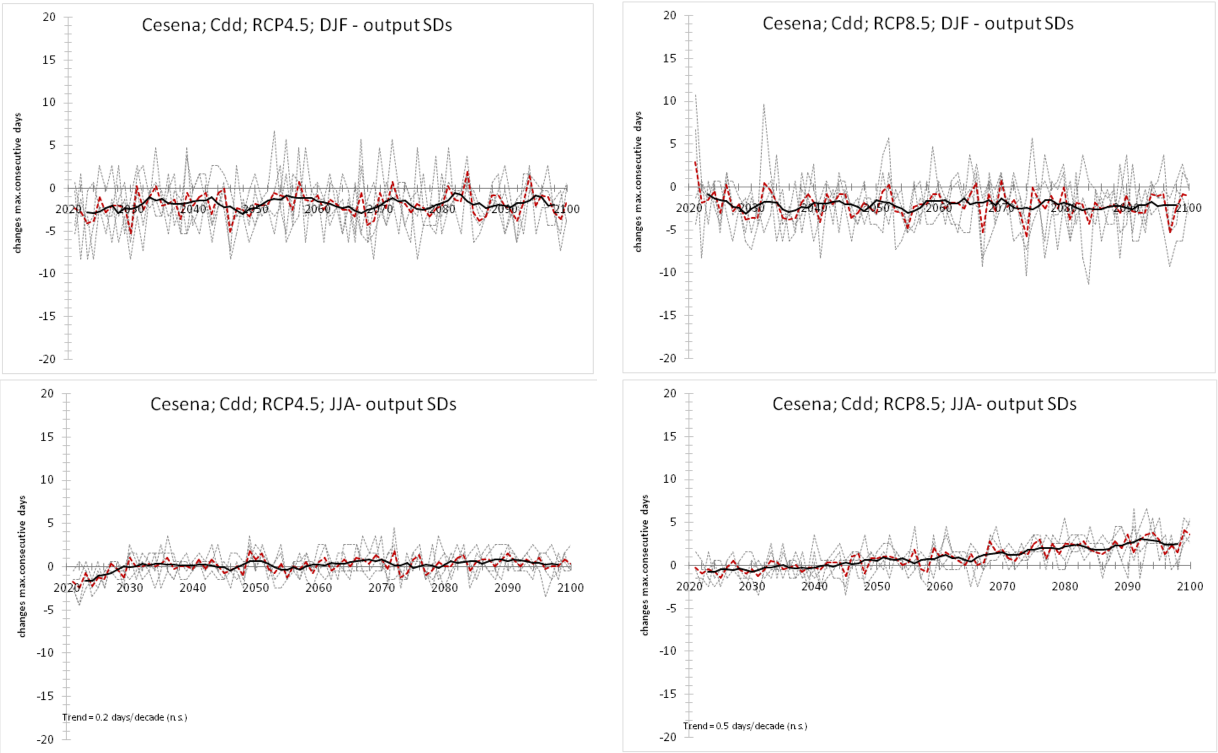

Figure 5-210: Variability of future changes of winter (DJF) and summer (JJA) max. number of consecutive dry days projected through SDs applied to 4GCMs (grey lines); the Ensemble Mean (red line) and moving average (black line) - scenario RCP4.5 (left) and RCP8.5 (right), 2021-2100 period Significant trend is marked with star while n.s. means not significant (source Arpae-Simc).

6.6 Case study 6: Verghereto

6.6.1 Dynamically downscaled results

In this section we present future climate change of temperature and precipitation related indices, extra rare humidex and wind projections for Verghereto. All indices are calculated from the available data set of regional climate models for the grid point that is representing the location of case study Verghereto. Data set is obtained by bilinear interpolation. All data are presented as follows:

- Climate change diagram of an individual index in seasons and on annual basis for four considered future periods, for two emission scenarios RCP4.5 and RCP8.5. Climate change is calculated as difference between future and reference period relative difference for precipitation indices, surface relative humidity and wind projections). Reference period is presented as ensemble mean of available regional climate models (Ref.mean), while climate change is shown for different models as well as for ensemble mean of models (ENSMEAN). Two sample Wilcoxon test is applied to test statistical significance of climate change for individual models (for 95 % confidence level). Significant change is marked by star
- Time series of future anomaly of an individual index for DJF and JJA and for two emission scenarios RCP4.5 and RCP8,5. Anomaly is calculated respect to the reference period and shown for individual models, ensemble mean and 5-year moving average. Mann Kendall trend test is applied to ensemble mean (for 95 % confidence level). Significant trend is marked with star (ns if not significant).

6.6.1.1 *Temperature related indices projections*

6.6.1.1.1 *Averaged 2 meter air temperature*

Averaged temperature change (Figure 5-211) in Verghereto shows increase in all seasons and on annual scale, for all future periods (exception is in winter for one model realisation in P1 and P2 periods). Although each model gives different amplitude of change, in ensemble mean the change is highest during summer or autumn and the smallest in winter and spring, for RCP4.5. The temperature increase is more pronounced towards the end of the century when the increase in the ensemble mean is from 1.4 °C in DJF and MAM to 2.0 °C in JJA. On annual scale for RCP4.5 temperature increase is for 1.7 °C. The amplitude of temperature change is more pronounced for RCP8.5 scenario, from 3.0 °C in MAM to 4.3 °C in JJA, on annual scale 3.6 °C at the end of 21st century for ensemble mean. The linear trend of temperature anomaly (Figure 5-212) in the future shows increase which is statistically significant for both considered seasons and both scenarios; for DJF ensemble is 0.20 °C / 10 year for RCP4.5 and 0.51 °C / 10 year for RCP8.5; for JJA ensemble is 0.18 °C / 10 year for RCP4.5 and 0.52 °C / 10 year.

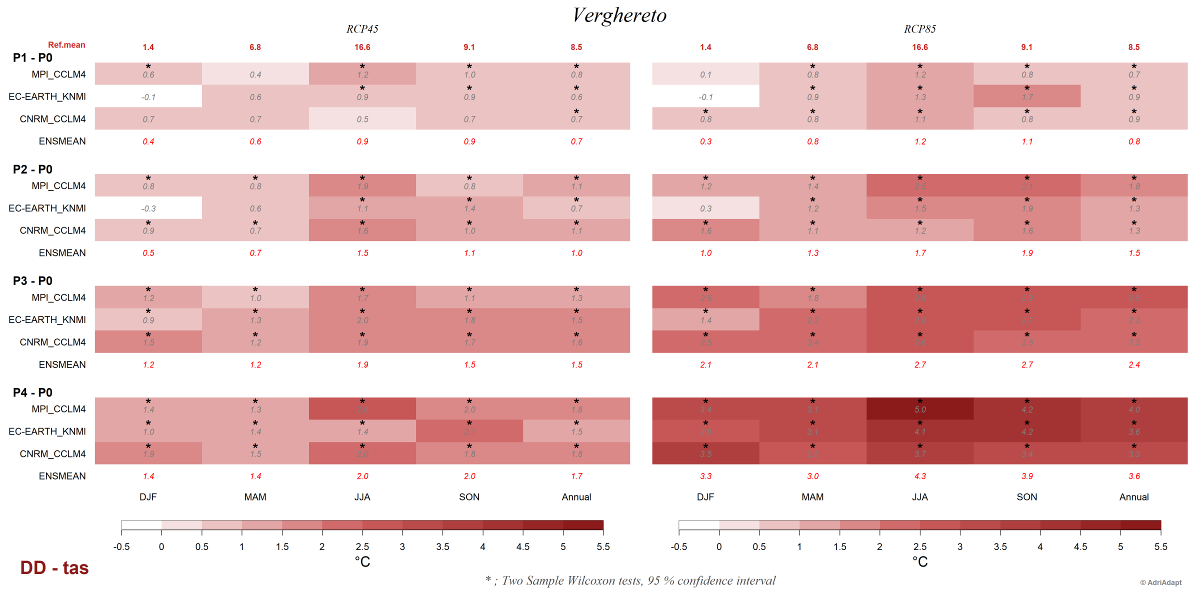

Figure 5-211: Averaged seasonal and annual 2m air temperature (in °C) obtained by dynamical downscaling for Verghereto: Ref. mean is 20 year simulated period (1986-2005) for ensemble mean; P1-P0, P2-P0, P3-P0, P4-P0 are changes in the future for following periods P1: 2021-2040, P2: 2041-2060, P3: 2061-2080, P4: 2081-2100. Differences are shown for individual models. Significant change is marked by star. Change is also shown as ensemble mean (ENSMEAN), not tested for significance. Left column is for RCP4.5 scenario and right for RCP8.5 scenario.

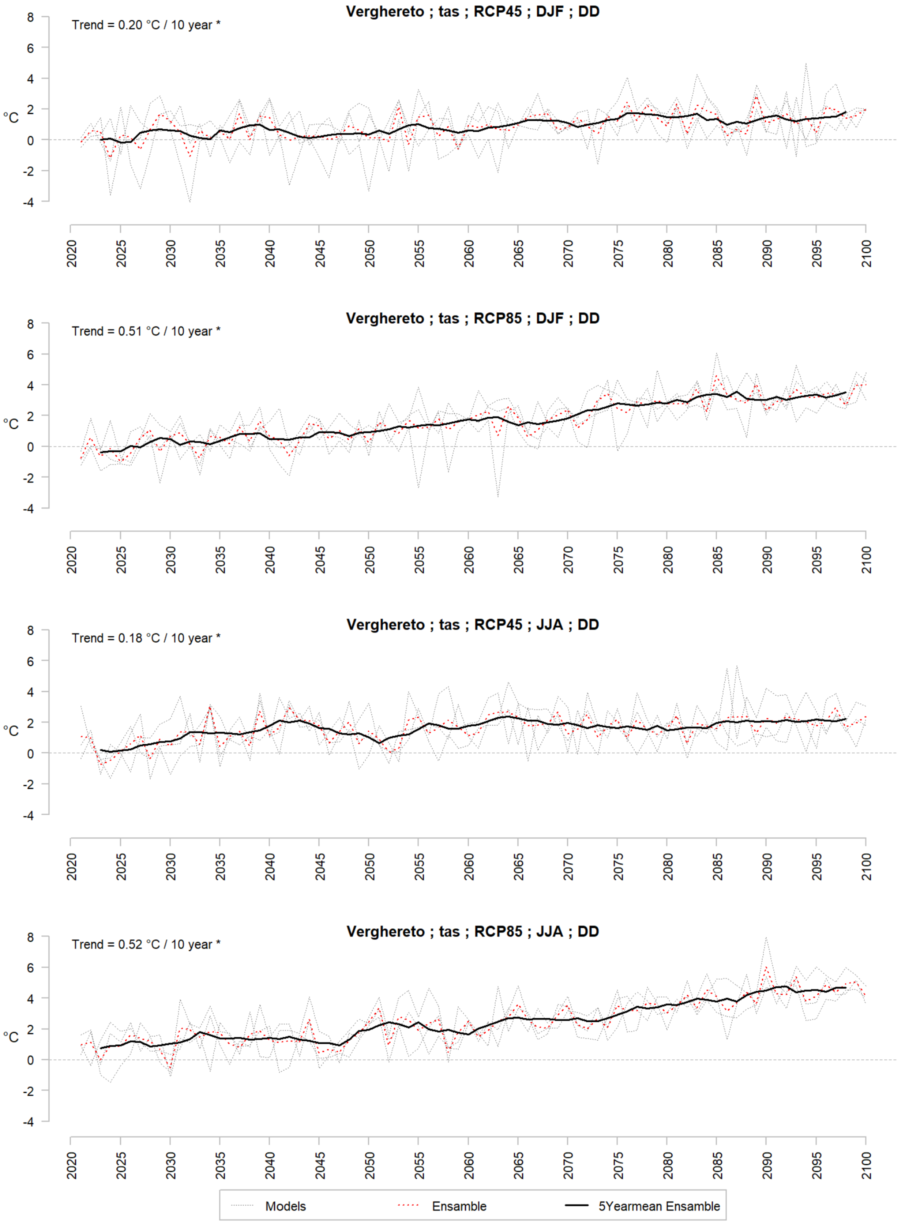

Figure 5-212: Variability of future 2m air temperature anomaly (in °C) in Verghereto for 2021-2100 obtained by dynamically downscaling for winter (DJF) and summer (JJA) and two RCP scenarios: individual models are in grey, the ensemble mean in red, 5-year moving average in black. Significant trend is marked with star (ns if not significant).

6.6.1.1.2 *High temperature*

High temperature change (Figure 5-213), defined as 95th percentile of 2m air temperature, in Verghereto is increasing from P1 to P4 future periods with the different amplitudes for each model. In ensemble mean at the end of century increase is from 1.4 °C in DJF to 2.6 °C in SON; 2.3 °C on annual scale for RCP4.5. Amplitude of change is more pronounced for RCP8.5 and is between 3.2 °C in DJF and 5.0 °C in SON, 4.9 °C for annual change at the end of 21st century. Variability of future 95th percentile of 2m air temperature anomaly (Figure 5-214) shows linear trend in change of ensemble mean, 0.16 °C / 10 year in DJF for RCP4.5 and 0.49 °C / 10 year for RCP8.5; 0.19 °C / 10 year in JJA for RCP4.5 and 0.56 °C / 10 year for RCP8.5. All trends are statistically significant.

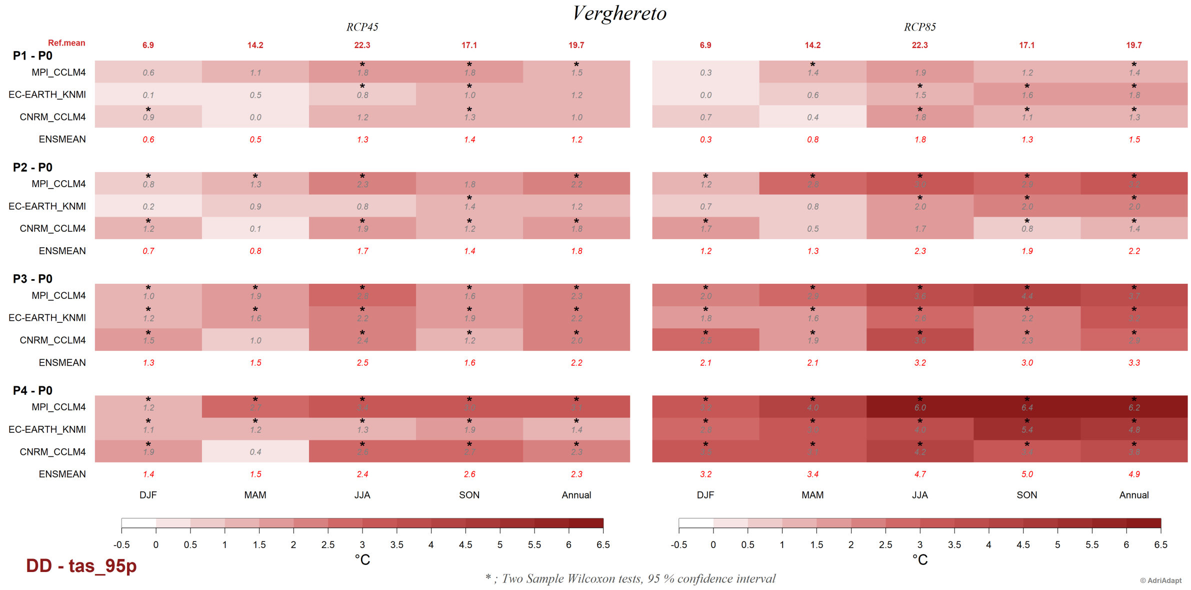

Verghereto

RCP45

	DJF	MAM	JJA	SON	Annual
Ref.mean	6.9	14.2	22.3	17.1	19.7
P1 - P0					
MPI_CCLM4	0.6	1.1	* 1.8	* 1.8	* 1.5
EC-EARTH_KNMI	0.1	0.5	* 0.8	* 1.0	1.2
CNRM_CCLM4	* 0.9	0.0	1.2	* 1.3	1.0
ENSMEAN	0.6	0.5	1.3	1.4	1.2
P2 - P0					
MPI_CCLM4	* 0.8	* 1.3	* 2.3	1.8	* 2.2
EC-EARTH_KNMI	0.2	0.9	0.8	* 1.4	1.2
CNRM_CCLM4	* 1.2	0.1	* 1.9	* 1.2	* 1.8
ENSMEAN	0.7	0.8	1.7	1.4	1.8
P3 - P0					
MPI_CCLM4	* 1.0	* 1.9	* 2.8	* 1.6	* 2.3
EC-EARTH_KNMI	* 1.2	* 1.6	* 2.2	* 1.9	* 2.2
CNRM_CCLM4	* 1.5	1.0	* 2.4	* 1.2	* 2.0
ENSMEAN	1.3	1.5	2.5	1.6	2.2
P4 - P0					
MPI_CCLM4	* 1.2	* 2.7	* 3.4	* 3.0	* 3.1
EC-EARTH_KNMI	* 1.1	* 1.2	* 1.3	* 1.9	* 1.4
CNRM_CCLM4	* 1.9	0.4	* 2.6	* 2.7	* 2.3
ENSMEAN	1.4	1.5	2.4	2.6	2.3

RCP85

	DJF	MAM	JJA	SON	Annual
Ref.mean	6.9	14.2	22.3	17.1	19.7
P1 - P0					
MPI_CCLM4	0.3	* 1.4	1.9	1.2	* 1.4
EC-EARTH_KNMI	0.0	0.6	* 1.5	* 1.6	* 1.8
CNRM_CCLM4	0.7	0.4	* 1.8	* 1.1	* 1.3
ENSMEAN	0.3	0.8	1.8	1.3	1.5
P2 - P0					
MPI_CCLM4	* 1.2	* 2.8	* 3.0	* 2.9	* 3.2
EC-EARTH_KNMI	0.7	0.8	* 2.0	* 2.0	* 2.0
CNRM_CCLM4	* 1.7	0.5	1.7	* 0.8	* 1.4
ENSMEAN	1.2	1.3	2.3	1.9	2.2
P3 - P0					
MPI_CCLM4	* 2.0	* 2.9	* 3.6	* 4.4	* 3.7
EC-EARTH_KNMI	* 1.8	* 1.6	* 2.6	* 2.2	* 3.2
CNRM_CCLM4	* 2.5	* 1.9	* 3.6	* 2.3	* 2.9
ENSMEAN	2.1	2.1	3.2	3.0	3.3
P4 - P0					
MPI_CCLM4	* 3.2	* 4.0	* 6.0	* 6.4	* 6.2
EC-EARTH_KNMI	* 2.8	* 3.0	* 4.0	* 5.4	* 4.8
CNRM_CCLM4	* 3.5	* 3.1	* 4.2	* 3.4	* 3.8
ENSMEAN	3.2	3.4	4.7	5.0	4.9

* ; Two Sample Wilcoxon tests, 95 % confidence interval

Figure 5-213: Seasonal and annual 95th percentile of 2m air temperature (high temperature, in °C) obtained by dynamical downscaling for Verghereto: Ref. mean is 20 year simulated period (1986-2005) for ensemble mean; P1-P0, P2-P0, P3-P0, P4-P0 are changes in the future for following periods P1: 2021-2040, P2: 2041-2060, P3: 2061-2080, P4: 2081-2100. Differences are shown for individual models. Significant change is marked by star. Change is also shown as ensemble mean (ENSMEAN), not tested for significance. Left column is for RCP4.5 scenario and right for RCP8.5 scenario.

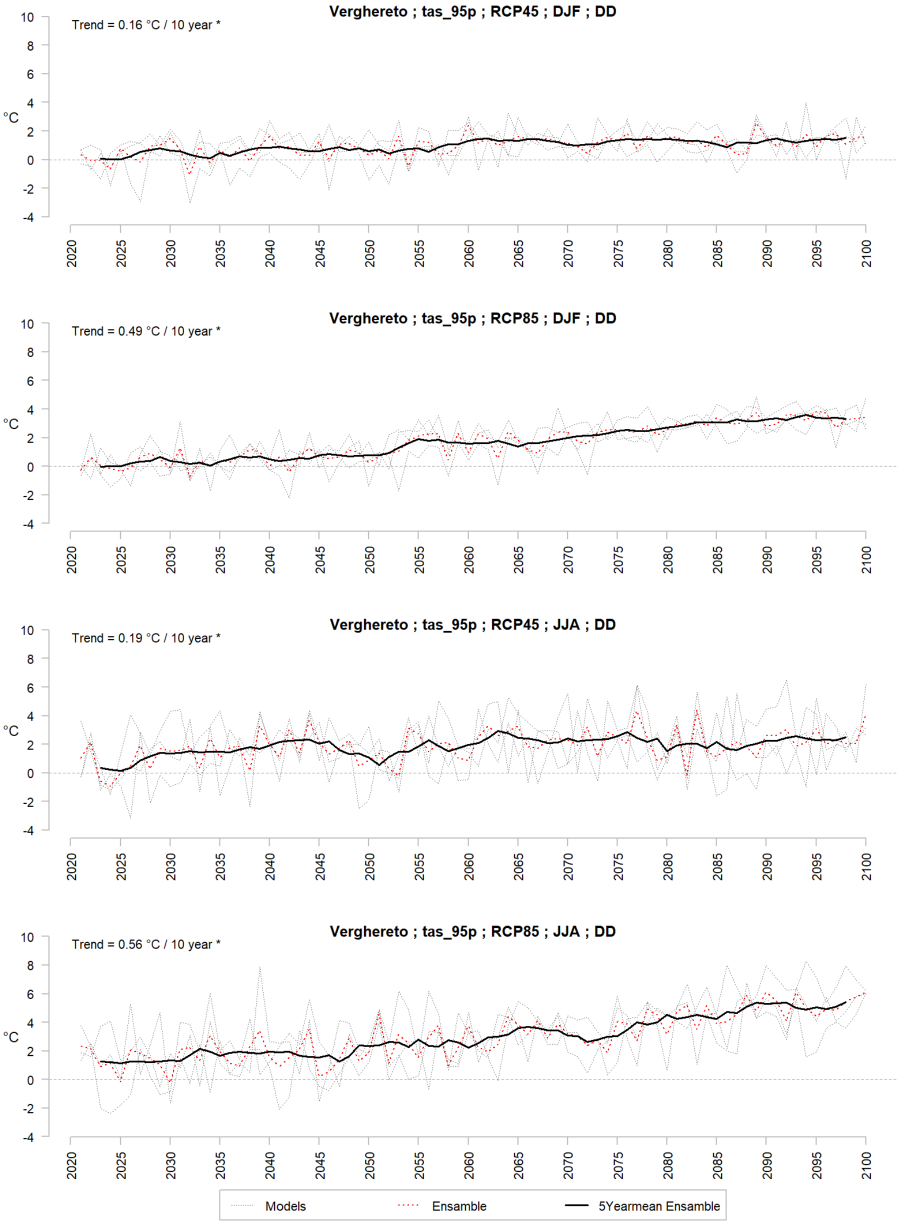

Figure 5-214: Variability of future 95th percentile of 2m air temperature (high temperature) anomaly (in °C) in Verghereto for 2021-2100 obtained by dynamically downscaling for winter (DJF) and summer (JJA) and two RCP scenarios: individual models are in grey, the ensemble mean in red, 5-year moving average in black. Significant trend is marked with star (ns if not significant).

6.6.1.1.3 *High maximum temperature*

High maximum temperature change (Figure 5-215), defined as 95th percentile of 2m maximum air temperature, in Verghereto is increasing from P1 to P4 future periods with the different amplitudes for each model. In ensemble mean at the end of century increase is from 1.5 °C in MAM to 2.9 °C in SON; 2.4 °C on annual scale for RCP4.5. Amplitude of change is more pronounced for RCP8.5 and is between 3.4 °C in DJF and MAM and 5.7 °C in SON; 5.2 °C for annual change at the end of 21st century. Variability of future 95th percentile of 2m maximum air temperature anomaly (Figure 5-216) shows linear trend in change of ensemble mean, 0.21 °C / 10 year in DJF for RCP4.5 and 0.49 °C / 10 year for RCP8.5; 0.20 °C / 10 year in JJA for RCP4.5 and 0.58 °C / 10 year for RCP8.5. All trends are statistically significant.

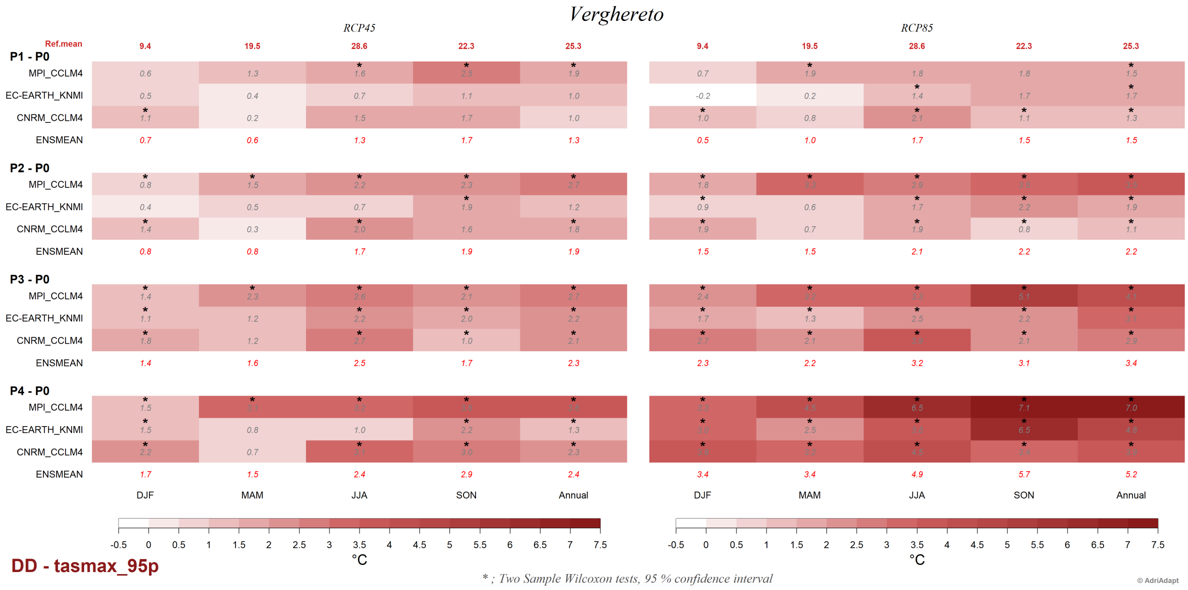

Figure 5-215: Seasonal and annual 95th percentile of 2m maximum air temperature (high maximum temperature, in °C) obtained by dynamical downscaling for Verghereto: Ref. mean is 20 year simulated period (1986-2005) for ensemble mean; P1-P0, P2-P0, P3-P0, P4-P0 are changes in the future for following periods P1: 2021-2040, P2: 2041-2060, P3: 2061-2080, P4: 2081-2100. Differences are shown for individual models. Significant change is marked by star. Change is also shown as ensemble mean (ENSMEAN), not tested for significance. Left column is for RCP4.5 scenario and right for RCP8.5 scenario.

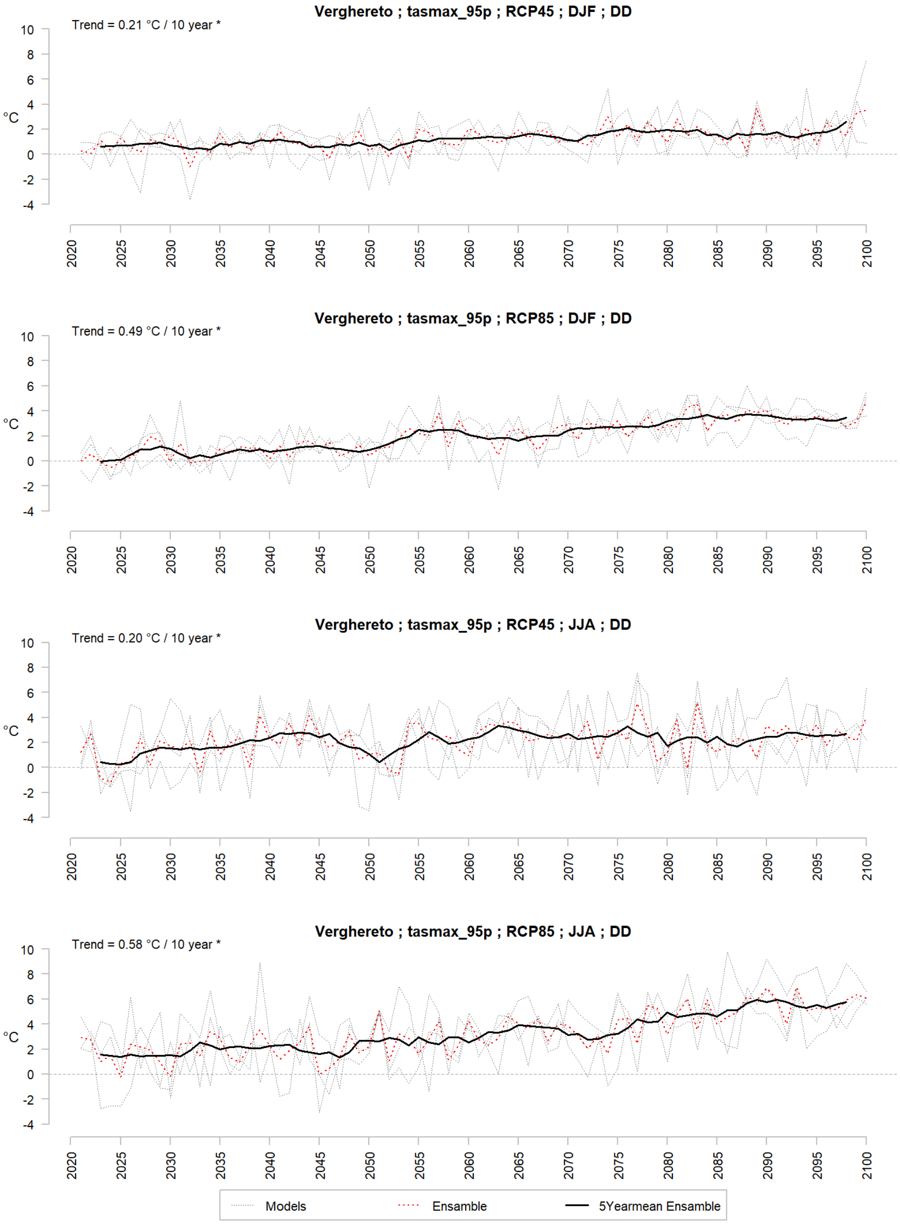

Figure 5-216: Variability of future 95th percentile of 2m maximum air temperature (high maximum temperature) anomaly (in °C) in Verghereto for 2021-2100 obtained by dynamically downscaling for winter (DJF) and summer (JJA) and two RCP scenarios: individual models are in grey, the ensemble mean in red, 5-year moving average in black. Significant trend is marked with star (ns if not significant).

https://www.italy-croatia.eu/adriadapt

6.6.1.1.4 *Extreme high temperature*

99th percentile of 2m air temperature (Figure 5-217) in Verghereto is increasing from P1 to P4 future periods with the different amplitudes for each model. In ensemble mean at the end of century increase is from 2.2 in JJA to 3.0 °C in SON; 2.3 °C on annual scale for RCP4.5. Amplitude of change is more pronounced for RCP8.5 and is between 3.3 °C in DJF and 5.7 °C in SON; 4.8 °C for annual change at the end of 21st century. Variability of future 99th percentile of 2m air temperature anomaly (Figure 5-218) shows linear trend in change of ensemble mean, 0.24 °C / 10 year in DJF for RCP4.5 and 0.52 °C / 10 year for RCP8.5; 0.18 °C / 10 year in JJA for RCP4.5 and 0.635 °C / 10 year for RCP8.5. All trends are statistically significant.

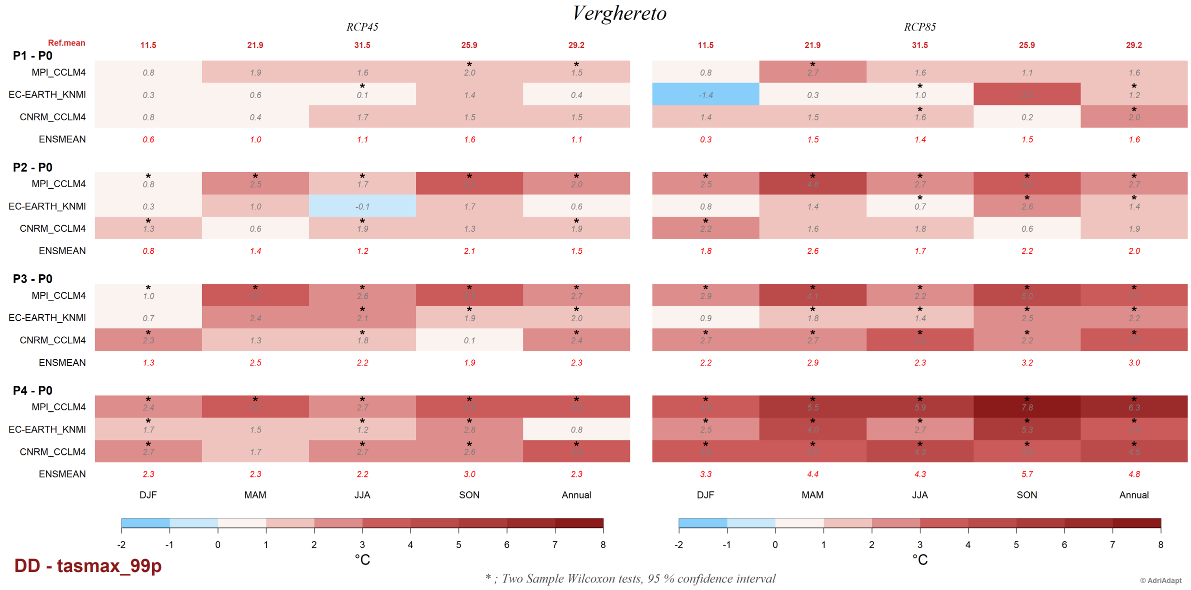

Figure 5-217: Seasonal and annual 99th percentile of 2m air temperature (extreme high temperature, in °C) obtained by dynamical downscaling for Verghereto: Ref. mean is 20 year simulated period (1986-2005) for ensemble mean; P1-P0, P2-P0, P3-P0, P4-P0 are changes in the future for following periods P1: 2021-2040, P2: 2041-2060, P3: 2061-2080, P4: 2081-2100. Differences are shown for individual models. Significant change is marked by star. Change is also shown as ensemble mean (ENSMEAN), not tested for significance. Left column is for RCP4.5 scenario and right for RCP8.5 scenario.

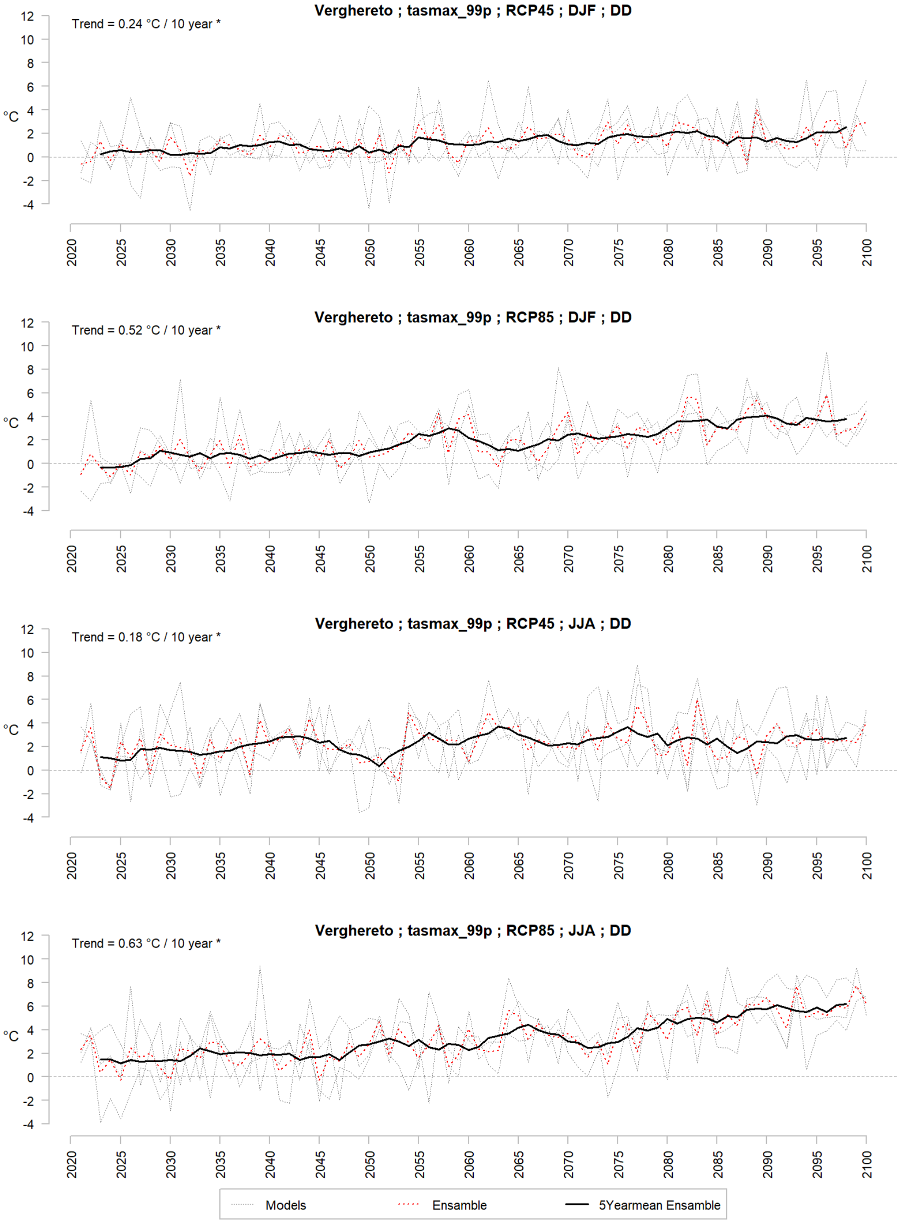

Figure 5-218: Variability of future 99th percentile of 2m air temperature (extreme high temperature) anomaly (in °C) in Verghereto for 2021-2100 obtained by dynamically downscaling for winter (DJF) and summer (JJA) and two RCP scenarios: individual models are in grey, the ensemble mean in red, 5-year moving average in black. Significant trend is marked with star (ns if not significant).

6.6.1.1.5 *Extreme high maximum temperature*

Future change of 99th percentile of 2m maximum air temperature (Figure 5-219) in Verghereto is changing from P1 to P4 periods with the different amplitudes for each model and mostly increase. Ensemble mean of change is positive for all periods. At the end of century increase is from 2.2 °C in JJA to 3.0 °C in SON; 2.3 °C on annual scale for RCP4.5. Amplitude of change is more pronounced for RCP8.5 and is between 3.3 °C in DJF and 5.7 °C in SON, 4.8 °C for annual change at the end of 21st century. Variability of future 99th percentile of 2m maximum air temperature anomaly (Figure 5-220) shows linear trend in change of ensemble mean, 0.24 °C / 10 year in DJF for RCP4.5 and 0.52 °C / 10 year for RCP8.5; 0.18 °C / 10 year in JJA for RCP4.5 and 0.63 °C / 10 year for RCP8.5. All trends are statistically significant.

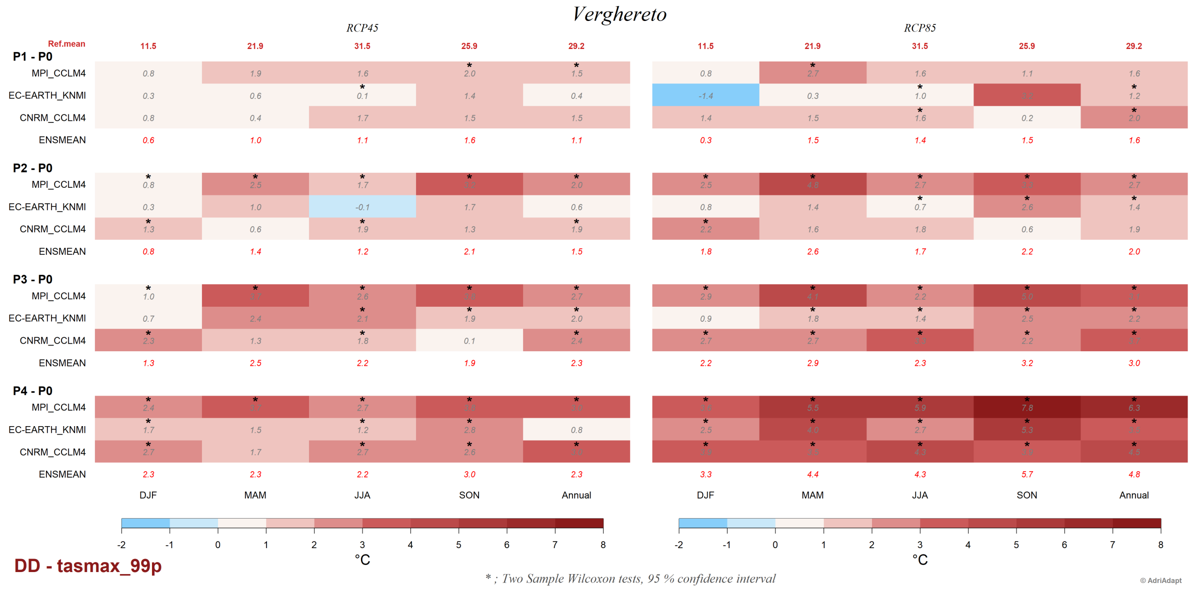

Figure 5-219: Seasonal and annual 99th percentile of 2m maximum air temperature (extreme high maximum temperature, in °C) obtained by dynamical downscaling for Verghereto: Ref. mean is 20 year simulated period (1986-2005) for ensemble mean; P1-P0, P2-P0, P3-P0, P4-P0 are changes in the future for following periods P1: 2021-2040, P2: 2041-2060, P3: 2061-2080, P4: 2081-2100. Differences are shown for individual models. Significant change is marked by star. Change is also shown as ensemble mean (ENSMEAN), not tested for significance. Left column is for RCP4.5 scenario and right for RCP8.5 scenario.

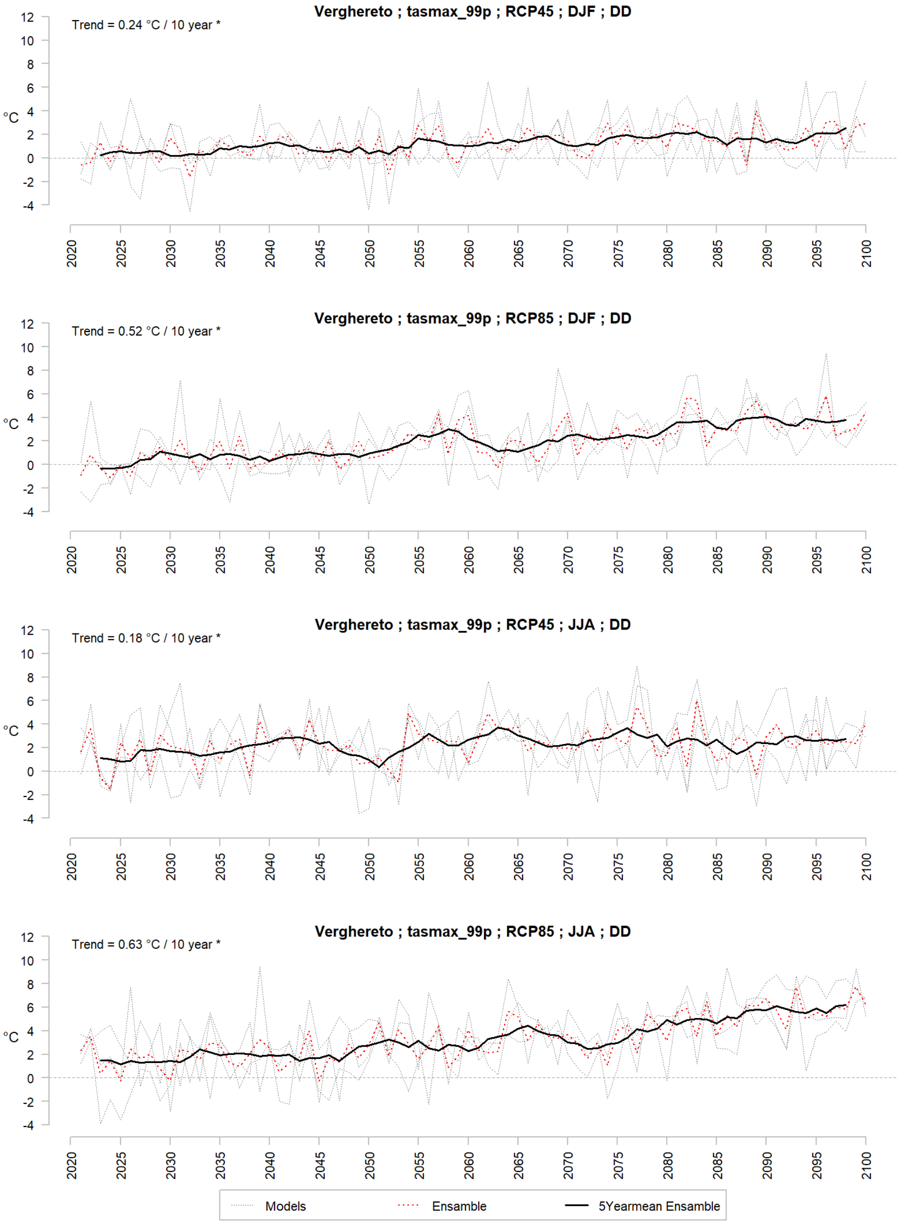

Figure 5-220: Variability of future 99th percentile of 2m maximum air temperature (extreme high maximum temperature) anomaly (in °C) in Verghereto for 2021-2100 obtained by dynamically downscaling for winter (DJF) and summer (JJA) and two RCP scenarios: individual models are in grey, the ensemble mean in red, 5-year moving average in black. Significant trend is marked with star (ns if not significant).

6.6.1.1.6 *Extreme rare high temperature*

Future change of 99.9th percentile of 2m air temperature (Figure 5-221) in Verghereto is increasing from P1 to P4 periods with the different amplitudes for each model. Slightly negative change appears for some seasons and some models in three first periods, but the change of ensemble mean is positive for all periods. At the end of century increase is from 1.3 °C in JJA to 3.2 °C in MAM; 2.3 °C on annual scale for RCP4.5. Amplitude of change is more pronounced for RCP8.5 and is between 2.8 °C in JJA and 5.2 °C in MAM; 3.9 °C for annual change at the end of 21st century. Variability of future 99.9th percentile of 2m air temperature anomaly (Figure 5-222) shows linear trend in change of ensemble mean, 0.21 °C / 10 year in DJF for RCP4.5 and 0.50 °C / 10 year for RCP8.5; 0.17 °C / 10 year in JJA for RCP4.5 and 0.53 °C / 10 year for RCP8.5. All trends are statistically significant.

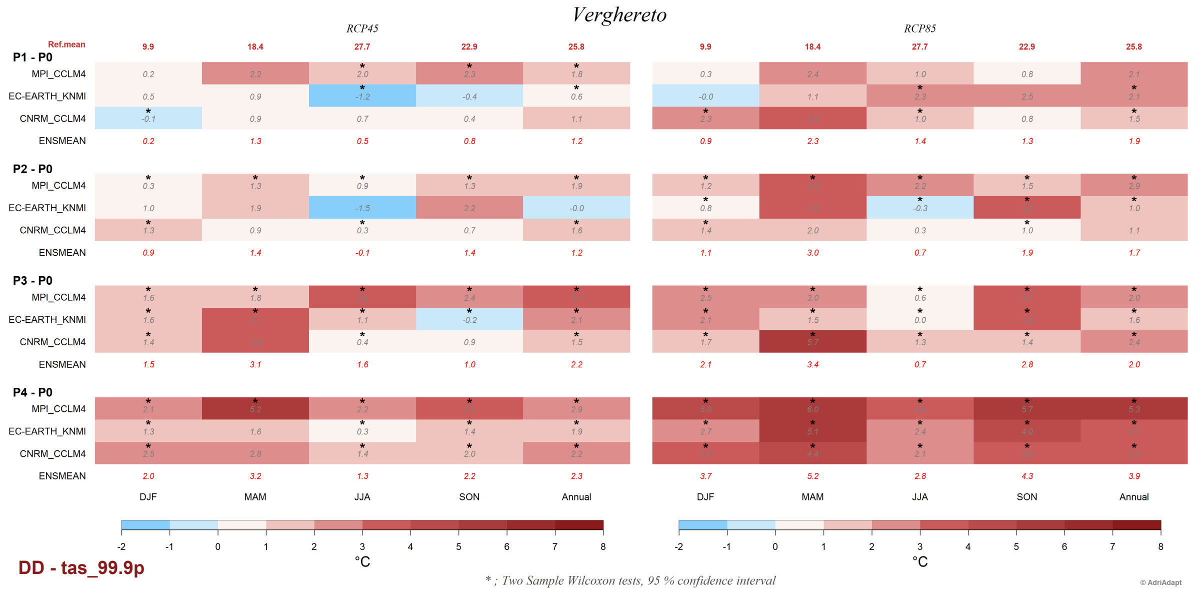

* ; Two Sample Wilcoxon tests, 95 % confidence interval

Figure 5-221: Seasonal and annual 99.9th percentile of 2m air temperature (extreme rare high temperature, in °C) obtained by dynamical downscaling for Verghereto: Ref. mean is 20 year simulated period (1986-2005) for ensemble mean; P1-P0, P2-P0, P3-P0, P4-P0 are changes in the future for following periods P1: 2021-2040, P2: 2041-2060, P3: 2061-2080, P4: 2081-2100. Differences are shown for individual models. Significant change is marked by star. Change is also shown as ensemble mean (ENSMEAN), not tested for significance. Left column is for RCP4.5 scenario and right for RCP8.5 scenario.

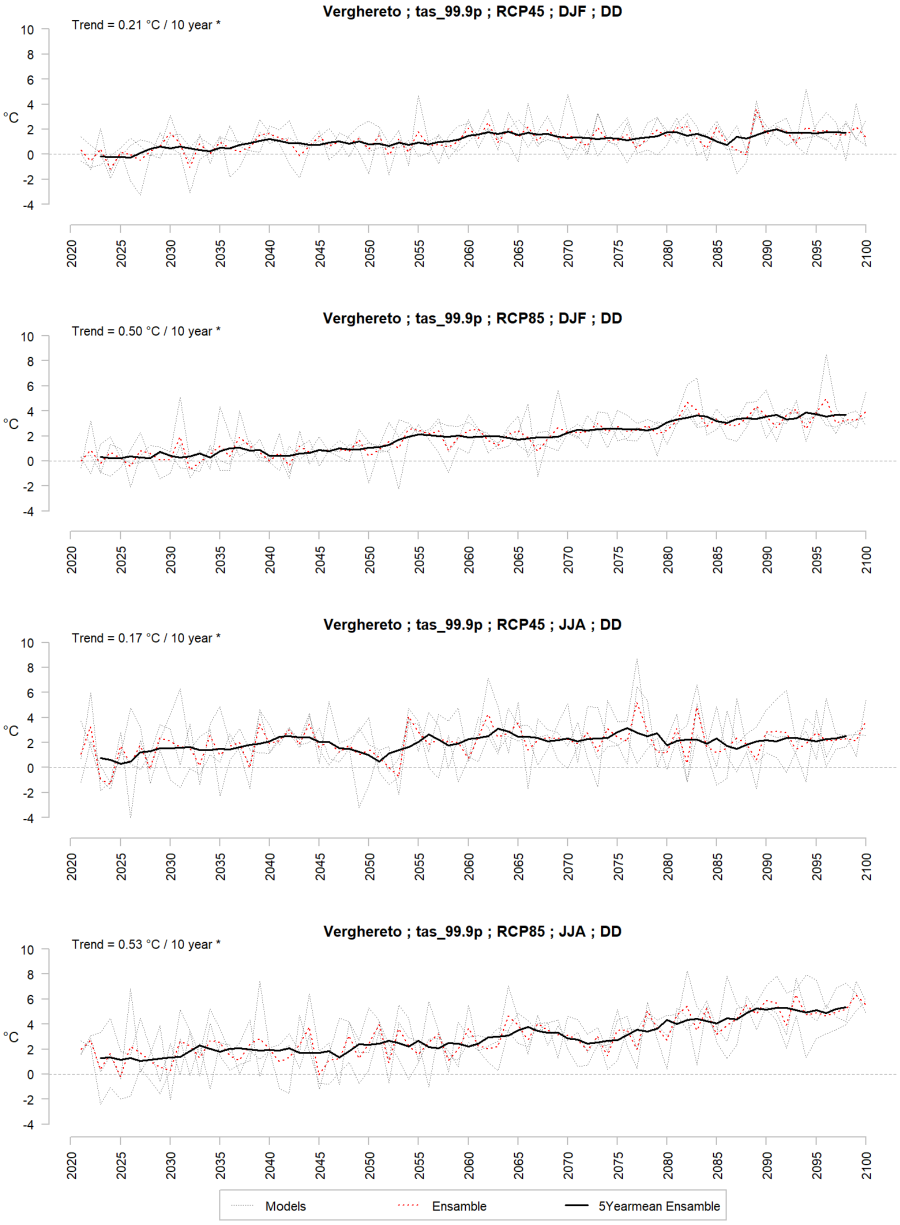

Figure 5-222: Variability of future 99.9th percentile of 2m air temperature (extreme rare high temperature) anomaly (in °C) in Verghereto for 2021-2100 obtained by dynamically downscaling for winter (DJF) and summer (JJA) and two RCP scenarios: individual models are in grey, the ensemble mean in red, 5-year moving average in black. Significant trend is marked with star (ns if not significant).

6.6.1.1.7 *Extreme rare high maximum temperature*

Future change of 99.9th percentile of 2m maximum air temperature (Figure 5-223) in Verghereto is changing from P1 to P4 periods with the different amplitudes for each model. Some models show for some time slices negative change, but in general ensemble mean for all season and annual change are positive. At the end of 21st century changes are between 0.7 °C in JJA and 3.4 °C in MAM; 2.0 °C for annual for RCP4.5 scenario. Amplitude of change is more pronounced for RCP8.5 and is between 2.9 °C in JJA and 5.0 °C in MAM; 4.2 °C for annual change at the end of 21st century. Variability of future 99.9th percentile of 2m maximum air temperature anomaly (Figure 5-224) shows linear trend in change of ensemble mean, 0.24 °C / 10 year in DJF for RCP4.5 and 0.52 °C / 10 year for RCP8.5; 0.18 °C / 10 year in JJA for RCP4.5 and 0.63 °C / 10 year for RCP8.5. All trends are statistically significant.

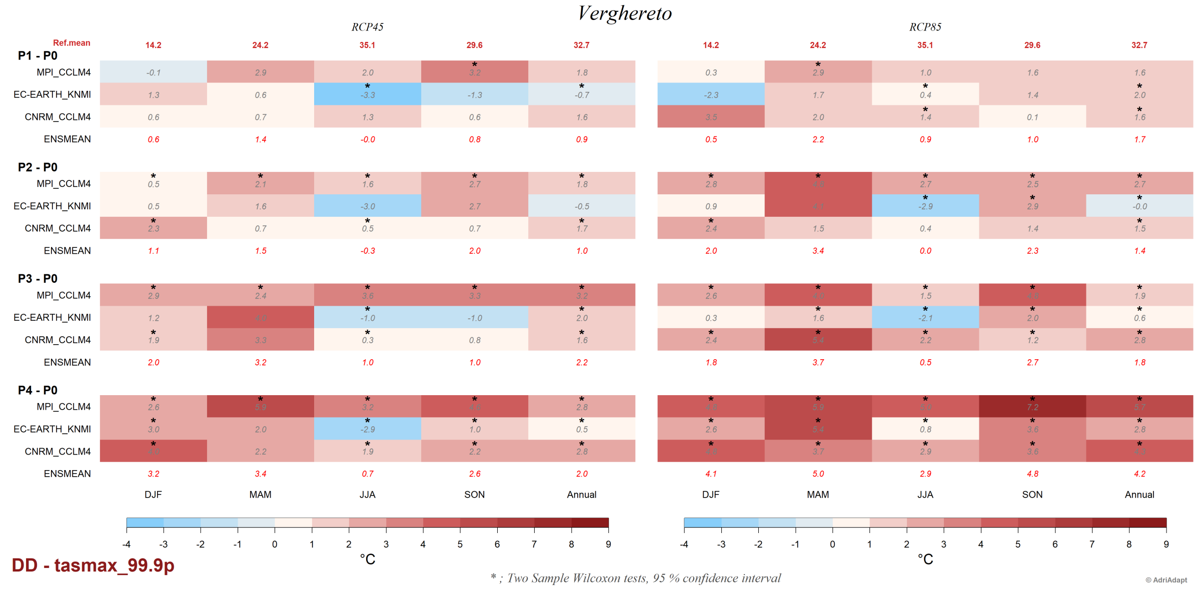

Figure 5-223: Seasonal and annual 99.9th percentile of 2m maximum air temperature (extreme rare high maximum temperature, in °C) obtained by dynamical downscaling for Verghereto: Ref. mean is 20 year simulated period (1986-2005) for ensemble mean; P1-P0, P2-P0, P3-P0, P4-P0 are changes in the future for following periods P1: 2021-2040, P2: 2041-2060, P3: 2061-2080, P4: 2081-2100. Differences are shown for individual models. Significant change is marked by star. Change is also shown as ensemble mean (ENSMEAN), not tested for significance. Left column is for RCP4.5 scenario and right for RCP8.5 scenario.

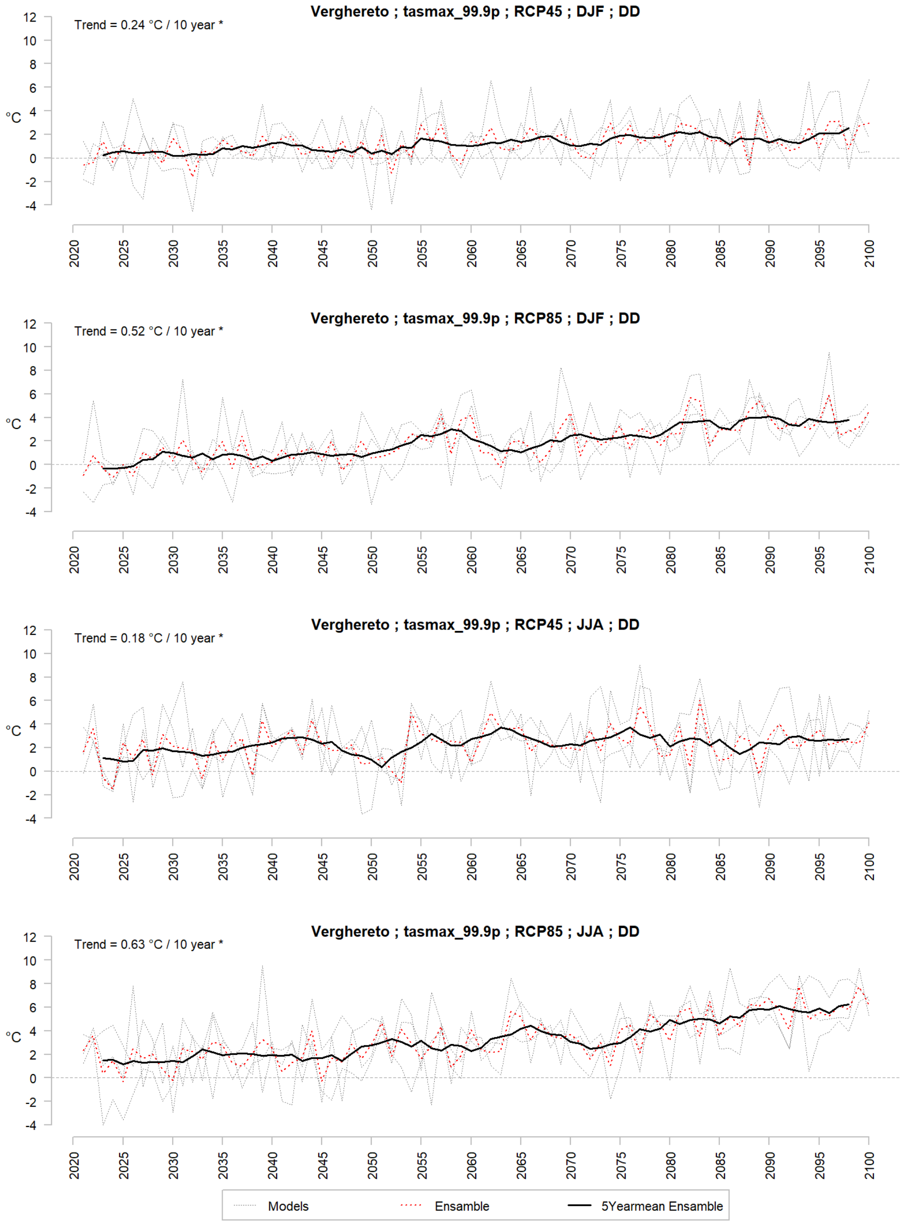
Verghereto ; tasmax_99.9p ; RCP45 ; DJF ; DD

Verghereto ; tasmax_99.9p ; RCP85 ; DJF ; DD

Verghereto ; tasmax_99.9p ; RCP45 ; JJA ; DD

Verghereto ; tasmax_99.9p ; RCP85 ; JJA ; DD

Figure 5-224: Variability of future 99.9th percentile of 2m maximum air temperature (extreme rare high maximum temperature) anomaly (in °C) in Verghereto for 2021-2100 obtained by dynamically downscaling for winter (DJF) and summer (JJA) and two RCP scenarios: individual models are in grey, the ensemble mean in red, 5-year moving average in black. Significant trend is marked with star (ns if not significant).

6.6.1.1.8 *Warm spell days index*

Warm spell days index (Figure 5-225) in Verghereto shows increase in all seasons and on annual scale, for all future period. Amplitude of change is increasing towards the end of 21st century, for RCP4.5 scenario is between 6.8 days in DJF and 11.0 in JJA; 36.7 days on annual scale. Amplitude of change is more pronounced for RCP8.5 and is between 19.2 days in MAM and 32.4 days in JJA, 101.6 days for annual change at the end of 21st century. Variability of future warm spell days index anomaly (Figure 5-226) shows linear trend in change of ensemble mean, 0.89 days/ 10 year in DJF for RCP4.5 and 2.96 days/ 10 year for RCP8.5; 0.78 days/10 year in JJA for RCP4.5 and 3.88 days/10 year for RCP8.5. All trends are statistically significant.

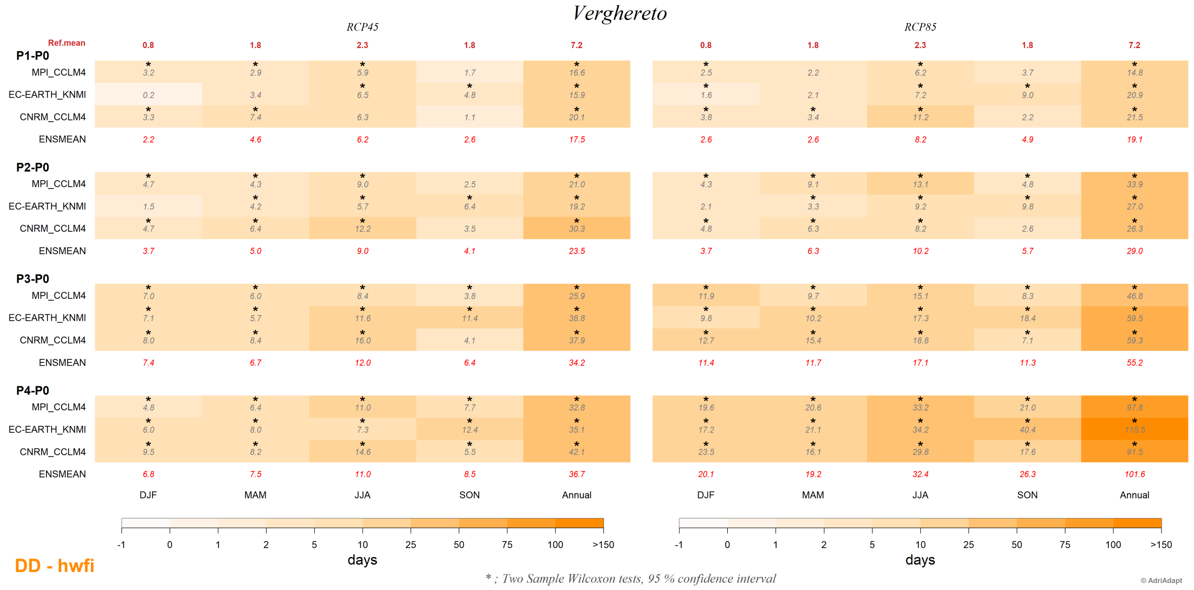

RCP45

	DJF	MAM	JJA	SON	Annual
Ref.mean	0.8	1.8	2.3	1.8	7.2
P1-P0					
MPI_CCLM4	* 3.2	* 2.9	* 5.9	1.7	* 16.6
EC-EARTH_KNMI	0.2	3.4	* 6.5	* 4.8	* 15.9
CNRM_CCLM4	* 3.3	* 7.4	6.3	1.1	* 20.1
ENSMEAN	2.2	4.6	6.2	2.6	17.5
P2-P0					
MPI_CCLM4	* 4.7	* 4.3	* 9.0	2.5	* 21.0
EC-EARTH_KNMI	1.5	* 4.2	* 5.7	* 6.4	* 19.2
CNRM_CCLM4	* 4.7	* 6.4	* 12.2	3.5	* 30.3
ENSMEAN	3.7	5.0	9.0	4.1	23.5
P3-P0					
MPI_CCLM4	* 7.0	* 6.0	* 8.4	* 3.8	* 25.9
EC-EARTH_KNMI	* 7.1	* 5.7	* 11.6	* 11.4	* 38.8
CNRM_CCLM4	* 8.0	* 8.4	* 16.0	4.1	* 37.9
ENSMEAN	7.4	6.7	12.0	6.4	34.2
P4-P0					
MPI_CCLM4	* 4.8	* 6.4	* 11.0	* 7.7	* 32.8
EC-EARTH_KNMI	* 6.0	* 8.0	* 7.3	* 12.4	* 35.1
CNRM_CCLM4	* 9.5	* 8.2	* 14.6	* 5.5	* 42.1
ENSMEAN	6.8	7.5	11.0	8.5	36.7

RCP85

	DJF	MAM	JJA	SON	Annual
Ref.mean	0.8	1.8	2.3	1.8	7.2
P1-P0					
MPI_CCLM4	* 2.5	2.2	* 6.2	3.7	* 14.8
EC-EARTH_KNMI	* 1.6	2.1	* 7.2	* 9.0	* 20.9
CNRM_CCLM4	* 3.8	* 3.4	* 11.2	2.2	* 21.5
ENSMEAN	2.6	2.6	8.2	4.9	19.1
P2-P0					
MPI_CCLM4	* 4.3	* 9.1	* 13.1	* 4.8	* 33.9
EC-EARTH_KNMI	2.1	* 3.3	* 9.2	* 9.8	* 27.0
CNRM_CCLM4	* 4.8	* 6.3	* 8.2	2.6	* 26.3
ENSMEAN	3.7	6.3	10.2	5.7	29.0
P3-P0					
MPI_CCLM4	* 11.9	* 9.7	* 15.1	* 8.3	* 46.8
EC-EARTH_KNMI	* 9.8	* 10.2	* 17.3	* 18.4	* 59.5
CNRM_CCLM4	* 12.7	* 15.4	* 18.8	* 7.1	* 59.3
ENSMEAN	11.4	11.7	17.1	11.3	55.2
P4-P0					
MPI_CCLM4	* 19.6	* 20.6	* 33.2	* 21.0	* 97.8
EC-EARTH_KNMI	* 17.2	* 21.1	* 34.2	* 40.4	* 115.5
CNRM_CCLM4	* 23.5	* 16.1	* 29.8	* 17.6	* 91.5
ENSMEAN	20.1	19.2	32.4	26.3	101.6

Figure 5-225: Seasonal and annual warm spell days index (in days) obtained by dynamical downscaling for Verghereto: Ref. mean is 20 year simulated period (1986-2005) for ensemble mean; P1-P0, P2-P0, P3-P0, P4-P0 are changes in the future for following periods P1: 2021-2040, P2: 2041-2060, P3: 2061-2080, P4: 2081-2100. Differences are shown for individual models. Significant change is marked by star. Change is also shown as ensemble mean (ENSMEAN), not tested for significance. Left column is for RCP4.5 scenario and right for RCP8.5 scenario.

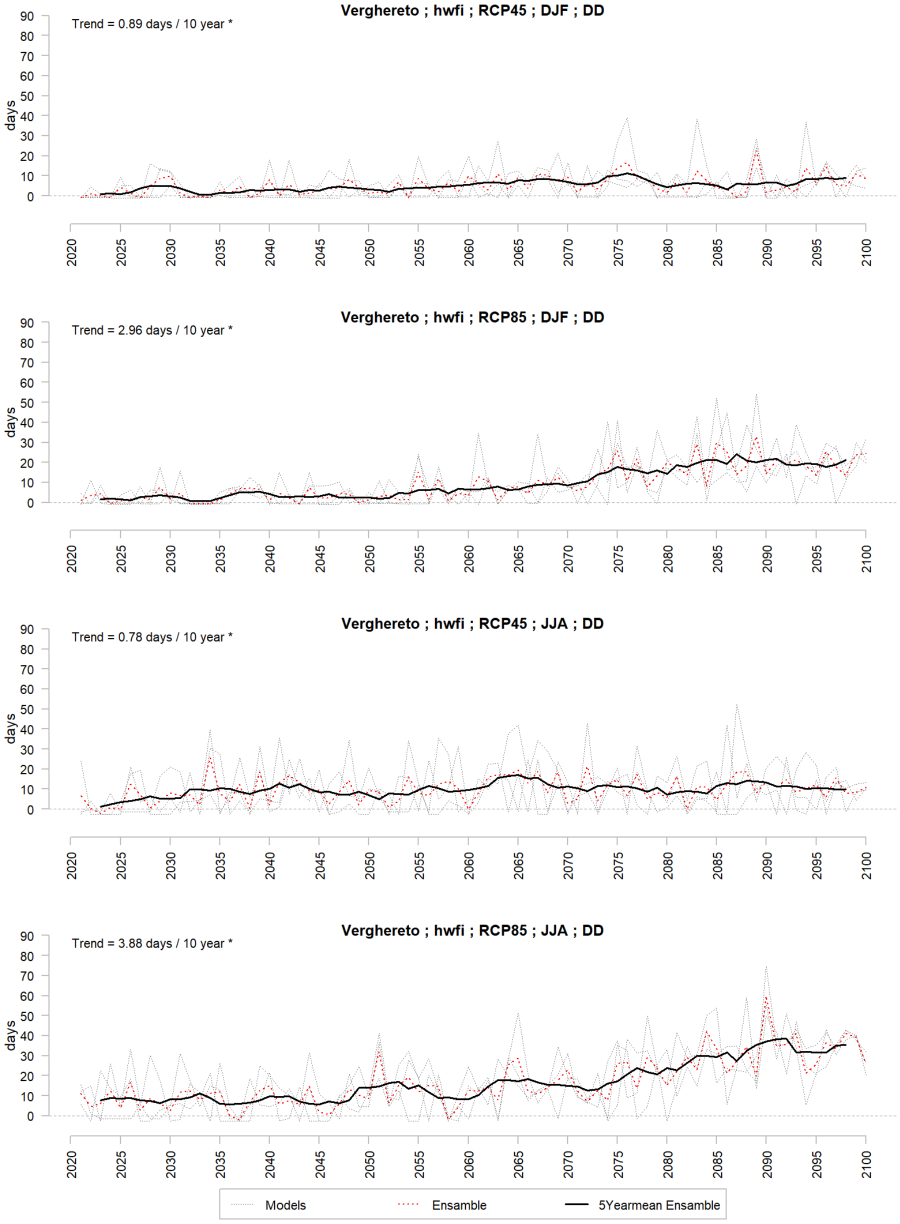

Figure 5-226: Variability of future warm spell days index anomaly in Verghereto (in days) for 2021-2100 obtained by dynamically downscaling for winter (DJF) and summer (JJA) and two RCP scenarios: individual models are in grey, the ensemble mean in red, 5-year moving average in black. Significant trend is marked with star (ns if not significant).

6.6.1.1.9 *Heat wave duration index*

Heat wave duration index (Figure 5-227) in Verghereto shows increase in all seasons and on annual scale, for all future periods. Amplitude of change is increasing towards the end of 21st century, for RCP4.5 scenario ensemble mean change is between 3.6 days in DJF and 6.7 in JJA; 21.4 days on annual scale. Amplitude of change is more pronounced for RCP8.5 and is between 11.4 days in MAM and 20.5 days in JJA, 64.0 days for annual change at the end of 21st century. Variability of future heat wave duration index anomaly (Figure 5-228) shows linear trend in change of ensemble mean, 0.45 days/ 10 year in DJF for RCP4.5 and 2.00 days/ 10 year for RCP8.5; 0.54 days/10 year in JJA for RCP4.5 and 2.62 days/10 year for RCP8.5. All trends are statistically significant.

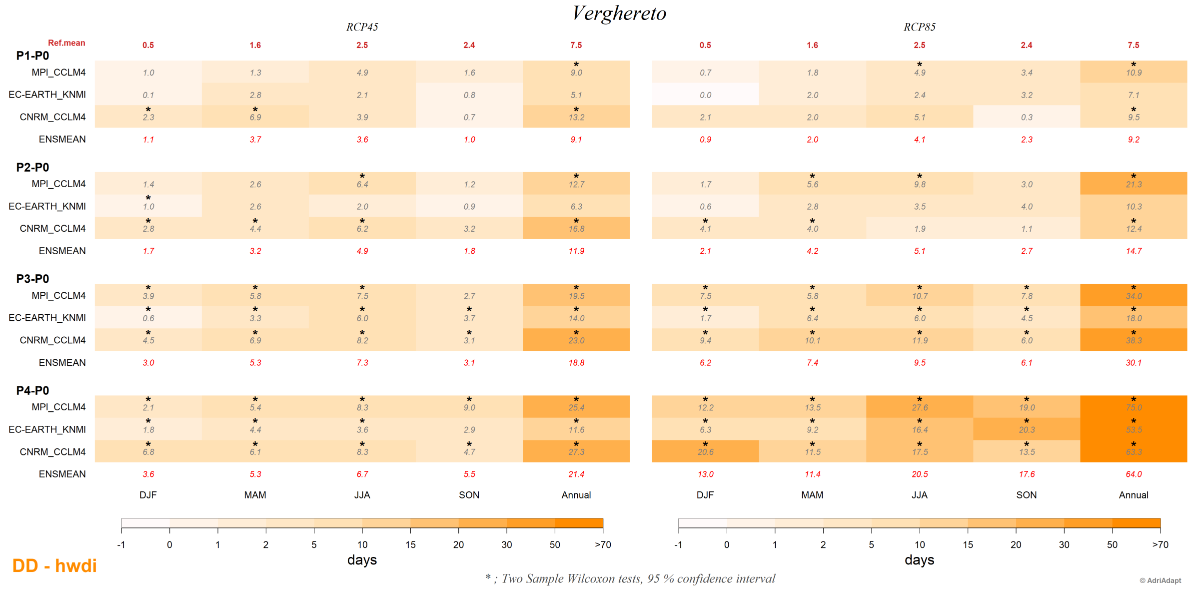

RCP45

	DJF	MAM	JJA	SON	Annual
Ref.mean	0.5	1.6	2.5	2.4	7.5
P1-P0					
MPI_CCLM4	1.0	1.3	4.9	1.6	* 9.0
EC-EARTH_KNMI	0.1	2.8	2.1	0.8	5.1
CNRM_CCLM4	* 2.3	* 6.9	3.9	0.7	* 13.2
ENSMEAN	1.1	3.7	3.6	1.0	9.1
P2-P0					
MPI_CCLM4	1.4	2.6	* 6.4	1.2	* 12.7
EC-EARTH_KNMI	* 1.0	2.6	2.0	0.9	6.3
CNRM_CCLM4	* 2.8	* 4.4	* 6.2	3.2	* 16.8
ENSMEAN	1.7	3.2	4.9	1.8	11.9
P3-P0					
MPI_CCLM4	* 3.9	* 5.8	* 7.5	2.7	* 19.5
EC-EARTH_KNMI	* 0.6	* 3.3	* 6.0	* 3.7	* 14.0
CNRM_CCLM4	* 4.5	* 6.9	* 8.2	* 3.1	* 23.0
ENSMEAN	3.0	5.3	7.3	3.1	18.8
P4-P0					
MPI_CCLM4	* 2.1	* 5.4	* 8.3	* 9.0	* 25.4
EC-EARTH_KNMI	* 1.8	* 4.4	* 3.6	2.9	* 11.6
CNRM_CCLM4	* 6.8	* 6.1	* 8.3	* 4.7	* 27.3
ENSMEAN	3.6	5.3	6.7	5.5	21.4

RCP85

	DJF	MAM	JJA	SON	Annual
Ref.mean	0.5	1.6	2.5	2.4	7.5
P1-P0					
MPI_CCLM4	0.7	1.8	* 4.9	3.4	* 10.9
EC-EARTH_KNMI	0.0	2.0	2.4	3.2	7.1
CNRM_CCLM4	2.1	2.0	5.1	0.3	* 9.5
ENSMEAN	0.9	2.0	4.1	2.3	9.2
P2-P0					
MPI_CCLM4	1.7	* 5.6	* 9.8	3.0	* 21.3
EC-EARTH_KNMI	0.6	2.8	3.5	4.0	10.3
CNRM_CCLM4	* 4.1	* 4.0	1.9	1.1	* 12.4
ENSMEAN	2.1	4.2	5.1	2.7	14.7
P3-P0					
MPI_CCLM4	* 7.5	* 5.8	* 10.7	* 7.8	* 34.0
EC-EARTH_KNMI	* 1.7	* 6.4	* 6.0	* 4.5	* 18.0
CNRM_CCLM4	* 9.4	* 10.1	* 11.9	* 6.0	* 38.3
ENSMEAN	6.2	7.4	9.5	6.1	30.1
P4-P0					
MPI_CCLM4	* 12.2	* 13.5	* 27.6	* 19.0	* 75.0
EC-EARTH_KNMI	* 6.3	* 9.2	* 16.4	* 20.3	* 53.5
CNRM_CCLM4	* 20.6	* 11.5	* 17.5	* 13.5	* 63.3
ENSMEAN	13.0	11.4	20.5	17.6	64.0

* ; Two Sample Wilcoxon tests, 95 % confidence interval

Figure 5-227: Seasonal and annual heat wave duration index (in days) obtained by dynamical downscaling for Verghereto: Ref. mean is 20 year simulated period (1986-2005) for ensemble mean; P1-P0, P2-P0, P3-P0, P4-P0 are changes in the future for following periods P1: 2021-2040, P2: 2041-2060, P3: 2061-2080, P4: 2081-2100. Differences are shown for individual models. Significant change is marked by star. Change is also shown as ensemble mean (ENSMEAN), not tested for significance. Left column is for RCP4.5 scenario and right for RCP8.5 scenario.

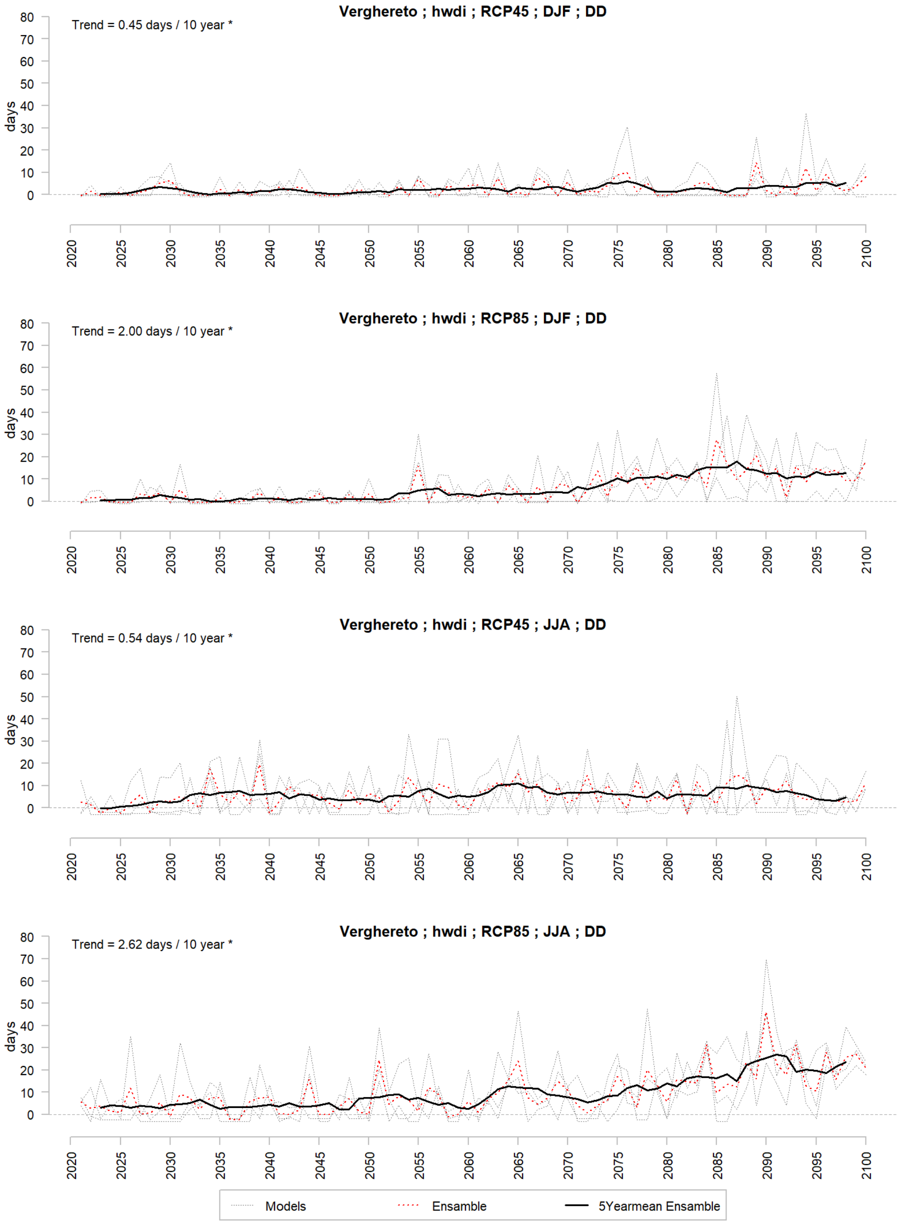

Figure 5-228: Variability of future heat wave duration index anomaly (in days) in Verghereto for 2021-2100 obtained by dynamically downscaling for winter (DJF) and summer (JJA) and two RCP scenarios: individual models are in grey, the ensemble mean in red, 5-year moving average in black. Significant trend is marked with star (ns if not significant).

6.6.1.2 *Precipitation related indices projections*

6.6.1.2.1 *Averaged precipitation*

Averaged precipitation obtained (Figure 5-229) by dynamical downscaling is expressed in mm/day and its change in the future is shown as relative to the P0 period. Precipitation is much more variable parameter in comparison to the temperature, therefore there is no always unique sign of change through the year as well as from model to model. The change in ensemble mean for Verghereto gives decrease of precipitation for all seasons except in DJF (2.3 %). Decrease will be between -2.7 % in SON and -9.3 % in JJA; -3.5 % on annual scale at the end of 21st century for RCP4.5 scenario. The same pattern of change is for RCP8.5 scenario. Precipitation will increase in DJF (2.4 %) and decrease between -9.1 % in SON and -28.0 % in JJA; -9.1 % on annual scale. Variability of future precipitation anomaly (Figure 5-230) for ensemble mean in Verghereto has positive linear trend in DJF for both scenarios. In JJA trend is changing sign from positive for RCP4.5 into negative for RCP8.5. Linear trend in JJA for RCP8.5 is statistically significant (-3.38 % / 10 year).

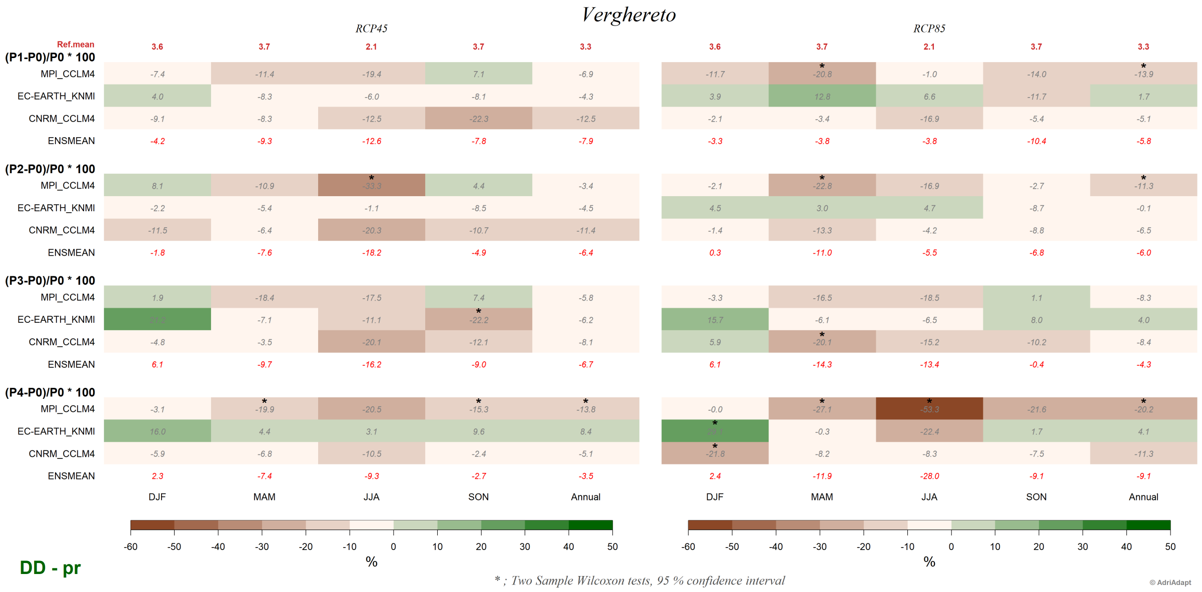

	RCP45					RCP85				
	DJF	MAM	JJA	SON	Annual	DJF	MAM	JJA	SON	Annual
Ref.mean	3.6	3.7	2.1	3.7	3.3	3.6	3.7	2.1	3.7	3.3
(P1-P0)/P0 * 100										
MPI_CCLM4	-7.4	-11.4	-19.4	7.1	-6.9	-11.7	* -20.8	-1.0	-14.0	* -13.9
EC-EARTH_KNMI	4.0	-8.3	-6.0	-8.1	-4.3	3.9	12.8	6.6	-11.7	1.7
CNRM_CCLM4	-9.1	-8.3	-12.5	-22.3	-12.5	-2.1	-3.4	-16.9	-5.4	-5.1
ENSMEAN	-4.2	-9.3	-12.6	-7.8	-7.9	-3.3	-3.8	-3.8	-10.4	-5.8
(P2-P0)/P0 * 100										
MPI_CCLM4	8.1	-10.9	* -33.3	4.4	-3.4	-2.1	* -22.8	-16.9	-2.7	* -11.3
EC-EARTH_KNMI	-2.2	-5.4	-1.1	-8.5	-4.5	4.5	3.0	4.7	-8.7	-0.1
CNRM_CCLM4	-11.5	-6.4	-20.3	-10.7	-11.4	-1.4	-13.3	-4.2	-8.8	-6.5
ENSMEAN	-1.8	-7.6	-18.2	-4.9	-6.4	0.3	-11.0	-5.5	-6.8	-6.0
(P3-P0)/P0 * 100										
MPI_CCLM4	1.9	-18.4	-17.5	7.4	-5.8	-3.3	-16.5	-18.5	1.1	-8.3
EC-EARTH_KNMI	21.2	-7.1	-11.1	* -22.2	-6.2	15.7	-6.1	-6.5	8.0	4.0
CNRM_CCLM4	-4.8	-3.5	-20.1	-12.1	-8.1	5.9	* -20.1	-15.2	-10.2	-8.4
ENSMEAN	6.1	-9.7	-16.2	-9.0	-6.7	6.1	-14.3	-13.4	-0.4	-4.3
(P4-P0)/P0 * 100										
MPI_CCLM4	-3.1	* -19.9	-20.5	* -15.3	* -13.8	-0.0	* -27.1	* -53.3	-21.6	* -20.2
EC-EARTH_KNMI	16.0	4.4	3.1	9.6	8.4	* 29.1	-0.3	-22.4	1.7	4.1
CNRM_CCLM4	-5.9	-6.8	-10.5	-2.4	-5.1	* -21.8	-8.2	-8.3	-7.5	-11.3
ENSMEAN	2.3	-7.4	-9.3	-2.7	-3.5	2.4	-11.9	-28.0	-9.1	-9.1

* ; Two Sample Wilcoxon tests, 95 % confidence interval

Figure 5-229: Averaged seasonal and annual precipitation obtained by dynamical downscaling for Verghereto: Ref. mean is 20 year simulated period (1986-2005) for ensemble mean in mmday^{-1}; P1-P0, P2-P0, P3-P0, P4-P0 are changes (in %) in the future for following periods P1: 2021-2040, P2: 2041-2060, P3: 2061-2080, P4: 2081-2100. Differences are shown for individual models. Significant change is marked by star. Change is also shown as ensemble mean (ENSMEAN), not tested for significance. Left column is for RCP4.5 scenario and right for RCP8.5 scenario.

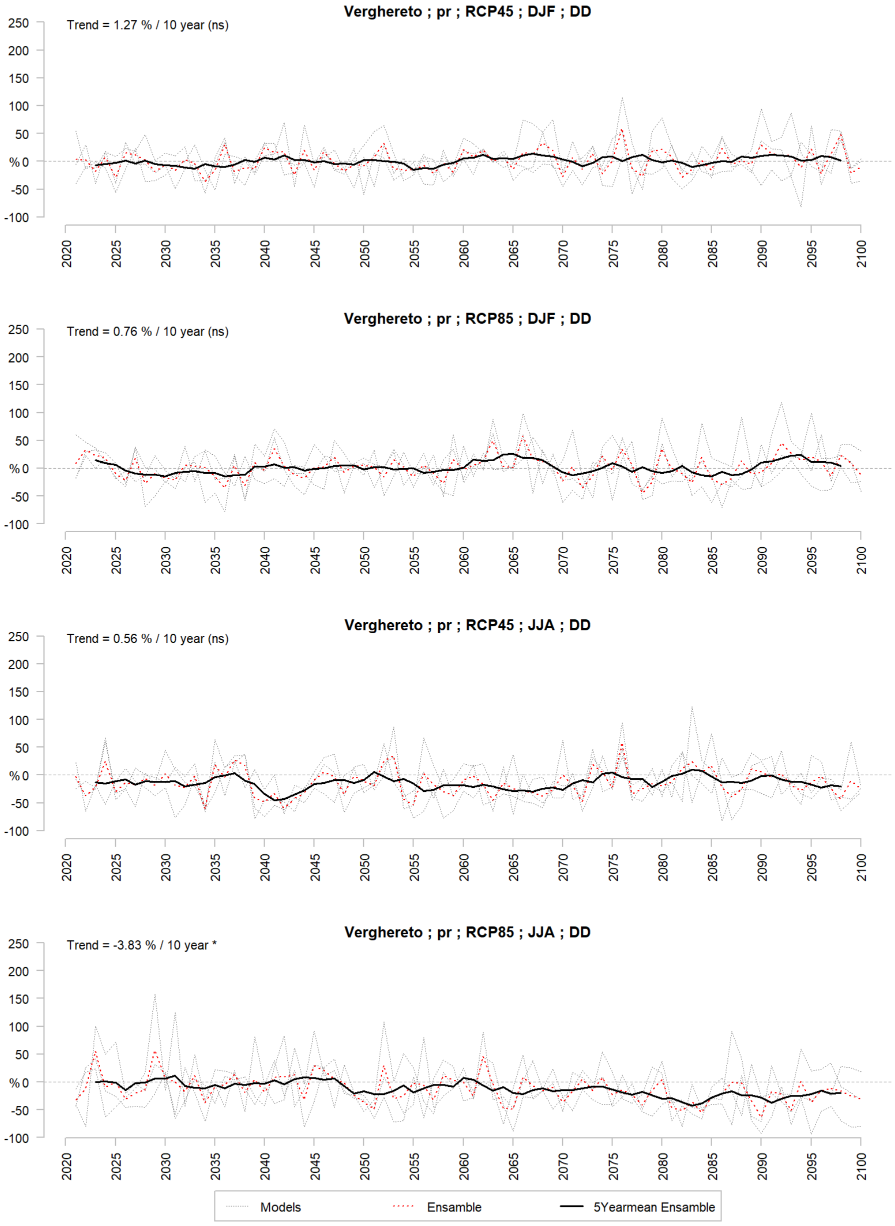

Figure 5-230: Variability of future precipitation anomaly (in %) in Verghereto for 2021-2100 obtained by dynamically downscaling for winter (DJF) and summer (JJA) and two RCP scenarios: individual models are

in grey, the ensemble mean in red, 5-year moving average in black. Significant trend is marked with star (ns if not significant).

6.6.1.2.2 *Intense precipitation*

Intense precipitation (Figure 5-231), defined by 95th percentile of precipitation in Verghereto, shows for ensemble mean at the end of 21st century that 95th percentile will increase in DJF (8.3 %) and SON (0.1 %), but decrease in MAM (-0.8 %) and JJA (-12.5 %); increase on annual scale (2.6 %) for RCP4.5 scenario. For RCP8.5 intense precipitation will decrease for all seasons except in DJF (14.0 %). Decrease will be between -1.5 % in SON and -29.4 % in JJA, -0.4 % on annual scale. Variability of future intense precipitation anomaly (Figure 5-232) for ensemble mean in Verghereto shows increase in precipitation in DJF for both scenarios, increase in JJA for RCP4.5 and decrease for RCP8.5 scenario. Linear trend in JJA for RCP8.5 is statistically significant (-3.96 % / 10 year).

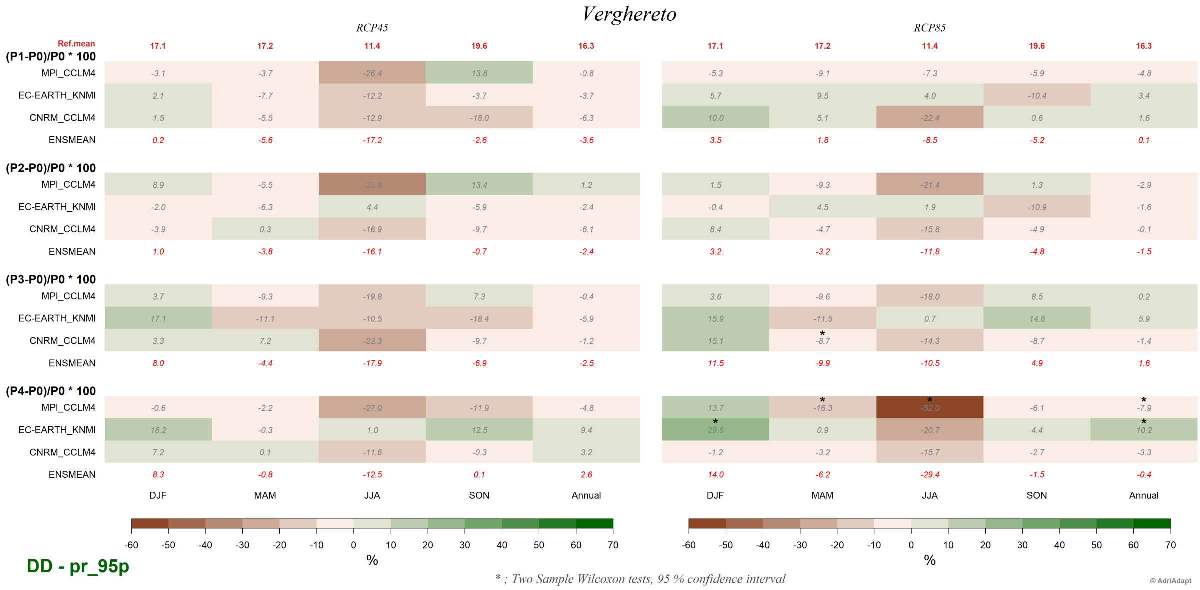

	RCP45					RCP85				
	DJF	MAM	JJA	SON	Annual	DJF	MAM	JJA	SON	Annual
Ref.mean	17.1	17.2	11.4	19.6	16.3	17.1	17.2	11.4	19.6	16.3
(P1-P0)/P0 * 100										
MPI_CCLM4	-3.1	-3.7	-26.4	13.8	-0.8	-5.3	-9.1	-7.3	-5.9	-4.8
EC-EARTH_KNMI	2.1	-7.7	-12.2	-3.7	-3.7	5.7	9.5	4.0	-10.4	3.4
CNRM_CCLM4	1.5	-5.5	-12.9	-18.0	-6.3	10.0	5.1	-22.4	0.6	1.6
ENSMEAN	0.2	-5.6	-17.2	-2.6	-3.6	3.5	1.8	-8.5	-5.2	0.1
(P2-P0)/P0 * 100										
MPI_CCLM4	8.9	-5.5	-35.9	13.4	1.2	1.5	-9.3	-21.4	1.3	-2.9
EC-EARTH_KNMI	-2.0	-6.3	4.4	-5.9	-2.4	-0.4	4.5	1.9	-10.9	-1.6
CNRM_CCLM4	-3.9	0.3	-16.9	-9.7	-6.1	8.4	-4.7	-15.8	-4.9	-0.1
ENSMEAN	1.0	-3.8	-16.1	-0.7	-2.4	3.2	-3.2	-11.8	-4.8	-1.5
(P3-P0)/P0 * 100										
MPI_CCLM4	3.7	-9.3	-19.8	7.3	-0.4	3.6	-9.6	-18.0	8.5	0.2
EC-EARTH_KNMI	17.1	-11.1	-10.5	-18.4	-5.9	15.9	-11.5	0.7	14.8	5.9
CNRM_CCLM4	3.3	7.2	-23.3	-9.7	-1.2	15.1	* -8.7	-14.3	-8.7	-1.4
ENSMEAN	8.0	-4.4	-17.9	-6.9	-2.5	11.5	-9.9	-10.5	4.9	1.6
(P4-P0)/P0 * 100										
MPI_CCLM4	-0.6	-2.2	-27.0	-11.9	-4.8	13.7	* -16.3	* -52.0	-6.1	* -7.9
EC-EARTH_KNMI	18.2	-0.3	1.0	12.5	9.4	* 29.6	0.9	-20.7	4.4	* 10.2
CNRM_CCLM4	7.2	0.1	-11.6	-0.3	3.2	-1.2	-3.2	-15.7	-2.7	-3.3
ENSMEAN	8.3	-0.8	-12.5	0.1	2.6	14.0	-6.2	-29.4	-1.5	-0.4

* ; Two Sample Wilcoxon tests, 95 % confidence interval

Figure 5-231: Seasonal and annual 95th percentile of precipitation (intense precipitation) obtained by dynamical downscaling for Verghereto: Ref. mean is 20 year simulated period (1986-2005) for ensemble mean in mmday^{-1}; P1-P0, P2-P0, P3-P0, P4-P0 are changes (in %) in the future for following periods P1: 2021-2040, P2: 2041-2060, P3: 2061-2080, P4: 2081-2100. Differences are shown for individual models. Significant change is marked by star. Change is also shown as ensemble mean (ENSMEAN), not tested for significance. Left column is for RCP4.5 scenario and right for RCP8.5 scenario.

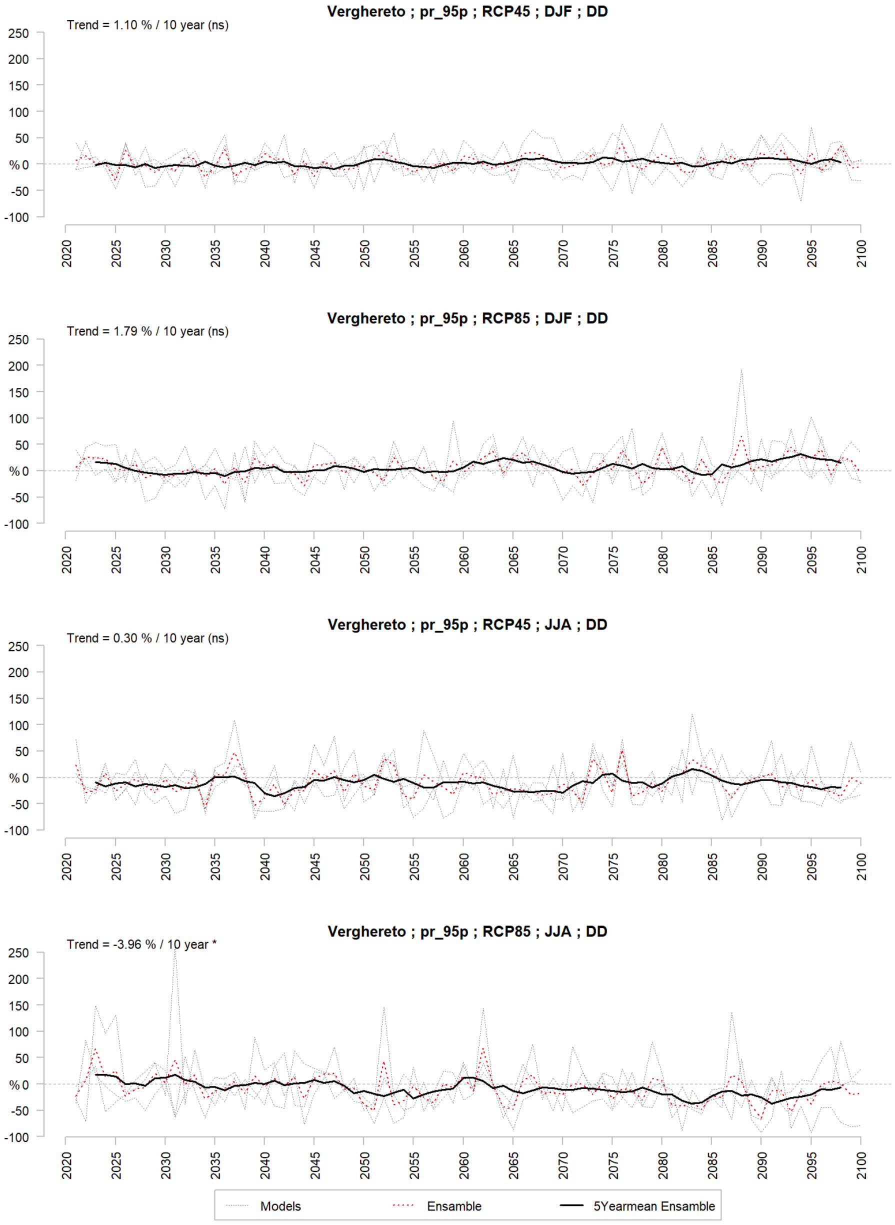

Figure 5-232: Variability of future 95th percentile of precipitation (intense precipitation) anomaly (in %) in Verghereto for 2021-2100 obtained by dynamically downscaling for winter (DJF) and summer (JJA) and two RCP scenarios: individual models are in grey, the ensemble mean in red, 5-year moving average in black. Significant trend is marked with star (ns if not significant).

6.6.1.2.3 *Extreme precipitation*

Extreme precipitation (Figure 5-233), defined by 99th percentile of precipitation in Verghereto, shows for ensemble mean decrease in all seasons except in DJF (14.8 %) for RCP4.5 scenario. Decrease will be between -2.0 % in JJA and -9.4 % in MAM; -0.5 % on annual scale. For RCP8.5 scenario ensemble mean change is positive for all seasons (except in MAM), Increase will be between 0.1 % in JJA and 14.4 % in DJF, 6.7 on annual scale. Decrease in MAM will be -1.5 %. Variability of future extreme precipitation anomaly (Figure 5-234) to the end of 21st century for ensemble mean in Verghereto has positive trends for DJF for both scenarios. In JJA variability of future extreme precipitation anomaly has positive trend for RCP4.5 but negative for RCP8.5. All trends are not statistically significant.

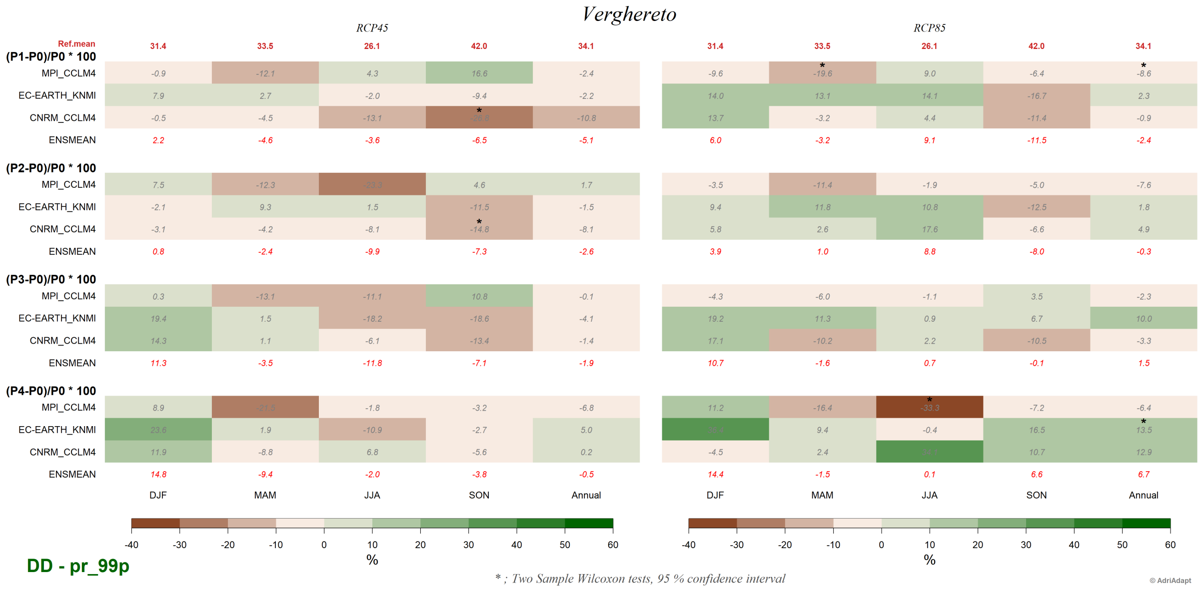

Verghereto

	RCP45					RCP85				
	DJF	MAM	JJA	SON	Annual	DJF	MAM	JJA	SON	Annual
Ref.mean	**31.4**	**33.5**	**26.1**	**42.0**	**34.1**	**31.4**	**33.5**	**26.1**	**42.0**	**34.1**
(P1-P0)/P0 * 100										
MPI_CCLM4	-0.9	-12.1	4.3	16.6	-2.4	-9.6	* -19.6	9.0	-6.4	* -8.6
EC-EARTH_KNMI	7.9	2.7	-2.0	-9.4	-2.2	14.0	13.1	14.1	-16.7	2.3
CNRM_CCLM4	-0.5	-4.5	-13.1	* -26.8	-10.8	13.7	-3.2	4.4	-11.4	-0.9
ENSMEAN	2.2	-4.6	-3.6	-6.5	-5.1	6.0	-3.2	9.1	-11.5	-2.4
(P2-P0)/P0 * 100										
MPI_CCLM4	7.5	-12.3	-23.3	4.6	1.7	-3.5	-11.4	-1.9	-5.0	-7.6
EC-EARTH_KNMI	-2.1	9.3	1.5	-11.5	-1.5	9.4	11.8	10.8	-12.5	1.8
CNRM_CCLM4	-3.1	-4.2	-8.1	* -14.8	-8.1	5.8	2.6	17.6	-6.6	4.9
ENSMEAN	0.8	-2.4	-9.9	-7.3	-2.6	3.9	1.0	8.8	-8.0	-0.3
(P3-P0)/P0 * 100										
MPI_CCLM4	0.3	-13.1	-11.1	10.8	-0.1	-4.3	-6.0	-1.1	3.5	-2.3
EC-EARTH_KNMI	19.4	1.5	-18.2	-18.6	-4.1	19.2	11.3	0.9	6.7	10.0
CNRM_CCLM4	14.3	1.1	-6.1	-13.4	-1.4	17.1	-10.2	2.2	-10.5	-3.3
ENSMEAN	11.3	-3.5	-11.8	-7.1	-1.9	10.7	-1.6	0.7	-0.1	1.5
(P4-P0)/P0 * 100										
MPI_CCLM4	8.9	-21.5	-1.8	-3.2	-6.8	11.2	-16.4	* -33.3	-7.2	-6.4
EC-EARTH_KNMI	23.6	1.9	-10.9	-2.7	5.0	36.4	9.4	-0.4	16.5	* 13.5
CNRM_CCLM4	11.9	-8.8	6.8	-5.6	0.2	-4.5	2.4	34.1	10.7	12.9
ENSMEAN	14.8	-9.4	-2.0	-3.8	-0.5	14.4	-1.5	0.1	6.6	6.7

* ; Two Sample Wilcoxon tests, 95 % confidence interval

Figure 5-233: Seasonal and annual 99th percentile of precipitation (extreme precipitation) obtained by dynamical downscaling for Verghereto: Ref. mean is 20 year simulated period (1986-2005) for ensemble mean in mmday^{-1}; P1-P0, P2-P0, P3-P0, P4-P0 are changes (in %) in the future for following periods P1: 2021-2040, P2: 2041-2060, P3: 2061-2080, P4: 2081-2100. Differences are shown for individual models. Significant change is marked by star. Change is also shown as ensemble mean (ENSMEAN), not tested for significance. Left column is for RCP4.5 scenario and right for RCP8.5 scenario.

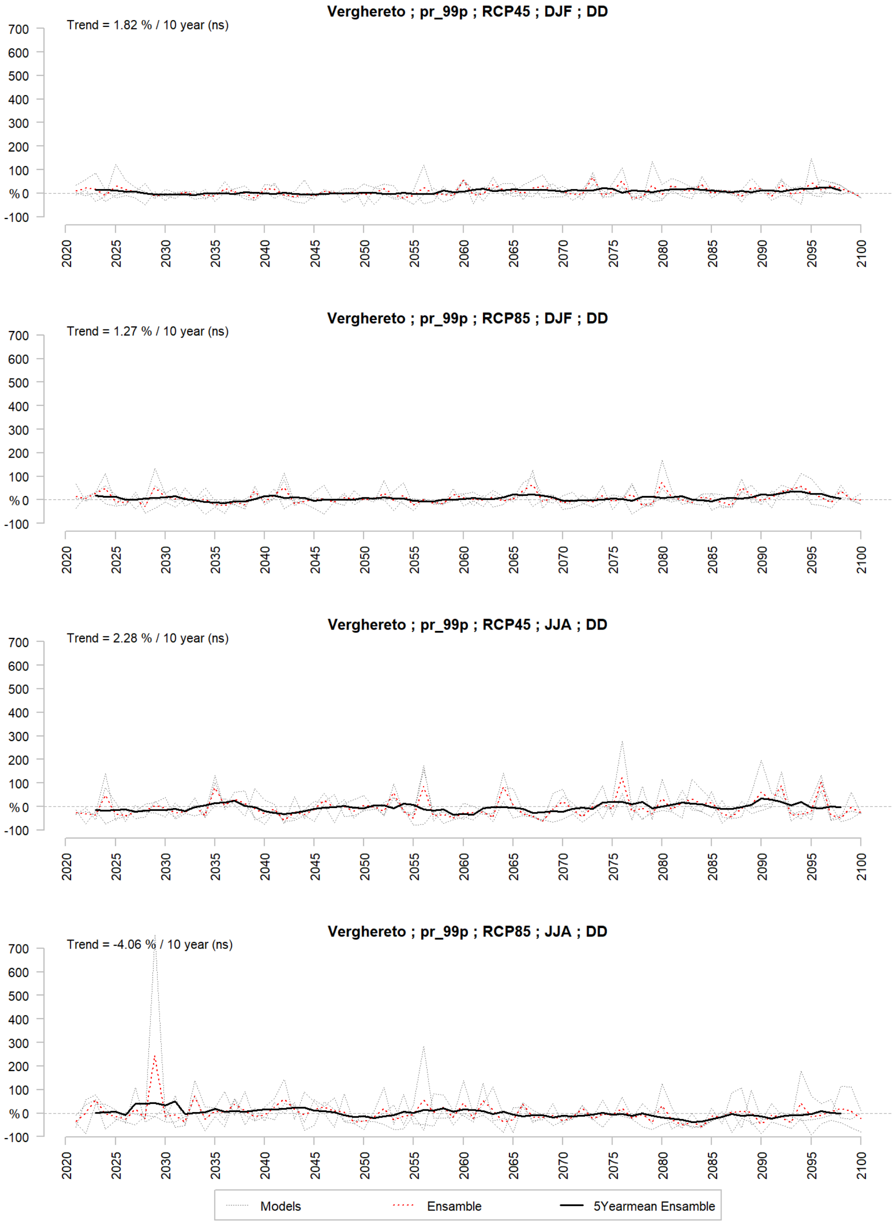

Figure 5-234: Variability of future 99th percentile of precipitation (extreme precipitation) anomaly (in %) in Verghereto for 2021-2100 obtained by dynamically downscaling for winter (DJF) and summer (JJA) and two RCP scenarios: individual models are in grey, the ensemble mean in red, 5-year moving average in black. Significant trend is marked with star (ns if not significant).

6.6.1.2.4 *Heavy precipitation index*

Heavy precipitation index (Figure 5-235), defined as number of days with precipitation greater than 10 mm, will change with no unique sign between models in all seasons. In ensemble mean change at the end of century, heavy precipitation index in Verghereto will decrease in MAM and JJA (-2.8 %, -12.6 % respectively) and increase in DJF and SON (4.9 %, 2.4 % respectively); decrease of -0.8 % on annual scale for RCP4.5 scenario. Worst case scenario RCP8.5 gives decrease in all seasons except DJF (2.3 %). Decrease will range from -7.2 % in SON to -34.2 % in JJA; -9.9 % on annual scale. Variability of future heavy precipitation index anomaly (Figure 5-236) to the end of 21st century for ensemble mean in Verghereto has positive trend for DJF for both scenarios, positive in JJA for RCP4.5 and negative for RCP8.5 scenario. Linear trend in JJA for RCP8.5 is statistically significant (-3.24 % / 10 year).

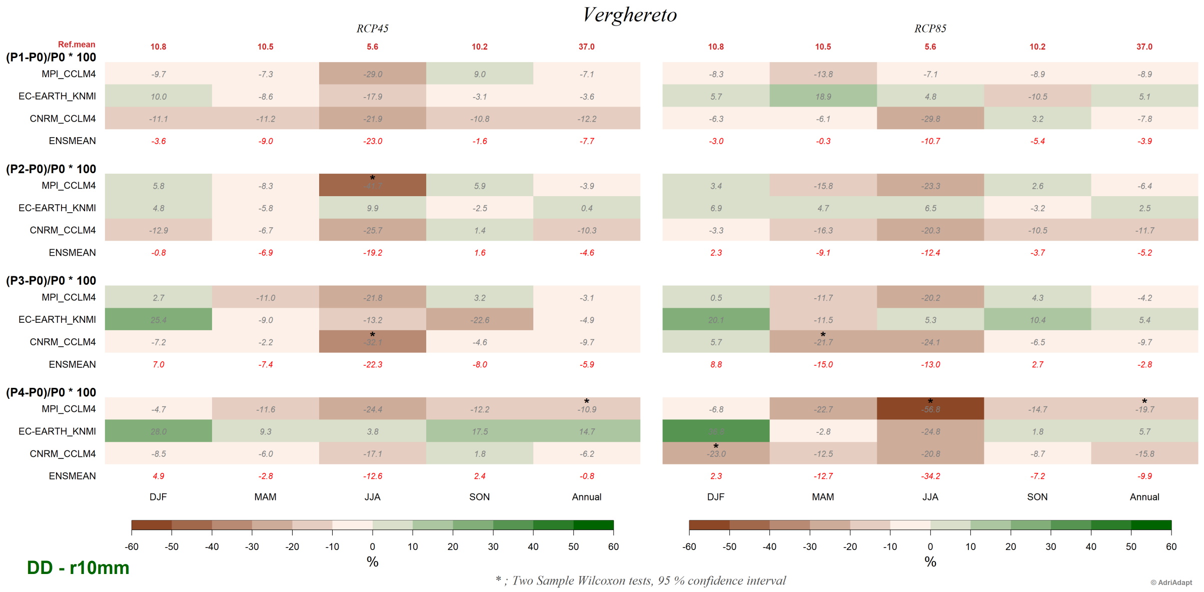

	RCP45					RCP85				
Ref.mean	10.8	10.5	5.6	10.2	37.0	10.8	10.5	5.6	10.2	37.0
(P1-P0)/P0 * 100										
MPI_CCLM4	-9.7	-7.3	-29.0	9.0	-7.1	-8.3	-13.8	-7.1	-8.9	-8.9
EC-EARTH_KNMI	10.0	-8.6	-17.9	-3.1	-3.6	5.7	18.9	4.8	-10.5	5.1
CNRM_CCLM4	-11.1	-11.2	-21.9	-10.8	-12.2	-6.3	-6.1	-29.8	3.2	-7.8
ENSMEAN	-3.6	-9.0	-23.0	-1.6	-7.7	-3.0	-0.3	-10.7	-5.4	-3.9
(P2-P0)/P0 * 100										
MPI_CCLM4	5.8	-8.3	* -41.7	5.9	-3.9	3.4	-15.8	-23.3	2.6	-6.4
EC-EARTH_KNMI	4.8	-5.8	9.9	-2.5	0.4	6.9	4.7	6.5	-3.2	2.5
CNRM_CCLM4	-12.9	-6.7	-25.7	1.4	-10.3	-3.3	-16.3	-20.3	-10.5	-11.7
ENSMEAN	-0.8	-6.9	-19.2	1.6	-4.6	2.3	-9.1	-12.4	-3.7	-5.2
(P3-P0)/P0 * 100										
MPI_CCLM4	2.7	-11.0	-21.8	3.2	-3.1	0.5	-11.7	-20.2	4.3	-4.2
EC-EARTH_KNMI	25.4	-9.0	-13.2	-22.6	-4.9	20.1	-11.5	5.3	10.4	5.4
CNRM_CCLM4	-7.2	-2.2	* -32.1	-4.6	-9.7	5.7	* -21.7	-24.1	-6.5	-9.7
ENSMEAN	7.0	-7.4	-22.3	-8.0	-5.9	8.8	-15.0	-13.0	2.7	-2.8
(P4-P0)/P0 * 100										
MPI_CCLM4	-4.7	-11.6	-24.4	-12.2	* -10.9	-6.8	-22.7	* -56.8	-14.7	* -19.7
EC-EARTH_KNMI	28.0	9.3	3.8	17.5	14.7	36.8	-2.8	-24.8	1.8	5.7
CNRM_CCLM4	-8.5	-6.0	-17.1	1.8	-6.2	* -23.0	-12.5	-20.8	-8.7	-15.8
ENSMEAN	4.9	-2.8	-12.6	2.4	-0.8	2.3	-12.7	-34.2	-7.2	-9.9
	DJF	MAM	JJA	SON	Annual	DJF	MAM	JJA	SON	Annual

* ; Two Sample Wilcoxon tests, 95 % confidence interval

Figure 5-235: Seasonal and annual heavy precipitation index obtained by dynamical downscaling for Verghereto: Ref. mean is 20 year simulated period (1986-2005) for ensemble mean in days; P1-P0, P2-P0, P3-P0, P4-P0 are changes (in %) in the future for following periods P1: 2021-2040, P2: 2041-2060, P3: 2061-2080, P4: 2081-2100. Differences are shown for individual models. Significant change is marked by star. Change is also shown as ensemble mean (ENSMEAN), not tested for significance. Left column is for RCP4.5 scenario and right for RCP8.5 scenario.

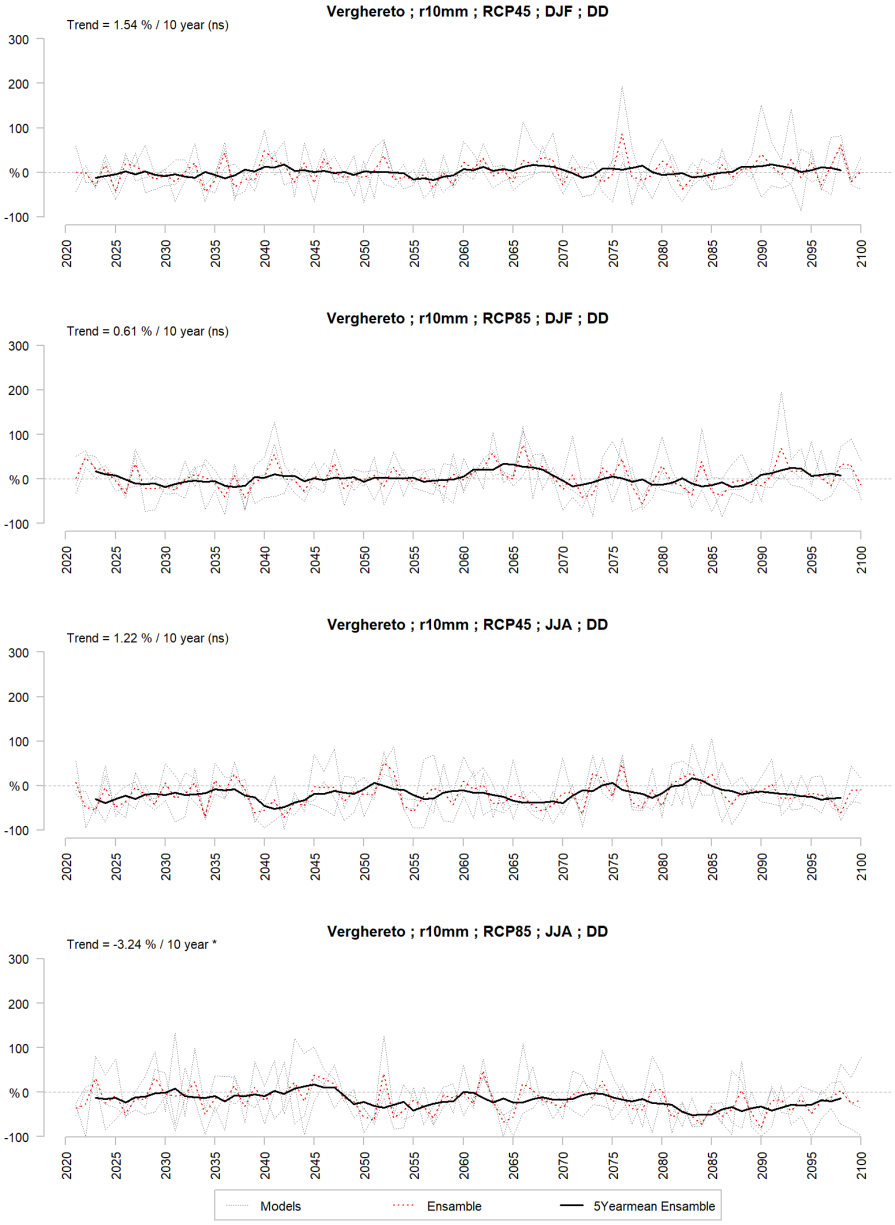

Figure 5-236: Variability of future heavy precipitation index anomaly (in %) in Verghereto for 2021-2100 obtained by dynamically downscaling for winter (DJF) and summer (JJA) and two RCP scenarios: individual models are in grey, the ensemble mean in red, 5-year moving average in black. Significant trend is marked with star (ns if not significant).

6.6.1.2.5 *Maximum number of consecutive dry days*

Maximum number of consecutive dry days (Figure 5-237) in Verghereto will quite differ from model to model. The ensemble mean change gives increase in all seasons for both scenarios at the end of 21st century. Increase will be between 3.3 % in SON and 17.9 % in JJA; 14.3 % on annual scale for RCP4.5 scenario. For RCP8.5 scenario ensemble mean change gives increase between 13.3 % in SON and 25.9 % in JJA, 22.9 % on annual scale. Variability of future maximum number of consecutive dry days anomaly (Figure 5-238) to the end of 21st century for ensemble mean in Verghereto has positive trends in both seasons for both scenarios. Linear trend in JJA for RCP8.5 scenario is statistically significant (2.54 % / 10 year).

Verghereto

	RCP45					*RCP85*				
Ref.mean	12.2	11.9	18.0	14.6	22.7	12.2	11.9	18.0	14.6	22.7
(P1-P0)/P0 * 100										
MPI_CCLM4	11.7	-11.5	1.8	11.0	11.0	39.1	14.0	8.9	19.2	20.5
EC-EARTH_KNMI	8.5	-3.6	-0.4	4.7	-4.0	-1.6	* -26.5	4.8	-2.6	-7.8
CNRM_CCLM4	-0.8	20.6	23.8	-8.9	2.1	7.0	20.1	* 29.1	-9.7	12.5
ENSMEAN	6.5	1.8	8.4	2.3	3.0	14.8	2.5	14.3	2.3	8.4
(P2-P0)/P0 * 100										
MPI_CCLM4	-5.3	-0.5	1.2	3.8	3.5	25.7	* 24.6	2.4	10.6	5.9
EC-EARTH_KNMI	-2.2	-3.2	-5.6	5.6	-6.4	3.6	* -8.3	2.7	15.4	9.7
CNRM_CCLM4	10.6	6.9	* 36.4	-11.0	8.5	-1.9	19.5	14.2	-8.7	5.8
ENSMEAN	1.0	1.1	10.7	-0.5	1.9	9.2	11.9	6.4	5.8	7.1
(P3-P0)/P0 * 100										
MPI_CCLM4	16.2	* 35.6	4.9	11.9	12.1	* 41.8	15.1	11.6	21.8	22.4
EC-EARTH_KNMI	-1.4	-7.9	3.3	24.5	-1.2	-13.1	-9.7	8.2	-0.8	-4.5
CNRM_CCLM4	7.2	19.0	28.9	-6.1	5.6	-6.8	33.4	42.9	-10.9	17.0
ENSMEAN	7.4	15.6	12.4	10.1	5.5	7.3	12.9	20.9	3.4	11.6
(P4-P0)/P0 * 100										
MPI_CCLM4	* 29.6	* 27.7	21.7	27.2	* 27.4	* 42.4	* 49.1	* 55.4	* 38.5	* 67.1
EC-EARTH_KNMI	-5.6	* -21.1	2.1	-16.1	-5.8	-10.1	-10.3	13.8	17.5	7.3
CNRM_CCLM4	26.0	7.3	29.8	-1.3	* 21.3	21.6	* 29.4	8.5	-16.2	-5.6
ENSMEAN	16.7	4.6	17.9	3.3	14.3	18.0	22.8	25.9	13.3	22.9
	DJF	MAM	JJA	SON	Annual	DJF	MAM	JJA	SON	Annual

** ; Two Sample Wilcoxon tests, 95 % confidence interval*

Figure 5-237: Seasonal and annual maximum number of consecutive dry days obtained by dynamical downscaling for Verghereto: Ref. mean is 20 year simulated period (1986-2005) for ensemble mean in days; P1-P0, P2-P0, P3-P0, P4-P0 are changes (in %) in the future for following periods P1: 2021-2040, P2: 2041-2060, P3: 2061-2080, P4: 2081-2100. Differences are shown for individual models. Significant change is marked by star. Change is also shown as ensemble mean (ENSMEAN), not tested for significance. Left column is for RCP4.5 scenario and right for RCP8.5 scenario.

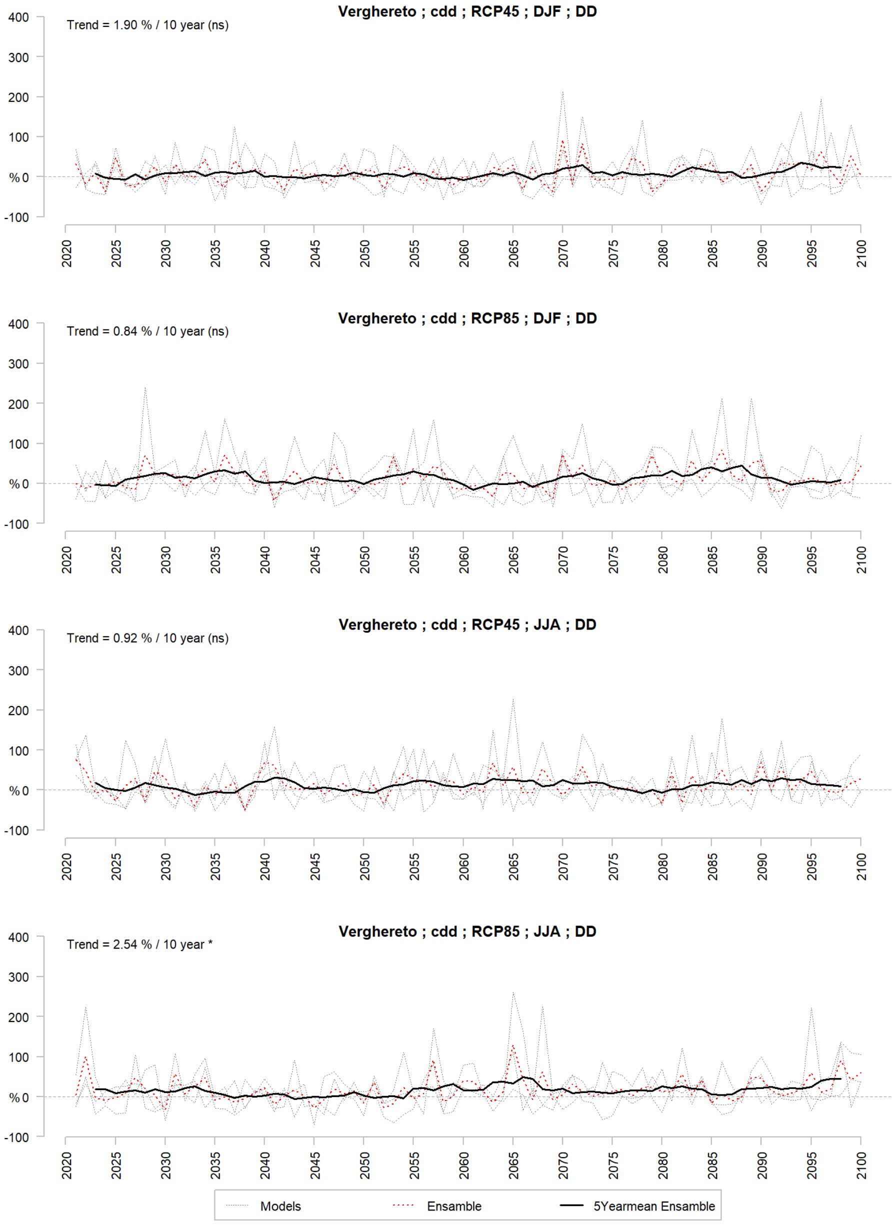

Figure 5-238: Variability of future maximum number of consecutive dry days anomaly (in %) in Verghereto for 2021-2100 obtained by dynamically downscaling for winter (DJF) and summer (JJA) and two RCP scenarios: individual models are in grey, the ensemble mean in red, 5-year moving average in black. Significant trend is marked with star (ns if not significant).

6.6.1.3 *Extra rare humidex projections*

Extra rare humidex change (defined by 99.9th percentile of humidex) in the future in Verghereto will increase towards the end of 21st century (Figure 5-239). Ensemble mean will increase between 0.5 in JJA and 3.0 in MAM; 1.1 on annual scale for RCP4.5 scenario. Scenario RCP8.5 gives higher positive amplitudes, from 3.9 in DJF to 6.3 in SON; 5.5 on annual scale. Variability of future 99.9th percentile of humidex anomaly (Figure 5-240) shows positive linear trend for both seasons and both considered scenarios. It is 0.26 [] / 10 year in DJF for RCP4.5 (0.67 [] /10 year for RCP8.5) and 0.20 [] /10 year in JJA for RCP4.5 (0.83 [] /10 year for RCP8.5). Trends are statistically significant.

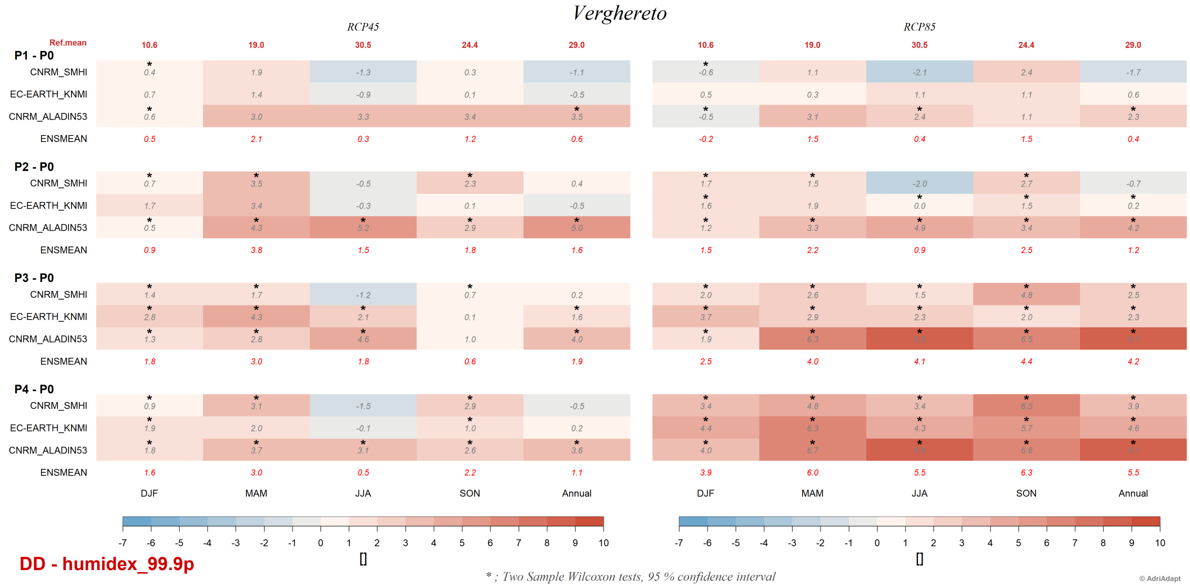

Figure 5-239: Seasonal and annual 99.9th percentile of humidex obtained by dynamical downscaling for Verghereto (in []): Ref. mean is 20 year simulated period (1986-2005); P1-P0, P2-P0, P3-P0, P4-P0 are changes in the future for following periods P1: 2021-2040, P2: 2041-2060, P3: 2061-2080, P4: 2081-2100. Differences are shown for individual models. Significant change is marked by star. Change is also shown as ensemble mean (ENSMEAN), not tested for significance. Left column is for RCP4.5 scenario and right for RCP8.5 scenario.

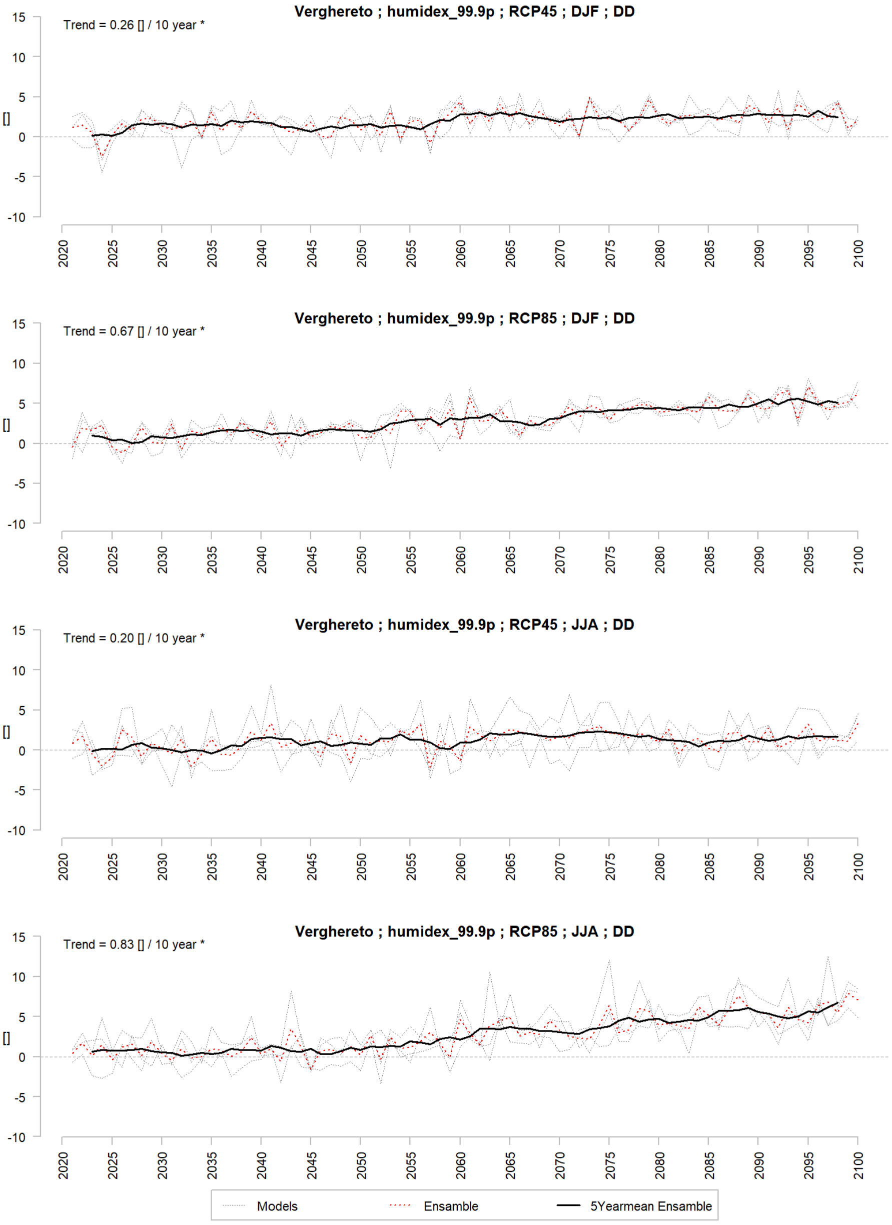

Figure 5-240: Variability of future 99.9th percentile of humidex anomaly (in []) in Verghereto for 2021-2100 obtained by dynamically downscaling for winter (DJF) and summer (JJA) and two RCP scenarios: individual models are in grey, the ensemble mean in red, 5-year moving average in black. Significant trend is marked with star (ns if not significant).

6.6.1.4 *Wind projections*

6.6.1.4.1 *Averaged wind module*

The change of wind speed at 10m high (Figure 5-241) is very variable from season to season and from model to model. It is expressed as relative difference to the wind speed in P0 period in percentage. At the end of 21st century wind speed in Verghereto will slightly decrease in all seasons except in MAM (1.3 %) and on annual scale. Decrease will be between -0.7 % in DJF and -2.9 % in SON; -0.9 % on annual scale for RCP4.5 scenario. For RCP8.5 scenario wind speed will increase in DJF and MAM (3.0 %, 1.1 % respectively) but decrease in JJA, SON and on the annual scale (-2.8 %, -3.8 %, -0.5 % respectively) at the end of 21st century. Variability of future wind speed at 10m high anomaly (Figure 5-242) shows positive linear trends in DJF and negative in JJA for both scenarios. Linear trends for RCP8.5 scenario in both seasons are statistically significant (1.09 % / 10 year in DJF; -0.66 % / 10 year).

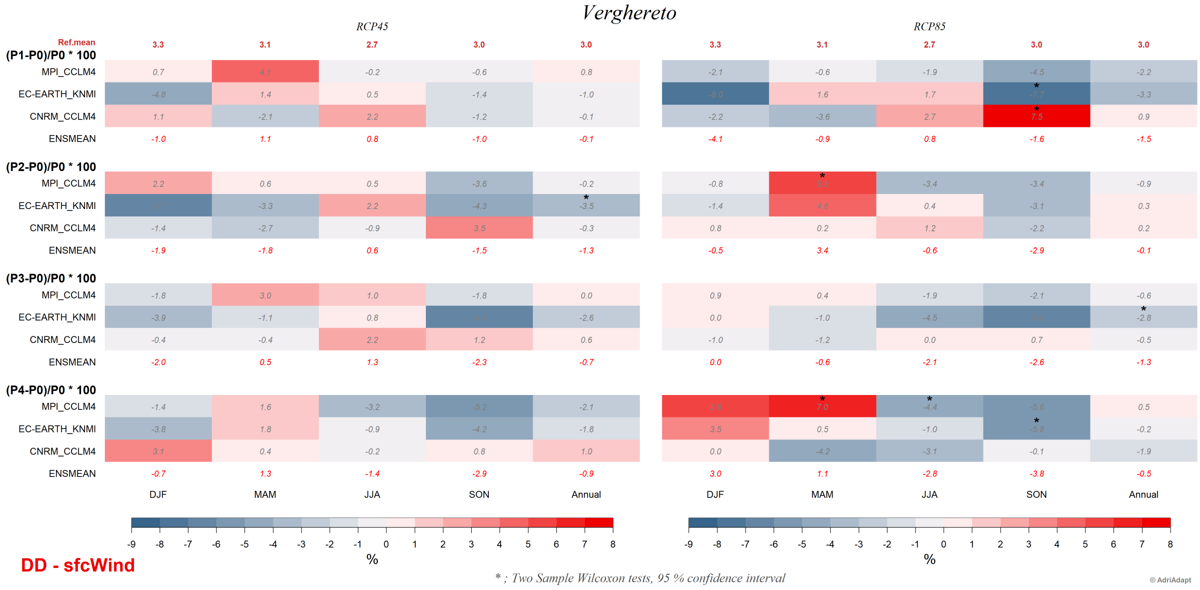

Verghereto

	RCP45					RCP85				
	DJF	MAM	JJA	SON	Annual	DJF	MAM	JJA	SON	Annual
Ref.mean	**3.3**	**3.1**	**2.7**	**3.0**	**3.0**	**3.3**	**3.1**	**2.7**	**3.0**	**3.0**
(P1-P0)/P0 * 100										
MPI_CCLM4	0.7	4.1	-0.2	-0.6	0.8	-2.1	-0.6	-1.9	-4.5	-2.2
EC-EARTH_KNMI	-4.8	1.4	0.5	-1.4	-1.0	-8.0	1.6	1.7	* -7.7	-3.3
CNRM_CCLM4	1.1	-2.1	2.2	-1.2	-0.1	-2.2	-3.6	2.7	* 7.5	0.9
ENSMEAN	-1.0	1.1	0.8	-1.0	-0.1	-4.1	-0.9	0.8	-1.6	-1.5
(P2-P0)/P0 * 100										
MPI_CCLM4	2.2	0.6	0.5	-3.6	-0.2	-0.8	* 5.3	-3.4	-3.4	-0.9
EC-EARTH_KNMI	-6.7	-3.3	2.2	-4.3	* -3.5	-1.4	4.6	0.4	-3.1	0.3
CNRM_CCLM4	-1.4	-2.7	-0.9	3.5	-0.3	0.8	0.2	1.2	-2.2	0.2
ENSMEAN	-1.9	-1.8	0.6	-1.5	-1.3	-0.5	3.4	-0.6	-2.9	-0.1
(P3-P0)/P0 * 100										
MPI_CCLM4	-1.8	3.0	1.0	-1.8	0.0	0.9	0.4	-1.9	-2.1	-0.6
EC-EARTH_KNMI	-3.9	-1.1	0.8	-6.4	-2.6	0.0	-1.0	-4.5	-6.5	* -2.8
CNRM_CCLM4	-0.4	-0.4	2.2	1.2	0.6	-1.0	-1.2	0.0	0.7	-0.5
ENSMEAN	-2.0	0.5	1.3	-2.3	-0.7	0.0	-0.6	-2.1	-2.6	-1.3
(P4-P0)/P0 * 100										
MPI_CCLM4	-1.4	1.6	-3.2	-5.2	-2.1	5.6	* 7.0	* -4.4	-5.6	0.5
EC-EARTH_KNMI	-3.8	1.8	-0.9	-4.2	-1.8	3.5	0.5	-1.0	* -5.8	-0.2
CNRM_CCLM4	3.1	0.4	-0.2	0.8	1.0	0.0	-4.2	-3.1	-0.1	-1.9
ENSMEAN	-0.7	1.3	-1.4	-2.9	-0.9	3.0	1.1	-2.8	-3.8	-0.5

* ; Two Sample Wilcoxon tests, 95 % confidence interval

Figure 5-241: Averaged seasonal and annual wind module (wind speed at 10m height) obtained by dynamical downscaling for Verghereto: Ref. mean is 20 year simulated period (1986-2005) in ms^{-1}; P1-P0, P2-P0, P3-P0, P4-P0 are changes (in %) in the future for following periods P1: 2021-2040, P2: 2041-2060, P3: 2061-2080, P4: 2081-2100. Differences are shown for individual models. Significant change is marked by star. Change is also shown as ensemble mean (ENSMEAN), not tested for significance. Left column is for RCP4.5 scenario and right for RCP8.5 scenario.

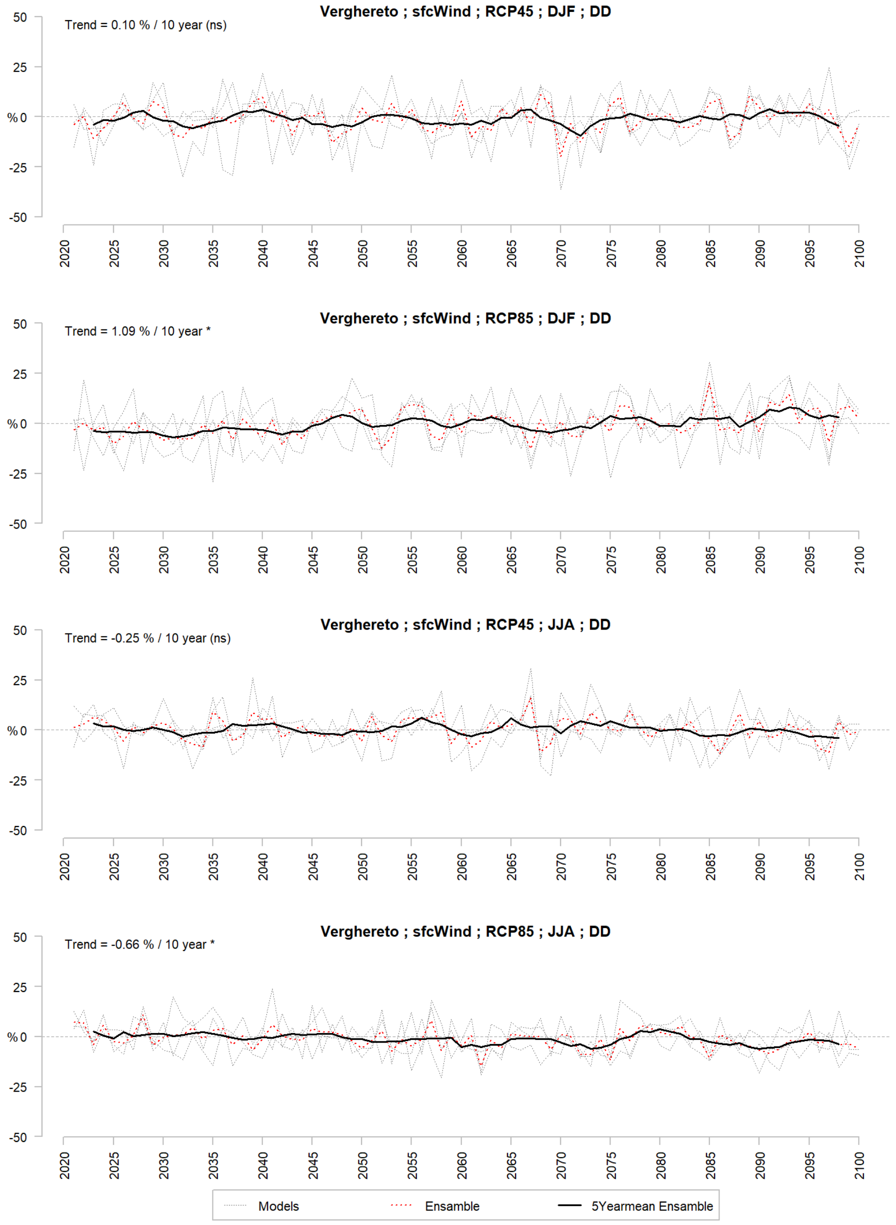

Verghereto ; sfcWind ; RCP45 ; DJF ; DD

Trend = 0.10 % / 10 year (ns)

Verghereto ; sfcWind ; RCP85 ; DJF ; DD

Trend = 1.09 % / 10 year *

Verghereto ; sfcWind ; RCP45 ; JJA ; DD

Trend = -0.25 % / 10 year (ns)

Verghereto ; sfcWind ; RCP85 ; JJA ; DD

Trend = -0.66 % / 10 year *

Figure 5-242: Variability of future wind module anomaly (wind speed at 10m height) anomaly (in %) in Verghereto for 2021-2100 obtained by dynamically downscaling for winter (DJF) and summer (JJA) and two RCP scenarios: individual models are in grey, the ensemble mean in red, 5-year moving average in black. Significant trend is marked with star (ns if not significant).

6.6.1.4.2 *Maximum wind module*

The change of maximum wind speed at 10m high (Figure 5-243) is very variable from season to season and from model to model. It is expressed as relative difference to the maximum wind speed in P0 period in percentage. At the end of 21st century maximum wind speed in Verghereto will slightly decrease in all seasons except in MAM (1.3 %). Decrease will be between -0.4 % in DJF and -3.1 % in SON; -0.8 % on annual scale for RCP4.5 scenario. For RCP8.5 scenario maximum wind speed will increase in DJF and MAM (3.0 %, 1.1 %, respectively) and decrease in JJA, SON and on annual scale (-2.0 %, -3.7 %, -0.4 % respectively). Variability of future maximum wind speed at 10m high anomaly (Figure 5-244) shows positive linear trend to the end of 21st century in DJF and negative in JJA. Linear trends for RCP8.5 scenario are statistically significant (0.96 % / 10 year in DJF; -0.48 % / 10 year in JJA).

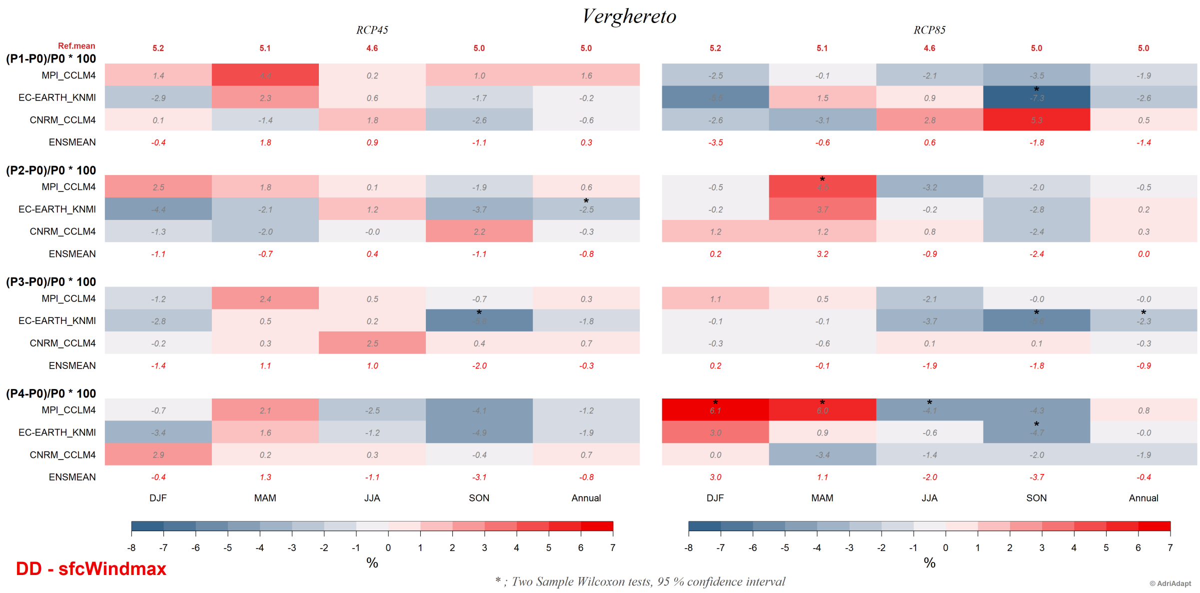

RCP45

	DJF	MAM	JJA	SON	Annual
Ref.mean	5.2	5.1	4.6	5.0	5.0
(P1-P0)/P0 * 100					
MPI_CCLM4	1.4	4.4	0.2	1.0	1.6
EC-EARTH_KNMI	-2.9	2.3	0.6	-1.7	-0.2
CNRM_CCLM4	0.1	-1.4	1.8	-2.6	-0.6
ENSMEAN	-0.4	1.8	0.9	-1.1	0.3
(P2-P0)/P0 * 100					
MPI_CCLM4	2.5	1.8	0.1	-1.9	0.6
EC-EARTH_KNMI	-4.4	-2.1	1.2	-3.7	* -2.5
CNRM_CCLM4	-1.3	-2.0	-0.0	2.2	-0.3
ENSMEAN	-1.1	-0.7	0.4	-1.1	-0.8
(P3-P0)/P0 * 100					
MPI_CCLM4	-1.2	2.4	0.5	-0.7	0.3
EC-EARTH_KNMI	-2.8	0.5	0.2	* -5.8	-1.8
CNRM_CCLM4	-0.2	0.3	2.5	0.4	0.7
ENSMEAN	-1.4	1.1	1.0	-2.0	-0.3
(P4-P0)/P0 * 100					
MPI_CCLM4	-0.7	2.1	-2.5	-4.1	-1.2
EC-EARTH_KNMI	-3.4	1.6	-1.2	-4.9	-1.9
CNRM_CCLM4	2.9	0.2	0.3	-0.4	0.7
ENSMEAN	-0.4	1.3	-1.1	-3.1	-0.8

RCP85

	DJF	MAM	JJA	SON	Annual
Ref.mean	5.2	5.1	4.6	5.0	5.0
(P1-P0)/P0 * 100					
MPI_CCLM4	-2.5	-0.1	-2.1	-3.5	-1.9
EC-EARTH_KNMI	-5.5	1.5	0.9	* -7.3	-2.6
CNRM_CCLM4	-2.6	-3.1	2.8	5.3	0.5
ENSMEAN	-3.5	-0.6	0.6	-1.8	-1.4
(P2-P0)/P0 * 100					
MPI_CCLM4	-0.5	* 4.5	-3.2	-2.0	-0.5
EC-EARTH_KNMI	-0.2	3.7	-0.2	-2.8	0.2
CNRM_CCLM4	1.2	1.2	0.8	-2.4	0.3
ENSMEAN	0.2	3.2	-0.9	-2.4	0.0
(P3-P0)/P0 * 100					
MPI_CCLM4	1.1	0.5	-2.1	-0.0	-0.0
EC-EARTH_KNMI	-0.1	-0.1	-3.7	* -5.6	* -2.3
CNRM_CCLM4	-0.3	-0.6	0.1	0.1	-0.3
ENSMEAN	0.2	-0.1	-1.9	-1.8	-0.9
(P4-P0)/P0 * 100					
MPI_CCLM4	* 6.1	* 6.0	* -4.1	-4.3	0.8
EC-EARTH_KNMI	3.0	0.9	-0.6	* -4.7	-0.0
CNRM_CCLM4	0.0	-3.4	-1.4	-2.0	-1.9
ENSMEAN	3.0	1.1	-2.0	-3.7	-0.4

DD - sfcWindmax

** ; Two Sample Wilcoxon tests, 95 % confidence interval*

Figure 5-243: Seasonal and annual maximum wind module (maximum wind speed at 10m height) obtained by dynamical downscaling for Verghereto: Ref. mean is 20 year simulated period (1986-2005) in ms^{-1}; P1-P0, P2-P0, P3-P0, P4-P0 are changes (in %) in the future for following periods P1: 2021-2040, P2: 2041-2060, P3: 2061-2080, P4: 2081-2100. Differences are shown for individual models. Significant change is marked by star. Change is also shown as ensemble mean (ENSMEAN), not tested for significance. Left column is for RCP4.5 scenario and right for RCP8.5 scenario.

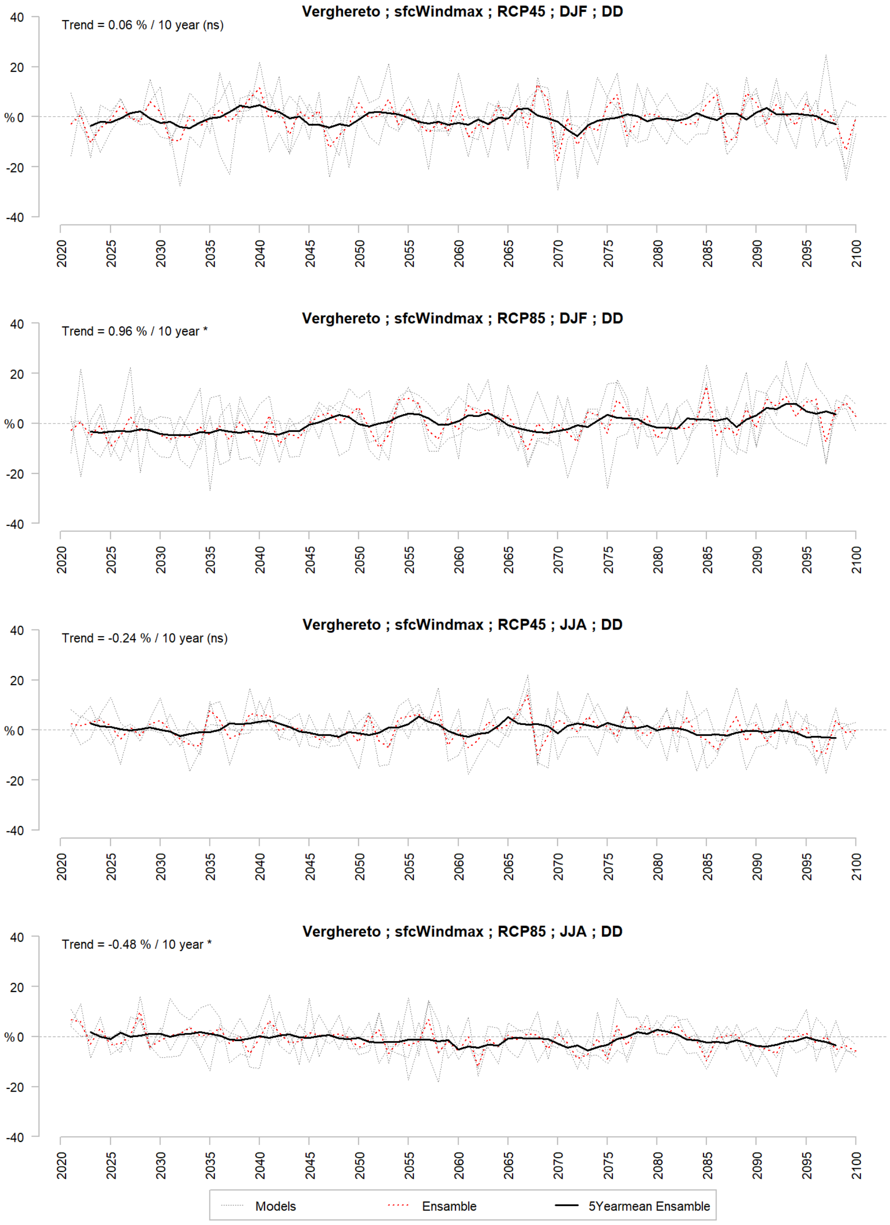

Figure 5-244: Variability of future maximum wind module (maximum wind speed at 10m height) (in %) in Verghereto for 2021-2100 obtained by dynamically downscaling for winter (DJF) and summer (JJA) and two RCP scenarios: individual models are in grey, the ensemble mean in red, 5-year moving average in black. Significant trend is marked with star (ns if not significant).

6.6.2 Statistically downscaled results

In this section we present future climate changes of temperature and precipitation related indices for Verghereto, as result from the statistical downscaling techniques constructed based on the observed local data/observed large scale circulation patterns and, applied then to future large-scale circulation patterns simulated by 4GCMs in the framework of CMIP5 experiments. The coordinates of the Verghereto grid point are included in table A from Annexes. The results are presented as follow:

- climate change diagram of an individual index for each season and on annual basis for four considered future periods (P1, P2, P3, P4), for two emission scenarios (RCP4.5 and RCP8.5). Climate change is calculated as difference between future (P1, P2, P3, P4) and reference period (P0) for temperature indices and some extreme precipitation indices, and as relative differences (expressed in %) for some precipitation indices. Reference period is 1986-2005, the Ref.mean (obs.) from the diagram (see below) is the climate observed value registered at station take into analysis, while climate changes (P1-P0; P2-P0,P3-P0;P4-P0) are shown for different models (SD_CMCC-CM, SD_CAN-ESM2, SD-MPI, SD_CNRM) as well as for ensemble mean of models (ENSMEAN). The t-Student test is applied to test the statistical significance of future climate (values from P1, or P2, or P3, or P4) with respect to present climate value (value from P0) and the results significant at 95% are marked by a star.
- time series of future anomaly of an individual index for DJF and JJA and for two emission scenarios RCP4.5 and RCP8.5; the anomaly is calculated respect to the reference period and shown for individual models, ensemble mean and 5-year moving average. Mann Kendall trend test is applied to ensemble mean (for 95 % confidence level). Significant trend is marked with star (n.s. if not significant).

6.6.2.1 *Temperature related indices projections*

6.6.2.1.1 *Seasonal minimum and maximum temperature*

Projected changes of seasonal and annual minimum temperature for Verghereto grid point are shown in figure 5-245, for RCP4.5 and RCP8.5 and over P1, P2, P3 and P4 with respect to present climate (P0). Following the moderate RCP4.5 scenario we expect an increase in annual minimum temperature between 1°C during P1 and up to 2.3°C going to the end of century (P4). The projected increase is higher for RCP8.5, especially for P3 and P4 when the simulations show changes in annual minimum temperature up to 4.6°C. Analysing in details the seasonal projected changes it could be observed that summer is season with higher magnitude of changes, up to 3°C for RCP4.5 and up to 5.7°C for RCP8.5 (P4 period, figure 5-245).

The temporal variability over 2021-2100 show positive and significant trends for winter and summer minimum temperature, more intense for RCP8.5 and especially in winter season, about 0.6°C/decade (figure 5-246).

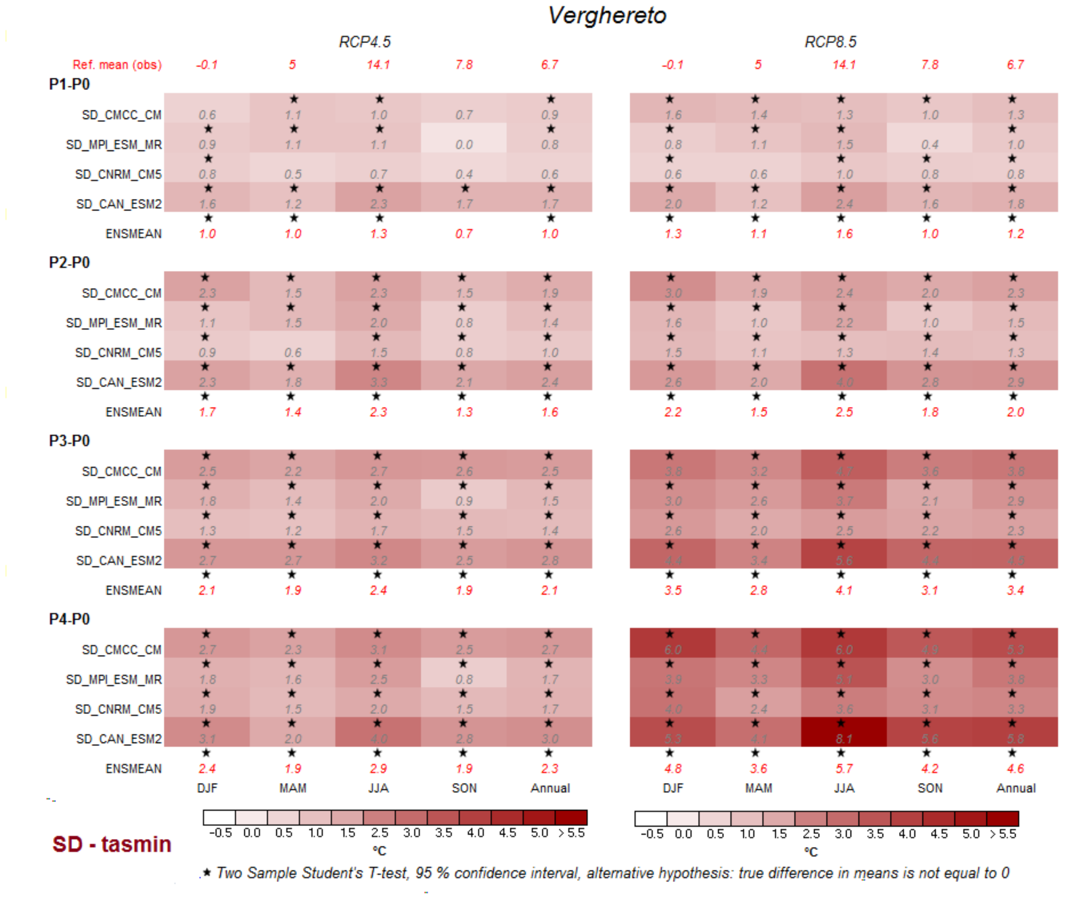

Verghereto

	RCP4.5					RCP8.5				
	DJF	MAM	JJA	SON	Annual	DJF	MAM	JJA	SON	Annual
Ref. mean (obs)	-0.1	5	14.1	7.8	6.7	-0.1	5	14.1	7.8	6.7
P1-P0										
SD_CMCC_CM	0.6	★ 1.1	★ 1.0	0.7	★ 0.9	★ 1.6	★ 1.4	★ 1.3	★ 1.0	★ 1.3
SD_MPI_ESM_MR	★ 0.9	★ 1.1	★ 1.1	0.0	★ 0.8	★ 0.8	★ 1.1	★ 1.5	0.4	★ 1.0
SD_CNRM_CM5	★ 0.8	0.5	0.7	0.4	0.6	★ 0.6	0.6	★ 1.0	★ 0.8	★ 0.8
SD_CAN_ESM2	★ 1.6	★ 1.2	★ 2.3	★ 1.7	★ 1.7	★ 2.0	★ 1.2	★ 2.4	★ 1.6	★ 1.8
ENSMEAN	★ 1.0	★ 1.0	★ 1.3	0.7	★ 1.0	★ 1.3	★ 1.1	★ 1.6	★ 1.0	★ 1.2
P2-P0										
SD_CMCC_CM	★ 2.3	★ 1.5	★ 2.3	★ 1.5	★ 1.9	★ 3.0	★ 1.9	★ 2.4	★ 2.0	★ 2.3
SD_MPI_ESM_MR	★ 1.1	★ 1.5	★ 2.0	★ 0.8	★ 1.4	★ 1.6	★ 1.0	★ 2.2	★ 1.0	★ 1.5
SD_CNRM_CM5	★ 0.9	0.6	★ 1.5	★ 0.8	★ 1.0	★ 1.5	★ 1.1	★ 1.3	★ 1.4	★ 1.3
SD_CAN_ESM2	★ 2.3	★ 1.8	★ 3.3	★ 2.1	★ 2.4	★ 2.6	★ 2.0	★ 4.0	★ 2.8	★ 2.9
ENSMEAN	★ 1.7	★ 1.4	★ 2.3	★ 1.3	★ 1.6	★ 2.2	★ 1.5	★ 2.5	★ 1.8	★ 2.0
P3-P0										
SD_CMCC_CM	★ 2.5	★ 2.2	★ 2.7	★ 2.6	★ 2.5	★ 3.8	★ 3.2	★ 4.7	★ 3.6	★ 3.8
SD_MPI_ESM_MR	★ 1.8	★ 1.4	★ 2.0	★ 0.9	★ 1.5	★ 3.0	★ 2.6	★ 3.7	★ 2.1	★ 2.9
SD_CNRM_CM5	★ 1.3	★ 1.2	★ 1.7	★ 1.5	★ 1.4	★ 2.6	★ 2.0	★ 2.5	★ 2.2	★ 2.3
SD_CAN_ESM2	★ 2.7	★ 2.7	★ 3.2	★ 2.5	★ 2.8	★ 4.4	★ 3.4	★ 5.6	★ 4.4	★ 4.5
ENSMEAN	★ 2.1	★ 1.9	★ 2.4	★ 1.9	★ 2.1	★ 3.5	★ 2.8	★ 4.1	★ 3.1	★ 3.4
P4-P0										
SD_CMCC_CM	★ 2.7	★ 2.3	★ 3.1	★ 2.5	★ 2.7	★ 6.0	★ 4.4	★ 6.0	★ 4.9	★ 5.3
SD_MPI_ESM_MR	★ 1.8	★ 1.6	★ 2.5	★ 0.8	★ 1.7	★ 3.9	★ 3.3	★ 5.1	★ 3.0	★ 3.8
SD_CNRM_CM5	★ 1.9	★ 1.5	★ 2.0	★ 1.5	★ 1.7	★ 4.0	★ 2.4	★ 3.6	★ 3.1	★ 3.3
SD_CAN_ESM2	★ 3.1	★ 2.0	★ 4.0	★ 2.8	★ 3.0	★ 5.3	★ 4.1	★ 8.1	★ 5.6	★ 5.8
ENSMEAN	★ 2.4	★ 1.9	★ 2.9	★ 1.9	★ 2.3	★ 4.8	★ 3.6	★ 5.7	★ 4.2	★ 4.6

SD - tasmin

★ Two Sample Student's T-test, 95 % confidence interval, alternative hypothesis: true difference in means is not equal to 0

Figure 5-245: Seasonal and annual minimum temperature: observed values over reference period (in red), changes projected by statistical downscaling applied to 4GCMs and the Ensemble Mean of changes over the four periods (P1, P2, P3, P4) projected in the framework of RCP4.5 (left) and RCP 8.5 (right). Significant change is marked by star (source Arpae-Simc)

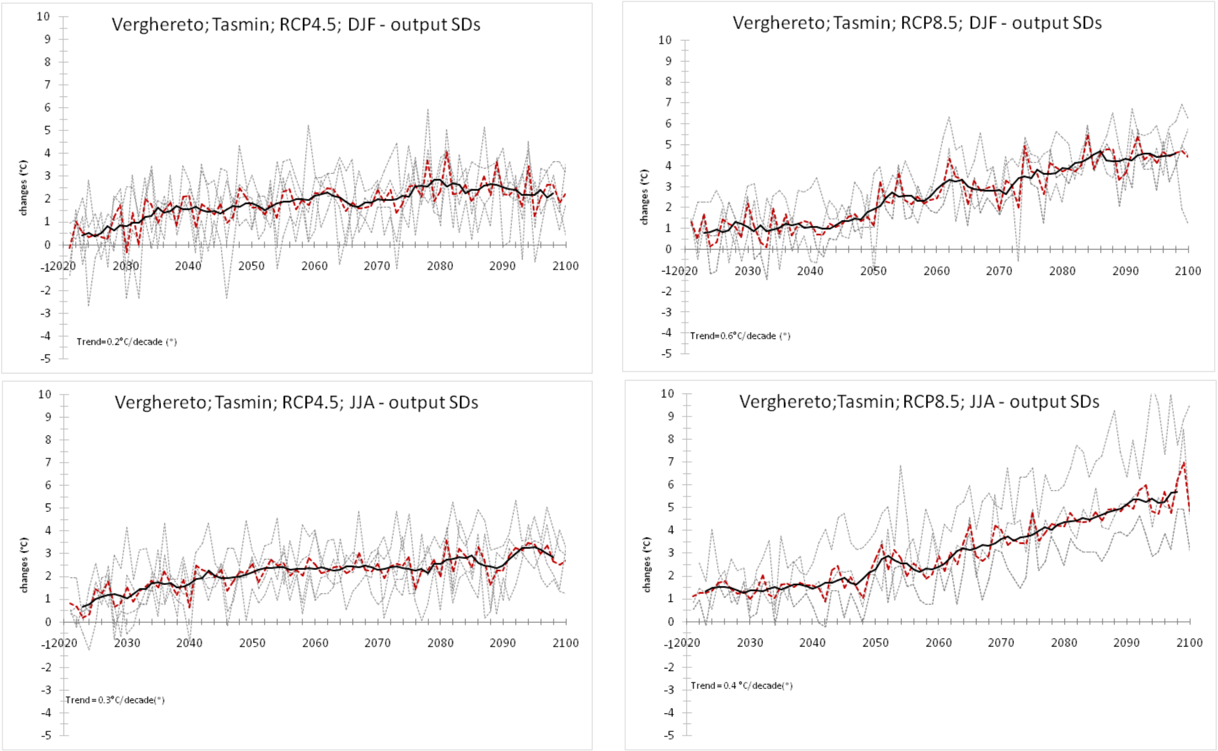

Figure 5-246: Variability of future changes of winter (DJF) and summer (JJA) minimum temperature projected through SDs applied to 4GCMs (grey lines); the Ensemble Mean (red line) and moving average (black line) - scenario RCP4.5 (left) and RCP8.5 (right), 2021-2100 period. Significant trend is marked with star while n.s. means not significant (source Arpae-Simc).

Projected changes of seasonal and annual maximum temperature for Verghereto are shown in figure 5-247, for RCP4.5 and RCP8.5 and over P1, P2, P3 and P4 with respect to present climate (P0). Following the moderate RCP4.5 scenario we expect an increase in annual maximum temperature between 1°C during P1 and up to 3°C going to the end of century (P4). The projected increase is higher for RCP8.5, especially for P3 and P4 when the simulations show changes in annual maximum temperature about 4.3°C and 6°C, respectively.

Analysing in details the seasonal projected changes of maximum temperature it could be observed that during summer the expected changes is very high, 3.9°C for RCP4.5 and 7°C for RCP8.5 at the end of century (P4). Considering that the climatological value of summer maximum temperature is 23°C (1985-2006) an increase of 7°C to the end of century for RCP8.5 means values around 30°C.

The temporal variability of the index over 2021-2100 show positive and significant trends for winter and summer maximum temperature, more intense for RCP8.5 and especially in summer season, about 1°C/decade (figure 5-248).

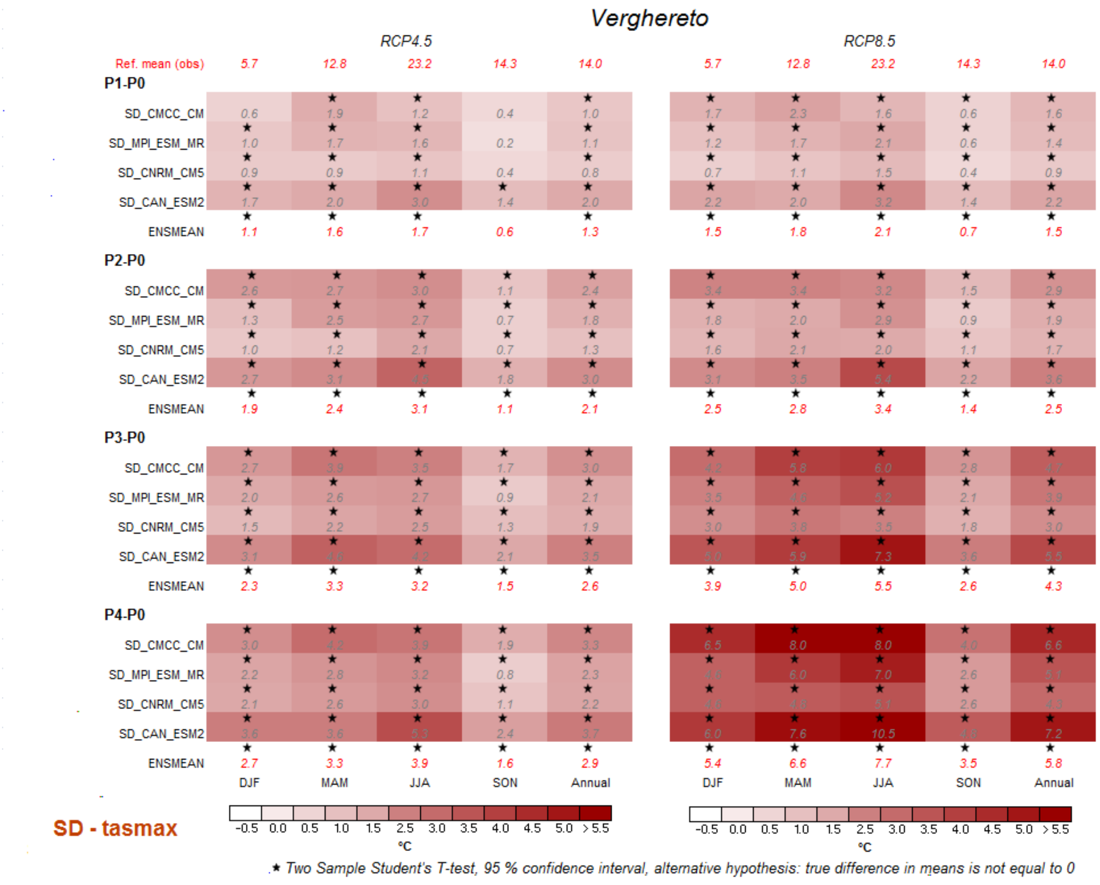

Figure 5-247: Seasonal and annual maximum temperature: observed values over reference period (in red), changes projected by statistical downscaling applied to 4GCMs and the Ensemble Mean of changes over the four periods (P1, P2, P3, P4) projected in the framework of RCP4.5 (left) and RCP 8.5 (right). Significant change is marked by star (source Arpae-Simc)

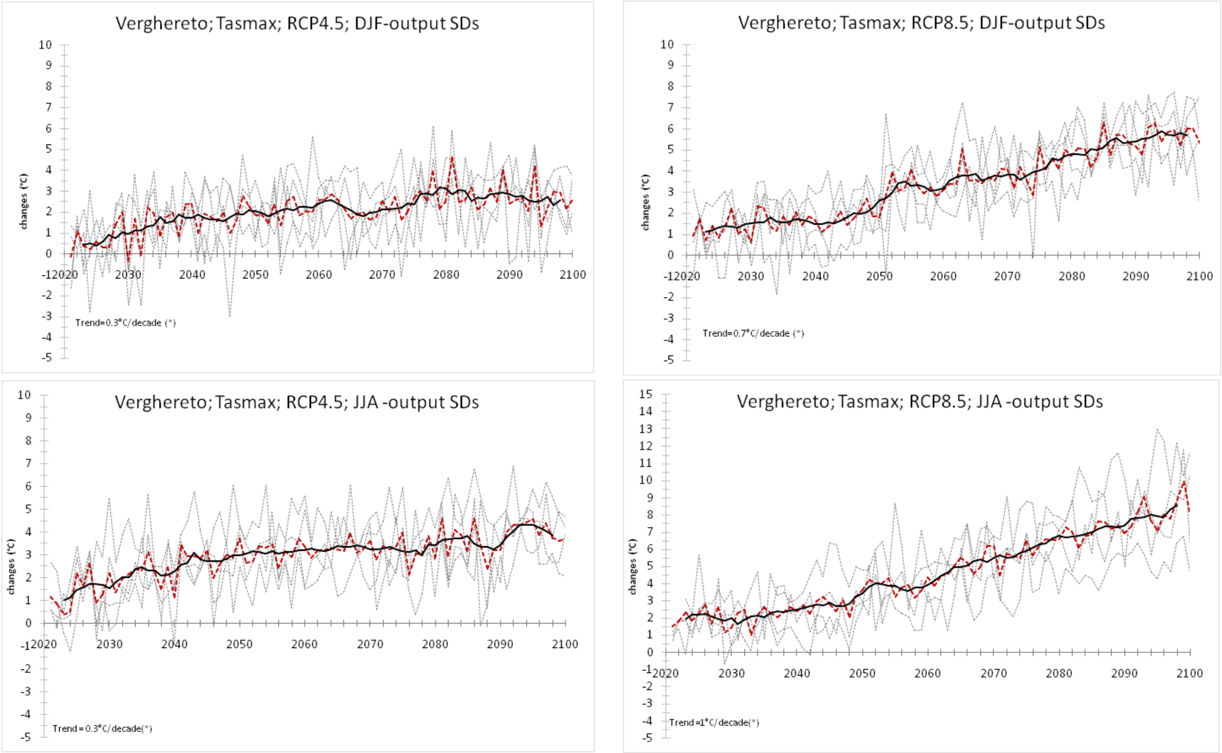

Figure 5-248: Variability of future changes of winter (DJF) and summer (JJA) maximum temperature projected through SDs applied to 4GCMs (grey lines); the Ensemble Mean (red line) and moving average (black line) - scenario RCP4.5 (left) and RCP8.5 (right), 2021-2100 period. Significant trend is marked with star while n.s. means not significant (source Arpae-Simc).

6.6.2.1.2 *Extreme temperature*

5th percentile of minimum temperature

The analysis performed on scenarios of extreme temperature, 5th minimum temperature and 95th maximum temperature reveals important future changes at Verghereto. An increase in *annual* 5th percentile of minimum temperature of 0.5°C is projected during the first period (2021-2040) and up to 1.5°C going to the end of century, in the framework of RP4.5 emission scenario. The signal became more intense for RCP8.5 emission scenario and especially during 2061-2080 and 2081-2100 periods, when the annual increases could reach 2.2°C during P3 and 3°C during P4 (see figure 5-249).

The projected changes are significant at seasonal level, with higher magnitude during winter and autumn followed by spring and summer. The long-term variability shows positive trends, both in winter and summer, statistically significant. only for RCP8.5 (see figure 5-250).

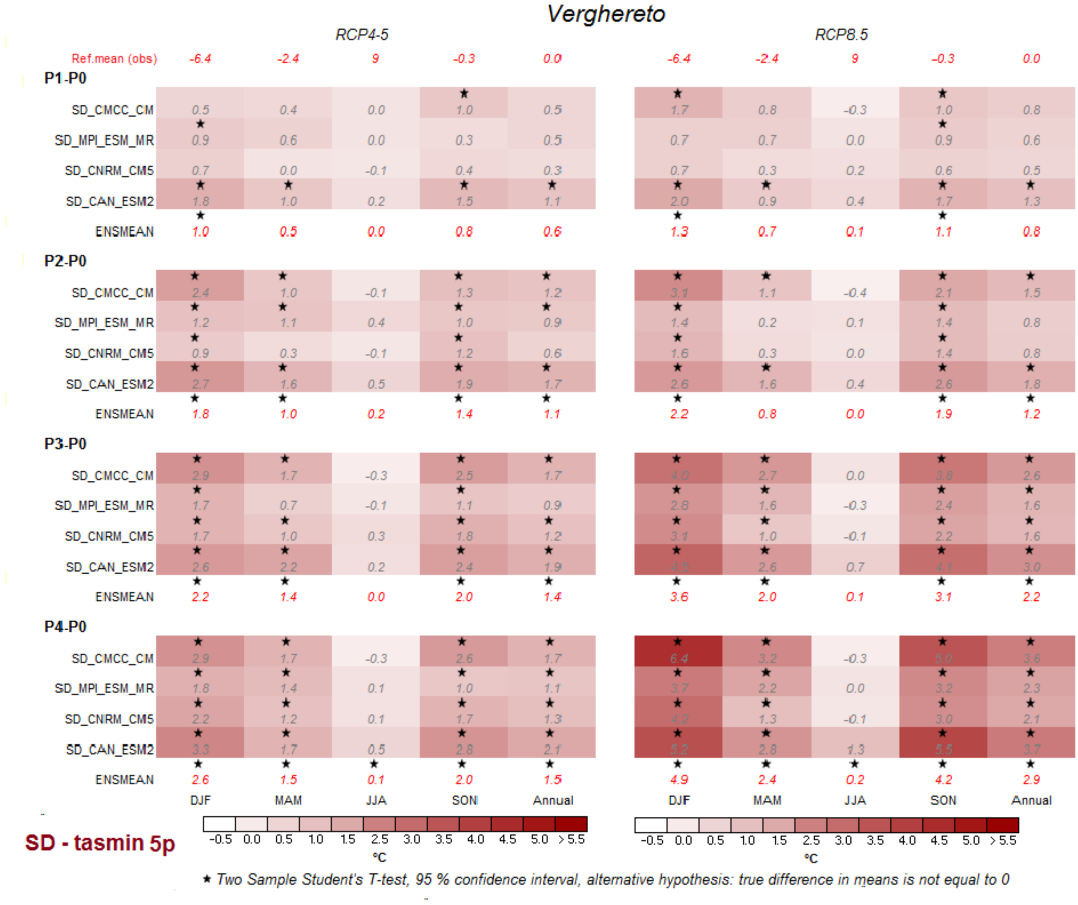

Verghereto

	RCP4-5					RCP8.5				
	DJF	MAM	JJA	SON	Annual	DJF	MAM	JJA	SON	Annual
Ref.mean (obs)	-6.4	-2.4	9	-0.3	0.0	-6.4	-2.4	9	-0.3	0.0
P1-P0										
SD_CMCC_CM	0.5	0.4	0.0	★ 1.0	0.5	★ 1.7	0.8	-0.3	★ 1.0	0.8
SD_MPI_ESM_MR	★ 0.9	0.6	0.0	0.3	0.5	0.7	0.7	0.0	★ 0.9	0.6
SD_CNRM_CM5	0.7	0.0	-0.1	0.4	0.3	0.7	0.3	0.2	0.6	0.5
SD_CAN_ESM2	★ 1.8	★ 1.0	0.2	★ 1.5	★ 1.1	★ 2.0	★ 0.9	0.4	★ 1.7	★ 1.3
ENSMEAN	★ 1.0	0.5	0.0	0.8	0.6	★ 1.3	0.7	0.1	★ 1.1	0.8
P2-P0										
SD_CMCC_CM	★ 2.4	★ 1.0	-0.1	★ 1.3	★ 1.2	★ 3.1	★ 1.1	-0.4	★ 2.1	★ 1.5
SD_MPI_ESM_MR	★ 1.2	★ 1.1	0.4	★ 1.0	★ 0.9	★ 1.4	0.2	0.1	★ 1.4	0.8
SD_CNRM_CM5	★ 0.9	0.3	-0.1	★ 1.2	0.6	★ 1.6	0.3	0.0	★ 1.4	0.8
SD_CAN_ESM2	★ 2.7	★ 1.6	0.5	★ 1.9	★ 1.7	★ 2.6	★ 1.6	0.4	★ 2.6	★ 1.8
ENSMEAN	★ 1.8	★ 1.0	0.2	★ 1.4	★ 1.1	★ 2.2	0.8	0.0	★ 1.9	★ 1.2
P3-P0										
SD_CMCC_CM	★ 2.9	★ 1.7	-0.3	★ 2.5	★ 1.7	★ 4.0	★ 2.7	0.0	★ 3.8	★ 2.6
SD_MPI_ESM_MR	★ 1.7	0.7	-0.1	★ 1.1	0.9	★ 2.8	★ 1.6	-0.3	★ 2.4	★ 1.6
SD_CNRM_CM5	★ 1.7	★ 1.0	0.3	★ 1.8	★ 1.2	★ 3.1	★ 1.0	-0.1	★ 2.2	★ 1.6
SD_CAN_ESM2	★ 2.6	★ 2.2	0.2	★ 2.4	★ 1.9	★ 4.5	★ 2.6	0.7	★ 4.1	★ 3.0
ENSMEAN	★ 2.2	★ 1.4	0.0	★ 2.0	★ 1.4	★ 3.6	★ 2.0	0.1	★ 3.1	★ 2.2
P4-P0										
SD_CMCC_CM	★ 2.9	★ 1.7	-0.3	★ 2.6	★ 1.7	★ 6.4	★ 3.2	-0.3	★ 5.0	★ 3.6
SD_MPI_ESM_MR	★ 1.8	★ 1.4	0.1	★ 1.0	★ 1.1	★ 3.7	★ 2.2	0.0	★ 3.2	★ 2.3
SD_CNRM_CM5	★ 2.2	★ 1.2	0.1	★ 1.7	★ 1.3	★ 4.2	★ 1.3	-0.1	★ 3.0	★ 2.1
SD_CAN_ESM2	★ 3.3	★ 1.7	0.5	★ 2.8	★ 2.1	★ 5.2	★ 2.8	1.3	★ 5.5	★ 3.7
ENSMEAN	★ 2.6	★ 1.5	★ 0.1	★ 2.0	★ 1.5	★ 4.9	★ 2.4	★ 0.2	★ 4.2	★ 2.9

★ Two Sample Student's T-test, 95 % confidence interval, alternative hypothesis: true difference in means is not equal to 0

Figure 5-249: 5th percentile of seasonal and annual minimum temperature: observed values over reference period (in red), changes projected by statistical downscaling applied to 4GCMs and the Ensemble Mean of changes over the four periods (P1, P2, P3, P4) projected in the framework of RCP4.5 (left) and RCP 8.5 (right). Significant change is marked by star (source Arpae-Simc)

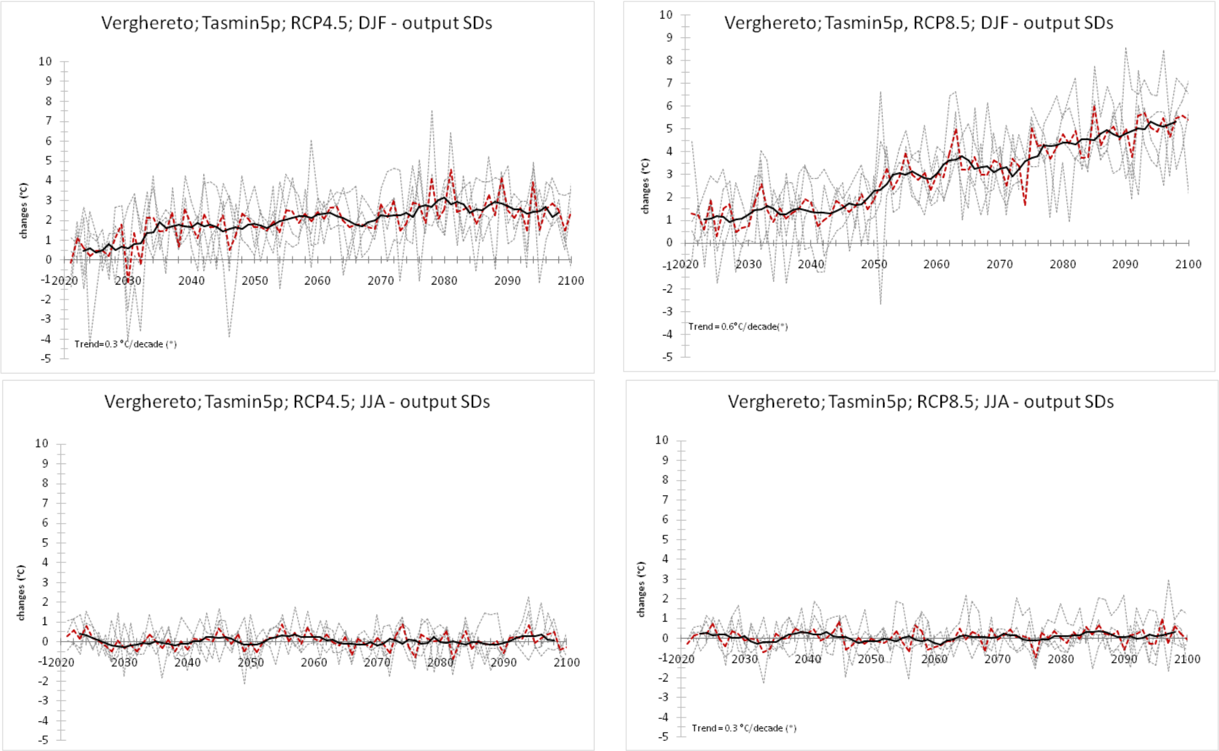

Figure 5-250: Variability of future changes of winter (DJF) and summer (JJA) of 5th minimum temperature projected through SDs applied to 4GCMs (grey lines); the Ensemble Mean (red line) and moving average (black line) - scenario RCP4.5 (left) and RCP8.5 (right), 2021-2100 period. Significant trend is marked with star while n.s. means not significant (source Arpae-Simc).

95th percentile of maximum temperature

Future change of 95th percentile of maximum temperature in Verghereto grid point is projected to increase from P1 to P4 periods, with amplitudes that vary from model to model.

The Ensemble Mean shows an increase in annual value of changes between 0.8 and 1.8°C for RCP4.5 and, between 1°C and 3.5°C in the framework of RCP8.5 (Figure 5-251). A deep analysis on projected changes reveals that higher values are expected to occur during summer season with peak of changes for RCP8.5 around 4.7°C during 2081-2100 with respect to 1986-2005. In addition, as could be noted the projected changes are similar for P1 and P2 in the framework of RCP4.5 and RCP8.5, but starting with P3 the changes have higher magnitude in RCP8.5.

Variability of future changes of 95th percentile of maximum temperature shows positive and significant trends especially during summer and RCP8.5 scenario (see figure 5-252)

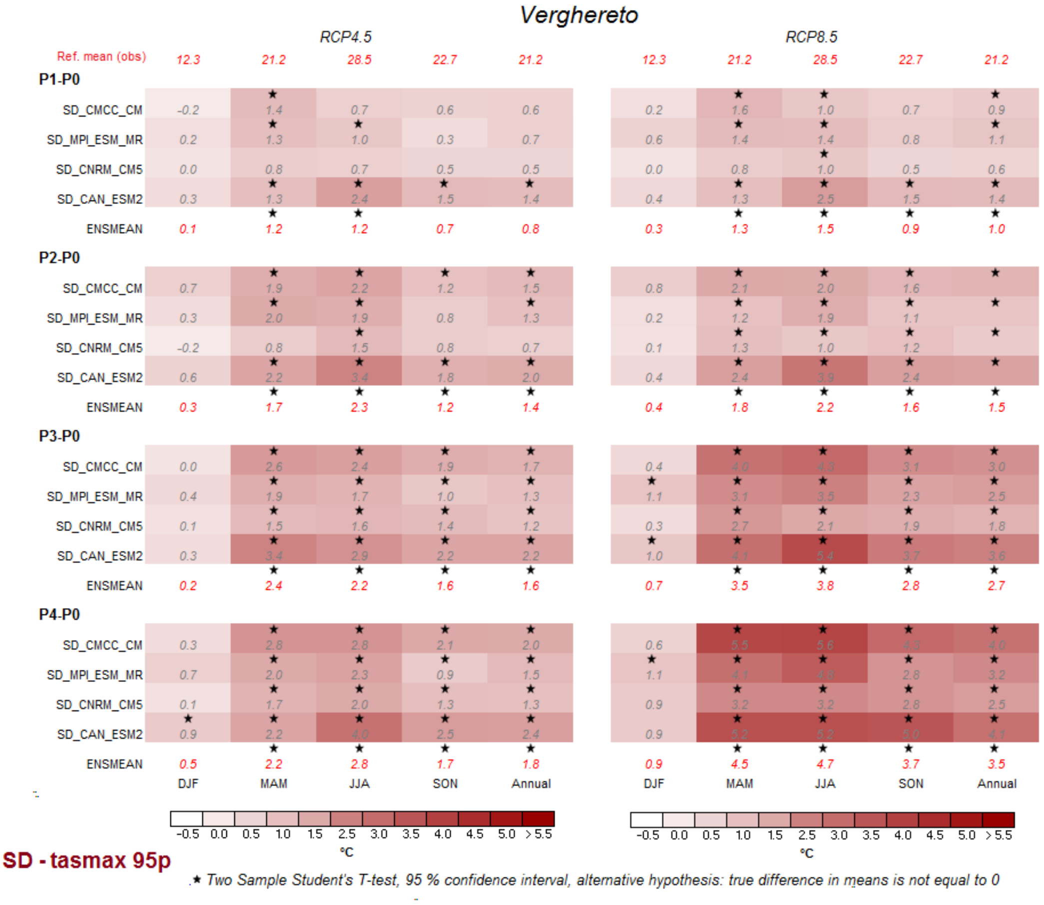

Verghereto

	RCP4.5					RCP8.5				
Ref. mean (obs)	12.3	21.2	28.5	22.7	21.2	12.3	21.2	28.5	22.7	21.2
P1-P0										
SD_CMCC_CM	-0.2	★ 1.4	0.7	0.6	0.6	0.2	★ 1.6	★ 1.0	0.7	★ 0.9
SD_MPI_ESM_MR	0.2	★ 1.3	★ 1.0	0.3	0.7	0.6	★ 1.4	★ 1.4	0.8	★ 1.1
SD_CNRM_CM5	0.0	0.8	0.7	0.5	0.5	0.0	0.8	★ 1.0	0.5	0.6
SD_CAN_ESM2	0.3	★ 1.3	★ 2.4	★ 1.5	★ 1.4	0.4	★ 1.3	★ 2.5	★ 1.5	★ 1.4
ENSMEAN	0.1	★ 1.2	★ 1.2	0.7	0.8	0.3	★ 1.3	★ 1.5	★ 0.9	★ 1.0
P2-P0										
SD_CMCC_CM	0.7	★ 1.9	★ 2.2	★ 1.2	★ 1.5	0.8	★ 2.1	★ 2.0	★ 1.6	★
SD_MPI_ESM_MR	0.3	★ 2.0	★ 1.9	0.8	★ 1.3	0.2	★ 1.2	★ 1.9	★ 1.1	★
SD_CNRM_CM5	-0.2	0.8	★ 1.5	0.8	0.7	0.1	★ 1.3	★ 1.0	★ 1.2	★
SD_CAN_ESM2	0.6	★ 2.2	★ 3.4	★ 1.8	★ 2.0	0.4	★ 2.4	★ 3.9	★ 2.4	★
ENSMEAN	0.3	★ 1.7	★ 2.3	★ 1.2	★ 1.4	0.4	★ 1.8	★ 2.2	★ 1.6	★ 1.5
P3-P0										
SD_CMCC_CM	0.0	★ 2.6	★ 2.4	★ 1.9	★ 1.7	0.4	★ 4.0	★ 4.3	★ 3.1	★ 3.0
SD_MPI_ESM_MR	0.4	★ 1.9	★ 1.7	★ 1.0	★ 1.3	★ 1.1	★ 3.1	★ 3.5	★ 2.3	★ 2.5
SD_CNRM_CM5	0.1	★ 1.5	★ 1.6	★ 1.4	★ 1.2	0.3	★ 2.7	★ 2.1	★ 1.9	★ 1.8
SD_CAN_ESM2	0.3	★ 3.4	★ 2.9	★ 2.2	★ 2.2	★ 1.0	★ 4.1	★ 5.4	★ 3.7	★ 3.6
ENSMEAN	0.2	★ 2.4	★ 2.2	★ 1.6	★ 1.6	0.7	★ 3.5	★ 3.8	★ 2.8	★ 2.7
P4-P0										
SD_CMCC_CM	0.3	★ 2.8	★ 2.8	★ 2.1	★ 2.0	0.6	★ 5.5	★ 5.6	★ 4.3	★ 4.0
SD_MPI_ESM_MR	0.7	★ 2.0	★ 2.3	★ 0.9	★ 1.5	★ 1.1	★ 4.1	★ 4.8	★ 2.8	★ 3.2
SD_CNRM_CM5	0.1	★ 1.7	★ 2.0	★ 1.3	★ 1.3	0.9	★ 3.2	★ 3.2	★ 2.8	★ 2.5
SD_CAN_ESM2	★ 0.9	★ 2.2	★ 4.0	★ 2.5	★ 2.4	0.9	★ 5.2	★ 5.2	★ 5.0	★ 4.1
ENSMEAN	0.5	★ 2.2	★ 2.8	★ 1.7	★ 1.8	0.9	★ 4.5	★ 4.7	★ 3.7	★ 3.5
	DJF	MAM	JJA	SON	Annual	DJF	MAM	JJA	SON	Annual

SD - tasmax 95p

★ Two Sample Student's T-test, 95 % confidence interval, alternative hypothesis: true difference in means is not equal to 0

Figure 5-251: 95th percentile of seasonal and annual maximum temperature: observed values over reference period (in red), changes projected by statistical downscaling applied to 4GCMs and the Ensemble Mean of changes over the four periods (P1, P2, P3, P4) projected in the framework of RCP4.5 (left) and RCP 8.5 (right). Significant change is marked by star (source Arpae-Simc)

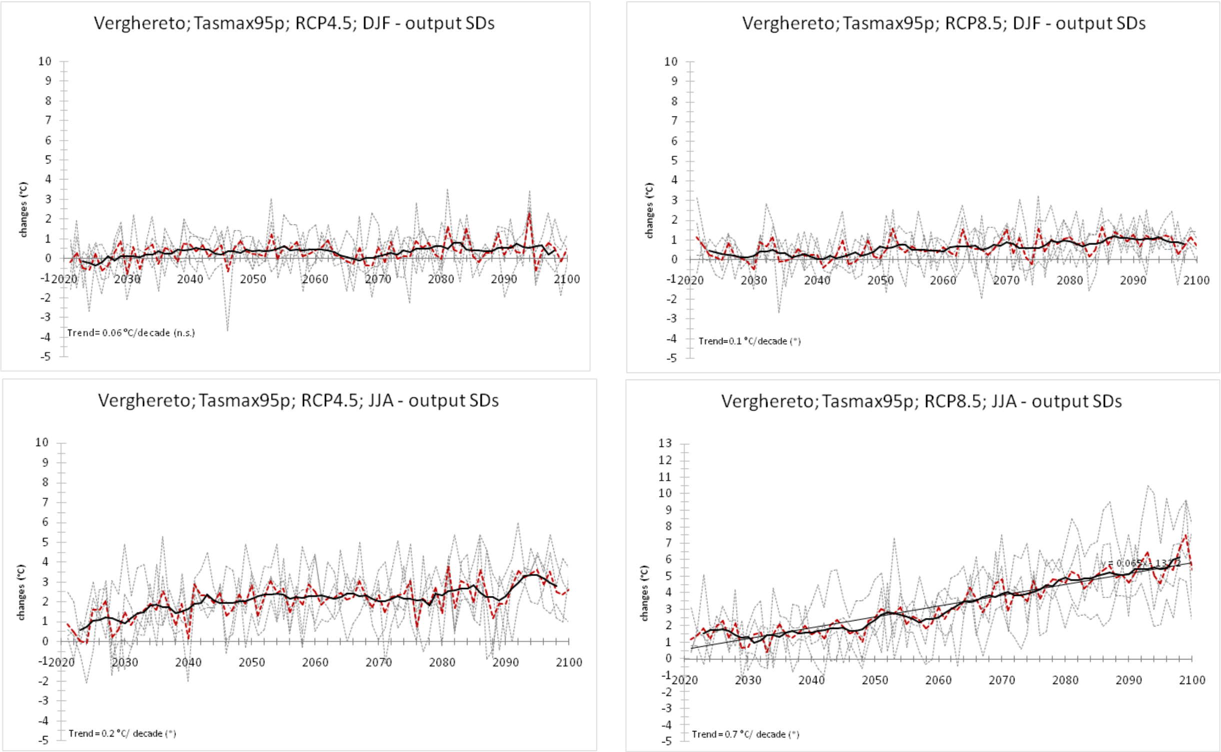

Figure 5-252: Future changes of winter (DJF) and summer (JJA) of 95th percentile of maximum temperature projected through SDs applied to 4GCMs (grey lines); the Ensemble Mean (red line) and moving average (black line) - scenario RCP4.5 (left) and RCP8.5 (right), 2021-2100 period. Significant trend is marked with star while n.s. means not significant (source Arpae-Simc).

6.6.2.1.3 *Heat wave duration*

The projection of the heat wave duration, index defined as the maximum number of consecutive days with maximum temperature greater than 90th daily percentile, shows an increase during all seasons and for both RCPs. Figure 5-253 includes the projected changes for Verghereto. As could be noted the magnitude is higher during spring followed by summer and autumn.
During spring, the increase could reach 16 consecutive days (P4) in RCP4.5 while in the framework of RCP8.5 could reach 59 consecutive days; in summer the projected changes is up to 2 consecutive days (P4) for RCP4.5 and up to 7 days for RCP8.5 (P4). As regards long term variability (see figure 5-254) the trend is positive during summer, higher in summer especially for RCP8.5 (1 days/decade)

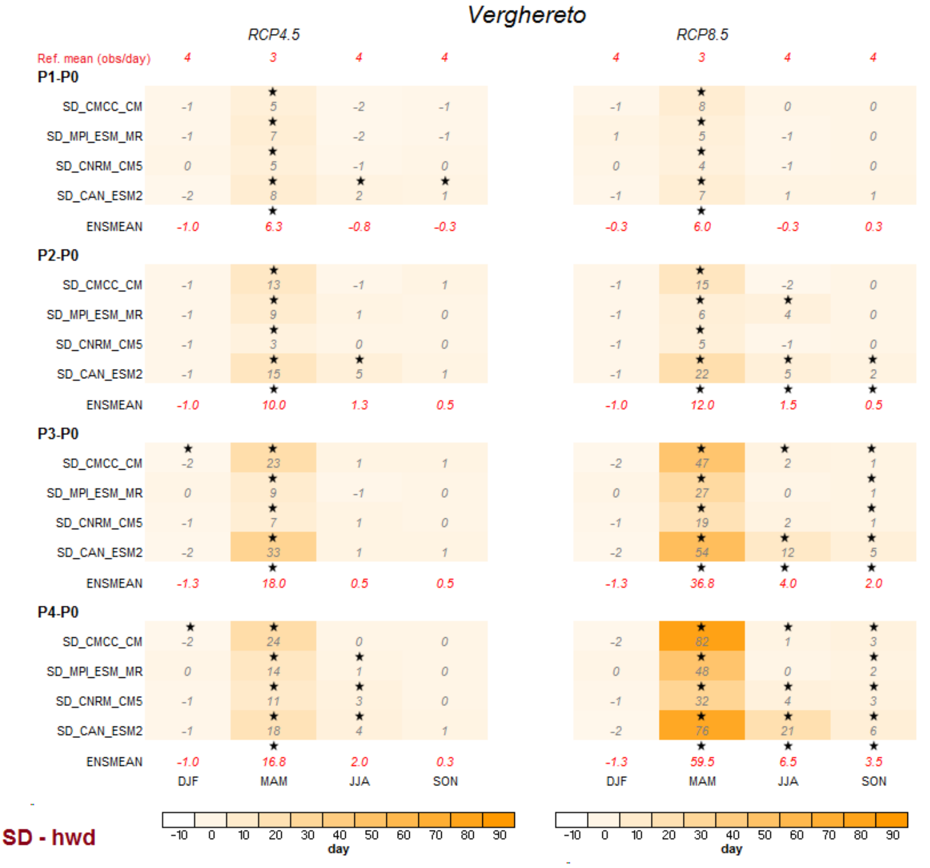

★ Two Sample Student's T-test, 95 % confidence interval, alternative hypothesis: true difference in means is not equal to 0

Figure 5-253: Seasonal heat wave duration: observed values over reference period (in red), changes projected by statistical downscaling applied to 4GCMs and the Ensemble Mean of changes over the four periods (P1, P2, P3, P4) projected in the framework of RCP4.5 (left) and RCP 8.5 (right). Significant change is marked by star (source Arpae-Simc)

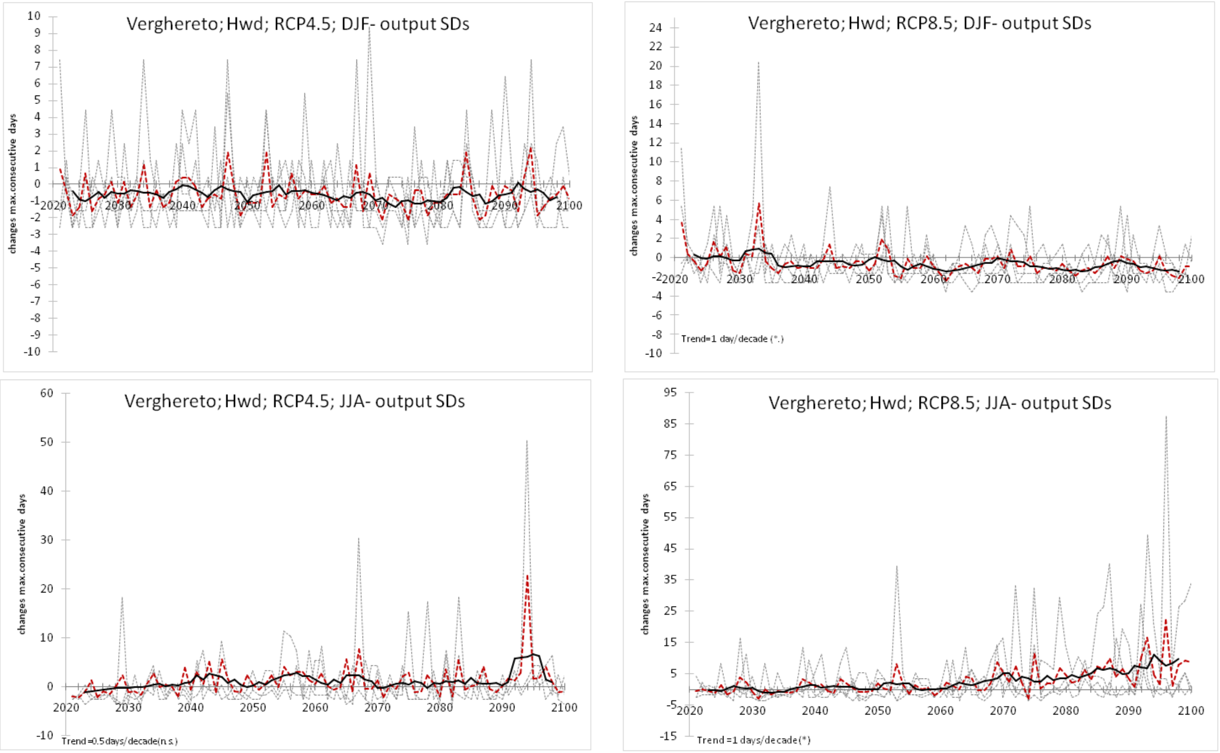

Figure 5-254: Variability of future changes of winter (DJF) and summer (JJA) heat wave duration projected through SDs applied to 4GCMs (grey lines); the Ensemble Mean (red line) and moving average (black line) - scenario RCP4.5 (left) and RCP8.5 (right), 2021-2100 period. Significant trend is marked with star while n.s. means not significant (source Arpae-Simc).

6.6.2.1.4 *Tropical nights*

Seasonal changes of tropical nights (tr) in terms of differences between P1-P0, P2-P0, P3-P0, P4-P0 are shown in figures 5-255, relative to the RCP4.5 and RCP8.5 scenarios. An increase is noted during summer, especially after 2041 up to the end of century. The increase varies between 5 to 14 days for RCP4.5 (from P2 to P4) and between 10 to 58 for RCP8.5 (from P2 to P4)

As concerns long term variability positive trend is observed during summer and statistically significant for RCP8.5, (up to 8 days/decade), over 2021-2100 (see figure 5-256).

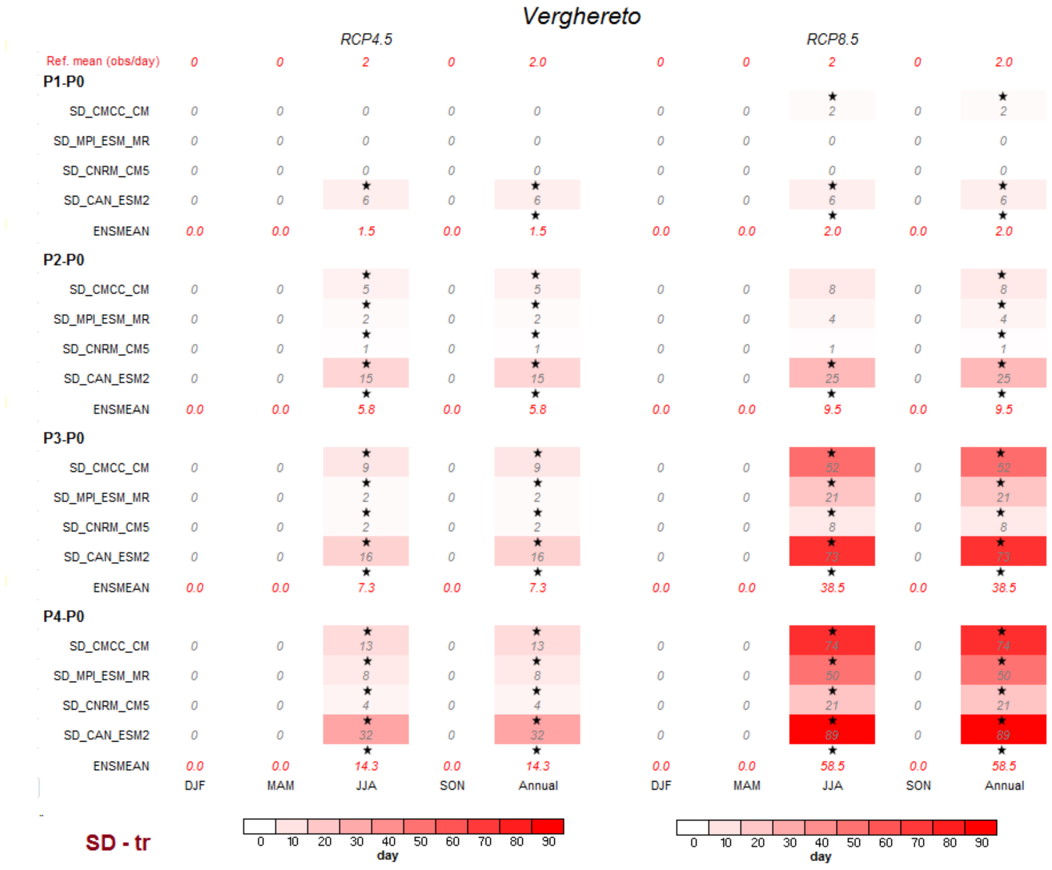

★ *Two Sample Student's T-test, 95 % confidence interval, alternative hypothesis: true difference in means is not equal to 0*

Figure 5-255: Seasonal and annual tropical nights: observed values over reference period (in red), changes projected by statistical downscaling applied to 4GCMs and the Ensemble Mean over the four periods (P1, P2,P3,P4) projected in the framework of RCP4.5 (left) and RCP8.5 (right). Significant change is marked by star (source Arpae-Simc)

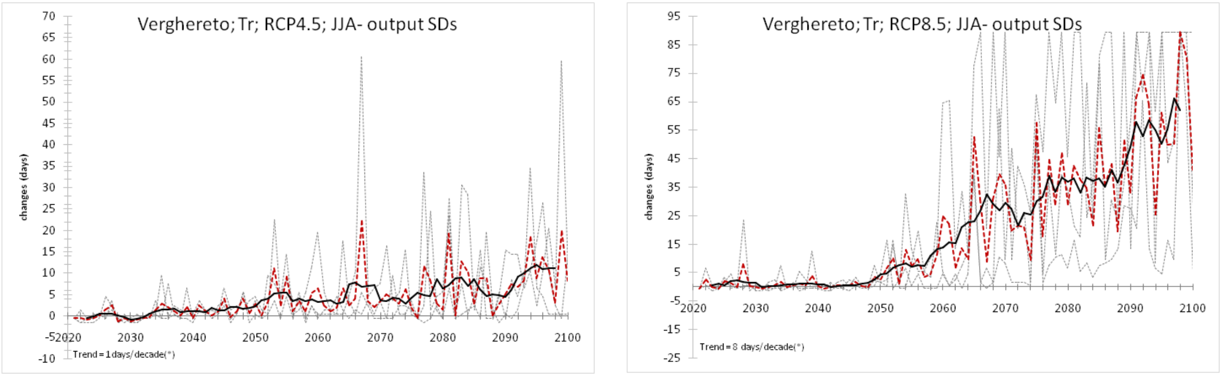

Figure 5-256: Variability of future changes of summer (JJA) tropical nights projected through SDs applied to 4GCMs (grey lines); the Ensemble Mean (red line) and moving average (black line) - scenario RCP4.5 (left) and RCP8.5 (right), 2021-2100 period. Significant trend is marked with star while n.s. means not significant (source Arpae-Simc).

6.6.2.1.5 *Frost days*

Seasonal changes of tropical nights (fd) in terms of differences between future and present period relative to the RCP4.5 and RCP8.5 scenarios. A decrease is noted at annual level, statistically significant, up to -27 days for RCP4.5 and -39days for RCP8.5. At seasonal level, is projected a significant decrease during winter, spring and autumn (see figure 5-257)
As concerns long term variability, negative trend is observed during winter, trend statistically significant for both RCPs(see figure 5-258).

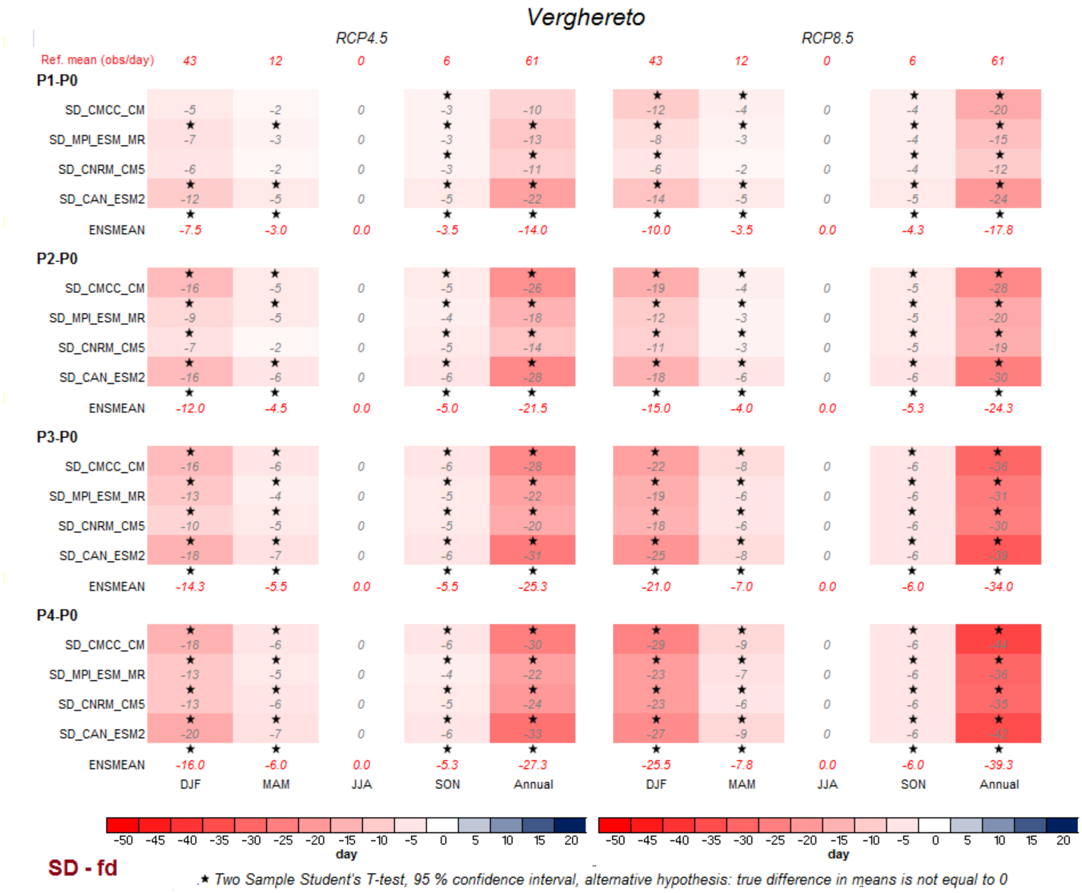

Verghereto

	RCP4.5					RCP8.5				
	DJF	MAM	JJA	SON	Annual	DJF	MAM	JJA	SON	Annual
Ref. mean (obs/day)	43	12	0	6	61	43	12	0	6	61
P1-P0										
SD_CMCC_CM	-5	-2	0	★ -3	-10	★ -12	★ -4	0	★ -4	★ -20
SD_MPI_ESM_MR	★ -7	★ -3	0	★ -3	★ -13	★ -8	★ -3	0	★ -4	★ -15
SD_CNRM_CM5	-6	-2	0	★ -3	★ -11	★ -6	-2	0	★ -4	★ -12
SD_CAN_ESM2	★ -12	★ -5	0	★ -5	★ -22	★ -14	★ -5	0	★ -5	★ -24
ENSMEAN	★ -7.5	★ -3.0	0.0	★ -3.5	★ -14.0	★ -10.0	★ -3.5	0.0	★ -4.3	★ -17.8
P2-P0										
SD_CMCC_CM	★ -16	★ -5	0	★ -5	★ -26	★ -19	★ -4	0	★ -5	★ -28
SD_MPI_ESM_MR	★ -9	★ -5	0	★ -4	★ -18	★ -12	★ -3	0	★ -5	★ -20
SD_CNRM_CM5	★ -7	-2	0	★ -5	★ -14	★ -11	★ -3	0	★ -5	★ -19
SD_CAN_ESM2	★ -16	★ -6	0	★ -6	★ -28	★ -18	★ -6	0	★ -6	★ -30
ENSMEAN	★ -12.0	★ -4.5	0.0	★ -5.0	★ -21.5	★ -15.0	★ -4.0	0.0	★ -5.3	★ -24.3
P3-P0										
SD_CMCC_CM	★ -16	★ -6	0	★ -6	★ -28	★ -22	★ -8	0	★ -6	★ -36
SD_MPI_ESM_MR	★ -13	★ -4	0	★ -5	★ -22	★ -19	★ -6	0	★ -6	★ -31
SD_CNRM_CM5	★ -10	★ -5	0	★ -5	★ -20	★ -18	★ -6	0	★ -6	★ -30
SD_CAN_ESM2	★ -18	★ -7	0	★ -6	★ -31	★ -25	★ -8	0	★ -6	★ -39
ENSMEAN	★ -14.3	★ -5.5	0.0	★ -5.5	★ -25.3	★ -21.0	★ -7.0	0.0	★ -6.0	★ -34.0
P4-P0										
SD_CMCC_CM	★ -18	★ -6	0	★ -6	★ -30	★ -29	★ -9	0	★ -6	★ -44
SD_MPI_ESM_MR	★ -13	★ -5	0	★ -4	★ -22	★ -23	★ -7	0	★ -6	★ -36
SD_CNRM_CM5	★ -13	★ -6	0	★ -5	★ -24	★ -23	★ -6	0	★ -6	★ -35
SD_CAN_ESM2	★ -20	★ -7	0	★ -6	★ -33	★ -27	★ -9	0	★ -6	★ -42
ENSMEAN	★ -16.0	★ -6.0	0.0	★ -5.3	★ -27.3	★ -25.5	★ -7.8	0.0	★ -6.0	★ -39.3

*

★ Two Sample Student's T-test, 95 % confidence interval, alternative hypothesis: true difference in means is not equal to 0

Figure 5-257: Seasonal and annual frost days: observed values over reference period (in red), changes projected by statistical downscaling applied to 4GCMs and the Ensemble Mean over the four periods (P1, P2,P3,P4) projected in the framework of RCP4.5 (left) and RCP 8.5 (right). Significant change is marked by star (source Arpae-Simc)

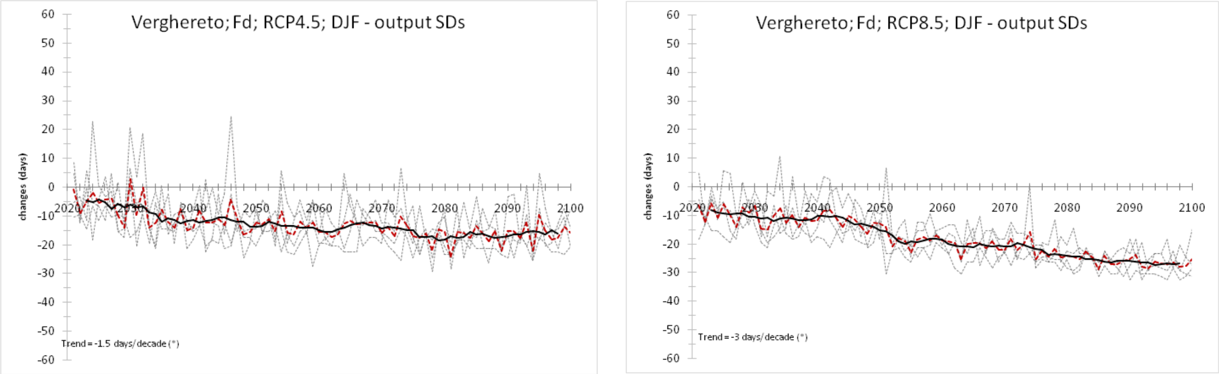

Figure 5-258: Future changes of winter (DJF) frost days projected through SDs applied to 4GCMs (grey lines); the Ensemble Mean (red line) and moving average (black line) - scenario RCP4.5 (left) and RCP8.5 (right), 2021-2100 period. Significant trend is marked with star while n.s. means not significant (source Arpae-Simc).

6.6.2.2 *Precipitation related indices projection*

6.6.2.2.1 *Amount of precipitation*

The projected changes for amount of precipitation at Verghereto show a general decrease over all period, seasons and for both emission scenarios. Analysing the changes presented in figure 5-259 it could be observed that generally, the signal is significant in spring and summer and, all SDs agree with this signal. Higher decrease is expected to occur during summer, between -25 % (P1) up to -38% (P4) for RCP4.5 and between -28 % (P1) up to -60% (P4) for RCP8.5 (see figure 5-259). Long term variability underlies negative trends during winter and summer, significant for both seasons and scenarios (see figure 5-260).

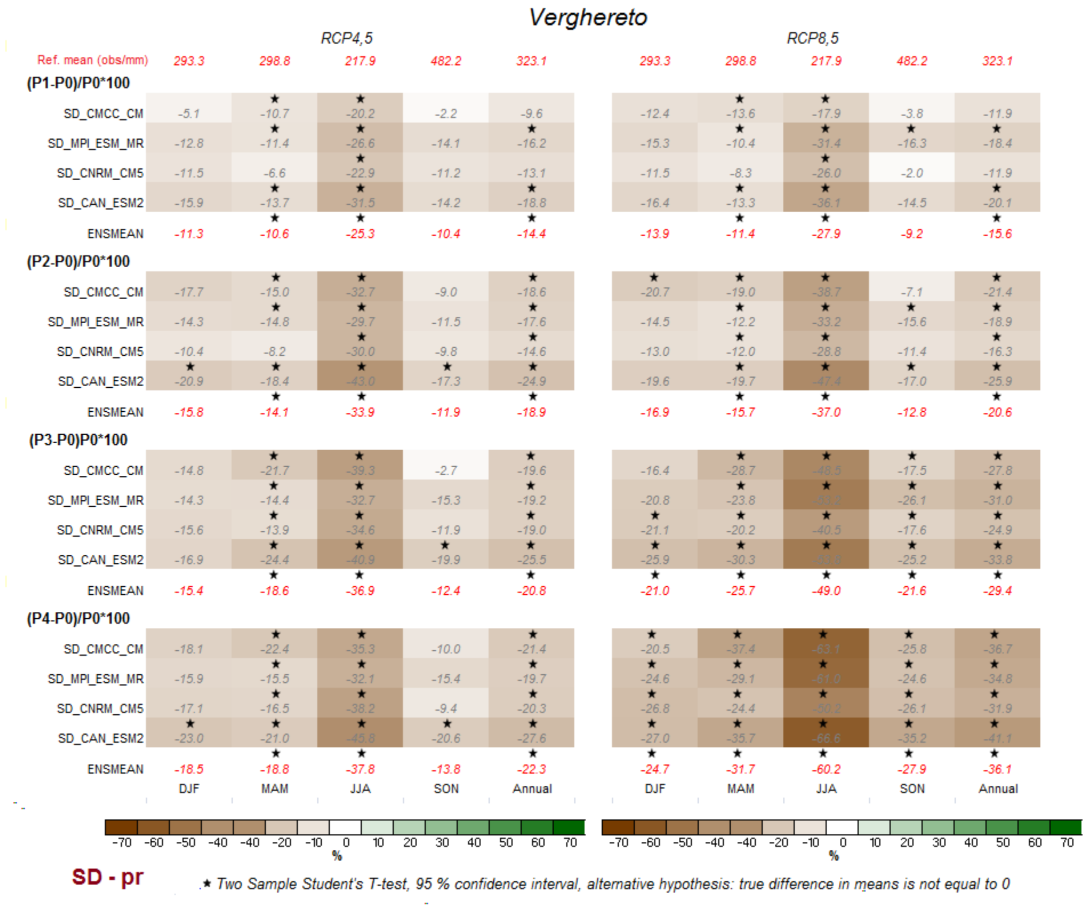

Verghereto

	RCP4,5					RCP8,5				
	DJF	MAM	JJA	SON	Annual	DJF	MAM	JJA	SON	Annual
Ref. mean (obs/mm)	293.3	298.8	217.9	482.2	323.1	293.3	298.8	217.9	482.2	323.1
(P1-P0)/P0*100										
SD_CMCC_CM	-5.1	★ -10.7	★ -20.2	-2.2	-9.6	-12.4	★ -13.6	★ -17.9	-3.8	-11.9
SD_MPI_ESM_MR	-12.8	★ -11.4	★ -26.6	-14.1	★ -16.2	-15.3	★ -10.4	★ -31.4	★ -16.3	★ -18.4
SD_CNRM_CM5	-11.5	-6.6	★ -22.9	-11.2	-13.1	-11.5	-8.3	★ -26.0	-2.0	-11.9
SD_CAN_ESM2	-15.9	★ -13.7	★ -31.5	-14.2	★ -18.8	-16.4	★ -13.3	★ -36.1	-14.5	★ -20.1
ENSMEAN	-11.3	★ -10.6	★ -25.3	-10.4	★ -14.4	-13.9	★ -11.4	★ -27.9	-9.2	★ -15.6
(P2-P0)/P0*100										
SD_CMCC_CM	-17.7	★ -15.0	★ -32.7	-9.0	★ -18.6	★ -20.7	★ -19.0	★ -38.7	-7.1	★ -21.4
SD_MPI_ESM_MR	-14.3	★ -14.8	★ -29.7	-11.5	★ -17.6	-14.5	★ -12.2	★ -33.2	★ -15.6	★ -18.9
SD_CNRM_CM5	-10.4	-8.2	★ -30.0	-9.8	★ -14.6	-13.0	★ -12.0	★ -28.8	-11.4	★ -16.3
SD_CAN_ESM2	★ -20.9	★ -18.4	★ -43.0	★ -17.3	★ -24.9	-19.6	★ -19.7	★ -47.4	★ -17.0	★ -25.9
ENSMEAN	-15.8	★ -14.1	★ -33.9	-11.9	★ -18.9	-16.9	★ -15.7	★ -37.0	-12.8	★ -20.6
(P3-P0)P0*100										
SD_CMCC_CM	-14.8	★ -21.7	★ -39.3	-2.7	★ -19.6	-16.4	★ -28.7	★ -48.5	★ -17.5	★ -27.8
SD_MPI_ESM_MR	-14.3	★ -14.4	★ -32.7	-15.3	★ -19.2	-20.8	★ -23.8	★ -53.2	★ -26.1	★ -31.0
SD_CNRM_CM5	-15.6	★ -13.9	★ -34.6	-11.9	★ -19.0	★ -21.1	★ -20.2	★ -40.5	★ -17.6	★ -24.9
SD_CAN_ESM2	-16.9	★ -24.4	★ -40.9	★ -19.9	★ -25.5	★ -25.9	★ -30.3	★ -53.8	★ -25.2	★ -33.8
ENSMEAN	-15.4	★ -18.6	★ -36.9	-12.4	★ -20.8	★ -21.0	★ -25.7	★ -49.0	★ -21.6	★ -29.4
(P4-P0)/P0*100										
SD_CMCC_CM	-18.1	★ -22.4	★ -35.3	-10.0	★ -21.4	★ -20.5	★ -37.4	★ -63.1	★ -25.8	★ -36.7
SD_MPI_ESM_MR	-15.9	★ -15.5	★ -32.1	-15.4	★ -19.7	★ -24.6	★ -29.1	★ -61.0	★ -24.6	★ -34.8
SD_CNRM_CM5	-17.1	★ -16.5	★ -38.2	-9.4	★ -20.3	★ -26.8	★ -24.4	★ -50.2	★ -26.1	★ -31.9
SD_CAN_ESM2	★ -23.0	★ -21.0	★ -45.8	★ -20.6	★ -27.6	★ -27.0	★ -35.7	★ -66.6	★ -35.2	★ -41.1
ENSMEAN	-18.5	★ -18.8	★ -37.8	-13.8	★ -22.3	★ -24.7	★ -31.7	★ -60.2	★ -27.9	★ -36.1

SD - pr

★ *Two Sample Student's T-test, 95 % confidence interval, alternative hypothesis: true difference in means is not equal to 0*

Figure 5-259: Seasonal and annual amount of precipitation: observed values over reference period (in red), changes projected by statistical downscaling applied to 4GCMs and the Ensemble Mean of changes over the four periods (P1, P2, P3, P4) expressed in % RCP4.5 (left) and RCP 8.5 (right) scenarios. Significant change is marked by star (source Arpae-Simc)

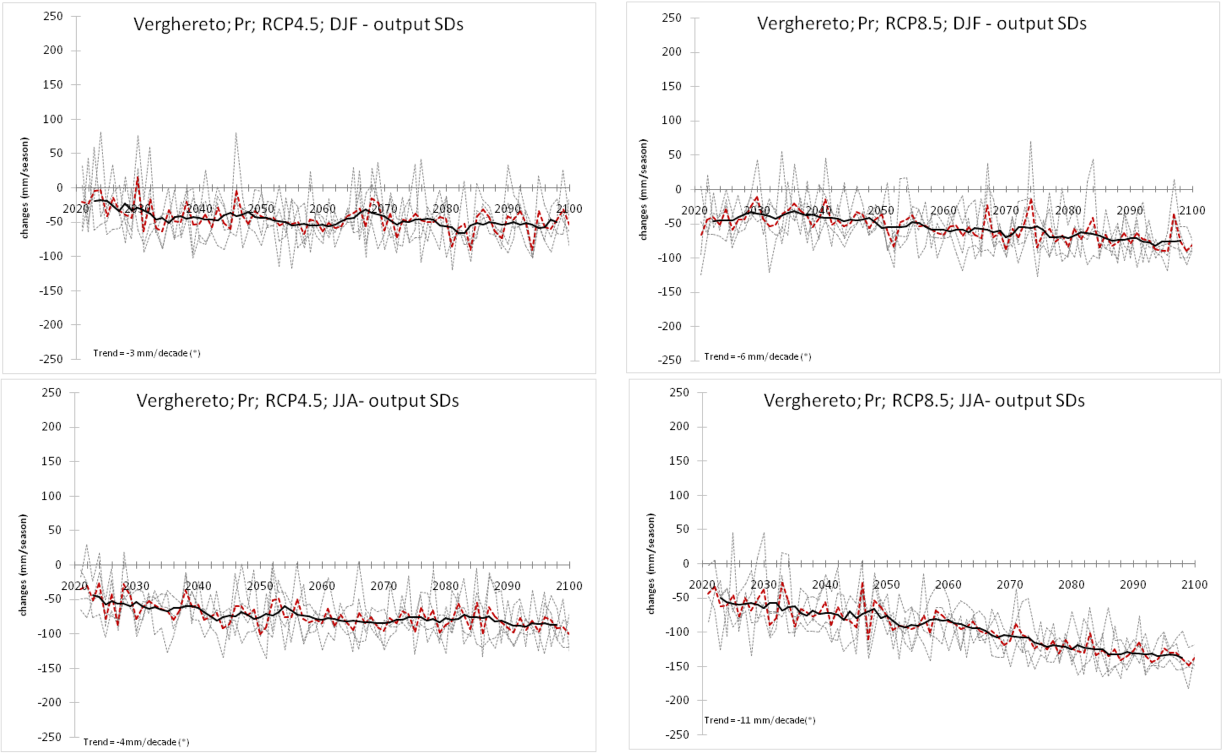

Figure 5-260: Variability of future changes of winter (DJF) and summer (JJA) precipitation projected through SDs applied to 4GCMs (grey lines); the Ensemble Mean (red line) and moving average (black line) - scenario RCP4.5 (left) and RCP8.5 (right), 2021-2100 period Significant trend is marked with star while n.s. means not significant (source Arpae-Simc).

6.6.2.2.2 *Intense precipitation*

90th percentile of seasonal amount of precipitation

Intense precipitation (Figure 5-261), defined by 90th percentile of precipitation in Verghereto- show in generally a decreases except autumn when an increase is projected especially on P3 and P4. The changes are not significant at seasonal and annual level. The long-term variability over 2021-2100 shows negative trend during winter and no signal of trend during summer (see figure 5-262).

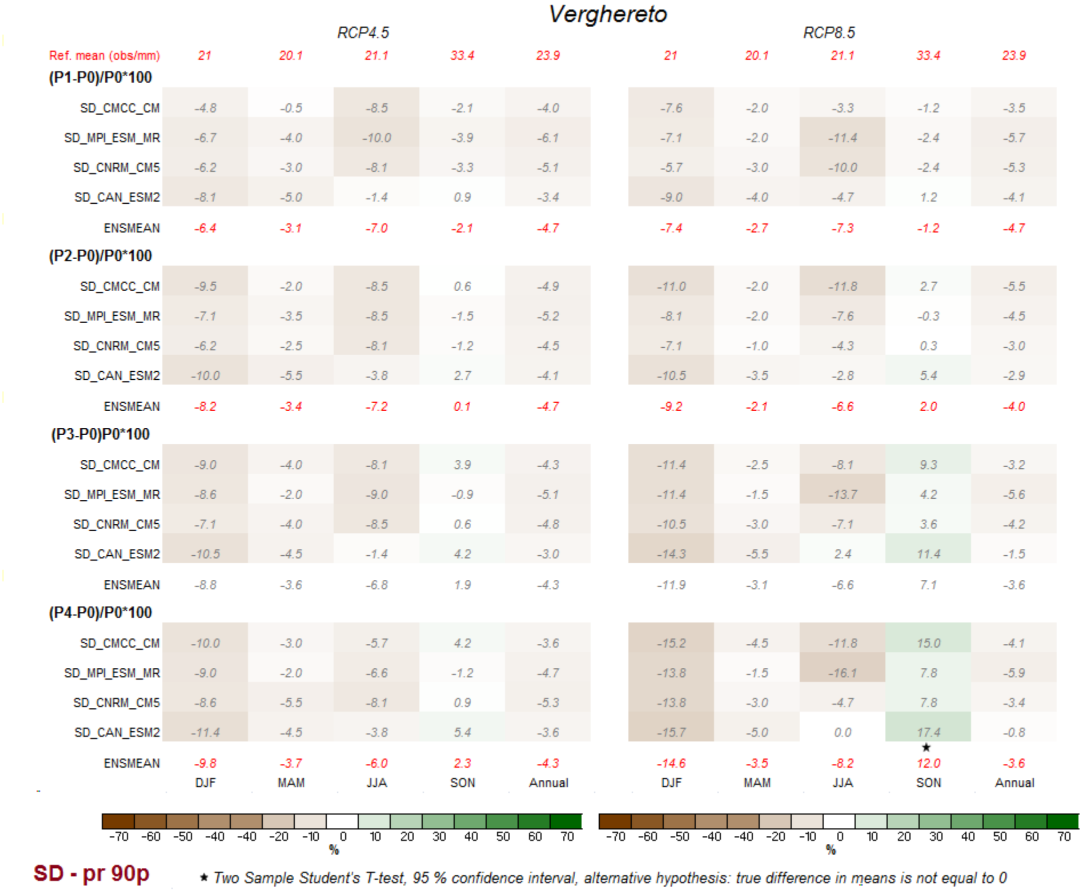

Verghereto

	RCP4.5					RCP8.5				
	DJF	MAM	JJA	SON	Annual	DJF	MAM	JJA	SON	Annual
Ref. mean (obs/mm)	21	20.1	21.1	33.4	23.9	21	20.1	21.1	33.4	23.9
(P1-P0)/P0*100										
SD_CMCC_CM	-4.8	-0.5	-8.5	-2.1	-4.0	-7.6	-2.0	-3.3	-1.2	-3.5
SD_MPI_ESM_MR	-6.7	-4.0	-10.0	-3.9	-6.1	-7.1	-2.0	-11.4	-2.4	-5.7
SD_CNRM_CM5	-6.2	-3.0	-8.1	-3.3	-5.1	-5.7	-3.0	-10.0	-2.4	-5.3
SD_CAN_ESM2	-8.1	-5.0	-1.4	0.9	-3.4	-9.0	-4.0	-4.7	1.2	-4.1
ENSMEAN	-6.4	-3.1	-7.0	-2.1	-4.7	-7.4	-2.7	-7.3	-1.2	-4.7
(P2-P0)/P0*100										
SD_CMCC_CM	-9.5	-2.0	-8.5	0.6	-4.9	-11.0	-2.0	-11.8	2.7	-5.5
SD_MPI_ESM_MR	-7.1	-3.5	-8.5	-1.5	-5.2	-8.1	-2.0	-7.6	-0.3	-4.5
SD_CNRM_CM5	-6.2	-2.5	-8.1	-1.2	-4.5	-7.1	-1.0	-4.3	0.3	-3.0
SD_CAN_ESM2	-10.0	-5.5	-3.8	2.7	-4.1	-10.5	-3.5	-2.8	5.4	-2.9
ENSMEAN	-8.2	-3.4	-7.2	0.1	-4.7	-9.2	-2.1	-6.6	2.0	-4.0
(P3-P0)P0*100										
SD_CMCC_CM	-9.0	-4.0	-8.1	3.9	-4.3	-11.4	-2.5	-8.1	9.3	-3.2
SD_MPI_ESM_MR	-8.6	-2.0	-9.0	-0.9	-5.1	-11.4	-1.5	-13.7	4.2	-5.6
SD_CNRM_CM5	-7.1	-4.0	-8.5	0.6	-4.8	-10.5	-3.0	-7.1	3.6	-4.2
SD_CAN_ESM2	-10.5	-4.5	-1.4	4.2	-3.0	-14.3	-5.5	2.4	11.4	-1.5
ENSMEAN	-8.8	-3.6	-6.8	1.9	-4.3	-11.9	-3.1	-6.6	7.1	-3.6
(P4-P0)/P0*100										
SD_CMCC_CM	-10.0	-3.0	-5.7	4.2	-3.6	-15.2	-4.5	-11.8	15.0	-4.1
SD_MPI_ESM_MR	-9.0	-2.0	-6.6	-1.2	-4.7	-13.8	-1.5	-16.1	7.8	-5.9
SD_CNRM_CM5	-8.6	-5.5	-8.1	0.9	-5.3	-13.8	-3.0	-4.7	7.8	-3.4
SD_CAN_ESM2	-11.4	-4.5	-3.8	5.4	-3.6	-15.7	-5.0	0.0	17.4 ★	-0.8
ENSMEAN	-9.8	-3.7	-6.0	2.3	-4.3	-14.6	-3.5	-8.2	12.0	-3.6

SD - pr 90p

★ Two Sample Student's T-test, 95 % confidence interval, alternative hypothesis: true difference in means is not equal to 0

Figure 5-261: Seasonal and annual amount of 90th precipitation: observed values over reference period (in red), changes projected by statistical downscaling applied to 4GCMs and the Ensemble Mean over the four periods (P1, P2, P3, P4) projected in the framework of RCP4.5 (left) and RCP 8.5 (right). Significant change is marked by star Significant trend is marked with star while n.s. means not significant (source Arpae-Simc).

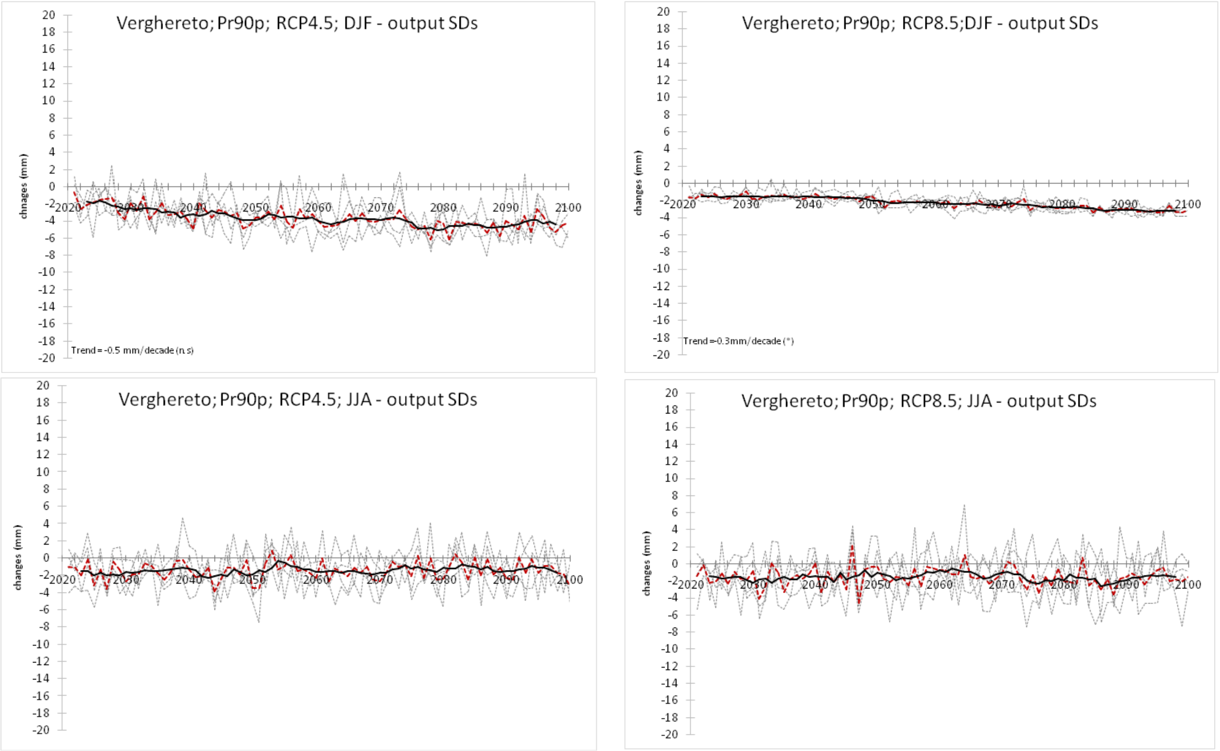

Figure 5-262: Future changes of winter (DJF) and summer (JJA) 90th perc. of precipitation projected through SDs applied to 4GCMs (grey lines); the Ensemble Mean (red line) and moving average (black line) - scenario RCP4.5 (left) and RCP8.5 (right), 2021-2100 period. Significant trend is marked with star while n.s. means not significant (source Arpae-Simc).

6.6.2.2.3 *Consecutive dry days*

The projected changes of consecutive dry days at Verghereto, index defined as the maximum number of consecutive days without precipitation, is presented in figure 5-263. Significant increase is projected in spring and summer for RCP4.5 and RCP8.5 (starting from P1 to P4), while winter and autumn could expect a decrease even if this is not statistically significant.
Long term variability presented in figure 5-264 shows a significant positive trend detected in RCP8.5 scenario (1 days/decade).

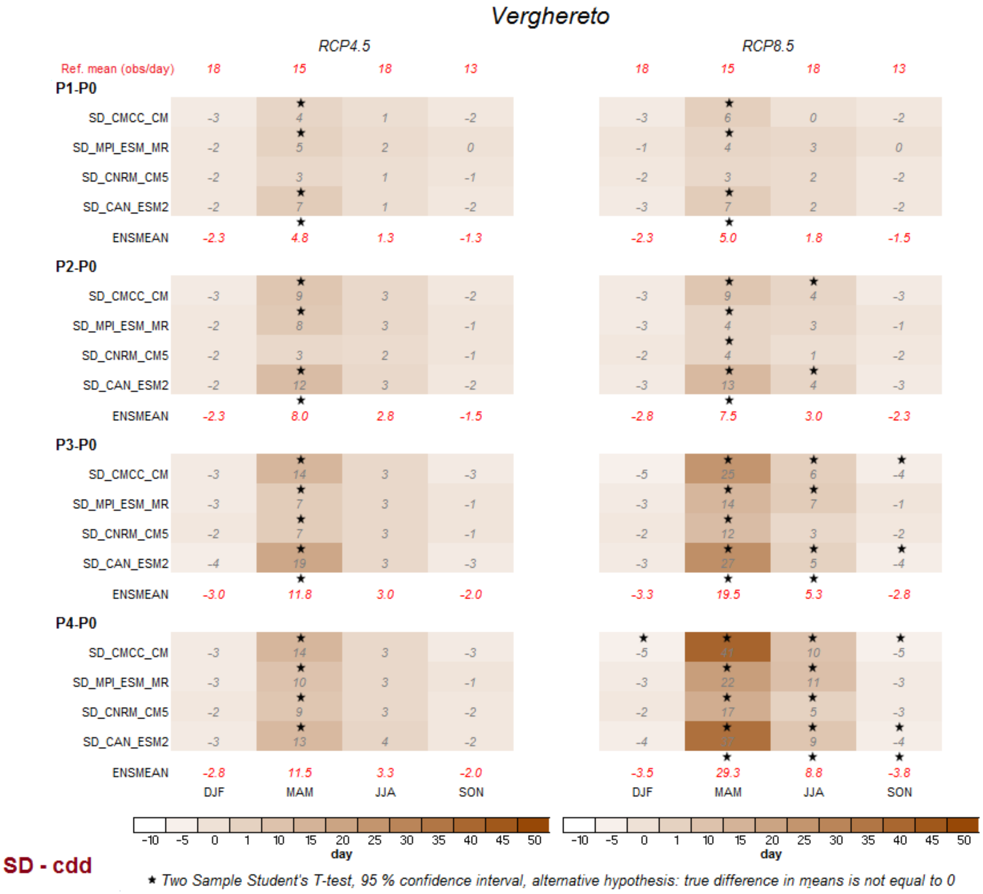

Verghereto

	RCP4.5				RCP8.5			
	DJF	MAM	JJA	SON	DJF	MAM	JJA	SON
Ref. mean (obs/day)	18	15	18	13	18	15	18	13
P1-P0								
SD_CMCC_CM	-3	★ 4	1	-2	-3	★ 6	0	-2
SD_MPI_ESM_MR	-2	★ 5	2	0	-1	★ 4	3	0
SD_CNRM_CM5	-2	3	1	-1	-2	3	2	-2
SD_CAN_ESM2	-2	★ 7	1	-2	-3	★ 7	2	-2
ENSMEAN	-2.3	★ 4.8	1.3	-1.3	-2.3	★ 5.0	1.8	-1.5
P2-P0								
SD_CMCC_CM	-3	★ 9	3	-2	-3	★ 9	★ 4	-3
SD_MPI_ESM_MR	-2	★ 8	3	-1	-3	★ 4	3	-1
SD_CNRM_CM5	-2	3	2	-1	-2	★ 4	1	-2
SD_CAN_ESM2	-2	★ 12	3	-2	-3	★ 13	★ 4	-3
ENSMEAN	-2.3	★ 8.0	2.8	-1.5	-2.8	★ 7.5	3.0	-2.3
P3-P0								
SD_CMCC_CM	-3	★ 14	3	-3	-5	★ 25	★ 6	★ -4
SD_MPI_ESM_MR	-3	★ 7	3	-1	-3	★ 14	★ 7	-1
SD_CNRM_CM5	-2	★ 7	3	-1	-2	★ 12	3	-2
SD_CAN_ESM2	-4	★ 19	3	-3	-3	★ 27	★ 5	★ -4
ENSMEAN	-3.0	★ 11.8	3.0	-2.0	-3.3	★ 19.5	★ 5.3	-2.8
P4-P0								
SD_CMCC_CM	-3	★ 14	3	-3	★ -5	★ 41	★ 10	★ -5
SD_MPI_ESM_MR	-3	★ 10	3	-1	-3	★ 22	★ 11	-3
SD_CNRM_CM5	-2	★ 9	3	-2	-2	★ 17	★ 5	-3
SD_CAN_ESM2	-3	★ 13	4	-2	-4	★ 37	★ 9	★ -4
ENSMEAN	-2.8	11.5	3.3	-2.0	-3.5	★ 29.3	★ 8.8	★ -3.8

SD - cdd

★ Two Sample Student's T-test, 95 % confidence interval, alternative hypothesis: true difference in means is not equal to 0

Figure 5-263: Seasonal and annual max. consecutive dry days: observed values over reference period (in red), changes projected by statistical downscaling applied to 4GCMs and the Ensemble Mean over the four periods (P1, P2, P3, P4) projected in the framework of RCP4.5 (left) and RCP 8.5 (right). Significant change is marked by star (source Arpae-Simc)

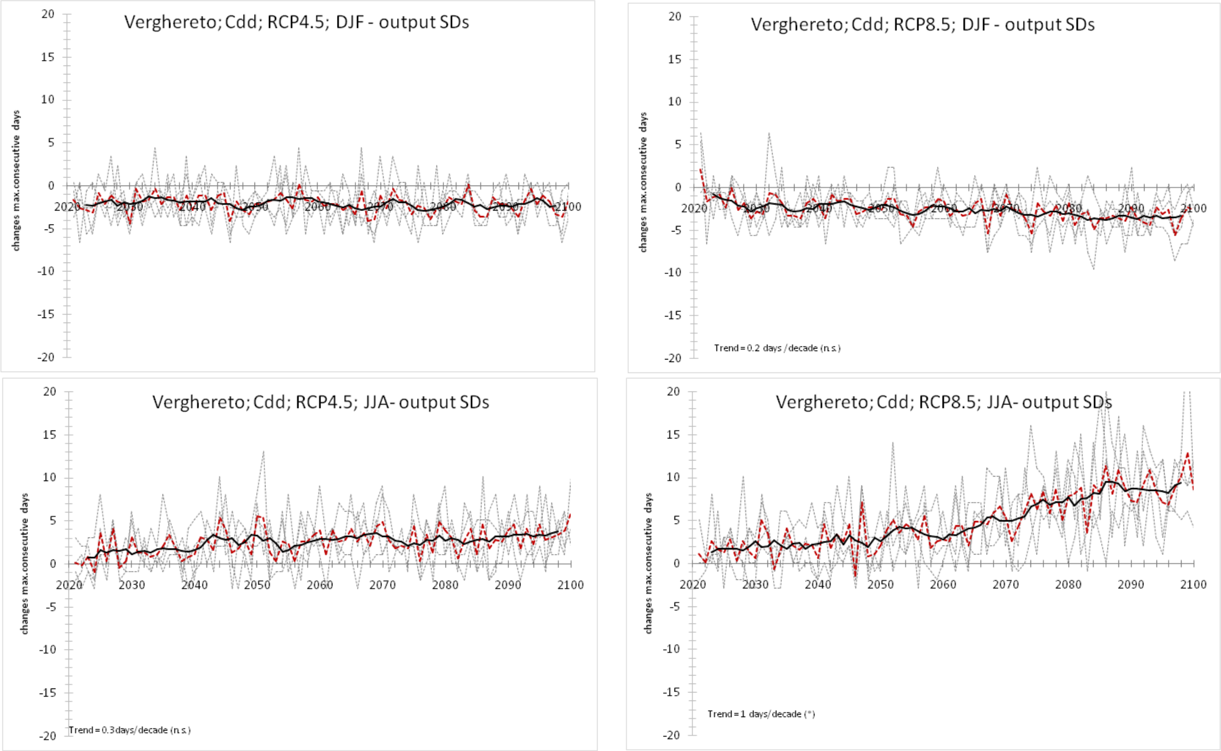

Figure 5-264: Variability of future changes of winter (DJF) and summer (JJA) max. number of consecutive dry days projected through SDs applied to 4GCMs (grey lines); the Ensemble Mean (red line) and moving average (black line) - scenario RCP4.5 (left) and RCP8.5 (right), 2021-2100. Significant trend is marked with star while n.s. means not significant (source Arpae-Simc).

7 Conclusions

This document provides a description of the projections of climate indicators over different periods and radiative scenarios based on data delivered by CMCC, Arpae and DHMZ to the ADRIADAPT project users, both in terms of dynamical (see deliverables D3.2.1), and statistical (see deliverable D3.2.2) downscaling outputs. Within the ADRIADAPT project, the simulated data cover the period 1961 to 2100, following historical forcing up to 2005 and two different possible radiative emission scenarios to the end of the century: a business as usual (RCP8.5) and a more moderate one (RCP4.5). Result for future periods are mainly presented as deviation from the base line historical period (1986-2005, named P0) over different time slices: 2021:2040, 2041:2060, 2061:2080, 2081:2100 named respectively P1, P2, P3, P4.

Projections resulting from the statistical downscaling over the case studies cities are reasonably consistent with what expected based on dynamical downscaling. Projections for the main parameters required by stakeholders and project users, case study by case study, are shown, also considering the significance of the differences found between the considered periods and the detected tendencies.

Within the current large document, the different stakeholders now have the possibility to get the necessary information on multi-scenario climate projection for future planning, selecting the domain and parameters of interest within chapter 5 and chapter 6.

8 Acknowledgements

We acknowledge the World Climate Research Programme's Working Group on Coupled Modelling, which is responsible for CMIP, and we thank the climate modeling groups (listed in Tables 1 and 3 of this document) for producing and making available their model output. For CMIP the U.S. Department of Energy's Program for Climate Model Diagnosis and Intercomparison provides coordinating support and led development of software infrastructure in partnership with the Global Organization for Earth System Science Portals.

9 References

- Antolini G, Auteri L, Pavan V, Tomei F, Tomozeiu R, Marletto V (2015): A daily high-resolution gridded climatic data set for Emilia-Romagna, Italy, during 1961–2010 International Journal of Climatology 08/2015; DOI:10.1002/joc.4473

- Cornes, R., G. van der Schrier, E.J.M. van den Besselaar, and P.D. Jones. 2018: An Ensemble Version of the E-OBS Temperature and Precipitation Datasets, J. Geophys. Res. Atmos., 123. doi:10.1029/2017JD028200

- Kobayashi S et al 2015 The JRA-55 re-analyses: general specifications and basic characteristics J. Meteor. Soc. Jpn. 93-5-48.

- Kotlarski, S., Keuler, K., Christensen, O. B., Colette, A., Déqué, M., Gobiet, A., Goergen, K., Jacob, D., Lüthi, D., van Meijgaard, E., Nikulin, G., Schär, C., Teichmann, C., Vautard, R., Warrach-Sagi, K., and Wulfmeyer, V. 2014: Regional climate modeling on European scales: a joint standard evaluation of the EURO-CORDEX RCM ensemble, Geosci. Model Dev., 7, 1297-1333, doi:10.5194/gmd-7-1297-2014.

- Nikulin, G., Jones, C., Giorgi, G., Asrar, G., Büchner, M., Cerezo- Mota, R., Christensen, O., Déqué, M., Fernandez, J., Hänsler, A., van Meijgaard, E., Samuelsson, P., Sylla, M., and Sushama, L., 2012: Precipitation Climatology in an Ensemble of CORDEX- Africa Regional Climate Simulations, J. Climate, 25, 6057–6078, doi:10.1175/JCLI-D-11-00375.1.

- Rummukainen 2010: State-of-the-art with regional climate models, WIREs Clim Change, 1:82-96

- Scoccimarro E., P.G. Fogli, S. Gualdi, 2017. The role of humidity in determining scenarios of perceived temperature extremes in Europe Environ. Res. Lett. 12 114029.

- Simmons A J, Berrisford P, Dee D P, Hersbach H, Hirahara S and Th´epaut J N 2017 A reassessment of temperature variations and trends from global reanalyses and monthly surface climatological datasets Q. J. R. Meteorolog. Soc. 143.

- Tomozeiu R, Cacciamani C, Pavan V, Morgillo A and Busuioc A (2007) Climate change scenarios for surface temperature in Emilia-Romagna (Italy) obtained using statistical downscaling models. Theor Appl Climatol 90:25-47

- Tomozeiu R, Agrillo G, Cacciamani C, Pavan V. (2014): Statistically downscaled climate change projections of surface temperature over Northern Italy for the periods 2021-2050 and 2071-2099. Nat Hazards 72:143-168. doi: 10.1007/s11069-013-0552-y
- Vautard et al., 2013: The simulation of European heat waves from an ensemble of regional climate models within the EURO-CORDEX project. Volume 41, Issue 9-10, pp 2555-2575.Von Storch H and Zwiers FW(1999) Statistical Analysis in Climate Research, Cambridge University Press
- Von Storch H (1995): Spatial Patterns: EOFs and CCA. In: von Storch H, Navarra A (eds) Analysis of climate variability. Application of statistical techniques. Springer pp 227–258
- Wilks DS (2006) Statistical Methods in the Atmospheric Sciences, 2nd Ed. International Geophysics Series, Vol. 59, Academic Press

10 ANNEXES

Table A: Coordination of grid points that belong to Cervia (***C***) and Savio Valley Union Municipalities (***SVMU)***

No.	Code	Nome	Comune	Prov	Lat.	Lon	Height(m)
1	1755	RIDRACOLI	BAGNO DI ROMAGNA	FORLI-CESENA	43.8675	11.8447	740.8
2	1756	LA LAMA	BAGNO DI ROMAGNA	FORLI-CESENA	43.8225	11.8447	1058.8
3	1794	POGGIO ALLA LASTRA	BAGNO DI ROMAGNA	FORLI-CESENA	43.9125	11.9077	524.9
4	1795	STRABATENZA	BAGNO DI ROMAGNA	FORLI-CESENA	43.8675	11.9077	716.7
5	1796	PIETRAPAZZA	BAGNO DI ROMAGNA	FORLI-CESENA	43.8225	11.9077	922.9
6	1835	S.PIERO IN BAGNO	BAGNO DI ROMAGNA	FORLI-CESENA	43.8675	11.9708	611.8
7	1836	BAGNO DI ROMAGNA	BAGNO DI ROMAGNA	FORLI-CESENA	43.8225	11.9708	719
8	1837	VERGHERETO	VERGHERETO	FORLI-CESENA	43.7775	11.9708	915.4
9	1874	MONTE MASCOLINO	BAGNO DI ROMAGNA	FORLI-CESENA	43.9125	12.0338	655.4
10	1875	PASSO DELL'INCISA	BAGNO DI ROMAGNA	FORLI-CESENA	43.8675	12.0338	662.6
11	1876	MONTE COMERO	VERGHERETO	FORLI-CESENA	43.8225	12.0338	1058.9
12	1877	MONTECORONARO	VERGHERETO	FORLI-CESENA	43.7775	12.0338	920.7
13	1912	MERCATO SARACENO	MERCATO SARACENO	FORLI-CESENA	44.0025	12.0969	299
14	1913	RULLATO	CIVITELLA DI ROMAGNA	FORLI-CESENA	43.9575	12.0969	457.4
15	1914	RUSCELLO	SARSINA	FORLI-CESENA	43.9125	12.0969	473.2
16	1915	LAGO DI QUARTO	SARSINA	FORLI-CESENA	43.8675	12.0969	542.1
17	1916	RIOFREDDO	VERGHERETO	FORLI-CESENA	43.8225	12.0969	862.3
18	1917	MONTE FUMAIOLO	VERGHERETO	FORLI-CESENA	43.7775	12.0969	1050.3

No.	Code	Nome	Comune	Prov	Lat.	Lon	Height(m)
19	1950	POLENTA	CESENA	FORLI-CESENA	44.0925	12.1599	193.5
20	1951	BORELLO	CESENA	FORLI-CESENA	44.0475	12.1599	179.8
21	1952	MONTE IOTTONE	MERCATO SARACENO	FORLI-CESENA	44.0025	12.1599	246
22	1953	MERCATO SARACENO OVEST	MERCATO SARACENO	FORLI-CESENA	43.9575	12.1599	388.2
23	1954	SARSINA	SARSINA	FORLI-CESENA	43.9125	12.1599	316.9
24	1988	MARTORANO	CESENA	FORLI-CESENA	44.1825	12.2230	23.3
25	1989	CESENA	CESENA	FORLI-CESENA	44.1375	12.2230	43.9
26	1990	MONTEREALE	CESENA	FORLI-CESENA	44.0925	12.2230	138.4
27	1991	SORRIVOLI	CESENA	FORLI-CESENA	44.0475	12.2230	240.6
28	2026	CASTIGLIONE DI CERVIA	CERVIA	RAVENNA	44.2725	12.2860	-0.1
29	2027	PISIGNANO	CESENA	FORLI-CESENA	44.2275	12.2860	4.4
30	2028	S.GIORGIO	CESENA	FORLI-CESENA	44.1825	12.2860	13.4
31	2029	CESENA EST	CESENA	FORLI-CESENA	44.1375	12.2860	31.3
32	2030	CALISESE	CESENA	FORLI-CESENA	44.0925	12.2860	101.9
33	2066	MILANO MARITTIMA	CERVIA	RAVENNA	44.2725	12.3491	0
34	2067	PINARELLA	CERVIA	RAVENNA	44.2275	12.3491	-1.2
35	2069	BULGARNO'	CESENA	FORLI-CESENA	44.1375	12.3491	15.7

Table B: Coordination of Sibenik and Knin stations (Croatia case studies)

No.	Nome	Lat.	Lon	Height(m)

1	SIBENIK	43°43'41''	15°54'23''	77
2	KNIN	44°2'27''	16°12'25''	255